

Issues 1-3

2024 | Volume 20

The Journal on Advanced Studies in Theoretical and Experimental Physics,
including Related Themes from Mathematics

PROGRESS IN PHYSICS



“All scientists shall have the right to present their scientific research results, in whole or in part, at relevant scientific conferences, and to publish the same in printed scientific journals, electronic archives, and any other media.” — Declaration of Academic Freedom, Article 8

ISSN 1555-5534

PROGRESS IN PHYSICS

A Scientific Journal on Advanced Studies in Theoretical and Experimental Physics, including Related Themes from Mathematics. This journal is registered with the Library of Congress (DC, USA).

Electronic version of this journal:
<https://www.progress-in-physics.com>

Editorial Board

Dmitri Rabounski
rabounski@yahoo.com
Pierre Millette
pierremillette@sympatico.ca
Andreas Ries
andreasries@yahoo.com
Florentin Smarandache
fsmarandache@gmail.com
Larissa Borissova
lborissova@yahoo.com
Ebenezer Chifu
ebenechifu@yahoo.com

Postal Address

Department of Mathematics and Science,
University of New Mexico,
705 Gurley Ave., Gallup, NM 87301, USA

Copyright © *Progress in Physics*, 2024

All rights reserved. The authors of the articles do hereby grant *Progress in Physics* non-exclusive, worldwide, royalty-free license to publish and distribute the articles in accordance with the Budapest Open Initiative: this means that electronic copying, distribution and printing of both full-size version of the journal and the individual papers published therein for non-commercial, academic or individual use can be made by any user without permission or charge. The authors of the articles published in *Progress in Physics* retain their rights to use this journal as a whole or any part of it in any other publications and in any way they see fit. Any part of *Progress in Physics* howsoever used in other publications must include an appropriate citation of this journal.

This journal is powered by L^AT_EX

A variety of books can be downloaded free from the Digital Library of Science:
<http://fs.gallup.unm.edu/ScienceLibrary.htm>

ISSN: 1555-5534 (print)
ISSN: 1555-5615 (online)

Standard Address Number: 297-5092
Printed in the United States of America

June 2024

Vol. 20, Issue 1

CONTENTS

Smarandache F., Ries A., Millette P., Chifu E. Progress in Physics: Twentieth Year of Publication	3
Rabounski D., Borissova L. On the Lambda Term in Einstein's Equations and Its Influence on the Cosmological Redshift	4
Rabounski D., Borissova L. Cosmological Redshift: Which Cosmological Model Best Explains It?	13
Noh Y. J. Interpretation of Quantum Mechanics in Terms of Discrete Time II	21
Dvoeglazov V. V. Addendum to "The Feynman-Dyson propagators for neutral particles (locality or non-locality?)"	24
Muktibodh A. Santilli's Recovering of Einstein's Determinism	26
Smarandache F. Partial Collisions of Unmatter-Matter, Unmatter-Antimatter, and Unmatter1-Unmatter2 to Generate High Energy	33
Marquet P. The Vacuum Stress-Energy Tensor in General Relativity	36
Marquet P. Gödel Time Travel: New Highlights	41
Abbey G. F., Simfukwe J., Simpemba P. C., Phiri S. P., Srivastava A., Nyambuya G. G. Inference of Plausible Spatial Sizes of GRB Systems Using Newly Proposed FDSL-Model for GRB Time Delays	47
Potter F. Graph Theory Entropy Values for Lepton and Quark Discrete Symmetry Quantum States and Their Decay Channels	61

Information for Authors

Progress in Physics has been created for rapid publications on advanced studies in theoretical and experimental physics, including related themes from mathematics and astronomy. All submitted papers should be professional, in good English, containing a brief review of a problem and obtained results.

All submissions should be designed in L^AT_EX format using *Progress in Physics* template. This template can be downloaded from *Progress in Physics* home page <http://www.ptep-online.com>

Preliminary, authors may submit papers in PDF format. If the paper is accepted, authors can manage L^AT_EX typing. Do not send MS Word documents, please: we do not use this software, so unable to read this file format. Incorrectly formatted papers (i.e. not L^AT_EX with the template) will not be accepted for publication. Those authors who are unable to prepare their submissions in L^AT_EX format can apply to a third-party payable service for LaTeX typing. Our personnel work voluntarily. Authors must assist by conforming to this policy, to make the publication process as easy and fast as possible.

Abstract and the necessary information about author(s) should be included into the papers. To submit a paper, mail the file(s) to the Editor-in-Chief.

All submitted papers should be as brief as possible. Short articles are preferable. Large papers can also be considered. Letters related to the publications in the journal or to the events among the science community can be applied to the section *Letters to Progress in Physics*.

All that has been accepted for the online issue of *Progress in Physics* is printed in the paper version of the journal. To order printed issues, contact the Editors.

Authors retain their rights to use their papers published in *Progress in Physics* as a whole or any part of it in any other publications and in any way they see fit. This copyright agreement shall remain valid even if the authors transfer copyright of their published papers to another party.

Electronic copies of all papers published in *Progress in Physics* are available for free download, copying, and re-distribution, according to the copyright agreement printed on the titlepage of each issue of the journal. This copyright agreement follows the *Budapest Open Initiative* and the *Creative Commons Attribution-Noncommercial-No Derivative Works 2.5 License* declaring that electronic copies of such books and journals should always be accessed for reading, download, and copying for any person, and free of charge.

Consideration and review process does not require any payment from the side of the submitters. Nevertheless the authors of accepted papers are requested to pay the page charges. *Progress in Physics* is a non-profit/academic journal: money collected from the authors cover the cost of printing and distribution of the annual volumes of the journal along the major academic/university libraries of the world. (Look for the current author fee in the online version of *Progress in Physics*.)

LETTERS TO PROGRESS IN PHYSICS**Progress in Physics: Twentieth Year of Publication**Florentin Smarandache¹, Andreas Ries², Pierre Millette³, and Ebenezer Chifu⁴

Progress in Physics Editorial Team

¹fsmarandache@gmail.com, ²ries@ptep-online.com, ³millette@ptep-online.com, ⁴ebenechifu@yahoo.com

“All scientists shall have the right to present their scientific research results, in whole or in part, at relevant scientific conferences, and to publish the same in printed scientific journals, electronic archives, and any other media.”

Declaration of Academic Freedom, Article 8 [1]

With this inauguration of Volume 20 of *Progress in Physics*, the journal starts its twentieth year of publication, offering a much-needed avenue for the dissemination of truly scientific submissions that are written as proper scientific papers that are free of logical, mathematical and physical errors.

The journal *Progress in Physics* was created in January 2005 on behalf of many influential scientists with whom we were in correspondence. The main reason was that publications in other journals were allowed only if the submitter was affiliated with a scientific institution or research organization. Given this situation, many working scientists finding themselves partially employed or unemployed, such as in between research grants, find themselves unable to publish their research results. Even e-print archives such as Cornell’s arXiv required scientific affiliation and still follow this policy. This is why the Declaration of Academic Freedom was written and published in ten languages in *Progress in Physics* [1], and why the journal was started.

Since commencing in 2005, we have published 967 articles till now, which are accessed free of charge online. We have also distributed printed copies of the journal to major libraries of science throughout the world and offer open access online based on library preferences. The journal has a stable position among other scientific journals published by scientific institutions, and at the same time remains absolutely independent from any bureaucratic influence on the part of scientific organizations.

Our aim is to publish a professional journal by keeping a high professional level of operation. Therefore, we always review submitted papers accepting those that meet the requirements stated above, and rejecting those that are not written as proper scientific papers or that contain formal errors. We follow our major principle according to which we consider submissions on the basis of what has been written in the submissions, without any connection with the submitter’s affiliation, personality and other considerations.

This has allowed us to make our journal a repository for high quality scientific research over the last two decades. We still do everything to keep the high level of the journal, which is a great advantage for our authors. Our Editorial Team as-

ures our readers and authors that we will continue to adhere to this independent editorial policy in the future, thereby following the Declaration of Academic Freedom.

In conclusion, we have done, and will continue to do, everything to support the principles of open and free dissemination of scientific information in the future. We open this 20th anniversary volume of our journal with faith in the future and invite all researchers who want to publish their scientific results to submit their manuscripts to our journal.

Submitted on January 2, 2024

References

1. Rabounski D. Declaration of Academic Freedom (Scientific Human Right). *Progress in Physics*, 2006, v. 2(1), 57–60.

LETTERS TO PROGRESS IN PHYSICS

On the Lambda Term in Einstein's Equations and Its Influence on the Cosmological Redshift

Dmitri Rabounski and Larissa Borissova

Puschino, Moscow Region, Russia

E-mail: rabounski@yahoo.com, lborissova@yahoo.com

Here we analyze our theory of the physical vacuum (λ -field filling de Sitter spaces), in which we calculated its physically observable properties (2001) and the parabolic (non-linear) cosmological redshift specific to de Sitter spaces (2013). To explain the recently discovered non-linear cosmological redshift, we consider the following options: 1) our Universe is a de Sitter world with $\lambda > 0$ and, therefore, with a parabolic cosmological redshift (because with $\lambda > 0$ the non-Newtonian gravitational forces acting in a de Sitter world are forces of repulsion, which decelerate photons), but in this case the physical vacuum has a negative density $\check{\rho} < 0$, and the observable curvature radius of space is imaginary (the space geometry is hyperbolic); 2) our Universe is a de Sitter world with $\lambda < 0$, where the physical vacuum has a positive density $\check{\rho} > 0$, and the observable curvature radius is real (the space geometry is spherical), but with a parabolic cosmological blueshift (and not a redshift) because with $\lambda < 0$ the non-Newtonian forces are forces of attraction (they accelerate photons); 3) our Universe is a de Sitter world with $\lambda > 0$ and, hence, a parabolic cosmological redshift, but the $\lambda g_{\alpha\beta}$ term in Einstein's field equations has the opposite (negative) sign. We vote for the 3rd option, because in this case a) the physical vacuum has a positive density $\check{\rho} > 0$, which satisfies the physical requirement that any kind of observable matter must have a positive mass and density, b) the observable curvature radius of space is real (and not imaginary) and, hence, the space geometry is spherical (and not hyperbolic), c) the non-Newtonian gravitational forces are forces of repulsion (they decelerate photons, thereby producing a redshift), d) the event horizon in such a universe is outlined by the gravitational radius of the de Sitter sphere. All this confirms the supposition that our Universe is a huge de Sitter gravitational collapsar with $\lambda > 0$ and a non-linear (parabolic) cosmological redshift.

In the late 1980s and 1990s, we undertook a massive theoretical research on the motion of particles in the space-time of General Relativity, which we published in 2001 in our two monographs [1, 2]. In particular, we created a theory of the physical vacuum (λ -field filling de Sitter spaces), in which we calculated its physically observable properties such as density, pressure, etc. [2, Chapter 5]. In 2010, using the mentioned theory of the physical vacuum, Larissa created a theory of the de Sitter gravitational collapsar (de Sitter bubble), which she suggested as a model of the observable Universe [3]. In our third monograph [4], published in 2013, we predicted a parabolic (non-linear) cosmological redshift in a de Sitter space [4, §6.4–§6.5]. In 2018, we also published a short paper on the mentioned parabolic redshift [5].

Meanwhile there was a serious problem with determining the cosmological shift in the frequency of photons travelling in a de Sitter world. This problem arose due to the sign of the λ -term, because it is not specified in de Sitter's metric. So, our closest colleagues drew our attention to some confusion in our sequential publications on this subject.

First, in our theory of the physical vacuum, where we did not consider the cosmological redshift, we assumed $\lambda < 0$ and,

therefore, a positive vacuum density $\check{\rho} > 0$ in our Universe [2, §5.3]. In this case, the non-Newtonian gravitational forces acting in any de Sitter space are forces of attraction, and the physically observable three-dimensional curvature is positive $C > 0$. Since $C = \frac{1}{\mathfrak{R}^2}$, the latter means that such a universe has a real observable curvature radius \mathfrak{R} , and, therefore, the space geometry is spherical (this is what the geometry of a de Sitter space should be). But a few years later, when Larissa suggested a collapsed de Sitter sphere as a model of the observable Universe [3], and then, in our monograph on the internal constitution of stars, where we considered de Sitter collapsars [4, Chapter 6], and also in our subsequent paper on the cosmological redshift [5], it was assumed that $\lambda > 0$. This is because forces of attraction ($\lambda < 0$) accelerate photons, thereby producing a photon blueshift (gain of the photon energy), and forces of repulsion ($\lambda > 0$) decelerate photons, thereby producing a photon redshift (loss of the photon energy). But in the case of $\lambda > 0$ we should expect a negative vacuum density $\check{\rho} < 0$, a negative physically observable curvature $C < 0$ and, hence, an imaginary numerical value of the observable curvature radius \mathfrak{R} of such a universe (this means that the space geometry is hyperbolic).

To resolve this contradiction, a solution was proposed in §6.5 of our book [4] (§5.1 in the 1st edition, 2013). But this solution was not well recognized by the readers, because it was “lost” among many other new results presented in that book. As a result, the above confusion has created a problem in understanding the parabolic cosmological redshift that we had predicted for a de Sitter universe.

Note that the cosmological redshift problem was never our task or field of interest. The parabolic redshift in a de Sitter universe was just one of the spin-off theoretical results that we obtained in the course of our long-term work on other, much more important mathematical and applied problems in the General Theory of Relativity.* On the other hand, we must respond to our colleagues regarding the parabolic cosmological redshift in a de Sitter universe, which we had predicted “at the tip of the pen”. It looks like it is time to dot all the i’s in this problem.

Let us begin. The λ -term was introduced in 1917 by Albert Einstein [6]. He added it multiplied by the fundamental metric tensor $g_{\alpha\beta}$ to the right-hand side of the field equations (known also as Einstein’s equations), which thus acquired their final well-known form†

$$R_{\alpha\beta} - \frac{1}{2} g_{\alpha\beta} R = -\kappa T_{\alpha\beta} + \lambda g_{\alpha\beta}.$$

He did this, because the metric of a static finite spherically symmetric space filled with a homogeneous and isotropic distribution of substance — Einstein’s metric, which he initially considered as the basic cosmological model of our Universe, — does not satisfy the original field equations (which do not contain the λ -term). Mathematically, this means that substituting the components of the fundamental metric tensor $g_{\alpha\beta}$, taken from Einstein’s metric, into the original field equations (without the λ -term), the left-hand side of the field equations does not equalize the right-hand side. But with the λ -term

*“As you know, our success depends on the fact that nearly all major scientific advances have been made while looking for something else, or following up curious observations.” — David Jones, Editor of *New Scientist*, May 1981. Cited from: Jones D. *The Inventions of Daedalus*. W. H. Freeman & Co., Oxford, 1982, page 3.

†Here $R_{\alpha\sigma} = R_{\alpha\beta\gamma\sigma}^{\dots\beta}$ [cm⁻²] is Ricci’s tensor (obtained as the contraction of the Riemann-Christoffel curvature tensor $R_{\alpha\beta\gamma\delta}$ by one index in each pair of its four indices), $R = g^{\alpha\beta} R_{\alpha\beta}$ is the scalar curvature, $\kappa = 8\pi G/c^2 = 1.862 \times 10^{-27}$ [cm/gram] is Einstein’s constant, $G = 6.672 \times 10^{-8}$ [cm³/gram sec²] is Gauss’ gravitational constant, and $T_{\alpha\beta}$ [gram/cm³] is the energy-momentum tensor of a distributed matter that fills the space.

Einstein’s field equations show how in a Riemannian space the field of its four-dimensional curvature depends on the field of a distributed matter (substance or, say, electromagnetic field) that fills this space. Note that Einstein’s field equations are not some kind of physical hypothesis. They follow mathematically from the geometric structure characteristic of any Riemannian space (as well as the Riemannian quadratic metric and its invariance throughout the entire space). For example, let us have a space determined by a metric. In order for this space to be Riemannian, it is necessary that its metric has the Riemannian quadratic form $ds^2 = g_{\alpha\beta} dx^\alpha dx^\beta$, be invariant throughout the entire space, and satisfy the field equations.

added to the right-hand side of the field equations, the fundamental metric tensor $g_{\alpha\beta}$ of a spherically symmetric static homogeneous and isotropic universe (*Einstein’s cosmological model*) makes both sides of the equations equal to each other, so the equations vanish. For detail, see Einstein’s 1917 paper [6] and the comprehensive review on this subject [7].

A year later, in 1918, Willem de Sitter [8] mathematically deduced that, in addition to Einstein’s metric (which determines a space filled with a static finite spherically homogeneous and isotropic distribution of substance), there is also another space metric satisfying the field equations containing the λ -term. De Sitter’s space metric has the form

$$ds^2 = \left(1 - \frac{\lambda r^2}{3}\right) c^2 dt^2 - \frac{dr^2}{1 - \frac{\lambda r^2}{3}} - r^2 (d\theta^2 + \sin^2\theta d\varphi^2)$$

and describes a static finite spherically symmetric space filled with a homogeneous and isotropic distribution of the λ -field (determined by the λ -term) without any islands of mass or distributed substance. The above metric then became known as *de Sitter’s cosmological model*.

Since the zero component T_{00} of the energy-momentum tensor of a distributed matter is associated with the density of the matter [6], then, according to the right-hand side of the field equations, the λ -term divided by Einstein’s constant κ should be associated with the density of the λ -field. Over the last century many astronomers tried to measure the numerical value of the λ -term, using various measurement methods; see the 2001 review on this subject [9]. However, all that they achieved does not differ from the result known in already the 1950s, according to which even the sign of the λ -term is under question, and the upper limit of its numerical value is $|\lambda| \leq 10^{-56}$ [cm⁻²]. Even now the astronomers can only say that the λ -field is an extremely rarefied medium, the density of which cannot be surely detected within the current accuracy of astronomical measurements.

There was no theory of the λ -field until the mid-1990s, when we began our own research on this subject. As a result of our research, in Chapter 5 of our monograph [2], first published in 2001, we presented a mathematical theory of the λ -field. In the framework of this theory, we theoretically determined the physically observable properties of the λ -field and much more. As always in our studies, we used the mathematical apparatus of physically observable quantities in General Relativity, known also as the Zelmanov chronometric invariants [10–12]; see the most comprehensive review of this mathematical technique in our survey [13].

In [2] we called the λ -field the *physical vacuum*, because it has vacuum-like properties. We relied on the works of Erast Gliner [14, 15], announced in 1966 by Andrew Sakharov [16]. Gliner selected and then studied a special state of distributed matter for which the energy-momentum tensor is $T_{\alpha\beta} = \mu g_{\alpha\beta}$, where μ is a constant number‡. He called this state of matter

‡Gliner used the space signature $(-+++)$, resulting in $T_{\alpha\beta} = -\mu g_{\alpha\beta}$.

the μ -vacuum, because it is related to vacuum-like states of substance ($T_{\alpha\beta} \sim g_{\alpha\beta}$, which means $R_{\alpha\beta} = k g_{\alpha\beta}$, $k = const$), but is not the vacuum (because $T_{\alpha\beta} = 0$ in the vacuum). Following this way, we introduced a new geometric classification of the states of distributed matter (and of space-time itself) according to the form of the energy-momentum tensor. We called this new classification the *T-classification of matter*:

- I. The emptiness is the state of space-time, for which the Ricci tensor is zero $R_{\alpha\beta} = 0$, which means the absence of both distributed substance ($T_{\alpha\beta} = 0$) and the physical vacuum ($\lambda = 0$).^{*} So, the emptiness is the state of a space-time without any kind of distributed matter;
- II. The physical vacuum or, simply, the vacuum is the state of distributed matter (space-time), which is determined by only the λ -field ($\lambda = const \neq 0$);
- III. The μ -vacuum is the state of distributed matter (space-time), which is determined by the energy-momentum tensor of the form $T_{\alpha\beta} = \mu g_{\alpha\beta}$ (where $\mu = const$). This is a vacuum-like state of matter, because $T_{\alpha\beta} \sim g_{\alpha\beta}$;
- IV. Substance is the state of distributed matter (space-time) for which $T_{\alpha\beta} \neq 0$, but $T_{\alpha\beta} \neq g_{\alpha\beta}$. This state comprises both ordinary substance and electromagnetic fields.

For the above reasons, we called the mathematical theory of the λ -term, which we presented in Chapter 5 of our monograph [2], the *theory of the physical vacuum*.

The energy-momentum tensor and physical properties of the physical vacuum (λ -field) were derived as follows. We presented the field equations in the form

$$R_{\alpha\beta} - \frac{1}{2} g_{\alpha\beta} R = -\kappa \tilde{T}_{\alpha\beta},$$

where $\tilde{T}_{\alpha\beta} = T_{\alpha\beta} + \check{T}_{\alpha\beta}$ is the joint energy-momentum tensor that describes both distributed substance and the physical vacuum, and

$$\check{T}_{\alpha\beta} = -\frac{\lambda}{\kappa} g_{\alpha\beta}$$

is the energy-momentum tensor of the physical vacuum. The physically observable properties of a medium are expressed with the projections of its energy-momentum tensor $T_{\alpha\beta}$ onto the time line and the three-dimensional spatial section of the observer [10–13]: the observable density ρ , the observable momentum density J^i and the observable stress tensor U^{ik}

$$\rho = \frac{T_{00}}{g_{00}}, \quad J^i = \frac{c T_0^i}{\sqrt{g_{00}}}, \quad U^{ik} = c^2 T^{ik},$$

Since the observable density of matter is positive, $\rho = \frac{T_{00}}{g_{00}} = -\mu > 0$, he obtained negative numerical values of μ . We always use the space signature (+---), because in this case the three-dimensional observable interval is positive [10–13]. Therefore, we have $\mu > 0$ and $T_{\alpha\beta} = \mu g_{\alpha\beta}$.

^{*}In an empty space, we have the field equations $R_{\alpha\beta} - \frac{1}{2} g_{\alpha\beta} R = 0$ or, in the mixed form, $R_\alpha^\beta - \frac{1}{2} g_\alpha^\beta R = 0$. After their contraction $R_\alpha^\alpha - \frac{1}{2} g_\alpha^\alpha R = 0$, we obtain $R - \frac{1}{2} 4R = 0$. Hence, the scalar curvature of any empty space is $R = 0$, and the field equations in an empty space have the form $R_{\alpha\beta} = 0$.

which, when calculated for the energy-momentum tensor of the physical vacuum $\check{T}_{\alpha\beta} = -\frac{\lambda}{\kappa} g_{\alpha\beta}$, have the form

$$\check{\rho} = \frac{\check{T}_{00}}{g_{00}} = -\frac{\lambda}{\kappa},$$

$$\check{J}^i = \frac{c \check{T}_0^i}{\sqrt{g_{00}}} = 0,$$

$$\check{U}^{ik} = c^2 \check{T}^{ik} = \frac{\lambda}{\kappa} c^2 h^{ik} = -\check{\rho} c^2 h^{ik},$$

where h^{ik} is the upper-index form of the physically observable three-dimensional metric tensor $h_{ik} = -g_{ik} + \frac{1}{c^2} v_i v_k$.[†]

From here we see that the physical vacuum (λ -field) is a *uniformly distributed matter* (since it has a constant density $\check{\rho} = const$), and also is a *non-emitting medium* (the energy flux in the physical vacuum is zero $c^2 \check{J}^i = 0$).

The equation of state of the physical vacuum[‡] follows from the general formula of the stress tensor

$$U_{ik} = p_0 h_{ik} - \alpha_{ik} = p h_{ik} - \beta_{ik},$$

which is applicable to any medium [12]. Here p_0 is the equilibrium pressure of the medium, p is the true pressure, α_{ik} is the viscosity of the 2nd kind, and $\beta_{ik} = \alpha_{ik} - \frac{1}{3} \alpha h_{ik}$ is the anisotropic part of α_{ik} ($\alpha = \alpha_i^i$ is its trace), called the viscosity of the 1st kind and manifested in anisotropic deformations of the medium. Since the physical vacuum (λ -field) is the only filler of any de Sitter space, and de Sitter's metric means a spherically symmetrical, homogeneous, isotropic and static (non-deforming) space, then in the physical vacuum $\check{\alpha}_{ik} = 0$ and $\check{\beta}_{ik} = 0$ (it is a *non-viscous medium*). Hence, the energy-momentum tensor of the physical vacuum has the form

$$\check{U}_{ik} = \check{p} h_{ik} = -\check{\rho} c^2 h_{ik},$$

and the equation of state of the physical vacuum is

$$\check{p} = -\check{\rho} c^2,$$

which means the *state of inflation*: if the density of a medium is positive, then the pressure inside it is negative (the medium expands).

So, we have obtained that the physical vacuum has the following physical properties:

[†]The physically observable three-dimensional spatial interval is determined as $d\sigma^2 = h_{ik} dx^i dx^k$, where $h_{ik} = -g_{ik} + \frac{1}{c^2} v_i v_k$ for which $h^{ik} = -g^{ik}$ and $h_k^i = -g_k^i = \delta_k^i$. Here $v_i = -c \frac{g_{0i}}{\sqrt{g_{00}}}$ is the linear velocity with which the reference space of the observer rotates (in the case, if it rotates), for which $v^i = -c g^{0i} \sqrt{g_{00}}$, $v_i = h_{ik} v^k$, $v^2 = v_k v^k = h_{ik} v^i v^k$. See the mathematical apparatus of chronometric invariants [10–13] for detail.

[‡]The equation of state of a distributed matter is the relationship between the pressure and density in the medium. For instance, $p = 0$ is the equation of state of a dust medium, $p = \rho c^2$ is the equation of state of a matter inside atomic nuclei, $p = \frac{1}{3} \rho c^2$ is the equation of state of an ultra-relativistic gas.

The physical vacuum, i.e., the λ -field, is a homogeneous ($\check{\rho} = const$), non-viscous ($\check{\alpha}_{ik} = 0, \check{\beta}_{ik} = 0$) and non-emitting ($\check{J}^i = 0$) medium, which is in the state of inflation ($\check{p} = -\check{\rho}c^2$).

We are able to calculate the numerical value of the physically observable density of the physical vacuum $\check{\rho} = -\frac{\lambda}{\kappa}$ and, therefore, the numerical value of the λ -term, if the physically observable three-dimensional curvature of the observable space will once be somehow measured in astronomical observations. How to do this is explained below.

In constant curvature spaces such as de Sitter spaces the Riemann-Christoffel curvature tensor is [17, Chapter VII]

$$R_{\alpha\beta\gamma\delta} = K(g_{\alpha\gamma}g_{\beta\delta} - g_{\alpha\delta}g_{\beta\gamma}), \quad K = const,$$

where K is a constant number proportional to the constant scalar curvature R . Contracting it step-by-step we obtain the Ricci tensor $R_{\alpha\beta} = -3K g_{\alpha\beta}$, the scalar curvature $R = -12K$ (because $g_{\alpha\beta}g^{\alpha\beta} = 4$) and, as a result, the field equations in a constant curvature space

$$3K g_{\alpha\beta} = -\kappa T_{\alpha\beta} + \lambda g_{\alpha\beta},$$

which mean $(\lambda - 3K)g_{\alpha\beta} = \kappa T_{\alpha\beta}$. Because $T_{\alpha\beta} = 0$ in any de Sitter space (its only filler is the λ -field), then the observable density of the physical vacuum in a de Sitter space is

$$\check{\rho} = -\frac{\lambda}{\kappa} = -\frac{3K}{\kappa} = -\frac{3Kc^2}{8\pi G},$$

and, since the physically observable three-dimensional curvature C of a de Sitter space is $C = -6K$,* we obtain the physically observable density of the physical vacuum $\check{\rho}$, the λ -term and the pressure \check{p} inside the vacuum (the latter follows from the equation of state of the physical vacuum, $\check{p} = -\check{\rho}c^2$), expressed with the physically observable space curvature C

$$\check{\rho} = \frac{C}{2\kappa}, \quad \lambda = -\frac{C}{2}, \quad \check{p} = -\frac{c^2 C}{2\kappa},$$

or, since C is known to be related to the physically observable curvature radius \mathfrak{R} of a three-dimensional constant curvature space as follows $C = \frac{1}{\mathfrak{R}^2}$,

$$\check{\rho} = \frac{1}{2\kappa\mathfrak{R}^2}, \quad \lambda = -\frac{1}{2\mathfrak{R}^2}, \quad \check{p} = -\frac{c^2}{2\kappa\mathfrak{R}^2}.$$

Astronomical observations performed over the last century indicate that the physically observable event horizon in our Universe is approximately 10^{28} cm (within one order of magnitude). Therefore, if we assume that our Universe is a de Sitter sphere with the observable curvature radius 10^{28} cm,

*It was obtained by projecting the Riemann-Christoffel curvature tensor $R_{\alpha\beta\gamma\delta}$ onto the time line and the three-dimensional spatial section of the observer; see [2, §5.3] for detail.

then we should expect (all within one order of magnitude):

$$\begin{aligned} \check{\rho} &\approx 3 \times 10^{-30} \text{ gram/cm}^3, \\ \check{p} &\approx -2 \times 10^{-9} \text{ gram/cm sec}^2, \\ |\lambda| &\approx 5 \times 10^{-57} \text{ cm}^{-2}. \end{aligned}$$

Gravitational forces act in any de Sitter space, but they are non-Newtonian gravitational forces because they arise due to the non-Newtonian gravitational potential created by the physical vacuum (λ -field). Below explains why.

In general, gravitational forces are forces caused by the non-uniform distribution of the gravitational potential w determined by the zero component g_{00} of the fundamental metric tensor $g_{\alpha\beta}$. As is known, in a general case [18],

$$g_{00} = \left(1 - \frac{w}{c^2}\right)^2, \quad \text{hence } w = c^2(1 - \sqrt{g_{00}}),$$

and the physically observable vector of the gravitational inertial force, determined in the framework of the the mathematical apparatus of chronometric invariants [10–13], is

$$F_i = \frac{1}{\sqrt{g_{00}}} \left(\frac{\partial w}{\partial x^i} - \frac{\partial v_i}{\partial t} \right).$$

In a space of de Sitter's metric (see the metric in the beginning of this article) we have

$$g_{00} = 1 - \frac{\lambda r^2}{3}, \quad \text{hence } w = c^2 \left(1 - \sqrt{1 - \frac{\lambda r^2}{3}} \right)$$

is the *non-Newtonian gravitational potential* specific to de Sitter metric spaces. The mixed components g_{0i} are zero in de Sitter's metric, hence $v_i = -c \frac{g_{0i}}{\sqrt{g_{00}}} = 0$ (which means that de Sitter spaces do not rotate). Using the above, we obtain that the physically observable gravitational inertial force in a de Sitter space has the following non-zero components

$$F_1 = \frac{\lambda c^2}{3} \frac{r}{1 - \frac{\lambda r^2}{3}}, \quad F^1 = \frac{\lambda c^2}{3} r,$$

or, when expressed with the physically observable density of the physical vacuum $\check{\rho}$ and the observable curvature radius of space \mathfrak{R} ,

$$\begin{aligned} F_1 &= -\frac{\kappa\check{\rho}c^2}{3} \frac{r}{1 + \frac{\kappa\check{\rho}r^2}{3}} = -\frac{c^2}{6\mathfrak{R}^2} \frac{r}{1 + \frac{r^2}{6\mathfrak{R}^2}}, \\ F^1 &= -\frac{\kappa\check{\rho}c^2}{3} r = -\frac{c^2}{6\mathfrak{R}^2} r. \end{aligned}$$

This is a *non-Newtonian gravitational force*, because it arises due to the non-Newtonian gravitational potential specific to de Sitter spaces, and also increases with the distance over which it acts (the force is proportional to r).

Based on the results presented above, we arrive at the following conclusions:

1. If the λ -term is negative $\lambda < 0$, then the density of the physical vacuum is positive $\check{\rho} > 0$, the pressure inside it is negative $\check{p} < 0$ (which means that the vacuum expands), the non-Newtonian gravitational forces acting in the space are negative $F^i < 0$ (this means that they are forces of attraction), and the three-dimensional observable curvature is positive $C > 0$;
2. On the contrary, if the λ -term is positive $\lambda > 0$, then the density of the physical vacuum is negative $\check{\rho} < 0$, the pressure inside it is positive $\check{p} > 0$ (the vacuum contracts), and the non-Newtonian gravitational forces acting in the space are positive $F^i > 0$ (therefore, they are forces of repulsion). But in this case, the physically observable three-dimensional curvature is negative $C < 0$ and, therefore, the observable curvature radius of space \mathfrak{R} has an imaginary numerical value $\mathfrak{R} = \frac{1}{\sqrt{C}} = \frac{1}{\sqrt{-2\lambda}}$, which means that the three-dimensional space geometry is hyperbolic (but not spherical, how the geometry of a de Sitter space should be).

Let us now study how the sign of the λ -term affects the frequency shift gained by a photon travelling in a de Sitter universe. It is called the *cosmological frequency shift*, because it is calculated for a photon fled a “cosmological” distance comparable to the radius of the Universe.

As we have shown and applied in our previous studies since 2009 [3–5], the physically observable cosmological frequency shift in photons is deduced by integrating the scalar equation of isotropic geodesic lines (trajectories of free light-like particles, e.g., free photons), which is the equation of the physically observable photon energy. This equation follows from the theory of chronometric invariants [10–13] (physical observables in the space-time of General Relativity), and is the chronometrically invariant (physically observable) projection of the four-dimensional equations of isotropic geodesics (the four-dimensional equations of motion of free photons) onto the time line of the observer, while the chronometrically invariant projection of the four-dimensional equations of isotropic geodesics onto the three-dimensional spatial section associated with the observer gives the three-dimensional physically observable equations of motion of free photons.

In particular, in 2011, following this calculation method applied to the equations of motion of mass-bearing particles, the cosmological mass defect of mass-bearing particles had been predicted [19]. The *cosmological mass-defect* is a new effect predicted according to General Relativity.

In short, the aforementioned calculation method applied to photons is as follows.

The four-dimensional (general covariant) equations of an isotropic geodesic line, which is the four-dimensional trajectory of a free photon*, when projected onto the time line and

*This is a photon, the motion of which is non-deviated by another force than the forces caused by the space itself (gravitation, rotation and deformation), so it travels along a shortest (geodesic) trajectory. If a photon is also

the three-dimensional spatial section associated with an observer, have two physically observable (chronometrically invariant) projections, which are[†]

$$\frac{d\omega}{d\tau} - \frac{\omega}{c^2} F_i c^i + \frac{\omega}{c^2} D_{ik} c^i c^k = 0,$$

$$\frac{d(\omega c^i)}{d\tau} - \omega F^i + 2\omega (D_k^i + A_k^i) c^k + \omega \Delta_{nk}^i c^n c^k = 0,$$

where ω is the photon’s frequency, c^i is the physically observable chr.inv.-vector of the light velocity ($h_{ik} c^i c^k = c^2$), and

$$d\tau = \sqrt{g_{00}} dt - \frac{1}{c^2} v_i dx^i$$

is the physically observable time interval. The factors under which photons move freely, aside of the chr.inv.-gravitational inertial force F_i (explained above), are the chr.inv.-angular velocity tensor of the space rotation A_{ik} , the chr.inv.-tensor of the space deformation D_{ik} and the chr.inv.-Christoffel symbols Δ_{jk}^i (they mean the non-uniformity of space)[‡]

$$A_{ik} = \frac{1}{2} \left(\frac{\partial v_k}{\partial x^i} - \frac{\partial v_i}{\partial x^k} \right) + \frac{1}{2c^2} (F_i v_k - F_k v_i),$$

$$D_{ik} = \frac{1}{2} \frac{\partial h_{ik}}{\partial t}, \quad D^{ik} = -\frac{1}{2} \frac{\partial h^{ik}}{\partial t},$$

$$\Delta_{jk}^i = h^{im} \Delta_{jk,m} = \frac{1}{2} h^{im} \left(\frac{\partial h_{jm}}{\partial x^k} + \frac{\partial h_{km}}{\partial x^j} - \frac{\partial h_{jk}}{\partial x^m} \right).$$

We call the time projection (first equation) the *chr.inv.-energy equation*, because it gives the physically observable energy $E = \hbar\omega$ of the photon as it travels. The spatial (second) projection represents the chr.inv.-equations of the photon’s motion in the three-dimensional space.

We calculate the cosmological frequency shift of a photon by integrating the chr.inv.-energy equation. De Sitter metric spaces do not rotate or deform[§], therefore the only acting

under the action of another additional force, that force deviates it from the geodesic (shortest) path thereby making the photon’s motion non-geodesic. Such a deviating non-geodesic force or forces appear in the right-hand side of the equations of motion thereby making the right-hand side of the equations nonzero and, thus, transforming them into the non-geodesic equations of motion. See our monograph [2] for detail.

[†]For details on how these projections are deduced, see our first monograph [1], in which we considered geodesic particle motion in terms of chronometric invariants (physically observable quantities in General Relativity), and also our second monograph [2] focused on non-geodesic motion.

[‡]The chr.inv.-derivation operators with respect to time and the spatial coordinates have the form: $\frac{\partial}{\partial t} = \frac{1}{\sqrt{g_{00}}} \frac{\partial}{\partial t}$ and $\frac{\partial}{\partial x^i} = \frac{\partial}{\partial x^i} + \frac{1}{c^2} v_i \frac{\partial}{\partial t}$.

[§]In de Sitter’s metric (see it in the beginning of this article), we have $g_{0i} = 0$. This means that the linear rotational velocity of such a space is zero $v_i = -c \frac{g_{0i}}{\sqrt{g_{00}}} = 0$ and also the angular velocity tensor $A_{ik} = 0$. Hence, de Sitter metric spaces do not rotate. In addition, the chr.inv.-metric tensor in a de Sitter space has the form $h_{ik} = -g_{ik} + \frac{1}{c^2} v_i v_k = -g_{ik}$. It does not depend on time because the non-zero g_{ik} components of de Sitter’s metric, which are $g_{11} = -(1 - \frac{\lambda r^2}{3})^{-1}$, $g_{22} = -r^2$, $g_{33} = -r^2 \sin^2\theta$, do not depend on time. Hence, the space deformation tensor is zero $D_{ik} = 0$. This means that de Sitter metric spaces do not deform, i.e., they are a kind of static spaces.

factor in the chr.inv.-energy equation is the non-Newtonian gravitational force F_i . Because the force and the physically observable time interval in a de Sitter space are

$$F_1 = \frac{\lambda c^2}{3} \frac{r}{1 - \frac{\lambda r^2}{3}}, \quad d\tau = \sqrt{g_{00}} dt = \sqrt{1 - \frac{\lambda r^2}{3}} dt,$$

we obtain the chr.inv.-energy equation of a photon travelling along the radial direction $x^1 = r$ in a de Sitter space

$$\frac{d\omega}{d\tau} - \frac{\omega}{c^2} F_1 c^1 = 0$$

in the form

$$d \ln \omega = \frac{\lambda r}{3} \frac{dr}{1 - \frac{\lambda r^2}{3}}$$

or, since $d \ln \left(1 - \frac{\lambda r^2}{3}\right) = -\frac{2\lambda r}{3} \frac{dr}{1 - \frac{\lambda r^2}{3}}$,

$$d \ln \omega = -\frac{1}{2} d \ln \left(1 - \frac{\lambda r^2}{3}\right),$$

integrating which we obtain the photon's frequency ω and its cosmological shift z (without specifying the sign of λ)*

$$\omega = \frac{\omega_0}{\sqrt{1 - \frac{\lambda r^2}{3}}} \approx \omega_0 \left(1 + \frac{\lambda r^2}{6}\right),$$

$$z = \frac{\omega - \omega_0}{\omega_0} = \frac{1}{\sqrt{1 - \frac{\lambda r^2}{3}}} - 1 \approx \frac{\lambda r^2}{6}.$$

As you can see from the above formula, we have obtained that in any de Sitter universe there is a parabolic (non-linear) cosmological shift in the frequency of photons. Two options of the cosmological frequency shift are conceivable, depending on the sign of λ :

1. In a de Sitter universe with $\lambda > 0$, we have $z > 0$ that means a *parabolic cosmological redshift* — the frequency of a photon decreases as it travels, because with $\lambda > 0$ the non-Newtonian gravitational forces acting in a de Sitter world are forces of repulsion, which decelerate photons travelling towards the observer. In this case, the physical vacuum has a negative density $\check{\rho} < 0$,

*The above z is not a kind of the Doppler frequency shift and is therefore calculated using a different formula. The Doppler redshift z is a decrease in the frequency of the signal emitted by a source moving away from the observer, and the Doppler blueshift is an increase in the signal's frequency when its source moves towards the observer. In contrast, in the case of a de Sitter space under consideration, the source of photons neither moves away nor approaches the observer (the distance r between them remains unchanged). In this case, the photon frequency shift is due only to the non-Newtonian gravitational field attributed to such a space (see the chr.inv.-energy equation that above). In the formula for z , which we have obtained, ω_0 is the frequency of the photon in the case, where its source coincides with the observer ($r=0$), and ω is the photon's frequency in the case, where the source of the photon is located at a distance r from him.

the pressure inside it is positive $\check{p} = -\check{\rho}c^2 > 0$ (which means that the physical vacuum contracts), the three-dimensional physically observable curvature $C = \frac{1}{\mathfrak{R}^2}$ is negative $C < 0$ and, therefore, the observable curvature radius of space \mathfrak{R} has an imaginary numerical value. The latter means that the space geometry is hyperbolic (what the geometry of a de Sitter space should not be). In addition, $\check{\rho} < 0$ contradicts the physical requirement that any kind of observable matter must have a positive mass and density;

2. In a de Sitter universe with $\lambda < 0$, we have $z < 0$ that means a *parabolic cosmological blueshift* — the frequency of a photon increases as it travels, since with $\lambda < 0$ the non-Newtonian gravitational forces acting in a de Sitter world are forces of attraction (they accelerate photons travelling towards the observer). In this case, the physical vacuum has a positive density $\check{\rho} > 0$, its pressure is negative $\check{p} = -\check{\rho}c^2 < 0$ (which means that the physical vacuum is an expanding medium), the three-dimensional physically observable curvature is positive $C = \frac{1}{\mathfrak{R}^2} > 0$ and, therefore, the observable curvature radius of space \mathfrak{R} has a real numerical value (this means that the space geometry is spherical as it should be in a de Sitter space).

In other words, in a de Sitter world with $\lambda > 0$ there is a non-linear (parabolic) cosmological redshift, and this our theoretical finding corresponds to the non-linearity of the cosmological redshift in the spectra of distant galaxies, which was recently discovered by astronomers[†]. But the $\lambda > 0$ case considered above does not satisfy such obvious physical requirements as a positive density of distributed matter and the real radius of the Universe. On the other hand, despite the fact that in a de Sitter world with $\lambda < 0$ there are no violations of the above physical requirements, in such a universe we have a parabolic cosmological blueshift.

We were looking for a solution that would resolve this dilemma. As a result, we have arrived at a conclusion that the above contradiction is resolved if we take Einstein's field equations in the following form

$$R_{\alpha\beta} - \frac{1}{2} g_{\alpha\beta} R = -\varkappa T_{\alpha\beta} - \lambda g_{\alpha\beta},$$

where the last term $\lambda g_{\alpha\beta}$ is taken with the opposite (negative) sign unlike Einstein's original equations, in which this term is positive. In this case,

$$R_{\alpha\beta} - \frac{1}{2} g_{\alpha\beta} R = -\varkappa \left(T_{\alpha\beta} + \frac{\lambda}{\varkappa} g_{\alpha\beta} \right),$$

where the right-hand side contains the sum $T_{\alpha\beta} + \frac{\lambda}{\varkappa} g_{\alpha\beta}$ (as it should be according to the logic of things) and the energy-

[†]See, for example, the surveys [20–22] and the original research results referred therein.

momentum tensor of the physical vacuum is*

$$\check{T}_{\alpha\beta} = \frac{\lambda}{\varkappa} g_{\alpha\beta}.$$

In this case, in a de Sitter world with $\lambda > 0$ and, therefore, with a parabolic cosmological redshift, we have

$$\check{\rho} = \frac{\lambda}{\varkappa} > 0, \quad \check{p} = -\check{\rho}c^2 < 0,$$

and, therefore (following the same deduction as on page 7),

$$\check{\rho} = \frac{C}{2\varkappa} = \frac{1}{2\varkappa\mathfrak{R}^2}, \quad \lambda = \frac{C}{2} = \frac{1}{2\mathfrak{R}^2},$$

$$\check{p} = -\frac{c^2C}{2\varkappa} = -\frac{c^2}{2\varkappa\mathfrak{R}^2},$$

from which we obtain positive numerical values of the three-dimensional physically observable curvature $C = \frac{1}{\mathfrak{R}^2}$ and the observable curvature radius of space \mathfrak{R}

$$C = 2\lambda > 0, \quad \mathfrak{R} = \frac{1}{\sqrt{C}} > 0.$$

In addition, there is one more property of de Sitter worlds with $\lambda > 0$. As follows from de Sitter's metric (see it in the beginning of this article) that the state of gravitational collapse (it is characterized by the condition $g_{00} = 0$) arises in a de Sitter space with $\lambda > 0$ under the obvious condition $\frac{\lambda r^2}{3} = 1$. As Larissa obtained in 2010 [3], "...since Schwarzschild's metric of the space inside a sphere of incompressible liquid transforms into de Sitter's metric by the collapse condition and the condition $\lambda = \frac{3}{a^2}$, we arrive at the conclusion: space inside a sphere of incompressible liquid, which is in the state of gravitational collapse, is described by de Sitter's metric, where the λ -term is $\lambda = \frac{3}{a^2}$. All these can be applied to the Universe as a whole, because it has mass, density, and radius such as those of a collapsar. Therefore, the Universe is a collapsar, whose internal space, being assumed to be a sphere of incompressible liquid, is a de Sitter space with $\lambda = \frac{3}{a^2}$ (here a is the radius of the Universe)." Larissa called this model the *de Sitter bubble*.

Let us calculate the physically observable curvature radius \mathfrak{R} of such a de Sitter space (it does not coincide with the metric radius a of the de Sitter sphere). Since the collapse condition in a de Sitter world arises under $\frac{\lambda r^2}{3} = 1$, where the radial coordinate r meets the metric radius a of the de Sitter sphere ($r = a$), we have $\lambda = \frac{3}{a^2}$. On the other hand, the λ -term expressed with the three-dimensional physically observable curvature radius $C = \frac{1}{\mathfrak{R}^2}$ has the form $\lambda = \frac{C}{2} = \frac{1}{2\mathfrak{R}^2}$ (see the deduction above). As a result, we obtain that the observable

*And not $\check{T}_{\alpha\beta} = -\frac{\lambda}{\varkappa} g_{\alpha\beta}$ as in the original version of Einstein's equations $R_{\alpha\beta} - \frac{1}{2} g_{\alpha\beta} R = -\varkappa T_{\alpha\beta} + \lambda g_{\alpha\beta}$ that means $R_{\alpha\beta} - \frac{1}{2} g_{\alpha\beta} R = -\varkappa (T_{\alpha\beta} - \frac{\lambda}{\varkappa} g_{\alpha\beta})$, where on the right-hand side is the energy-momentum tensor of distributed matter $T_{\alpha\beta}$, from which $\frac{\lambda}{\varkappa} g_{\alpha\beta}$ is subtracted.

curvature radius of a de Sitter space with $\lambda > 0$, expressed with the metric radius a of the de Sitter sphere in the state of gravitational collapse, is

$$\mathfrak{R} = \frac{a}{\sqrt{6}} \approx 0.41 a,$$

which means that from the point of view of an observer located inside such a de Sitter bubble, the curvature radius of the bubble \mathfrak{R} is less than its metric radius a (which is the greatest metric distance in the space).[†] As is seen from the above deduction, this is an observable effect of General Relativity due to the physically observable distortion of space caused by the gravitational field (λ -field, in this case).

Let us provide astronomers with a formula of physically observable cosmological distances inside a de Sitter universe with $\lambda > 0$. The theory of chronometric invariants (physical observables in the space-time of General Relativity) determines the square of the three-dimensional physically observable interval as $d\sigma^2 = h_{ik} dx^i dx^k$, where $h_{ik} = -g_{ik} + \frac{1}{c^2} v_i v_k$ is the chr.inv.-metric tensor, and $v_i = -c \frac{g_{0i}}{\sqrt{g_{00}}}$ is the linear rotational velocity of space. Since $g_{0i} = 0$ in de Sitter's metric (see the metric in the beginning of this article), de Sitter metric spaces do not rotate ($v_i = 0$). Therefore, $h_{ik} = -g_{ik}$ in any de Sitter space and, hence, $d\sigma^2 = h_{ik} dx^i dx^k = -g_{11} dr^2$ along the radial direction $x^1 = r$ in it. As a result, the three-dimensional physically observable interval along the radial direction in a de Sitter space has the form

$$d\sigma = \frac{dr}{\sqrt{1 - \frac{\lambda r^2}{3}}},$$

the integration of which together with the collapse condition $\frac{\lambda a^2}{3} = 1$ gives the formula of physically observable cosmological distances inside the de Sitter bubble

$$\sigma = a \arcsin \frac{r}{a}.$$

At small metric distances $r \ll a$ between cosmic objects and an observer (compared to the metric radius of the de Sitter sphere a , which is the metric radius of the Universe), we have $\arcsin \frac{r}{a} \approx \frac{r}{a}$. Therefore, at small metric distances $r \ll a$, the physically observable distances σ to the cosmic objects are $\sigma \approx r$. The farther a cosmic object is located from the observer, the greater the physically observed distance σ to this object is than the metric distance r to it. For the ultimately distant cosmic objects that are located at the distance equal to the metric radius of the Universe $r = a$ (the radius of the de Sitter bubble), the physically observable distance to them is

$$\sigma = a \arcsin 1 = \frac{\pi}{2} a \approx 1.57 a.$$

[†]Note that the observable curvature radius is constant $\mathfrak{R} = \text{const}$ throughout a de Sitter space, because de Sitter metric spaces are a kind of constant curvature spaces by definition.

Finally, assuming the corrected version of Einstein's field equations (see above), we arrive at the third option to represent the observable Universe as a de Sitter world:

3. Our Universe is a de Sitter world with $\lambda > 0$, but the $\lambda g_{\alpha\beta}$ term in Einstein's field equations has the opposite (negative) sign unlike Einstein's original equations (in which this term is positive). In this case, the physical vacuum has a positive density $\check{\rho} > 0$, the pressure inside it is negative $\check{p} = -\check{\rho}c^2 < 0$ (the physical vacuum expands), the three-dimensional physically observable curvature is positive $C = \frac{1}{\mathfrak{R}^2} > 0$ and, therefore, the observable curvature radius of space \mathfrak{R} has a real numerical value (this means that the space geometry is spherical as it should be in a de Sitter space). Since $\lambda > 0$ the non-Newtonian gravitational forces acting in the space are forces of repulsion. They decelerate photons travelling towards the observer (the frequency of the photons decreases as they travel). As a result, the observer should register a *parabolic (non-linear) cosmological redshift* in the frequency of the photons arriving at him from the far cosmos.

We vote for the above 3rd option as a model of the observable Universe, because in this case:

- a) the physical vacuum has a positive density $\check{\rho} > 0$, which satisfies the obvious physical requirement that any kind of observable matter in the Universe must have a positive mass and density,
- b) the observable curvature radius of space \mathfrak{R} is real (and not imaginary) and, hence, the space geometry is spherical (and not hyperbolic),
- c) the forces acting in such a space are the non-Newtonian gravitational forces of repulsion: they decelerate photons travelling towards the observer, thereby causing a non-linear (parabolic) redshift in the frequency of the photons,
- d) the entire observable Universe is located inside a huge de Sitter gravitational collapsar (its gravitational radius outlines the observable event horizon).

Let us apply this model to calculate the metric distance r to the galaxy JADES-GS-z13-0 that is the highest redshift galaxy known to date. It was discovered by astronomers in 2022, and its redshift is $z = 13.2$ [23]. Therefore, applying our parabolic redshift formula for this galaxy, we have

$$z = \frac{1}{\sqrt{1 - \frac{\lambda r^2}{3}}} - 1 = 13.2,$$

which with $\lambda = \frac{3}{a^2}$ taken into account (where a is the metric radius of the collapsed de Sitter sphere, i.e., the metric radius of the Universe) gives

$$r = a \sqrt{1 - \frac{1}{(z+1)^2}} = 0.998 a,$$

i.e., this galaxy is located on the very edge of the Universe. This fact is consistent with the observed non-linearity of the cosmological redshift discovered by astronomers [20–22] in the spectra of distant galaxies.

Even if galaxies with redshifts higher than $z = 13.2$ are discovered in the future, we will find that they are not much farther away from us than the aforementioned galaxy. This is thanks to our redshift formula, according to which the parabolic redshift curve z rises very strongly upward at large distances r even for very small increments of r . For example, a galaxy, the redshift of which is $z = 25$, according to our redshift formula is located at the distance $r = 0.999a$ from us, and the distance to a galaxy with $z > 100$ is $r = 0.99(9)a$.

For more or less nearby galaxies, the redshift of which is $z \approx 0.1$, our formula that above gives $r \approx 0.4a$.

All this confirms Larissa's suggestion, made in 2010 [3], according to which the observable Universe is a huge de Sitter gravitational collapsar (de Sitter bubble) with $\lambda > 0$, the gravitational radius of which outlines the observable event horizon.

We thank Pierre A. Millette for discussion and comments.

Submitted on January 7, 2024

References

1. Rabounski D. and Borissova L. Particles Here and Beyond the Mirror. The 4th revised edition, New Scientific Frontiers, London, 2023 (the 1st edition was issued in 2001).
Rabounski D. et Larissa Borissova L. Particules de l'Univers et au delà du miroir. La 2ème édition révisée en langue française, New Scientific Frontiers, Londres, 2023 (French translation).
2. Borissova L. and Rabounski D. Fields, Vacuum, and the Mirror Universe. The 3rd revised edition, New Scientific Frontiers, London, 2023 (the 1st edition was issued in 2001).
Borissova L. et Rabounski D. Champs, Vide, et Univers miroir. La 2ème édition révisée en langue française, New Scientific Frontiers, Londres, 2023 (French translation).
3. Borissova L. De Sitter bubble as a model of the observable Universe. *The Abraham Zelmanov Journal*, 2010, v. 3, 3–24.
4. Borissova L. and Rabounski D. Inside Stars. The 3rd edition, revised and expanded, New Scientific Frontiers, London, 2023 (the 1st edition was issued in 2013).
5. Borissova L. and Rabounski D. Cosmological redshift in the de Sitter stationary Universe. *Progress in Physics*, 2018, no. 1, 27–29.
6. Einstein A. Kosmologische Betrachtungen zur allgemeinen Relativitätstheorie. *Sitzungsberichte der Königlich Preußischen Akademie der Wissenschaften*, 142–152.
7. O'Raifeartaigh C., O'Keefe M., Nahm W., Mitton S. Einstein's 1917 static model of the Universe: a centennial review. *The European Physical Journal H*, 2017, v. 42, 431–474; arXiv: 1701.07261.
8. De Sitter W. On the curvature of space. *Koninklijke Nederlandsche Akad. van Wetenschappen, Proceedings*, 1918, vol. XX, part I, no. 2, 229–243.
9. Carroll S. M. The cosmological constant. *Living Reviews in Relativity*, 2001, v. 4, 1–56.
10. Zelmanov A. L. Chronometric Invariants. Translated from the 1944 PhD thesis, American Research Press, Rehoboth, New Mexico, 2006.
11. Zelmanov A. L. Chronometric invariants and accompanying frames of reference in the General Theory of Relativity. *Soviet Physics Doklady*, 1956, v. 1, 227–230 (translated from *Doklady Akademii Nauk USSR*, 1956, v. 107, issue 6, 815–818).

12. Zelmanov A. L. On the relativistic theory of an anisotropic inhomogeneous universe. *The Abraham Zelmanov Journal*, 2008, vol. 1, 33–63 (translated from the thesis of the 6th Soviet Conference on the Problems of Cosmogony, USSR Academy of Sciences Publishers, Moscow, 1957, 144–174).
13. Rabounski D. and Borissova L. Physical observables in General Relativity and the Zelmanov chronometric invariants. *Progress in Physics*, 2023, no. 1, 3–29.
14. Gliner E. B. Algebraic properties of energy-momentum tensor and vacuum-like states of matter. *Journal of Experimental and Theoretical Physics*, 1966, v. 22, no. 2, 378–382.
Translated from: *Zhurnal Eksperimental'noi i Teoreticheskoi Fiziki*, 1966, v. 49, no. 2, 543–548.
15. Gliner E. B. Vacuum-like state of medium and Friedmann's cosmology. *Soviet Physics Doklady*, 1970, v. 15, 559–562.
Translated from: *Doklady Akademii Nauk SSSR*, 1970, v. 192, no. 4, 771–774.
16. Sakharov A. D. The initial stage of an expanding Universe and the appearance of a nonuniform distribution of matter. *Journal of Experimental and Theoretical Physics*, 1966, v. 22, no. 1, 241–249.
Translated from: *Zhurnal Eksperimental'noi i Teoreticheskoi Fiziki*, 1966, v. 49, no. 1, 345–357.
17. Synge J. L. *Relativity: the General Theory*. North Holland, Amsterdam, 1960.
18. Landau L. D. and Lifshitz E. M. *The Classical Theory of Fields*. The 4th edition, Butterworth-Heinemann, 1979 (the first English edition was issued in 1951, translated from the 1939 Russian edition).
19. Rabounski D. Cosmological mass-defect — a new effect of General Relativity. *The Abraham Zelmanov Journal*, 2011, v. 4, 137–161.
20. Heavens A. F., Matarrese S., Verde L. The non-linear redshift-space power spectrum of galaxies. *Monthly Notices of the Royal Astron. Society*, 1998, v. 301, 797–808.
21. Sigad Y., Branchini E., Dekel A. Measuring the nonlinear biasing function from a galaxy redshift survey. *The Astronomical Journal*, 2000, v. 540, 62–73.
22. Gebhardt H. and Jeong D. Nonlinear redshift-space distortions in the harmonic-space galaxy power spectrum. *Physical Review D*, 2020, v. 102, 083521; arXiv: 2008.08706.
23. Curtis-Lake E., Carniani S., Cameron A. et al. Spectroscopic confirmation of four metal-poor galaxies at $z = 10.3$ – 13.2 . *Nature Astronomy*, 2023, v. 7, 622–632; arXiv: 2212.04568.

LETTERS TO PROGRESS IN PHYSICS

Cosmological Redshift: Which Cosmological Model Best Explains It?

Dmitri Rabounski and Larissa Borissova

Puschino, Moscow Region, Russia

E-mail: rabounski@yahoo.com, lborissova@yahoo.com

Here we list three options that General Relativity has proposed over the past decade to explain the non-linear cosmological redshift, observed by astronomers. 1) If the redshift law is linear for nearby galaxies, then turns into exponential for distant galaxies, and triangulation of galaxies reveals non-zero curvature of space, then our Universe is an expanding Friedmann world. 2) If the linear redshift law turns into parabolic for distant galaxies, then our Universe is a static de Sitter world with $\lambda > 0$, in which the physical vacuum has a positive density, the observable curvature of space is positive, and the non-Newtonian gravitational forces acting there are repulsive forces increasing with distance (which cause photons to lose energy as they move). 3) If for distant galaxies the linear redshift law turns into exponential, but triangulation of galaxies does not reveal even the slightest curvature of space, then our Universe has a flat space, where the redshift in the spectra of distant objects is due only to the fact that the light-like sub-space (home of photons) of any metric space-time rotates with the speed of light, thereby creating a repulsive centrifugal force (which causes photons to lose energy as they move). In this case, any particular space metric creates only an addition to the exponential redshift law, which must take place even in a flat unperturbed space.

Cosmological redshift was discovered by Vesto Slipher (Flagstaff Observatory, Arizona), who first registered it on September 17, 1912 in the spectrum of Andromeda Nebula M31 [1], then over subsequent years in the spectra of other galaxies [2, 3]. Slipher's discovery of the cosmological redshift and the key contribution of his measurements into the discovery of the redshift law are explained in detail in the comprehensive 2013 surveys [4–6].

Slipher explained this result by the Doppler effect, saying that most galaxies move away from the observer with high velocities (therefore their spectra become redshifted). A few years after the discovery in the early 1920s, a number of scientists came up with the idea of explaining the cosmological redshift in the framework of one of the cosmological models proposed by the General Theory of Relativity. They all tried to deduce the dependence of the redshift and the corresponding radial velocity of galaxies on their distance from the observer as the Doppler effect in the framework of de Sitter's cosmological model. These were researchers such as Ludwik Silberstein, Knut Lundmark, Carl Wirtz, Edwin Hubble, Willem de Sitter. Their work is discussed in detail in recent historical studies by Michael Way, Harry Nussbaumer, Cormac O'Raiheartaigh and their co-authors (if any), which are referred here in context of the discovery of the redshift law (see References).

Abbé Georges Lemaître was one of the researchers. After his "Docteur en Sciences" graduation from Université catholique de Louvain à Bruxelles and being ordained as a diocesan (secular) priest, he spent 1923–1925 outside Belgium. During

1923 he was a research associate in astronomy with Arthur Eddington at the Cambridge Observatory in England, then during 1924 — with Harlow Shapley at the Harvard Observatory (Massachusetts). Eddington introduced Lemaître to the General Theory of Relativity and relativistic cosmology, and with Shapley he studied the spectra of galaxies.

Returning to Belgium in 1925, Lemaître, like his aforementioned predecessors, tried to explain the observed cosmological redshift in the framework of de Sitter's cosmological model. This is a spherical universe of constant curvature filled with the physical vacuum called the λ -field, which is given by the λ -term in de Sitter's space metrics. Such a universe is usually static ($\lambda = const$), but can also be expanding if the λ -term and the space curvature (it is proportional to λ), having the same numerical value at any point in space, are proportional to the expansion rate, i.e., they depend on time (the case considered by Lemaître and his predecessors). Galaxies in an expanding universe are scattering away from the observer, so their observed spectra must be redshifted due to the Doppler effect. But, following his predecessors, Lemaître had come to an unsatisfactory result. He had deduced the same linear redshift law as Silberstein before him. But the obtained solution becomes invalid at the coordinate origin and even at a small distance from it, and also there the light source and the observer cannot be swapped (the solution depends on the coordinates). This means that, if the λ -term and the space curvature depend on time (the universe is expanding or compressing), then they can have the same numerical values at any point in space only if the space is either inhomogeneous or

anisotropic (or both) thereby contradicting the conditions of spherical symmetry and isotropy, which are assumed in de Sitter's metric. In other words, Lemaître had proved that the studies of his predecessors, in which they tried to deduce the Doppler redshift in an expanding de Sitter universe, lead to nonsense. Lemaître explained all of the above in his 1925 paper [7], which was then reprinted in 1926 [8].

The mentioned defeat does not mean that de Sitter's metric itself is bad, but is due to the fact that this metric can only be static. Whereas the Doppler redshift, which Lemaître and his predecessors tried to deduce, is specific to such a space metric that initially depends on time.

Therefore in 1926, Lemaître immediately turned to Friedmann's cosmological model of an expanding (or compressing) universe [9, 10], since the Doppler redshift naturally accompanies the expansion of space. This model describes an approximately empty spherical universe (with no islands of mass or distributed substance), which is expanding or contracting on its own. Success awaited Lemaître on this path. He assumed that the Friedmann universe is expanding with a constant radial velocity, then easily expressed the expansion velocity from Friedmann's space metric and substituted it into the Doppler law known from classical physics. As a result, Lemaître had obtained a linear relationship between the cosmological redshift in the spectra of galaxies and the distance from them to the observer, which means a linear redshift law according to which the redshift for distant galaxies is greater than for nearby ones and increases proportionally to the distance. Then, using Slipher's measurements, he had estimated the numerical value of the constant coefficient in this linear relationship, which is now known as the *Hubble constant*. Lemaître reported these results, including the discovery of the redshift law and the estimation of the redshift law constant, in his fundamental 1927 paper published in *Annales de la Societe Scientifique de Bruxelles* [11]. But this publication in the obscure French-language journal was not noticed in the scientific community.

Two years later, Edwin Hubble published his 1929 paper [12] that brought him worldwide fame. In this paper, with a number of omissions because he was never fluent in General Relativity, Hubble repeated the results obtained by Lemaître, including the linear redshift law and the redshift law constant estimated using Slipher's measurement data. Hubble did not refer to his use of Slipher's measurements and Lemaître's 1927 paper in which Lemaître reported his discovery of the redshift law. Therefore, the redshift law later became known as *Hubble's law* or the *Hubble redshift*.

When in 1931 an English translation of Lemaître's 1927 paper was submitted through Eddington to the *Monthly Notices of the Royal Astronomical Society*, the passages about his discovery of the redshift law and his estimate of the redshift law constant were removed by the editor because these results had already been attributed to Hubble. Finally, the English translation of Lemaître's 1927 paper was published [13],

but with significant censorship. In the same issue of the journal, Lemaître also published another paper [14], in which he outlined the details of his theory of the expanding Universe; a short version of the second article was then reprinted in French [15]. Lemaître did not discuss the above editorial decision: as a truly good Catholic, he always believed that "God hath commanded so" and never tried to defend his authorship of the redshift law and the redshift constant.

This story was known to a narrow circle of scientists back in the 1980s [16]. Then in the early 2000s, Hubble's authorship of the redshift law was publicly questioned in favour of Lemaître in the 2003 article [17] and the detailed 2009 book [18] on this subject. This drama was revealed in full power in 2011 by two historians of science [19, 20], which caused widespread resonance in the scientific community in the same 2011 thanks to the science news reports on this subject, which were first published in *Forbes* [21], then — in *Nature News* [22, 23] and *Nature* [24]. All this in 2011–2013 led to a revision of Hubble's rôle in this discovery and the recognition of Lemaître's authorship of the redshift law with the key contribution of Slipher's measurements; see [25–29] for example.

In the century passed since Slipher's measurements, observational astronomy techniques and observational equipment have made significant progress. Astronomers now have a vast amount of data on the redshifts and radial velocities of galaxies (instead of only a few dozens known in the 1920s). As a result, in the last two decades, astronomers claim about the possible existence of a deviation from the linear redshift law, which needs a theoretical explanation: see, for example, the surveys [30–32] on this subject and the original research results referred therein.

However, if following the same way of theoretical explanation as Lemaître and his predecessors did, we arrive at a problem. The essence of the problem is that neither Lemaître nor his predecessors deduced the cosmological redshift law directly from the specific space metric that they chose. In essence, they merely postulated that the redshift occurs in the spectra of galaxies due to their scattering away from the observer, i.e., due to the Doppler effect. They followed the "two-step path" of mathematical deduction. At the first stage of their deduction, they somehow extracted the expansion rate of the Universe from the specific space metric that they chose (as the change rate of the curvature radius of space). Then they merely substituted this speed into the Doppler effect formula known from classical physics, and thus obtained the cosmological redshift law. This is what Lemaître did, and this is what his predecessors did. It cannot be said that such a method is very consistent with theoretical physics, since the origin of the cosmological redshift is initially postulated as a result of the Doppler effect in scattering galaxies in an expanding universe, and also a "mixture" of classical physics and General Relativity is used in the derivation.

If, in solving a physics problem, we decide to solve, say, the forced oscillation equation, we are essentially postulating that the cause of this effect lies in forced oscillations, and then we obtain a solution that automatically “confirms” the initially postulated forced oscillations. In other words, if we initially postulate the origin of the cosmological redshift effect, say, as a result of the Doppler effect or something else, then no matter what mathematical operations we perform next, we get the same effect that we postulated at the beginning, but only expressed in a mathematically more extended and elegant form.

Therefore, if we like to find the truly origin of the cosmological redshift effect, we should never postulate its origin. In addition, in order to be honest, if we like to deduce the cosmological redshift law as a space-time effect, i.e., as an effect in the framework of a cosmological model provided by General Relativity, we should follow only with the equations of General Relativity, and never use the equations and laws of classical physics (such as the Doppler effect formula). In other words, the cosmological redshift law should be obtained from the equations of General Relativity, and without any preliminary assumptions about its origin. This is the solely right way how to do things in theoretical physics.

In this letter, we list the newest solutions that are most fit for explaining the observed cosmological redshift, including its non-linearity. These solutions have been obtained since 2009 using the same original derivation method that has never been used for this purpose before — solving the scalar geodesic equation (energy equation) for a photon travelling from a source to an observer in the space-time of General Relativity. These solutions were obtained using only the equations of General Relativity, and without any prior assumptions about the nature of the cosmological redshift.

The solutions are different only because of the geometric structure of space, which is different for different space metrics (cosmological models). In other words, the mathematical derivation merely follows the geometric structure of the space in which it is performed. Thus, the resulting redshift law merely shows how the frequency of a travelling photon changes according to the geometric structure of the particular space (cosmological model) in which the photon travels.

The mentioned new method used to derive the cosmological redshift law dates back to our research studies of the 1990s, which we summarized in 2001 in our two monographs [33, 34]. The first monograph focuses on the geodesic (free) motion of mass-bearing and massless (light-like) particles in the space-time of General Relativity, and the second monograph examines their non-geodesic (non-free) motion.

As always in our studies we used the mathematical apparatus of chronometric invariants, which are physically observable quantities in the space-time of General Relativity. Such quantities are obtained as the projections of four-dimensional

(general covariant) quantities onto the three-dimensional spatial section and the time line associated with a particular observer and his laboratory. Such quantities depend on the geometric and physical properties of the real physical space of the observer, as well as the laboratory standards to which he compares his measurement results. Therefore, if we have all quantities and equations of General Relativity expressed in the chronometrically invariant form, then we do not need to think about which of the obtained solutions are physically observable (that was a common problem in General Relativity in the past), since all the obtained solutions are, by definition, measurable on practice. The mathematical apparatus of chronometric invariants is also known as the Zelmanov chronometric invariants in honor of Abraham Zelmanov, who developed it in 1944; see our detailed survey of chronometric invariants [35] and references therein.

As for the mentioned new method used to derive the cosmological redshift law, it is simple.

The four-dimensional equations of motion of a particle in space-time have two physically observable projections. The projection onto the time line of the observer is a scalar equation showing how the particle’s energy changes in time, depending on the properties of the observer’s space. In other words, this is the *energy equation* of the particle. The projection onto the spatial section associated with the observer (his three-dimensional space) is the three-dimensional vector equation of motion of the particle, which also depends on the properties of the observer’s space.

Integrating the scalar equation of motion (energy equation) of mass-bearing particles, Dmitri in 2009–2011 derived that the observable masses of cosmic bodies depend on their distance from the observer. He had called this the *cosmological mass-defect* [36], which is a new effect predicted according to General Relativity. The cosmological mass-defect depends on the specific metric of space, i.e., on the geometric structure of the specific space (particular cosmological model). Dmitri had calculated the cosmological mass-defect in the space of the most commonly used space metrics (cosmological models), such as Schwarzschild’s mass-point metric, Reissner-Nordström’s metric of the space of an electrically charged mass-point, Gödel’s metric of the rotating space with self-closed time-like geodesics, Schwarzschild’s metric inside a sphere filled with an incompressible liquid, de Sitter’s metric inside a sphere filled with the physical vacuum, Einstein’s metric inside a sphere filled with an ideal liquid and the physical vacuum, and also Friedmann’s metric of a deforming (expanding or compressing) space.

Accordingly, by integrating the scalar equation of motion (energy equation) of a massless light-like particle, such as a photon, we obtain its physically observable frequency as a function of the travelled distance. This is the way to derive the cosmological redshift law in the space of any specific metric (particular cosmological model), without any prior assumptions about the nature of the cosmological redshift. This is

how Dmitri in 2011 derived the cosmological redshift law in the space of each of the aforementioned cosmological models [37] (see also his 2012 short paper [38]), by analogy with the cosmological mass-defect.

The above work [37] has its own background and continuation. A year earlier, in 2010, Larissa considered a Sitter sphere in the state of gravitational collapse (its radius coincides with its gravitational radius). She showed that a de Sitter collapsar (*de Sitter bubble*) is fit to the observed Universe [39]. Integrating the scalar equation of motion (energy equation) of photons, based on her *de Sitter bubble model*, showed a parabolic redshift law [37, §6], which remains valid outside the state of gravitational collapse. Then in 2013, in our monograph on astrophysics [40, §6.4–6.5] (§5.1 in the 1st edition), we proved that the parabolic redshift law takes place a de Sitter space, in which $\lambda > 0$, the physical vacuum has a positive density, and the observable curvature radius of space is positive (otherwise it is a blueshift). Our redshift studies in a de Sitter universe were summarized in a short paper in 2018 [41] and then in an extended paper in 2023 [42].

The same method as above for deriving the cosmological redshift law was used in the 2009 papers [43–45], in which Dmitri had derived an exponential cosmological redshift due to the global non-holonomy of space.

The term *holonomy* dates back to Schouten's theory of non-holonomic manifolds and was first used in General Relativity in 1944 by Zelmanov [35]. If the time lines that "pierce" a three-dimensional spatial section are everywhere orthogonal to it, then the space (space-time) is *holonomic*. Otherwise it is *non-holonomic*. Zelmanov had proved that $g_{0i} \neq 0$ in non-holonomic spaces, which manifests itself in the form of a rotation of the spatial section (three-dimensional space) with a speed depending on g_{0i} , and this rotation cannot be removed by coordinate transformations. See [35] for detail.

Dmitri had showed in the third paper [45] that although each particular space (space-time) has its own specific metric and does not necessarily have a three-dimensional rotation, its light-like sub-space (home of photons) always rotates with the speed of light (varying depending on the gravitational potential). The light-speed rotation of the light-like space cannot be removed by coordinate transformations and is due to the sign-alternating structure of any space-time metric (which distinguishes the time axis from the spatial coordinate axes). In other words, the light-like space (in which photons travel) is always strictly non-holonomic. This rotation creates a centrifugal force that affects only particles in the light-like space (such as photons). By assuming the mentioned rotation when integrating the scalar equation of motion (energy equation) of photons, Dmitri had derived the exponential redshift law. This law should take place even in a flat unperturbed space (space-time), while each particular space metric creates only an addition to the exponent.

As for the origin of the cosmological redshift and the cosmological mass-defect, it can be understood from the scalar

equation of motion (energy equation), which for photons and mass-bearing particles has the form, respectively,

$$\frac{d\omega}{d\tau} - \frac{\omega}{c^2} F_i c^i + \frac{\omega}{c^2} D_{ik} c^i c^k = 0,$$

$$\frac{dm}{d\tau} - \frac{m}{c^2} F_i v^i + \frac{m}{c^2} D_{ik} v^i v^k = 0,$$

in which m is the relativistic mass of a mass-bearing particle, travelling with the velocity $v^i = \frac{dx^i}{d\tau}$, and ω is the frequency of a photon (photons travel with the velocity of light $c^i = \frac{dx^i}{d\tau}$, for which $c_i c^i = c^2 = \text{const}$).

If the space is static (the tensor of the space deformation rate is $D_{ik} = 0$), then $d\tau$ is reduced in the equations, which then are integrated with respect to the radial coordinate $x^1 = r$. As a result, we obtain the mass-bearing particle's mass m and the photon's frequency ω as a function of the distance r from the observer (for whom $r = r_0 = 0$).

If the gravitational inertial force is $F_i = 0$ (there is no gravitational field and rotation of space), but the space is deforming (expanding or compressing), then when multiplying the equations by the metric tensor h_{ik} , the multiplier $h_{ik} c^i c^k = c^2$ is reduced and the equations are integrated with respect to the travel time τ . In this case, we obtain the mass-bearing particle's mass m and the photon's frequency ω as a function of the time t travelled from the source (where $t = t_0 = 0$) to the observer (which is the reverse path of integration, changing the sign of the integration result).

Therefore, the origin of the cosmological redshift and the cosmological mass-defect is clearly seen from the equations. If the gravitational inertial force, consisting of a term given by the gravitational potential and a term given by the centrifugal force, is a force of repulsion ($F_1 > 0$) or the space is expanding ($D_{11} > 0$), then the repulsive force decelerates photons travelling to the observer, thereby producing a loss of the photon energy $E = \hbar\omega$ (*photon redshift*). In the case of mass-bearing particles such as cosmic bodies, their masses (and energies $E = mc^2$) registered by the observer are less than their actual masses (and energies) at their distant locations.

Otherwise, if the gravitational inertial force is a force of attraction ($F_1 < 0$) or the space is compressing ($D_{11} < 0$), then the force accelerates photons travelling to the observer, thereby producing a gain of their energy (*photon blueshift*), and the masses of distant cosmic bodies registered by the observer are greater than their actual masses at their distant locations.

This means that both the cosmological mass-defect and the cosmological redshift arise from the specific geometric structure of each particular space.

Below we list three different solutions for the cosmological redshift law, which can be considered to fit to the observed Universe. The first two were derived in 2011 [37], while the third solution — in 2009 [43–45], all using the above method of integrating the scalar equation of motion (energy equation) for photons.

Cosmological redshift in an expanding Friedmann universe. In such a universe, the frequency ω of a photon registered by an observer away from the emitted photon is

$$\omega = \omega_0 e^{-\frac{\dot{R}}{R} t},$$

where R is the curvature radius of space (the Universe's radius in this case), and \dot{R} is the rate of its expansion. This exponential law transforms into the linear

$$\omega \simeq \omega_0 \left(1 - \frac{\dot{R}}{R} t\right)$$

at short duration of the photon's travel (and, respectively, at small distances from the photon's emitter to the observer).

We see from the above formulae that the photon's frequency ω registered by the observer is lower than its frequency ω_0 at the initial moment of time $t = t_0 = 0$, when it was emitted by a source in the far cosmos. The farther the photon's emitter is located from the observer, the lower the photon's frequency ω registered by him: the photon's frequency is redshifted upon arrival at the observer.

The above formulae for the photon's frequency result in the *exponential redshift law*

$$z = \frac{\omega_0 - \omega}{\omega} = e^{\frac{\dot{R}}{R} t} - 1, \quad z > 0,$$

which transforms into the *linear redshift law* at short duration (and small distances) of the photon's travel

$$z \simeq \frac{\dot{R}}{R} t.$$

As was shown in [37], the above formulae for the photon's frequency and redshift are the same in both a constant-speed expanding Friedmann universe ($\dot{R} = \text{const}$) and a constant-deformation Friedmann universe (where $\frac{\dot{R}}{R} = \text{const}$).

So, the cosmological redshift in an expanding Friedmann universe increases with distance to cosmic bodies according to the *exponential redshift law*, which transforms into the *linear redshift law* at short duration (and small distances) of photons' travel.

Here we should make a short remark about Lemaître's linear redshift law. With all our respect to Georges Lemaître, he did not solve any equations. His 1927 paper focused on how to find the expansion rate of the Universe from Friedmann's metric. Then he substituted this rate into the Doppler redshift formula taken from classical physics. In fact, he merely renamed the emitter's velocity in Doppler's formula as the expansion rate of the Universe (and justified this renaming by showing how the expansion rate is found from Friedmann's metric). But by doing this, Lemaître could not obtain anything other than the linear redshift law, because it initially follows from Doppler's formula at the velocity of the emitter, much lower than the velocity of light.

In contrast to what Lemaître did, the exponential redshift law formula that above is a mathematical solution obtained directly by solving the scalar equation of motion (energy equation) for photons travelling in an expanding Friedmann universe. It was derived without any prior assumptions about the form of the redshift law. This is the solely right way how to do things in theoretical physics.

The said does not affect the memory about Abbé Lemaître as an outstanding scientist and good Catholic, an exemplar of human decency and honesty, and does not diminish his fundamental contribution to relativistic cosmology.

Cosmological redshift in a static de Sitter universe. In a de Sitter universe, the frequency ω_0 of a photon registered by an observer (for whom $r = r_0 = 0$) upon its arrival is also lower than its frequency ω at the location of its distant source, from which it was emitted. This dependence is expressed with the parabolic (square) law

$$\omega = \frac{\omega_0}{\sqrt{1 - \frac{\lambda r^2}{3}}},$$

which at small distances r between the photon's source and the observer transforms into the simplified law

$$\omega \simeq \omega_0 \left(1 + \frac{\lambda r^2}{6}\right).$$

The farther the emitter is located from the observer, the lower the photon's frequency ω_0 registered by him. Thus, the photon's frequency is redshifted upon arrival at the observer in a de Sitter universe.

These formulae for the photon's frequency result in the *parabolic (square) redshift law*

$$z = \frac{\omega - \omega_0}{\omega_0} = \frac{1}{\sqrt{1 - \frac{\lambda r^2}{3}}} - 1, \quad z > 0,$$

which at small distances r takes the simplified form

$$z \simeq \frac{\lambda r^2}{6}.$$

At the ultimately large distance in space (event horizon, where $r = a$), which is determined in a de Sitter universe by the condition $\frac{\lambda r^2}{3} = \frac{\lambda a^2}{3} = 1$, the photon's frequency and redshift are maximum: $\omega_{\max} = \infty$ and $z_{\max} = \infty$.

So, the cosmological redshift in a static de Sitter universe increases with distance to cosmic bodies according to the *parabolic (square) redshift law*.

This redshift law depends on the sign of the λ -term and, accordingly, the sign of the density of the physical vacuum (which is the filler of de Sitter space) and the sign of the physically observable curvature of space (since these quantities are connected with λ). It was proved in [40, §6.4–6.5] (§5.1 in the 2013 edition) and then summarized in [41, 42] that the

cosmological redshift ($z > 0$) takes place in a de Sitter universe, where $\lambda > 0$, the physical vacuum has a positive density (like substance, and not a negative density like field), the curvature radius of space is positive (the geometry of space is spherical, and not hyperbolic), and the non-Newtonian gravitational forces that act in any de Sitter space and increase with distance from the observer are repulsive forces. These repulsive forces cause photons to lose energy as they travel to the observer, thereby producing a redshift in the frequency of the photons. Otherwise (if $\lambda < 0$), there is not a cosmological redshift, but a blueshift ($z < 0$) and the curvature radius of space takes an imaginary numerical value (the geometry of space is hyperbolic).

Cosmological redshift due to the global non-holonomy of the light-like space. The term *non-holonomy* dates back to Schouten's theory of non-holonomic manifolds and was first used in General Relativity in 1944 by Zelmanov. If the time lines that "pierce" a three-dimensional spatial section are everywhere orthogonal to it, then the space (space-time) is *holonomic*. Otherwise it is *non-holonomic*. Zelmanov had proved that $g_{0i} = 0$ in holonomic spaces and $g_{0i} \neq 0$ in non-holonomic spaces. The latter manifests itself as a rotation of the spatial section (three-dimensional space) with a speed depending on g_{0i} , which cannot be removed by coordinate transformations. For detail, see our survey [35] and references therein.

It was proved [45] that the light-like sub-space of any space-time metric rotates with the speed of light, thereby creating a repulsive centrifugal force. This repulsive force only acts on particles in the light-like space (i.e., photons) in the direction away from the observer (coordinate origin), thereby causing photons to lose energy and frequency as they travel to him

$$\omega = \omega_0 e^{-\Omega t}, \quad \Omega \equiv H_0,$$

resulting in the *exponential redshift law*

$$z = \frac{\omega_0 - \omega}{\omega} = e^{\Omega t} - 1, \quad z > 0,$$

where ω_0 is the photon's frequency at the initial moment of time $t = t_0 = 0$, when it was emitted by a distant source in the cosmos, ω is its frequency upon arrival at the observer, and Ω is the angular rotational velocity of the light-like space due to its global non-holonomy (light-speed rotation), which is equal to the Lemaître-Hubble constant $H_0 = 2.3 \pm 0.3 \times 10^{-18} \text{ sec}^{-1}$ (as measured in the framework of the Hubble Space Telescope Key Project for 2001 [46]).

We see that the repulsive centrifugal force, which is always present in the light-like space (home of photons) due to its light-speed rotation, causes a redshift (loss of energy) in the frequency of a photon arrived from a distant source at the observer. The farther the photon's emitter (and longer is its travel time t), the lower the photon's frequency ω registered by the observer upon its arrival.

At short duration (and small distances) of the photon's travel we have the linear approximation for the photon's frequency

$$\omega \simeq \omega_0 (1 - H_0 t)$$

and the *linear redshift law*

$$z \simeq H_0 t.$$

So, the cosmological redshift due to the light-speed rotation of the light-like space (its global non-holonomy) increases with distance to cosmic bodies according to the *exponential redshift law*, which at short duration (and small distances) of photons' travel transforms into the *linear redshift law*.

Since the light-like space rotates with the speed of light due to only the sign-alternating structure of any space-time metric (which distinguishes the time axis from the spatial coordinate axes), and this rotation cannot be removed by coordinate transformations, the above exponential redshift law and its linear approximation at small distances should take place even in a flat unperturbed space. Any particular space metric should create only an addition to the above exponential redshift law, straightening this exponential curve or making it more curved.

Thus, the following three versions have been proposed according to General Relativity to explain the observed non-linear cosmological redshift law.

1. If the redshift in the spectra of nearby galaxies increases linearly with distance to them, then it turns into exponential for distant galaxies, and triangulation of galaxies reveals non-zero curvature of space, then our Universe is an expanding Friedmann world. In this case, photons lose energy as they travel to the observer due to the fact that they are decelerated by the expansion of space.

2. If the linear redshift law turns into parabolic for distant galaxies, then our Universe is a static de Sitter world with $\lambda > 0$, in which the physical vacuum has a positive density, the observable curvature is positive, and the non-Newtonian gravitational forces acting there are repulsive forces increasing with distance from the observer (which cause photons to lose energy as they travel to the observer).

3. If for distant galaxies the linear redshift law turns into exponential, but triangulation of galaxies does not reveal even the slightest curvature of space, then our Universe has a flat space, where the redshift in the spectra of distant objects is due only to the light-speed rotation of the light-like sub-space (home of photons) in any metric space-time, which creates a repulsive centrifugal force causing photons to lose energy as they travel to the observer. But in this case we should assume that the device with which the observer measures the redshift is connected with a light-like reference frame, which creates a problem for an ordinary observer, since he and his laboratory reference frame are related to ordinary substance.

Which of the above three options best explains the cosmological redshift in our Universe will be decided in accordance with astronomical observations.

Submitted on February 5, 2024

References

- Slipher V. M. The radial velocity of the Andromeda Nebula. *Lowell Observatory Bulletin*, 1913, v. 2, no. 8, 56–57.
- Slipher V. M. Spectrographic observations of nebulae (Reports of the 17th Meeting of the American Astron. Society). *Popular Astronomy*, 1915, v. 23, 21–24.
- Slipher V. M. Radial velocity observations of spiral nebulae. *The Observatory*, 1917, v. 40, 304–306.
- Peacock J. A. Slipher, galaxies, and cosmological velocity fields. *Astronomical Society of the Pacific Conference Series*, 2013, v. 471 “Origins of the Expanding Universe 1912–1923”, 3–23; arXiv: 1301.7286 (2013).
- Nussbaumer H. Slipher’s redshifts as support for de Sitter’s model and the discovery of the dynamic Universe. *Astronomical Society of the Pacific Conference Series*, 2013, v. 471 “Origins of the Expanding Universe 1912–1923”, 25–38; arXiv: 1303.1814 (2013).
- O’Raifeartaigh C. The contribution of V. M. Slipher to the discovery of the expanding Universe. *Astronomical Society of the Pacific Conference Series*, 2013, v. 471 “Origins of the Expanding Universe 1912–1923”, 49–61; arXiv: 1212.5499 (2013).
- Lemaître G. Note on de Sitter’s universe. *Journal of Mathematical Physics*, 1925, v. 4, no. 3, 188–192.
- Lemaître G. Note on de Sitter’s universe. *Publications du Laboratoire d’astronomie et de géodésie de l’Université de Louvain*, 1926, v. 2, 37–41 (reprinted from *Journal of Math. Physics*, see above).
- Friedmann A. Über die Krümmung des Raumes. *Zeitschrift für Physik*, 1922, Band 10, No. 1, 377–386 (published in English as: Friedman A. On the curvature of space. *General Relativity and Gravitation*, 1999, vol. 31, no. 12, 1991–2000).
- Friedmann A. Über die Möglichkeit einer Welt mit konstanter negativer Krümmung des Raumes. *Zeitschrift für Physik*, 1924, Band 21, No. 1, 326–332 (published in English as: Friedmann A. On the possibility of a world with constant negative curvature of space. *General Relativity and Gravitation*, 1999, vol. 31, no. 12, 2001–2008).
- Lemaître G. Un Univers homogène de masse constante et de rayon croissant rendant compte de la vitesse radiale des nébuleuses extragalactiques. *Annales de la Société Scientifique de Bruxelles*, ser. A, 1927, tome 47, 49–59.
- Hubble E. A relation between distance and radial velocity among extragalactic nebulae. *Proceedings of the National Academy of Sciences*, 1929, v. 15, 168–173.
- Lemaître G. A homogeneous universe of constant mass and increasing radius accounting for the radial velocity of extra-galactic nebulae. *Monthly Notices of the Royal Astronomical Society*, 1931, v. 91, no. 5, 483–490 (this is a substantially shortened English translation of the 1927 paper).
- Lemaître G. The expanding universe. *Monthly Notices of the Royal Astronomical Society*, 1931, v. 91, no. 5, 490–501.
- Lemaître G. L’expansion de l’espace. *Publications du Laboratoire d’astronomie et de géodésie de l’Université de Louvain*, 1931, v. 8, 101–120.
- Peebles P. J. E. Impact of Lemaître’s ideas on modern cosmology. In: “The Big Bang and Georges Lemaître”, Proceedings of the Symposium (Louvain-la-Neuve, Belgium, October 10–13, 1983), D. Reidel Publishing Co., Dordrecht, 1984, 23–30.
- Kragh H. and Smith R. W. Who discovered the expanding universe? *History of Science*, 2003, v. 41, 141–162.
- Nussbaumer H. and Bieri L. Discovering the Expanding Universe. Cambridge University Press, Cambridge, 2009.
- Van den Bergh S. The curious case of Lemaître’s equation no. 24. *Journal of the Royal Astronomical Society of Canada*, 2011, v. 105, 151; arXiv: 1106.1195 (2011).
- Block D. L. Georges Lemaître and Stigler’s law of eponymy. In the paper collection: “Georges Lemaître: Life, Science and Legacy”, *Astrophysics and Space Science Library*, 2012, v. 395, 89–96; Initially posted under the title “A Hubble eclipse: Lemaître and censorship”, arXiv: 1106.3928 (2011).
- Farrell J. Why Hubble’s law... wasn’t really Hubble’s. *Forbes*, June 15, 2011.
- Reich E. S. Edwin Hubble in translation trouble. Amateur historians say famed astronomer may have censored a foreign rival. *Nature News*, 27 June 2011.
- Reich E. S. Letter sheds light on alleged censorship by Hubble. *Nature News*, 11 July 2011.
- Livio M. Lost in translation: Mystery of the missing text solved. *Nature*, v. 479, 10 November 2011, 171–173.
- Shaviv G. Did Edwin Hubble plagiarize? arXiv: 1107.0442 (2011).
- Way M. J. and Nussbaumer H. Lemaître’s Hubble relationship. arXiv: 1104.3031 (2011).
- Nussbaumer H. and Bieri L. Who discovered the expanding universe? arXiv: 1107.2281 (2011).
- Way M. J. Dismantling Hubble’s legacy? *Astronomical Society of the Pacific Conference Series*, 2013, v. 471 “Origins of the Expanding Universe 1912–1923”, 97–132; arXiv: 1301.7294 (2013).
- Luminet J.-P. Editorial note to: Georges Lemaître, A homogeneous universe of constant mass and increasing radius accounting for the radial velocity of extra-galactic nebulae. *General Relativity and Gravitation*, 13 June 2013, v. 45, 1619–1633; arXiv: 1305.6470 (2013).
- Heavens A. F., Matarrese S., Verde L. The non-linear redshift-space power spectrum of galaxies. *Monthly Notices of the Royal Astronomical Society*, 1998, v. 301, 797–808.
- Sigad Y., Branchini E., Dekel A. Measuring the nonlinear biasing function from a galaxy redshift survey. *The Astronomical Journal*, 2000, v. 540, 62–73.
- Gebhardt H. and Jeong D. Nonlinear redshift-space distortions in the harmonic-space galaxy power spectrum. *Physical Review D*, 2020, v. 102, 083521; arXiv: 2008.08706.
- Rabounski D. and Borissova L. Particles Here and Beyond the Mirror. The 4th revised edition, New Scientific Frontiers, London, 2023 (the 1st edition was issued in 2001).
- Rabounski D. et Larissa Borissova L. Particules de l’Univers et au delà du miroir. La 2ème édition révisée en langue française, New Scientific Frontiers, Londres, 2023 (French translation).
- Borissova L. and Rabounski D. Fields, Vacuum, and the Mirror Universe. The 3rd revised edition, New Scientific Frontiers, London, 2023 (the 1st edition was issued in 2001).
- Borissova L. et Rabounski D. Champs, Vide, et Univers miroir. La 2ème édition révisée en langue française, New Scientific Frontiers, Londres, 2023 (French translation).
- Rabounski D. and Borissova L. Physical observables in General Relativity and the Zelmanov chronometric invariants. *Progress in Physics*, 2023, no. 1, 3–29.
- Rabounski D. Cosmological mass-defect — a new effect of General Relativity. *The Abraham Zelmanov Journal*, 2011, v. 4, 137–161.
- Rabounski D. Non-linear cosmological redshift: The exact theory according to General Relativity. *The Abraham Zelmanov Journal*, 2012, v. 5, 3–30.
- Rabounski D. On the exact solution explaining the accelerate expanding Universe according to General Relativity. *Progress in Physics*, 2012, no. 2, L1–L6.

39. Borissova L. De Sitter bubble as a model of the observable Universe. *The Abraham Zelmanov Journal*, 2010, v. 3, 3–24.
 40. Borissova L. and Rabounski D. *Inside Stars*. The 3rd edition, revised and expanded, New Scientific Frontiers, London, 2023 (the 1st edition was issued in 2013).
 41. Borissova L. and Rabounski D. Cosmological redshift in the de Sitter stationary Universe. *Progress in Physics*, 2018, no. 1, 27–29.
 42. Rabounski D. and Borissova L. On the lambda term in Einstein's equations and its influence on the cosmological redshift. *Progress in Physics*, 2023, no. 2, 4–12.
 43. Rabounski D. An explanation of Hubble redshift due to the global non-holonomy of space. *Progress in Physics*, 2009, no. 1, L1–L2.
 44. Rabounski D. Hubble redshift due to the global non-holonomy of space. *The Abraham Zelmanov Journal*, 2009, v. 2, 11–28.
 45. Rabounski D. On the speed of rotation of the isotropic space: Insight into the redshift problem. *The Abraham Zelmanov Journal*, 2009, v. 2, 208–223.
 46. Freedman W. L., Madore B. F., Gibson B. K., et al. Final results from the Hubble Space Telescope Key Project to measure the Hubble constant. *Astrophysical Journal*, 2001, v. 553, no. 1, 47–72.
-

Interpretation of Quantum Mechanics in Terms of Discrete Time II

Young Joo Noh

E-mail : yjnoh777@gmail.com, Seongnam, Korea.

From the perspective of discrete time, the macroscopic world and the microscopic world are divided using the Planck mass as a reference point. The microscopic world is a world where the nature of time is discrete and non-locality dominates, and the macroscopic world is a world where the nature of time is continuous and locality dominates. The macroscopic world is not reduced to the result of the order of the microscopic world, and the physical laws of both worlds are real. The differences between the two worlds lead to limitations in applying physical intuition formed in the macroscopic world to the microscopic world. As an alternative to this, a new model of the physical reality of matter in the microscopic world was proposed.

1 Boundary between the macroscopic world and the microscopic world

From a discrete time perspective, quantum waves are formed by the contributions of Δt future and past spinors, and can be expressed as follows [1]:

$$\begin{aligned} (x^\mu + \Delta x^\mu) \Psi(x^\mu) - x^\mu \Psi(x^\mu + \Delta x^\mu) \\ = \Delta x^\mu \exp\left(-\frac{i}{\hbar} \Delta x^\alpha P_\alpha\right) \Psi(x^\mu). \end{aligned} \quad (1)$$

In (1), the time component of Δx^μ is $c\Delta t$.

In order for (1) to be established, the following two assumptions are necessary:

1. $\Psi(x^\mu)$ is an analytic function.
2. $[x^\mu, P_\nu] = -i\hbar\delta_\nu^\mu$, where $P_\nu = i\hbar\frac{\partial}{\partial x^\nu}$.

Mathematically, there is no limit to the lower limit of Δx^μ , or Δt , in the Taylor expansion of $\Psi(x^\mu + \Delta x^\mu)$. However, there is a physical constraint on the lower limit of Δt . Δt is defined as the time taken for light to pass through the reduced Compton wavelength λ_c [2]:

$$\Delta t = \frac{\lambda_c}{c} = \frac{\hbar}{mc^2}. \quad (2)$$

As mass increases, λ_c decreases. However, physically, this process cannot proceed without limitations, because a black hole is formed when λ_c becomes the Schwarzschild radius r_s . Therefore, λ_c must satisfy the following conditions:

$$\left(\lambda_c = \frac{\hbar}{mc}\right) > \left(r_s = \frac{2Gm}{c^2}\right). \quad (3)$$

Since the mass at $\lambda_{c,p}$, the lower limit of λ_c , is the Planck mass m_p , the lower limit of Δt is the Planck time t_p .

$$\begin{aligned} \lambda_{c,p} &= \frac{\hbar}{m_p c} = \frac{2Gm_p}{c^2} \\ \Delta t_{\text{lower limit}} &= \frac{\hbar}{m_p c^2} = \sqrt{\frac{2\hbar G}{c^5}} = t_p. \end{aligned} \quad (4)$$

If $\Delta t \leq t_p$, the analytic expansion of $\Psi(x^\mu + \Delta x^\mu)$ is mathematically possible, but physically not possible. This means that (1) is not possible, so it can be said that plane waves as harmonic oscillations are not formed. In other words, $\Delta t = t_p$ becomes the boundary point of whether a quantum wave is formed or not. Since Δt is inversely proportional to mass, this boundary is determined only by mass. That is, the Planck mass. Using this as a reference point, the quantum world and the non-quantum world are divided.

The Planck mass is the boundary, but there is one more thing to consider. Eq. (1) is for a plane wave of a single wavelength. If the mass is close to the Planck mass (1.5×10^{-8} kg), it is of course not an elementary particle but a composite. In this case as well, for (1) to hold, the waves of all components must be in a coherent state. Therefore, the Planck mass is theoretically the maximum value of a quantum system where quantum waves can be formed. However, for actual composites in thermal equilibrium, even if the mass is less than the Planck mass, quantum waves may be canceled out and quantum phenomena may not appear. This tendency will be greater as the mass of the system or the number of components increases.

In fact, it can be inferred from existing quantum mechanics that the Planck mass is the boundary between the quantum world and the non-quantum world. The Compton wavelength of matter is defined as the wavelength of a photon with energy equal to its rest energy. However, when the wavelength of the photon becomes the Schwarzschild radius, the photon is confined by its own gravitational field. Therefore, the Compton wavelength is limited by the Planck length, and the mass at this point is the Planck mass. This means that the Planck mass represents the limit to which the Compton wavelength, which refers to the quantum characteristics of matters, can be achieved.

Now, I will discuss the properties of time when $m \geq m_p$. In (1) and the physical constraints of Δt , it was discussed that if $m < m_p$ ($\Delta t > t_p$), a quantum wave is formed, and if $m \geq m_p$ ($\Delta t \leq t_p$), a quantum wave is not formed. In the latter

case, Δt is not defined by physical constraints. In other words, the concept of discrete time does not apply to the physical system. If the concept of discrete time is not applied, there is only one possibility. That is continuous time. This means that if the mass of a physical system is greater than the Planck mass, the time applied to the system must be continuous. As a result of this discussion, the following conclusions can be drawn. With the Planck mass as the reference point, elementary particles in the microscopic world have their own discrete time, while the macroscopic world has continuous time. Since the characteristics of continuous time are independent of the mass of the object, all macroscopic objects have the same continuous time in their stationary inertial frames. This is why the time we experience feels as if it is universal.

The above contents are summarized and shown in the figure below. In Fig. 1, $\Delta t = 0$ in the $m \geq m_p$ range does not mean that (1) is applied, but simply represents continuous time.

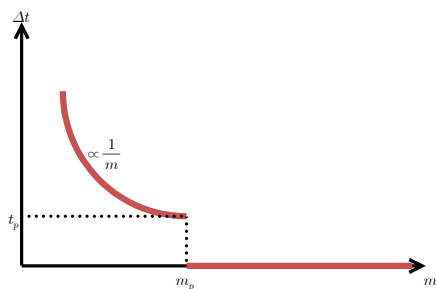


Fig. 1: $\Delta t - m$ graph

As you can see from Fig. 1, the macroscopic world is not on a continuous line with the microscopic world. In other words, the limit of any variable in the microscopic world cannot become the macroscopic world. Since the properties of time are completely different in the two worlds, the dynamical principles based on them are also bound to be different. Both the macroscopic world and the microscopic world are real worlds with their own unique characteristics. This perspective is very different from existing quantum mechanical interpretations. Most existing quantum mechanical interpretations (Copenhagen, many worlds, decoherence, etc.) view the macroscopic world as the limit of the continuum of the microscopic world.

In the microscopic world, the nature of time is discrete, and as discussed in the previous paper [4], matter in this discrete time repeats the process of wave collapse and propagation as a non-local wave. Thus, the characteristic of the microscopic world is non-locality. Meanwhile, in the macroscopic world, the nature of time is continuous. Since local principles naturally apply to fields defined in continuous time, the characteristic of the macroscopic world is locality. Naturally, the physical intuition of the world where locality ap-

plies and the world where non-locality applies is bound to be different. The physical intuition of the macroscopic world dominated by classical mechanics is clear. Things like particles, waves, and determined trajectories are concepts based on local principles. However, according to the discussion so far, the microscopic world is non-local, so intuition with concepts based on local principles is bound to have limitations. In the next section, I will present a model for a new physical intuition based on the non-locality of the microscopic world.

2 The new quantum mechanical reality of matter

As mentioned in the previous section, concepts such as particles, waves, and trajectories are concepts established in the macroscopic world where local principles are applied. They are concepts of physical reality that humans, as beings in the macroscopic world, infer from their experiences. However, there are bound to be limitations in describing the microscopic world with these concepts. One solution to this difficulty is Heisenberg’s method as follows [5]:

We can no longer speak of the behaviour of the particle independently of the process of observation. As a final consequence, the natural laws formulated mathematically in quantum theory no longer deal with the elementary particles themselves but with our knowledge of them.

But I think more can be said about reality. We may think of the microscopic world as something that cannot be directly experienced. However, in reality, all parts of our body act according to the order of the microscopic world, and the basic parts of living things experience quantum phenomena. I think that what can be experienced can be drawn.

As can be seen in Fig. 2, the quantum mechanical reality presented here is composed of Compton sphere, spinor, and matter wave (i.e. de Broglie wave). The Compton sphere is a sphere with the reduced Compton wavelength as its radius, and as presented in the previous paper [4], it is a sphere formed by points contributing to the past and future of Δt at the center point. All points on the hemisphere are simultaneous events in discrete time Δt . Spinors contributing from the future hemisphere and spinors contributing from the past hemisphere combine at the center to form spinors at the central point. The spinors at this central point have phases according to (1), and a collection of identical phases forms a matter wave.

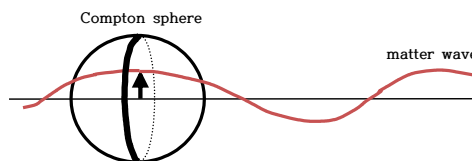


Fig. 2: The new quantum mechanical reality of matter

The wavefront of the same phase as a matter wave has the characteristics of a non-local wave. Due to their inherent characteristics, these non-local waves cause simultaneous wave collapse when they interact. (Please refer to the previous paper [4] for the process of non-local wave formation and propagation from the Compton sphere.) The start of wave propagation is the Compton sphere. While the wave is propagating, the Compton sphere no longer exists, but only a matter wave as a non-local wave. The interaction (inelastic scattering) causes an instantaneous collapse of the matter wave, and the resulting collapsed state is assumed to become a Compton sphere again. This is because the Compton sphere is the beginning of a non-local wave and can be viewed as an indecomposable elementary particle. Absorption of energy through interaction increases the frequency of the spinor phase within the Compton sphere. As a result, a matter wave as a new non-local wave with a shorter wavelength is formed and propagated. Meanwhile, electromagnetic waves are also non-local waves, but since they have no rest mass, the Compton sphere does not exist. It is assumed that the contraction of the wave due to interaction will result in only a localized electromagnetic field, the size of which will be determined by the size of the interacting matter. If there is a change in energy after interaction, it propagates as a wave with a new wavelength.

3 Conclusions

The distinction between the macroscopic world and the microscopic world has been interpreted from various perspectives since the beginning of quantum mechanics, and most perspectives have attempted to understand the macroscopic world as a continuation of the microscopic world. However, from the perspective of discrete time, the two worlds are not on a continuous line and take on completely different appearances with the Planck mass as the reference point. In the macroscopic world, the nature of time is continuous, and the principle of locality governs. In the microscopic world, the nature of time is discrete, and non-locality becomes the basic principle of existence. The macroscopic world cannot be reduced to the result of the order of the microscopic world, and the two worlds form a kind of hierarchical relationship of existence.

From the above perspective, it can be said that it is natural that concepts such as particles, waves, and trajectories, which are concepts of physical reality in the macroscopic world, that is, classical mechanics, will be difficult to apply to the microscopic world. The concept of physical reality in the microscopic world, inferred from a discrete time perspective, is quite different from that in the macroscopic world. As presented in the previous paper [4], the wave concept of the microscopic world is not a wave concept based on local principles of the macroscopic world, but a non-local wave. There are also many differences in the concept of particles. The

concept of a particle in the macroscopic world is a particle without an internal structure of finite size or a point particle with no size. These particle concepts are abstracted on the basis of continuous space and time. The concept of a particle of a finite size without an internal structure still has the meaning of an internal area, and a point particle without size is premised on the meaning of an infinite division of continuous space. From a discrete time perspective, an elementary particle in the microscopic world, in the case of matter, is a Compton sphere. The size of the Compton sphere is determined by the rest mass, and although it is an elementary particle that cannot be resolved, it has an internal structure. The internal structure mentioned here does not mean a composite such as an atom. The Compton sphere consists of two hemispheres with time differences, and has an internal structure in the sense that a spinor field is formed at the center. Since the spinor formed at the center has a phase, the Compton sphere as a particle is not maintained and propagates as a matter wave over time. Due to interaction (this corresponds to the case of inelastic scattering; during elastic scattering, it maintains its wave properties without wave collapse), the matter wave collapses into a Compton sphere again. And this process repeats. This is a new physical intuition from a discrete time perspective on the microscopic world.

Received on January 26, 2024

References

1. Noh Y.J. Propagation of a Particle in Discrete Time. *Progress in Physics*, 2020, v. 16, 116–122.
2. Noh Y.J. Anomalous Magnetic Moment in Discrete Time. *Progress in Physics*, 2021, v. 17, 207–209.
3. Noh Y.J. Lamb Shift in Discrete Time. *Progress in Physics*, 2022, v. 18, 126–130.
4. Noh Y.J. Interpretation of Quantum Mechanics in Terms of Discrete Time I. *Progress in Physics*, 2023, v. 19, 109–114.
5. Heisenberg W. The Physicist's Conception of Nature. Hutchinson, 1958, p. 15.

Addendum to “The Feynman-Dyson propagators for neutral particles (locality or non-locality?)”

Valeriy V. Dvoeglazov

UAF, Universidad de Zacatecas, Apartado Postal 636, Suc. 3, Zacatecas 98061, Zac., México. E-mail: valeri@fisica.uaz.edu.mx

We answer several questions of the referees and readers that arose after publication of the commented article [1]. Moreover, we see that it is impossible to consider correct relativistic quantum mechanics without negative energies, tachyons, and without appropriate forms of discrete symmetries.

Why did we consider four field functions in the propagator for spin-1 in [1, 2]?* Let us make some observations for spin-1/2 and spin 1.

We have 4 solutions in the original Dirac equation for u – and 4 solutions for $v = \gamma^5 u$ (remember we have $p_0 = \pm E_p = \pm \sqrt{\mathbf{p}^2 + m^2}$). See, for example, [3]. In the $S = 1$ Weinberg equation [4], we have 12 solutions†. Apart from $p_0 = \pm E_p$, we have tachyonic solutions $p_0 = \pm E'_p = \pm \sqrt{\mathbf{p}^2 - m^2}$, i.e. $m \rightarrow im$. This is easily checked on using the algebraic equations and solving them with respect to p_0 :

$$\text{Det} [\gamma^\mu p_\mu \pm m] = 0, \quad (1)$$

and

$$\text{Det} [\gamma^{\mu\nu} p_\mu p_\nu \pm m^2] = 0. \quad (2)$$

In the construction of the field operator [3], we generally need $u(-p) = u(-p_0, -\mathbf{p}, m)$ which should be transformed to $v(p) = \gamma^5 u(p) = \gamma^5 u(+p_0, +\mathbf{p}, m)$. On the other hand, when we calculate the parity properties we need $\mathbf{p} \rightarrow -\mathbf{p}$. The $u(p_0, -\mathbf{p}, m)$ satisfies

$$[\tilde{\gamma}^{\mu\nu} p_\mu p_\nu + m^2] u(p_0, -\mathbf{p}, m) = 0. \quad (3)$$

The $u(-p_0, \mathbf{p}, m)$ “spinor” satisfies:

$$[\tilde{\gamma}^{\mu\nu} p_\mu p_\nu + m^2] u(-p_0, +\mathbf{p}, m) = 0, \quad (4)$$

that is the same as above. The tilde signifies $\tilde{\gamma}^{\mu\nu} = \gamma_{00} \gamma^{\mu\nu} \gamma_{00}$ that is analogous to the $S = 1/2$ case $\tilde{\gamma}^\mu = \gamma_0 \gamma^\mu \gamma_0$. The $u(-p_0, -\mathbf{p}, m)$ satisfies:

$$[\gamma^{\mu\nu} p_\mu p_\nu + m^2] u(-p_0, -\mathbf{p}, m) = 0. \quad (5)$$

This case is opposite to the spin-1/2 case where the spinor $u(-p_0, \mathbf{p}, m)$ satisfies

$$[\tilde{\gamma}^\mu p_\mu + m] u(-p_0, +\mathbf{p}, m) = 0, \quad (6)$$

and $u(p_0, -\mathbf{p}, m)$,

$$[\tilde{\gamma}^\mu p_\mu - m] u(p_0, -\mathbf{p}, m) = 0, \quad (7)$$

*See also references therein.

†In [5], we have causal solutions only for the $S=1$ Tucker-Hammer equation.

and

$$[\gamma^\mu p_\mu + m] u(-p_0, -\mathbf{p}, m) = 0. \quad (8)$$

In general, we can use $u(-p_0, +\mathbf{p}, m)$ or $u(p_0, -\mathbf{p}, m)$ to construct the causal propagator in the spin-1/2 case. However, we need not use both because a) $u(-p_0, +\mathbf{p}, m)$ satisfies a similar equation as $u(+p_0, -\mathbf{p}, m)$ and b) we have the integration over \mathbf{p} . This integration is invariant with respect $\mathbf{p} \rightarrow -\mathbf{p}$:

$$S_F(x_2, x_1) = \sum_\sigma \int \frac{d^3 \mathbf{p}}{(2\pi)^3} \frac{m}{E_p} \times \left[\theta(t_2 - t_1) a u^\sigma(p) \bar{u}^\sigma(p) e^{-i\mathbf{p} \cdot (\mathbf{x}_2 - \mathbf{x}_1)} + \theta(t_1 - t_2) b v^\sigma(p) \bar{v}^\sigma(p) e^{+i\mathbf{p} \cdot (\mathbf{x}_2 - \mathbf{x}_1)} \right]. \quad (9)$$

So the result for the causal propagator

$$S_F(x) = \int \frac{d^4 p}{(2\pi)^4} e^{-ip \cdot x} \frac{\hat{p} + m}{p^2 - m^2 + i\epsilon} \quad (10)$$

seems to not change.

The situation is different for spin 1. The tachyonic solutions of the original Weinberg equation

$$[\gamma^{\mu\nu} p_\mu p_\nu + m^2] u(p_0, +\mathbf{p}, m) = 0 \quad (11)$$

are just the solutions of the equation with the opposite square of mass ($m \rightarrow im$):

$$[\gamma^{\mu\nu} p_\mu p_\nu - m^2] u(p_0, \mathbf{p}, im) = 0. \quad (12)$$

We cannot transform the propagator of the original equation (11) to that of (12) just by the change of the variables \mathbf{p} as in the spin-1/2 case. The mass square changed the sign, just as in the case of v – “spinors”. When we construct the propagator we have to take into account this solution and, possibly, the superposition $u(p, m)$ and $u(p, im)$, and corresponding equations.

The conclusion is paradoxical: in order to construct the causal propagator for the spin 1 we have to take acausal (tachyonic) solutions of homogeneous equations into account. It is not surprising that the propagator is not causal for the Tucker-Hammer equation because the latter does not contain the tachyonic solutions. Probably, this statement is valid for all higher spins.

Received on February 20, 2024

References

1. Dvoeglazov V.V. *Rev. Mex. Fis.*, 2017, v. 65, 612.
 2. Dvoeglazov V.V. *Int. J. Theor. Phys.*, 1998, v. 37, 1915.
 3. Cázares J. A. and Dvoeglazov V, V. *Rev. Mex. Fis.*, 2023, v. 69, 050703, 1–9.
 4. Weinberg S. *Phys. Rev. B*, 1964, v. 133, 1318.
 5. Tucker R. H. and Hammer C. L. *Phys. Rev. D*, 1971, v. 3, 2448.
-

Santilli's Recovering of Einstein's Determinism

Arun Muktibodh

Department of Mathematics, Mohota College of Science, Nagpur, India. E-mail: amukti2000@yahoo.com

We study the recent series of papers by the Italian-American physicist, Ruggero Maria Santilli based on the Lie-isotopic branch of hadronic mechanics, which imply that a system of extended protons and neutrons in conditions of partial mutual penetration in a nuclear structure verifies the following properties: 1) Admits, for the first time, explicit and concrete realizations of Bohm's hidden variables. 2) Violates Bell's inequalities by therefore admitting classical counterparts. 3) Verifies the broadening of Heisenberg's indeterminacy principle for electromagnetic interactions of point-like particles in vacuum into the *isouncertainty principle* of hadronic mechanics, also called *Einstein's isodeterminism*, for extended hadrons in conditions of partial mutual penetration, which new principle allows a progressive recovering of Einstein's determinism in the transition from hadrons to nuclei and stars and its full recovering at the limit of Schwarzschild's horizon. We then indicate some of the far reaching advances that are possible for hadronic mechanics and Einstein's isodeterminism but impossible for quantum mechanics and Heisenberg's indeterminacy principle.

1 Hadronic mechanism

Experimental foundations. This paper is based on the experimental evidence that protons [1] and neutrons [2] (collectively called nucleons) have an *extended* charge distribution with the radius $R_N = 0.87$ fm in conditions of partial mutual penetration when they are members of a nuclear structure [3–5] (e.g., the charge radius of the Helium [4] $R_{He} = 1.67$ fm is 0.07 fm smaller than the nucleon diameter $D_N = 1.74$ fm), resulting in the expectation that strong nuclear interactions have a conventional potential, thus Hamiltonian component and a new, contact, thus zero-range and non-Hamiltonian component.

Origination of hadronic mechanics. The Italian-American physicist, R. M. Santilli initiated his studies on extended particles under potential/Hamiltonian and contact/non-Hamiltonian interactions during his graduate studies at the University of Torino, Italy. By recalling that quantum mechanics is reversible over time while nuclear fusions are known to be irreversible and inspired by the 1935 Einstein-Podolsky-Rosen (EPR) argument that *Quantum mechanics is not a complete theory*, [6] (see the recent studies [7–9]), Santilli dedicated his 1965 Ph.D. thesis to the EPR irreversible “completion” of quantum mechanics via the *Lie-admissible generalization of Lie's theory and Heisenberg's equation* [10–12]).

After joining Harvard University under DOE support in September 1977 for the study of irreversible processes, Santilli resumed his research on the Lie-admissible formulation of irreversibility as one can see from his 1978 papers [13, 14], his Springer-Verlag monographs [15, 16] and his axiomatic formulation of irreversibility in the 1981 paper [17] released under his affiliation at Harvard's Department of Mathematics and proposed the continuation of the studies under the name of *hadronic mechanics* which is intended to denote a mechanics for strong interactions (see p. 112 of [16] for the first ap-

pearance of the name “hadronic mechanics”).

Hamiltonian interactions, which are collectively referred to interactions that are linear, local and derivable from a potential, thus being fully representable by the conventional Hamiltonian of quantum mechanics.

Non-Hamiltonian interactions, which are collectively referred to interactions that are: *Nonlinear* (in the wave function) as pioneering by Werner Heisenberg [18]; *Nonlocal* (distributed in a volume not reducible to points) as pioneered by Louis de Broglie and David Bohm [19]; *Nonpotential* (of contact zero-range type) as pioneered by R. M. Santilli in the 1978 monograph [15] via the *conditions of variational self-adjointness* according to which Hamiltonian interactions are variationally selfadjoint (SA), while non-Hamiltonian interactions are variationally nonselfadjoint (NSA).

Lie-isotopic branch of hadronic mechanics. In this paper, we use the axiom-preserving, time reversible *Lie-isotopic branch of hadronic mechanics* introduced in Charts 5.2, 5.3 and 5.4, p. 165 on of [16] for the representation of *stable* (thus, time-reversal invariant) systems of *extended* collections of particles at short mutual distances under Hamiltonian/SA and non-Hamiltonian/NSA interactions.

Santilli's Lie-isotopic methods are based on the generalization of the conventional universal enveloping associative algebra ξ with generic product $AB = A \times B$ and related unit 1 , $1 \times A = A \times 1 \equiv A$ into the associativity-preserving isoenveloping algebra $\hat{\xi}$ with isoproduct and related isounit (first presented in Eq. (5), p. 71 of [16] and Chart. 5.2 p. 154 for treatment)

$$\begin{aligned} A \hat{\times} B &= A \hat{S} B, \quad \hat{S} > 0, \\ \hat{1} &= 1/\hat{S}, \quad \hat{1} \times A = A \times \hat{1} \equiv A, \end{aligned} \quad (1)$$

where S , called the isotopic element (or the Santillian) is positive-definite but possesses otherwise an unrestricted func-

tional dependence on all needed local variables.

The lifting $\xi \rightarrow \hat{\xi}$ was proposed for the consequential generalization of all branches of Lie's theory into the axiom-preserving *Lie-Santilli isothory* (presented in Charts 5.3, 5.4 from p.114 on of [16]) (see also [20, 21]) with particular reference to the lifting of n-dimensional Lie algebras with (Hermitian) generators $X_k, k = 1, 2, \dots, n$ and conventional brackets into the form

$$\begin{aligned} [X_i \hat{\times} X_j] &= X_i \hat{\times} X_j - X_j \hat{\times} X_i = \\ &= X_i \hat{S} X_j - X_j \hat{S} X_i = C_{ij}^k X_k. \end{aligned} \quad (2)$$

The fundamental dynamical equation of the isotopic methods are given by the *Lie-isotopic generalization of Heisenberg equation* (Eq. (18a), p. 153 of [16])

$$idA/dt = A \hat{\times} H - H \hat{\times} A = A \hat{S} H - H \hat{S} A, \quad (3)$$

where the Hamiltonian H represents all SA interactions while the Santillian \hat{S} represents the extended character of particles and their *new* class of NSA interactions.

Subsequent studies. For advances on hadronic mechanics that occurred in the decades following the 1978 proposal [13–16], the interested reader can inspect: the overview [8] with applications in various fields; the classification of hadronic mechanics [22] (including, in addition to the *Lie-isotopic branch*, the *Lie-admissible branch* for the representation of irreversible processes; *hyperstructural branch* for biological structures and the *isodual branch* for antiparticles); the introductory reviews [23–25]; the AO collection of recent papers [26]; the list of early workshops and conferences [27]; independent monographs [28–36]; and the general presentation [37–39].

Realization of the isotopic element. To render this paper minimally self-sufficient, let us recall the generally used realization of the Santillian [8]

$$\begin{aligned} \hat{S} &= \hat{S}_{4 \times 4} = \Pi_{\alpha=1,2,3,4} \text{Diag} \left(\frac{1}{n_{1,\alpha}^2}, \frac{1}{n_{2,\alpha}^2}, \frac{1}{n_{3,\alpha}^2}, \frac{1}{n_{4,\alpha}^2} \right) \times \\ &\times e^{-\Gamma(r,p,a,E,d,\tau,\pi,\psi,\dots)} > 0, \\ n_{\mu,\alpha} &> 0, \quad \Gamma > 0, \end{aligned} \quad (4)$$

where:

- 1) The representation of the dimension and shape of the individual nucleons is done via semi-axes $n_{k,\alpha}^2, k = 1, 2, 3$ (with n_3 parallel to the spin) and normalization for the vacuum $n_{k,\alpha}^2 = 1$.
- 2) The representation of the density is done via the characteristic quantity $n_{4,\alpha}^2$ per individual nucleons with normalization for the vacuum $n_{4,\alpha}^2 = 1$.
- 3) The representation of the nonlinear, nonlocal and non-potential interactions between extended nucleons is done via the positive-definite exponential term Γ with

an arbitrary dependence on relative coordinates r , momenta p , accelerations a , energy E , density d , temperature τ , pressure, π , wave functions ψ or any needed local variable.

When representing nucleons and their NSA interactions, the space dimension of the isotopic element is restricted not to surpass the range of strong interactions $R = 1 \text{ fm} = 10^{-13} \text{ cm}$. However, the space dimension of the isotopic element can be, in general, infinite.

Elementary construction of hadronic mechanics. Despite their apparent mathematical complexity, all isotopic formulations can be constructed via the following simple *quantum mechanical nonunitary transformation* unit $1 = \hbar$, and therefore, of all related formulations according to the simple rules [40]

$$\begin{aligned} 1 &\rightarrow U1U^\dagger = \hat{1} \neq 1, \\ AB &\rightarrow U(AB)U^\dagger = \\ &= (UAU^\dagger)(UU^\dagger)^{-1}(UBU^\dagger) = \hat{A}\hat{S}\hat{B}, \\ [X_i, X_j] &\rightarrow U[X_i, X_j]U^\dagger = [\hat{X}_i, \hat{X}_j], \end{aligned} \quad (5)$$

which transformations essentially complete a quantum mechanical model for point-like particles into a hadronic model for extended particles under new interactions.

Invariance of isotopic formulations. All quantum mechanical nonunitary models, thus including models (5), are affected by serious inconsistency problems, such as the general lack of conservation of Hermiticity/observability, causality, etc. These problems were resolved by Santilli in the 1998 Ref. [40] via the completion of unitary law (4) into the *isounitary law*

$$\hat{W} \hat{\times} \hat{W}^\dagger = \hat{W}^\dagger \hat{\times} \hat{W} = \hat{1}, \quad (6)$$

completed by the identical reformulation of transformations (5) into the isounitary form

$$\begin{aligned} U &= \hat{W} \hat{S}^{1/2}, \\ UU^\dagger &= \hat{1} \rightarrow \hat{W} \hat{\times} \hat{W}^\dagger = \hat{W}^\dagger \hat{\times} \hat{W} = \hat{1}, \\ \hat{1} &\rightarrow \hat{W} \hat{\times} \hat{1} \hat{\times} \hat{W}^\dagger = \hat{1}' \equiv \hat{1}, \\ \hat{A} \hat{\times} \hat{B} &\rightarrow \hat{W} \hat{\times} (\hat{A} \hat{\times} \hat{B}) \hat{\times} \hat{W}^\dagger = \hat{A}' \hat{\times}' \hat{B}' = \hat{A}' \hat{S}' \hat{B}', \\ \hat{S}' &\equiv \hat{S} = (\hat{W}^\dagger \hat{\times} \hat{W})^{-1}, \end{aligned} \quad (7)$$

with consequential resolution of the problematic aspects of quantum nonunitary models (5), as well as the prediction by isotopic formulations, in view of properties (7), of the same numerical values under the same conditions at different times.

Experimental verifications. Santilli hadronic mechanics has been verified in virtually all physics fields by the exact and invariant representation of experimental data generally not representable via quantum mechanics, such as: direct experimental verifications of the EPR argument [41–43]; electrodynamics [44–47]; large ion physics [48]; particle physics

[49, 50]; Bose-Einstein correlation [51, 52]; propagation of light within physical media [53]; cosmology [54, 55]; neutron synthesis from the Hydrogen [56]; Deuteron magnetic moment [57]; Deuteron spin and rest energy [58]; and other fields.

2 Einstein's isodeterminism

EPR entanglement. Experimental evidence well known since Einstein's times establishes that particles, which are initially bounded together and then separated, can influence each other continuously and instantaneously at arbitrary distances [59]. Albert Einstein strongly objected against the very terms "quantum entanglement" on grounds that the sole possible representation of particle entanglements via the Copenhagen interpretation of quantum mechanics would require superluminal communications that violate special relativity.

For the intent of honoring the generally forgotten Einstein's view, Santilli [62] proved that the sole possible representation of particle entanglement by the Copenhagen interpretation of quantum mechanics is that for which *the particles are free*, evidently because the sole possible interactions admitted by said interpretation are those derivable from a potential which is identically null for particles at large mutual distances.

By recalling that the wave packet of particles is identically null solely at infinite distance, Ref. [62] then pointed out that the sole interactions that are continuous, instantaneous and at arbitrary distances are given by the mutual penetration of wave packets of particles which, being nonlinear, nonlocal and nonpotential, thus NSA [15], are beyond any hope of treatment via quantum mechanics.

Thanks to the prior development of isomathematics for the representation of NSA interactions [33, 36, 37], Santilli [62] proposed the axiom-preserving completion of quantum into hadronic entanglement under the suggested name of *EPR entanglements* which does indeed represent particle entanglements with non-zero, yet non-Hamiltonian-NSA interactions.

Note that the EPR entanglement of particles requires a conceptual and technical revision of the notion of interactions, e.g., because nuclear constituents admit nontrivial NSA interactions even when they are at a mutual distance bigger than that of strong interactions.

More recently, the EPR entanglement has been experimentally proved to hold at arbitrary *classical* distances [60]. This important feature appears to support Santilli's suggestion [15] that contact forces dating back to Newton, when turned into an operator form, are plausible candidates for the *fifth interactions* intended as *nonlinear, nonlocal, continuous and instantaneous interactions at arbitrary distances* due to the overlapping of the wave packets of particles (see Sect. 1.5.C of [80]). Their lack of identification to date is easily explained by their lack of existence in quantum mechanics. Therefore, in the event such a view is accepted, Santilli's

1978 monograph [15] can be considered the birth of the fifth interactions.

Note also that paper [62] confirms Einstein's additional view that "*The wave function of quantum mechanics does not provide a complete description of the entire physical reality*" [6].

Bohm's hidden variables. As it is well known, in an attempt of reconciling Einstein's determinism with quantum mechanics, D. Bohm [63, 64] submitted in 1952 the hypothesis that quantum mechanics admits *hidden variables* λ , that is, variables which are hidden in its formalism. Following half a century of failure to achieve explicit realizations, a rather general consensus (confirmed by Bell's inequalities outlined next) is that *Bohm's hidden variables do not exist within the formalism of quantum mechanics*.

In 1995, R. M. Santilli [38] proved that *hidden variables do exist within the context of hadronic mechanics, they are hidden in the axiom of associativity of quantum mechanics and are quantitatively represented by the isotopic element* (Sect. 4.C.3, p. 170 on and Sect. 6.8, p. 254 on of [38], e.g.,

$$\lambda = \hat{S}, \quad (8)$$

$$A \hat{\times} B = A \lambda B, \quad A \hat{\times} (B \hat{\times} C) = (A \hat{\times} B) \hat{\times} C.$$

It should be noted that, despite its apparent elementary character of the isotopic product (1), the quantitative study of the indicated realization of Bohm's hidden variables required collegial efforts in the nonlocal lifting of the entire 20th century applied mathematics, including the Newton-Leibnitz differential calculus [65] (see also studies [36]). Nowadays, there exists a number of explicit and concrete realization of hidden variables, among which we mention the realization used for the first numerically exact and time invariant representation of the Deuteron magnetic moment [66, 67] which achievement resulted to be impossible for quantum mechanics in one century.

Bell's inequalities. In the 1964, J. S. Bell [68] proved a number of quantum mechanical inequalities, the first one of which essentially states that systems of point like particles with spin 1/2 represented via quantum mechanics do not admit classical counterparts. This view was assumed by mainstream physicists for over half a century to be the final disproof of the EPR argument and of Bohm's hidden variables.

Again thanks to the prior development of isomathematics as well as of explicit and concrete realizations of hidden variables, Santilli [71] proved in 1998 a number of hadronic inequalities essentially stating that *systems of extended particles with spin 1/2 represented via the Lie-isotopic branch of hadronic mechanics do indeed admit classical counterparts*, while providing explicit examples.

Santilli's hadronic inequalities are confirmed by the direct experimental verifications of the EPR-argument [41–43] establishing the existence in nature of particle conditions which violate Bell's inequalities.

Note that the above theoretical and experimental works imply the expectation that Heisenberg’s uncertainties principle is correspondingly violated by strong interactions between extended nucleons in conditions of mutual penetration.

Einstein’s isodeterminism. Soon after joining Harvard University in late 1977, R. M. Santilli expressed doubts on the exact validity for strong interactions of Heisenberg’s uncertainty principle (also called indeterminacy principle) and other quantum mechanical laws, as one can see from the *titles* of the 1978 memoir [14] (see also the subsequent papers [69, 70]). Santilli’s argument underlying such a conviction is that Heisenberg’s standard deviations for coordinates Δr , momenta Δp and their product are certainly valid for the conditions of their original conception, i.e., for point-like charged particles under electromagnetic interactions, because a point-like particle can move within a star by solely sensing action-at-a-distance interactions due to its dimensionless character.

The situation is conceptually, mathematically, theoretically and experimentally different when considering extended nucleons in conditions of mutual penetration because, in view of their “strength”, strong interactions imply the creation of a *pressure* on a given nucleon by its surrounding nucleons, according to a view pioneered by L. de Broglie and D. Bohm with their nonlocal theory [19]. It is then evident that the standard deviations for the indicated nucleon Δr and Δp *cannot* be the same as the corresponding deviations for an electron in vacuum, thus implying the need for a suitable completion of Heisenberg’s uncertainty principle for strong interactions.

Thanks to the original works [14, 69, 70] and the recent works [62, 71], Santilli [72] finally achieved in 2019 the axiom-preserving EPR completion of Heisenberg’s uncertainty principle into the *isouncertainty principle of hadronic mechanics*, also called *Einstein’s isouncertainties*, for extended nucleons under electromagnetic, weak and strong interactions whose derivation can be outlined as follows.

Let \mathcal{H} be the Hilbert-Myung-Santilli isospace [73] of isomechanics with *isostates* $|\hat{\psi}\rangle$ and isoinner product $\langle\hat{\psi}|\hat{\times}|\hat{\psi}\rangle$ (for a review, see Sect. 4 of [23]). Assume the isonormalization which is necessary for a constant Santillian

$$\langle\hat{\psi}|\hat{\times}|\hat{\psi}\rangle = \langle\hat{\psi}|\hat{S}|\hat{\psi}\rangle = \hat{S}, \tag{9}$$

the Schrödinger-Santilli isoequation [16, 38]

$$\begin{aligned} \hat{H}\hat{\times}|\hat{\psi}\rangle &= \\ &= [\sum_{k=1,2,\dots,n} \frac{1}{2m_k} \hat{p}_k\hat{\times}\hat{p}_k + \hat{V}(r)] \hat{S}(r, p, \psi, \dots) |\hat{\psi}\rangle = \\ &E \times |\hat{\psi}\rangle, \end{aligned} \tag{10}$$

the isolinear momentum [65]

$$\hat{p}\hat{\times}|\hat{\psi}\rangle = -i\hat{1}\partial_r\hat{\psi}, \tag{11}$$

and the isocommutation rules

$$\begin{aligned} [\hat{r}_i, \hat{p}_j]\hat{\times}|\hat{\psi}\rangle &= -i\hat{1}\delta_{i,j}|\hat{\psi}\rangle, \\ [\hat{r}_i, \hat{r}_j]\hat{\times}|\hat{\psi}\rangle &= [\hat{p}_i, \hat{p}_j]\hat{\times}|\hat{\psi}\rangle = 0. \end{aligned} \tag{12}$$

Then the isounitary transformation (7) of Heisenberg’s uncertainty principle

$$\Delta r \Delta p = \frac{1}{2} |\langle\psi|[r, p]|\psi\rangle| \geq \frac{1}{2} \hbar, \tag{13}$$

uniquely and unambiguously yields the *isouncertainty principle of hadronic mechanics*, also called *Einstein’s isodeterminism*, whose projection on our spacetime (as needed for experiments) is given by [72] (see [23] for an extended derivation)

$$\begin{aligned} \hat{\Delta r} \hat{\Delta p} &= \frac{1}{2} |\langle\hat{\psi}|\hat{\times}[\hat{r}, \hat{p}]\hat{\times}|\hat{\psi}\rangle| = \\ &= \frac{1}{2} |\langle\hat{\psi}|\hat{S}[\hat{r}, \hat{p}]\hat{S}|\hat{\psi}\rangle| \approx \frac{1}{2} \hbar \hat{S} = \frac{1}{2} \hbar e^{-\Gamma(r, p, a, E, d, \tau, \pi, \psi, \dots)} \approx \\ &\approx \frac{1}{2} \hbar [1 - \Gamma(r, p, a, E, d, \tau, \pi, \psi, \dots) + \dots] \ll \frac{1}{2} \hbar, \end{aligned} \tag{14}$$

where the Santillian \hat{S} is given by Eq. (4) and we assumed, in first approximation, that all nucleons are perfectly spherical.

It should be mentioned that completion (14) of Heisenberg’s uncertainty principle includes as particular cases most of the existing generalized uncertainty relations known to this author (see, e.g., [74–76] and papers quoted therein).

In particular, the standard isodeviations $\hat{\Delta r}$ and $\hat{\Delta p}$ progressively and individually tend to zero with the increase of the density of the hadronic medium, thus in the transition from hadrons to nuclei and stars.

Note that the completion of the value $\geq \frac{1}{2} \hbar$ into the form $\approx \frac{1}{2} \hbar \hat{S}$ is due to the nonlocality of hadronic mechanics which requires a redefinition of the very notion of standard deviations due to the very big pressure exercised on a nucleon by the surrounding nucleons under “strong” interactions [24, 72].

To achieve the full validity of Einstein’s determinism, Santilli [77, 78] decomposes the Riemannian metric $g(x)$ in four dimensions into then product of the Minkowskian metric $\eta = -\text{Diag}(1, 1, 1, -1)$ and the gravitational isotopic element \hat{S}

$$g(x) = \hat{S}_{4 \times 4} \eta_{4 \times 4}, \tag{15}$$

with particular values for the Schwartzschild metric

$$\hat{S}_{kk} = \frac{1}{1 - 2M/r}, \quad \hat{S}_{44} = 1 - 2M/r. \tag{16}$$

It is then easy to see that Einstein’s determinism [6] is fully recovered at the limit of the Schwartzschild horizon.

3 Concluding remarks

Despite one century of studies under large public funds, nuclear physics has been unable to achieve the controlled nuclear fusion; the recycling of radioactive nuclear waste; the

exact representations of nuclear data; the synthesis of the neutron from the Hydrogen atom in the core of stars; the nuclear stability despite the natural instability of the neutron and extremely repulsive protonic Coulomb forces; and other open problems.

A main point which is attempted to convey in this paper is that the indicated open nuclear problems appear to be due to the *theoretical assumption* that Heisenberg's uncertainty principle for point-like particles under electromagnetic interactions is also valid for extended nucleons under strong interactions.

As an illustration, Heisenberg's uncertainty principle prohibits a structural representation of the synthesis of the neutron from the electron and the proton in the core of stars, because the standard deviation Δr_e for the coordinate of the electron is much bigger than the size of the neutron and the standard deviation Δp_e of the momentum implies a kinetic energy of the electron bigger than the rest energy of the neutron,

$$\begin{aligned}\Delta r_e &> R_n = 0.87 \times 10^{-13} \text{ cm}, \\ \Delta v_e &> \frac{\hbar}{\Delta r_e \times m_e} > 10^{10} \text{ m/s}, \\ \Delta K_e &= \frac{1}{2m_e} \times (\Delta p_e)^2 > m_n = 939.56 \text{ MeV}/c^2.\end{aligned}\quad (17)$$

By comparison, the study of the neutron synthesis via hadronic mechanics under isouncertainty principle (14), implies standard isodeviations for which Eqs. (17) become

$$\begin{aligned}\hat{\Delta} r_e &= \hat{S} \Delta r_e \leq R_n = 0.87 \times 10^{-13} \text{ cm}, \\ \hat{\Delta} v &= \hat{S} \Delta v_e \ll 10^{10} \text{ m/s}, \\ \hat{\Delta} K_e &= \hat{S} \Delta K_e \ll m_n = 939.56 \text{ MeV}/c^2,\end{aligned}\quad (18)$$

thus allowing a quantitative representation of the neutron synthesis from the Hydrogen [79] with far reaching advances that cannot be formulated in quantum mechanics, let alone treated, such as [80–82]: 1) The prediction of means for recycling radioactive nuclear waste by nuclear power plants via *new* stimulated decays; 2) The possible return to the continuous creation of matter in the universe to explain the 0.782 MeV missing in the neutron synthesis; 3) The apparent reduction of all matter in the universe to protons and electrons.

Acknowledgments

The author would like to express sincere thanks to Dr. R. Anderson of the R. M. Santilli Foundation for continuous help in the preparation of this paper, particularly for historical aspects on hadronic mechanics and related documentation. Additional thanks are due to Prof. R. M. Santilli for continuous technical assistance on hadronic mechanics, including consultations and technical controls. The author is solely respon-

sible of the content of the paper due to numerous final revisions.

Received on March 4, 2024

References

- Pohl R., Antognini A. and Kottmann F. The size of the proton. *Nature*, 2010, v. 466, 213–216. www.nature.com/articles/nature09250
- Wietfeldt F.E. Measurements of the Neutron Lifetime. *Atoms*, 2018, v. 6, 1–19. www.mdpi.com/2218-2004/6/4/70
- IAEA, Nuclear data. www.iaea.org/about/organizational-structure/department-of-nuclear-sciences-and-applications/division-of-physical-and-chemical-sciences/nuclear-data-section
- ScienceDirect, Helium nucleus. www.sciencedirect.com/topics/mathematics/helium-nucleus
- Rau S. et al. Penning trap measurements of the deuteron and the HD^+ molecular ion. *Nature*, 2020, v. 585, 43–47. doi.org/10.1038/s41586-020-2628-7
- Einstein A., Podolsky B. and Rosen N. Can quantum-mechanical description of physical reality be considered complete? *Phys. Rev.*, 1935, v. 47, 777–780. www.eprdebates.org/docs/epr-argument.pdf
- Beghella-Bartoli S. and Santilli R. M., Ed. Proceedings of the 2020 Teleconference on the Einstein-Podolsky-Rosen argument that “Quantum mechanics is not a complete theory”. Curran Associates, New York, NY, 2021. Printed version: www.proceedings.com/59404.html
- Santilli R. M. Overview of historical and recent verifications of the Einstein-Podolsky-Rosen argument and their applications to physics, chemistry and biology. APAV - Accademia Piceno Aprutina dei Velati, Pescara, Italy, 2021. www.santilli-foundation.org/epr-overview-2021.pdf
- Dunning-Davies J. A. Present Day Perspective on Einstein-Podolsky-Rosen and its Consequences. *Journal of Modern Physics*, 2021, v. 12, 887–936. www.scirp.org/journal/paperinformation.aspx?paperid=109219
- Santilli R. M. Embedding of Lie-algebras into Lie-admissible algebras. *Nuovo Cimento*, 1967, v. 51, 570–585. [//www.santilli-foundation.org/docs/Santilli-54.pdf](http://www.santilli-foundation.org/docs/Santilli-54.pdf)
- Santilli R. M. Dissipativity and Lie-admissible algebras. *Meccanica*, 1969, v. 1, 3–12.
- Santilli R. M. An introduction to Lie-admissible algebras. *Suppl. Nuovo Cimento*, 1968, v. 6, 1225.
- Santilli R. M. On a possible Lie-admissible covering of Galilei's relativity in Newtonian mechanics for nonconservative and Galilei form-non-invariant systems. *Hadronic Journal*, 1978, v. 1, 223–423. www.santilli-foundation.org/docs/Santilli-58.pdf
- Santilli R. M. Need of subjecting to an experimental verification the validity within a hadron of Einstein special relativity and Pauli exclusion principle. *Hadronic Journal* 1978, v. 1, 574–901. www.santilli-foundation.org/docs/santilli-73.pdf
- Santilli R. M. Foundation of Theoretical Mechanics, Vol. I, The Inverse Problem in Newtonian Mechanics. *Springer-Verlag*, Heidelberg, Germany, 1978. www.santilli-foundation.org/docs/Santilli-209.pdf
- Santilli R. M. Foundation of Theoretical Mechanics. Vol. II, Birkhoffian Generalization of Hamiltonian Mechanics. *Springer-Verlag*, Heidelberg, Germany, 1983. www.santilli-foundation.org/docs/santilli-69.pdf
- Santilli R.M. Initiation of the representation theory of Lie-admissible algebras of operators on bimodular Hilbert spaces. *Hadronic J.*, 1979, v. 3, 440–467. www.santilli-foundation.org/docs/santilli-1978-paper.pdf
- Heisenberg W. *Nachr. Akad. Wiss. Gottingen*, 1953, v. IIa, 111–133. www.link.springer.com/chapter/10.1007/978-3-642-70079-8_23

19. Stanford Encyclopedia of Philosophy, Bohmian (de Broglie-Bohm) Mechanics. 2021. plato.stanford.edu/entries/qm-bohm
20. Sourlas D.S and Tsagas Gr. T. Mathematical Foundation of the Lie-Santilli Theory. Ukraine Academy of Sciences, 1993. www.santilli-foundation.org/docs/santilli-70.pdf
21. Kadeisvili J. V. An introduction to the Lie-Santilli isotopic theory. *Mathematical Methods in Applied Sciences*, 1996, v. 19, 134–172. www.santilli-foundation.org/docs/Santilli-30.pdf
22. Anderson R. Outline of Hadronic Mathematics, Mechanics and Chemistry as Conceived by Santilli R. M. *American Journal of Modern Physics*, 2016, v. 6, 1–16. www.santilli-foundation.org/docs/HMMC-2017.pdf
23. Santilli R. M. Studies on A. Einstein, B. Podolsky and N. Rosen prediction that quantum mechanics is not a complete theory, I: Basic methods. *Ratio Mathematica*, 2020, v. 38, 5–69. eprdebates.org/docs/epr-review-i.pdf
24. Santilli R. M. Studies on A. Einstein, B. Podolsky and N. Rosen prediction that quantum mechanics is not a complete theory, II: Apparent proof of the EPR argument. *Ratio Mathematica*, 2020, v. 38, 71–138. eprdebates.org/docs/epr-review-ii.pdf
25. Santilli R. M. Studies on A. Einstein, B. Podolsky and N. Rosen prediction that quantum mechanics is not a complete theory, III: Illustrative examples and applications. *Ratio Mathematica*, 2020, v. 38, 139–222. eprdebates.org/docs/epr-review-iii.pdf
26. Anderson A. Collected OA Papers on Hadronic Mathematics, Mechanics and Chemistry. www.santilli-foundation.org/docs/HMMC.pdf
27. Anderson R. List of early OA international workshops and conferences in hadronic mechanics. www.santilli-foundation.org/docs/workshops-conf-hm.pdf
28. Aringazin A. K, Jannussis A., Lopez F., Nishioka M. and Veljanosky B. Santilli's Lie-Isotopic Generalization of Galilei and Einstein Relativities. Kostakaris Publishers, Athens, Greece, 1991. www.santilli-foundation.org/docs/Santilli-108.pdf
29. Sourlas D.S. and Tsagas Gr. T. Mathematical Foundation of the Lie-Santilli Theory. Ukraine Academy of Sciences, 1993. www.santilli-foundation.org/docs/santilli-70.pdf
30. Lohmus J., Paal E. and Sorgsepp L. Nonassociative Algebras in Physics. Hadronic Press, Palm Harbor, 1994. www.santilli-foundation.org/docs/Lohmus.pdf
31. Kadeisvili J. V. Santilli's Isotopies of Contemporary Algebras, Geometries and Relativities. Ukraine Academy of Sciences, Second edition, 1997. www.santilli-foundation.org/docs/Santilli-60.pdf
32. Jiang C-X. Foundations of Santilli Isonumber Theory. International Academic Press, 2001. www.i-b-r.org/docs/jiang.pdf
33. Ganfornina R. M. F. and Valdes J. N. Fundamentos de la Isotopia de Santilli. International Academic Press, 2001. www.i-b-r.org/docs/spanish.pdf
English translation: *Algebras, Groups and Geometries*, 2015, v. 32, 135–308. www.i-b-r.org/docs/Aversa-translation.pdf
34. Davvaz B. and Vougiouklis Th. A Walk Through Weak Hyperstructures and H_p -Structures. World Scientific, 2018.
35. Gandzha I. and Kadeisvili J. V. New Sciences for a New Era: Mathematical, Physical and Chemical Discoveries by Ruggero Maria Santilli. Sankata Printing Press, Nepal, 2011. www.santilli-foundation.org/docs/RMS.pdf
36. Georgiev S. Foundations of IsoDifferential Calculus. Nova Publishers, New York:
Vol. 1: Iso-Differential and Iso-Integral Calculus for Iso-Functions in One Variable. 2014;
Vol. 2: Iso-Differential and Iso-Integral Calculus for Iso-Functions in Several Variables. 2014;
Vol. 3: Iso-Ordinary Iso-Differential Equations. 2014;
Vol. 4: Iso-Difference Equations. 2015;
Vol. 5: Iso-Stochastic Iso-Differential Equations. 2015;
Vol. 6: Theory of Iso-Measurable Iso-Functions. 2016.
New Edition of Vol. 1: Iso-Differential and Iso-Integral Calculus for Iso-Functions in One Variable. 2022. Iso-Mathematics. Lambert Academic Publishing, 2022.
37. Santilli R. M. Elements of Hadronic Mechanics. Vol. I, Mathematical Foundations. Ukraine Academy of Sciences, Kiev, 1995. www.santilli-foundation.org/docs/Santilli-300.pdf
38. Santilli R. M. Elements of Hadronic Mechanics. Vol. II, Theoretical Foundations. Ukraine Academy of Sciences, Kiev, 1995. www.santilli-foundation.org/docs/Santilli-301.pdf
39. Santilli R. M. Elements of Hadronic Mechanics. Vol. III, Experimental verifications. Ukraine Academy of Sciences, Kiev, 2016. www.santilli-foundation.org/docs/elements-hadronic-mechanics-iii.compressed.pdf
40. Santilli R. M. Invariant Lie-isotopic and Lie-admissible formulation of quantum deformations. *Found. Phys.*, 1997, v. 27, 1159–1177. www.santilli-foundation.org/docs/Santilli-06.pdf
41. Fadel M. et al. Spatial entanglement patterns and Einstein-Podolsky-Rosen steering in Bose-Einstein condensates. *Science*, 2018, v. 360, 409–415. www.santilli-foundation.org/Basel-paper.pdf
42. Colciaghi P. et al. Einstein-Podolsky-Rosen Experiment with Two Bose-Einstein Condensates. *Phys. Rev. X*, 2023, v. 13, 021031, 10 pp. journals.aps.org/prx/pdf/10.1103/PhysRevX.13.021031
43. Aspect A. et al. Experimental Realization of Einstein-Podolsky-Rosen-Bohm Gedankenexperiment: A New Violation of Bell's Inequalities. *Phys. Rev. Lett.*, 1982, v. 49, 91–94. ui.adsabs.harvard.edu/abs/1982PhRvL..49...91A
44. Miller J. P. et al. Muon ($g-2$): experiment and theory. *Rep. Prog. Phys.*, 2007, v. 70, 795–881. news.fnal.gov/2021/04/first-results-from-fermilabs-muon-g-2-experiment-strengthen-evidence-of-new-physics
45. Santilli R. M. Apparent Unsettled Value of the Recently Measured Muon Magnetic Moment. *Progress in Physics*, 2022, v. 18, 15–18. www.santilli-foundation.org/docs/muon-meanlife-2022.pdf
46. Santilli R. M. Representation of the anomalous magnetic moment of the muons via the Einstein-Podolsky-Rosen completion of quantum into hadronic mechanics. *Progress in Physics*, 2021, v. 17, 210–215. www.progress-in-physics.com/2021/PP-62-13.PDF
47. Santilli R. M. Representation of the anomalous magnetic moment of the muons via the novel Einstein-Podolsky-Rosen entanglement in: Garcia H. M. C., Guzman J. J. C., Kauffman L. H. and Makaruk H., Eds. Scientific Legacy of Professor Zbigniew Oziewicz. World Scientific, 2024. [www.santilli-foundation.org/docs/santilli-546-\(1\).pdf](http://www.santilli-foundation.org/docs/santilli-546-(1).pdf)
48. Schukraft K. Heavy-ion physics with the ALICE experiment at the CERN Large Hadron Collider. *Trans. Royal Soc.*, 2012, v. A370, 917–932. royalsocietypublishing.org/doi/10.1098/rsta.2011.0469
49. Cardone F., Mignani R. and Santilli R. M. On a possible energy-dependence of the K^0 lifetime. Part I. *J. Phys. G: Part. Phys.*, 1992, v. 18, L141–L144. www.santilli-foundation.org/docs/Santilli-32.pdf
50. Cardone F., Mignani R. and Santilli R. M. On a possible energy-dependence of the K^0 lifetime. Part II. *J. Phys. G: Part. Phys.*, 1992, v. 18, L61–L65. www.santilli-foundation.org/docs/Santilli-32.pdf
51. Santilli R. M. Nonlocal formulation of the Bose-Einstein correlation within the context of hadronic mechanics. *Hadronic J.*, 1992, v. 5, 1–50 and v. 15, 81–133. www.santilli-foundation.org/docs/Santilli-116.pdf
52. Cardone F. and Mignani R. Nonlocal approach to the Bose-Einstein correlation. *JETP*, 1996, v. 83, 435. www.santilli-foundation.org/docs/Santilli-130.pdf
53. Ahmar H. et al. Additional experimental confirmations of Santilli's IsoRedShift and the consequential lack of expansion of the universe. *Journal of Computational Methods in Sciences and Engineering*, 2013, v. 13, 321–375. www.santilli-foundation.org/docs/IRS-confirmations-212.pdf

54. Mignani R. Quasars redshift in isominkowski space. *Physics Essay*, 1992, v. 5, 531. www.santilli-foundation.org/docs/Santilli-31.pdf
55. Santilli R. M. Experimental Verifications of IsoRedShift with Possible Absence of Universe Expansion, Big Bang, Dark Matter and Dark Energy. *The Open Astronomy Journal*, 2010, v. 3, 124–132. www.santilli-foundation.org/docs/IsoRedshift-Letter.pdf
56. Norman R., Beghella Bartoli S., Buckley B., Dunning-Davies J., Rak J. and Santilli R. M. Experimental Confirmation of the Synthesis of Neutrons and Neutroids from a Hydrogen Gas. *American Journal of Modern Physics*, 2017, v. 6, 85–104. www.santilli-foundation.org/docs/confirmation-neutron-synthesis-2017.pdf
57. Santilli R. M. A quantitative isotopic representation of the Deuteron magnetic moment. In: Proceedings of the International Symposium “Dubna Deuteron-3e”. Joint Institute for Nuclear Research, Dubna, Russia, 1994. www.santilli-foundation.org/docs/Santilli-134.pdf
58. Santilli R. M. The Physics of New Clean Energies and Fuels According to Hadronic Mechanics. Special issue of the Journal of New Energy, 1998. www.santilli-foundation.org/docs/Santilli-114.pdf
59. Bengtsson I. and Życzkowski K. An Introduction to Quantum Entanglement, second, revised edition. Cambridge University Press, 2006. chaos.if.uj.edu.pl/~karol/geometry.htm
60. Berkowitz R. Macroscopic systems can be controllably entangled and limitlessly measured. *Physics Today*, July 2021, 16–18. www.santilli-foundation.org/docs/particle-entanglement.pdf
61. Santilli R. M. Elements of nuclear physics according to hadronic mechanics. I: Exact Lie-isotopic representation of nuclear data. submitted for publication.
62. Santilli R. M. A quantitative representation of particle entanglements via Bohm’s hidden variables according to hadronic mechanics. *Progress in Physics*, 2022, v. 18, 131–137. www.santilli-foundation.org/docs/pip-entanglement-2022.pdf
63. Bohm D. A Suggested Interpretation of the Quantum Theory in Terms of “Hidden Variables”. *Phys. Rev.*, 1952, v. 85, 166–182. journals.aps.org/pr/abstract/10.1103/PhysRev.85.166
64. Bohm D. Quantum Theory. Prentice-Hall, New York, 1951.
65. Santilli R. M. Nonlocal-Integral Isotopies of Differential Calculus, Mechanics and Geometries. *Rendiconti Circolo Matematico Palermo, Suppl.*, 1996, v. 42, 7–82. www.santilli-foundation.org/docs/Santilli-37.pdf
66. Santilli R. M. Iso-Representation of the Deuteron Spin and Magnetic Moment via Bohm’s Hidden Variables. *Progress in Physics*, 2022, v. 18, 74–81. www.progress-in-physics.com/2022/PP-63-12.PDF
67. Santilli R. M. and Sobczyk G. Representation of nuclear magnetic moments via a Clifford algebra formulation of Bohm’s hidden variables. *Scientific Reports*, 2022, v. 12, 1–10. www.santilli-foundation.org/Santilli-Sobczyk.pdf
68. Bell J. S. On the Einstein Podolsky Rosen paradox. *Physics*, 1964, v. 1, 195. cds.cern.ch/record/111654/files/vol1p195-200.001.pdf
69. Santilli R. M. Generalization of Heisenberg’s uncertainty principle for strong interactions. *Hadronic Journal*, 1981, v. 4, 642. www.santilli-foundation.org/docs/generalized-uncertainties-1981.pdf
70. Santilli R. M. Isotopic lifting of Heisenberg’s uncertainties for gravitational singularities. *Communications in Theoretical Physics*, 1994, v. 3, 47–66. santilli-foundation.org/docs/santilli-511.pdf
71. Santilli R. M. Isorepresentation of the Lie-isotopic $SU(2)$ Algebra with Application to Nuclear Physics and Local Realism. *Acta Applicandae Mathematicae*, 1998, v. 50, 177–190. www.santilli-foundation.org/docs/Santilli-27.pdf
72. Santilli R. M. Studies on the classical determinism predicted by A. Einstein, B. Podolsky and N. Rosen. *Ratio Mathematica*, 2019, v. 37, 5–23. www.eprdebates.org/docs/epr-paper-ii.pdf
73. Myung H. C. and Santilli R. M. Modular-isotopic Hilbert space formulation of the exterior strong problem. *Hadronic Journal*, 1982, v. 5, 1277. www.santilli-foundation.org/docs/myung-santilli-1982.pdf
74. Liang S.-D., Lake M. J. and Harko T., Eds. Generalized uncertainty relations: Existing paradigms and new approaches. Special Issue of *Frontiers in Astronomy and Space Sciences*, 2023. www.frontiersin.org/research-topics/25805/generalized-uncertainty-relations-existing-paradigms-and-new-approaches
75. Li J.-L., and Qiao C.-F. The Generalized Uncertainty Principle. *Annalen der Physik*, 2021, v. 533, 2000335. ui.adsabs.harvard.edu/abs/2021AnP...53300335L/abstract
76. Herdegen A. and Ziobro P. Generalized uncertainty relations. *Letters in Mathematical Physics*, 2017, v. 107, 659–671. link.springer.com/article/10.1007/s11005-016-0916-9
77. Santilli R. M. Isotopic quantization of gravity and its universal isopoincaré symmetry, in the Proceedings of The Seventh Marcel Grossmann Meeting on Gravitation. SLAC, 1992, Jantzen R. T., Keiser G. M. and Ruffini R., Editors, *World Scientific Publishers*, p. 500–505, 1994. www.santilli-foundation.org/docs/Santilli-120.pdf
78. Santilli R. M. Unification of gravitation and electroweak interactions, in the Proceedings of the Eight Marcel Grossmann Meeting on Gravitation. Israel, 1997, Piran T. and Ruffini R. Editors, *World Scientific*, p. 473–475, 1999. www.santilli-foundation.org/docs/Santilli-137.pdf
79. Santilli, R. M. Reduction of Matter in the Universe to Protons and Electrons via the Lie-isotopic Branch of Hadronic Mechanics. *Progress in Physics*, 2023, v. 19, 73–99. www.progress-in-physics.com/2023/PP-65-09.PDF
80. Santilli R. M. Elements of nuclear physics according to hadronic mechanics. I: Apparent insufficiencies of quantum mechanics in nuclear physics. *Acta Mathematica*, 2024, v. 52, in press. www.santilli-foundation.org/docs/RM-santilli-paper-1.pdf
81. Santilli R. M. Elements of nuclear physics according to hadronic mechanics. II: Exact Lie-isotopic representation of Deuteron data. *Acta Mathematica*, 2024, v. 52, in press. www.santilli-foundation.org/docs/RM-santilli-paper-2.pdf
82. Santilli R. M. Elements of nuclear physics according to hadronic mechanics. III: Exact Lie-isotopic representation of nuclear stability. *Acta Mathematica*, 2024, v. 52, in press. www.santilli-foundation.org/docs/RM-santilli-paper-3.pdf

Partial Collisions of Unmater-Matter, Unmatter-Antimatter, and Unmatter1-Unmatter2 to Generate High Energy

Florentin Smarandache

Mathematics, Physics, and Natural Science Division, University of New Mexico, Gallup, NM 87301, USA
E-mail: smarand@unm.edu

In this paper we present the possibility of partial collisions between unmatter with matter, and unmatter with antimatter, and two or more different types of unmaters colliding between themselves to create high energy. In general, the collisions between unmatter with matter, or with antimatter, or with other type of unmatter, because being partial, they release less energy than the matter-unmatter collision which is a total collision. But the unmatter may be easier to produce in laboratory than antimatter.

1 Introduction

According to the CERN website [1], the universe is composed from 5% matter, 26.8% dark matter, and 68.2% dark energy.

The antimatter (also called dark matter) is composed from antiparticles.

The matter-antimatter asymmetry is enormous, contrary to the Big Bang Theory, which sustains that it should have been created equal amounts of matter and antimatter.

The unmatter-matter and unmatter-antimatter asymmetries should also be studied. At the Big Bang, if any, not only matter and antimatter would have been generated, but unmatter as well. Similarly, Unmatter Plasma [8, 9, 10] is a novel form of plasma, exclusively made of matter and its antimatter counterpart. It was first generated in the 2015 experiment.

The Big Bang Theory would have occurred 13.7 billion years ago, and the accelerated expansion of the universe would be due to dark matter — which contradicts the hypothesis of the initial explosion, according to which the universe should slow down. . .

The antimatter is considered a doppelganger of the matter. According to [2], “a gram of antimatter colliding with a gram of matter would produce as much energy as a nuclear bomb”.

2 Elementary Particles

The smallest units of matter (i.e., not made up by other smaller units of matter) are called elementary particles. A particle has: charge, mass, and angular momentum (spin).

The building blocks of matter, or most elementary particles known today are:

6 quarks and 6 leptons

with their corresponding antiparticles

6 antiquarks and 6 antileptons

(see Table 1 and Table 2 on top of the next Page).

The quarks are bonded together by *gluons*, and the study of strong interactions between quarks is called Quantum Chromodynamics (QCD).

In an atom, the electrons are leptons, while the protons, neutrons, and pions are made up of quarks.

A *baryon* is made up of an odd number of quarks (usually three); while a *meson* is made up of an even number of quarks (usually a quark and an antiquark, therefore such a meson is the most elementary form of unmatter, let us call it *unmatter-meson*.

A *pion* (or *pi-meson*) is an unstable subatomic particle of one of the following three forms: and each one is composed from a quark and an antiquark (as such, they are mesons, and therefore elementary forms of unmatter, let us call them *unmatter-pions*.

The *hadron* is a particle made up of two or more quarks that, through a strong interaction, are hold together.

Antimatter is matter composed of antiparticles.

While the *antiparticle*, as partner of a particle, is matter with reversed charge, parity, and time of its corresponding particle.

The *photon particle* is its own photon antiparticle, but this is an exception. All other particles have different corresponding antiparticles.

In collision, particle and antiparticle annihilate each other and produce gamma photons, neutrinos, and other particles.

3 Standard Model

According to the Standard Model, there are 17 distinct subatomic particles:

12 fermions and 5 bosons.

The fermion is a particle that only in combination with its antiparticle can be created or destroyed. Like the electron.

While the boson is a particle that can be created and destroyed in arbitrary numbers. Like photon.

Boson is in general a force carrier particle.

The fundamental forces that act in the nature are: gravity, electromagnetism, strong force, and weak force.

4 Defining Unmatter

In short, unmatter is formed by matter and antimatter that bind together and it was introduced by Smarandache in 2004 on the CERN website [4], and developed later [5–17].

Quarks	up (u)	down (d)	charm (c)	strange (s)	top (t)	bottom (b)
Antiquarks	up	down	charm	strange	top	bottom

Table 1: Quarks and antiquarks.

Leptons	charged	antielelectron	antimuon	antitau
Antileptons	neutrals	anti-electron-neutrino	anti-muon-neutrino	anti-tau-neutrino

Table 2: Leptons and antileptons.

The building blocks of matter and antimatter (most elementary particles known today) are 6 quarks and 6 leptons; their 12 antiparticles also exist.

Then *unmatter* will be formed by at least a building block and at least an antibuilding block which can bind together.

Let us start from neutrosophy [3], which is a generalization of dialectics, i.e., not only the opposites are combined but also the neutralities. Why? Because when an idea is launched, a category of people will accept it, others will reject it, and a third one will ignore it (don't care). But the dynamics between these three categories changes, so somebody accepting it might later reject or ignore it, or an ignorant will accept it or reject it, and so on. Similarly the dynamicity of <A>, <antiA>, <neutA>, where <neutA> means neither <A> nor <antiA>, but in between (neutral). Neutrosophy considers a kind not of di-alectics but tri-alectics (based on three components: <A>, <antiA>, <neutA>).

Hence unmatter is a kind of intermediary (not referring to the charge) between matter and antimatter, i.e. neither one, nor the other.

Neutrosophic Logic (NL) is a generalization of fuzzy logic (especially of intuitionistic fuzzy logic) in which a proposition has a degree of truth, a degree of falsity, and a degree of neutrality (neither true nor false); in the normalized NL the sum of these degrees is 1.

5 Unmatter Atom

It is possible to define the unmatter in a more general way, using the exotic atom. The exotic atom is an atom obtained after substituting one or more particles by other particles of the same charge (constituents).

The classical unmatter atoms were formed by particles like (a) electrons, protons, and antineutrons, or (b) antielectrons, antiprotons, and neutrons.

In a more general definition, an unmatter atom is a system of particles as above, or such that one or more particles are replaced by other particles of the same charge.

Other categories would be (c) a matter atom with where one or more (but not all) of the electrons and/or protons are replaced by antimatter particles of the same corresponding charges, and (d) an antimatter atom such that one or more (but not all) of the antielectrons and/or antiprotons are replaced by matter particles of the same corresponding charges.

In a more composed system we can substitute a particle by an unmatter particle and form an unmatter atom.

Of course, not all of these combinations are stable, semi-stable, or quasi-stable, especially when their time to bind together might be longer than their lifespan.

6 Unmatter Charge

The charge of unmatter may be positive as in the pentaquark Theta-plus, 0 (as in the atom of positronium), or negative as in anti-Rho meson, i.e. $u^{\bar{d}}$, (M. Jordan).

7 Containment

The unmatter could be store as the antimatter atom “by atomic traps (based on electric or magnetic dipoles) and by lasers (magneto-optical traps and optical tweezers)” [18].

8 Matter and Antimatter

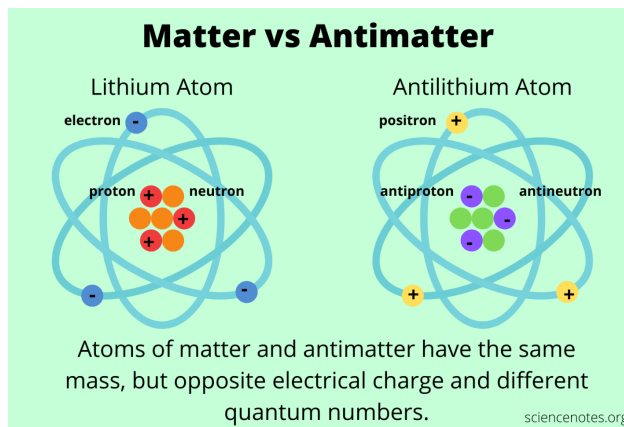


Fig. 1: Matter vs Antimatter. Courtesy of Anne Helmenstine, “What Is Antimatter? Definition and Examples” [18].

Lithium Atom:

- electron1 (-), electron2 (-), electron3 (-);
- proton1 (+), proton2 (+), proton3 (+);
- neutron1 (0), neutron2 (0), neutron3 (0), neutron4 (0).

Lithium Antiatom:

- positon1 (+), positon2 (+), positon3 (+);
- antiproton1 (-), antiproton2 (-), antiproton3 (-);
- antineutron1 (0), antineutron2 (0), antineutron3 (0), antineutron4 (0).

9 Proton and AntiProton

The Proton is made up of: up-quark, up-quark, down-quark; and AntiProton is made up of: anti-up-quark, anti-up-quark, anti-down-quark.

10 Real Examples of Unmatter

- (i) Meson, which in general is made up of: quark and anti-quark, and as particular cases of mesons one has:
Pion1 = anti-up-quark, down-quark;
Pion2 = up-quark, anti-down-quark. Pion2 is the Anti-Pion1.
- (ii) **Pentaquark**, which is made up of:
up-quark, up-quark, down-quark, down-quark, anti-strange-quark.

11 Partial Collisions of Unmatter-Unmatter

- (i) Pion1 vs. Pentaquark: anti-up-quark vs. up-quark (only), since between down-quark and down-quark there is no collision.
- (ii) Pion2 vs. Pentaquark: anti-down-quark vs. down-quark (only), since between up-quark and up-quark there is no collision.

12 Total Collision of Unmatter-Unmatter

Pion1 vs. Pion2: anti-up-quark vs. up-quark; and down-quark vs. anti-down-quark.

13 Partial Collisions of Unmatter-Matter

- (i) Pion1 vs. Proton: anti-up-quark vs. up-quark (only), since between down-quark and down-quark there is no collision.
- (ii) Pion2 vs. Proton: anti-down-quark vs. down-quark (only), since between up-quark and up-quark there is no collision.

14 Partial Collisions of Unmatter-Antimatter

- (i) Pion1 vs. Antiproton: down-quark vs. anti-down-quark (only), since between anti-up-quark and anti-up-quark there is no collision.
- (ii) Pion2 vs. Antiproton: up-quark vs. anti-up-quark (only), since between anti-down-quark and anti-down-quark there is no collision.

Submitted on May 5, 2024

References

1. ALPHA collaboration at CERN reports first measurements of certain quantum effects in antimatter. The measurements are consistent with predictions for “normal” matter and pave the way for future precision studies. 19 February 2020; <https://home.cern/news/news/physics/alpha-collaboration-cern-reports-first-measurements-certain-quantum-effects>
2. Levana Z. Ce mai face lumea de eclipsa (II): CERN si semnele Minunatei Lumi Noi, Active News, 07 aprilie 2024; <https://www.activenews.ro/opinii/Ce-mai-face-lumea-de-eclipsa-II-CERN-si-semnele-Minunatei-Lumi-Noi-188590>
3. Smarandache F. A unifying field in logics, neutrosophic logic. Neutrosophy, neutrosophic set, neutrosophic probability. Am. Res. Press, 1998; <https://fs.unm.edu/eBook-Neutrosophics6.pdf>
4. Smarandache F. Matter, antimatter, and unmatter. CDS-CERN, EXT-2005-142, 2004; *Bulletin of Pure and Applied Sciences*, 2004, v. 23D, no. 2, 173–177; <http://cdsweb.cern.ch/record/798551>
5. Goldfain E. and Smarandache F. On emergent physics, “unparticles” and exotic “unmatter” states. *Progress in Physics*, 2008, no. 4, 10–15.
6. Smarandache F. Verifying unmatter by experiments, more types of unmatter, and a quantum chromodynamics formula. *Progress in Physics*, 2005, no. 2, 113–116; *Infinite Energy*, 2006, v. 12, no. 67, 36–39.
7. Smarandache F., Rabounski D. Discovered “Angel Particle”, which is both matter and antimatter, as a new experimental proof of unmatter. 2017 APS Annual Meeting of the Far West Section, Merced, California, Nov. 3–4, 2017; <http://meetings.aps.org/Meeting/FWS17/Session/E1.16>
8. Smarandache F. Unmatter plasma revisited. 59th Annual Meeting of the APS Division of Plasma Physics, Milwaukee, Wisconsin, Oct. 23–27, 2017; <http://meetings.aps.org/Meeting/DPP17/Session/YP11.35>
9. Smarandache F., Ali M. Neutrosophic triplet as extension of matter plasma, unmatter plasma, and antimatter plasma. 69th Annual Gaseous Electronics Conference, Bochum, Germany, v. 61, no. 9, Oct. 10–14, 2016; <http://meetings.aps.org/Meeting/GEC16/Session/HT6.111>
10. Smarandache F. Unmatter plasma. 57th Annual Meeting of the APS Division of Plasma Physics, Savannah, Georgia, Nov. 16–20, 2015; <http://meetings.aps.org/Meeting/DPP15/Session/UP12.46>
11. Smarandache F. Unmatter as a consequence of the law of included multiple-middles. Annual Meeting of the APS Four Corners Section, Tempe, Arizona, Oct. 16–17, 2015; <http://meetings.aps.org/Meeting/4CF15/Session/F1.66>
12. Smarandache F. Unparticle, a special case of unmatter. 53rd Annual Meeting of the APS Division of Plasma Physics, Salt Lake City, Utah, Nov. 14–18, 2011; <http://meetings.aps.org/Meeting/DPP11/Event/153509>
13. Rabounski D., Smarandache F. The Brightsen nucleon cluster model predicts unmatter entities inside nuclei. 2008 Annual Meeting of the Division of Nuclear Physics, Oakland, California, Oct. 23–26, 2008; <http://meetings.aps.org/Meeting/DNP08/Event/87738>
14. Goldfain E., Smarandache F. On emergent physics, unparticles and exotic unmatter states. 2009 Joint Spring Meeting of the New England Section of APS and AAPT, Boston, Massachusetts, May 8–9, 2009; <http://meetings.aps.org/link/BAPS.2009.NES.APSP.2>
15. Smarandache F. Verifying unmatter by experiments, more types of unmatter, and a quantum chromodynamics formula. 62nd Annual Gaseous Electronics Conference, Saratoga Springs, New York, Oct. 20–23, 2009; <http://meetings.aps.org/link/BAPS.2009.GEC.KTP.110>
16. Smarandache F. A new form of matter — Unmatter, composed of particles and anti-particles. 40th Annual Meeting of the APS Division of Atomic, Molecular and Optical Physics, Charlottesville, Virginia, May 19–23, 2009; <http://meetings.aps.org/link/BAPS.2009.DAMOP.E1.97>
17. Smarandache F. Unparticle, a special case of unmatter. 53rd Annual Meeting of the APS Division of Plasma Physics, Salt Lake City, Utah, Nov. 14–18, 2011; <http://meetings.aps.org/Meeting/DPP11/Session/Index3/?SessionEventID=158034>
18. Helmenstine A. What Is Antimatter? Definition and Examples. <https://sciencenotes.org/what-is-antimatter-definition-and-examples>

The Vacuum Stress-Energy Tensor in General Relativity

Patrick Marquet

Calais, France. E-mail: patrick.marquet6@wanadoo.fr

In General Relativity, the Einstein field equations with a massive term source are plagued with the non conservation of this energy-momentum tensor. To remedy this problem, a pseudo-tensor of the gravitational field is classically added so that the global right hand side is conserved. Using Cartan's calculus, we derive here the differential form of the Einstein field equations which provides the Landau-Lifshitz symmetric (pseudo) 3-form of the gravitational field. Assuming a slightly variable cosmological term, we then infer a vacuum energy-momentum (real) 3-form so that the global r.h.s. of the field equations eventually exhibits a full real 3-form that satisfies the conserved property. In the early phase of the universe's expansion it is suggested that the cosmological term was huge and constant, before becoming variable to yield the estimated value predicted to-day.

Notations

Space-time Greek indices α, β, \dots are 0, 1, 2, 3 for local coordinates.
Space-time Latin indices a, b, \dots are 0, 1, 2, 3 for a general basis.
The space-time signature is -2 .
Einstein's constant is denoted by \varkappa .
The velocity of light is $c = 1$.

1 Differential calculus

1.1 The classical field equations in GR (short overview)

In General Relativity (GR), any line element on the 4-pseudo-Riemannian manifold (M, \mathbf{g}) is given by $ds^2 = g_{ab} dx^a dx^b$. By varying the action $\mathcal{S} = \mathcal{L}_E d^4x$ with respect to the g_{ab} where the lagrangian density is given by

$$\mathcal{L}_E = g^{ab} \sqrt{-g} \left[\{^e_{ab}\} \{^d_{de}\} - \{^d_{ae}\} \{^e_{bd}\} \right] \quad (1)$$

one infers the symmetric Einstein tensor

$$G_{ab} = R_{ab} - \frac{1}{2} g_{ab} R, \quad (2)$$

where

$$R_{bc} = \partial_a \{^a_{bc}\} - \partial_c \{^a_{ba}\} + \{^d_{bc}\} \{^a_{da}\} - \{^d_{ba}\} \{^a_{dc}\} \quad (3)$$

is the (symmetric) Ricci tensor whose contraction gives the curvature scalar R . (Here $\{^e_{ab}\}$ denote the Christoffel symbols of the second kind.)

The source free field equations are

$$G_{ab} = R_{ab} - \frac{1}{2} g_{ab} R + \Lambda g_{ab} = 0, \quad (4)$$

where Λ is the Einstein cosmological constant.

The second rank tensor G_{ab} is symmetric and is only function of the metric tensor components g_{ab} and their first and second order derivatives. Due to Bianchi's identities the Einstein tensor is conceptually conserved

$$\nabla_a G^a_b = 0, \quad (5)$$

where ∇_a is the Riemann covariant derivative.

When a massive source is present, the field equations become

$$G_{ab} = R_{ab} - \frac{1}{2} g_{ab} (R - 2\Lambda) = \varkappa T_{ab}. \quad (6)$$

If ρ is the matter density, then T_{ab} is here the tensor describing a pressure free fluid

$$T_{ab} = \rho u_a u_b. \quad (7)$$

1.2 The Cartan structure equations

Let us now consider a 4-manifold M referred to a vector basis e_α . The dual basis θ^β of one-forms (pfaffian forms) are related to the local coordinates x^α by

$$\theta^\beta = a^\beta_a dx^a. \quad (8)$$

These are called *vierbein* or *tetrad fields* [1].

In a dual basis θ^a , to any parallel transported vector along a closed path, can be then associated the following 2-forms:

— A *rotation curvature form*

$$\Omega^\alpha_\beta = \frac{1}{2} R^\alpha_{\beta\gamma\delta} \theta^\gamma \wedge \theta^\delta; \quad (9)$$

— A *torsion form*

$$\Omega^\alpha = \frac{1}{2} T^\alpha_{\gamma\delta} \theta^\gamma \wedge \theta^\delta. \quad (10)$$

Introducing the Cartan procedure one first defines the connection forms

$$\Gamma^\alpha_\beta = \{^\alpha_{\gamma\beta}\} \theta^\gamma. \quad (11)$$

The first Cartan structure equation is related to the torsion by [2, p.40]

$$\Omega^\alpha = \frac{1}{2} T^\alpha_{\gamma\delta} \theta^\gamma \wedge \theta^\delta = d\theta^\alpha + \Gamma^\alpha_\gamma \wedge \theta^\gamma. \quad (12)$$

The second Cartan structure equation is defined as follows [2, p.42] so that

$$\Omega_\beta^\alpha = \frac{1}{2} R_{\beta\gamma\delta}^\alpha \theta^\gamma \wedge \theta^\delta = d\Gamma_\beta^\alpha + \Gamma_\gamma^\alpha \wedge \Gamma_\beta^\gamma, \quad (13)$$

where $R_{\beta\gamma\delta}^\alpha$ are the components of the curvature tensor in the most general sense.

Within the Riemannian framework alone (torsion free), $R_{\beta\gamma\delta}^\alpha$ reduce to the Riemann curvature tensor components and the first structure equation (12) becomes:

$$d\theta^\alpha = -\Gamma_\gamma^\alpha \wedge \theta^\gamma. \quad (14)$$

2 Differential equations of General Relativity

2.1 The Einstein field equations

We first recall the Hodge star operator definition for an oriented 4-dimensional pseudo-Riemannian manifold (M, \mathbf{g}) with volume element determined by \mathbf{g}

$$\boldsymbol{\eta} = \sqrt{-g} \theta^0 \wedge \theta^1 \wedge \theta^2 \wedge \theta^3. \quad (15)$$

Let $\Lambda_k(\mathbf{E})$ be the subspace of completely antisymmetric multilinear forms on the real vector space \mathbf{E} .

The Hodge star operator $*$ is a linear isomorphism, i.e., $L_k(M) \rightarrow L_{n-k}(M)$ (where $k \leq n$).

If $\theta^0, \theta^1, \theta^2, \theta^3$ is an oriented basis of 1-forms, then this operator is defined by

$$\begin{aligned} *(\theta^{i1} \wedge \theta^{i2} \wedge \theta^{ik}) &= \\ &= \frac{\sqrt{-g}}{(n-k)!} \varepsilon_{j1\dots jn} g^{j1i1} \dots g^{jkik} \theta^{jk+1} \wedge \dots \wedge \theta^{jn}. \end{aligned} \quad (16)$$

With this preparation, the Einstein action simply reads

$$*R = R\boldsymbol{\eta}. \quad (17)$$

Varying this action with respect to $\delta\theta^\beta$ of the orthonormal tetrad fields, eventually leads to the field equations under the differential form

$$-\frac{1}{2} \eta_{\beta\gamma\delta} \wedge \Omega^{\gamma\delta} = \varkappa *T_\beta, \quad (18)$$

where T_α is related to the energy-momentum tensor $T_{\alpha\beta}$ by $T_\alpha = T_{\alpha\beta} \theta^\beta$ and include all other contributions.

In the same manner, one has for the Einstein tensor $G_\alpha = G_{\alpha\beta} \theta^\beta$. For all detailed derivations refer to [3].

2.2 The energy-momentum tensor

In the field equations (18), we insert $\eta^{\alpha\beta\gamma} = \eta^{\alpha\beta\gamma\delta} \theta_\delta$. Then, we use the second structure equation under the following form

$$\Omega_{\beta\gamma} = d\Gamma_{\beta\gamma} - \Gamma_{\mu\beta} \wedge \Gamma_\gamma^\mu, \quad (19)$$

$$-\frac{1}{2} \eta^{\alpha\beta\gamma\delta} \theta_\delta \wedge (d\Gamma_{\beta\gamma} - \Gamma_{\mu\beta} \wedge \Gamma_\gamma^\mu) = \varkappa *T_\alpha, \quad (20)$$

leading to

$$-\frac{1}{2} \eta^{\alpha\beta\gamma\delta} d(\Gamma_{\beta\gamma} \wedge \theta_\delta) = \varkappa (*T_\alpha + *t_\alpha), \quad (21)$$

where [4]

$$*t^\alpha = -\frac{1}{2\varkappa} \eta^{\alpha\beta\gamma\delta} (\Gamma_{\mu\beta} \wedge \Gamma_\gamma^\mu \wedge \theta_\delta - \Gamma_{\beta\gamma} \wedge \Gamma_{\mu\delta} \wedge \eta^\mu). \quad (22)$$

We see that $*t^\alpha$ is unaffected by the exterior product terms in the bracket, therefore $t_{\alpha\beta}$ is symmetric.

In that case, we identify $*t^\alpha$ with the Landau-Lifshitz 3-form $*t_{L-L}^\alpha$ which yields the corresponding pseudo-tensor $t_{L-L}^{\alpha\beta}$ [5, eq.101.7]

$$\begin{aligned} (-g) t_{L-L}^{\alpha\nu} &= \frac{1}{2\varkappa} \left\{ \#g_{,\lambda}^{\alpha\nu} \#g_{,\mu}^{\lambda\mu} - \#g_{,\lambda}^{\alpha\lambda} \#g_{,\mu}^{\nu\mu} + \right. \\ &+ \frac{1}{2} g^{\alpha\nu} g_{\lambda\mu} \#g_{,\rho}^{\lambda\theta} \#g_{,\theta}^{\rho\mu} - (g^{\alpha\lambda} g_{\mu\theta} \#g_{,\rho}^{\nu\theta} \#g_{,\lambda}^{\mu\rho} \\ &+ g^{\nu\lambda} g_{\mu\theta} \#g_{,\rho}^{\alpha\theta} \#g_{,\lambda}^{\mu\rho}) + g_{\mu\lambda} g^{\theta\rho} \#g_{,\theta}^{\alpha\lambda} \#g_{,\rho}^{\nu\mu} \\ &\left. + \frac{1}{8} (2g^{\alpha\lambda} g^{\nu\mu} - g^{\alpha\nu} g^{\lambda\mu}) (2g_{\theta\rho} g_{\delta\tau} - g_{\rho\delta} g_{\theta\tau}) \#g_{,\lambda}^{\theta\tau} \#g_{,\mu}^{\rho\delta} \right\}, \end{aligned} \quad (23)$$

where

$$\#g^{\alpha\nu} = \sqrt{-g} g^{\alpha\nu}. \quad (24)$$

3 The vacuum energy

3.1 The gravitational field tensor

In General Relativity, it is well known, that the Einstein tensor $G_{\alpha\beta}$ is intrinsically conserved, while the massive tensor $T_{\alpha\beta}$ is not. This is because the gravitational field is not included in $T_{\alpha\beta}$. If so, then one obtains the conservation law

$$\partial_\beta \sqrt{-g} (T^{\alpha\beta} + t^{\alpha\beta}) = 0. \quad (25)$$

The tensor $t_{\alpha\beta}$ describes the gravitational field, derived from the Einstein-Dirac pseudo-tensor density [6, p.61]

$$\sqrt{-g} t_a^\beta = \frac{1}{2\varkappa} \left\{ \frac{(\partial_\alpha \#g^{\sigma\tau}) \partial \mathcal{L}_E}{\partial (\partial_\beta \#g^{\sigma\tau})} - \delta_\alpha^\beta \mathcal{L}_E \right\}. \quad (26)$$

However, the Einstein field equations are yet unbalanced since they do not exhibit a full real tensor as a source.

To remedy this problem, we showed that a slightly variable cosmological term Λ -term induces a stress energy tensor of vacuum which restores a true gravitational tensor on the r.h.s. of the equation (6) as it should be [7, 8].

This real vacuum tensor was given by

$$(t_{\alpha\beta})_{\text{vac}} = -\frac{1}{2\kappa} \Lambda g_{\alpha\beta}, \quad (27)$$

where the term Λ was found to be [9]

$$\Lambda = \nabla_{\alpha} K^{\alpha} = \theta^2, \quad (28)$$

where K^{α} is a 4-vector, and

$$\theta = X^{\alpha}_{;\alpha} \quad (29)$$

is the space-time volume scalar expansion characterizing the vacuum stress-energy tensor $(t_{\alpha\beta})_{\text{vac}}$. X^{α} is a congruence of non-intersecting unit time lines: $X^{\alpha} X_{\alpha} = 1$

$$X^{\alpha}_{;\alpha} = h^{\alpha\beta} \theta_{\alpha\beta}, \quad (30)$$

where $\theta_{\alpha\beta}$ stands for the expansion tensor, and $h_{\alpha\beta} = g_{\alpha\beta} - X_{\alpha} X_{\beta}$ is the projection tensor. Due to the form of (28), the lagrangian (1) differs only from a divergence and varying its action generates the same Einstein equations.

The real tensor $t^{\alpha\beta}_{\text{vac}}$ corresponding to the vacuum stress energy tensor can be added to $t^{\alpha\beta}$ without affecting the Einstein tensor inferred from the variational principle. So the final (real) gravitational tensor density is given by

$$\sqrt{-g} (t^{\beta}_{\alpha})_{\text{G}} = \frac{1}{2\kappa} \left\{ \left(\partial_{\alpha}^{\#} g^{\sigma\tau} \right) \frac{\partial \mathcal{L}_{\text{E}}}{\partial (\partial_{\beta}^{\#} g^{\sigma\tau})} - \delta_{\alpha}^{\beta} (\mathcal{L}_{\text{E}} - \sqrt{-g} \Lambda) \right\}. \quad (31)$$

The real tensor $(t^{\beta}_{\alpha})_{\text{G}}$ is afterwards conveniently symmetrized through the Belinfante procedure [10].

With this definition the field equations can be finally written

$$R^{\alpha\beta} - \frac{1}{2} g^{\alpha\beta} R = \kappa (T^{\alpha\beta} + t^{\alpha\beta}_{\text{G}}). \quad (32)$$

Sufficiently far from this matter we always have

$$R^{\alpha\beta} - \frac{1}{2} g^{\alpha\beta} R = \kappa t^{\alpha\beta}_{\text{vac}}. \quad (33)$$

Inspection shows that each energy-momentum tensor is conserved.

3.2 The vacuum stress-energy 3-form

Here we adopt the Landau-Lifshitz symmetric pseudo-3-form $*t^{\alpha}_{\text{L-L}}$ instead of the Einstein-Dirac pseudo-density. We then determine a vacuum energy 3-form designed to render the r.h.s. of (21) fully real according to the previous derivation.

To this end, we first regard the variable cosmological term Λ as inducing a given space-time curvature. This is legitimized by the fact that the real tensor $(t_{\alpha\beta})_{\text{vac}}$ is *a priori* persistent throughout the vacuum.

Since Λ is a scalar, let us then set the resulting curvature 2-form as

$$\Omega = \frac{1}{2} R^{\delta}_{\sigma\delta\tau} \theta^{\sigma} \wedge \theta^{\tau}. \quad (34)$$

By analogy with the classical formalism (4) we then apply the quantity $g^{\gamma\delta} \Omega$ to the field equations (18) as follows

$$\left. \begin{aligned} -\frac{1}{2} \eta_{\alpha\mu\nu} \wedge (\Omega^{\mu\nu} + g^{\mu\nu} \Omega) &= \kappa *T_{\alpha} \\ -\frac{1}{2} \eta^{\mu}_{\alpha\nu} \wedge (\Omega^{\nu}_{\mu} + \delta^{\nu}_{\mu} \Omega) &= \kappa *T_{\alpha} \end{aligned} \right\}. \quad (35)$$

Using $\Omega^{\nu}_{\mu} = \frac{1}{2} R^{\nu}_{\beta\gamma\delta} \theta^{\gamma} \wedge \theta^{\delta}$, these equations can be written in the form

$$-\frac{1}{4} \eta^{\mu}_{\alpha\nu} \wedge \theta^{\sigma} \wedge \theta^{\tau} (R^{\nu}_{\mu\sigma\tau} + \delta^{\nu}_{\mu} R^{\delta}_{\sigma\delta\tau}) = \kappa T_{\alpha\beta} \eta^{\beta}. \quad (36)$$

To $R^{\nu}_{\mu\sigma\tau}$ is now added a new 4th rank curvature tensor which is noted

$$2\Lambda^{\nu}_{\mu\sigma\tau} = -\delta^{\nu}_{\mu} R^{\delta}_{\sigma\delta\tau}. \quad (37)$$

To make it apparent, we first use the following relations

$$\eta^{\alpha} \equiv * \theta^{\alpha} \quad (38)$$

$$\eta_{\alpha} = \frac{1}{3!} (\eta_{\alpha\beta\gamma\delta} \theta^{\beta} \wedge \theta^{\gamma} \wedge \theta^{\delta}) = \frac{1}{3!} \theta^{\beta} \wedge \eta_{\alpha\beta}. \quad (39)$$

Then, we apply the following identities

$$\theta^{\beta} \wedge \eta_{\alpha} = \delta_{\alpha}^{\beta} \eta,$$

$$\theta^{\gamma} \wedge \eta_{\alpha\beta} = \delta_{\beta}^{\gamma} \eta_{\alpha} - \delta_{\alpha}^{\gamma} \eta_{\beta},$$

$$\theta^{\delta} \wedge \eta_{\alpha\beta\gamma} = \delta_{\gamma}^{\delta} \eta_{\alpha\beta} + \delta_{\beta}^{\delta} \eta_{\gamma\alpha} + \delta_{\alpha}^{\delta} \eta_{\beta\gamma},$$

$$\theta^{\varepsilon} \wedge \eta_{\alpha\beta\gamma\delta} = \delta_{\delta}^{\varepsilon} \eta_{\alpha\beta\gamma} - \delta_{\gamma}^{\varepsilon} \eta_{\delta\alpha\beta} + \delta_{\beta}^{\varepsilon} \eta_{\gamma\delta\alpha} - \delta_{\alpha}^{\varepsilon} \eta_{\beta\gamma\delta}.$$

With this preparation, (36) reads

$$\begin{aligned} & -\frac{1}{4} (R^{\mu\nu}_{\sigma\tau} - 2\Lambda^{\mu\nu}_{\sigma\tau}) [\delta^{\tau}_{\nu} (\delta^{\sigma}_{\mu} \eta_{\alpha} - \delta^{\sigma}_{\nu} \eta_{\mu}) + \\ & + \delta^{\tau}_{\mu} (\delta^{\sigma}_{\alpha} \eta_{\nu} - \delta^{\sigma}_{\nu} \eta_{\alpha}) + \delta^{\tau}_{\alpha} (\delta^{\sigma}_{\nu} \eta_{\mu} - \delta^{\sigma}_{\mu} \eta_{\nu})] = \\ & = -\frac{1}{2} (R^{\mu\nu}_{\mu\nu} - 2\Lambda^{\mu\nu}_{\mu\nu}) \eta_{\alpha} + (R^{\mu\nu}_{\alpha\nu} - 2\Lambda^{\mu\nu}_{\alpha\nu}) \eta_{\nu} = \\ & = (R^{\beta\nu}_{\alpha\nu} - 2\Lambda^{\beta\nu}_{\alpha\nu}) \eta_{\beta} - \frac{1}{2} \delta_{\alpha}^{\beta} (R^{\mu\nu}_{\mu\nu} - 2\Lambda^{\mu\nu}_{\mu\nu}) \eta_{\beta}. \end{aligned} \quad (40)$$

As a contributing curvature tensor, $2\Lambda^{\beta\nu}_{\alpha\nu}$ must be included in $R^{\beta\nu}_{\alpha\nu}$ so that we eventually retrieve the classical field equations with a cosmological term

$$\left(R^{\beta}_{\alpha} - \frac{1}{2} \delta_{\alpha}^{\beta} R + \delta_{\alpha}^{\beta} \Lambda \right) \eta_{\beta} = \kappa T^{\beta}_{\alpha} \eta_{\beta}. \quad (41)$$

Taking account of $\Omega_{\beta\gamma} = d\Gamma_{\beta\gamma} - \Gamma_{\mu\beta} \wedge \Gamma^{\mu}_{\gamma}$, we revert to the field equations (22) which are also expressed as

$$-\frac{1}{2} \eta^{\alpha\beta\gamma\delta} \theta_{\delta} \wedge (d\Gamma_{\beta\gamma} - \Gamma_{\mu\beta} \wedge \Gamma^{\mu}_{\gamma}) = \kappa *T^{\alpha}. \quad (42)$$

Adding the extra-curvature yields

$$-\frac{1}{2} \eta^{\alpha\beta\gamma\delta} \theta_{\delta} \wedge [(d\Gamma_{\beta\gamma} - \Gamma_{\mu\beta} \wedge \Gamma^{\mu}_{\gamma}) + g_{\beta\gamma} \Omega] = \kappa *T^{\alpha}. \quad (43)$$

that is according to (21)

$$-\frac{1}{2} \eta^{\alpha\beta\gamma\delta} \left[d(\Gamma_{\beta\gamma} \wedge \theta_\delta) + \theta_\delta \wedge g_{\beta\gamma} \Omega \right] = \kappa \left({}^*T^\alpha + {}^*t_{L-L}^\alpha \right). \quad (44)$$

Therefore

$$\begin{aligned} -\frac{1}{2} \eta^{\alpha\beta\gamma\delta} d(\Gamma_{\beta\gamma} \wedge \theta_\delta) &= \\ &= \kappa \left[{}^*T^\alpha + {}^*t_{L-L}^\alpha + \frac{1}{2\kappa} \eta^{\alpha\beta\gamma\delta} (\theta_\delta \wedge g_{\beta\gamma} \Omega) \right], \\ -\frac{1}{2} \eta^{\alpha\beta\gamma\delta} \delta(\Gamma_{\beta\gamma} \wedge \theta_\delta) &= \\ &= \kappa \left[{}^*T^\alpha + {}^*t_{L-L}^\alpha - \frac{1}{4\kappa} \eta^{\alpha\beta\gamma\delta} (\theta_\delta \wedge g_{\beta\gamma} R_{\lambda\sigma\tau}^\lambda \theta^\sigma \wedge \theta^\tau) \right]. \end{aligned}$$

In the expression $-\frac{1}{4\kappa} \eta^{\alpha\beta\gamma\delta} \theta_\delta \wedge g_{\beta\gamma} R_{\lambda\sigma\tau}^\lambda \theta^\sigma \wedge \theta^\tau$, we make the substitution

$$-g_{\beta\gamma} R_{\lambda\sigma\tau}^\lambda = 2\Lambda_{\beta\gamma\sigma\tau}. \quad (45)$$

We eventually find the *vacuum stress-energy momentum 3-form*

$${}^*t_{\text{vac}}^\alpha = \frac{1}{2\kappa} \eta^{\alpha\beta\gamma\delta} \theta_\delta \wedge \Lambda_{\beta\gamma\sigma\tau} \theta^\sigma \wedge \theta^\tau. \quad (46)$$

Therefore the global gravitational field is described by the (real) 3-form

$${}^*t_G^\alpha = -\frac{1}{2\kappa} \eta^{\alpha\beta\gamma\delta} \left[(\Gamma_{\mu\beta} \wedge \Gamma_\gamma^\mu \wedge \theta_\delta - \Gamma_{\beta\gamma} \wedge \Gamma_{\mu\delta} \wedge \theta^\mu) - \theta_\delta \wedge \Lambda_{\beta\gamma\sigma\tau} \theta^\sigma \wedge \theta^\tau \right]. \quad (47)$$

3.3 The complete Einstein equations

The field equations are

$$-\frac{1}{2} \eta^{\alpha\beta\gamma\delta} d(\Gamma_{\beta\gamma} \wedge \theta_\delta) = \kappa ({}^*T^\alpha + {}^*t_G^\alpha). \quad (48)$$

As per (33) far from matter, we always have

$$-\frac{1}{2} \eta^{\alpha\beta\gamma\delta} d(\Gamma_{\beta\gamma} \wedge \theta_\delta) = \kappa {}^*t_{\text{vac}}^\alpha. \quad (49)$$

Now, let us multiply equation (48) with $\sqrt{-g}$, then taking into account $\eta_{\alpha\beta\gamma\delta} = -\frac{1}{2\sqrt{-g}} \varepsilon_{\alpha\beta\gamma\delta}$, we find a new form for the field equations

$$-d(\sqrt{-g} \eta^{\alpha\beta\gamma\delta} \Gamma_{\beta\gamma} \wedge \theta_\delta) = 2\kappa \sqrt{-g} ({}^*T^\alpha + {}^*t_G^\alpha) \quad (50)$$

or

$$-d(\sqrt{-g} \Gamma^{\beta\gamma} \wedge \eta_{\beta\gamma}^\alpha) = 2\kappa \sqrt{-g} ({}^*T^\alpha + {}^*t_G^\alpha). \quad (51)$$

From these equations follows immediately the differential conservation law

$$d[\sqrt{-g} ({}^*T^\alpha + {}^*t_G^\alpha)] = 0. \quad (52)$$

If we integrate equation (51) over a 3-dimensional space-like region D_3 , then we obtain

$$P^\alpha = -\frac{1}{2\kappa} \int \sqrt{-g} \Gamma^{\beta\gamma} \wedge \eta_{\beta\gamma}^\alpha, \quad (53)$$

which is the total 4-momentum of the isolated system. Inspection shows that P^α is gauge invariant in the following sense

$$\theta(x) \rightarrow A(x) \theta(x), \quad (54)$$

$$\Gamma(x) \rightarrow A(x) \Gamma(x) A^{-1}(x) - dA(x) A^{-1}(x), \quad (55)$$

where $A(x)$ is a local transformation matrix (A_β^α).

General Relativity is invariant with respect to such transformations and is thus a non-abelian gauge theory.

3.4 The early cosmological expansion evolution

The singularity of our universe is generally set at 10^{-43} seconds corresponding to the Planck era.

At this epoch, the size of our universe is predicted to be 10^{-35} meters with an energy of 10^{19} GeV and a temperature amounting to 10^{32} K. We postulate that the cosmological term was present and constant in the early stage of the singularity possessing a huge value. As time was the very first parameter to appear, the cosmological constant Λ would be associated to a large ‘‘pre’’ 3-form time component ${}^*t_{\text{vac}}^0$ with no further explicit structure. At 10^{-35} seconds, strong force and electro-weak force decoupled and at 10^{-12} seconds, the electro-weak force splits into weak and electromagnetic forces. Over this period of time, the cosmological term drastically decreases and becomes slightly variable. These processes cause the Universe’s expansion to accelerate and ${}^*t_{\text{vac}}^0$ would deploy according to equation (46)

$${}^*t_{\text{vac}}^\alpha = \frac{1}{2\kappa} \eta^{\alpha\beta\gamma\delta} \theta_\delta \wedge \Lambda_{\beta\gamma\sigma\tau} \theta^\sigma \wedge \theta^\tau. \quad (56)$$

Such a hypothesis would lend support to the inflation scenario recently suggested by the astronomer Claude Poher. His theory is based on the detection of massless particles moving at the speed of light which are assumed to propagate throughout the entire vacuum [11, 12]. According to Poher, these particles act as a gravitational isotropic flux and each one bears an individual energy measured at $\text{Eu} = 8.5 \times 10^{-21}$ Joules [13–15]. Without invoking a quantum aspect, the corpuscular nature of this flux might well appear as a piecewise structure of the vacuum field we have inferred in the above.

Conclusion

If one relaxes our demand on the cosmological term constancy, it is possible to define a real homogeneous vacuum stress-energy tensor which is by essence a pervasive field. In our picture, the gravitational field of a matter appears as an excited state of this field. Far from its matter source, the gravitational field pseudo-tensor asymptotically decreases down

to the level of the vacuum energy-momentum tensor leaving the field equations with a non-zero right hand side. In here, we have shown that starting with the Landau-Lifshitz 3-form, it is also possible to infer a real 3-form representing the vacuum energy-momentum to restore a real r.h.s. of the field equations. The vacuum energy field hypothesis is rewarding in terms of several physical advantages:

- The ill-defined gravitational pseudo-tensor remains here a true tensor restoring the consistency in the field equations with a massive source;
- The inferred global energy-momentum tensor always satisfies the conservation law as well as the vacuum tensor alone;
- Because of the nature of this vacuum tensor there is no need to introducing any other arbitrary ingredients or modification of the general theory of relativity. Despite its smallness, a cosmological term seems to be badly needed to ascertain some major astrophysical observations which are all related to the FLRW expanding model of universe.

The Lambda-CDM model, which uses the FLRW metric, currently measures the cosmological constant to be on the order of 10^{-52} m^{-2} . However, there is no reason “à priori” to consider this term as a constant everywhere which would constitute a strong physical evidence for the vacuum field to exist in General Relativity.

Submitted on May 31, 2024

References

1. Marquet P. Lichnerowicz’ theory of spinors in General Relativity. The Zelmanov approach. *The Abraham Zelmanov Journal*, 2012, v. 5, 117–133.
2. Kramer D., Stephani H., Hertl E., MacCallum M. Exact Solutions of Einstein’s Field Equations. Cambridge University Press, 1979.
3. Marquet P. Twin universes: a new approach confirmed by General Relativity. *Progress in Physics*, 2019, v. 15, no. 2, 64–67.
4. Marquet P. Twin universes confirmed by General Relativity. *Progress in Physics*, 2022, v. 18, no.1, 89–94.
5. Landau L., Lifshitz E. The Classical Theory of Fields. Addison-Wesley, Reading, 1962.
6. Dirac P.A.M. General Theory of Relativity. Princeton University Press, 2nd edition, 1975.
7. Marquet P. The gravitational field: a new approach. *Progress in Physics*, 2013, v.9, no.3, 62–66.
8. Marquet P. Vacuum background field in General Relativity. *Progress in Physics*, 2016, v. 12, no. 4, 314–316.
9. Marquet P. Some Insights on the Nature of the Vacuum Background Field in General Relativity. *Progress in Physics*, 2016, v. 12, no. 4, 366–367.
10. Rosenfeld L. Sur le tenseur d’impulsion-énergie. *Acad. Roy. de Belgique (Mémoires de la Classe des Sciences)*, 1940, t. 18, 1–30.
11. Poher C. European Patent Publication WO 2007/093 699 A2, PCT FR 2007/000249 (February 14, 2006); <https://www.epo.org/searching-for-patents.html>
12. Poher C., Poher D. Physical phenomena observed during strong electric discharges into layered Y123 superconducting devices at 77K. *Applied Physics Research*, 2011, v. 3, no. 2, 51–66.
13. Poher C., Modanese G. Enhanced induction into distant coils by YBCO and silicon-graphite electrodes under large current pulses. *Physics Essays*, 2017, v. 30, no. 4, 435–441.
14. Poher C., Poher D. Gravity and matter quantum behavior from accelerations during electric discharges into graphite-based super conductor. *Applied Physics Research*, 2020, v. 12, no. 3, 48–79.
15. Poher C., Poher D. Quantum model of inertia-predictions-confirmations, consequences for gravitation into galaxies and CDM cosmology models. *Applied Physics Research*, 2020, v. 12, no. 4, 8–62.

Gödel Time Travel: New Highlights

Patrick Marquet

Calais, France. E-mail: patrick.marquet6@wanadoo.fr

The history of fascinating idea of time travel can be traced back to Kurt Gödel who found a solution of Einstein’s field equations that contains closed time-like curves (CTCs). Those make it theoretically feasible to go on journey into one’s own past. In what follows, we establish a realistic way to provide the required conditions to achieve this time displacement. After having given Gödel’s model a physical meaning, we assign an object to move along a closed time-like curve using the warp drive technique. Provided the object bears circulating charges interacting with a surrounding electromagnetic field, it is possible to extract a negative energy necessary to sustain the warp drive without resorting to the hypothetical “exotic matter”. In addition, this field/charge interaction has the virtue to drastically reduce the amount of required negative energy. Lastly, the entropy of the system is shown to be negative during the time journey into the past.

Notations

Space-time indices are: $\mu, \nu = 0, 1, 2, 3$.

Spatial indices are: $a, b = 1, 2, 3$.

The space signature is -2 (unless otherwise specified).

Newton’s constant is G .

1 The generalized Gödel metric

The classical Gödel line element is generically given by the interval [1]

$$ds^2 = a^2 \left(dx_0^2 - dx_1^2 + dx_2^2 \frac{1}{2} e^{2x_1} - dx_3^2 + 2 e^{x_1} dx_0 dx_2 \right), \quad (1)$$

or equivalently

$$ds^2 = a^2 \left[-dx_1^2 - dx_3^2 - dx_2^2 \frac{1}{2} e^{2x_1} + (e^{x_1} dx_2 + dx_0)^2 \right] \quad (2)$$

expliciting x_0

$$ds^2 = a^2 \left[c^2 dt^2 + \frac{1}{2} e^{2x} dy^2 - 2 e^x c dt dy - dx^2 - dz^2 \right], \quad (2bis)$$

where $a > 0$.

In the cylindrical coordinates (t, r, ϕ) with the transformations

$$e^x = \cosh 2r + \cosh \phi \sinh 2r,$$

$$ye^x = \sqrt{2} \sinh \phi \sinh 2r,$$

$$\tan \frac{1}{2} \left[\phi + \left(ct - \frac{2t'}{2\sqrt{2}} \right) \right] = e^{-2r} \tan \frac{\phi}{2},$$

the metric reads

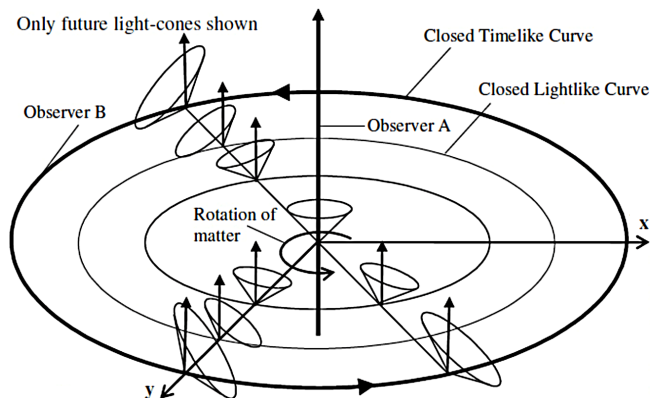
$$ds^2 = 4a^2 \left[(dt')^2 - dr^2 + (\sinh^4 r - \sinh^2 r) d\phi^2 + 2\sqrt{2} \sinh^2 r d\phi dt' \right] \quad (3)$$

(the inessential coordinate z is here suppressed).

In its original formulation, the Gödel universe describes a set of masses (such as galaxies, stars and planets) rotating about arbitrary axes.

The metric (3) exhibits a rotational symmetry about the axis $r = 0$ since we clearly see that the components of the metric tensor do not depend on ϕ .

For $r \geq 0$, we have $0 \leq \phi \leq 2\pi$. If a curve r_G is defined by $\sinh r = 1$ that is $r_G = \log(1 + \sqrt{2})$, then for any curve $r > r_G$ we have $\sinh^4 r - \sinh^2 r > 0$. Such a curve which materializes in the “plane” $t = const$ is a closed time-like curve (CTC). The radius r_G referred to as the Gödel radius, induces a light-like curve or closed null curve where the light cones are tangential to the plane of constant t . With increasing $r > r_G$, the light cones continue to keel over and their opening angles widen until their future parts reach the negative numerical values of t .



As a consequence a spacecraft can move in such way that its chronological order with the positive cosmic time is reversed.

In order to make his metric compatible solution to Einstein’s field equations, Gödel is led to introduce the cosmo-

logical constant Λ as

$$G_{\mu\beta} = \frac{8\pi G}{c^4} \rho c^2 u_\mu u_\beta + \Lambda g_{\mu\beta}. \quad (4)$$

To achieve this compatibility he then further sets

$$a^{-2} = \frac{8\pi G}{c^2} \rho, \\ \Lambda = -\frac{1}{2} R = -\frac{1}{2a^2} = -\frac{4\pi G}{c^2} \rho.$$

Finetuning the hypothetical cosmological constant with the (mean) density of the universe and the Ricci scalar R , appears as a rather dubious physical argument.

In our publication [2], we assumed that a is slightly space-time variable and we set

$$a^2 = e^2. \quad (5)$$

As a result, the Gödel metric tensor components are conformal to the real Gödel metric tensor $g_{\mu\nu}$

$$(g_{\mu\nu})' = e^{2U} g_{\mu\nu}, \quad (g^{\mu\nu})' = e^{-2U} g^{\mu\nu}.$$

The exact Gödel metric reads now

$$ds^2 = e^{2U} \left[c^2 dt^2 + \frac{1}{2} e^{2x} dy^2 - 2e^x c dt dy - dx^2 - dz^2 \right] \quad (6)$$

or

$$ds^2 = 4e^{2U} \left[(dt')^2 - dr^2 + (\sinh^4 r - \sinh^2 r) d\phi^2 + 2\sqrt{2} \sinh^2 r d\phi dt' \right]. \quad (7)$$

This implies that this metric is a straightforward solution of the field equations describing a peculiar perfect fluid [3–5]

$$G_{\mu\beta} = \frac{8\pi G}{c^4} \left[(\rho c^2 + P) u_\mu u_\beta - P g_{\mu\beta} \right]. \quad (8)$$

The model is now likened to a fluid in rotation with mass density ρ and pressure P with an equation of state $\rho = f(P)$.

The positive scalar U is shown to be

$$U(x^\mu) = \int \frac{dP}{\rho c^2 + P}. \quad (9)$$

From (7) one formally infers that the flow lines of matter of the fluid follow conformal geodesics given by

$$s' = \int e^U ds. \quad (10)$$

The 4-vector $K_\nu = \partial_\nu U$ is regarded as the 4-acceleration of the flow lines [6]. The hallmark of the theory is the substitution (5). With this new definition, the Gödel space-time is no longer the representation of a cosmological model but it is

relegated to the rank of an ordinary metric where its physical properties could allow for a possible replication.

Rotation of the model and closed curves now depend on the fluid characteristics.

To this effect consider the metric

$$ds^2 = c^2 (dt'')^2 - \frac{(dr'')^2}{1 + (r''/2e^U)^2} - r'' \left[1 - (r''/2e^U)^2 \right] d\phi^2 + 2(r'')^2 \frac{c}{\sqrt{2}e^U} d\phi dt''. \quad (11)$$

As easily verified it is equivalent to the metric (7) if we set [7]

$$r'' = 2e^U \sinh r, \quad t'' = \frac{2e^U t'}{c}. \quad (12)$$

In this new representation, we see that when $r'' = 2e^U$, the coefficient in front of $d\phi^2$ vanishes. If we choose the cosmic time t'' describing the evolution of our universe as the rotation-axis, then $r''_G = 2e^U$ constitutes the Gödel radius for which the time lines close up and are tangential to the light cones (null curves). These curves are contained in the plane $t'' = const.$ in the same way as detailed above. Inspection shows that the fluid rotates with the angular velocity

$$\omega = \frac{c}{\sqrt{2}e^U}. \quad (13)$$

Through the equation of state $\rho = f(P)$, the Gödel radius will be set by tuning the pressure parameter P of the considered fluid.

Referring to the work initiated in [8], we complete hereinafter our last publication [9] in which a spacecraft moves along a Gödel trajectory by using a warp drive propulsion. The required negative energy will be now given a physical meaning.

2 A short review on Alcubierre's theory

2.1 The ADM formalism

Arnott, Deser and Misner (ADM) suggested to construct a space-time foliation of hypersurfaces parametrized by an arbitrarily chosen time coordinate value x^0 [10]. This foliation is characterised by a proper time $d\tau$ between two nearby hypersurfaces

$$x^0 = const, \quad \text{and} \quad x^0 + dx^0 = const, \quad (14)$$

where $cd\tau$ is proportionnal to dx^0

$$cd\tau = N(x^a, x^0) dx^0, \quad (15)$$

and in the ADM terminology, N is called the *lapse function*.

Let us evaluate the 3-vector whose spatial coordinates x^a are lying in the hypersurface $x^0 = const$, and the vector is normal to the hypersurface on the second hypersurface $x^0 + dx^0 = const$, where those coordinates become

$$N^a dx^0,$$

and the vector N^a is called the *shift vector*.

From these definitions follows the derivation of the 3-tensor

$$K_{ab} = (2N)^{-1} (-N_{a;b} - N_{b;a} + \partial_0 g_{ab}), \quad (16)$$

It represents the “extrinsic curvature”, and as such describes the manner in which the hypersurface $x^0 = \text{const}$ is embedded in the surrounding space-time.

With this brief preparation we are now able to tackle our topic.

2.2 Alcubierre’s function

In 1994, M. Alcubierre showed that a superluminal velocity can be achieved without violating the laws of Relativity. He considered a perturbed space-time region likened to bubble (“warp drive”) which could transport a spacecraft in a surfing mode inside the bubble, the proper time $d\tau$ is the coordinate time element dt measured by an external observer called “Eulerian”.

The motion is only achieved by the space wave, so that the occupants of the spacecraft are at rest and would not suffer any acceleration nor time dilation in the displacement [11]. This process requires a front contraction of the space while subject to a rear expansion. The spacecraft center distance located in the bubble

$$r_s(t) = \sqrt{(x - x_s(t))^2 + y^2 + z^2} \quad (17)$$

varies until R_e , which is the external radius of the bubble.

With respect to the distant observer the apparent velocity of the spacecraft is

$$v_s(t) = \frac{dx_s(t)}{dt}, \quad (18)$$

where $x_s(t)$ is the coordinate of the bubble’s trajectory along the x -direction.

Alcubierre then defined the step function $f(r_s, t)$

$$f(r_s, t) = \frac{\tanh[\sigma(r_s + R_e)] - \tanh[\sigma(r_s - R_e)]}{2 \tanh(\sigma R_e)}, \quad (19)$$

where $R_e > 0$ is the external radius of the bubble, and σ is a “bump” parameter used to tune the wall thickness of the bubble. The larger the parameter σ , the greater the contained energy density; for its shell thickness decreases. Moreover, the absolute increase of σ means a faster approach of the condition

$$\left. \begin{array}{l} \lim_{\sigma \rightarrow \infty} f(r_s, t) = 1 \text{ for } r_s \in [-R_e, R_e] \\ \text{and is 0 everywhere else} \end{array} \right\}. \quad (20)$$

The Alcubierre metric is

$$(ds^2)_{\text{AL}} = -c^2 dt^2 + [dx - v_s f(r_s, t) c dt]^2 + dy^2 + dz^2. \quad (21)$$

Inspection shows that

$$K_{ab} = -u_{a;b}, \quad (22)$$

which is sometimes called the second fundamental form of the 3-space.

Within this formalism, the expansion scalar becomes

$$\theta = \partial_1 N^1 = -\text{tr } K_{ab} \quad (23)$$

that with (20) is

$$\theta = v_s \frac{df}{dr_s} \frac{x_s}{r_s}. \quad (24)$$

Let us now write the Alcubierre metric in the following equivalent form

$$(ds^2)_{\text{AL}} = -\left[(1 - v_s^2 f^2(r_s, t)) c^2 dt^2 - 2 v_s f c dt dx + dx^2 + dy^2 + dz^2 \right]. \quad (25)$$

Taking account of (20) one finally find the energy density

$$(T^{00})_{\text{AL}} = -\frac{c^4}{32\pi G} v_s^2 \left(\frac{df}{dr_s} \right)^2 \frac{y^2 + z^2}{r_s^2}. \quad (26)$$

This expression is unfortunately negative as measured by the Eulerian observer and therefore it violates the weak energy conditions (WEC) [12]. Notwithstanding this violation, one is nevertheless forced to introduce a way to obtain a negative energy density. This possibility is examined below.

2.3 Nature of the negative energy

We consider a spacecraft having a shell whose thickness is $R_e - R_i$, where R_e is the external radius, while R_i is the inner radius. R_e coincides with the Alcubierre bubble which thus constitutes the whole spacecraft contour.

Consider now a charge μ circulating within the shell thus giving rise of a 4-current density

$$j^\alpha = \mu u^\alpha. \quad (27)$$

This current is coupled to a co-moving electromagnetic field characterized with the 4-potential A^a which yields the interacting energy-momentum tensor

$$(T^{\alpha\beta})_{\text{elec}} = \frac{1}{4\pi} \left(\frac{1}{4} g^{\alpha\beta} F_{\gamma\delta} F^{\gamma\delta} + F^{\alpha\sigma} F^\beta{}_\sigma \right) + g^{\alpha\beta} j_\nu A^\nu - j^\alpha A^\beta. \quad (28)$$

The extracted energy density is

$$(T^{00})_{\text{elec}} = \frac{1}{4\pi} \left(\frac{1}{4} F_{\gamma\delta} F^{\gamma\delta} + F^{0\nu} F_\nu^0 \right) + j_\nu A^\nu - j^0 A^0. \quad (29)$$

Since we chose an orthonormal basis, we have

$$(T^{00})_{\text{elec}} = \frac{1}{8\pi} (\mathbf{E}^2 + \mathbf{B}^2) \frac{1}{4\pi} \Delta(\Phi \mathbf{E}), \quad (30)$$

where \mathbf{E} and \mathbf{B} are respectively the electric and magnetic field strengths derived from the Maxwell tensor

$$F_{\gamma\delta} = \partial_\gamma A_\delta - \partial_\delta A_\gamma. \quad (31)$$

We assume that the field potential $A^\alpha(\Phi, \mathbf{A})$ is given in the Lorentz gauge.

The charge density is derived from

$$\Delta \mathbf{E} = 4\pi\mu, \quad (32)$$

which is just the time component of the 4-current density inferred from Maxwell's equations

$$\nabla_\alpha F^{\alpha\beta} = \frac{4\pi}{c} j^\beta. \quad (33)$$

Therefore negative energy density may be shown explicitly by the interaction tensor

$$(T^{00})_{\text{electint}} = \frac{1}{4\pi} \mathbf{E} \Delta \Phi + \mu \Phi, \quad (34)$$

$$(T^{00})_{\text{elecint}} = \frac{1}{4\pi} \left(-\Delta \Phi - \frac{1}{c} \partial_t \mathbf{A} \right) \Delta \Phi + \mu \Phi \quad (35)$$

since $\mathbf{E} = -\Delta \Phi - \frac{1}{c} \partial_t \mathbf{A}$.

In (35) the first term in the brackets is always negative. As to the last term, it is made negative when the time varying charge density μ and the scalar potential Φ are 180° out of phase (method reached by the use of phasors).

We now suppose that the positive free radiative energy density

$$(T^{00})_{\text{elecrad}} = \frac{1}{8\pi} (\mathbf{E}^2 + \mathbf{B}^2)$$

is confined within the spacecraft, i.e., right to the inner side of the shell wall. The interacting tensor $(T^{00})_{\text{elecint}}$ is set so as to exhibit its energy density part on the *external side* of the shell. This is made consistent since the charges are circulating *inside* the surrounding shell of the spacecraft.

So we see that negative energy production can be achieved with such a configuration. The higher the charge density and the higher the scalar potential, then the most effective negative energy density.

The local field equations read

$$G_{\mu\beta} = \frac{8\pi G}{c^4} [(\rho c^2 + P)u_\mu u_\beta - P g_{\mu\beta} + (T_{\mu\beta})_{\text{elec}}]. \quad (36)$$

Remains now the energy density level $(T^{00})_{\text{elecint}}$ which is anticipated to be very huge. There is however a possible drastic reduction which adequately exploits the contribution of the electromagnetic field interacting with the charges.

2.4 Reducing the required negative energy

The spacecraft bubble is externally charged surrounded by a comoving electromagnetic field. As such it follows a *finslerian geodesic* [13] provided the ratio $\frac{\mu}{\rho}$ remains constant along the trajectory

$$(ds)_{\text{shell}} = ds + \frac{\mu}{\rho} A_\alpha dx^\alpha, \quad ds = \sqrt{\eta_{\alpha\beta} dx^\alpha dx^\beta}. \quad (37)$$

Neglecting the non-quadratic terms the metric reads

$$(ds^2)_{\text{shell}} = ds^2 + \left(\frac{\mu}{\rho} A_\alpha dx^\alpha \right)^2. \quad (38)$$

The interacting charge of the spacecraft must now be included in the metric (25).

Because we are considering only the energy density of the spacecraft-bubble as a whole, the spatial components of $\frac{\mu}{\rho} A_\alpha dx^\alpha$ in (38) can be neglected and the interaction term reduces to its time component

$$\frac{\mu}{\rho} A_0 dx^0 = \frac{\Phi\mu}{\rho} c dt. \quad (39)$$

The metric (37) becomes now

$$ds^2 = - \left(1 + \frac{\Phi\mu}{\rho} \right)^2 c^2 dt^2 + dz^2 + dx^2 + dy^2. \quad (40)$$

Notice that the time component of the metric tensor

$$g_{00} = - \left(1 + \frac{\Phi\mu}{\rho} \right)^2 \quad (41)$$

can be expressed by the following formula

$$M = -(1 + N), \quad (42)$$

where the lapse function is defined as

$$N = \Phi \frac{\mu}{\rho}. \quad (43)$$

The Alcubierre metric (25) reads now

$$ds^2 = - [M^2 - v_s^2 f^2(r_s)] c^2 dt^2 - 2v_s f(r_s) c dt dx + dz^2 + dx^2 + dy^2. \quad (44)$$

The interaction term should be only function of r_s , R_e , σ , and of the thickness $(R_e - R_i)$, but not depending on the velocity v_s .

Here, our analysis is not too dissimilar to the approach detailed in [14, 15].

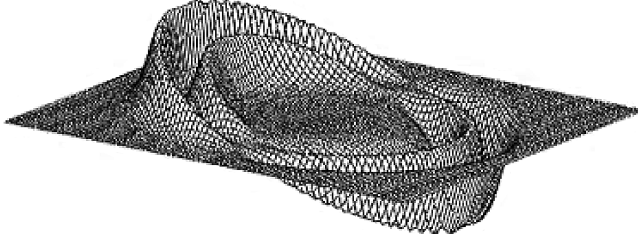
Finally, the negative energy density requirement is

$$\frac{c^4}{8G} v_s^2 \left(\frac{df}{dr_s} \right)^2 \frac{y^2 + z^2}{r_s^2} = \left(\Delta \Phi + \frac{1}{c} \partial_t \mathbf{A} \right) \Delta \Phi + \mu \Phi. \quad (45)$$

The splitting shell/inner part of the spacecraft frame, is really the hallmark of the theory here it implies that the proper time τ of the inner part of the spacecraft is not affected by the term N .

The spacecraft-bubble follows the trajectory $x_s(t)$. Therefore For $R \leq R_e$, the bubble is assumed to be ruled by the new Alcubierre metric (44) expressed with the signature -2

$$ds^2 = (M^2 - v_s^2 f^2) c^2 dt^2 - 2v_s f(r_s) c dt dx - dz^2 - dx^2 - dy^2. \quad (46)$$



A 2D representation of the warped region according to (44). Propagation is from left (expansion) to right (contraction). The groove corresponds to the shell thickness determined by the function N .

This space-time is thus regarded as *globally hyperbolic* and the bubble will never know whether it moves along a CTC. As a result, the bubble is seen by a specific observer (see below) as being transported forward along the x -direction *tangential* to a CTC beyond the Gödel radius r_G .

We may now write down the *Gödel-Alcubierre metric*

$$ds^2 = e^{2U(1-f)} \left\{ \left[\left(1 + \frac{\Phi\mu}{\rho} \right)^2 - v_s^2 f^2 \right] c^2 dt^2 - \left[f - \frac{1}{2} (1-f) e^{2x} \right] dy^2 - 2 [v_s f + (1-f) e^x] c dt dy - dx^2 - dz^2 \right\}. \quad (47)$$

In the absence of charge, beyond the distance R_e , we have $R > R_e \rightarrow \infty$ and $f = 0$ outside of the spacecraft-bubble and we retrieve Gödel's original modified metric (6).

3 Entropy along a Gödel trajectory

3.1 Relativistic thermodynamics

Consider a fluid that consists of n particles in motion within a given region. The primary variables are:

- The particle current

$$I^\mu = n u^\mu; \quad (48)$$

- The energy-momentum $T^{\mu\nu}$;
- The entropy flux S^μ ,

where, obviously, $T^{\mu\nu}$ and I^μ are conserved

$$T_{;\nu}^{\mu\nu} = 0 \quad I_{;\mu}^\mu = 0.$$

In a relativistic situation, the second law of thermodynamics requires

$$S_{;\mu}^\mu \geq 0. \quad (49)$$

For equilibrium states we have

$$S^\mu = n s u^\mu, \quad (50)$$

where s is the entropy per particle.

Denoting Q as the chemical potential and T the heat quantity (temperature) of the medium, the Euler relation reads

$$n s = \frac{\rho + P}{T} - \frac{Q n}{T}, \quad (51)$$

where ρ and P are respectively the density and pressure of the medium. We also have the Gibbs fundamental thermodynamic equation

$$T ds = ds \left(\frac{\rho}{n} \right) + P d \left(\frac{1}{n} \right) \quad (52)$$

or

$$T n ds = d\rho - \frac{\rho + P}{n} + dn. \quad (53)$$

From (51), we get

$$S^\mu = - \frac{Q I^\mu}{T} + \frac{(\rho + P) u^\mu}{T}. \quad (54)$$

Since in the rest system, the matter energy flux must vanish, we have

$$u_\lambda T^{\lambda\mu} = \rho u^\mu \quad (55)$$

and thus, we find the following expression for the entropy vector in equilibrium

$$S^\mu = - \frac{Q I^\mu}{T} + \frac{u_\lambda T^{\lambda\mu}}{T} + \frac{P u^\mu}{T}. \quad (56)$$

3.2 Applying to the time travel trajectory

Let us consider a spacecraft moving along a Gödel trajectory. We obviously neglect the chemical potential of the spacecraft's bodyframe as well as the pressure and the entropy vector reduces to

$$S^\mu = \frac{u_\lambda T^{\lambda\mu}}{T}. \quad (57)$$

This vector must be measured by the Eulerian observer which travels along the trajectory tangential to u^μ , where he "sees"

$$\frac{dt}{d\tau} = M^{-1}. \quad (58)$$

With this definition, it is easy to show that its velocity components are

$$(u^\mu)_E = [cM^{-1}, v_s f cM^{-1}, 0, 0] \quad (59)$$

$$(u_\mu)_E = [cM, 0, 0, 0]. \quad (59bis)$$

We are interested in the entropy scalar part

$$(S^0)_E = \frac{(u_0)_E (T^{00})_{AL}}{T} \quad (60)$$

with

$$(T^{00})_{AL} = - \frac{c^4}{32\pi G} \frac{v_s^2 (y^2 + z^2)}{M^4 r_s^2} \left(\frac{df}{dr_s} \right)^2, \quad (61)$$

$$(u_0)_E = cM. \quad (62)$$

We clearly see that the entropy $(S^0)_E$ of the system is negative. Hence, the entropy S^0 attached to the spacecraft is seen negative with respect to the Eulerian observer which thus measures a “negentropy”. While travelling to the past, the occupants of the spacecraft experience a positive entropy, i.e., they are ageing in their own proper time.

Conclusions

In the novel “The time machine” (1895) by H. G. Wells, an english scientist constructs a machine which allows him to travel back and forth in time.

Closed time-like curves were discovered in the 1920’s, but it is really in 1988 that time travel possibility was seriously considered by physicists in the stunning article [16]. The Gödel solution was mainly regarded as a mathematical curiosity and thus it was almost forgotten. We have succeeded in reviving his work by using some transformations which give Gödel’s mathematical derivation a full physical significance. In this view, the major contribution of J. Natário’s work [17, 18] introduces now a complementary perspective.

So far, Gödel’s model only depicts a travel into the past. What about the journey home? If advanced civilizations harness the time travel technology, they must be able to return to their own present, meaning a reversed time orientation. In the light of the aforementioned derivations we conclude that they should take another path. A possibility arises by considering our recent publication [19]. In this article, we recalled that the current Einstein’s field equations are inferred from the second Bianchi’s identity which is verified by the Riemann tensor. The latter tensor can be particularized to the *Landau-Lifchitz superpotential* [20], which is shown to yield two opposite field equations (not necessarily symmetrical) coupled with a common index.

Identifying the time coordinate chosen as the cosmic time-axis, to this common index, the solution of the second field equation would then display a reversed time orientation. In this case an advanced civilization could adequately exploit this circumstance to return to its epoch.

Much remains to be worked out on the subject, but we trust that Gödel’s legacy will continue to stimulate my fundamental researches in this field.

Submitted on May 31, 2024

References

- Gödel K. An example of a new type of cosmological solutions of Einstein’s field equations of gravitation. *Review of Modern Physics*, 1949, v. 21, no. 3, 447–450.
- Marquet P. The exact Gödel solution. *Progress in Physics*, 2021, v. 17, no. 2, 133–138.
- Eisenhart L.P. Space-time continua of perfect fluids in General Relativity. *Trans. Amer. Math. Soc.*, 1924, v. 26, 205–220.
- Synge J.L. Relativistic hydrodynamics. *Proc. Lond. Math. Soc.*, 1937, v. 43, 376–416.
- Lichnerowicz A. Les Théories Relativistes de la Gravitation et de l’Electromagnétisme. Masson et Cie, Paris, 1955.
- Hawking S.W., Ellis G.F.R. The Large Scale Structure of Space time. Cambridge University Press, 1987.
- Kajari E., Walser R., Schleich P., Delgado A. Sagnac effect of Gödel’s universe. arXiv: 0404032 (2004).
- Tippett B.J., Tsang D. Traversable achronal retrograde domain in space-time. arXiv: 1310.7985 (2013).
- Marquet P. Gödel time travel with warp drive propulsion. *Progress in Physics*, 2022, v. 18, no.1, 82–88.
- Arnowitz R., Deser S., Misner C. Dynamical structure and definition of energy in General Relativity. *Physical Review*, 1959, v. 116, no. 5, 1322–1330.
- Alcubierre M. The warp drive: hyper fast travel within General Relativity. *Classical and Quantum Gravity*, 1994, v. 11, L73–L77.
- Marquet P. The generalized warp drive concept in the EGR theory. *The Abraham Zelmanov Journal*, 2009, v. 2, 261–287.
- Marquet P. Geodesics and Finslerian equations in the EGR theory. *The Abraham Zelmanov Journal*, 2010, v. 3, 90–100.
- Loup F., Waite D., Held R., Halerewicz E.Jr., Stabno M., Kuntzman M., Sims R. A causally connected superluminal Warp Drive spacetime. arXiv: 020.2021 (2002).
- Loup F., Waite D., Halerewicz E.Jr. Reduced total energy requirements for a modified Alcubierre warp drive spacetime. arXiv: 010.70975 (2001).
- Morris M.S., Thorne K.S., Yurtsever U. Wormholes, time machine and the weak energy condition. *Phys. Rev. Let.*, 1988, v. 61, no. 13, 1446–1449.
- Natário J. Optimal time travel in the Gödel universe. arXiv: 1105.619 (2011).
- Natario J. Warp Drive with zero expansion. arXiv: 01.10086 (2002).
- Marquet P. Twin universes confirmed by General Relativity. *Progress in Physics*, 2022, v. 18, no. 1, 89–94.
- Landau L., Lifshitz E. The Classical Theory of Fields. Addison-Wesley, Reading, 1962.

Inference of Plausible Spatial Sizes of GRB Systems Using Newly Proposed FDSL-Model for GRB Time Delays

Godson Fortune Abbey¹, Joseph Simfukwe¹, Prosperity Christopher Simpemba¹, Saul Paul Phiri¹, Alok Srivastava¹
and Golden Gadzirayi Nyambuya^{1,2}

¹Copperbelt University, School of Mathematics and Natural Sciences, Department of Physics, P. O. Box 21692, Jambo Drive Riverside, Kitwe, Republic of Zambia. E-mail: godsonabbey88@gmail.com, josephsimfukwe2013@gmail.com

²National University of Science & Technology, Faculty of Applied Sciences, Department of Applied Physics, P. O. Box AC 939, Ascot, Bulawayo, Republic of Zimbabwe. E-mail: physicist.ggn@gmail.com

We have used regression analysis to establish a time correction mechanism for four GRBs (030329, 980425, 000418, and 021004) employed from literature on the basis of a frequency-dependent speed of light (FDSL) model which we developed entirely from Maxwell's electromagnetic equations in conjunction with plasma and dispersion effects. In our first instalment (Paper 1), on the assumption that these GRBs all leave the source at the same time we obtained good positive correlations and hence justified the reliability of our fitting model. In this paper, however, on the assumption that each photon leaves the GRB source at different times, we modify the previous model to obtain a more fitting model. Furthermore, the modification led to the unification of the four GRBs into a homogenous albeit perfect correlation leading to the determination of the frequency equivalent of the ISM ($v_* = 1.507 \pm 0.0009$ Hz) and hence, the spatial sizes (ΔD) of the internal and external shocks wherein we obtain for the four GRBs $\Delta D = 838.90, 39.00, 7804.00$ and 19188.00 for GRBs 030329, 980425, 000418, and 021004 respectively. If the results provided herein are deemed acceptable or reasonable — *one can on this basis* — say that the relationship we have established from our analysis for the four GRBs supports two GRB models, “the framework of the fireball model” and “the multiple shock wave model” of GRBs production and their afterglow. Additionally, the implications are evident in the variations of relativistic outflows within the jets offering valuable insights into the acceleration mechanisms and interactions between the jet and its surrounding medium.

1 Introduction

One of the most puzzling phenomena in modern astrophysics is perhaps γ -ray bursts (GRBs). These brief flashes of non-thermal γ -ray energy which occur about once a day have consistently defied the *laws of physics* in their explanation. GRBs are highly concentrated high-energy explosions from distant objects deep within space. These explosions create a relativistic blastwave which inevitably collides with the circumburst medium resulting in internal and external shocks [1]. The photons emanating from these shocks possess enormous energies typically on the order of 10^{42} – 10^{47} J [2, 3], and arrive at Earth as cosmic snipers that are uniformly distributed on the sky [4]. Due to these extreme energies, the prompt emission observed in these GRBs before now was believed to have been generated by a relativistic jet from their central engine [5–7]. Similarly, an afterglow is likely produced by external shocks from the interaction between the jet material and the circumburst medium [3].

Despite decades of research, the precise mechanisms driving GRBs and the characteristics of their progenitors remain a subject of intense investigation. One crucial aspect of understanding GRBs lies in estimating the spatial size of the shock waves they generate, as it provides invaluable insights

into their physics and progenitor environments. Recent advancements in time-delay models, e.g. [8–11], have offered a promising avenue to infer the spatial scales of GRBs phenomena. These delays, resulting from the differential arrival times of photons emitted from different parts of the shock region encode valuable information about the size and structure of the emitting source. By exploiting the temporal behaviour of GRB emissions across different frequencies and utilizing theoretical models of light propagation and interaction with the surrounding medium, we can be able to constrain the spatial dimensions of GRB shockwaves.

However, such methods face limitations in resolving the intrinsic size of the shock region, often convoluted by the surrounding environment and instrumental effects. An alternative approach gaining traction involves exploiting the time delay phenomena observed in photons of different frequencies from GRB shocks as they propagate via the Interstellar Medium (ISM). This paper aims to provide an independent method formulated from relativistic mechanics in estimating the spatial size of GRB shocks using one of such time-delay models [8]. We will explore the theoretical foundations underpinning this model, the observational data utilized [12], and the constraints derived from such analyses. Additionally, we will discuss the implications of these spatial estimates on

our understanding of GRB physics, progenitor systems, and their broader astrophysical implications. In the end, we aim to provide insights into the spatial characteristics of GRB shocks and their implications for understanding the physics of these extraordinary cosmic events.

Penultimately, we shall give a synopsis of the remainder of the present article. To begin, in §2 we take a critical look at the GRB time delay shock models to understand the role these shocks play in the generation of photons of different frequencies as they travel through the ISM. §3 gives a brief overview of the fireball model with special emphasis on how the internal and external shock mechanism gives strong support for our ideas on the non-simultaneous release of the photon pairs. §4 discusses our proposed FSDL time delay model and how it all fits into our current instalment. In §5, we give a *step-by-step* process of the current time rectification methodology we adopted, the fitting procedure used to obtain ν_* and the constraints imposed on our parameters. §6, §7 and §8, present our results, the justification of our rectification mechanism and the general discussion accompanying our results. Thereafter, we conclude with §9.

Lastly, we perhaps must hasten and say that, throughout this paper, we assume a flat *Standard Λ CDM-Cosmology Model* where we take [13]: $H_0 = 67.40 \pm 0.50 \text{ km} \times \text{s}^{-1} \times \text{Mpc}^{-1}$, $\Omega_\Lambda = 0.685 \pm 0.007$, and $\Omega_m = 0.315$ and that, for all our calculations of the luminosity distances (D_L) to the different GRBs and their host galaxies, we shall use Wright's [14] online cosmology calculator.*

2 GRB Time Delay Models

Several studies provide valuable insights into the time delay mechanism of GRB shocks. e.g. [15] introduced an improved model-independent method based on time-delay measurements of GRBs at different energy bands. This method allows for probing the energy-dependent velocity due to modified dispersion relations for photons. Additionally, [16] discussed estimating the number of emitting electrons in GRBs based on fitted parameters and assuming specific emission radii predicted by shock models within the outflow. Moreover, [17] demonstrated how delayed and long-lasting afterglow emissions in certain GRBs could be interpreted through a synchrotron forward-shock model. This interpretation was supported by the analysis of radio, optical, and X-ray light curves. Many other authors have also studied time delay models in probing GRB to mention but a few [18]

This paper aims to provide an independent method formulated from relativistic mechanics in estimating the spatial size of GRB shocks using one of such time-delay models [8]. We will explore the theoretical foundations underpinning this model, the observational data utilized [12], and the constraints derived from such analyses. Additionally, we will discuss the implications of these spatial estimates on our

understanding of GRB physics, progenitor systems, and their broader astrophysical implications. In the end, we aim to provide insights into the spatial characteristics of GRB shocks and their implications for understanding the physics of these extraordinary cosmic events. To begin, we will first take a critical look at the GRB fireball model with specific reference to the internal and external shock models to understand the role these shocks play in the generation of photons of different frequencies as they travel through the ISM.

3 Fireball Model

As is well known, a highly effective framework for interpreting observations of GRBs has been made available in the form of the fireball model [19–22]. The fireball model is commonly employed to explain the mechanism that produces the radiation we detect from most GRBs. The most widely accepted, and almost certain explanation for GRB production according to the fireball model is that when there is an ejection of extremely high energetic jets due to the merger of two neutron stars (NS-NS) [23], or a neutron star and a black hole (NS-BH) [4, 23] and a supernova [24] explosion as depicted in Fig. 1, the enormous release of energy gives rise to a Poynting-flux-dominated Magneto-hydrodynamics (MHD) wind with a luminosity of approximately $10^{50} \text{ erg} \times \text{s}^{-1}$ [25] within the ISM confined to the jet cone. These MHD winds generate the GRBs when the kinetic energy of these ultra-relativistic particles, or potentially the electromagnetic energy of the Poynting flux, is converted to radiation [21, 26].

The GRB fireball model is essential for understanding the nature and implications of GRB shocks. In a bid to demystify the radiation mechanism, [27, 28] compared the fireball-shock and millisecond-magnetar models by fitting them to X-ray data of specific GRBs, emphasizing the importance of different shock models in explaining GRB phenomena. Similarly, [29] used a “boosted fireball” model to replicate the hydrodynamics of GRB outflows, highlighting the necessity for comprehensive models to decode the complexities of GRBs. In the same light, [30] provides a comprehensive review of γ -ray bursts and related transients, discussing theoretical models for prompt and afterglow emissions, including the standard fireball model with internal and external shocks. Their study highlights the role of synchrotron radiation from relativistic electrons accelerated in the shocks, emphasizing the importance of magnetic fields in these processes, and the internal and external shock mechanisms for γ -ray burst emission.

Additionally, [31] discussed utilizing GRB emissions as a test-bed for modified gravity theories, demonstrating how GRBs can offer insights into fundamental physics beyond standard models [32–35] and many more have also explored how gravitational wave observations can enhance our understanding of the intrinsic properties of the shock waves from GRBs, showcasing the interdisciplinary nature of studying

*<https://www.astro.ucla.edu/~wright/CosmoCalc.html>

these phenomena. To describe both the initial burst of γ -rays and the lengthy afterglow, the fireball model employs two separate shock wave models — namely, the *internal and external shock wave models* [36, 37].

3.1 Internal Shock

As depicted in Fig. 1, internal shocks are responsible for the high energy of γ -ray particles. Moments after the incident, shock waves (fronts) with a Lorentz factor (Γ) close to 100 are emitted from the inner engine at relativistic speeds leading to multiple shock waves, each travelling at a different relativistic speeds. These shock fronts result in energetic γ -ray emissions which are principally caused by thermal magnetic reconnection activities and relativistic processes. In this process, baryonic mass will be added to the emission, thus helping to convert some radiation energy into relativistic kinetic energy, which in turn increases the γ -ray burst flux. As illustrated in Fig. 1, a significant portion of the initial energy released by the freshly generated BH is transformed straight into photons in a pure radiation fireball [37, 38].

3.2 External Shock

On the other hand, external shocks are predominantly thermal emissions produced as the energy transferred from the shock waves is deposited into the interstellar medium (ISM). The spilt substance can then be trapped in the shock front and release radiation as the shock travels in the outward direction. The resulting broadband synchrotron radiation evolves as the external shock propagates outward into the surrounding medium, depending on various fundamental characteristics of the explosion, the specifics of the shock evolution, and the density profile of the medium into which it expands [26, 40]. When shocks from this external surrounding circumburst matter delay this flow of electrons, the afterglow appears with varying frequencies ranging from X-ray to optical wavelengths. It is generally assumed that most of the GRBs we detect are triggered by internal shocks, while the slow afterglow emanates from the external shocks [41].

It is on this theoretical explanation of this fireball model that we anchor our modified time delay emission model, wherein we now have the radio photon pairs not simultaneously leaving the GRB event as has been assumed in our previous papers [8]. We aim to show that under the above-stated new assumption of non-simultaneous emission of the radio photon pair, the time delay experienced by these photons may very well be a result of the series of shock waves generated by the internal and external production mechanism as is assumed in the fireball model. This may also lead us to understand the shock dynamics and/or the spatial sizes of the shocks.

4 Our Proposed FSDL Model

Here, we adopt a standard fireball scenario for the GRBs afterglow, where a relativistic shock with (Γ) expands into the

circumburst medium (CBM). The afterglow flux arises from the radiation (synchrotron and possibly also inverse Compton) emitted by relativistic electrons accelerated from the internal to the external shocks. To describe the spatial size of these jets, we account for the effects of the conductance of the medium through which these radiations pass en route to the detector and model the shock dynamics using our FSDL-model.

The formulation we came up with was simple and elaborate which is: In [8], without any exogenous or exotic ideas being brought in, the following dispersion relation was derived directly from Maxwell's four fundamental equations of Electrodynamics

$$\omega^2 - c_0^2 \kappa^2 = -4\omega_* \omega, \quad (1)$$

where $\omega_* = 2\pi\nu_* = \mu c^2 \sigma / 4$, $\omega = 2\pi\nu$, with ν being the frequency of the Photon and k its wave-number. Given that the group velocity v_g of a wave is given by $v_g = \partial\omega/\partial k$, thus differentiating Eq. (1) throughout with respect to k and rearranging, it follows that

$$v_g = \frac{c_0^2}{\omega/k} \frac{1}{2\omega_* / \omega} = \frac{c_0^2}{v_p} \frac{1}{1 + 2\omega_* / \omega} = \frac{c_0^2}{v_p} \frac{1}{1 + 2v_* / v}, \quad (2)$$

where $v_p = \omega/k$, is the phase velocity. In a vacuum, we have that $v_g = v_p = c_0$. This assumption (of $v_g = v_p$) was extended to the scenario of a non-vacuum medium and so doing (i.e., maintaining this condition $v_g \neq v_p$, in the non-vacuum medium), one obtains

$$\frac{v_g}{c_0} = \frac{1}{\sqrt{1 + \frac{2v_*}{v}}}. \quad (3)$$

From Eq. (3), it follows that if D is the distance between the Earth and the GRB, and v_l and v_h are the group velocities for the lower and higher frequency Photons, then - to first order approximation we have that $c_0/v_g \simeq 1 + v_*/v$, which in turns implies that for two photons with varying velocities, the time delay Δt is such that

$$\Delta t = \frac{D}{v_l} - \frac{D}{v_h} = \frac{Dv_*}{c} \left(\frac{1}{v_l} - \frac{1}{v_h} \right). \quad (4)$$

It is clear that if the laid down theory has any correspondence with physical and natural reality, then, a plot of $\Delta t \propto (v_l^{-1} - v_h^{-1})$ for the same source (i.e., same D) should accordingly yield a straight-line graph with a slope equal to Dv_*/c_0 . Eq. (4) implies that the time delay will be given by

$$\Delta t = \frac{Dv_*}{C} \left(\frac{1}{v_l} - \frac{1}{v_h} \right). \quad (5)$$

The relation in Eq. (5) was applied to the following GRBs GRB 030329, GRB 980425, GRB 000418 and GRB 021004

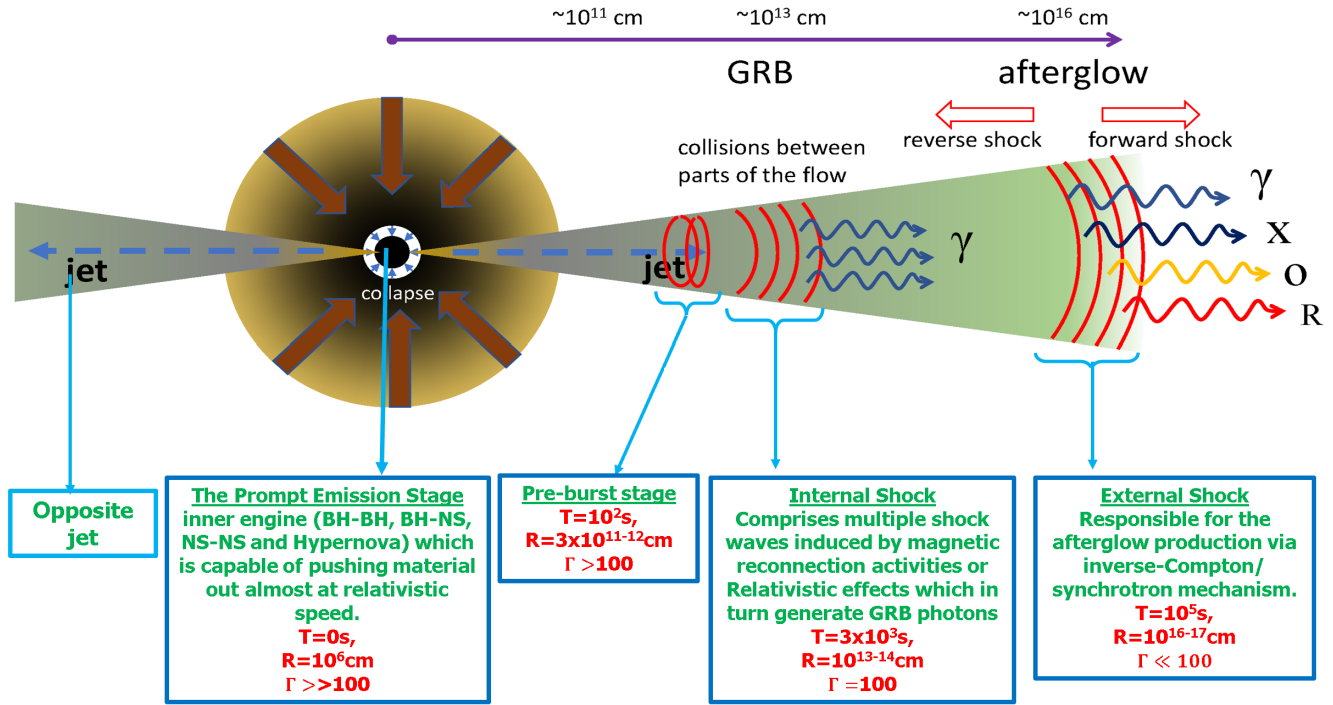


Fig. 1: A Modified cartoon depiction showing schematics description of and the basic mechanism of the GRB fireball model [39], <https://www.swift.ac.uk/about/grb.php>.

obtained from [12] and the result was a strong linear correlation between Δt and Δv^{-1} .

The obtained linear correlation confirms the theory on which Eq. (5) has been derived. Furthermore, in [8], as a major step, Eq. (5) assumes that the pair of GRB photons leave the event simultaneously. The above-stated assumption leads to a biased fit wherein the intercept of the graph of Δt vs Δv^{-1} was made to pass through the point of origin (0, 0) for there to be a zero y-intercept (see Fig. 2). Despite them giving a good correlation, the four graphs also yield slopes which were used to estimate the conductance of the ISM through which these GRB travel (see [8]).

In this current instalment, we develop a model that does not assume a simultaneous release of these pairs of photons. Rather preemptively, we must say that — this new assumption of a non-simultaneous — *albeit systematic* — emission of these photon pairs allows us to obtain a much more convincing and stronger correlation in the time delay. That is to say, this new correlation allows us to build a unified model of the four GRBs in our present sample wherein, we obtain two major results, mainly

1. A constant v_* called the frequency equivalence of the interstellar medium (ISM)'s conductance which allows us to estimate every other parameter involved with the four GRBs in question;
2. The spatial sizes of the internal and external shocks of our four GRB samples.

One significant step involved in our modified FSDL model is the estimation of the time correction parameter t_c . In this modified model, we believe that a pair of events coming from the same shock front will lie on the same slope on a Δt vs Δv^{-1} graph. In the case of our four GRB samples, the GRBs will be delayed by a fraction of the difference between the spatial sizes obtained from our calculation. Furthermore, in line with this assumption, the earlier photon leaves now while the latter leaves a time, t later. We can show that under the above-stated assumption, Eq. (5) will be modified to be

$$\Delta t = \frac{\mathcal{D}v_*}{c_0} \left(\frac{1}{v_l} - \frac{1}{v_h} \right) + t_c, \quad (6)$$

where t_c is a two-fold correction factor we introduced to rectify the time delay in the photon arrival times. Additionally, t_c is the y-intercept of this unbiased* linear regression model. This t_c will turn out to be the time difference between the emission of the photon pair from the internal and external shocks. This time difference is depicted in Figures 5 to 8 as the internal and external shock. We will briefly present our justification for our Non-simultaneous emission model.

4.1 Data Sampling and Description

As pointed out in Paper 1 [8], our data sample is wholly drawn from [12], wherein [12] draw their data from 304 GRB sam-

*By "unbiased plot", we mean a plot that does not force the linear graph to pass through the (0, 0)-point of origin as has been done on Paper 1.

ples compelled from 1997 to 2011 by [42]. From [12], eight of these GRB samples were used by [8] to investigate correlations in γ -ray burst time delays between pairs of radio photons as Paper 1 of a series of research geared towards investigating the cause of time delay in the arrival time of photons of different frequencies emanating from γ -ray burst.

In the said Paper 1 [8], in ascending order, the eight distinct GRBs we selected were 980425, 991208 000418, 000926, 021004, 030329, 031203 and 060218 making a total sample size of 52. Amongst these eight GRB samples, four of them GRB 980425, 000418, 021004 and 030329 when applied to our FDSL model gave good positive linear correlations as expected, which in turn provides a sound basis for our work and reliability of our model. The remaining four samples GRB 991208, 000926, 031203 and 060218 showed a weak correlation, so we didn't include them in our first instalment. In this present instalment, our aim was to put up a working model first with the 4 GRBs that gave a good positive correlation. To avoid constraints, we will differ the remaining weak correlated GRB samples to a later instalment where we can systematically test our model on all the data set in [12]. Additionally, we can now apply this model to recent data.

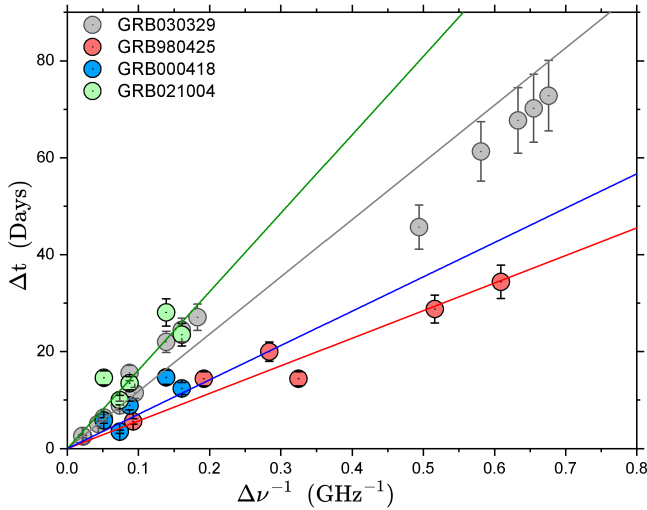


Fig. 2: Graph for Events GRB 030329, 980425, 000418, and 021004. The BLF were made to all passes through the origin.

5 Non-Simultaneous Photon Emission Model

Here we present a brief overview of our modified model as stated in the introductory section — the assumption that the low (ν_l) and high (ν_h) frequency photons are released simultaneously is to be done away with because it is very much possible that the low (or perhaps the high) frequency photon is released first, with the high (low) frequency photon is released a time t_c later (or *vice-versa*). In this event, the photon travel times t_l and t_h of the low and high frequency photons,

respectively — will be related as follows

$$t_l = \frac{D}{v_l} + t_c, \quad (7a)$$

$$t_h = \frac{D}{v_h}, \quad (7b)$$

where, likewise v_l and v_h are the speed of the low and high-frequency photons, respectively. From the foregoing, it follows from Eq. (7), that

$$\Delta t = t_l - t_h = \frac{D}{v_l} - \frac{D}{v_h} + t_c. \quad (8)$$

As given in [8], if we are to substitute into Eq. (8), the following

$$\frac{1}{v_l} = \frac{1}{c_0} \left(1 + \frac{v_*}{v_l} \right), \quad (9a)$$

$$\frac{1}{v_h} = \frac{1}{c_0} \left(1 + \frac{v_*}{v_h} \right), \quad (9b)$$

then, one will be led to Eq. (5). In this way — as promised, we have justified Eq. (6).

It is important to note that if t_c is a random variable — *the meaning of which is that this time is not the same for each photon pair* — it would give rise to a clearly visible scatter in the data points along some imagined average straight line. If t_c is uniform for all the data points — imply some welcome define and systematic origin, then, the resulting data points — *if plotted in an unbiased manner* — they would lie on a straight line that does not pass through the (0, 0)-point of origin as is the case with the data point of the GRBs in our sample. In the next subsection, we will briefly describe how we obtained the v_* from our t_c .

5.1 Fitting Procedures

As promised above, we here describe, in §5.1.1 & 5.1.1, the fitting procedures employed to arrive at a value for the time delay correction t_c and the value of the frequency equivalent of the ISM's conductance (v_*).

5.1.1 Time Delay Correction (t_c)

To obtain t_c , the following procedures were carried out

1. First, we isolated the different subgroups of the individual GRBs as shown in Fig. 2. That is to say, we noted that for each GRB source, there exist two distinct subgroups — were for:
 - (a) GRB 030329, as can be seen in Fig. 5, we have ($a, b, c, d, e, f, l, m, n, o$) and (g, h, i, j) data points forming the two subgroups with GRB 0302329k being an outlier data point;

- (b) GRB 980425, as can be seen in Fig. 6, we have (a, c, d) and (b, e, f) forming the two distinct subgroups;
 - (c) GRB 000418 of Fig. 7, have (a, d) and (b, c, e) forming the two distinct subgroups;
 - (d) Finally, GRB 021004, in Fig. 8 have (a, b, d) and (c, e) forming the two distinct subgroups;
2. Upon a meticulous observation of Fig. 5 to 8, one can see that the data points for the four GRBs were grouped in two; events group 1 representing the internal shocks and event group 2 representing the external shocks. The idea behind this grouping is to enable us to see the data points that are aligned so we can correct for the time delay (Fig. 7);
 3. When the time delay (t_c) is corrected, one can see that each group's data points have been aligned into an almost straight line. Fig. 3 shows the same four GRBs in Figures 5 to 8 after t_c correction. The scattered and group events have been aligned almost perfectly to a straight line indicating a nearly perfect linear correlation amongst the four samples respectively.

5.1.2 Calculation of the Conductance (ν_*) of the ISM

At this point, we must say that, if our model is correct or has any meaningful correspondence with physical and natural reality, then ν_* can be obtained thus

1. First — we note that the slope of the time delay corrected graphs of Fig. 3 is proportional to the distances to the respective GRBs, i.e.

$$S = \frac{D\nu_*}{c_0}. \quad (10)$$

From this Eq. (10), it is clear that if the distance to the GRB is known, the value of ν_* can be computed. Further, if cosmological space is homogeneous, then ν_* must have a constant value in any given cosmological direction that one chooses. Assuming a homogeneous space as is the case in the Λ CDM-model [43], it follows that $S \propto D$, the meaning of which is that if the distance (D_{\dagger}) to just one GRB is known, then, the distance (D_k) to the rest of the GRBs can be inferred from this Eq. (10).

That is to say: let S_{\dagger} be the slope on the graph of the GRB whose distance D_{\dagger} is known and if S_k is the slope on the graph of the GRB whose distance D_k is unknown, then, we can deduce this distance D_k from the GRB whose slope S_{\dagger} and distance D_{\dagger} are known, i.e.,

$$D_k = \left(\frac{S_{\dagger}}{S_k}\right)D_{\dagger}. \quad (11)$$

From Eq. (10), it is abundantly clear that — *in-order to deduce ν_** — one needs not know the actual distance to the GRB whose distance D_{\dagger} is known, but a relative distance — e.g., $D_{\dagger} \equiv 1$, can be assigned, so that the relative distance $D_{\text{rel}}(k)$, to the k^{th} GRB on our list can be computed, i.e.,

$$D_{\text{rel}}(k) = \frac{S_{\dagger}}{S_k}. \quad (12)$$

From (11) and (12), it follows that

$$D_k = D_{\text{rel}}(k)D_{\dagger}. \quad (13)$$

It must be noted that $D_{\text{rel}}(k)$ is a dimensionless quantity while D_{\dagger} has the dimensions of length;

2. Inserting D_k as given in Eq. (13) into Eq. (10), where Δt has been corrected for the non-simultaneous time delay, we will have

$$\frac{\Delta t}{D_{\text{rel}}} = \frac{D_{\dagger}\nu_*}{c_0} \left(\frac{1}{v_l} - \frac{1}{v_h}\right). \quad (14)$$

What Eq. (14) implies is that if all our assumptions are correct or have a meaningful correspondence with physical and natural reality, then, a plot of $\Delta t/D_{\text{rel}}$ vs $\Delta\nu^{-1}$ should yield a straight line graph. the result of the assumption is evident in (3);

3. In the present, for our standard GRB with distance D_{\dagger} and slope S_{\dagger} , we took the GRB with the smallest redshift, namely GRB 980425, which has a redshift $z = 0.009$. The justification for doing this is spelt out in §7;
4. On careful observation of Fig. 4b one can see that the scatter in the plots has all been fully corrected into an almost perfectly straight line graph. A *t-test* was carried out on the combined plot to test for statistical significance. The result was not only consistent but also significant at a 95% confidence level. The complete regression fittings and other regression parameters are shown in Table 1 and 3;
5. Therefore, From the foregoing, we have that $D_{\dagger} = 40.00$ Mpc, and $S_{\dagger} = 70.00 \pm 2.00$ GHz \times Days. Substituting these numerical values into 10 and converting to standard units we calculated ν_* to be 1.507 ± 0.0009 as the frequency equivalence of the conductance of the ISM. Following we now estimate the spatial sizes of the internal and external shocks as presented in §6.

6 Result and Analysis

According to the Fireball model depicted in Fig. 1, a GRB will have two shock fronts, the internal and external. The events emanating from these shock fronts will have a large gradient on the Δt vs $\Delta\nu^{-1}$ graph. Given that in the present GRB time delay model, the distance (D) of the group events

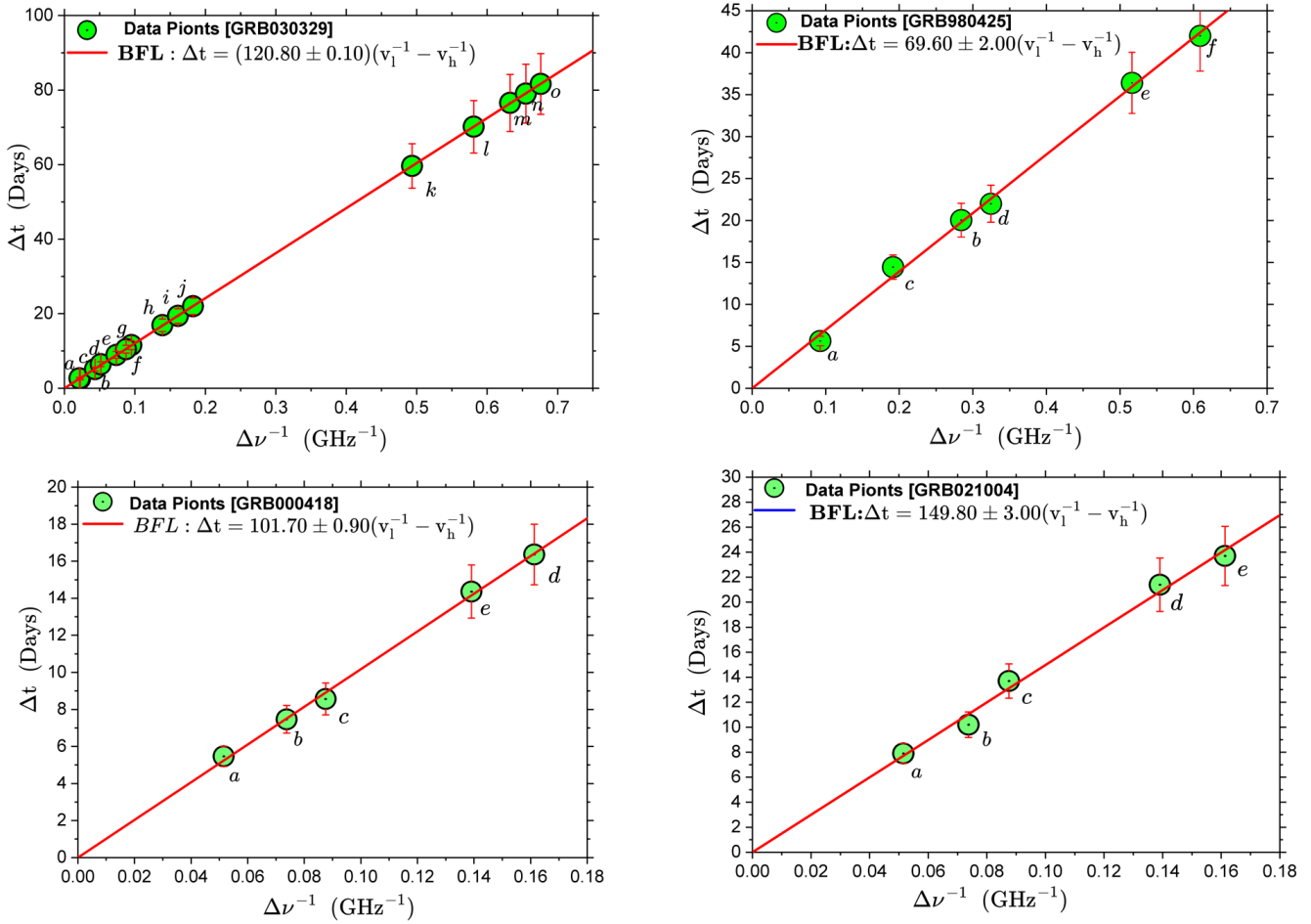


Fig. 3: Graph of GRB 030329, 980425, 000418, and 021004 events after t_C correction.

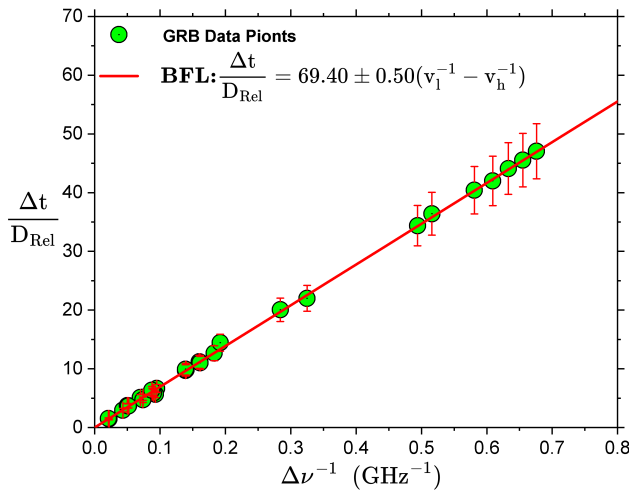


Fig. 4: Relative distance Plot. The combined scatter plots for GRB 030329, GRB 980425, GRB 000418 and GRB 021004 after relative distance correction respectively. Regression fitting for this plot passes through the (0,0)-point of origin unbiased showing that the t_c has been eliminated naturally via our correction procedure

emanating from the same shock front is such that $D = c_0 S / v_*$. It follows from the foregoing that event group (1) must therefore be emanating from the internal shock while event group (2) are coming from the external shock. If both events have slopes S_1 and S_2 , from the bare facts at hand, the spatial size, ΔD , between these two shocks is such that

$$\Delta D = \left(\frac{c_0 \Delta S}{v_*} \right) \quad (15)$$

where $\Delta S = S_2 - S_1$, $\Delta D = D_2 - D_1$ and $v_* = 1.507 \pm 0.009$ Hz (see [8]). Under the above premise, we now present the results of the spatial sizes of the four GRBs in question.

6.1 Estimating the Spatial Size

Following the procedures laid down so far, the spatial size (ΔD) can be estimated from the plot of Δt vs $\Delta \nu^{-1}$ as shown in Fig. 5 to 8 while keeping v_* as a constant. Fig. 5 to 8 shows a scattered plot of GRB 030329, GRB 980425, GRB 000418 and GRB 021004, with two fittings representing both the internal shocks (red line with yellow data points) and external shock (blue line with red data points). Regression analysis and fittings in accordance with the FDSL model yield the following result.

6.1.1 GRB 030329

GRB 030329 have a set of two events, namely — events ($a, b, c, d, e, f, l, m, n, o$) and (g, h, i, j) as shown in Fig. 5, each with slopes $S_1 = 105.90 \pm 0.60$, and $S_2 = 120.80 \pm 2.00$ respectively. Substituting these values into Eq. 15 after converting to SI units with $v_* = 1.507 \pm 0.009$ Hz, we obtain the spatial

size $\Delta D = 8.00 \pm 1.00$ Mpc. What this implies is that the spatial size between the jets is occurring at megaparsec scales. However, from the fireball model, this value seems to be very large compared to what has been obtained [49–51]. The significance is that the time delay is a result of the distance the Photons travel from the internal to the external shocks due to the reduction in their velocity as they travel via the ISM, thus making our fitting model more significant. It is also important to note that such distinct results greatly improve our understanding of GRBs if these results are to be corroborated with more data points.

6.1.2 GRB 980425

GRB 980425 have two events, namely — (a, c, d) and (b, e, f) forming the two distinct subgroups. as shown in Fig. 6, each with slopes $S_1 = 71.00 \pm 4.00$, and $S_2 = 75.00 \pm 8.00$ respectively. we obtain $\Delta D = 2.00 \pm 5.00$ Mpc. This GRB is also of the mega Parsec scale as expected.

6.1.3 GRB 000418

In the case of GRB 000418, we have two events, namely — events (a, d) and (b, c, e) as shown in Fig. 7, each with slopes $S_1 = 101.70 \pm 0.00$, and $S_2 = 102.40 \pm 7.00$ respectively. Substituting these parameters into 15, we obtain $\Delta D = 1.00 \pm 4.00$ Mpc. Similarly, the spatial size of this GRB is also of the mega Parsec scale as expected.

6.1.4 GRB 021004

Regression fittings for both the internal and external shocks for GRB 021004 are shown in Fig. 8. with $S_1 = 150.00 \pm 20.00$ and $S_2 = 154.00 \pm 0.00$ respectively, we obtain the spatial size to be $\Delta D = 13.00 \pm 4.00$ Mpc.

7 Interim Discussion

For the distances to the GRBs, we can use the Λ CDM-redshift distance estimates. Our reservation with this is that distances deduced using high redshift (i.e., $z > 0.009$) may not be accurate. For example, over the years, there has been a raging debate on this [52, 53]. This debate has somehow subsided with most astrophysicists and cosmologists accepting the Λ CDM-redshift distance estimates [54]. If any, there has not been any controversy with low redshifts and using these for distance determinations via Hubble's law [55, 56].

Rather fortuitously, we have in our four sample GRB the source GRB 980425 with a low redshift of $z = 0.0090$. This redshift is small enough so much that, one can easily apply the usual *Hubble law** to determine the distance to this

*On 26 October 2018, through an electronic vote conducted among all members of the International Astronomical Union (IAU), the resolution to recommend renaming the *Hubble law* as the *Hubble-Lemaître law* was accepted. This resolution was proposed in order to pay tribute to both —

Table 1: Result Table. In column 2 the number (1) is the internal shock and (2) is the external shock

Events	Shocks	Slopes for Shocks (S_1, S_2) (GHz \times Days)	Slope ΔS ($S_2 - S_1$) (GHz \times Days)	y -Intercept (t_c) (t_{c1}, t_{c2}) (Days)	R^2
GRB 030329	(1)	105.90 ± 0.60	15.00 ± 2.00	$+0.70 \pm 0.20$	0.9997
	(2)	120.80 ± 2.00		$+5.00 \pm 0.20$	0.9997
GRB 980425	(1)	71.00 ± 4.00	4.00 ± 9.00	-9.00 ± 2.00	0.9975
	(2)	75.00 ± 8.00		-1.00 ± 2.00	0.9884
GRB 000418	(1)	102.00 ± 7.00	1.00 ± 7.00	-4.00 ± 0.00	1.0000
	(2)	102.00 ± 0.00		$+0.30 \pm 0.70$	0.9949
GRB 021004	(1)	150.00 ± 20.00	10.00 ± 20.00	-0.30 ± 2.00	0.9889
	(2)	154.00 ± 0.00		$+7.00 \pm 0.00$	1.0000

Table 2: Summary Table. Columns (1)-(4) lists (1) Source name, (2) Cosmological redshift of the host galaxies [44–48], (3) Distance to the GRB as obtained from Wright’s cosmological calculator (4) the Spatial Size of the GRB shocks. The last row of the table presents the error-weighted average of the frequency equivalence of the conductance of the ISM, which we find to be $\nu_* = 1.507 \pm 0.009$ Hz.

Source	Host Galaxy Redshift	Distance (\mathcal{D}_L) (Mpc)	Spatial size (ΔD) (Mpc)
GRB 030329	0.1683 ± 0.0001	838.9000	8.0000 ± 1.0000
GRB 980425	0.0087 ± 0.0000	39.0000	2.0000 ± 5.0000
GRB 000418	1.1181 ± 0.0001	7804.0000	1.0000 ± 4.0000
GRB 021004	2.3304 ± 0.0005	19188.0000	13.0000 ± 3.0000

source without the need e.g. for Wright’s [14] online cosmology calculator. If we can have confidence in the distance to this GRB as determined by Hubble’s law, it means we can safely estimate the the ISM conductance σ . Taking $\mathcal{H}_0 = 67.4 \text{ km} \times \text{s}^{-1} \times \text{Mpc}^{-1}$ [57], we obtain that the source GRB 980425 is at a distance of approximately, $\mathcal{D} = 40 \text{ Mpc}$. Given that for this GRB, we have $\mathcal{D}v_*/c_0 = (6.00 \pm 2.00) \times 10^{15}$, it follows from all this — that, we will have that $\sigma = (1.0800 \pm 0.0400) \times 10^{-11} \Omega^{-1} \times \text{m}^{-1}$. If what we have obtained is to be taken seriously, not only are these results consistent, but they also show a great possibility of querying the standard distance method adopted over the years for GRBs using redshift and cosmological methods.

8 General Discussion

The results we have obtained so far not only justify the authenticity of our model but also support the fireball model

Georges Henri Joseph Édouard Lemaître (1894–1966), and, Edwin Powell Hubble (1889–1953), for their fundamental contributions to the development of the modern expanding cosmology model.

for the internal and external shock mechanism. Similar work has been done to understudy the mechanism of the internal and external shocks e.g. [33, 58–63]. One such major work by [64] delves into the width of γ -ray burst spectra as a measure to understand the emission processes in highly relativistic jets. Although the study highlights the differences in spectra widths, one can infer from this that such width may be a result of the large distances travelled by the photons indicating a large fraction across the jets. Similarly, [58] in a recent study investigated the long-term evolution of relativistic collisionless shocks in electron-positron plasma using 2D particle-in-cell simulations. Their results reveal the generation of intermittent magnetic structures by the shock, with magnetic coherence scales increasing over time as the photons travel along the jet cone. Their findings further suggest implications for γ -ray burst afterglow models, particularly in understanding the interplay between internal prompt emission and external shock mechanisms that power the afterglows in these astrophysical phenomena. Our findings and results also underscores the ongoing debate surrounding the

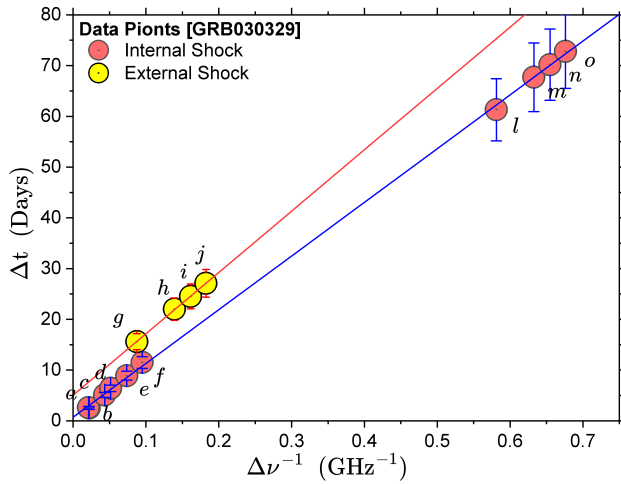


Fig. 5: Graph for Events GRB 030329 ($a, b, c, d, e, f, l, m, n, o$) and (g, h, i, j). The BLF yields slopes of $S_1 = (105.90 \pm 0.60)x + (0.70 \pm 0.20) @ R^2 = 9.9997$ and $S_2 = (120.80 \pm 2.00)x + (5.00 \pm 0.20) @ R^2 = 0.9997$.

internal and external shock mechanisms responsible for GRB emission which we believe is a step forward in the right direction.

For the internal shocks, one approach is to consider the variability timescale of the burst, which is related to the spatial size of the emitting region. On the other hand, the external shocks, are formed when the GRB outflow interacts with the surrounding medium, leading to a slower, and more prolonged emission phase.

This slowing down of the photons we believe is due to the vast difference between the internal and external shock which our model is accounting for. [65] has already shown that the radius of the external shocks can be estimated based on the deceleration timescale, which depends on the density of the surrounding medium. His findings agree with our rarified plasma model as the interactions of the photons and the plasma medium through which these photons travel can significantly affect their propagation.

Additionally, as far back as the mid and late 1990's (see e.g. [21, 66]), it has been shown that the "fireball model" often used in GRB studies suggests that the internal shocks occur within the relativistic outflow produced during the GRB event. [67] further highlighted the transition from a stratified stellar wind to a homogeneous interstellar medium (ISM) and concluded that favourable parameters could lead to the detection of GRBs at hundreds of GeVs, emphasizing the importance of considering both internal and external shock mechanisms in understanding GRB emission dynamics. In both cases (internal and external shock mechanisms), detailed modelling and analysis of observational data, such as light curves and spectra, are necessary to constrain the parameters and obtain accurate estimates of the shock radii and possibly

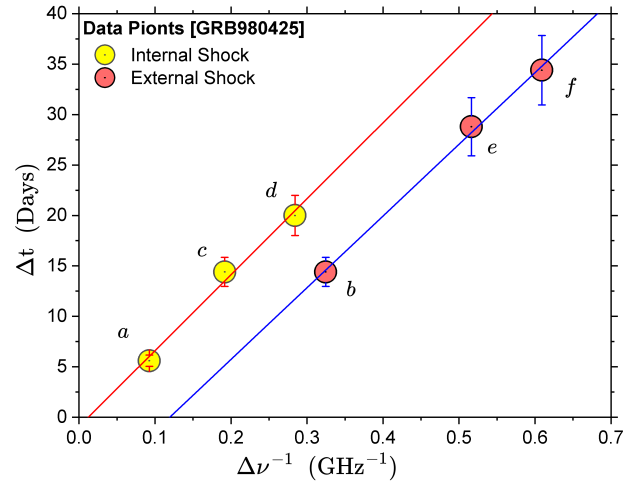


Fig. 6: Graph for Events GRB 980425 (a, c, d) and (b, e, f). The BLF yields slopes of $S_1 = (71.00 \pm 4.00)x + (9.00 \pm 2.00) @ R^2 = 0.9975$ and $S_2 = (75.00 \pm 8.00)x + (1.00 \pm 2.00) @ R^2 = 0.9884$.

the spatial sizes.

This is the next phase of this work as we work to gather more data to carry out further analysis. What our model presents so far is in support of the fireball model but on a much larger scale. It is our hope that as we fine-tune this model and incorporate more data in subsequent work, we can be able to come close to what has been established and possibly improve on the existing knowledge of these extreme astrophysical phenomena.

It is paramount we bring this to the reader for better clarity that the spatial size of the internal and external shocks plays a significant role in determining how the photons and plasma interact and propagate through the ISM. Now, with regard to the interaction mechanism between the Photon and the plasma in the present model, one will rightly ask: *Since the Photon and the plasma are here interacting, what is different between this proposed interaction mechanism and the Plasma Effect?* To that, we have the following to say. The Compton wavelength of Photon — or more so, its radius — is much smaller than the wavelength of radio waves. From an intuitive physical standpoint, it is possible to imagine an Electron being engulfed by the Photon in such a manner that the Electron can be pictured to be moving inside the \vec{E} and \vec{B} -fields of the Photon. Succinctly stated, the Electron is absorbed by the Photon in much the same manner as the Photon is absorbed by the Electron in such phenomenon as the *Photoelectric effect* [68], i.e., this simple but elaborate explanation will lead to our next instalment "can a photon absorb an electron".

It is our hope that our FSDL time delay model if properly fine-tuned with the right dataset will demystify the interaction mechanism between the photons and the plasma as they travel via the ISM.

Table 3: Combined Data Table [12]. Columns (1)-(8) list the (1) Initial/low frequency of the burst, (2) Final/high frequency of the burst (3) Initial time of the burst (4) Final time of the burst (5) Difference in the frequency (6) Values obtain from the two-fold correction (7) Relative distance obtained from the slopes of the four GRBs (8) Final values obtained from the relative distance correction

GRB Event Label	ν_1 (GHz)	ν_2 (GHz)	t_1 (Days)	t_2 (Days)	$\Delta\nu^{-1}$ (GHz ⁻¹)	Δt_c (Days)	D_{rel}	$\Delta t_c/D_{rel}$ (Days)
GRB030329a	15.00	22.50	8.40	10.90	0.022	2.56	1.7360 ± 0.0030	2.00 ± 0.10
GRB030329b	22.50	43.00	5.80	8.40	0.021	2.64	1.7360 ± 0.0030	2.00 ± 0.20
GRB030329c	15.00	43.00	5.80	10.90	0.043	5.14	1.7360 ± 0.0030	3.00 ± 0.30
GRB030329d	8.46	15.00	10.90	17.30	0.052	6.44	1.7360 ± 0.0030	4.00 ± 0.40
GRB030329e	8.46	22.50	8.40	17.30	0.074	8.94	1.7360 ± 0.0030	5.00 ± 0.50
GRB030329f	8.46	43.00	5.80	17.30	0.095	11.54	1.7360 ± 0.0030	7.00 ± 0.70
GRB030329g	4.86	8.46	17.30	32.90	0.088	10.49	1.7360 ± 0.0030	6.00 ± 0.60
GRB030329h	4.86	15.00	10.90	32.90	0.139	16.89	1.7360 ± 0.0030	10.00 ± 1.00
GRB030329i	4.86	22.50	8.40	32.90	0.161	19.39	1.7360 ± 0.0030	11.00 ± 1.00
GRB030329j	4.86	43.00	5.80	32.90	0.183	21.99	1.7360 ± 0.0030	13.00 ± 1.00
GRB030329k	1.43	4.86	32.90	78.60	0.494	59.65	1.7360 ± 0.0030	34.00 ± 3.00
GRB030329l	1.43	8.46	17.30	78.60	0.581	70.15	1.7360 ± 0.0030	40.00 ± 4.00
GRB030329m	1.43	15.00	10.90	78.60	0.633	76.55	1.7360 ± 0.0030	44.00 ± 4.00
GRB030329n	1.43	22.50	8.40	78.60	0.655	79.05	1.7360 ± 0.0030	46.00 ± 5.00
GRB030329o	1.43	43.00	5.80	78.60	0.676	81.65	1.7360 ± 0.0030	47.00 ± 5.00
GRB980425a	4.80	8.64	12.70	18.30	0.093	5.65	1.0000 ± 0.0000	6.00 ± 0.60
GRB980425c	2.50	4.80	18.30	32.70	0.192	14.45	1.0000 ± 0.0000	14.00 ± 1.00
GRB980425d	2.50	8.64	12.70	32.70	0.284	20.05	1.0000 ± 0.0000	20.00 ± 2.00
GRB980425b	1.38	2.50	32.70	47.10	0.325	21.60	1.0000 ± 0.0000	22.00 ± 2.00
GRB980425e	1.38	4.80	18.30	47.10	0.516	36.40	1.0000 ± 0.0000	36.00 ± 4.00
GRB980425f	1.38	8.64	12.70	47.10	0.609	42.00	1.0000 ± 0.0000	42.00 ± 4.00
GRB000418e	4.86	15.00	12.30	27.00	0.140	14.36	1.4600 ± 0.0100	10.00 ± 1.00
GRB000418b	8.46	15.00	12.30	18.10	0.050	5.46	1.4600 ± 0.0100	4.00 ± 0.40
GRB000418c	4.86	8.46	18.10	27.00	0.090	8.56	1.4600 ± 0.0100	6.00 ± 0.60
GRB000418d	4.86	22.50	14.60	27.00	0.160	16.37	1.4600 ± 0.0100	11.00 ± 1.00
GRB000418a	8.46	22.50	14.60	18.10	0.070	7.47	1.4600 ± 0.0100	5.00 ± 0.50
GRB021004a	8.46	22.50	8.70	18.70	0.074	10.2	2.1500 ± 0.0300	5.00 ± 0.50
GRB021004b	4.86	8.46	18.70	32.20	0.088	13.7	2.1500 ± 0.0300	6.00 ± 0.60
GRB021004d	4.86	22.50	8.70	32.20	0.161	23.7	2.1500 ± 0.0300	11.00 ± 1.00
GRB021004c	8.46	15.00	4.10	18.70	0.052	7.89	2.1500 ± 0.0300	4.00 ± 0.40
GRB021004e	4.86	15.00	4.10	32.20	0.139	21.39	2.1500 ± 0.0300	10.00 ± 1.00

9 Conclusion

We have used regression analysis to establish a time correction mechanism for four GRBs (030329, 980425, 000418, and 021004) employed from [12] on the basis of a frequency-dependent speed of light model (FDSL model) which we developed entirely from Maxwell's electromagnetic equations in conjunction with plasma and dispersion effects. In line with this model, on the assumption that these GRBs all leave the source at the same time, we have shown in our previous paper [8] that these four GRBs gave good positive correlations and hence reliable for testing our model. In this paper, however, on the assumption that each individual photon leaves the GRB source at different times, we modify the previous model to obtain a more fitting model. Additionally, the

correction led to the unification of the four GRB into a homogenous albeit perfect correlation which led to the determination of the frequency equivalent of the ISM (ν_s) and hence, the spatial sizes of the internal and external shocks.

If the results provided herein are deemed acceptable or reasonable — *one can on this basis* — make the following tentative conclusion regarding the implication of the spatial sizes of GRB internal and external shocks using our FSDL time delay model:

1. The relationship we have established from our analysis for the four GRBs, clearly supports two GRB models “the framework of the fireball model” and “the multiple shock wave model” of GRBs production and their afterglow.
2. From our regression analysis that here, we can infer that not only is our model reliable and consistent but was used to

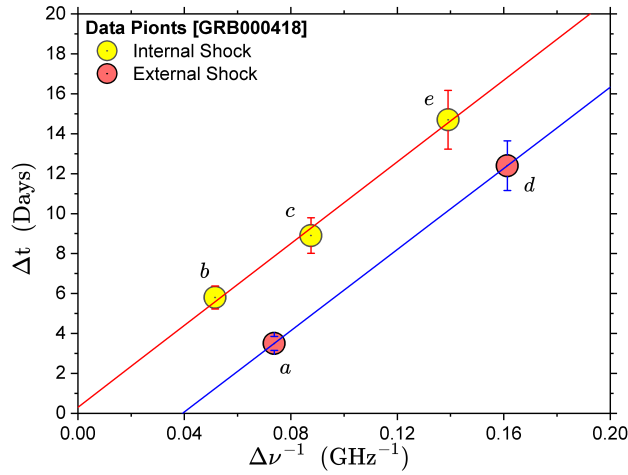


Fig. 7: Graph for Events GRB 000418 (b, c, e) and (a, d). The BLF yields slopes of $S_1 = (102.00 \pm 7.00)x + (4.00 \pm 0.00)$ @ $R^2 = 1.0000$ and $S_2 = (102.00 \pm 0.00)x - (0.30 \pm 0.70)$ @ $R^2 = 0.9949$.

estimate the spatial sizes between the internal and external shocks.

- From our FSDL time delay models and the fitting procedures we employ, we are able to say unequivocally that the internal shocks arise from variations in the relativistic outflows within the jet itself, which offer valuable insights into the acceleration mechanisms and particle interactions occurring within the jet. On the other hand, the external shocks, result from the interaction between the jet and its surrounding medium, which shed light on the environmental conditions and the impact of the jet on its surroundings. This we are able to deduce due to the nature of the differential time in the arrival time of the photons and the vast distances obtained in the spatial sizes between the internal and external shocks.

Furthermore, the determination of the spatial size of γ -ray jets for both internal and external shocks is a crucial endeavour in understanding the dynamics and emission processes of astrophysical jets. We believe that through meticulous observations, corroboration of more data sets and sophisticated modelling techniques for e.g. intense spectral analysis of the radiations from these shocks, 3D modelling of the particle dynamics emanating from the shocks, and magneto-hydrodynamic (MHD) effects, we can be able to unravel the complexities of these high-energetic phenomena.

Acknowledgements

We hereby acknowledge the financial support rendered by the Education, Audio and Culture Executive Agency of the European Commission through the Pan-African Planetary and Space Science Network under funding agreement number 6242.24-PANAF-12020-1-BW-PANAF-MOBAF. Also, we would like to acknowledge the invaluable support from our workstations — The Copperbelt University (Republic of

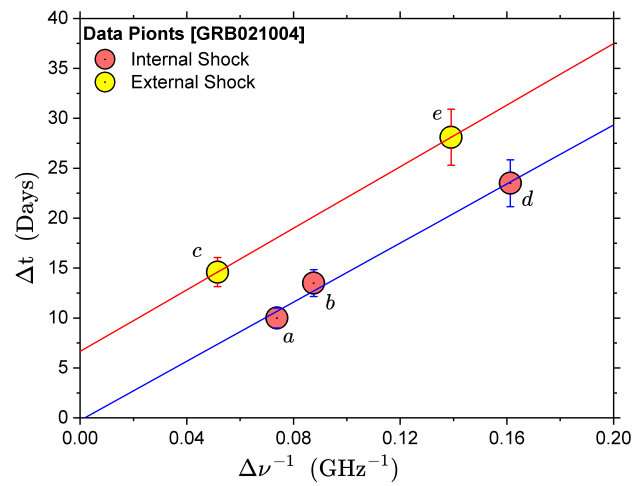


Fig. 8: Graph for Events GRB 021004 (b, c, e) and (a, d). The BLF yields slopes of $S_1 = (150.00 \pm 20.00)x + (0.30 \pm 2.00)$ @ $R^2 = 9.889$ and $S_2 = (154 \pm 0.00)x - (7.00 \pm 0.00)$ @ $R^2 = 1.0000$.

Zambia) and the National University of Science and Technology (Republic of Zimbabwe) for the support rendered in making this work possible.

Submitted on June 17, 2024

References

- Joshi J.C., Chand V., and Razzaque S. Synchrotron and synchrotron self-compton emission components in GRBs detected at very high energies. *Proceedings of the 16th Marcel Grossmann Meeting*, 5–10 July 2021, World Scientific, 2023, 3009–3016.
- Piro L., De Pasquale M., Soffitta P., et al. Probing the environment in gamma-ray bursts: the case of an x-ray precursor, afterglow late onset, and wind versus constant density profile in GRB 011121 and GRB 011211. *The Astrophysical Journal*, 2005, v.623, no.1, 314–324.
- Ze-Cheng Zou, Bin-Bin Zhang, Yong-Feng Huang, and Xiao-Hong Zhao. Gamma-ray burst in a binary system. *The Astrophysical Journal*, 2021, v.921, id2, 1–7.
- Janiuk A. Many faces of accretion in gamma ray bursts. arXiv: 2112.14086, 2021.
- Bromberg O., Nakar E., and Piran T. Are low-luminosity gamma-ray bursts generated by relativistic jets? *The Astrophysical Journal Letters*, 2011, v.739, no.2, L55, 1–12.
- Königl A. Relativistic jets as X-ray and gamma-ray sources. *The Astrophysical Journal*, 1981, v.243, 700–709.
- Kumar P., Zhang B. The physics of gamma-ray bursts & relativistic jets. *Physics Reports*, 2015, v.561, no.12, 1–109.
- Nyambuya G.G., Marusenga S., Abbey G.F., Simpemba P., Simfukwe J. Correlation in gamma-ray burst time delays between pairs of radio photons. *International Journal of Astronomy and Astrophysics*, 2023, v.13, 195–216.
- Hao J.M., Yuan Y.F. Progenitor delay-time distribution of short gamma-ray bursts: Constraints from observations. *Astronomy & Astrophysics*, 2013, v.558, A22.
- Mao Shude. Gravitational lensing, time delay, and gamma-ray bursts. *The Astrophysical Journal*, 1992, v.389, no.2, L41–L44.

11. Zhang B., Zhang B. Gamma-ray burst prompt emission light curves and power density spectra in the ICMART model. *The Astrophysical Journal*, 2014, v.782, no.2, id92, 1–11.
12. Zhang B., Chai Y.T., Zou Y.C., Wu X.F. Constraining the mass of the photon with gamma-ray bursts. *Journal of High Energy Astrophysics*, 2016, v.11–12, 20–28.
13. Ade P.A., Aghanim N., Alves M.I., et al. Planck 2013 results. I. Overview of products and scientific results. *Astronomy & Astrophysics*, 2014, v.571, A1, 1–66.
14. Wright E.L. A cosmology calculator for the world wide web. *Publications of the Astronomical Society of the Pacific*, 2006 v.118, no.850, 1711–1715.
15. Pan Y., Qi J., Cao S., Liu T., Liu Y., Geng S., Lian Y., Zhu Z.H. Model-independent constraints on Lorentz invariance violation: implication from updated Gamma-ray burst observations. *The Astrophysical Journal*, 2020 v.890, no.2, id169, 1–7.
16. Burgess J.M., Bégué D., Greiner J., Giannios D., Bacelj A., Berlato F. Gamma-ray bursts as cool synchrotron sources. *Nature Astronomy*, 2020 v.4, no.2, 174–179.
17. Fraija N., De Colle F., Veres P., Dichiaro S., Duran R.B., A.C. Caligula do E.S. Pedreira, Galvan-Gamez A., Kamenetskaia B.B. Description of atypical bursts seen slightly off-axis. *The Astrophysical Journal*, 2020, v.896, no.1, id25, 1–22.
18. Alexander K.D., Laskar T., Berger E., Johnson M.D., Williams P.K., Dichiaro S., Fong W.F., Gomboc A., Kobayashi S., Margutti R., Mundell C.G. An unexpectedly small emission region size inferred from strong high-frequency diffractive scintillation in GRB 161219B. *The Astrophysical Journal*, 2019, v.870, no.2, id67, 1–12.
19. Taylor G.B., Frail D.A., Berger E., Kulkarni S.R. The angular size and proper motion of the afterglow of GRB 030329. *The Astrophysical Journal*, 2004 v.609, no.1, L1, 1–3.
20. Eichler D., Levinson A. A compact fireball model of gamma-ray bursts. *The Astrophysical Journal*, 2000, v.529, no.1, 146–150.
21. Piran T. Gamma-ray bursts and the fireball model. *Physics Reports*, 1999, v.314, no.6, 575–667.
22. Fox D.B., Mészáros P. GRB fireball physics: prompt and early emission. *New Journal of Physics*, 2006, v.8, 199–223.
23. Ciolfi R. Short gamma-ray burst central engines. *International Journal of Modern Physics D*, 2018, v.27, no.13, 1842004.
24. Levan A.J., Tanvir N.R., Starling R.L., Wiersema K., Page K.L., Perley D.A., Schulze S., Wynn G.A., Chornock R., Hjorth J., Cenko S.B. A new population of ultra-long duration gamma-ray bursts. *The Astrophysical Journal*, 2014, v.781, no.1, A13, 1–13.
25. Thompson C. A model of gamma-ray bursts. *Monthly Notices of the Royal Astronomical Society*, 1994, v.270, no.3, 480–498.
26. Mészáros P. The fireball shock model of gamma ray bursts. *AIP Conference Proceedings 2000, Jun 23*, v.522, no.1, 213–225.
27. Sarin N., Lasky P.D., Ashton G. X-ray afterglows of short gamma-ray bursts: Magnetar or Fireball? *The Astrophysical Journal*, 2019, v.872, no.1, id114, 1–6.
28. Kopač D., Mundell C.G., Japelj J., Arnold D.M., Steele I.A., Guidorzi C., Dichiaro S., Kobayashi S., Gomboc A., Harrison R.M., Lamb G.P. Limits on optical polarization during the prompt phase of GRB 140430A. *The Astrophysical Journal*, 2015, v.813, no.1, id1, 1–14.
29. McDowell A., MacFadyen A. Revisiting the parameter space of binary neutron star merger event GW170817. *The Astrophysical Journal*, 2023, v.945, no.2, id135, 1–8.
30. Willingale R., Mészáros P. Gamma-ray bursts and fast transients: multi-wavelength observations and multi-messenger signals. *Space Science Reviews*, 2017, v.207, 63–86.
31. Capozziello S., Lambiase G. The emission of Gamma Ray Bursts as a test-bed for modified gravity. *Physics Letters B*, 2015, v.750, 344–347.
32. Wang Y., Jiang L.Y., Ren J. GRB 201104A: A “repetitive” short gamma-ray burst? *The Astrophysical Journal*, 2022, v.935, no.2, id179, 1–10.
33. Fraija N., Veres P. The origin of the optical flashes: The case study of GRB 080319B and GRB 130427A. *The Astrophysical Journal*, 2018, v.859, no.1, id70, 1–9.
34. Fan X., Messenger C., Heng I.S. Probing intrinsic properties of short gamma-ray bursts with gravitational waves. *Physical Review Letters*, 2017, v.119, no.18, 181102.
35. Abbott B.P., Abbott R., Abbott T.D., et al. Gravitational waves and gamma-rays from a binary neutron star merger: GW170817 and GRB 170817A. *The Astrophysical Journal Letters*, 2017, v.848, no.2, L13, 1–7.
36. Pe’Er A. Physics of Gamma-Ray Bursts Prompt Emission. *Advances in Astronomy*, 2015, no.1, 907321.
37. Piran T. The physics of gamma-ray bursts. *Reviews of Modern Physics*, 2004 v.76, no.4, 1143–1210.
38. Yu Y.W., Gao H., Wang F.Y., Zhang B.B. Gamma-Ray Bursts. *Handbook of X-ray and Gamma-ray Astrophysics*, Springer Nature Reference Book, Singapore, 2022, 34 pages.
39. Dado S., Dar A., De Rújula A. Critical Tests of Leading Gamma Ray Burst Theories. *Universe*, 2022, v.8, no.7, 350–395.
40. Yost S.A., Harrison F.A., Sari R., Frail D.A. A study of the afterglows of four gamma-ray bursts: constraining the explosion and fireball model. *The Astrophysical Journal*, 2003, v.597, no.1, 459–473.
41. Oates S.R., Page M.J., Schady P., et al. A statistical study of gamma-ray burst afterglows measured by the Swift Ultraviolet Optical Telescope. *Monthly Notices of the Royal Astronomical Society*, 2009, 395, no.1, 490–503.
42. Chandra P., Frail D.A. A radio-selected sample of gamma-ray burst afterglows. *The Astrophysical Journal*, 2012, v.746, no.2, id156, 1–28.
43. Fay S. Λ CDM periodic cosmology. *Monthly Notices of the Royal Astronomical Society*, 2020, v.494, no.2, 2183–2190.
44. Stanek K.Z., Matheson T., Garnavich P.M., et al. Spectroscopic discovery of the supernova 2003dh associated with GRB 030329. *The Astrophysical Journal*, 2003, v.591, no.1, L17, 1–3.
45. Hurley K., Sommer M., Atteia J.L., Boer M., Cline T., Cotin F., Henoux J.C., Kane S., Lowes P., Niel M. The solar X-ray/cosmic gamma-ray burst experiment aboard ULYSSES. *Astronomy and Astrophysics Supplement Series*, 1992, v.92, no.2, 401–410.
46. Bloom J.S., Berger E., Kulkarni S.R., Djorgovski S.G., Frail D.A. The redshift determination of GRB 990506 and GRB 000418 with the Echelle Spectrograph Imager on Keck. *The Astronomical Journal*, 2003, v.125, no.3, 999–1005.
47. Klose S., Stecklum B., Masetti N., et al. The very red afterglow of GRB 000418: Further evidence for dust extinction in a gamma-ray burst host galaxy. *The Astrophysical Journal*, 2000, v.545, no.1, 271–276.
48. Waxman E. The nature of GRB 980425 and the search for off-axis gamma-ray burst signatures in nearby Type Ib/c supernova emission. *The Astrophysical Journal*, 2004, v.602, no.2, 886–891.
49. Aad G., Abajyan T., Abbott B., Abdallah J., Khalek S.A., Abdelalim A.A., Aben R., Abi B., Abolins M., AbouZeid O.S., Abramowicz H. Observation of a new particle in the search for the Standard Model Higgs boson with the ATLAS detector at the LHC. *Physics Letters B*, 2012, v.716, no.1, 1–29.
50. Zhang B. A possible connection between fast radio bursts and gamma-ray bursts. *The Astrophysical Journal Letters*, 2013, v.780, no.2, L21, 1–4.
51. Jackson N. The hubble constant. *Living Reviews in Relativity*, 2015, v.18, v.1, 1–52.

52. Parker B.R. *The Vindication of the Big Bang: Breakthroughs and Barriers*. Springer Verlag, 2013.
53. Lian Y., Cao S., Biesiada M., Chen Y., Zhang Y., Guo W. Probing modified gravity theories with multiple measurements of high-redshift quasars. *Monthly Notices of the Royal Astronomical Society*, 2021, v.505, no.2, 2111–2123.
54. Salpeter E.E., Hoffman Jr G.L. The galaxy luminosity function and the redshift-distance controversy (a review). *Proceedings of the National Academy of Sciences*, 1986, v.83, no.10, 3056-3063.
55. Hubble E. A relation between distance and radial velocity among extragalactic nebulae. *Proceedings of the National Academy of Sciences*, 1929, v.15, no.3, 168-173.
56. Davis T. An expanding controversy. *Science*, 2019 v.365, no.6458, 1076–1077.
57. Aghanim N., Akrami Y., Ashdown M., et al. Planck 2018 results-VI. Cosmological parameters. *Astronomy & Astrophysics*, 2020, v.641, A6, 1–67.
58. Grošelj D., Sironi L., Spitkovsky A. Long-term evolution of relativistic unmagnetized collisionless shocks. *The Astrophysical Journal Letters*, 2024, v.963, no.2, L44, 1–8.
59. Kathirgamaraju A., Duran R.B., Giannios D. GRB off-axis afterglows and the emission from the accompanying supernovae. *Monthly Notices of the Royal Astronomical Society*, 2016, v.461, no.2, 1568-1575.
60. Bégué D., Burgess J.M. The anatomy of a long gamma-ray burst: a simple classification scheme for the emission mechanism(s). *The Astrophysical Journal*, 2016, v.820, no.1, id68, 1–6.
61. Sarin N., Hamburg R., Burns E., Ashton G., Lasky P.D., Lamb G.P. Low-efficiency long gamma-ray bursts: a case study with AT2020blt. *Monthly Notices of the Royal Astronomical Society*, 2022, v.512, no.1, 1391-1399.
62. Arimoto M., Asano K., Ohno M., Veres P., Axelsson M., Bissaldi E., Tachibana Y., Kawai N. High-energy non-thermal and thermal emission from GRB 141207A detected by Fermi. *The Astrophysical Journal*, 2016, v.833, no.2, id139, 1–13.
63. Zhang B.T., Murase K., Ioka K., Song D., Yuan C., Mészáros P. External inverse-Compton and proton synchrotron emission from the reverse shock as the origin of VHE gamma rays from the hyper-bright GRB 221009A. *The Astrophysical Journal Letters*, 2023, v.947, no.1, L14, 1–7.
64. Axelsson M., Borgonovo L. The width of gamma-ray burst spectra. *Monthly Notices of the Royal Astronomical Society*, 2015, v.447, no.4, 3150–3154.
65. Re'em S., Piran T. Hydrodynamic timescales and temporal structure of gamma-ray bursts. *The Astrophysical Journal*, 1995, v.455, no.2, L143–L146.
66. Rees M.J., Mészáros P. Unsteady outflow models for cosmological gamma-ray bursts. arXiv: astro-ph/9404038, 1994.
67. Fraija N., Duran R.B., Dichiara S., Beniamini P. Synchrotron self-Compton as a likely mechanism of photons beyond the synchrotron limit in GRB 190114C. *The Astrophysical Journal*, 2019, v.883, no.2, id162, 1–13.
68. Lenard P. Ueber die lichtelektrische Wirkung. *Annalen der Physik*, 1902, Bd.313, No.5, 149–198.

Graph Theory Entropy Values for Lepton and Quark Discrete Symmetry Quantum States and Their Decay Channels

Franklin Potter

Sciencegems, 8642 Marvale Drive, Huntington Beach, CA, United States. E-mail: frank11hb@yahoo.com

We assume that each lepton family and each quark family represents its own unique discrete symmetry modular group, one which is also a binary subgroup of SU(2). Equivalently, we have a different regular 3-D polyhedral group for each lepton family and a different regular 4-D polytope group for each quark family. Being discrete symmetry subgroups representing 3-D and 4-D geometric objects that are known also as complete graphs, they each possess a different graph theory entropy based upon the number of connected paired vertices. We examine the various decay channels of the leptons and the quarks that obey all the conservation laws as well as the special theory of relativity to look for a violation of a fundamental graph theory entropy inequality constraint. Such a violation and its experimental verification would confirm the importance of graph theory entropy in particle physics.

1 Introduction

The identification of the symmetry group or groups for the lepton families and for the quark families of the Standard Model (SM) has been an interesting challenge for decades. In recent years there has been an emphasis on the discrete symmetry modular groups [1] such as $\Gamma_3 = A_4$, $\Gamma_4 = S_4$, $\Gamma_5 = A_5$, as well as their double groups Γ'_3 , Γ'_4 , and Γ'_5 , where the A_4 , S_4 , and A_5 refer to equivalent permutation groups. These discrete symmetry modular groups not only connect directly to a top-down approach using superstring concepts (see e.g. [2, 3] for recent reviews) but also represent the discrete symmetries of the regular polyhedrons in R^3 . However, no discrete symmetry group or set of discrete symmetry groups has been accepted yet, even though neutrino mass values are predicted, because the true mass values for the neutrinos are not known for direct comparison [4].

In a series of articles and conference presentations since 1987 we have proposed [5–7] that each lepton family represents a unique discrete symmetry binary subgroup of the continuous group SU(2), or equivalently, of the quaternion group Q and the modular group. That is, they represent the only finite quaternion subgroups that enclose a 3-D volume. Specifically, the electron family (ν_e, e^-) represents $2T = (3,3,2) = \Gamma'_3$, the muon family (ν_μ, μ^-) represents $2O = (3,4,2) = \Gamma'_4$, and the tau family (ν_τ, τ^-) represents $2I = (3,5,2) = \Gamma'_5$, where the first and second group notations are also the familiar geometrical names for the 3-D regular polyhedron groups, i.e. the Platonic solids in R^3 . As subgroups of SU(2), there is an upper and lower quantum state in each family.

We proposed also [5, 6] that quark families represent the related discrete symmetry groups for the 4-D regular polytopes that enclose a volume, (3,3,3) for the (u, d) family, (3,3,4) for the (c, s) family, (3,4,3) for the (t, b) family, and (3,3,5) for the predicted 4th quark family, i.e. a top/bottom family (t', b') or (T, B). Of course, the predicted 4th quark






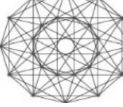
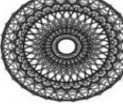
family (T, B) has not been discovered yet, but its existence might resolve several problems within the SM and would increase the value of the Jarlskog constant for the baryon asymmetry of the Universe (BAU) by a factor of about 10^{13} [8].

How do we know that the lepton families and the quark families represent these particular discrete symmetry groups? By imposing the conservation of total lepton family number as the rationale for lepton family mixing and the conservation of total baryon number as the rationale for quark family mixing, we derived the lepton mixing matrix and the quark mixing matrix from first principles without any free parameters [6]. That is, with these discrete symmetry groups, by having a linear superposition of their quaternion group generators for the lepton families and separately for the quark families, we could mimic the continuous symmetry group SU(2) for each and therefore meet the continuous symmetry requirement of Noether's theorem [9] for a conservation law.

All 9 predicted elements of the lepton 3x3 Pontecorvo-Maki-Nakagawa-Sakata (PMNS) mixing matrix match the experimentally determined value ranges, while 8 of 9 elements in the quark 3x3 Cabibbo-Kobayashi-Maskawa (CKM) agree with experimentally determined value ranges, with only the V_{ub} element disagreeing. Of course, with 4 quark families predicted, one has a 4x4 quark mixing matrix CKM4, and we predict reasonable values for the 4th column and the 4th row. Our values also agree with recent concerns that the first row of the normal 3x3 CKM matrix does not sum to unity (for a review see [10, 11]).

However, this mismatch of family numbers, 4 to 3, might raise concerns for triangle anomaly cancellations, which normally cancel with 3 lepton families matching 3 quark families 1-to-1. But we have the cancellation because the lepton families and quark families separately form linear superpositions to each collectively mimic SU(2), so the anomaly cancellation still occurs via quark SU(2) negative contribution against lepton SU(2) positive contribution.

Table 1: Fermion Group and Graph Entropy Assignments

Family	ν_e, e^-	ν_μ, μ^-	ν_τ, τ^-	u, d	c, s	t, b	T, B
Group	(332)	(342)	(352)	(333)	(334)	(343)	(335)
Graph							
n	4	6	12	5	8	24	120
H	2.0	2.585	3.585	2.322	3.0	4.585	6.907

In addition to providing the rationale for the lepton family mixing and for the quark family mixing, we predicted [7] a normal neutrino mass hierarchy (NH) to the neutrino mass values with $m_1 = 0.3$ meV, $m_2 = 8.9$ meV, and $m_3 = 50.7$ meV, reasonable mass values just within the proposed cosmological constraint limit of 60 meV [12]. We await further experiments that will determine the actual neutrino mass values in the near future.

In the following, we utilize the mathematical graph theory property that each discrete symmetry group represents a 3-D or 4-D complete graph and that graph theory identifies an entropy for each complete graph that is determined by its number of vertices, or nodes. This graph theory entropy is not the entropy normally considered in the decay of particles but is an additional entropy to be considered.

Why do we investigate graph theory entropy for these lepton family and quark family discrete symmetries? Because if space happens to be discrete at the Planck scale of about 10^{-35} meters, then this graph entropy could be important. The hope is that we might encounter a graph theory entropy forbidden decay that is allowed by all the known conservation laws and the special theory of relativity (STR). This constraint placed by these graph entropy values for the decays of the leptons and the quarks could either provide further support for the possible existence of a 4th quark family or possibly eliminate a 4th quark family. Therefore, an investigation into the properties and predictions of graph theory entropy seems justified.

2 Graph entropy

Each lepton family and each quark family is represented by a complete undirected graph as illustrated in Table 1, meaning that every pair of distinct vertices is connected by a unique edge [13]. A complete graph G with n vertices has a graph theory entropy

$$H(G) = \log_2 n, \tag{1}$$

and given two complete graphs G_1 and G_2 their union entropy

$$H(G_1 \cup G_2) \leq H(G_1) + H(G_2). \tag{2}$$

Therefore the two resulting graphs must have at least the entropy of the original graph. So when a lepton or a quark decays, the total graph entropy of the particle products of the

decay must be at least equal to the graph entropy of the decaying particle or else the decay cannot occur.

As an example, consider the weak interaction decay of the muon μ^- first to the W^- plus the muon neutrino, and then the W decays:

$$\mu^- \rightarrow W^- + \nu_\mu \rightarrow e^- + \bar{\nu}_e + \nu_\mu. \tag{3}$$

In Table 1 are given the entropy values for the lepton families and the quark families. The entropy $H(\mu^-) = 2.585$, and the final products of the decay sum to a total entropy 6.585, so the entropy inequality condition is met,

$$H(e^- + \bar{\nu}_e + \nu_\mu) > H(\mu^-) \tag{4}$$

as expected for this prevalent decay channel for the muon.

Tables 2 and 3 contain the entropy values for spontaneous decay channels for the leptons and for spontaneous semileptonic decay channels for the quarks that obey the conservation laws and the special theory of relativity (STR). I have included decay channels for a predicted 4th quark family (T,B).

The up quark in the 1st quark family has a smaller mass than its down quark partner, so a spontaneous decay channel is not available to the down quark, and therefore no decay channel is shown even though given enough energy in a proton-proton collision, for example, the up quark in a proton can change into a down quark to produce a neutron plus a positron and electron neutrino.

Table 4 provides the entropy values for spontaneous quark decays to a different quark plus a meson. With no evidence for the predicted 4th quark family and for the mass values of the T and B quarks, the last two columns contain entropy values for both reasonable decay channels as well as possibly some forbidden decay channels. The predicted mass values for the B and T quarks are estimated by using a four family Koide formula [14].

Intermediate stages in each decay process involve a weak interaction boson, a W or a Z, which have the extremely short lifetime [4] of about 3×10^{-25} seconds. Alternative quantum states for the W's and Z can be expressed in terms of the discrete symmetry of the 2I group as the direct product $2I \times 2I'$, where $2I'$ is the group 2I with one of its quaternion generators modified to provide "reciprocal" operations to ensure that

Table 2: Final Graph Entropy Values for Lepton Decays

Particle	Mass (MeV)	Group	H	Decay Channel Total H	
				$e^- + \bar{\nu}_e + \nu_\mu$	$\mu^- + \bar{\nu}_\mu + \nu_\tau$
e^-	0.511	(332)	2.0		
μ^-	105.66	(342)	2.585	6.585	
τ^-	1776.84	(352)	3.585	7.585	8.755

all 7 families properly experience the weak interaction [15]. Therefore,

$$W^+ = |\nu_\tau\rangle|\tau^+\rangle \quad (5)$$

$$Z^0 = (|\nu_\tau\rangle|\bar{\nu}_\tau\rangle + |\tau^-\rangle|\tau^+\rangle)/\sqrt{2} \quad (6)$$

$$W^- = |\tau^-\rangle|\bar{\nu}_\tau\rangle \quad (7)$$

$$\gamma = (|\nu_\tau\rangle|\bar{\nu}_\tau\rangle - |\tau^-\rangle|\tau^+\rangle)/\sqrt{2}. \quad (8)$$

In each expression for an electroweak (EW) boson there exists the product of two identical complete graphs for the tau family representing the discrete symmetry groups 2I and 2I'. Each group in the product uses the same 12 vertices as the single tau family graph for 2I and therefore this product has the same graph theory entropy value as the tau family entropy $H = 3.585$. The W and Z bosons, having the extremely short lifetimes, immediately decay to the various long-lived final states which have final graph theory entropies that are expected to obey the graph entropy inequality in (2).

3 Discussion

We have applied graph theory entropy to lepton and quark decay channels. We had hoped to encounter some forbidden decays as a result of additional graph theory entropy restrictions for decays that are allowed by the normal conservation laws and STR. That is, we looked for forbidden decays that would violate the final state graph entropy inequality in (2):

$$H(G_1 \cup G_2) \leq H(G_1) + H(G_2)$$

where $G_1 \cup G_2$ represents the initial decaying particle state graph and G_1 and G_2 are the final state particle graphs.

We did find two decays that are in violation of this graph entropy inequality in two separate channels, both of them for 4th quark family T and B semileptonic decays to the (u, d) quark family plus the electron family as shown by the two underlined and bold entries in Table 3. These decays:

$$T^{+2/3} \rightarrow d^{-1/3} + W^+ \rightarrow d^{-1/3} + e^+ + \nu_e \quad (9)$$

$$B^{-1/3} \rightarrow u^{+2/3} + W^- \rightarrow u^{+2/3} + e^- + \bar{\nu}_e \quad (10)$$

satisfy all normal constraints but would be prohibited in graph theory because the initial graph entropy of 6.907 would result in a final graph entropy of 6.322, a violation of the graph entropy inequality rule. No other violations were found in the decay channels.

Unfortunately, we have no evidence that the 4th quark family actually exists, so we cannot check Nature for this violation yet. Therefore, we must wait for the opportunity in the future should the T and B quarks make their existence known.

Acknowledgements

We thank Sciencegems for continued support and for encouragement to investigate various challenges in particle physics.

Received on July 18, 2024

References

1. Feruglio F. Are neutrino masses modular forms? arXiv: hep-ph/1706.08749.
2. Ding G. J. and King S. F. Neutrino Mass and Mixing with Modular Symmetry. arXiv: hep-ph/2311.09282.
3. Kobayashi T. and Tanimoto M. Modular flavor symmetric models. arXiv: hep-ph/2307.03384.
4. Navas S. *et al.* (Particle Data Group) Neutrino Properties. *Phys. Rev. D*, 2024, v. 110, 030001.
5. Potter F. Geometrical Basis for the Standard Model. *Int. J. of Theor. Phys.*, 1994, v. 33, 279–305.
6. Potter F. CKM and PMNS mixing matrices from discrete subgroups of SU(2). *J. Phys: Conf. Ser.*, 2015, v. 631, 012024.
7. Potter F. Fermion Mass Derivations: I. Neutrino Masses via the Linear Superposition of the 2T, 2O, and 2I Discrete Symmetry Subgroups of SU(2). *Prog. in Phys.*, 2023, v. 19 (1), 55–61. Online: <https://progress-in-physics.com/2023/PP-65-06.PDF>
8. Hou W. S. Source of CP Violation for the Baryon Asymmetry of the Universe. *Int. J. of Mod. Phys.*, v. D20, 2011, 1521–1532. arXiv: hep-ph/1101.2161v1.
9. Baez J. Noether's Theorem in a Nutshell. accessed 12 July 2024. <https://math.ucr.edu/home/baez/noether.html>.
10. Kitahara T. Theoretical point of view on Cabibbo angle anomaly. arXiv: hep-ph/2407.00122v1.
11. Alexandrou C. *et al.* Inclusive hadronic decay rate of the τ lepton from lattice QCD: the $\bar{u}s$ flavour channel and the Cabibbo angle. arXiv: hep-ph/2403.05404v2.
12. Noriega H. E. and Aviles A. Unveiling Neutrino Masses: Insights from Robust (e)BOSS Data Analysis and Prospects for DESI and Beyond. arXiv: astro-ph/2407.06117v1.
13. Wikipedia contributors. Graph Entropy. In *Wikipedia, the Free Encyclopedia*. 2024 May 15, retrieved 14:02, July 13, 2024, from <https://w.wiki/Aewq>.
14. Kocik J. The Koide Lepton Mass Formula and the Geometry of Circles. arXiv: physics.gen-ph/1201.2067v1.
15. Potter F. Elimination of Anomalies Reported for $b \rightarrow s\ell\ell$ and $b \rightarrow c\ell\bar{\nu}_\ell$ Semi-Leptonic Decay Ratios $R(K, K^*)$ and $R(D, D^*)$ when the Lepton Families Represent Discrete Symmetry Binary Subgroups 2T, 2O, 2I of SU(2). *Prog. in Phys.*, 2018, v. 14 (4), 185–188. Online: <https://progress-in-physics.com/2018/PP-55-01.PDF>.

Table 3: Final Graph Entropy Values for Quark Semileptonic Decays

Quark	$u^{+2/3}$	$d^{-1/3}$	$c^{+2/3}$	$s^{-1/3}$	$t^{+2/3}$	$b^{-1/3}$	$T^{+2/3}$	$B^{-1/3}$
Mass	2.3 MeV	4.8 MeV	127.5 MeV	95 MeV	173.2 GeV	4.8 GeV	3.4 TeV	95 GeV
Group <i>H</i>	(333) 2.322	(334) 3.0	(343) 4.585	(335) 6.907				
Decay Channel								
$d^{-1/3} + e^+ + \nu_e$			6.322		6.322		<u>6.322</u>	
$u^{+2/3} + e^- + \bar{\nu}_e$	6.322			6.322		6.322		<u>6.322</u>
$s^{-1/3} + e^+ + \nu_e$			7.0		7.0		7.0	
$c^{+2/3} + e^- + \bar{\nu}_e$						7.0		7.0
$b^{-1/3} + e^+ + \nu_e$					8.585		8.585	
$t^{+2/3} + e^- + \bar{\nu}_e$					10.907		10.907	
$B^{-1/3} + e^+ + \nu_e$								
$T^{+2/3} + e^- + \bar{\nu}_e$								
$d^{-1/3} + \mu^+ + \nu_\mu$			7.492		7.492		7.492	
$u^{+2/3} + \mu^- + \bar{\nu}_\mu$						7.492		7.492
$s^{-1/3} + \mu^+ + \nu_\mu$					8.17		8.17	
$c^{+2/3} + \mu^- + \bar{\nu}_\mu$						8.17		8.17
$b^{-1/3} + \mu^+ + \nu_\mu$					9.755		9.755	
$t^{+2/3} + \mu^- + \bar{\nu}_\mu$					12.077		12.077	
$B^{-1/3} + \mu^+ + \nu_\mu$								
$T^{+2/3} + \mu^- + \bar{\nu}_\mu$								
$d^{-1/3} + \tau^+ + \nu_\tau$					9.492		9.492	
$u^{+2/3} + \tau^- + \bar{\nu}_\tau$						9.492		9.492
$s^{-1/3} + \tau^+ + \nu_\tau$					10.17		10.17	
$c^{+2/3} + \tau^- + \bar{\nu}_\tau$						10.17		10.17
$b^{-1/3} + \tau^+ + \nu_\tau$					11.755		11.755	
$t^{+2/3} + \tau^- + \bar{\nu}_\tau$					14.077		14.077	
$B^{-1/3} + \tau^+ + \nu_\tau$								
$T^{+2/3} + \tau^- + \bar{\nu}_\tau$								

Table 4: Final Graph Entropy Values for Quark Decay Channels to Mesons

Quark	$u^{+2/3}$	$d^{-1/3}$	$c^{+2/3}$	$s^{-1/3}$	$t^{+2/3}$	$b^{-1/3}$	$T^{+2/3}$	$B^{-1/3}$
Mass	2.3 MeV	4.8 MeV	127.5 MeV	95 MeV	173.2 GeV	4.8 GeV	3.4 TeV	95 GeV
Group H	(333) 2.322		(334) 3.0		(343) 4.585		(335) 6.907	
Decay Channel								
$u + d\bar{u}$				6.966		6.966		6.966
$u + s\bar{c}$						8.322		8.322
$c + d\bar{u}$						7.644		7.644
$c + s\bar{c}$						9.0		9.0
$d + d\bar{u}$			6.966		6.966		6.966	
$d + s\bar{c}$			8.322		8.322		8.322	
$d + b\bar{t}$							11.492	
$s + d\bar{u}$					7.644		7.644	
$s + s\bar{c}$					9.0		9.0	
$s + b\bar{t}$							12.17	
$b + d\bar{u}$					9.229		9.229	
$b + s\bar{c}$					10.585		10.585	
$b + b\bar{t}$							13.755	
$B + d\bar{u}$							11.551	
$B + s\bar{c}$							12.907	
$B + b\bar{t}$							16.077	

PROGRESS IN PHYSICS

A Scientific Journal on Advanced Studies in Theoretical and Experimental Physics, including Related Themes from Mathematics. This journal is registered with the Library of Congress (DC, USA).

Electronic version of this journal:
<https://www.progress-in-physics.com>

Editorial Board

Dmitri Rabounski
rabounski@yahoo.com
Pierre Millette
pierremillette@sympatico.ca
Andreas Ries
andreasries@yahoo.com
Florentin Smarandache
fsmarandache@gmail.com
Larissa Borissova
lborissova@yahoo.com
Ebenezer Chifu
ebenechifu@yahoo.com

Postal Address

Department of Mathematics and Science,
University of New Mexico,
705 Gurley Ave., Gallup, NM 87301, USA

Copyright © *Progress in Physics*, 2024

All rights reserved. The authors of the articles do hereby grant *Progress in Physics* non-exclusive, worldwide, royalty-free license to publish and distribute the articles in accordance with the Budapest Open Initiative: this means that electronic copying, distribution and printing of both full-size version of the journal and the individual papers published therein for non-commercial, academic or individual use can be made by any user without permission or charge. The authors of the articles published in *Progress in Physics* retain their rights to use this journal as a whole or any part of it in any other publications and in any way they see fit. Any part of *Progress in Physics* howsoever used in other publications must include an appropriate citation of this journal.

This journal is powered by L^AT_EX

A variety of books can be downloaded free from the Digital Library of Science:
<http://fs.gallup.unm.edu/ScienceLibrary.htm>

ISSN: 1555-5534 (print)
ISSN: 1555-5615 (online)

Standard Address Number: 297-5092
Printed in the United States of America

December 2024

Vol. 20, Issue 2

CONTENTS

Borissova L., Rabounski D. Galileo's Principle and the Origin of Gravitation According to General Relativity	69
Rabounski D. Introducing the Space Metric of a Rotating Massive Body and Four New Effects of General Relativity	79
Potter F. Galaxy Clusters: Quantum Celestial Mechanics (QCM) Rescues MOND? ...	100
Morozov N. A. On the Possibility of a Scientific Prognosis of the Weather with the Introduction of Galactic Impacts into Analysis	103
Marquet P. Yang-Mills Theory in the Framework of General Relativity	108
Nyambuya G. G. On a Plausible Solution to the Hubble Tension via the Hypothesis of Cosmologically Varying Fundamental Natural Constants	112
Ellis R. I: Evidence for Phenomena, Including Magnetic Monopoles, Beyond 4-D Space-Time, and Theory Thereof	127
Ellis R. II: Preliminary Evidence for a Second Time Dimension Directed from the Future to the Past, and for Unification	135

Information for Authors

Progress in Physics has been created for rapid publications on advanced studies in theoretical and experimental physics, including related themes from mathematics and astronomy. All submitted papers should be professional, in good English, containing a brief review of a problem and obtained results.

All submissions should be designed in L^AT_EX format using *Progress in Physics* template. This template can be downloaded from *Progress in Physics* home page <http://www.ptep-online.com>

Preliminary, authors may submit papers in PDF format. If the paper is accepted, authors can manage L^AT_EX typing. Do not send MS Word documents, please: we do not use this software, so unable to read this file format. Incorrectly formatted papers (i.e. not L^AT_EX with the template) will not be accepted for publication. Those authors who are unable to prepare their submissions in L^AT_EX format can apply to a third-party payable service for LaTeX typing. Our personnel work voluntarily. Authors must assist by conforming to this policy, to make the publication process as easy and fast as possible.

Abstract and the necessary information about author(s) should be included into the papers. To submit a paper, mail the file(s) to the Editor-in-Chief.

All submitted papers should be as brief as possible. Short articles are preferable. Large papers can also be considered. Letters related to the publications in the journal or to the events among the science community can be applied to the section *Letters to Progress in Physics*.

All that has been accepted for the online issue of *Progress in Physics* is printed in the paper version of the journal. To order printed issues, contact the Editors.

Authors retain their rights to use their papers published in *Progress in Physics* as a whole or any part of it in any other publications and in any way they see fit. This copyright agreement shall remain valid even if the authors transfer copyright of their published papers to another party.

Electronic copies of all papers published in *Progress in Physics* are available for free download, copying, and re-distribution, according to the copyright agreement printed on the titlepage of each issue of the journal. This copyright agreement follows the *Budapest Open Initiative* and the *Creative Commons Attribution-Noncommercial-No Derivative Works 2.5 License* declaring that electronic copies of such books and journals should always be accessed for reading, download, and copying for any person, and free of charge.

Consideration and review process does not require any payment from the side of the submitters. Nevertheless the authors of accepted papers are requested to pay the page charges. *Progress in Physics* is a non-profit/academic journal: money collected from the authors cover the cost of printing and distribution of the annual volumes of the journal along the major academic/university libraries of the world. (Look for the current author fee in the online version of *Progress in Physics*.)

Galileo's Principle and the Origin of Gravitation According to General Relativity

Larissa Borissova and Dmitri Rabounski

Puschino, Moscow Region, Russia

E-mail: rabounski@yahoo.com, lborissova@yahoo.com

Using the chronometrically invariant notation of General Relativity (chronometric invariants are the physically observable projections of four-dimensional quantities onto the time line and the three-dimensional space of an observer), we deduce Galileo's principle and Newton's law of gravitation as a particular case of the chr.inv.-formula for the gravitational inertial force acting in the four-dimensional pseudo-Riemannian space (space-time of General Relativity). This is a "mathematical bridge", connecting the empirical laws of Newton's theory of gravitation with the purely geometric laws of General Relativity. We also show that the origin of the gravitational field in the space of the Schwarzschild mass-point metric is a spherical surface that surrounds any mass-point at a very small radius, equal to the gravitational radius calculated for the mass. There, on the spherical surface, a breaking of the three-dimensional observable space takes place, and the observer's physical observable time stops. It is not possible to get these results using the general covariant notation of General Relativity, because physically observable quantities in the general covariant notation are not mathematically defined.

We dedicate this article to Prof. Kyril Stanyukovich (1916–1989), our long friendly conversations with whom in the 1980s formed the basis of this study 40 years later and prompted us to write this article.

1 Problem statement

Our closest colleague, patron and friend over decades was Prof. Kyril Stanyukovich (1916–1989). In addition to his groundbreaking works on gas dynamics and super-powerful non-nuclear ammunition, he was also a prominent researcher in the field of General Relativity; see [1–4] and References therein. Over many years in the 1980s, he repeatedly focused our attention onto a still unsolved problem: in the framework of Riemannian geometry (which is the basis of General Relativity), the fundamental laws of Newtonian classical mechanics have not yet been mathematically deduced as an unambiguous special case of the purely geometric laws of General Relativity.

This problem was also pointed out earlier by Alexei Petrov (1910–1972), the outstanding scientist in the field of General Relativity, who in 1950 introduced an algebraic classification of the spaces (and the gravitational fields) known in the framework of General Relativity [5–8]. This classification is called the Petrov classification of Einstein spaces thanks to his monograph *Einstein Spaces* [7], first published in 1961.

In our personal opinion, the fundamental laws of Newtonian classical mechanics have not yet been deduced as a special case of the geometric laws of General Relativity only because the researchers, who worked on this problem earlier, used the *general covariant notation* of General Relativity. In the framework of the general covariant notation, physically observable quantities are not mathematically determined. As

a result, there is no clear mathematical transition from the four-dimensional quantities of General Relativity to the three-dimensional quantities of Newton's theory, which are measurable in experiment.

In this paper, we will solve the mentioned problem using the *chronometrically invariant notation* of General Relativity, i.e., the mathematical apparatus of chronometric invariants, which are mathematically determined as physically observable quantities in the four-dimensional pseudo-Riemannian space (space-time). To do this, we compare the mathematical basis of Newton's theory of gravitation with the mathematical basis of General Relativity. This comparison will allow us to consider the fundamental laws of Newton's theory as the three-dimensional spatial projections of the four-dimensional (space-time) laws of General Relativity.

2 The mathematical basis of Newton's theory of gravitation and that of Einstein's theory of relativity

It is well known that Newton's theory of gravitation and Einstein's theory of relativity are based on different mathematical foundations. The bases of both theories are sets, each of which has its own method of measuring infinitely small distances ds between its elements (points). Such sets are called *metric spaces*, and the quantity ds^2 is called the *space metric*. Metric spaces play a huge rôle in topology, geometry, and in the sections of theoretical physics where we study the structure of space and time.

Newton's fundamental laws, including the Law of Universal Gravitation, are formulated in the framework of the three-dimensional flat, homogeneous and isotropic (Euclidean) space E_3 . Such a space allows the existence of *inertial reference frames*: in an inertial reference frame, free bodies

either travel uniformly and rectilinearly or are at rest relative to the observer. In any inertial reference frame, time is homogeneous, and space is homogeneous and isotropic. The homogeneity of time means uniformity of its pace. The homogeneity of a space means the equality of all its points, and the isotropy of a space means the equality of all directions in it. The homogeneity and isotropy of space follow from Newton's first law (the law of inertia), which says: "if in the region, where inertial reference frames exist, no forces act on a body, or all forces acting on the body balance each other, then the body is either at rest or travels rectilinearly and uniformly".

In a three-dimensional flat space E_3 (Euclidean space), the square of the length of an elementary three-dimensional interval ds , characterizing the distance between two infinitely close points of the space, in the Cartesian coordinates x, y, z has the form

$$ds^2 = dx^2 + dy^2 + dz^2, \quad (1)$$

where the numerical value of ds^2 can only be *positive* and, hence, the three-dimensional interval ds is always a *substantial quantity*. The metric (1) is called *positive definite*, and the space E_3 described by it is *properly Euclidean*. Here the word "properly" means that all basis vectors of E_3 have substantial lengths. The three-dimensional curvature of the space E_3 is zero. For this reason, the space E_3 is flat. The condition $ds^2 = 0$ is satisfied only in the coordinate origin $x = y = z = 0$.

The laws of Newtonian classical mechanics, including Newton's law of gravitation, are formulated in the framework of a flat three-dimensional (Euclidean) space E_3 .

Einstein's theory of relativity was created to describe space and time as a single entity, which is "space-time". The necessary prerequisites for Einstein's theory were obtained in the works of several other scientists, mainly in the works authored by Hermann Minkowski and Henri Poincaré. The basis of the theory is the four-dimensional curved pseudo-Riemannian space V_4 . The prefix "pseudo" in this case indicates the fundamental difference between the mathematical basis of Newton's theory and the mathematical basis of Einstein's theory: this prefix means that one coordinate basis vector (time basis vector) has an imaginary length, and three other three-dimensional (spatial) basis vectors have substantial lengths (or vice versa, which is the same).

Initially, Einstein created the Special Theory of Relativity, the mathematical basis of which is the flat four-dimensional pseudo-Euclidean space E_4 , later called the *Minkowski space*. The Minkowski space is a simplest particular case of four-dimensional pseudo-Riemannian spaces, which is homogeneous and isotropic, while its four-dimensional curvature is zero: the three-dimensional subspace of the Minkowski space may be non-uniform and anisotropic in one reference frame, but these factors in the Minkowski space depend on the observer's reference frame and, therefore, they can be re-

duced to zero simply by choosing another different reference frame. Bodies that are not affected by external forces travel uniformly and rectilinearly in the Minkowski space.

The Minkowski space is described by the metric

$$ds^2 = -(dx^0)^2 + (dx^1)^2 + (dx^2)^2 + (dx^3)^2, \quad (2)$$

where $x^0 = ct$ is the time coordinate, in which c is the velocity of light, t is the ideal (uniform) coordinate time, and $x^1 = x$, $x^2 = y$, $x^3 = z$ are the Cartesian three-dimensional (spatial) coordinates. In this notation, each of the three-dimensional spatial basis vectors e^i (where $i = 1, 2, 3$) has a substantial unit length, and the time basis vector e^0 has an imaginary unit length $(e^0)^2 = -1$ or vice versa, depending on the choice for the space signature $(-+++)$ as in (2) above or $(+---)$ as is most commonly used in General Relativity.

The basic space (space-time) of the General Theory of Relativity is the curved four-dimensional pseudo-Riemannian space V_4 — the generalization of the flat four-dimensional pseudo-Euclidean (Minkowski) space E_4 , which can be inhomogeneous, anisotropic, etc. per se, i.e., independently of the choice of the observer's reference frame. The laws of General Relativity are formulated in the framework of the curved four-dimensional pseudo-Riemannian space V_4 .

The square of the elementary distance ds between two infinitely close points (i.e., the space metric) in V_4 is expressed as follows

$$\begin{aligned} ds^2 &= g_{\alpha\beta} dx^\alpha dx^\beta = \\ &= g_{00} dx^0 dx^0 + 2g_{0i} dx^0 dx^i + g_{ik} dx^i dx^k, \end{aligned} \quad (3)$$

where $\alpha, \beta = 0, 1, 2, 3$ are the space-time (four-dimensional) indices, $i, k = 1, 2, 3$ are the spatial (three-dimensional) indices, and $g_{\alpha\beta}$ is the fundamental metric tensor of the space (it is a symmetric tensor, i.e., $g_{\alpha\beta} = g_{\beta\alpha}$). In the pseudo-Riemannian space, the time basis vector e^0 has the length dependent on the gravitational field potential, and the lengths of the three-dimensional spatial basis vectors e^i depend on the inhomogeneity and anisotropy of space, i.e., they are not unit length vectors, in contrast to the four-dimensional pseudo-Euclidean (Minkowski) space. The factors that deviate the lengths of the space basis vectors from unit are determined by the components of the fundamental metric tensor $g_{\alpha\beta}$ (while in the Minkowski space we can always find an inertial reference frame, in which the diagonal components of $g_{\alpha\beta}$ are units, and its non-diagonal components are zero). The time component g_{00} characterizes the gravitational field potential, the spatial components g_{ik} characterize the inhomogeneity and anisotropy of the observer's three-dimensional space, and the mixed (space-time) components g_{0i} characterize the angle of inclination of his three-dimensional space to the lines of time (the spaces in which this inclination takes place are called *non-holonomic spaces*; see Section 3, where we explain the basics of the theory of physically observable quantities in the space-time of General Relativity). In particular,

the physically observable time of the observer depends on the magnitude of the gravitational potential at the place of observation, and also on the magnitude and direction of the rotation speed of his three-dimensional physical space (its inclination to the time line).

As a result of the aforementioned absolute factors of $g_{\alpha\beta}$, which cannot vanish by choosing an inertial reference frame in the pseudo-Riemannian space (in contrast to the pseudo-Euclidean space of Special Relativity), we formulate Newton's first law (the law of inertia) in General Relativity as follows: "a body can be at rest or travelling rectilinearly and uniformly only in the absence of the gravitational field, inhomogeneity and isotropy of space and its rotation (the latter means the absence of the inclination of the three-dimensional space to the time lines)".

3 Physically observable quantities in the space-time of General Relativity

Before comparing the mathematical foundations of Newton's theory of gravitation and Einstein's theory of relativity, we must explain the basics of the theory of physically observable quantities in the four-dimensional pseudo-Riemannian space (which are also known as the Zelmanov chronometric invariants).

This mathematical apparatus that uniquely determines physically observable quantities in the space-time of General Relativity was created in 1944 by Abraham Zelmanov [9–11], who was our teacher. In addition to Zelmanov's original publications, which were very concise, this mathematical apparatus was explained in detail by us in a special Chapter given in each of our three research monographs, originally published in 2001 [12, 13] and 2013 [14]. The most comprehensive survey of Zelmanov's mathematical apparatus was published by us in 2023, in the special paper [15], where we collected everything (or almost everything) that we know about this mathematical apparatus personally from Zelmanov and on the basis of our own research studies.

Over the past decades, the following problems of General Relativity have been solved using the mathematical apparatus of chronometric invariants:

- The theory of non-quantum teleportation in the space-time of General Relativity [12, 16, 17], the basics of which were first outlined in 2001 in our book [12] and then developed in all necessary details in 2022 [17];
- The theory of the direct and opposite flow of time, and also the three kinds of particles in the space-time of General Relativity, published in 2001, in the book [12];
- The theory of frozen/stopped light according to General Relativity, which explained the frozen light experiment (2000). This theory was first drafted in 2001, in the 1st edition of our book [12], then in 2011 published in all necessary details in our paper [18] and since 2012 added to all subsequent editions of the book [12];
- The cosmological mass-defect — a new effect of General Relativity, predicted in 2011 [19], according to which the observed masses of cosmic bodies depend on their distance from the observer if they are at cosmological large-scale distances from him (depending on the specific metric of space);
- The non-linear cosmological redshift, deduced in 2012 [20] for various space metrics, including the Friedmann expanding universe and the de Sitter static universe. Three short papers [21–23] were then focused on specific aspects of the obtained solutions, and a final analysis of those of them that are most suitable for explaining the non-linear cosmological redshift observed by astronomers was given in 2013, in the paper [24];
- The deflection of light rays and mass-bearing particles, and also the length stretching and time dilation in the field of a rotating body — these are three new effects of General Relativity, deduced in 2023 [25, 26];
- The condensed matter model of the Sun, created in the framework of General Relativity, according to which the space breaking in the gravitational field of the Sun meets the maximum concentration of the asteroids in the Asteroid belt. This study was first published in 2009–2010 [27, 28];
- The theory of the internal constitution of stars and the sources of stellar energy according to General Relativity, which was first published in 2013, in the book [14];
- The exact solutions, obtained in 2005 to the equations of deviating geodesics for solid-body and free-mass gravitational wave detectors [29, 30] (different from the approximate solutions presumed in 1961 by Joseph Weber). Since 2008, this study was added to all subsequent editions of our book [12]. The obtained solutions are based on the comprehensive theoretical study of gravitational waves performed during a decade in 1968–1978 [31–33];
- "Zitterbewegung" of travelling electrons, explained in 2023 by Pierre Millette [34] on the basis of the theory of spin-particles in General Relativity, published in 2001 [13, Chapter 4].

For a complete list of the published research studies performed using the mathematical apparatus of chronometric invariants as of January 2023, see Bibliography in our comprehensive paper on this subject [15].

In short, the essence of Zelmanov's mathematical apparatus of chronometric invariants (known also as the chronometrically invariant formalism) is as follows. Zelmanov unambiguously determined physically observable quantities in the space-time of General Relativity as the projections of four-dimensional tensor quantities onto the time line and the three-dimensional spatial section of the space-time, which are associated with an observer. Such projections remain invariant

throughout the three-dimensional spatial section associated with the observer (his observable three-dimensional physical space), i.e., they are “chronometric invariants” in the physical reference frame of the observer and depend on the physical and geometric properties of his space, such as the gravitational potential, rotation, curvature, etc., which are determined by the respective components of the fundamental metric tensor $g_{\alpha\beta}$ and their derivatives.

The “chronometrically invariant” projections of any four-dimensional tensor quantity onto the time line and the three-dimensional spatial section associated with an observer are calculated using the Zelmanov operators of projection, which take the physical and geometric properties of the observer’s space into account (see our comprehensive survey [15] of the chronometrically invariant formalism for detail).

As a result, the square of the four-dimensional (space-time) interval $ds^2 = g_{\alpha\beta} dx^\alpha dx^\beta$, expressed with chronometrically invariant (physically observable) quantities, has the form

$$ds^2 = c^2 d\tau^2 - d\sigma^2, \quad (4)$$

where $d\tau$ is the chr.inv.-time interval (physically observable time interval), obtained as the chr.inv.-projection of the four-dimensional displacement vector dx^α onto the observer’s time line

$$d\tau = \sqrt{g_{00}} dt - \frac{1}{c^2} v_i dx^i, \quad \sqrt{g_{00}} = 1 - \frac{w}{c^2}, \quad (5)$$

and $d\sigma^2$ is the square of the chr.inv.-spatial interval (physically observable three-dimensional spatial interval)

$$d\sigma^2 = h_{ik} dx^i dx^k, \quad (6)$$

created using the chr.inv.-metric three-dimensional tensor h_{ik}

$$h_{ik} = -g_{ik} + \frac{1}{c^2} v_i v_k, \quad h^{ik} = -g^{ik}, \quad h_k^i = \delta_k^i, \quad (7)$$

which is the chr.inv.-projection of the fundamental metric tensor $g_{\alpha\beta}$ onto the observer’s three-dimensional space (the spatial section of the space-time, which is associated with him). So forth, w is the physically observable chr.inv.-potential of the gravitational field that fills the observer’s space, and v_i is the three-dimensional vector of the linear velocity of rotation of the observer’s space

$$w = c^2 (1 - \sqrt{g_{00}}), \quad v_i = -\frac{c g_{0i}}{\sqrt{g_{00}}}, \quad (8)$$

dx^i is the elementary interval of the three-dimensional spatial coordinates ($i = 1, 2, 3$), and $v^i = dx^i/d\tau$ is the chr.inv.-velocity vector (physically observable three-dimensional velocity), which is different from the three-dimensional coordinate velocity vector $u^i = dx^i/dt$.

If all g_{0i} of a four-dimensional (space-time) metric ds^2 are zero, then such space-time is *holonomic*. In this case the three-dimensional spatial section associated with the observer

(his observed three-dimensional space) is everywhere orthogonal to the time lines $x^0 = ct = const$ that pierce it. If at least one of the components g_{0i} of the four-dimensional metric is different from zero, then such space-time is *non-holonomic*. In such a (non-holonomic) space-time, the observer’s three-dimensional spatial section $x^0 = const$ is inclined to the time lines. In this case, at different points the observed three-dimensional space can be inclined to the time lines at different angles depending on the local geometric structure of the particular four-dimensional space-time.

The formula for the physically observable time interval $d\tau$ (5) can therefore be re-written as

$$d\tau = \left(1 - \frac{w + v_i u^i}{c^2}\right) dt, \quad (9)$$

where $v_i u^i$ is the scalar product of the linear rotational velocity of the observer’s space v_i and the three-dimensional coordinate velocity vector u^i

$$v_i u^i = |v_i| |u^i| \cos(v_i u^i), \quad (10)$$

which means that if the vectors v_i and u^i are orthogonal to each other, then their scalar product $v_i u^i = 0$. In this case, the rotation of the three-dimensional reference space does not contribute to the change in the observer’s physically observable time τ . If the vectors v_i and u^i are inclined to each other, then their mutual orientation in space affects the physically observable time τ , as well as its direction to the future or to the past: in the case, where the vector of the linear rotational velocity of the observer’s reference space v_i is inclined in the same direction as the velocity motion vector of his reference body u^i (i.e., $v_i u^i > 0$), the observer’s physical time τ flows faster; in the case, where the vectors v_i and u^i are inclined in opposite directions ($v_i u^i < 0$), the observed time τ flows slower. This purely theoretical conclusion was confirmed by the Hafele and Keating experiment (1971, repeated in 2005), in which they compared the readings of atomic clocks installed on board a jet airplane flying along a parallel around the globe with the readings of atomic clocks left on the surface of the Earth [35–39]. Thus, it was proven that the observed time on our planet depends on the following physical factors: 1) the magnitude of the gravitational field potential at the place of observation; 2) the speed of the Earth’s rotation around its own axis (diurnal rotation); 3) the speed of the observer’s motion relative to the Earth’s rotation. For detail, see our recent publication on this subject [26].

In the theory of chronometric invariants, there are physically observable (chronometrically invariant) analogues of the quantities known in Newtonian classical mechanics. This fact will help us to find a connexion between Newton’s theory of gravitation and General Relativity.

So, the physical reference space of a real observer (which is his physical reference frame) is characterized by the following physically observable chr.inv.-quantities. These are

the chr.inv.-vector of the physically observable gravitational inertial force F_i acting in the observer's space, the first (gravitational) term of which is created by the gradient of the gravitational potential w and the second (inertial) term is created by the centrifugal force of inertia

$$F_i = \frac{1}{\sqrt{g_{00}}} \left(\frac{\partial w}{\partial x^i} - \frac{\partial v_i}{\partial t} \right), \quad \sqrt{g_{00}} = 1 - \frac{w}{c^2}, \quad (11)$$

the antisymmetric chr.inv.-tensor A_{ik} of the physically observable three-dimensional angular velocity of rotation of the observer's space

$$A_{ik} = \frac{1}{2} \left(\frac{\partial v_k}{\partial x^i} - \frac{\partial v_i}{\partial x^k} \right) + \frac{1}{2c^2} (F_i v_k - F_k v_i), \quad (12)$$

the symmetric chr.inv.-tensor D_{ik} of the physically observable deformation rate of the space

$$\left. \begin{aligned} D_{ik} &= \frac{1}{2} \frac{\partial h_{ik}}{\partial t}, & D^{ik} &= -\frac{1}{2} \frac{\partial h^{ik}}{\partial t} \\ D &= h^{ik} D_{ik} = \frac{\partial \ln \sqrt{h}}{\partial t}, & h &= \det \| h_{ik} \| \end{aligned} \right\}, \quad (13)$$

the chr.inv.-Christoffel symbols of the 1st rank $\Delta_{jk,m}$ and the 2nd rank Δ_{nk}^i (they are the coefficients of the physically observable inhomogeneity of the observer's space)

$$\Delta_{nk}^i = h^{im} \Delta_{nk,m} = \frac{1}{2} h^{im} \left(\frac{\partial h_{nm}}{\partial x^k} + \frac{\partial h_{km}}{\partial x^n} - \frac{\partial h_{nk}}{\partial x^m} \right), \quad (14)$$

and the physically observable chr.inv.-curvature of the observer's space, which is expressed with the chr.inv.-curvature tensor C_{lkij} that has all properties of the Riemann-Christoffel curvature tensor throughout the entire three-dimensional spatial section associated with the observer, whereas its subsequent contractions produce the chr.inv.-curvature scalar C

$$\begin{aligned} C_{lkij} &= \frac{1}{4} (H_{lkij} - H_{jkil} + H_{klji} - H_{iljk}) = \\ &= H_{lkij} - \frac{1}{2} (2A_{ki} D_{jl} + A_{ij} D_{kl} + A_{jk} D_{il} + \\ &\quad + A_{kl} D_{ij} + A_{li} D_{jk}), \end{aligned} \quad (15)$$

$$C_{lk} = C_{lki}^{\dots i} = H_{lk} - \frac{1}{2} (A_{kj} D_l^j + A_{lj} D_k^j + A_{kl} D), \quad (16)$$

$$C = h^{lk} C_{lk} = h^{lk} H_{lk}, \quad (17)$$

where it is denoted, for brevity and a better association with the Riemann-Christoffel curvature tensor,

$$H_{lki}^{\dots j} = \frac{\partial \Delta_{il}^j}{\partial x^k} - \frac{\partial \Delta_{kl}^j}{\partial x^i} + \Delta_{il}^m \Delta_{km}^j - \Delta_{kl}^m \Delta_{im}^j, \quad (18)$$

and the operators

$$\frac{\partial}{\partial t} = \frac{1}{\sqrt{g_{00}}} \frac{\partial}{\partial t}, \quad \frac{\partial}{\partial x^i} = \frac{\partial}{\partial x^i} + \frac{v_i}{c^2} \frac{\partial}{\partial t} \quad (19)$$

are the chr.inv.-operators of derivation with respect to time t and the spatial coordinates x^i .

It should be noted that the physically observable chr.inv.-curvature of the observer's space is depended on not only the space inhomogeneity (Christoffel symbols), but also on the rotation A_{ik} and deformation D_{ik} of the space, and, therefore, does not vanish in the absence of the gravitational field.

Since the task here is to find a connexion between Einstein's theory of relativity and Newton's theory of gravitation, in which space-time is static (non-deforming) and flat, we will not consider the deformation and curvature of space (i.e., we will assume that $D_{ik} = 0$ and $C_{lkij} = 0$). In addition, if in this particular case the three-dimensional observable space does not rotate or if its rotation velocity does not depend on time, then the gravitational inertial force F_i depends only on the numerical value of the gravitational potential w and its spatial derivatives. We will therefore consider this particular case in the next Section to deduce Galileo's principle and Newton's law of gravitation as consequences of the purely geometric laws of General Relativity.

4 Galileo's principle and Newton's law of gravitation in the framework of General Relativity

According to the biography of Galileo, in 1589 he conducted his famous experiments with bodies falling from the Leaning Tower of Pisa to the surface of the Earth. Galileo wanted to prove his case in a correspondence dispute with Aristotle, who, in turn, about 2000 years before Galileo, in 360–330 B.C., argued that the motion speed of falling bodies depends on the magnitude of their masses: he argued the greater the mass of a falling body, the faster it falls down.

In contrast to Aristotle, Galileo made a supposition that the fall time of bodies does not depend on their masses. In support of his hypothesis, Galileo dropped down balls of different masses from the Leaning Tower of Pisa. With this experiment, Galileo established that bodies of different masses, dropped down to the surface of the Earth simultaneously from the same altitude above the Earth's surface, access the ground simultaneously. Since the Tower's height h is much less than the radius of the Earth ($h \ll R_{\oplus}$), it can be assumed that any body located at a small altitude above the Earth's surface is attracted to the centre of the Earth with a force proportional to the numerical value of the body's mass. In fact, Galileo had discovered that the fall time of the body does not depend on the numerical value of its mass. Therefore, he had arrived at the conclusion that is now called *Galileo's principle*:

All bodies, regardless of the numerical values of their masses, fall to the surface of the Earth with the same acceleration, called the *free-fall acceleration*.

Later, in 1666, Isaac Newton formulated the Law of Universal Gravitation. According to this law, the force of attraction F between two material points with masses m_1 and m_2 , located at a distance r from each other, acts along the line

connecting their centres. This force is formulated as

$$F = -\frac{Gm_1m_2}{r^2}, \quad (20)$$

where $G = 6.67 \times 10^{-8}$ cm³/gram sec² is the Newton gravitational constant. From the above formula (20) it follows that in a flat (Euclidean) space E_3 the gravitational force of attraction F is determined only by the numerical values of the interacting masses and the distance between them, and does not depend on the size of the bodies. Such an interaction is called *point interaction*. Thus, in Newton's theory of gravitation, the gravitational interaction between two bodies is "point-like", i.e., it is carried out between the gravitating centres of these bodies (material points).

Applying (20) to the gravitational interaction between the Earth and a body of mass m falling to the Earth's surface, we obtain

$$F = -\frac{GmM_{\oplus}}{R_{\oplus}^2} = -mg, \quad (21)$$

where $g = GM_{\oplus}/R_{\oplus}^2$ is the free-fall acceleration due to the Earth's gravitation, $M_{\oplus} = 5.97 \times 10^{27}$ gram is the mass of the Earth, $R_{\oplus} = 6.37 \times 10^8$ cm is the radius of the Earth, and m is the mass of the body falling down to the Earth's surface. Formula (4.2) explains the results of Galileo's experiments under the condition that the bodies fall on the surface of the Earth from a small altitude $h \ll R_{\oplus}$. In this case, it is easy to calculate the magnitude of the free-fall acceleration on the Earth's surface: $g = 981$ cm/sec².

Formula (21) is the mathematical expression of Galileo's principle in the framework of Newton's theory of gravitation.

Let us now deduce Galileo's principle and Newton's law of gravitation in the framework of the four-dimensional space (space-time) of General Relativity. To do this, we consider Schwarzschild's mass-point metric. This metric is an exact solution of Einstein's field equations, which describes a spherically symmetric gravitational field created in an empty space (space-time) by a spherical island of substance, the mass of which is M , and which is approximated by a mass-point. The Schwarzschild mass-point metric in the spherical coordinates r, θ, φ has the form

$$ds^2 = \left(1 - \frac{r_g}{r}\right) c^2 dt^2 - \frac{dr^2}{1 - \frac{r_g}{r}} - r^2 (d\theta^2 + \sin^2\theta d\varphi^2), \quad (22)$$

where $r_g = 2GM/c^2$ is the so-called *gravitational radius* calculated here for a spherical body of the mass M (which we approximate by a mass-point). The polar coordinate angle θ is measured from the North pole to the equator.

Since, according to the chronometrically invariant formalism, the component g_{00} in a general case is expressed with the gravitational field potential w as

$$g_{00} = \left(1 - \frac{w}{c^2}\right)^2, \quad (23)$$

and according to the Schwarzschild mass-point metric (22) we have

$$g_{00} = 1 - \frac{r_g}{r}, \quad (24)$$

then in the space of the Schwarzschild mass-point metric the gravitational field potential $w = c^2(1 - \sqrt{g_{00}})$ has the form

$$w = c^2 \left(1 - \sqrt{1 - \frac{r_g}{r}}\right) = c^2 \left(1 - \sqrt{1 - \frac{2GM}{c^2 r}}\right), \quad (25)$$

which in the quasi-Newtonian approximation ($r_g \ll r$), where the ratio r_g/r takes small numerical values and, therefore,

$$\sqrt{1 - \frac{2GM}{c^2 r}} \approx 1 - \frac{GM}{c^2 r}, \quad (26)$$

takes the form

$$w = c^2 \left(1 - \sqrt{1 - \frac{2GM}{c^2 r}}\right) \approx \frac{GM}{r}, \quad (27)$$

which coincides with the gravitational field potential according to Newton's theory of gravitation.

So forth, looking at the Schwarzschild mass-point metric (22), we realize that it is static, since all components of its fundamental metric tensor $g_{\alpha\beta}$ do not depend on the time coordinate $x^0 = ct$. This means that the space of the Schwarzschild mass-point metric does not deform ($D_{ik} = 0$). In addition, since all space-time components of the fundamental metric tensor of the metric are zero ($g_{0i} = 0$), such a space does not rotate ($v_i = 0, A_{ik} = 0$). As a result of the above, the physically observable time interval $d\tau$ in the Schwarzschild mass-point field has the form

$$\begin{aligned} d\tau &= \sqrt{g_{00}} dt - \frac{1}{c^2} v_i dx^i = \sqrt{g_{00}} dt = \left(1 - \frac{w}{c^2}\right) dt = \\ &= \sqrt{1 - \frac{r_g}{r}} dt = \sqrt{1 - \frac{2GM}{c^2 r}} dt, \quad (28) \end{aligned}$$

which means that the flow of the physically observable time τ in the Schwarzschild mass-point field is determined only by the numerical value of the gravitational field potential w .

Since the space of the Schwarzschild mass-point metric is static ($D_{ik} = 0$) and does not rotate ($v_i = 0, A_{ik} = 0$), the components of the chr.inv.-vector of the physically observable gravitational inertial force F_i (11) that acts on a unit mass in such a space take the form

$$F_1 = \frac{1}{\sqrt{g_{00}}} \frac{\partial w}{\partial r}, \quad F_2 = 0, \quad F_3 = 0, \quad (29)$$

where $w = c^2(1 - \sqrt{g_{00}})$ is the gravitational field potential. Therefore, in terms of the gravitational radius $r_g = 2GM/c^2$ calculated for the mass M , the solely non-zero component of the physically observable gravitational inertial force acting in

the space of the Schwarzschild mass-point metric is

$$F_1 = -\frac{c^2}{2g_{00}} \frac{\partial g_{00}}{\partial r} = -\frac{c^2}{2\left(1 - \frac{r_g}{r}\right)} \frac{r_g}{r^2}. \quad (30)$$

Apply the obtained formula (30) to a body having a mass m (different from unit mass) and located on the Earth's surface ($r = R_\oplus$) or at a small altitude h above it ($h \ll R_\oplus$). Since the radius of the Earth is $R_\oplus = 6.37 \times 10^8$ cm, and its gravitational radius is $r_g = 0.89$ cm, the ratio r_g/R_\oplus on the Earth's surface takes a very small numerical value $r_g/R_\oplus = 1.4 \times 10^{-9}$ that can be neglected. In this case, the formula for the gravitational force F_1 (30), which we have obtained in the framework of General Relativity, takes the following form

$$\Phi_1 = mF_1 = -\frac{c^2}{2\left(1 - \frac{r_g}{r}\right)} \frac{mr_g}{r^2} = -\frac{GmM_\oplus}{R_\oplus^2} = -mg, \quad (31)$$

which coincides with the formula (21), which, in turn, is the mathematical expression of Galileo's principle in the framework of Newton's theory of gravitation.

This means that, according to General Relativity, all bodies located on the surface of the Earth or at a small altitude above it are attracted to the centre of the Earth with the same acceleration, equal to the free-fall acceleration $g = GM_\oplus/R_\oplus^2 = 981$ cm/sec² (which is a conclusion, analogous to Galileo's principle in Newton's theory of gravitation).

In fact, using the chronometrically invariant notation of General Relativity, we have just deduced the following:

Both Galileo's principle and Newton's law of gravitation (empirical laws of classical mechanics) are direct consequences of the geometric structure of the four-dimensional pseudo-Riemannian space (space-time of General Relativity), since the force of gravity, which attracts material bodies to the Earth, is the chr.inv.-vector of the physically observable gravitational inertial force acting in the space (gravitational field) of the Schwarzschild mass-point metric.

This cannot be shown using the general covariant notation of General Relativity, because it does not include physical observable quantities. This is why there is no unambiguous mathematical transition from General Relativity to Newton's theory of gravitation in the framework of the general covariant notation of General Relativity.

5 The origin of the gravitational field according to General Relativity

Let us now consider the origin of gravitation using the chronometrically invariant notation of General Relativity.

In the space of the Schwarzschild mass-point metric, on a spherical surface of the radius $r = r_g$ from the coordinate origin (which is the centre of the gravitating body approximated by a mass-point), the time component g_{00} of the fundamental

metric tensor is zero ($g_{00} = 0$), and the radial component g_{11} becomes infinitely large ($g_{11} \rightarrow \infty$)

$$r = r_g, \quad g_{00} = 1 - \frac{r_g}{r} = 0, \quad g_{11} = \frac{1}{1 - \frac{r_g}{r}} \rightarrow \infty, \quad (32)$$

and, since the Schwarzschild space does not rotate ($v_i = 0$), hence the radial component h_{11} of the chr.inv.-metric tensor $h_{ik} = -g_{ik} + \frac{1}{c^2} v_i v_k$ becomes also infinite ($h_{11} \rightarrow -\infty$).

This means that on the spherical surface $r = r_g$ that surrounds any mass-point (located at the coordinate origin in the space of the Schwarzschild mass-point metric) the following conditions take place:

- 1) The three-dimensional observable space (and the gravitational field of the mass-point, which fills the space) has a space breaking ($g_{11} \rightarrow \infty$, $h_{11} \rightarrow -\infty$);
- 2) The physically observable time τ of the observer stops ($d\tau = 0$) on this surface

$$d\tau = \sqrt{g_{00}} dt - \frac{1}{c^2} v_i dx^i = \sqrt{g_{00}} dt = 0. \quad (33)$$

That is, there on the surface of the gravitational radius $r = r_g$, which surrounds the centre of gravity inside any material body, the physically observable time stops ($d\tau = 0$), and the observable three-dimensional space is expanded infinitely in the radial direction $x^1 = r$ since the three-dimensional physically observable chr.inv.-interval $d\sigma$ that is determined as $d\sigma^2 = h_{ik} dx^i dx^k$ (6) on such a surface is

$$d\sigma = \sqrt{h_{11} x^1 x^1} = \frac{dr}{\sqrt{1 - \frac{r_g}{r}}} \rightarrow \infty. \quad (34)$$

Equating $d\tau$ in the Schwarzschild mass-point field, which is $d\tau = \left(1 - \frac{w}{c^2}\right) dt$ (28), to zero (since $d\tau = 0$ on the surface of the gravitational radius), we obtain

$$E = Mw = Mc^2, \quad (35)$$

i.e., the energy $E = Mw$ of the gravitational field, created by a body having a non-unit mass M , on the surface of the gravitational radius $r = r_g$ (which surrounds the centre of gravity inside any material body) is the same as the total energy of the body $E = Mc^2$.

We therefore arrive at the following conclusion:

The gravitational field of any body is originated in the surface of the gravitational radius $r = r_g$, which is surrounding the centre of gravity inside the body.

This is the origin of the gravitational field according to General Relativity. Since the gravitational radius of an ordinary body is incomparably smaller than its physical radius, the conclusion we have obtained in the framework of General Relativity is completely consistent with Newton's theory of gravitation, according to which the gravitational field of any

body is originated in its center of gravity (which coincides with its geometric center in the case, where the body has a spherically symmetrical shape).

For example, the surface of the gravitational radius, which is surrounding the centre of gravity of the planet Earth, is the origin of the Earth's gravitational field attracting to this surface near the centre of the planet everything that is underground, grows on the Earth's surface, moves along it and above it (in the Earth's atmosphere and in the cosmos). Trees indicate this fact: their trunks are always directed from the centre of the Earth, and not at an angle to this direction. This is especially clearly seen in cases, where the ground on which the tree grows lies at an angle to a flat surface, for example, on a mountain slope: in this case, the tree does not grow perpendicular to the slope, but its trunk is oriented strictly in the direction from the centre of the Earth.

From the above conclusion about the origin of the gravitational field it also follows that a *collapse surface* (in terms of General Relativity, this is a surface on which $g_{00} = 0$ and, as a result, the physically observable time stops $d\tau = 0$) is not exclusively the surface of a black hole (gravitational collapsar) — a body, the substance of which is compressed to such a super-dense state that it is concentrated under its gravitational radius. Indeed, ordinary bodies are not in the state of gravitational collapse, since almost all mass of an ordinary body is located above its gravitational radius (which is very small compared to its physical radius). However, the tiny sphere of the gravitational radius that takes place at the centre of every ordinary body is also a *collapse surface*, because the physically observable time stops and the spatial metric has a breaking on this tiny sphere, just like on the surface of a black hole (gravitational collapsar).

The same conclusion about the origin of the gravitational field follows from the geodesic equations (equations of motion of free particles) in the space of the Schwarzschild mass-point metric. "Free" here means that the moving particle is affected only by the forces, the source of which is the geometric structure of the space itself (i.e., in the absence of extraneous fields).

The geodesic equations in the chronometrically invariant notation are a system of the chr.inv.-projections onto the time line (the chr.inv.-scalar projection) and onto the three-dimensional space (the chr.inv.-vector projection) associated with a particular observer. They have the following form (see References to the Zelmanov chronometric invariants)

$$\frac{dm}{d\tau} - \frac{m}{c^2} F_i v^i + \frac{m}{c^2} D_{ik} v^i v^k = 0, \quad (36)$$

$$\frac{d(mv^i)}{d\tau} - mF^i + 2m(D_k^i + A^i_k)v^k + m\Delta_{nk}^i v^n v^k = 0, \quad (37)$$

where m is the relativistic mass of the particle, τ is the physically observable time of its motion, $v^i = dx^i/d\tau$ is its physically observable chr.inv.-velocity, F_i is the chr.inv.-vector of

the gravitational inertial force, A_{ik} is the chr.inv.-tensor of the angular velocity of rotation of the observer's space, D_{ik} is the chr.inv.-tensor of the rate of its deformation, and Δ_{nk}^i are the chr.inv.-Christoffel symbols of the 2nd rank (which are the coefficients of the physically observable inhomogeneity of the observer's space).

The chr.inv.-geodesic equations (36, 37) are simplified in the space of the Schwarzschild mass-point metric

$$\frac{dm}{d\tau} - \frac{m}{c^2} F_i v^i = 0, \quad (38)$$

$$\frac{d(mv^i)}{d\tau} - mF^i + m\Delta_{nk}^i v^n v^k = 0, \quad (39)$$

since such a space does not rotate or deform (see above). Here $v^1 = dr/d\tau$, $v^2 = d\theta/d\tau$, $v^3 = d\varphi/d\tau$. In addition, only the radial component F_1 of the gravitational inertial force F_i is non-zero. According to (29), it is

$$F_1 = \frac{1}{\sqrt{g_{00}}} \frac{\partial w}{\partial r} = \frac{c^2}{c^2 - w} \frac{\partial w}{\partial r}, \quad (40)$$

where $w = c^2(1 - \sqrt{g_{00}})$ is the potential of the gravitational field (created by a massive body, approximated by a mass-point), in which the particle travels. Therefore, the scalar geodesic equation (38) takes the form

$$\frac{dm}{m} = \frac{1}{c^2} F_1 dr, \quad (41)$$

which can be re-written as

$$\frac{dm}{m} = -\frac{d(c^2 - w)}{c^2 - w}, \quad (42)$$

which is the same as

$$d(\ln m) = -d[\ln(c^2 - w)]. \quad (43)$$

Integrating (43), we obtain the solution

$$mc^2 - mw = C, \quad (44)$$

where C in the integration constant. Since $w = c^2(1 - \sqrt{g_{00}})$, $g_{00} = 1 - r_g/r$, and $r_g = 2GM/c^2$, then $C = 0$ under the condition $g_{00} = 0$, which satisfies at the spherical surface of the gravitational radius $r = r_g$ (where $w = c^2$).

From the obtained solution (44) we see that a particle of mass m , which travels in the gravitational field of a mass M , has a maximum energy $mw = mc^2$ under the condition $g_{00} = 0$, which satisfies on the surface of the gravitational radius $r = r_g = 2GM/c^2$ from this mass-point (on which the physically observable time stops $d\tau = 0$, and the space and the gravitational field have a breaking $g_{11} = -h_{11} \rightarrow \infty$).

In particular, the above solution is applicable to the Earth, planets, the Sun, stars, galaxies and generally any bodies in the Universe.

In conclusion, we note that Riemannian spaces are non-degenerate by definition: the determinant $g = \det \|g_{\alpha\beta}\|$ of the fundamental metric tensor satisfies the condition $g < 0$. In addition, Zelmanov had obtained a relation connecting the determinants of the four-dimensional metric tensor $g_{\alpha\beta}$ and the three-dimensional chr.inv.-metric tensor h_{ik}

$$h = -\frac{g}{g_{00}}, \quad (45)$$

where $h = \det \|h_{ik}\|$, $g = \det \|g_{\alpha\beta}\|$, and g_{00} is the time component of the four-dimensional Riemannian metric.

These quantities in the space of the Schwarzschild mass-point metric (22) are

$$h = \frac{r^4 \sin^2 \theta}{1 - \frac{r_g}{r}}, \quad g_{00} = 1 - \frac{r_g}{r}, \quad g = -r^4 \sin^2 \theta. \quad (46)$$

From this we see that the numerical values of h and g depend on the location of the observer with respect to the polar coordinate θ (which is opposite to the geographic latitude, because it is measured from the North pole to the equator). At the North and South poles, where $\theta = 0^\circ$ and 180° , respectively, the space-time of the Schwarzschild mass-point metric is *completely degenerate*, since in this case $g = 0$. The observable three-dimensional space is also degenerate ($h = 0$) at the North and South poles. In addition, the radial component h_{11} becomes infinite over the entire surface of the gravitational radius $r = r_g$ that means a breaking in the space (and the gravitational field) on this surface.

It should be noted that the complete degeneration of the four-dimensional space-time and the three-dimensional observable space takes place in the Schwarzschild mass-point field not only on the spherical surface of the gravitational radius $r = r_g$ (around the centre of gravity of the mass-point), but also everywhere along the radial coordinate r directed to North and South. But even with a tiny deviation from the polar direction $\theta = 0^\circ$ or $\theta = 180^\circ$ (i.e., from the polar axis of the coordinate frame) the space is already non-degenerate.

The above conclusion means that the surface of the gravitational radius $r = r_g$ is not only the origin of the gravitational field of any body, which spreads outside and inside the surface, but is also the special space-time “membrane” separating the external space (gravitational field) of the body, where $r > r_g$, from its internal space (gravitational field), where $r < r_g$. Since both the space-time metric and the spatial metric are degenerate inside the “membrane”, the space (space-time) inside the “membrane” is different from the ordinary pseudo-Riemannian space (space-time) and is a completely degenerate space-time.

6 Conclusion

So, using the chronometrically invariant notation of General Relativity (chronometric invariants are the physically observable projections of four-dimensional quantities onto the time

line and the three-dimensional space of an observer), we have deduced Galileo’s principle and Newton’s law of gravitation as a particular case of the chr.inv.-formula for the gravitational inertial force acting in the four-dimensional pseudo-Riemannian space (space-time of General Relativity).

In fact, by doing this, we have created a “mathematical bridge”, connecting Newton’s theory of gravitation with General Relativity. This “mathematical bridge” is important for theoretical physics, since no one earlier than us had derived the empirical laws of Newton’s theory of gravitation as a particular case of the purely geometric laws of General Relativity.

We have also showed that on the spherical surface that surrounds any mass-point at a very small radius, equal to the gravitational radius calculated for the mass, a space breaking takes place in the gravitational field of the mass-point (and in its three-dimensional observable space), and the observer’s physical observable time stops. That is, the gravitational field of any mass-point extends both inward from the mentioned spherical surface to the coordinate origin (which coincides with the mass-point), and outward from the mentioned surface into the surrounding space to infinity, but is absent on the surface itself. This theoretical result leads us to the conclusion that the origin of the gravitational field in the space of the Schwarzschild mass-point metric is a spherical surface that surrounds any mass-point at the gravitational radius calculated for the mass.

The above results were obtained only thanks to the chronometrically invariant notation of General Relativity, which provides an unambiguous mathematical definition of physically observable quantities in the four-dimensional pseudo-Riemannian space (space-time). It would be impossible to get these results using the conventional general covariant notation of General Relativity, because physically observable quantities in the general covariant notation are not mathematically defined.

Submitted on July 21, 2024

References

1. Stanyukovich K.P. The gravitational field and elementary particles. Science Press, Moscow, 1965.
2. Stanyukovich K. On the problem of the existence of stable particles in the Metagalaxy. *The Abraham Zelmanov Journal*, 2008, v. 1, 99–110 (translated from *Problemy Teorii Gravitazii i Elementarnykh Chastiz*, v. 1, Atomizdat, Moscow, 1966, 267–279).
3. Stanyukovich K. On increasing entropy in an infinite universe. *The Abraham Zelmanov Journal*, 2008, v. 1, 111–117 (translated from the extended draft of the publication in *Doklady Akademii Nauk SSSR*, 1949, v. LXIX, no. 6, 793–796).
4. Stanyukovich K. On the evolution of the fundamental physical constants. *The Abraham Zelmanov Journal*, 2008, v. 1, 118–126 (translated from the presentation held on May 12, 1971, in Kiev, at the seminar on General Relativity maintained by Alexei Z. Petrov in the Institute of Theoretical Physics).
5. Petrov A.Z. On the spaces determining the gravitational fields. *Doklady Akademii Nauk USSR*, 1951, v. XXXI, 149–152.

6. Petrov A. The classification of spaces determining the fields of gravitation. *The Abraham Zelmanov Journal*, 2008, v. 1, 81–98 (translated from *Uchenye Zapiski Kazanskogo Gosudarstvennogo Universiteta*, 1954, v. 114, book 8, 55–69).
7. Petrov A.Z. Einstein Spaces. Pergamon Press, Oxford, 1969 (translated from the 1st Russian edition, Moscow, 1961).
8. Rabounski D. Biography of Alexei Petrov (1910–1972). *The Abraham Zelmanov Journal*, 2008, v. 1, xxvii–xxix.
9. Zelmanov A. L. Chronometric Invariants. Translated from the 1944 PhD thesis, American Research Press, Rehoboth, New Mexico, 2006.
10. Zelmanov A. L. Chronometric invariants and accompanying frames of reference in the General Theory of Relativity. *Soviet Physics Doklady*, 1956, v. 1, 227–230 (translated from *Doklady Akademii Nauk USSR*, 1956, v. 107, issue 6, 815–818).
11. Zelmanov A. L. On the relativistic theory of an anisotropic inhomogeneous universe. *The Abraham Zelmanov Journal*, 2008, vol. 1, 33–63 (translated from the thesis of the 6th Soviet Conference on the Problems of Cosmogony, USSR Academy of Sciences Publishers, Moscow, 1957, 144–174).
12. Rabounski D. and Borissova L. Particles Here and Beyond the Mirror. The 4th revised edition, New Scientific Frontiers, London, 2023 (the 1st edition was issued in 2001).
Rabounski D. et Larissa Borissova L. Particules de l’Univers et au delà du miroir. La 2ème édition révisée en langue française, New Scientific Frontiers, Londres, 2023.
13. Borissova L. and Rabounski D. Fields, Vacuum, and the Mirror Universe. The 3rd revised edition, New Scientific Frontiers, London, 2023 (the 1st edition was issued in 2001).
Borissova L. et Rabounski D. Champs, Vide, et Univers miroir. La 2ème édition révisée en langue française, New Scientific Frontiers, Londres, 2023.
14. Borissova L. and Rabounski D. Inside Stars. The 3rd edition, revised and expanded, New Scientific Frontiers, London, 2023 (the 1st edition was issued in 2013).
15. Rabounski D. and Borissova L. Physical observables in General Relativity and the Zelmanov chronometric invariants. *Progress in Physics*, 2023, v. 19, issue 1, 3–29.
16. Borissova L. and Rabounski D. On the possibility of instant displacements in the space-time of General Relativity. *Progress in Physics*, 2005, v. 1, issue 1, 17–19.
17. Rabounski D. and Borissova L. Non-quantum teleportation in a rotating space with a strong electromagnetic field. *Progress in Physics*, 2022, v. 18, issue 1, 31–49.
18. Rabounski D. and Borissova L. A theory of frozen light according to General Relativity. *The Abraham Zelmanov Journal*, 2011, v. 4, 3–27.
19. Rabounski D. Cosmological mass-defect — a new effect of General Relativity. *The Abraham Zelmanov Journal*, 2011, v. 4, 137–161.
20. Rabounski D. Non-linear cosmological redshift: the exact theory according to General Relativity. *The Abraham Zelmanov Journal*, 2012, v. 5, 3–30.
21. Rabounski D. On the exact solution explaining the accelerate expanding Universe according to General Relativity. *Progress in Physics*, 2012, v. 8, issue 2, L1–L6.
22. Borissova L. and Rabounski D. Cosmological redshift in the de Sitter stationary Universe. *Progress in Physics*, 2018, v. 14, issue 1, 27–29.
23. Rabounski D. and Borissova L. On the lambda term in Einstein’s equations and its influence on the cosmological redshift. *Progress in Physics*, 2024, v. 20, issue 2, 4–12.
24. Rabounski D. and Borissova L. Cosmological redshift: which cosmological model best explains it? *Progress in Physics*, 2024, v. 20, issue 2, 13–20.
25. Rabounski D. and Borissova L. Deflection of light rays and mass-bearing particles in the field of a rotating body. *Progress in Physics*, 2022, v. 18, issue 1, 50–55.
26. Rabounski D. and Borissova L. Length stretching and time dilation in the field of a rotating body. *Progress in Physics*, 2022, v. 18, issue 1, 62–65.
27. Borissova L. The gravitational field of a condensed matter model of the Sun: the space breaking meets the Asteroid strip. *The Abraham Zelmanov Journal*, 2009, v. 2, 224–260.
28. Borissova L. The Solar System according to General Relativity: the Sun’s space breaking meets the Asteroid strip. *Progress in Physics*, 2010, v. 6, issue 2, 43–47.
29. Borissova L. Gravitational waves and gravitational inertial waves in the General Theory of Relativity: A theory and experiments. *Progress in Physics*, 2005, no. 2, 30–62.
30. Rabounski D. and Borissova L. Exact theory of a gravitational wave detector. New experiments proposed. *Progress in Physics*, 2006, v. 2, issue 2, 31–38.
31. Borissova L. B. Relative oscillations of test particles in comoving reference frames. *Soviet Physics Doklady*, 1976, v. 20, 816–819 (translated from *Doklady Acad. Nauk SSSR*, 1975, v. 225, no. 4, 786–789).
32. Borissova L. B. Quadrupole mass-detector in field of weak plane gravitational fields. *Russian Physics Journal*, 1978, v. 21, no. 10, 1341–1344 (translated from *Izvestiia Vysshikh Uchebnykh Zavedenii, Fizika*, 1978, no. 10, 109–114).
33. Borissova L. Gravitational waves and gravitational inertial waves according to the General Theory of Relativity. *The Abraham Zelmanov Journal*, 2010, v. 3, 25–70.
34. Millette P. A. Zitterbewegung and the non-holonomy of pseudo-Riemannian spacetime. *Progress in Physics*, 2023, v. 19, issue 1, 66–72.
35. Hafele J. Performance and results of portable clocks in aircraft. *PTTI 3rd Annual Meeting*, November 16–18, 1971, 261–288.
36. Hafele J. and Keating R. Around the world atomic clocks: predicted relativistic time gains. *Science*, July 14, 1972, v. 177, 166–168.
37. Hafele J. and Keating R. Around the world atomic clocks: observed relativistic time gains. *Science*, July 14, 1972, v. 177, 168–170.
38. Demonstrating relativity by flying atomic clocks. *Metromnia, the UK’s National Measurement Laboratory Newsletter*, issue 18, Spring 2005.
39. Rabounski D. and Borissova L. In memoriam of Joseph C. Hafele (1933–2014). *Progress in Physics*, 2015, v. 11, issue 2, 136.

Introducing the Space Metric of a Rotating Massive Body and Four New Effects of General Relativity

Dmitri Rabounski

Puschino, Moscow Region, Russia. E-mail: rabounski@yahoo.com

This paper introduces and proves the space metric of a rotating spherical body (approximated by a mass-point). This is a new metric to General Relativity, which is an extension and replacement of Schwarzschild's mass-point metric (since all cosmic bodies rotate). Physically observable characteristics of such a space are calculated, including the curvature of space and others. It is shown that the curvature of such a space has two components: a component created by the gravitational field (it decreases with distance from the body) and a constant curvature component created by the rotation of space (it does not depend on distance). Using Einstein's equations, the Riemannian conditions are calculated under which the introduced metric is valid (with the conditions, the Einstein equations vanish). Four new effects of General Relativity are calculated: the deflection of light rays and mass-bearing particles near a rotating body, a length-stretching effect along the geographical longitudes, a time-loss effect in the clocks co-moving with the Earth's rotation (to the East) and a time increment when moving to the West.

1 Introduction

This is the fourth paper in the series of papers on the effects of the space curvature, caused by the rotation of space.

The first [1] of these studies, besides many other scientific results obtained in it, showed that the rotation of space makes it curved. Then, two subsequent studies [2, 3] predicted four new effects of General Relativity, the origin of which is the space curvature caused by the rotation of space.

The first two effects are the deflection of light rays and mass-bearing particles in the field of a rotating body [2].

When a body rotates, the space around it curves towards the direction of its rotation and the centre of the body (around which it rotates), thereby creating a "slope of the hill" descending "down" along the equator in the direction, in which the body rotates, and also to the centre of the body. Therefore, when a particle travels freely to a rotating body, it "rolls down" the slope of the space curvature along the equator in the direction, in which the body rotates, as well as to the centre of the body. As a result, the following two effects should occur in the field of a rotating body:

1. A particle travelling freely to a rotating body should be deflected slightly from its radial trajectory in the equatorial direction, in which the body rotates, i.e., along the geographical longitudes;
2. The particle should gain a small increase of its velocity, and its path should become physically "stretched" for a little, causing the particle to reach the body with a delay in time compared to if the body did not rotate.

That is, light rays and mass-bearing particles should be deflected near a rotating body due to the curvature of space caused by its rotation. These two effects should take place both for mass-bearing particles and for light rays (massless light-like particles such as photons).

The other two effects are the length stretching and time loss/gain, expected in the field of a rotating body due to the curvature of its space, caused by its rotation [3]:

3. Since the diurnal rotation of the Earth around its axis curves the Earth's space making it "stretched" along the geographical longitudes, then the measured length of a standard rod should be greater when the rod is installed in the longitudinal direction;
4. Due to the same reason, there should be a time loss on board an airplane flying to the East (the direction in which the Earth's space rotates), and also a time increment when flying in the opposite direction, to the West.

Both of the effects are maximum at the equator (where the curvature of the Earth's space caused by its rotation is maximum and, therefore, space is maximally "stretched") and decrease towards the North and South Poles.

The above four effects, namely — the deflection of light rays and mass-bearing particles in the field of a rotating body, and also the length stretching and time loss/gain in the field of a rotating body — are new fundamental effects of the General Theory of Relativity, which were predicted "au bout d'un stylo". These four effects can be considered as an addition to the well-known Einstein effect of the deflection of light rays in the field of a gravitating body (which does not take the rotation of space into account).

2 Problem statement

When calculating the mentioned four new effects in the field of a rotating body, our task was to deduce the effects in their "pure form", i.e., without any other factors taken into account. To do this, the simplest metric was used, which described the four-dimensional space (space-time) of a rotating body, the mass of which is so small that the gravitational field it creates

can be neglected.

This space metric is easy to deduce. Consider the metric of an empty space, which does not rotate or deform

$$ds^2 = c^2 dt^2 - dr^2 - r^2 (d\theta^2 + \sin^2\theta d\varphi^2), \quad (1)$$

where and below, in terms of the spherical coordinates, r is the radial coordinate, dr is the elementary segment length along the radial r -axis, θ is the polar coordinate angle measured from the North Pole to the equator, $r d\theta$ is the elementary arc length along the θ -axis (along the geographical latitudes), φ is the geographical longitude (equatorial coordinate axis), and $r \sin\theta d\varphi$ is the elementary arc length along the equatorial φ -axis.

Assume that the space rotates along the equatorial axis φ , i.e., along the geographical longitudes, with the linear velocity $v_3 = \omega r^2 \sin^2\theta$, where $\omega = \text{const}$ is the angular velocity of this rotation. Since by definition of v_i (13)

$$v_3 = \omega r^2 \sin^2\theta = -\frac{c g_{03}}{\sqrt{g_{00}}} \quad (2)$$

then we have

$$g_{03} = -\frac{1}{c} v_3 \sqrt{g_{00}} = -\frac{\omega r^2 \sin^2\theta}{c}, \quad (3)$$

and the metric of such a rotating empty space has the form

$$ds^2 = c^2 dt^2 - 2\omega r^2 \sin^2\theta dt d\varphi - dr^2 - r^2 (d\theta^2 + \sin^2\theta d\varphi^2). \quad (4)$$

As you can see, the non-zero components of the fundamental metric tensor $g_{\alpha\beta}$ of this metric are

$$\left. \begin{aligned} g_{00} &= 1, & g_{03} &= -\frac{\omega r^2 \sin^2\theta}{c} \\ g_{11} &= -1, & g_{22} &= -r^2, & g_{33} &= -r^2 \sin^2\theta \end{aligned} \right\}, \quad (5)$$

where $g_{00} = 1$ means that the space is free of gravitational fields or such fields can be neglected: with $g_{00} = 1$ the gravitational field potential w , the general formula of which for any space metric is $w = c^2 (1 - \sqrt{g_{00}})$ (12), is either equal to zero $w = 0$ or approaches zero $w \rightarrow 0$.

The deflection of light rays and mass-bearing particles in the field of a rotating body [2], and also the length stretching and time loss/gain in the field of a rotating body [3] were obtained in the space of the above metric (4). Thanks to the above approximation, expressed with the simplest metric (4) describing a rotating empty space, it was possible to obtain the mentioned effects of the space curvature created by the rotation of space in their "pure form", without adding any other geometric or physical factors.

But real experiments conducted in an Earth-bound laboratory must take the gravitational field of the Earth into account. From this follows the problem statement for this paper:

PROBLEM STATEMENT

Our task now is to re-calculate the space curvature effects caused by the rotation of space — the deflection of light rays and mass-bearing particles, and also the length stretching and time loss/gain in the field of a rotating body — for the case, where the gravitational field of the rotating body is taken into account.

To do this, we need the metric of such a space. We deduce it from Schwarzschild's mass-point metric, which describes a spherically symmetric space filled with the gravitational field created in emptiness by a spherical massive island of substance (approximated by a mass-point)

$$ds^2 = \left(1 - \frac{r_g}{r}\right) c^2 dt^2 - \frac{dr^2}{1 - \frac{r_g}{r}} - r^2 (d\theta^2 + \sin^2\theta d\varphi^2), \quad (6)$$

where r is the radial distance from the centre of the massive island, $r_g = 2GM/c^2$ is its gravitational radius, calculated for its mass M , and the non-zero components of the fundamental metric tensor $g_{\alpha\beta}$ are

$$\left. \begin{aligned} g_{00} &= 1 - \frac{r_g}{r}, & g_{11} &= -\frac{1}{1 - \frac{r_g}{r}} \\ g_{22} &= -r^2, & g_{33} &= -r^2 \sin^2\theta \end{aligned} \right\}. \quad (7)$$

As before, we assume that the space rotates along the equatorial axis φ (along the geographical longitudes) with the linear velocity $v_3 = \omega r^2 \sin^2\theta$, where $\omega = \text{const}$ is the angular velocity of this rotation. Since by definition of v_i (13)

$$v_3 = \omega r^2 \sin^2\theta = -\frac{c g_{03}}{\sqrt{g_{00}}}, \quad (8)$$

and, hence,

$$g_{03} = -\frac{1}{c} v_3 \sqrt{g_{00}} = -\frac{\omega r^2 \sin^2\theta}{c} \sqrt{1 - \frac{r_g}{r}} \neq 0, \quad (9)$$

then we obtain the desired metric

$$ds^2 = \left(1 - \frac{r_g}{r}\right) c^2 dt^2 - 2\omega r^2 \sin^2\theta \sqrt{1 - \frac{r_g}{r}} dt d\varphi - \frac{dr^2}{1 - \frac{r_g}{r}} - r^2 (d\theta^2 + \sin^2\theta d\varphi^2), \quad (10)$$

which describes a spherically symmetric space, which is filled with the gravitational field created in emptiness by a rotating spherical island of matter (approximated by a mass-point) and rotates together with this body.

It is the metric (10), in the space of which we are going to re-calculate the space curvature effects, created due to the rotation of space.

We will do this in the following steps. First, we need to give a short description of the mathematical formalism we are

using — the mathematical apparatus of chronometric invariants, which are physically observable quantities in the space-time of General Relativity.

Second, we calculate the physically observable chr.inv.-characteristics of the space of a rotating mass-point, which is the space of the metric (10).

Third, it is not a fact that the space described by the introduced metric of a rotating mass-point (10) is Riemannian. By definition, a Riemannian space is such one, the metric of which has the Riemannian square form $ds^2 = g_{\alpha\beta} dx^\alpha dx^\beta$, determined by the Riemann fundamental metric tensor $g_{\alpha\beta}$, is invariant $ds^2 = inv$ everywhere in the space, and also satisfies Einstein's field equations, which are the specific relation between the Ricci curvature tensor, the fundamental metric tensor multiplied by the curvature scalar, and the energy-momentum tensor of the "space filler" (the latter targets non-empty Riemannian spaces filled with distributed matter). The above three requirements are specific to the family of Riemannian spaces.

Finding a metric that satisfies the first two conditions is easy, but satisfying the third condition (Einstein's field equations) is problematic. This is why, until now, only a small number of space metrics have been proven to be Riemannian and used in the General Theory of Relativity.

A space metric satisfies the field equations, if the components of the fundamental metric tensor $g_{\alpha\beta}$ (specific to this metric) and the components of the energy-momentum tensor of the medium (that fills the space), substituted into the field equations, make the left-hand and right-hand sides of the equations identical (the field equations vanish). In an empty Riemannian space, the left-hand side of the field equations itself after the above substitution must become zero (since in this case the energy-momentum tensor of distributed matter on the right-hand side is zero).

Most likely, the introduced metric of the space of a rotating mass-point (10) does not satisfy the field equations. For this reason, at our third step, we will substitute the $g_{\alpha\beta}$ components from the introduced metric (10) into the left-hand terms of the field equations (the right-hand side of the equations is zero, since the space of a rotating mass-point we are considering is not filled with distributed matter). The relations (particular conditions) that vanish the resulting field equations are *Riemannian conditions*, under which the introduced metric (10) is Riemannian and, therefore, can be used in the framework of General Relativity.

At our fourth step, we will deduce formulae for the space curvature effects in the field of a rotating massive body, i.e., in the space of the metric (10), which is the final task of this research.

3 Chronometrically invariant quantities

We use the mathematical apparatus of chronometric invariants, which uniquely determines physically observable quantities

in the four-dimensional pseudo-Riemannian space (space-time of General Relativity). This mathematical formalism was created in 1944 by Abraham Zelmanov.

In addition to the publications by Zelmanov [4–6], which were very concise, an extended review of the chronometrically invariant formalism was given in each of our three research monographs (together with L. Borissova), originally published in 2001 [7, 8] and 2013 [9]. In 2023 we published the most comprehensive survey of the Zelmanov formalism [10], where we collected almost everything that we know in this field personally from Zelmanov and based on our own research studies. The most complete list of the research studies performed using the chronometrically invariant formalism as of January 2023 can be found in the Bibliography to our survey [10].

In short, Zelmanov unambiguously determined physically observable quantities in the space-time of General Relativity as the projections of four-dimensional tensor quantities onto the time line and the three-dimensional spatial section, associated with an observer. Such projections remain invariant throughout the observer's three-dimensional spatial section (his observable three-dimensional physical reference space), i.e., they are "chrono-metric invariants" in his reference frame and depend on the properties of his physical reference space, such as the gravitational potential, rotation, deformation, curvature, etc.

The chronometrically invariant projections of any four-dimensional tensor quantity are calculated using operators of projection, which take the physical properties and geometric structure of the observer's space into account. For detail, see the References to chronometric invariants, e.g., the most detailed survey [10].

Below you can find only the necessary minimum of this mathematical formalism, which is necessary for understanding and reproducing the results obtained in this study.

Projecting the four-dimensional displacement vector dx^α ($\alpha = 0, 1, 2, 3$) onto the time line of an observer gives the physically observable chr.inv.-time interval $d\tau$

$$d\tau = \sqrt{g_{00}} dt - \frac{1}{c^2} v_i dx^i, \quad i = 1, 2, 3, \quad (11)$$

where g_{00} is expressed with the chr.inv.-potential w (physically observable potential) of the gravitational field that fills the space of the observer as

$$w = c^2 (1 - \sqrt{g_{00}}), \quad \sqrt{g_{00}} = 1 - \frac{w}{c^2}, \quad (12)$$

and v_i is the three-dimensional vector of the linear velocity of rotation of the observer's space

$$v_i = -\frac{c g_{0i}}{\sqrt{g_{00}}}, \quad v^i = -c g^{0i} \sqrt{g_{00}}, \quad v_i = h_{ik} v^k. \quad (13)$$

Projecting dx^α onto the observer's three-dimensional spatial section gives the three-dimensional chr.inv.-displacement

vector dx^i (which coincides with the three-dimensional coordinate displacement vector). As a result, $d\tau$ distinguishes the chr.inv.-velocity vector $v^i = dx^i/d\tau$ (physically observable three-dimensional velocity) from the three-dimensional coordinate velocity vector $u^i = dx^i/dt$.

The three-dimensional chr.inv.-spatial interval $d\sigma$ (physically observable three-dimensional interval) is determined

$$d\sigma^2 = h_{ik} dx^i dx^k, \quad (14)$$

using the three-dimensional chr.inv.-metric tensor h_{ik}

$$h_{ik} = -g_{ik} + \frac{1}{c^2} v_i v_k, \quad h^{ik} = -g^{ik}, \quad h_k^i = \delta_k^i, \quad (15)$$

which is the chr.inv.-projection of the fundamental metric tensor $g_{\alpha\beta}$ onto the observer's spatial section and possesses all properties of $g_{\alpha\beta}$ throughout the spatial section (the observer's three-dimensional space).

The square of the four-dimensional (space-time) interval $ds^2 = g_{\alpha\beta} dx^\alpha dx^\beta$ is therefore expressed with chronometrically invariant (physically observable) quantities as

$$ds^2 = c^2 d\tau^2 - d\sigma^2. \quad (16)$$

Thanks to the splitting of space-time into three-dimensional spatial sections pierced by time lines, which is specific to the chronometrically invariant formalism, we can reveal the true nature of three-dimensional rotations. When $v_i \neq 0$, i.e., the reference body of an observer rotates (together with his reference space), then this rotation cannot be vanished by a coordinate transformation (by moving the observer to another reference frame within his three-dimensional spatial section). This happens because the rotation speed v_i (13) is determined by the mixed (space-time) components g_{0i} of the fundamental metric tensor $g_{\alpha\beta}$, and not by its three-dimensional spatial components g_{ik} dependent on time (as it is considered in classical mechanics, where time is just a parameter, and not the fourth coordinate). Since the components of $g_{\alpha\beta}$ are cosines of the angles between the respective coordinate lines, then three-dimensional rotations are due to the *non-holonomy* of space-time, which means that time lines are not orthogonal to three-dimensional spatial sections.

If all g_{0i} are zero, then such space-time is *holonomic*. In this case the three-dimensional spatial section is everywhere orthogonal to the time lines that pierce it. If at least one of the components g_{0i} is different from zero, then such space-time is *non-holonomic*, and the spatial section $x^0 = \text{const}$ is inclined to the time lines (at different points it can be inclined to the time lines at different angles depending on the local geometric structure of the particular four-dimensional space-time).

In general, the physical reference space of a real observer can be filled with a gravitational field, rotate, deform, be inhomogeneous and curved.

The chr.inv.-vector of the gravitational inertial force F_i , where the first (gravitational) term is created by the gradient

of the gravitational potential w and the second (inertial) term is created by the centrifugal force of inertia, is

$$F_i = \frac{1}{\sqrt{g_{00}}} \left(\frac{\partial w}{\partial x^i} - \frac{\partial v_i}{\partial t} \right), \quad \sqrt{g_{00}} = 1 - \frac{w}{c^2}. \quad (17)$$

The antisymmetric chr.inv.-tensor A_{ik} of the angular velocity of rotation of space is

$$A_{ik} = \frac{1}{2} \left(\frac{\partial v_k}{\partial x^i} - \frac{\partial v_i}{\partial x^k} \right) + \frac{1}{2c^2} (F_i v_k - F_k v_i), \quad (18)$$

which is related to F_i by two identities

$$\frac{* \partial A_{ik}}{\partial t} + \frac{1}{2} \left(\frac{* \partial F_k}{\partial x^i} - \frac{* \partial F_i}{\partial x^k} \right) = 0, \quad (19)$$

$$\frac{* \partial A_{km}}{\partial x^i} + \frac{* \partial A_{mi}}{\partial x^k} + \frac{* \partial A_{ik}}{\partial x^m} + \frac{1}{2} (F_i A_{km} + F_k A_{mi} + F_m A_{ik}) = 0, \quad (20)$$

where asterisk denotes the chr.inv.-derivation operators

$$\frac{* \partial}{\partial t} = \frac{1}{\sqrt{g_{00}}} \frac{\partial}{\partial t}, \quad \frac{* \partial}{\partial x^i} = \frac{\partial}{\partial x^i} + \frac{1}{c^2} v_i \frac{\partial}{\partial t}. \quad (21)$$

Antisymmetric chr.inv.-tensors can be used to create the corresponding chr.inv.-pseudovectors (marked with an asterisk) using the antisymmetric chr.inv.-discriminant tensor

$$\varepsilon^{ikm} = \frac{e^{ikm}}{\sqrt{h}}, \quad \varepsilon_{ikm} = e_{ikm} \sqrt{h}, \quad (22)$$

where $h = \det \| h_{ik} \|$. This tensor is the chr.inv.-analogy of the Levi-Civita antisymmetric unit tensor e^{ikm} (the components of e^{ikm} are either +1 or -1 depending on the transposition of its indices).^{*} For example, the antisymmetric chr.inv.-tensor A_{ik} of the angular velocity of rotation of space has the corresponding chr.inv.-pseudovector Ω^{*i} of this rotation

$$\left. \begin{aligned} \Omega^{*i} &= \frac{1}{2} \varepsilon^{ikm} A_{km}, & \Omega_{*i} &= \frac{1}{2} \varepsilon_{imn} A^{mn} \\ \varepsilon^{ipq} \Omega_{*i} &= \frac{1}{2} \varepsilon^{ipq} \varepsilon_{imn} A^{mn} = \\ &= \frac{1}{2} (\delta_m^p \delta_n^q - \delta_m^q \delta_n^p) A^{mn} = A^{pq} \end{aligned} \right\}. \quad (23)$$

The symmetric chr.inv.-tensor D_{ik} of the deformation rate of space is formulated as

$$\left. \begin{aligned} D_{ik} &= \frac{1}{2} \frac{* \partial h_{ik}}{\partial t}, & D^{ik} &= -\frac{1}{2} \frac{* \partial h^{ik}}{\partial t} \\ D &= h^{ik} D_{ik} = \frac{* \partial \ln \sqrt{h}}{\partial t}, & h &= \det \| h_{ik} \| \end{aligned} \right\}. \quad (24)$$

^{*}For detail, see pages 14–16 in our comprehensive survey of the Zelmanov chronometric invariants [10], or §2.3 in our monograph [8].

The chr.inv.-Christoffel symbols of the 1st rank $\Delta_{jk,m}$ and the 2nd rank Δ_{nk}^i (their physical sense is the coefficients of inhomogeneity of space) are

$$\Delta_{nk}^i = h^{im} \Delta_{nk,m} = \frac{1}{2} h^{im} \left(\frac{* \partial h_{nm}}{\partial x^k} + \frac{* \partial h_{km}}{\partial x^n} - \frac{* \partial h_{nk}}{\partial x^m} \right). \quad (25)$$

The physically observable curvature of space is expressed with the chr.inv.-curvature tensor C_{lkij} that possesses all properties of the Riemann-Christoffel curvature tensor throughout the three-dimensional spatial section associated with the observer. Its subsequent contractions give the chr.inv.-Ricci curvature tensor C_{ik} and the chr.inv.-scalar curvature C

$$\begin{aligned} C_{lkij} &= \frac{1}{4} (H_{lkij} - H_{jkil} + H_{klji} - H_{ijlk}) = \\ &= H_{lkij} - \frac{1}{2} (2A_{ki} D_{jl} + A_{ij} D_{kl} + A_{jk} D_{il} + \\ &\quad + A_{kl} D_{ij} + A_{li} D_{jk}), \end{aligned} \quad (26)$$

$$C_{lk} = C_{lki}^{\dots i} = H_{lk} - \frac{1}{2} (A_{kj} D_l^j + A_{lj} D_k^j + A_{kl} D), \quad (27)$$

$$C = h^{lk} C_{lk} = h^{lk} H_{lk}, \quad (28)$$

where, for a better association with the Riemann-Christoffel curvature tensor, we denote

$$H_{lki}^{\dots j} = \frac{* \partial \Delta_{il}^j}{\partial x^k} - \frac{* \partial \Delta_{kl}^j}{\partial x^i} + \Delta_{il}^m \Delta_{km}^j - \Delta_{kl}^m \Delta_{im}^j. \quad (29)$$

From the above definitions we see that the physically observable curvature of space depends on not only the gravitational inertial force (hidden in the second chr.inv.-derivatives of the chr.inv.-metric tensor), but also the rotation, deformation and inhomogeneity of space and, therefore, does not vanish in the absence of the gravitational field.

By analogy with absolute (general covariant) derivatives, the corresponding chr.inv.-derivatives are introduced

$$* \nabla_i Q_k = \frac{* \partial Q_k}{\partial x^i} - \Delta_{ik}^l Q_l, \quad (30)$$

$$* \nabla_i Q^k = \frac{* \partial Q^k}{\partial x^i} + \Delta_{il}^k Q^l, \quad (31)$$

$$* \nabla_i Q_{jk} = \frac{* \partial Q_{jk}}{\partial x^i} - \Delta_{ij}^l Q_{lk} - \Delta_{ik}^l Q_{jl}, \quad (32)$$

$$* \nabla_i Q_j^k = \frac{* \partial Q_j^k}{\partial x^i} - \Delta_{ij}^l Q_l^k + \Delta_{il}^k Q_j^l, \quad (33)$$

$$* \nabla_i Q^{jk} = \frac{* \partial Q^{jk}}{\partial x^i} + \Delta_{il}^j Q^{lk} + \Delta_{il}^k Q^{jl}, \quad (34)$$

$$* \nabla_i Q^j = \frac{* \partial Q^j}{\partial x^i} + \Delta_{ji}^j Q^i, \quad \Delta_{ji}^j = \frac{* \partial \ln \sqrt{h}}{\partial x^i}, \quad (35)$$

$$* \nabla_i Q^{ji} = \frac{* \partial Q^{ji}}{\partial x^i} + \Delta_{il}^j Q^{il} + \Delta_{li}^j Q^{ji}, \quad \Delta_{li}^j = \frac{* \partial \ln \sqrt{h}}{\partial x^i}, \quad (36)$$

which, in particular, exhibit some properties of the chr.inv.-metric tensor h_{ik} and the chr.inv.-discriminant tensor ε_{ijk} (used further in calculations)

$$* \nabla_i h_{jk} = 0, \quad * \nabla_i h_j^k = 0, \quad * \nabla_i h^{jk} = 0, \quad (37)$$

$$* \nabla_l \varepsilon_{ijk} = 0, \quad * \nabla_l \varepsilon^{ijk} = 0, \quad (38)$$

Einstein's field equations, having the well-known general covariant (four-dimensional) form

$$R_{\alpha\beta} - \frac{1}{2} g_{\alpha\beta} R = -\kappa T_{\alpha\beta} + \lambda g_{\alpha\beta} \quad (39)$$

can also be presented in chr.inv.-form, i.e., in the form of their physically observable chr.inv.-projections.

Note, that the Zelmanov formalism uses $\kappa = \frac{8\pi G}{c^2}$, but not $\kappa = \frac{8\pi G}{c^4}$ as Landau and Lifshitz did in their *The Classical Theory of Fields* [11]. This is because, since Ricci's tensor $R_{\alpha\beta}$ has the dimension $[\text{cm}^{-2}]$ and the energy-momentum tensor $T_{\alpha\beta}$ has the dimension of mass density $[\text{gram}/\text{cm}^3]$, if we used $\kappa = \frac{8\pi G}{c^4}$ on the right-hand side of the field equations, then we would not use the energy-momentum tensor $T_{\alpha\beta}$ itself, but $c^2 T_{\alpha\beta}$ as Landau and Lifshitz did (which is not correct at all from the point of view of physical sense and physically observable quantities).

To understand the chr.inv.-Einstein equations that below, we should note that any tensor or tensor equation of the 2nd rank has three chr.inv.-projections: the time projection, the space-time (mixed) projection and the spatial projection; for detail, see [10]. So, the energy-momentum tensor $T_{\alpha\beta}$ of a distributed matter has the following chr.inv.-projections

$$\varrho = \frac{T_{00}}{g_{00}}, \quad J^i = \frac{c T_0^i}{\sqrt{g_{00}}}, \quad U^{ik} = c^2 T^{ik}, \quad (40)$$

where ϱ is the observable mass density of the distributed matter, J^i is its observable momentum density, and U^{ik} is the observable stress-tensor of the matter field.

The general covariant Einstein field equations (39) also have three chr.inv.-projections, which are called the chr.inv.-Einstein equations

$$\begin{aligned} \frac{* \partial D}{\partial t} + D_{jl} D^{jl} + A_{jl} A^{lj} + * \nabla_j F^j - \frac{1}{c^2} F_j F^j = \\ = -\frac{\kappa}{2} (\varrho c^2 + U) + \lambda c^2, \end{aligned} \quad (41)$$

$$* \nabla_j (h^{ij} D - D^{ij} - A^{ij}) + \frac{2}{c^2} F_j A^{ij} = \kappa J^i, \quad (42)$$

$$\begin{aligned} \frac{* \partial D_{ik}}{\partial t} - (D_{ij} + A_{ij}) (D_k^j + A_{k.}^j) + D D_{ik} + 3 A_{ij} A_{k.}^j - \\ - \frac{1}{c^2} F_i F_k + \frac{1}{2} (* \nabla_i F_k + * \nabla_k F_i) - c^2 C_{ik} = \\ = \frac{\kappa}{2} (\varrho c^2 h_{ik} + 2 U_{ik} - U h_{ik}) + \lambda c^2 h_{ik}. \end{aligned} \quad (43)$$

With the above mathematical tools, we now have everything we need to consider the space of a rotating massive body using the chronometrically invariant formalism.

4 Physically observable characteristics of the space of a rotating massive body

Consider a space of the rotating Schwarzschild metric, which we have introduced (10). It has the form

$$ds^2 = \left(1 - \frac{r_g}{r}\right) c^2 dt^2 - 2\omega r^2 \sin^2\theta \sqrt{1 - \frac{r_g}{r}} dt d\varphi - \frac{dr^2}{1 - \frac{r_g}{r}} - r^2 (d\theta^2 + \sin^2\theta d\varphi^2). \quad (44)$$

Such a space rotates in the equatorial plane along the geographical longitudes φ with an angular velocity $\omega = const.$ The linear velocity of this rotation is $v_3 = \omega r^2 \sin^2\theta$

$$v_3 = \omega r^2 \sin^2\theta = -\frac{c g_{03}}{\sqrt{g_{00}}}, \quad v_1 = v_2 = 0, \quad (45)$$

hence, non-zero components of the fundamental metric tensor of the above space metric are

$$\left. \begin{aligned} g_{00} &= 1 - \frac{r_g}{r}, & g_{03} &= -\frac{\omega r^2 \sin^2\theta}{c} \sqrt{1 - \frac{r_g}{r}} \\ g_{11} &= -\frac{1}{1 - \frac{r_g}{r}}, & g_{22} &= -r^2, & g_{33} &= -r^2 \sin^2\theta \end{aligned} \right\}. \quad (46)$$

Respectively, the chr.inv.-metric tensor $h_{ik} = -g_{ik} + \frac{1}{c^2} v_i v_k$ (15) of a rotating Schwarzschild space has only the following non-zero components

$$\left. \begin{aligned} h_{11} &= \frac{1}{1 - \frac{r_g}{r}}, & h_{22} &= r^2 \\ h_{33} &= r^2 \sin^2\theta \left(1 + \frac{\omega^2 r^2 \sin^2\theta}{c^2}\right) \end{aligned} \right\}, \quad (47)$$

and, respectively, calculating the determinant of the chr.inv.-metric tensor h_{ik} , we obtain

$$h = \det \| h_{ik} \| = h_{11} h_{22} h_{33} = \frac{r^4 \sin^2\theta}{1 - \frac{r_g}{r}} \left(1 + \frac{\omega^2 r^2 \sin^2\theta}{c^2}\right), \quad (48)$$

$$\sqrt{h} = \frac{r^2 \sin\theta}{\sqrt{1 - \frac{r_g}{r}}} \sqrt{1 + \frac{\omega^2 r^2 \sin^2\theta}{c^2}}. \quad (49)$$

As is seen from the above formulae, the matrix h_{ik} is strict diagonal: all of its non-diagonal components h_{ik} ($i \neq k$) are zero. Therefore, the upper-index components of h_{ik} are obtained just like the invertible matrix components to any diag-

onal matrix as $h^{ik} = (h_{ik})^{-1}$. They are

$$\left. \begin{aligned} h^{11} &= 1 - \frac{r_g}{r}, & h^{22} &= \frac{1}{r^2} \\ h^{33} &= \frac{1}{r^2 \sin^2\theta \left(1 + \frac{\omega^2 r^2 \sin^2\theta}{c^2}\right)} \end{aligned} \right\}. \quad (50)$$

In particular, as a result, the square of the linear velocity, with which the space rotates $v^2 = v_i v^i = v_i h^{ik} v_k$ (13) is

$$v^2 = v_3 h^{33} v_3 = \frac{\omega^2 r^2 \sin^2\theta}{1 + \frac{\omega^2 r^2 \sin^2\theta}{c^2}}. \quad (51)$$

As is seen from (47), the obtained chr.inv.-metric tensor h_{ik} does not depend on time. This means that the chr.inv.-tensor of the deformation rate of space D_{ik} (24) is zero

$$D_{ik} = \frac{1}{2} \frac{\partial h_{ik}}{\partial t} = 0, \quad (52)$$

i.e., a rotating Schwarzschild space does not deform.

Taking into account that the linear velocity $v_3 = \omega r^2 \sin^2\theta$ with which the space rotates does not depend on time

$$\frac{\partial v_3}{\partial t} = 0 \quad (53)$$

and also that the gravitational field potential $w = c^2 (1 - \sqrt{g_{00}})$ in the present case is

$$w = c^2 \left(1 - \sqrt{1 - \frac{r_g}{r}}\right), \quad (54)$$

we obtain the components of the chr.inv.-vector of the gravitational inertial force F_i (17). They are

$$F_1 = \frac{1}{\sqrt{g_{00}}} \frac{\partial w}{\partial r} = -\frac{c^2 r_g}{2r^2} \frac{1}{1 - \frac{r_g}{r}}, \quad F_2 = F_3 = 0, \quad (55)$$

$$F^1 = h^{11} F_1 = -\frac{c^2 r_g}{2r^2}, \quad F^2 = F^3 = 0. \quad (56)$$

Since the gravitational inertial force in the present case is a radially acting force F_1 that depends only on $x^1 = r$, i.e.

$$\frac{\partial F_k}{\partial x^i} = 0, \quad i \neq k, \quad (57)$$

then according to the 1st Zelmanov identity (19) we have

$$\frac{\partial A_{ik}}{\partial t} = 0, \quad (58)$$

i.e., the rotation of the space of the rotating Schwarzschild metric is stationary.

According to the definition of the chr.inv.-tensor of the angular velocity of rotation of space A_{ik} (18), only the following components of it are non-zero in the space of the rotating Schwarzschild metric: $A_{13} \neq 0$, $A_{31} \neq 0$, $A^{13} \neq 0$, $A^{31} \neq 0$,

$A_{23} \neq 0, A_{32} \neq 0, A^{23} \neq 0, A^{32} \neq 0$. Using the definition of A_{ik} (18), after some algebra we obtain

$$A_{13} = \frac{1}{2} \frac{\partial v_3}{\partial r} + \frac{1}{2c^2} F_1 v_3 = \omega r \sin^2 \theta - \frac{\omega r_g \sin^2 \theta}{4 \left(1 - \frac{r_g}{r}\right)}, \quad (59)$$

$$A_{31} = -A_{13} = -\omega r \sin^2 \theta + \frac{\omega r_g \sin^2 \theta}{4 \left(1 - \frac{r_g}{r}\right)}, \quad (60)$$

$$A^{13} = h^{11} h^{33} A_{13} = \frac{\left(1 - \frac{r_g}{r}\right) \omega}{r \left(1 + \frac{\omega^2 r^2 \sin^2 \theta}{c^2}\right)} - \frac{\omega r_g}{4r^2 \left(1 + \frac{\omega^2 r^2 \sin^2 \theta}{c^2}\right)}, \quad (61)$$

$$A^{31} = -A^{13} = -\frac{\left(1 - \frac{r_g}{r}\right) \omega}{r \left(1 + \frac{\omega^2 r^2 \sin^2 \theta}{c^2}\right)} + \frac{\omega r_g}{4r^2 \left(1 + \frac{\omega^2 r^2 \sin^2 \theta}{c^2}\right)}, \quad (62)$$

$$A_{23} = \frac{1}{2} \frac{\partial v_3}{\partial \theta} = \omega r^2 \sin \theta \cos \theta, \quad (63)$$

$$A_{32} = -A_{23} = -\omega r^2 \sin \theta \cos \theta, \quad (64)$$

$$A^{23} = h^{22} h^{33} A_{23} = \frac{\omega \cot \theta}{r^2 \left(1 + \frac{\omega^2 r^2 \sin^2 \theta}{c^2}\right)}, \quad (65)$$

$$A^{32} = -A^{23} = -\frac{\omega \cot \theta}{r^2 \left(1 + \frac{\omega^2 r^2 \sin^2 \theta}{c^2}\right)}. \quad (66)$$

Find the physically observable scalar angular velocity Ω , with which the space rotates. Its square is calculated as

$$\begin{aligned} \Omega^2 &= \Omega_{*i} \Omega^{*i} = \Omega_{*1} \Omega^{*1} + \Omega_{*2} \Omega^{*2} = \\ &= h_{11} \Omega^{*1} \Omega^{*1} + h_{22} \Omega^{*2} \Omega^{*2}. \end{aligned} \quad (67)$$

In the space of the rotating Schwarzschild metric, which we are considering, we have

$$\Omega^{*1} = \frac{1}{2} \varepsilon^{1km} A_{km} = \frac{e^{1km}}{2\sqrt{h}} A_{km} = \frac{e^{123}}{2\sqrt{h}} A_{23} + \frac{e^{132}}{2\sqrt{h}} A_{32} \quad (68)$$

and, taking into account that $e^{123} = +1$ and $e^{132} = -1$, and also $A_{32} = -A_{23}$, we obtain

$$\Omega^{*1} = \frac{e^{123}}{2\sqrt{h}} A_{23} + \frac{e^{123}}{2\sqrt{h}} A_{23} = \frac{e^{123}}{\sqrt{h}} A_{23} = \frac{A_{23}}{\sqrt{h}}. \quad (69)$$

In the same way, we obtain

$$\begin{aligned} \Omega^{*2} &= \frac{1}{2} \varepsilon^{2km} A_{km} = \frac{e^{2km}}{2\sqrt{h}} A_{km} = \\ &= \frac{e^{213}}{2\sqrt{h}} A_{13} + \frac{e^{231}}{2\sqrt{h}} A_{31} = \frac{e^{213}}{\sqrt{h}} A_{13} = -\frac{A_{13}}{\sqrt{h}}. \end{aligned} \quad (70)$$

Finally, substituting A_{13} (59), A_{23} (63), $h = \det \| h_{ik} \|$ (48), h_{11} and h_{22} (47) into Ω^2 (67), we obtain the physically observable scalar angular velocity Ω of the rotation of space

$$\begin{aligned} \Omega &= \sqrt{\Omega_{*i} \Omega^{*i}} = \frac{\omega}{\sqrt{1 + \frac{\omega^2 r^2 \sin^2 \theta}{c^2}}} \times \\ &\times \sqrt{1 - \frac{3r_g \sin^2 \theta}{2r} + \frac{r_g^2 \sin^2 \theta}{16r^2 \left(1 - \frac{r_g}{r}\right)}}. \end{aligned} \quad (71)$$

If there is no mass ($M = 0$), then the gravitational radius is $r_g = 2GM/c^2 = 0$. In this case, $g_{00} = 1 - \frac{r_g}{r} = 1$ and the formulae for h_{ik} (47–50), A_{ik} (59–66) and Ω (71) we have obtained in the space of the rotating Schwarzschild metric transform into the corresponding formulae in the spherically symmetric rotating space without the gravitational field, which we have obtained earlier; see page 43 in the previous paper [1].

To calculate the chr.inv.-Einstein equations in the space of the rotating Schwarzschild metric, we need the chr.inv.-Ricci curvature tensor C_{ik} containing in the third, tensor chr.inv.-Einstein equation (43). The chr.inv.-Ricci tensor C_{ik} (27) consists of the chr.inv.-derivatives of the chr.inv.-Christoffel symbols Δ_{nk}^i and the products of Δ_{nk}^i with each other. In turn, Δ_{nk}^i (25) are the re-combination of the chr.inv.-derivatives of the chr.inv.-metric tensor h_{ik} (47). Therefore, at first we calculate the non-zero chr.inv.-derivatives of h_{ik}

$$\frac{* \partial h_{11}}{\partial r} = -\frac{r_g}{\left(1 - \frac{r_g}{r}\right)^2 r^2}, \quad (72)$$

$$\frac{* \partial h_{22}}{\partial r} = 2r, \quad (73)$$

$$\frac{* \partial h_{33}}{\partial r} = 2r \sin^2 \theta \left(1 + \frac{2\omega^2 r^2 \sin^2 \theta}{c^2}\right), \quad (74)$$

$$\frac{* \partial h_{33}}{\partial \theta} = 2r^2 \sin \theta \cos \theta \left(1 + \frac{2\omega^2 r^2 \sin^2 \theta}{c^2}\right). \quad (75)$$

The chr.inv.-Christoffel symbols Δ_{nk}^i (25) in the rotating Schwarzschild metric space have the non-zero components

$$\left. \begin{aligned} \Delta_{11}^1 &= \frac{1}{2} h^{11} \frac{* \partial h_{11}}{\partial r}, & \Delta_{22}^1 &= \frac{1}{2} h^{11} \frac{* \partial h_{22}}{\partial r} \\ \Delta_{33}^1 &= -\frac{1}{2} h^{11} \frac{* \partial h_{33}}{\partial r}, & \Delta_{12}^2 &= \frac{1}{2} h^{22} \frac{* \partial h_{22}}{\partial r} \\ \Delta_{21}^2 &= \frac{1}{2} h^{22} \frac{* \partial h_{22}}{\partial r}, & \Delta_{33}^2 &= -\frac{1}{2} h^{22} \frac{* \partial h_{33}}{\partial \theta} \\ \Delta_{13}^3 &= \frac{1}{2} h^{33} \frac{* \partial h_{33}}{\partial r}, & \Delta_{23}^3 &= \frac{1}{2} h^{33} \frac{* \partial h_{33}}{\partial \theta} \\ \Delta_{31}^3 &= \frac{1}{2} h^{33} \frac{* \partial h_{33}}{\partial r}, & \Delta_{32}^3 &= \frac{1}{2} h^{33} \frac{* \partial h_{33}}{\partial \theta} \end{aligned} \right\}. \quad (76)$$

After some algebra using the obtained formulae for the non-zero components of h^{ik} (50) and the chr.inv.-derivatives of the non-zero components of h_{ik} (72–75), we obtain

$$\Delta_{11}^1 = -\frac{r_g}{2r^2\left(1 - \frac{r_g}{r}\right)}, \quad (77)$$

$$\Delta_{22}^1 = -r, \quad (78)$$

$$\Delta_{33}^1 = -r \sin^2\theta \left(1 + \frac{2\omega^2 r^2 \sin^2\theta}{c^2}\right), \quad (79)$$

$$\Delta_{12}^2 = \Delta_{21}^2 = \frac{1}{r}, \quad (80)$$

$$\Delta_{33}^2 = -\sin\theta \cos\theta \left(1 + \frac{2\omega^2 r^2 \sin^2\theta}{c^2}\right), \quad (81)$$

$$\Delta_{13}^3 = \Delta_{31}^3 = \frac{1}{r\left(1 + \frac{\omega^2 r^2 \sin^2\theta}{c^2}\right)} \left(1 + \frac{2\omega^2 r^2 \sin^2\theta}{c^2}\right), \quad (82)$$

$$\Delta_{23}^3 = \Delta_{32}^3 = \frac{\cot\theta}{1 + \frac{\omega^2 r^2 \sin^2\theta}{c^2}} \left(1 + \frac{2\omega^2 r^2 \sin^2\theta}{c^2}\right). \quad (83)$$

The non-zero contracted chr.inv.-Christoffel symbols Δ_{i1}^i and Δ_{i2}^i are calculated from their definition based on the determinant $h = \det \|h_{ik}\|$; see (35) or (36). Using the formulae for h (48) and its square root (49) obtained in the space of the rotating Schwarzschild metric, we obtain

$$\Delta_{i1}^i = \frac{\partial \ln \sqrt{h}}{\partial r} = \frac{2}{r\left(1 + \frac{\omega^2 r^2 \sin^2\theta}{c^2}\right)} \left(1 + \frac{3\omega^2 r^2 \sin^2\theta}{2c^2}\right) - \frac{r_g}{2r^2\left(1 - \frac{r_g}{r}\right)}, \quad (84)$$

$$\Delta_{i2}^i = \frac{\partial \ln \sqrt{h}}{\partial \theta} = \frac{\cot\theta}{1 + \frac{\omega^2 r^2 \sin^2\theta}{c^2}} \left(1 + \frac{2\omega^2 r^2 \sin^2\theta}{c^2}\right). \quad (85)$$

Based on the above formulae, we calculate the non-zero chr.inv.-derivatives of the contracted chr.inv.-Christoffel symbols Δ_{i1}^i and Δ_{i2}^i . After some algebra, we obtain

$$\frac{\partial \Delta_{i1}^i}{\partial r} = -\frac{2}{r^2\left(1 + \frac{\omega^2 r^2 \sin^2\theta}{c^2}\right)^2} - \frac{3\omega^2 \sin^2\theta}{c^2\left(1 + \frac{\omega^2 r^2 \sin^2\theta}{c^2}\right)^2} - \frac{3\omega^4 r^2 \sin^4\theta}{c^4\left(1 + \frac{\omega^2 r^2 \sin^2\theta}{c^2}\right)^2} + \frac{r_g}{r^3\left(1 - \frac{r_g}{r}\right)^2} \left(1 - \frac{r_g}{2r}\right), \quad (86)$$

$$\frac{\partial \Delta_{i1}^i}{\partial \theta} = \frac{2\omega^2 r \sin\theta \cos\theta}{c^2\left(1 + \frac{\omega^2 r^2 \sin^2\theta}{c^2}\right)^2}, \quad (87)$$

$$\frac{\partial \Delta_{i2}^i}{\partial r} = \frac{2\omega^2 r \sin\theta \cos\theta}{c^2\left(1 + \frac{\omega^2 r^2 \sin^2\theta}{c^2}\right)^2} = \frac{\partial \Delta_{i1}^i}{\partial \theta}, \quad (88)$$

$$\frac{\partial \Delta_{i2}^i}{\partial \theta} = -\frac{1}{\sin^2\theta\left(1 + \frac{\omega^2 r^2 \sin^2\theta}{c^2}\right)} - \frac{2\omega^2 r^2 \sin^2\theta}{c^2\left(1 + \frac{\omega^2 r^2 \sin^2\theta}{c^2}\right)^2} - \frac{2\omega^4 r^4 \sin^4\theta}{c^4\left(1 + \frac{\omega^2 r^2 \sin^2\theta}{c^2}\right)^2}. \quad (89)$$

Now, using the quantities calculated above, we calculate the chr.inv.-Ricci curvature tensor C_{ik} in the space of the rotating Schwarzschild metric. Since the space we are considering does not deform ($D_{ik} = 0$), then in this case the general formula for $C_{lk} = C_{lki}^{\dots i}$ (27) is simplified to

$$C_{lk} = H_{lk} = H_{lki}^{\dots i} = \frac{\partial \Delta_{il}^i}{\partial x^k} - \frac{\partial \Delta_{kl}^i}{\partial x^i} + \Delta_{il}^m \Delta_{km}^i - \Delta_{kl}^m \Delta_{im}^i, \quad (90)$$

which, according to the non-zero chr.inv.-Christoffel symbols calculated in the space of the rotating Schwarzschild metric (see above), has the following non-zero components

$$C_{11} = \frac{\partial \Delta_{i1}^i}{\partial r} + \Delta_{21}^2 \Delta_{12}^2 + \Delta_{31}^3 \Delta_{13}^3 - \frac{\partial \Delta_{11}^1}{\partial r} + \Delta_{11}^1 \Delta_{11}^1 - \Delta_{11}^1 \Delta_{i1}^i, \quad (91)$$

$$C_{12} = \frac{\partial \Delta_{i1}^i}{\partial \theta} + \Delta_{31}^3 \Delta_{23}^3 - \Delta_{21}^2 \Delta_{i2}^i, \quad (92)$$

$$C_{21} = \frac{\partial \Delta_{i2}^i}{\partial r} + \Delta_{32}^3 \Delta_{13}^3 - \Delta_{12}^2 \Delta_{i2}^i, \quad (93)$$

$$C_{22} = \frac{\partial \Delta_{i2}^i}{\partial \theta} - \frac{\partial \Delta_{22}^2}{\partial r} + 2\Delta_{12}^2 \Delta_{22}^2 + \Delta_{32}^3 \Delta_{23}^3 - \Delta_{22}^2 \Delta_{i1}^i, \quad (94)$$

$$C_{33} = -\frac{\partial \Delta_{33}^3}{\partial r} - \frac{\partial \Delta_{33}^3}{\partial \theta} + 2\Delta_{13}^3 \Delta_{33}^3 + 2\Delta_{23}^3 \Delta_{33}^3 - \Delta_{33}^3 \Delta_{i1}^i - \Delta_{33}^3 \Delta_{i2}^i. \quad (95)$$

To calculate these components, we calculate the unknown derivatives contained in them. We obtain

$$\frac{\partial \Delta_{11}^1}{\partial r} = \frac{r_g}{r^3\left(1 - \frac{r_g}{r}\right)^2} \left(1 - \frac{r_g}{2r}\right), \quad (96)$$

$$\frac{\partial \Delta_{33}^3}{\partial r} = -\sin^2\theta \left(1 + \frac{6\omega^2 r^2 \sin^2\theta}{c^2}\right), \quad (97)$$

$$\frac{\partial \Delta_{33}^3}{\partial \theta} = \sin^2\theta + \frac{2\omega^2 r^2 \sin^4\theta}{c^2} - \cos^2\theta - \frac{6\omega^2 r^2 \sin^2\theta \cos^2\theta}{c^2}. \quad (98)$$

Substituting the non-zero necessary chr.inv.-Christoffel symbols and their chr.inv.-derivatives into these general for-

mulae (91–95), after some algebra and non-trivial transformations we obtain formulae for the non-zero components of the chr.inv.-Ricci tensor in the space of the rotating Schwarzschild metric. They have the form

$$C_{11} = \frac{3\omega^2 \sin^2 \theta}{c^2 \left(1 + \frac{\omega^2 r^2 \sin^2 \theta}{c^2}\right)} - \frac{\omega^4 r^2 \sin^4 \theta}{c^4 \left(1 + \frac{\omega^2 r^2 \sin^2 \theta}{c^2}\right)^2} + \frac{r_g}{r^3 \left(1 - \frac{r_g}{r}\right) \left(1 + \frac{\omega^2 r^2 \sin^4 \theta}{c^2}\right)} \left(1 + \frac{3\omega^2 r^2 \sin^2 \theta}{2c^2}\right), \quad (99)$$

$$C_{12} = \frac{3\omega^2 r \sin \theta \cos \theta}{c^2 \left(1 + \frac{\omega^2 r^2 \sin^2 \theta}{c^2}\right)} - \frac{\omega^4 r^3 \sin^3 \theta \cos \theta}{c^4 \left(1 + \frac{\omega^2 r^2 \sin^2 \theta}{c^2}\right)^2}, \quad (100)$$

$$C_{21} = \frac{3\omega^2 r \sin \theta \cos \theta}{c^2 \left(1 + \frac{\omega^2 r^2 \sin^2 \theta}{c^2}\right)} - \frac{\omega^4 r^3 \sin^3 \theta \cos \theta}{c^4 \left(1 + \frac{\omega^2 r^2 \sin^2 \theta}{c^2}\right)^2}, \quad (101)$$

$$C_{22} = \frac{3\omega^2 r^2 \cos^2 \theta}{c^2 \left(1 + \frac{\omega^2 r^2 \sin^2 \theta}{c^2}\right)} - \frac{\omega^4 r^4 \sin^2 \theta \cos^2 \theta}{c^4 \left(1 + \frac{\omega^2 r^2 \sin^2 \theta}{c^2}\right)^2}, \quad (102)$$

$$C_{33} = \frac{3\omega^2 r^2 \sin^2 \theta}{c^2} - \frac{\omega^4 r^4 \sin^4 \theta}{c^4 \left(1 + \frac{\omega^2 r^2 \sin^2 \theta}{c^2}\right)}, \quad (103)$$

where $C_{12} = C_{21}$ means that the space of the rotating Schwarzschild metric has a certain curvature symmetry.

Using the obtained components of the chr.inv.-Ricci tensor C_{ik} (99–103) and the upper-index components h^{ik} (50) of the chr.inv.-metric tensor, we calculate the physically observable chr.inv.-scalar curvature $C = h^{ik} C_{ik}$ (28) of the space of the rotating Schwarzschild metric. Since only h^{11} , h^{22} , h^{33} are non-zero in such a space, then $C = h^{11} C_{11} + h^{22} C_{22} + h^{33} C_{33}$. After some algebra, we obtain

$$C = \frac{6\omega^2}{c^2 \left(1 + \frac{\omega^2 r^2 \sin^2 \theta}{c^2}\right)} - \frac{2\omega^4 r^2 \sin^2 \theta}{c^4 \left(1 + \frac{\omega^2 r^2 \sin^2 \theta}{c^2}\right)^2} + \frac{r_g}{r^3 \left(1 + \frac{\omega^2 r^2 \sin^2 \theta}{c^2}\right)} \times \left(1 - \frac{3\omega^2 r^2 \sin^2 \theta}{2c^2} + \frac{\omega^4 r^4 \sin^4 \theta}{c^4}\right), \quad (104)$$

where the first two terms are due only to the rotation of space, and the third term (in the second and third lines of the formula) is due to the combined action of the gravitational field and the rotation of space.

This is the *physically observable chr.inv.-scalar curvature* of the three-dimensional space of a rotating massive body. It is this curvature of space that is registered in astronomical observations and laboratory measurements in the space near such rotating massive bodies as stars and planets.

In the absence of a massive island of substance producing the gravitational field ($M = 0$, $r_g = 2GM/c^2 = 0$), the obtained formula (104) transforms into the formula

$$C = \frac{6\omega^2}{c^2 \left(1 + \frac{\omega^2 r^2 \sin^2 \theta}{c^2}\right)} - \frac{2\omega^4 r^2 \sin^2 \theta}{c^4 \left(1 + \frac{\omega^2 r^2 \sin^2 \theta}{c^2}\right)^2}, \quad (105)$$

obtained recently in a rotating spherically symmetric space without a gravitational field; see page 45 in the first paper [1] of this series of papers.

At small speeds of rotation, the obtained formula for the chr.inv.-scalar curvature (104) takes the simplified form

$$C = \frac{6\omega^2}{c^2} + \frac{r_g}{r^3}. \quad (106)$$

From the obtained simplified formula for C (106), we see that the rotation of a massive body at slow rotations creates a constant curvature field that does not depend on distance from its source (the rotating body), whereas the gravitational field of the body creates a curvature that decreases inversely proportional to r^3 from it.

If the massive body approximated by a mass-point does not rotate ($\omega = 0$), then the space metric of a rotating massive body (10), which we have introduced and considered here, transforms into the Schwarzschild mass-point metric (6). In this case the obtained formula for the physically observable chr.inv.-scalar curvature (104) transforms into

$$C = \frac{r_g}{r^3}, \quad (107)$$

which is the same as the three-dimensional scalar curvature of a spherically symmetric gravitational field, which Landau and Lifshitz give in their *The Classical Theory of Fields* [11]; see page 325 of §100 in the 4th final English edition, or pages 378–379 of §97 in the 3rd French edition. The only difference is that their curvature has a negative sign. This is because in the years, when they wrote their book (the 1st edition was issued in 1939), Zelmanov's chronometrically invariant formalism had not yet been created. Therefore, Landau and Lifshitz believed that the three-dimensional components g_{ik} of the fundamental metric tensor $g_{\alpha\beta}$ create an observable metric tensor. On the contrary, the chronometrically invariant formalism clearly proves that the physically observable metric tensor that possesses all properties of the fundamental metric tensor throughout the three-dimensional spatial section associated with an observer (his observable three-dimensional space) is $h_{ik} = -g_{ik} + \frac{1}{c^2} v_i v_k$ (15). This is why their curvature of a non-rotating centrally symmetric gravitational field is negative, and the truly physically observable chr.inv.-curvature (107), which we have just deduced using the chronometrically invariant formalism, has a positive sign, as it should be according to the physical sense of this quantity.

Consider a few typical numerical examples of the curvature of space caused by rotating cosmic bodies.

The first typical example is the Sun: $r_{\odot} \approx 7.0 \times 10^{10}$ cm, $M_{\odot} \approx 2.0 \times 10^{33}$ gram, $r_{g\odot} = 2GM_{\odot}/c^2 \approx 3.0 \times 10^5$ cm, $\omega_{\odot} \approx 2.87 \times 10^{-6}$ sec⁻¹ (we are considering the Carrington rotation of the Sun at the equator with a sidereal period of 25.38 days). According to the obtained formula (106), the expected constant curvature of space due to the proper rotation of the Sun is $C = 6\omega_{\odot}^2/c^2 \approx 5.6 \times 10^{-32}$ cm⁻², while the variable curvature of space due to the gravitational field of the Sun at a distance of one solar radius r_{\odot} from its centre (i.e., on the Sun's surface) is 4 orders of magnitude greater: $C = r_{g\odot}/r_{\odot}^3 \approx 8.8 \times 10^{-28}$ cm⁻².

Since the curvature of space due to the Sun's rotation is constant, and the curvature due to its gravitational field decreases inversely proportional to r^3 from it, then there is a spherical surface in the cosmos on which these curvatures are equal to each other: $C = r_g/r^3 = 6\omega^2/c^2$. For the Sun, this is a spherical surface surrounding the Sun at a distance of

$$r = \sqrt[3]{\frac{c^2 r_{g\odot}}{6\omega_{\odot}^2}} \approx 1.8 \times 10^{12} \text{ cm} \approx 25 r_{\odot}. \quad (108)$$

Starting from the distance $r \approx 1.8 \times 10^{12}$ cm $\approx 25 r_{\odot}$ from the centre of the Sun, the contribution of the Sun's rotation to the observable curvature of space (it remains constant with distance) exceeds the contribution of the Sun's gravitational field (since it decreases inversely proportional to r^3). For comparison: Mercury, the closest planet to the Sun, orbits the Sun at a distance of $r = 57.9$ mln km $= 82.7 r_{\odot}$.

For the Earth ($r_{\oplus} = 6.37 \times 10^8$ cm, $M_{\oplus} = 5.97 \times 10^{27}$ gram, $r_{g\oplus} = 0.884$ cm, $\omega_{\oplus} = 7.27 \times 10^{-5}$ sec⁻¹), the constant curvature of space caused by the Earth's rotation is $C = 6\omega_{\oplus}^2/c^2 \approx 3.5 \times 10^{-29}$ cm⁻² that is 3 orders of magnitude greater than the constant curvature $C = 6\omega_{\oplus}^2/c^2 \approx 5.6 \times 10^{-32}$ cm⁻² caused by the rotation of the Sun. The curvature of space caused by the Earth's gravitational field on the Earth's surface ($r = r_{\oplus}$) is $C = r_{g\oplus}/r_{\oplus}^3 \approx 3.4 \times 10^{-27}$ cm⁻².

At a distance of

$$r = \sqrt[3]{\frac{c^2 r_{g\oplus}}{6\omega_{\oplus}^2}} \approx 2.93 \times 10^9 \text{ cm} \approx 29\,300 \text{ km} \approx 4.6 r_{\oplus} \quad (109)$$

from the centre of the Earth (or at an altitude of $h = r - r_{\oplus} \approx 23\,000$ km $\approx 3.6 r_{\oplus}$ above the Earth's surface) the contributions of the Earth's rotation and its gravitational field to the curvature of space become equal to each other. At higher altitudes, the contribution of the Earth's rotation to the curvature of space, since it remains constant with altitude, is greater than the contribution of the Earth's gravitational field (the latter becomes comparatively negligible, since it decreases inversely proportional to r^3).

For our Galaxy ($r \approx 30\,000$ pc $\approx 10^{23}$ cm, $M \approx 2 \times 10^{11} M_{\odot}$, $r_g \approx 6 \times 10^{16}$ cm, $T \approx 200$ mln years, $\omega = 2\pi/T \approx 10^{-15}$ sec⁻¹), the constant curvature of space caused by its rotation is $C = 6\omega^2/c^2 \approx 7 \times 10^{-51}$ cm⁻², while the curvature caused by its gravitational field at its edge ($r \approx 30\,000$ pc $\approx 10^{23}$ cm) is 2

	* $C = \frac{r_g}{r^3}, \text{ cm}^{-2}$	† $C = \frac{6\omega^2}{c^2}, \text{ cm}^{-2}$	‡ $r = \sqrt[3]{\frac{c^2 r_g}{6\omega^2}}$
Galaxy	6×10^{-53}	7×10^{-51}	7 000 pc
Sun	8.8×10^{-28}	5.6×10^{-32}	$25 r_{\odot}$
Earth	3.4×10^{-27}	3.5×10^{-29}	$4.6 r_{\oplus}$
Pulsars (min)		1.9×10^{-21}	
Pulsars (max)		1.4×10^{-13}	

*The variable (decreasing) curvature of space caused by the gravitational field of the cosmic body at a distance equal to its radius from its centre.

†The constant curvature of space caused by the rotation of the cosmic body.

‡The distance from the centre of the cosmic body at which the contribution of its rotation to the curvature of space becomes equal to the contribution of its gravitational field.

orders of magnitude weaker: $C = r_g/r^3 \approx 6 \times 10^{-53}$ cm⁻². The distance from the Galactic centre, at which the contribution of the rotation of the Galaxy to the curvature of space becomes equal to the contribution of its gravitational field is

$$r = \sqrt[3]{\frac{c^2 r_g}{6\omega^2}} \approx 2.1 \times 10^{22} \text{ cm} \approx 7\,000 \text{ parsec}. \quad (110)$$

The observed frequencies of radio-pulsars are in the range from $\omega_{\min} = 0.53$ to $\omega_{\max} = 4501$ sec⁻¹. Therefore, the constant curvature of space caused by pulsars is in the range of magnitudes from $C \approx 1.9 \times 10^{-21}$ to $C \approx 1.4 \times 10^{-13}$ cm⁻².

As a result of the above calculation, we arrive at the following conclusion:

CONCLUSION ON THE BACKGROUND CURVATURE OF SPACE

The curvature of space caused by the gravitational field of rotating massive bodies decreases inversely proportional to r^3 and, therefore, becomes negligibly small already in the immediate vicinity of these bodies, at a distance of a few of their radii from them. However, the rotation of these bodies creates a constant curvature field, which is much weaker than the curvature caused by their gravitational fields near these bodies, but does not depend on the distance to them. Moreover, such rapidly rotating cosmic objects as pulsars create strong fields of a constant curvature, the magnitude of which is many orders greater than the constant curvature fields caused by other rotating stars and Galaxies.

It seems that the space of the entire Universe is filled with a constant curvature field that is the superposition of the constant curvature fields caused by rapidly rotating cosmic bodies such as pulsars. This is the basis for considering the background space of our Universe as a *constant curvature space*.

This is a very interesting theoretical discovery that requires further study and analysis by astronomers.

5 Einstein's field equations in the space of a rotating massive body

As mentioned on page 81, Einstein's equations are one of the necessary conditions for a space to be Riemannian. Therefore, the considered space metric of a rotating massive body (10) is Riemannian under some particular conditions (*Riemannian conditions*) by which the Einstein equations for this space metric vanish. Now our task is to find out the Riemannian conditions for the space metric (10).

As we showed above (52), the space of a rotating massive body, which we are considering, does not deform ($D_{ik} = 0$), and is not filled with any distributed matter such as gas, dust, electromagnetic fields, etc. The latter means that the energy-momentum tensor of distributed matter is zero ($T_{\alpha\beta} = 0$) and, hence, the entire right-hand side of the Einstein field equations is zero. With taking the above into account, the chr.inv.-Einstein equations (41–43) take the simplified form

$$A_{jl}A^{lj} + {}^* \nabla_j F^j - \frac{1}{c^2} F_j F^j = 0, \quad (111)$$

$${}^* \nabla_j A^{ij} - \frac{2}{c^2} F_j A^{ij} = 0, \quad (112)$$

$$2A_{ij}A_k{}^j - \frac{1}{c^2} F_i F_k + \frac{1}{2} ({}^* \nabla_i F_k + {}^* \nabla_k F_i) - c^2 C_{ik} = 0. \quad (113)$$

The *1st Riemannian condition* for the space metric of a rotating massive body (10), which we are considering, follows from the obtained scalar chr.inv.-Einstein equation (111). Since $A_{jl}A^{lj} = -A_{jl}A^{jl}$ is the square of the chr.inv.-tensor A_{jl} of the angular velocity of the rotation of space, taken with the opposite sign, and the Zelmanov operator of the chr.inv.-physical divergence (marked with a tilde)

$${}^* \widetilde{\nabla}_j = {}^* \nabla_j - \frac{1}{c^2} F_j, \quad (114)$$

gives a divergence that is physically registered by the observer, for instance, ${}^* \widetilde{\nabla}_j F^j$ according to (31) is

$$\begin{aligned} {}^* \widetilde{\nabla}_j F^j &= \frac{{}^* \partial F^j}{d x^j} + \Delta_{jl}^j F^l - \frac{1}{c^2} F_j F^j = \\ &= {}^* \nabla_j F^j - \frac{1}{c^2} F_j F^j, \end{aligned} \quad (115)$$

then the scalar chr.inv.-Einstein equation (111) gives:

THE 1ST RIEMANNIAN CONDITION

In the space of a rotating massive body, the physically observable rotation of space is always balanced by the physically observable divergence of the acting gravitational inertial force:

$$A_{jl}A^{jl} = {}^* \widetilde{\nabla}_j F^j, \quad (116)$$

or, which is the same,

$$2\Omega^2 = {}^* \widetilde{\nabla}_j F^j. \quad (117)$$

P.S. The alternative form (117) of the 1st Riemannian condition (116) is obtained using the components of A_{jl} (59–66) that we have calculated earlier in the space of a rotating massive body, after which we have

$$\begin{aligned} A_{jl}A^{jl} &= \frac{2\omega^2}{1 + \frac{\omega^2 r^2 \sin^2 \theta}{c^2}} - \frac{3\omega^2 r_g \sin^2 \theta}{r \left(1 + \frac{\omega^2 r^2 \sin^2 \theta}{c^2}\right)} + \\ &+ \frac{\omega^2 r_g^2 \sin^2 \theta}{8r^2 \left(1 + \frac{\omega^2 r^2 \sin^2 \theta}{c^2}\right) \left(1 - \frac{r_g}{r}\right)} = 2\Omega^2, \end{aligned} \quad (118)$$

where Ω^2 is the square of the physically observable scalar angular velocity Ω (71) with which the space rotates.

The *2nd Riemannian condition* for the space metric of a rotating massive body follows from the obtained vector chr.inv.-Einstein equation (112):

THE 2ND RIEMANNIAN CONDITION

In the space of a rotating massive body, the physically observable divergence of the rotation of space is always and everywhere equal to zero:

$${}^* \widetilde{\nabla}_j A^{ij} = 0, \quad (119)$$

which means that the physically observable rotation of such a space is *homogeneous* (i.e., such a space rotates always and everywhere homogeneously).

P.S. And here is why. Using the definition of the operator of the chr.inv.-physical divergence ${}^* \widetilde{\nabla}_j$ (114) that is physically registered by the observer, we calculate the chr.inv.-physical divergence of the contravariant tensor of the angular velocity of rotation of space A^{ij} . According to the general formula for the chr.inv.-derivative ${}^* \nabla_j$ of an arbitrary contravariant tensor of the 2nd rank (36), we obtain

$$\begin{aligned} {}^* \widetilde{\nabla}_j A^{ij} &= \frac{{}^* \partial A^{ij}}{\partial x^j} + \Delta_{jl}^i A^{jl} - \frac{1}{c^2} F_j A^{ij} + \\ &+ \Delta_{ij}^l A^{ij} - \frac{1}{c^2} F_j A^{ij} = {}^* \nabla_j A^{ij} - \frac{2}{c^2} F_j A^{ij}, \end{aligned} \quad (120)$$

which completely coincides with the left-hand side of the obtained vector chr.inv.-Einstein equation (112), while the right-hand side of the equation is zero.

The *3rd and 4th Riemannian conditions* for the space metric of a rotating massive body follow from the obtained tensor chr.inv.-Einstein equation (113), re-written in the expanded component notation

$$2A_{1j}A_1{}^j - \frac{1}{c^2} F_1 F_1 + {}^* \nabla_1 F_1 - c^2 C_{11} = 0, \quad (121)$$

$$2A_{1j}A_2{}^j - c^2 C_{12} = 0, \quad (122)$$

$$2A_{2j}A_2{}^j - c^2 C_{22} = 0, \quad (123)$$

$$2A_{3j}A_3{}^j - c^2 C_{33} = 0, \quad (124)$$

in accordance with the non-zero components of A_{ij} , F_i and C_{ik} , which we have calculated earlier (see above).

So, the 3rd Riemannian condition follows from the first component (124). It says:

THE 3RD RIEMANNIAN CONDITION

In the space of a rotating massive body, the physically observable curvature of space in the radial direction $x^1 = r$ from the body is caused by both the physically observable rotation of space (the first term of the equation) and the physically observable divergence of the gravitational inertial force acting in the same radial direction (the second term):

$$2A_{13}A_1^3 + \sqrt{\nabla_1} F_1 = c^2 C_{11}. \tag{125}$$

The 4th Riemannian condition follows from the rest three non-zero components (122–124) of the tensor chr.inv.-Einstein equation:

THE 4TH RIEMANNIAN CONDITION

In the space of a rotating massive body, the physically observable curvature of space in all other directions from the body, except for the radial direction $x^1 = r$ (in which the gravitational-inertial force acts), is caused only by the physically observable rotation of space:

$$\left. \begin{aligned} 2A_{13}A_2^3 &= c^2 C_{12} \\ 2A_{23}A_2^3 &= c^2 C_{22} \\ 2(A_{31}A_3^1 + A_{32}A_3^2) &= c^2 C_{33} \end{aligned} \right\}. \tag{126}$$

P.S. It should be noted that the components A_{13} and A^{31} (59–62) of the chr.inv.-tensor of the angular velocity of rotation of space A_{ij} contain both terms determined only by the rotation of space and terms dependent on $r_g = 2GM/c^2$ (which includes the mass M of the attracting body). This is because the chr.inv.-tensor A_{ij} (18) by definition takes into account the effect of the acting gravitational inertial force F_i onto the tensor A_{ij} , thereby making A_{ij} a truly physically observable quantity dependent on the physical properties of space.

Therefore, when we say a “physically observable rotation of space” or a “physically observable quantity” in general, we mean a chronometrically invariant physical quantity, actually registered by the observer in his real measurements and, therefore, dependent on the physical properties of space.

Finally, summing up the results obtained in this Section of the present work, we can state the following:

CONCLUSION

Under the four Riemannian conditions deduced above, the space metric of a rotating massive body (10) that we have introduced and studied in this paper satisfies Einstein’s field equations (thereby turning them into zero identities) and is therefore proven to be Riemannian and can be used in General Relativity.

The above conclusion has great significance for General Relativity, cosmology and astrophysics. This is because the introduced (and now proven) space metric of a rotating spherical body, approximated by a mass-point, is not only a new metric to General Relativity, which is an extension and replacement of the classical Schwarzschild mass-point metric (which does not take into account the rotation of space). The introduced space metric is the *main space metric in the Universe*, characterizing the physically observable field of any real cosmic body, be it a planet, star, galaxy or something else (since all real cosmic bodies rotate).

6 Deflection of light rays and mass-bearing particles in the space of a rotating massive body

In the previous study [2], we considered massless (light-like) and mass-bearing particles moving in the space of a rotating body, where the gravitational field created by the body was so weak that its influence on the moving particles could be neglected. The solutions obtained for the chronometrically invariant equations of motion of free massless and free mass-bearing particles in the space of a rotating body showed that their physically observable motion should deviate from a straight line due to the curvature of space caused by the rotation of space. In other words, the trajectories of light rays and mass-bearing particles should be deflected near a rotating body due to the curvature of space caused by its rotation.

These are two new fundamental effects of General Relativity, in addition to the deflection of light rays in the field of a gravitating body (known in Einstein’s theory from the very beginning).

In the paper [2], the mentioned two new effects were calculated in the space metric of a rotating body, where $g_{00} = 1$, i.e., the gravitational potential is zero $w = c^2(1 - \sqrt{g_{00}}) = 0$, in order to show these effects of the rotation of space in their “pure form” (i.e., in the absence of the gravitational field).

Now we are going to calculate these two new effects of General Relativity anew, now in the space of a rotating massive body, the metric of which (10) takes the gravitational field of the rotating body into account: the gravitational potential is $w \neq 0$ and, hence, $g_{00} < 1$; for details, see the space metric (10) that we are considering. This, in contrast to the abstract case considered in the previous work [2], is a *real physical case*, since all real cosmic bodies in the Universe such as planets, stars, galaxies and something else not only rotate, but also have their own gravitational field.

So, let us begin. The chr.inv.-equations of motion are the physically observable chr.inv.-projections of the general covariant four-dimensional equations of motion onto the time line and the three-dimensional spatial section associated with a particular observer. Such projections are invariant throughout the spatial section of the observer (his physically observable three-dimensional space) and are expressed through the physical properties of his local reference space. A detailed

derivation of the chr.inv.-equations of motion can be found in the monographs [7, 8], the first of which is devoted to free (geodesic) motion of particles, while the second is a study of non-geodesic motion.

The chr.inv.-equations of motion of a free mass-bearing particle have the form

$$\frac{dm}{d\tau} - \frac{m}{c^2} F_i v^i + \frac{m}{c^2} D_{ik} v^i v^k = 0, \quad (127)$$

$$\frac{d(mv^i)}{d\tau} + 2m(D_k^i + A_k^i)v^k - mF^i + m\Delta_{nk}^i v^n v^k = 0, \quad (128)$$

and the chr.inv.-equations of motion of a free massless (light-like) particle have the form

$$\frac{d\omega}{d\tau} - \frac{\omega}{c^2} F_i c^i + \frac{\omega}{c^2} D_{ik} c^i c^k = 0, \quad (129)$$

$$\frac{d(\omega c^i)}{d\tau} + 2\omega(D_k^i + A_k^i)c^k - \omega F^i + \omega\Delta_{nk}^i c^n c^k = 0, \quad (130)$$

where the first (scalar) chr.inv.-equation of motion is the projection of the general covariant equations of motion onto the observer's time line, and the second (vector) chr.inv.-equation of motion is the projection onto his spatial section (his three-dimensional space).

Here m is the relativistic mass of the mass-bearing particle, ω is the relativistic frequency of the massless (light-like) particle, the physically observable time interval $d\tau$ (11) is expressed through the gravitational potential w (12) and the linear velocity of the rotation of space v_i (13) as

$$d\tau = \left(1 - \frac{w}{c^2}\right) dt - \frac{1}{c^2} v_i dx^i, \quad (131)$$

and the chr.inv.-vector of the physically observable velocity of the particle has the form

$$v^i = \frac{dx^i}{d\tau}, \quad v_i v^i = h_{ik} v^i v^k = v^2,$$

which, in the case of massless (light-like) particles, transforms into the chr.inv.-vector of the physically observable velocity of light, for which $c_i c^i = h_{ik} c^i c^k = c^2 = const$ (despite the fact that its individual components c^i are variables depending on the properties of space).

Since the space of a rotating massive body, which we are considering, does not deform ($D_{ik} = 0$), then the chr.inv.-equations of motion simplify by vanishing D_{ik} . For a free mass-bearing particle they take the form

$$\frac{dm}{d\tau} - \frac{m}{c^2} F_i v^i = 0, \quad (132)$$

$$\frac{d(mv^i)}{d\tau} + 2mA_k^i v^k - mF^i + m\Delta_{nk}^i v^n v^k = 0, \quad (133)$$

while for a massless (light-like) particle they become

$$\frac{d\omega}{d\tau} - \frac{\omega}{c^2} F_i c^i = 0, \quad (134)$$

$$\frac{d(\omega c^i)}{d\tau} + 2\omega A_k^i c^k - \omega F^i + \omega\Delta_{nk}^i c^n c^k = 0. \quad (135)$$

6.1 Solving the chr.inv.-scalar equation of motion

Since the rotating massive body we are considering is not a gravitational collapsar, i.e., its physical radius r is much greater than its gravitational radius ($r \gg r_g$), then according to the formulae for F_i (55) and F^i (56) obtained for the field of a rotating massive body we have

$$F_1 = F^1 = -\frac{c^2 r_g}{2r^2} = -\frac{GM}{r^2}. \quad (136)$$

With this fact taken into account, the scalar equation of motion of a free mass-bearing particle (132), in the case when it travels along the radial direction $x^1 = r$ from the rotating massive body, takes the form

$$\frac{dm}{m} = -\frac{GM}{c^2} \frac{dr}{r^2}, \quad (137)$$

which is a simple differential equation $\frac{dy}{y} = -a \frac{dx}{x^2}$ or, which is the same, $d \ln m = -a \frac{dx}{x^2}$. It solves as $y = C e^{a/x}$, where the integration constant C in this case is $C = m_{(r=r_0=0)} = m_0$. As a result, we obtain that the scalar equation of motion of a free mass-bearing particle (132) solves as

$$m = m_0 e^{\frac{GM}{c^2 r}} \approx m_0 \left(1 + \frac{GM}{c^2 r}\right). \quad (138)$$

For example, according to the obtained solution, the mass of a body located on the Earth's surface ($M_\oplus = 5.97 \times 10^{27}$ gram, $r_\oplus = 6.37 \times 10^8$ cm) is greater than its mass, measured when the body was located at a distance of the Moon's orbit from the Earth ($r = 3.0 \times 10^{10}$ cm) by a value of $1.5 \times 10^{-11} m_0$ due to the greater magnitude of the Earth's gravitational field potential on the Earth's surface.

The scalar equation of motion of a free massless (light-like) particle (134), when it radially travels in space, solves in the same way. Its solution has the form

$$\omega = \omega_0 e^{\frac{GM}{c^2 r}} \approx \omega_0 \left(1 + \frac{GM}{c^2 r}\right). \quad (139)$$

This solution means that photons gain an additional energy (and frequency) from the gravitational field. For example, a photon with a frequency ω_0 at the moment of emission from the surface of a star has a lower frequency $\omega < \omega_0$ (and energy) when it moves away from this star at some distance. The greater the gravitational field potential (i.e., the closer the photon is to the source of the gravitational field), the more the photon's frequency is redshifted. According to the above so-

lution, the photon's redshift z in the field of a rotating massive body is determined as (where $r_0 < r_1$)

$$z = \frac{\omega_0 - \omega}{\omega} = e^{\frac{GM}{c^2 r_0} - \frac{GM}{c^2 r_1}} - 1 \approx \frac{GM}{c^2 r_0} - \frac{GM}{c^2 r_1}. \quad (140)$$

So, by solving the chr.inv.-scalar equation of free mass-bearing and massless (light-like) particles we have deduced two effects. First, we have deduced the well-known relativistic effect of the decrease in the mass of a body with height above the Earth's surface (138). Second, we have deduced the gravitational redshift (140), which is also the effect of General Relativity, known from the very beginning and first registered in the spectra of white dwarfs.

Landau and Lifshitz derived these effects from the conservation of energy of a free particle travelling in a stationary gravitational field; for example, see [11, §88]. Zelmanov followed the same way of derivation. However, the new derivation method presented here, based on the integration of the chr.inv.-scalar geodesic equation, allows us to represent the mentioned effects as something not specifically related to the stationary gravitational field, but as general effects of General Relativity that can be calculated in any metric space.

Note that the chr.inv.-scalar equation of motion does not take the rotation of space into account. Therefore, the obtained solutions of the equation (and the effects following from them) coincide with the solutions in a space of the Schwarzschild's mass-point field (which does not rotate).

6.2 Solving the chr.inv.-vector equation of motion

Let us now solve the chr.inv.-vector equation of motion. For a free mass-bearing particle, radially travelling in the space of a rotating massive body, this is the equation (133), while for a massless particle this is the equation (135).

Since the chr.inv.-vector equation of motion depends on the tensor of the angular velocity of rotation of space A_{ik} , we expect that its solution will reveal new effects of General Relativity, previously unknown in the framework of the non-rotating Schwarzschild mass-point metric.

The chr.inv.-vector equations of motion are unsolvable in their general form (133) and (135), because they require substitution of the solutions for the particle's mass m (138) and frequency ω (139) obtained from the chr.inv.-scalar equations of motion, which in turn contain an exponential function of distance r (as a result, each term of the vector equations of motion would contain this complicated function).

Therefore, we will solve the chr.inv.-vector equations of motion in an approximation that the mass-bearing particle's mass m and the massless (light-like) particle's frequency ω remain constant during the travel. This approximation can be used in problems of motion near planets and stars, because, as shown above, the mass m_0 of a body located on the surface of the Earth is only $1.5 \times 10^{-11} m_0$ greater than its mass measured when the body was at the distance of the Moon.

In addition to the assumed approximations $m = const$ and $\omega = const$, we assume, as well as when we solved the scalar equations of motion above, that the rotating massive body that is the source of the gravitational field is not a gravitational collapsar ($r \gg r_g$), so the acting gravitational inertial force is expressed in the simplified form (136).

Moreover, to further simplify the vector equations of motion, we assume that the particle travels at a very high radial velocity v_1 in the equatorial plane along the radial axis $x^1 = r$ towards the origin of the coordinates (the body's centre). For example, it could be a particle falling from the near-Earth space in the equatorial plane onto the Earth's surface. In this case: a) the polar angle is $\theta = \frac{\pi}{2}$ and, therefore, $\cos \theta = 0$ and $\sin \theta = 1$, b) the velocities v^2 and v^3 , with which the particle is deflected along the geographical latitudes and longitudes, are negligible compared to its radial velocity v^1 .

Finally, we assume that the body that is the source of the field rotates (synchronously with its entire space) with slow linear velocities compared to the velocity of light.

Now we substitute into the chr.inv.-vector equations of motion (133) and (135) the components of the gravitational inertial force F_i (136), the tensor of the angular velocity of rotation of space A_{ik} (59–66), and also the inhomogeneity coefficients of space, a.k.a. the Christoffel symbols Δ_{nk}^i (77–83), which we have calculated above in this paper in accordance with the space metric of a rotating massive body. As a result, after using the above approximations, we obtain the vector equations of motion in component notation.

The resulting chr.inv.-vector equation of motion of a free mass-bearing particle, in component notation derived after some algebra, has the form

$$\left. \begin{aligned} \frac{dv^1}{d\tau} - 2\omega r v^3 - r v^2 v^2 - r v^3 v^3 + \frac{GM}{r^2} &= 0 \\ \frac{dv^2}{d\tau} + \frac{2}{r} v^1 v^2 &= 0 \\ \frac{dv^3}{d\tau} + \frac{2\omega}{r} v^1 + \frac{2}{r} v^1 v^3 &= 0 \end{aligned} \right\}. \quad (141)$$

and for a massless (light-like) particle the resulting chr.inv.-vector equation of motion has the components

$$\left. \begin{aligned} \frac{dc^1}{d\tau} - 2\omega r c^3 - r c^2 c^2 - r c^3 c^3 + \frac{GM}{r^2} &= 0 \\ \frac{dc^2}{d\tau} + \frac{2}{r} c^1 c^2 &= 0 \\ \frac{dc^3}{d\tau} + \frac{2\omega}{r} c^1 + \frac{2}{r} c^1 c^3 &= 0 \end{aligned} \right\}. \quad (142)$$

As can be seen from the equations, the gravitational field of a rotating body makes a contribution in the form of only the last term in the first equation, i.e., it affects the motion of the particle only along the radial direction $x^1 = r$. On the

contrary, the rotation field of this body makes a contribution to the motion of the particle both along the radial axis r and along the equatorial (longitudinal) coordinate axis φ and the latitudinal coordinate axis θ .

As is seen, the vector equations of motion for a mass-bearing particle and a massless (light-like) particle are identical. The only difference is that the equations for a massless (light-like) particle contain the physically observable velocity of light c^i instead of the mass-bearing particle's physically observable velocity v^i . For this reason, we will solve only the equation of motion of a mass-bearing particle (the solution for a massless particle will coincide).

The problem is that this system of differential equations is unsolvable even when considered in the above simplified form. Therefore, we will solve them using the *small parameter method*.

Namely, — we assume that the radially travelling particle gains only a very small increment or decrement α' to its initial numerical value v^1 . This allows us to set $v^1 = const$ in the third equation of the system, which is the equation of motion along the equatorial (longitudinal) axis φ , and in the second equation that is the equation of motion along the latitudinal axis θ . Then, using the obtained solutions of the third and second equations, we will solve the first equation (the equation of motion along the radial axis r) with respect to $v^1 + \alpha'$, i.e., with respect to the small parameter α .

But even now, without solving the vector equations of motion, but only based on their general form given above, we see that three effects are possible, namely:

1. The deflection of a radially travelling particle along the geographic longitudes due to the influence of the rotation of space (the third equation);
2. The deflection of a radially travelling particle along the geographic latitudes due to the influence of the rotation of space (the second equation);
3. The acceleration or braking of a radially travelling particle in the radial direction due to both the gravitational field and the rotation of space (the first equation).

6.2.1 Solving the third vector equation of motion

The third equation is an equation of motion along the equatorial axis φ . This is a differential equation of the form

$$y' + ay + b = 0, \tag{143}$$

or, which is the same,

$$\varphi'' + a\varphi' + b = 0, \tag{144}$$

where the variable y and the constants used are

$$y = v^3 = \frac{d\varphi}{d\tau}, \tag{145}$$

$$a = \frac{2}{r} v^1 = const, \quad b = \frac{2\omega}{r} v^1 = const. \tag{146}$$

The above equations (143) and (144) solve as

$$y = \frac{C}{e^{ax}} - \frac{b}{a}, \quad \varphi = \frac{C_1}{e^{ax}} - \frac{bx}{a} + C_2. \tag{147}$$

Substituting the integration constants, calculated from the initial conditions $x = x_0 = 0$ and $y = y_0 = 0$,

$$C = \frac{b}{a} = \omega, \tag{148}$$

$$C_1 = -\frac{b}{a^2} = -\frac{\omega r}{2v^1}, \quad C_2 = -C_1 = \frac{\omega r}{2v^1}, \tag{149}$$

below we represent the above solutions of the equations (143) and (144) in their final form.

As a result, the obtained solution of the equation (143), which is the physically observable velocity $y = v^3$ of the radially travelling particle along the equatorial axis φ at the point of arrival on the surface of the rotating body (onto which the particle was falling down from the cosmos along the radial direction r), takes the final form

$$v^3 = -\omega + \omega e^{-\frac{2}{r} v^1 \tau}. \tag{150}$$

The first term here is the basic equatorial velocity of the particle, the cause of which is the shift of its equatorial coordinate φ towards negative numerical values due to the turn of the rotating massive body during the time of the particle's travel to the body's surface.

The second term is absent in the classical theory. This additional term reveals an additional velocity gained by the free falling mass-bearing particle along the equatorial coordinate φ (geographical longitudes) of the rotating massive body in the direction, opposite to its rotation.

In turn, the obtained solution for the equatorial coordinate φ of the particle's point of arrival, which is the solution of the equation (144), takes the final form as follows

$$\varphi = \varphi_0 - \omega\tau + \frac{\omega r}{2v^1} \left(1 - e^{-\frac{2}{r} v^1 \tau} \right). \tag{151}$$

The first and second terms of the solution are known in the classical theory.

The third, additional term of this solution, unknown in the classical theory, reveals a deflection of the free falling mass-bearing particle along the equatorial coordinate φ (geographical longitudes) of the rotating massive body in the direction, opposite to its rotation.

Respectively, the solutions of the third vector equation of motion for a massless (light-like) particle, such as a photon, have the same form

$$c^3 = -\omega + \omega e^{-\frac{2}{r} c^1 \tau}, \tag{152}$$

$$\varphi = \varphi_0 - \omega\tau + \frac{\omega r}{2c^1} \left(1 - e^{-\frac{2}{r} c^1 \tau} \right), \tag{153}$$

where the mass-bearing particle's velocity is replaced with the physically observable velocity of light.*

These solutions show another new effect of the rotation of space, which is absent in the classical theory and is revealed by the second term of the solution (152) and the third term of the solution (153). This is an additional deflection of a light ray travelling towards the surface of a rotating massive body, which occurs along the equatorial coordinate φ (geographical longitudes) of the body in the direction, in which the body rotates.

Note that the solutions of the third vector equation of motion, which we have derived above in the field of a rotating massive body with a significant gravitational field, coincide with those derived earlier [2] in the field of a rotating body, the gravitational field can be neglected (i.e., in the absence of the gravitational field). This is because the acting gravitational force takes effect on only the first vector equation of motion (along the radial axis r), but is not included into the second and third vector equations of motion (along the latitudinal polar coordinates θ and the equatorial longitudinal coordinates φ).

For this reason, the numerical examples of the solutions will be identical to those calculated in the previous paper [2] in the absence of the gravitational field. Therefore, we now reproduce the examples here in short from [2].

Thus, the curvature of space caused by the rotation of the Earth around its axis ($\omega_{\oplus} = 1 \text{ rev/day} = 1.16 \times 10^{-5} \text{ rev/sec}$, $r_{\oplus} = 6.37 \times 10^8 \text{ cm}$) deflects a light ray arriving at the Earth's surface from the Moon ($\tau = 1 \text{ sec}$) along the geographical longitudes φ in the direction of the Earth's rotation. The angle of deflection of the light ray is[†]

$$\Delta\varphi = \frac{\omega_{\oplus} r_{\oplus}}{2c^1} \left(1 - e^{-\frac{2}{r} c^1 \tau} \right) \approx 1.2 \times 10^{-7} \text{ rev} \approx 0.16'', \quad (154)$$

where the deflection of the light ray is mainly due to the first term, and the second term, depending on the travel time τ , is equal to 1.5×10^{-41} and, therefore, can be neglected.

The magnitude of this effect increases with the radius and rotation velocity of the cosmic body. Thus, a light ray arriving at the Sun ($\omega_{\odot} = 4.5 \times 10^{-7} \text{ rev/sec}$, $r_{\odot} = 7.0 \times 10^{10} \text{ cm}$) is deflected by the curvature of space caused by the Sun's rotation by an angle, the numerical value of which is

$$\Delta\varphi \approx 5.3 \times 10^{-7} \text{ rev} \approx 0.68'', \quad (155)$$

the value of which is much larger in the case of a rapidly rotating star, such as Wolf-Rayet stars or neutron stars.

*Note that, despite the components of the physically observable velocity of light are variables depending on the properties of space, its square remains constant $c_i c^i = h_{ik} c^i c^k = c^2 = \text{const}$.

[†]In this case, the physically observable velocity of light has a negative numerical value of $c^1 = -3 \times 10^{10} \text{ cm/sec}$, since the velocity of light vector is directed towards the Earth, i.e., opposite to the radial coordinates r measured from the centre of the Earth.

6.2.2 Solving the second vector equation of motion

The second vector equation of motion is an equation of motion along the geographical latitudes, where the latitudinal coordinate θ (polar angle) is measured from the North Pole. This is a differential equation of the form

$$y' + ay = 0, \quad (156)$$

or, with respect to the latitudinal coordinates θ ,

$$\theta'' + a\theta' = 0, \quad (157)$$

where the variable y and the constant a are

$$y = v^2 = \frac{d\theta}{d\tau}, \quad a = \frac{2}{r} v^1 = \text{const}. \quad (158)$$

These equations solve as

$$y = \frac{C}{e^{ax}}, \quad \theta = \frac{C_1}{e^{ax}} + C_2, \quad (159)$$

where the integration constants are calculated from the initial conditions $x = x_0 = 0$ and $y = y_0 = 0$. They are $C = 0$, $C_1 = 0$ and $C_2 = \theta_0$.

Thus, the final solutions of the second vector equation of motion have the following form

$$v^2 = 0, \quad \theta = \theta_0, \quad (160)$$

which means that a particle travelling radially towards the surface of a massive rotating body is not deflected along the geographical latitudes.

6.2.3 Solving the first vector equation of motion

The first vector equation of motion is an equation of motion along the first (radial) coordinate axis r .

This equation contains contributions from both the rotation of space (the second term) and the gravitational field (the last term of the equation). Therefore, its solution will differ from the solution of the first equation of motion in the field of a rotating body, the gravitational field of which can be neglected (i.e., in the absence of the gravitational field).

Assume that the particle's velocity in the radial direction gains only a very small increment or decrement α' to its initial numerical value v^1 . In other words, we assume $v^1 = \text{const}$ and, therefore, solve the first vector equation of motion with respect to the sum $v^1 + \alpha'$, i.e., with respect to the small parameter α .

Taking the obtained solutions $v^3 = -\omega$ and $v^2 = 0$ into account, the first vector equation of motion is reduced to

$$\frac{dv^1}{d\tau} + \omega^2 r + \frac{GM}{r^2} = 0, \quad (161)$$

where r is the radius of the rotating body, and M is its mass. This is a differential equation having the form

$$y' + b = 0, \quad (162)$$

or, with respect to the small parameter α ,

$$\alpha'' + b = 0, \tag{163}$$

where the variable y and the constant b are

$$y = \alpha', \quad b = \omega^2 r + \frac{GM}{r^2} = \text{const.} \tag{164}$$

The above equations (162) and (163) solve as

$$y = C - bx, \quad \alpha = -\frac{bx^2}{2} + C_2 x + C_1, \tag{165}$$

where the integration constants, calculated from the initial conditions $x = x_0 = 0$, $\alpha = \alpha_0 = 0$ and $y = y_0 = 0$, are zero. As a result, the solutions of the equations (162) and (163) take their final form

$$\alpha' = -\omega^2 r \tau - \frac{GM}{r^2} \tau, \quad \alpha = -\frac{\omega^2 r}{2} \tau^2 - \frac{GM}{2r^2} \tau^2. \tag{166}$$

The second terms in the solutions are the contribution of the gravitational field, created by the rotating massive body, which is the well-known effect of the classical theory. The terms reveal, respectively, the additional radial velocity gain by the falling particle (in the solution for α') and also the reduction of the distance travelled by the particle (in the solution for α), all due to the influence of the gravitational field attracting the particle to the rotating body.

However, the first terms in the solutions are absent in the classical theory. They show, respectively, the additional negative radial velocity (in the solution for α') and the stretching in the distance travelled by the particle (in the solution for α) due to the influence of the rotation of space of the gravitating body onto which the particle falls.

We see that here only the rotation of space produces a new effect of General Relativity in addition to the classical theory (i.e., the gravitational field of the rotating body does not produce a new additional effect).

In the absence of the gravitational field, the obtained solutions (166) coincide with those obtained in the previous paper [2] for a particle travelling towards a rotating body, the gravitational field of which can be neglected.

In fact, the new effect revealed by the first terms of the solutions (166) means that a mass-bearing particle or a light ray reaches a rotating massive body later due to the “stretching” of its path of travel due to the curvature of space caused by the rotation of space of the body, i.e., the mass-bearing particle or the light ray arrives at the rotating body with a time delay compared if the body did not rotate.

These new effects are the same for both mass-bearing and massless (light-like) particles. For example, the increment of the path length travelled by a light ray from the Moon to the Earth, and also the delay in its travel time are

$$\alpha = -\frac{\omega_{\oplus}^2 r_{\oplus}}{2} \tau^2 \simeq -1.7 \text{ cm}, \tag{167}$$

$$\Delta\tau = \frac{\alpha}{c^1} \simeq 5.7 \times 10^{-11} \text{ sec}, \tag{168}$$

and for a light ray that travelled from the Earth to the Sun the increment of the travelled path length and the delay in its travel time are

$$\alpha = -\frac{\omega_{\odot}^2 r_{\odot}}{2} \tau^2 \simeq -6.6 \times 10^4 \text{ cm}, \tag{169}$$

$$\Delta\tau = \frac{\alpha}{c^1} \simeq 2.2 \times 10^{-6} \text{ sec}, \tag{170}$$

which are the same as those calculated in the previous paper [2] in the field of a rotating body, the gravitational field of which can be neglected.

6.2.4 Conclusion

In concluding this Section of the present paper, let us formulate the two new effects of General Relativity calculated here in the field of a rotating massive body:

THE 1ST NEW EFFECT OF GENERAL RELATIVITY

A mass-bearing particle radially falling onto the surface of a rotating body gains an additional velocity, directed along the equatorial coordinate φ (geographical longitudes) of the body in the opposite direction of its rotation, thereby causing a deflection of the particle in the longitudinal direction φ .

In addition, the radially falling mass-bearing particle arrives at the rotating body with a time delay compared if the body did not rotate.

This happens due to the “stretching” of the rotating body’s space along the equatorial coordinate φ (along the geographical longitudes) and the radial direction r (towards the body) as a result of the curvature of space, caused by its rotation (together with the body).

THE 2ND NEW EFFECT OF GENERAL RELATIVITY

A light ray radially spreading towards the surface of a rotating body acquires an additional deflection upon arrival along the equatorial latitudinal coordinate φ of the body in the direction, in which the body rotates.

In addition, the radially spreading light ray arrives at the rotating body with a time delay compared if the body did not rotate.

This deflection of the light ray and the delay in its arrival at the rotating body occurs due to the “stretching” of the rotating body’s space along the equatorial coordinate φ (along the geographical longitudes) and the radial direction r (towards the body), which are the result of the curvature of space, caused by its rotation (together with the body).

The physical origin of the new effects is obvious from our above calculation of the curvature of space, which we found to be caused by not only the gravitational field but also the rotation of space:

ON THE ORIGIN OF THE NEW EFFECTS

As has been found, the rotation of any body curves space in the direction of its rotation and to the centre of this body (the centre of rotation), thereby creating a “slope of the hill” slowing “down” along the equator in the direction, in which this body rotates, and also to the centre of this body.

In addition, the gravitational field created by the rotating body also curves space, making its own contribution in the form of the curvature of space towards the body’s centre.

As a result, due to the created curvature of space, a mass-bearing particle or a light ray freely travelling towards a rotating massive body “rolls down the curvature hill” of space along the equator of the body in the direction of the body’s rotation (the contribution of the rotation of space), and also “rolls” towards the centre of the body (the combined contribution of the rotation of space and the gravitational field).

7 Length stretching and time loss/gain in the space of a rotating massive body

According to the chronometrically invariant formalism, the three-dimensional physically observable chr.inv.-interval $d\sigma$ (14) and the physically observable time interval $d\tau$ (11)

$$d\sigma^2 = h_{ik} dx^i dx^k, \quad d\tau = \left(1 - \frac{w}{c^2}\right) dt - \frac{1}{c^2} v_i dx^i \quad (171)$$

depend on the chr.inv.-metric tensor $h_{ik} = -g_{ik} + \frac{1}{c^2} v_i v_k$ (15), the gravitational field potential w (12) and the linear velocity of the rotation of space v_i (13). Thus, we can calculate $d\sigma$ and $d\tau$ in the space of any particular metric, for which we have previously calculated the quantities h_{ik} , w and v_i .

Let us now calculate the length of a rigid rod and the time interval in the field of a rotating massive body.

7.1 Length stretching

Let us substitute into the formula for $d\sigma$ the non-zero components h_{ik} (47) that we have calculated according to the space metric of a rotating massive body (10).

Thus, we obtain the physically observable length dl of a rigid rod, installed in stages along each of the coordinates

$$dl_r = \sqrt{h_{11} dr^2} = \frac{dr}{\sqrt{1 - \frac{r_g}{r}}} = \frac{dl_0}{\sqrt{1 - \frac{r_g}{r}}}, \quad (172)$$

$$dl_\theta = \sqrt{h_{22} d\theta^2} = r d\theta = dl_0, \quad (173)$$

$$\begin{aligned} dl_\varphi &= \sqrt{h_{33} d\varphi^2} = \sqrt{1 + \frac{\omega^2 r^2 \sin^2 \theta}{c^2}} r \sin \theta d\varphi = \\ &= \sqrt{1 + \frac{\omega^2 r^2 \sin^2 \theta}{c^2}} dl_0, \quad (174) \end{aligned}$$

where $dr = dl_0$ is the length of an elementary segment along the radial axis r , $r d\theta = dl_0$ is the length of an elementary arc along the latitudinal axis θ (the polar angle θ is measured from the North Pole), and $r \sin \theta d\varphi = dl_0$ is the length of an elementary arc along the equatorial latitudinal axis φ .

As is seen from the above calculation, a rigid rod located in the field of a rotating massive body (say, in the field of the Earth or the Sun) retains its original physically observable length dl_0 , when installed along the geographical latitudes ($dl_0 = dl_0$).

In contrast, when the rod installed in the position along the radial coordinate r , i.e., in the direction towards the centre of the rotating massive body (along its radius), its physically observable length dl_r is greater than its original length dl_0 by a small value δl_r

$$dl_r = \sqrt{h_{11} dr^2} = \frac{dl_0}{\sqrt{1 - \frac{r_g}{r}}} \approx \left(1 + \frac{r_g}{2r}\right) dl_0, \quad (175)$$

$$\delta l_r \approx \frac{r_g}{2r} dl_0 \approx \frac{1}{2} C r^2 dl_0, \quad (176)$$

which is determined by the curvature of space $C = \frac{r_g}{r^3}$ caused by the gravitational field of the rotating body. See the second term in the formula for the physically observable curvature C (106) of the space of a rotating massive body, which we have derived above in this paper.

And also, when the rod is installed in the position along the equatorial coordinate φ , i.e., in the direction along the geographical longitudes along which the massive body (say, the Earth or the Sun) rotates around its own axis, its physically observable length dl_φ is greater than its original length dl_0 by a small value δl_φ

$$dl_\varphi = \sqrt{1 + \frac{\omega^2 r^2 \sin^2 \theta}{c^2}} dl_0 \approx \left(1 + \frac{\omega^2 r^2 \sin^2 \theta}{2c^2}\right) dl_0, \quad (177)$$

$$\delta l_\varphi \approx \frac{\omega^2 r^2 \sin^2 \theta}{2c^2} dl_0 \approx \frac{1}{12} C r^2 \sin^2 \varphi dl_0, \quad (178)$$

determined by the curvature of space $C = \frac{6\omega^2}{c^2}$ created by its rotation (together with the massive body) and is expressed with the first term in the formula for the physically observable curvature C (106), which we have derived in this paper.

As a result of the above derivation, we obtain the 3rd new effect of General Relativity:

THE 3RD NEW EFFECT OF GENERAL RELATIVITY

A rigid rod installed along the radial coordinate in the field of a rotating massive body (i.e., in the direction to the body’s centre) acquires an additional length. This additional length is determined by the curvature of the body’s space caused by its gravitational field.

In addition, if the rod is installed along the equatorial coordinate φ (i.e., along the geographical longi-

tudes of the body), then its length acquires an additional length determined by the curvature of the body's space caused by its rotation.

This effect of length stretching of a rod in the field of a rotating massive body is due to the "stretching" of the body's space along the radial direction r (towards the body) caused by its gravitational field, and along the equatorial coordinate φ (along the geographical longitudes), caused by the rotation of the body's space (together with the body).

In other words, a rod in the field of a rotating massive body is "stretched" together with the "stretching" of the coordinate grid of space in the radial and equatorial directions. The "stretching" of the grid of space in the radial direction occurs due to the curvature of the body's space (the funnel of space) in this direction, caused by its gravitational field. Whereas the "stretching" of the coordinate grid of space along the equatorial coordinates is caused by the curvature of the body's space due to its rotation in this direction.

For example, the length stretching of a rod installed at the equator of the Earth ($\omega_{\oplus} = 1 \text{ rev/day} = 7.27 \times 10^{-5} \text{ sec}^{-1}$, $r_{\oplus} = 6.37 \times 10^8 \text{ cm}$) in the direction along the longitudinal axis φ , i.e., along the equator, has a numerical value of

$$\delta l_{\varphi} \approx \frac{\omega_{\oplus}^2 r_{\oplus}^2 \sin^2 \theta}{2c^2} dl_0 \approx 1.2 \times 10^{-12} dl_0 \quad (179)$$

of the original length dl_0 of the rod.

The length stretching of a rod installed vertically on the Earth's surface, has a numerical value of

$$dl_r \approx \frac{r_{g\oplus}}{2r_{\oplus}} dl_0 \approx 7.0 \times 10^{-10} dl_0. \quad (180)$$

This length stretching effect is maximum at the equator, where the curvature and "stretching" of the Earth's space caused by the Earth's gravitational field are maximum (since the Earth is oblate towards the equator), and the curvature and "stretching" of the Earth's space caused by the Earth's rotation are also maximum. This length stretching effect decreases towards the geographical poles, where the length stretching caused by the rotation of the Earth's space vanishes (since $\sin \theta = 0$ at the poles), and the length stretching caused by the gravitational field is a little lesser than at the equator.

7.2 Time loss/gain

Let us now substitute into the general formula for the physically observable interval $d\tau$ the gravitational potential w (54) and the linear velocity of the rotation of space $v_3 = \omega r^2 \sin^2 \theta$ (45) that we have calculated above in this paper among the other characteristic of the space metric of a rotating massive body (10).

Thus, we obtain the physically observable time interval $d\tau$, which will be registered by an observer travelling along

the equatorial direction φ (i.e., along the geographical longitudes) in the space of a rotating massive body

$$\begin{aligned} d\tau &= \sqrt{1 - \frac{r_g}{r}} dt - \frac{1}{c^2} v_3 u^3 dt = \\ &= \sqrt{1 - \frac{r_g}{r}} dt - \frac{\omega r^2 \sin^2 \theta}{c^2} u^3 dt, \quad (181) \end{aligned}$$

where $u^3 = \frac{d\varphi}{dt}$ is the coordinate velocity of the observer in the equatorial direction $x^3 = \varphi$, along which he travels.

The first term in this formula determines the known effect of time loss due to the curvature of the body's space $C = \frac{r_g}{r^3}$ caused by its the gravitational field: the stronger the gravitational field (the closer the observer is to a massive body), the shorter the time intervals registered by him

$$d\tau = \sqrt{1 - \frac{r_g}{r}} dt \approx \left(1 - \frac{r_g}{2r}\right) dt, \quad (182)$$

$$\delta\tau \approx -\frac{r_g}{2r} dt \approx -\frac{1}{2} C r^2 dt. \quad (183)$$

In other words, this is the known effect of the classical theory: the higher the observer is above the surface of a massive body, the weaker the curvature of the body's space and, consequently, the shorter the time intervals that the observer records.

However, the second term of (181) is absent in the classical theory. This term reveals the increment of the physically observable time, which is due to the curvature of the body's space $C = \frac{6\omega^2}{c^2}$ caused by its rotation (together with the massive body itself)

$$\delta\tau = -\frac{\omega r^2 \sin^2 \theta}{c^2} u^3 dt = -\frac{C r^2 \sin^2 \theta}{6\omega} u^3 dt. \quad (184)$$

The sign of this effect depends on the direction, in which the observer travels with respect to the rotation of space, i.e., on the sign of the observer's coordinate velocity u^3 (he travels along the equatorial axis $x^3 = \varphi$).

As a result, based on the second term in the obtained solution, we obtain the 4th new effect of General Relativity in addition to those three explained above. This effect says:

THE 4TH NEW EFFECT OF GENERAL RELATIVITY

A clock on board an airplane (or a spacecraft) flying in the field of a rotating massive body in the same direction in which the body's space rotates (together with the body itself) should register a time loss depending on the airplane's (or a spacecraft's) velocity and the rotation velocity of the body's space.

In contrast, a clock on board an airplane (or a spacecraft) flying in the direction, opposite to the body's space rotation should register a time increment, as well depending on the airplane's (or a spacecraft) velocity and the velocity, with which the body's space rotates.

This effect of time loss/gain in the field of a rotating massive body is due to the “stretching” of the body’s space along the equatorial direction φ (along the geographical longitudes), caused by the rotation of the body’s space along this axis. When, say, an airplane flies towards the Earth’s rotation, the magnitude of the total rotation of space registered on its board is less than the proper rotation of the Earth’s space at the point of departure/arrival and, therefore, the “stretching” (and curvature) of space registered on board the airplane is also less. In contrast, when an airplane flies backwards the Earth’s space rotation, the clock on its board registers a time increment due to the greater magnitude of the total rotation and, therefore, greater “stretching” (and curvature) of space.

For example, consider a typical commercial flight traveling at 10 000 m along the Earth’s equator ($\omega_{\oplus} = 1 \text{ rev/day} = 7.27 \times 10^{-5} \text{ sec}^{-1}$, $r_{\oplus} = 6.37 \times 10^8 \text{ cm}$) at a typical cruising speed of 800 km/hour, which means a flight time around the globe of $t \approx 1.8 \times 10^5 \text{ sec}$. Since the planet Earth rotates from West to East, the above 800 km/hour mean that the airplane’s velocity is $u^3 = +3.5 \times 10^{-5} \text{ sec}^{-1}$ when flying Eastward and $u^3 = -3.5 \times 10^{-5} \text{ sec}^{-1}$ when flying Westward.

Then, according to the second term (184) in the obtained solution for $d\tau$ (181) we have obtained in the field of a rotating massive body, a clock installed on board the airplane should register a time loss of

$$\delta\tau_{\text{East}} = -\frac{\omega_{\oplus} r_{\oplus}^2 \sin^2\theta}{c^2} u^3 t \approx -210 \text{ nanosec}, \quad (185)$$

when flying to the East (i.e., in the same direction, in which the Earth’s space rotates), and also a time increment

$$\delta\tau_{\text{West}} = +\frac{\omega_{\oplus} r_{\oplus}^2 \sin^2\theta}{c^2} u^3 t \approx +210 \text{ nanosec}, \quad (186)$$

when flying to the West (i.e., oppositely to the rotation of the Earth’s space).*

This effect is maximum at the equator (where the curvature of the Earth’s space caused by its rotation is maximum and, therefore, space is maximally “stretched”) and decreases towards the poles, where $\sin\theta = 0$ and, therefore, this effect vanishes.

This effect was first registered in the “around-the-world-clock experiment”, conducted in 1971 by Joseph C. Hafele and Richard E. Keating [12–14] and then repeated in 2005 by the UK’s National Measurement Laboratory [15], despite the fact that they did not know about the chronometrically invariant formalism and the effects caused by the rotation of space; I discussed this issue in extensive friendly correspon-

dence with Joseph C. Hafele in the last years of his life, before he passed away in 2014 [16]. Their flights took place in the Northern Hemisphere (not at the equator) and at different altitudes. In addition, the results of their measurements were affected by the relativistic addition of the airplane’s velocity to the Earth’s rotation velocity when flying Eastward (and subtraction when flying Westward), as well as the decrease in the Earth’s gravitational potential with flight altitude. That is their measurement results were not purely the effect of the rotation of space. The total effect registered in the Hafele-Keating experiment was a time loss of -59 ± 10 nanoseconds when flying Eastward and a time increment of $+273 \pm 7$ nanoseconds when flying Westward, which fits well with our above calculation of the new effect due to the rotation of space, if we take into account the relativistic addition of the airplane’s velocity to the Earth’s rotation velocity when flying Eastward and subtraction when flying Westward.

8 Conclusion

The main contribution of this paper is introducing and proving the space metric of a rotating massive body, approximated by a mass-point. This is a new space metric to General Relativity, the main purpose of which is to be a modern extension and replacement of the classical Schwarzschild mass-point metric (since in the space of the Schwarzschild metric a massive body creating gravitational field does not rotate).

We have proven that the introduced space metric of a rotating massive body satisfies Einstein’s field equations, and also derived the Riemann conditions under which this occurs. Therefore, the introduced metric can be legitimately used in General Relativity.

We have calculated all known physically observable properties of space determined by the introduced metric of a rotating massive body, including the physically observable curvature of space. And here is what is especially interesting: we have found that the curvature of space is caused not only by the gravitational field filling it, but also by the rotation of space (together with the massive body). Based on this theoretical discovery, we have predicted and calculated four new effects of General Relativity:

1. Deflection along the equatorial coordinate and time delay of mass-bearing particles falling onto a rotating massive body, which is due to the “stretching” (curvature) of space, caused by its rotation (together with the body itself);
2. Deflection along the equatorial coordinate and time delay of light rays spreading to a rotating massive body, which is due to the “stretching” (curvature) of space, caused by its rotation;
3. Length stretching of a rod installed along the radial and equatorial coordinates in the field of a rotating massive body due to the “stretching” (curvature) of space in these directions, caused by its rotation;

*The calculated numerical values are the same as those calculated in the previous paper [3] in the absence of the gravitational field, since the gravitational field produces an individual effect, expressed by the first term of the obtained solution for $d\tau$ (181).

4. The loss of time in a clock travelling in the direction of the body's space rotation, which is due to the increase in the "stretching" (curvature) of space in the direction of its rotation, and accordingly the increment of time when the clock travels oppositely to the rotation of space.

All real cosmic bodies in the Universe rotate. Therefore, the introduced and proved space metric is the *main space metric in the Universe*, characterizing the field of any real cosmic body, be it a planet, star, galaxy or something else.

Feel free to use this new metric instead of the classical Schwarzschild metric to solve problems in General Relativity and astrophysics, if you have the necessary mathematical skills and wishes to do so, of course.

Submitted on September 28, 2024

References

1. Rabounski D. and Borissova L. Non-quantum teleportation in a rotating space with a strong electromagnetic field. *Progress in Physics*, 2022, v. 18, issue 1, 31–49.
2. Rabounski D. and Borissova L. Deflection of light rays and mass-bearing particles in the field of a rotating body. *Progress in Physics*, 2022, v. 18, issue 1, 50–55.
3. Rabounski D. and Borissova L. Length stretching and time dilation in the field of a rotating body. *Progress in Physics*, 2022, v. 18, issue 1, 62–65.
4. Zelmanov A. L. Chronometric Invariants. Translated from the 1944 PhD thesis, American Research Press, Rehoboth, New Mexico, 2006.
5. Zelmanov A. L. Chronometric invariants and accompanying frames of reference in the General Theory of Relativity. *Soviet Physics Doklady*, 1956, v. 1, 227–230 (translated from *Doklady Akademii Nauk USSR*, 1956, v. 107, issue 6, 815–818).
6. Zelmanov A. L. On the relativistic theory of an anisotropic inhomogeneous universe. *The Abraham Zelmanov Journal*, 2008, vol. 1, 33–63 (translated from the thesis of the 6th Soviet Conference on the Problems of Cosmogony, USSR Academy of Sciences Publishers, Moscow, 1957, 144–174).
7. Rabounski D. and Borissova L. Particles Here and Beyond the Mirror. The 4th revised edition, New Scientific Frontiers, London, 2023 (the 1st edition was issued in 2001).
Rabounski D. et Larissa Borissova L. Particules de l'Univers et au delà du miroir. La 2ème édition révisée en langue française, New Scientific Frontiers, Londres, 2023.
8. Borissova L. and Rabounski D. Fields, Vacuum, and the Mirror Universe. The 3rd revised edition, New Scientific Frontiers, London, 2023 (the 1st edition was issued in 2001).
Borissova L. et Rabounski D. Champs, Vide, et Univers miroir. La 2ème édition révisée en langue française, New Scientific Frontiers, Londres, 2023.
9. Borissova L. and Rabounski D. Inside Stars. The 3rd edition, revised and expanded, New Scientific Frontiers, London, 2023 (the 1st edition was issued in 2013).
10. Rabounski D. and Borissova L. Physical observables in General Relativity and the Zelmanov chronometric invariants. *Progress in Physics*, 2023, v. 19, issue 1, 3–29.
11. Landau L. D. and Lifshitz E. M. The Classical Theory of Fields. First published in 1939 in Russian, and then in 1951 in English (Pergamon Press, Oxford). The section and page references are given here from the final, 4th, twice expanded and revised English edition (1979, Butterworth-Heinemann, Oxford).
12. Hafele J. Performance and results of portable clocks in aircraft. PTTI 3rd Annual Meeting, November 16–18, 1971, 261–288.
13. Hafele J. and Keating R. Around the world atomic clocks: predicted relativistic time gains. *Science*, July 14, 1972, v. 177, 166–168.
14. Hafele J. and Keating R. Around the world atomic clocks: observed relativistic time gains. *Science*, July 14, 1972, v. 177, 168–170.
15. Demonstrating relativity by flying atomic clocks. *Metromnia*, the UK's National Measurement Laboratory Newsletter, issue 18, Spring 2005.
16. Rabounski D. and Borissova L. In memoriam of Joseph C. Hafele (1933–2014). *Progress in Physics*, 2015, v. 11, issue 2, 136.

Galaxy Clusters: Quantum Celestial Mechanics (QCM) Rescues MOND?

Franklin Potter

Sciencegems, 8642 Marvale Drive, Huntington Beach, CA, USA. E-mail: frank11hb@yahoo.com

Although the MOND radial acceleration $g = \sqrt{g_N a_0}$ for the acceleration of objects in a low acceleration environment less than $a_0 = -1.2 \times 10^{-10} \text{ m/s}^2$ has been extremely successful for single galaxies, the much higher mass clusters of galaxies do not have enough baryonic mass to comply. We consider the possibility that the MOND a_0 value, instead of being a universal constant, actually depends upon both the total baryonic mass of the gravitationally bound system and its total angular momentum, as derived by Quantum Celestial Mechanics (QCM) from the general relativistic Hamilton-Jacobi equation. If the total angular momentum of the galaxy cluster is less than expected, then the MOND radial acceleration expression can remain valid.

1 Introduction

Galaxy rotation velocities do not match Newton's Law of Universal Gravitation, $g = -GM/r^2$, for stars experiencing low gravitational radial accelerations [1]. The stars at all large orbital radii where the radial acceleration is less than about 10^{-10} m/s^2 are moving at nearly identical velocities instead of decreasing to the lower velocity values predicted by Newton's Law.

Initial attempts to alter Newton's Law failed, so the dark matter hypothesis became the alternative explanation with the consequence that Newton's Law could apply once again [2]. However, two important challenges to dark matter continue to exist: (1) no predicted dark matter particle has ever been detected in at least 50 years of experimental searches [3, 4], and (2) a modification of gravitation called MOND (MODified Newtonian Dynamics) exists and agrees extremely well with single galaxy rotation curves [5] and has predicted many other physical properties that have been found to hold true for single galaxies and other gravitationally bound systems [6, 7].

Even though fitting the rotation curves of single galaxies is remarkably successful, MOND does not fit the radial acceleration values for clusters of galaxies [8, 9]. There is a significant disagreement with the MOND gravitational acceleration expression

$$g = \sqrt{g_N a_0}, \quad (1)$$

where the MOND acceleration constant $a_0 = -1.2 \times 10^{-10} \text{ m/s}^2$ and $g_N = -GM(< r)/r^2$ is the Newtonian acceleration for enclosed baryonic mass M . This gravitational expression using the a_0 value has been shown to hold true for all single galaxies and is assumed to be true for clusters of galaxies.

However, the measurements for galaxy clusters reveal that the observed acceleration g_{obs} is greater than the acceleration value g predicted by this MOND expression at the low radial acceleration environments where the expression should be true. Fig. 1 shows the discrepancy between the dynamic mass and all the observed mass of the baryons in the gas and the stars within the cluster, with the data from [8]. Some clusters need as much as a factor of 5 more baryonic mass for the

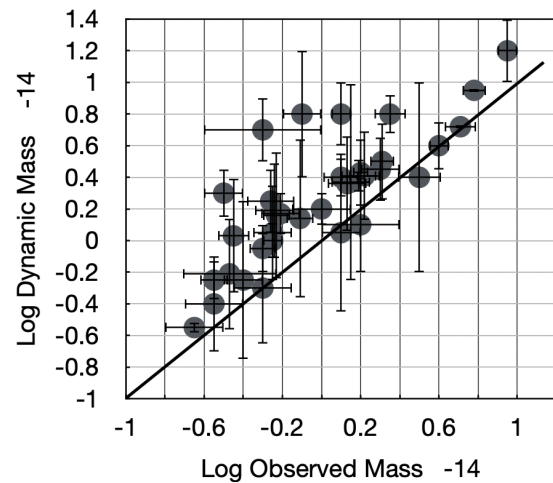


Fig. 1: Log scales around 10^{14} solar masses for galaxy clusters. If MOND is to prevail with its constant a_0 value, all the clusters should be at the straight line. Data is a representative selection from Sanders (2003).

MOND expression to hold true, i.e., be at the straight line where the dynamic mass and the observed mass values agree.

This discrepancy between g_{obs} and the MOND predicted g has been attributed to missing baryonic mass M in the cluster, but several searches have not found any more mass than already determined. Consequently, to fit the actual observed radial accelerations for all galaxy clusters, a distribution of dark matter has been proposed so that Newton's Law applies to galaxy clusters.

We propose a different explanation for the acceleration discrepancy, one that allows the MOND acceleration expression $g = \sqrt{g_N a_0}$ to be correct for galaxy clusters as well as for single galaxies. In 2003, H. G. Preston and I investigated [10] an approach to gravitation that we called quantum celestial mechanics (QCM) in which the general relativistic Hamilton-Jacobi equation is converted into a new scalar gravitational wave equation (GWE). In different metrics the GWE allows

us to propose some new explanations for specific types of gravitational behavior.

In the Schwarzschild metric the GWE leads to the quantization of angular momentum *per unit mass* because both Newtonian gravitational attraction and a QCM gravitational repulsion exists for orbiting bodies. All confirmed planetary systems, including the Solar System, have been shown to agree with this QCM prediction [11], i.e. the orbital planetary equilibrium radii of the multi-planetary systems are only at the QCM predicted subset of all possible equilibrium radii that are allowed by Newton's Law.

We also derived the above MOND gravitational expression, which revealed that the MOND acceleration a_0 will have slightly different values in different single galaxies depending on the total baryonic mass M_T of the gravitationally bound system and its total angular momentum L_T ,

$$a_0 = \frac{G^3 M_T^7}{n^4 L_T^4}, \quad (2)$$

with n an integer.

This dependency of a_0 upon both M_T and L_T will allow us to re-interpret the MOND expression for g so that clusters of galaxies, as well as single galaxies, satisfy $g_{obs} = g$ without the need for dark matter.

2 Derivation of QCM and MOND, a brief review

From the general relativistic Hamilton-Jacobi equation,

$$g^{\alpha\beta} \frac{\partial S}{\partial x^\alpha} \frac{\partial S}{\partial x^\beta} - \mu^2 c^2 = 0 \quad (3)$$

the transformation

$$\Psi = e^{iS'/\mu c H} \quad (4)$$

introduces a wave function Ψ , with S the action, μ the mass of the orbiting object, and $S' = S/\mu c$ so that the equivalence principle is obeyed. For a detailed derivation, see [10]. Here we have defined a system scale length H by

$$H = \frac{L_T}{M_T c} \quad (5)$$

for the total gravitationally bound system mass M_T having total angular momentum L_T and c being the speed of light in vacuum.

Following through with the mathematical steps produces a scalar gravitational wave equation (GWE)

$$g^{\alpha\beta} \frac{\partial^2 \Psi}{\partial x^\alpha \partial x^\beta} + \frac{\Psi}{H^2} = 0. \quad (\text{GWE}) \quad (6)$$

Expressing the GWE in the Schwarzschild metric, a separation of variables leads to differential equations in coordinates (t, r, θ, ϕ) that produce quantization conditions. The angular parts dictate the quantization of angular momentum *per unit mass* for orbital angular momentum L as

$$\frac{L}{\mu} = mcH \quad (7)$$

for integer m . The radial equation leads to the quantization of energy per unit mass

$$E_n = -\mu c^2 \frac{r_g^2}{8n^2 H^2} \quad (8)$$

for integer n .

Using the virial theorem and E_n , we obtain the velocity v in terms of the Schwarzschild radius r_g and H ,

$$v = \frac{r_g c}{2nH}. \quad (9)$$

Whence, with the radial acceleration $g = v^2/r$, we derive the MOND acceleration expression from

$$g = \frac{r_g^2 c^2}{4n^2 H^2 r} = \sqrt{\frac{GM}{r^2} \left(\frac{G^3 M_T^7}{n^4 L_T^4} \right)}. \quad (10)$$

Therefore, the MOND acceleration a_0 is not a universal constant but is determined to be

$$a_0 = \frac{G^3 M_T^7}{n^4 L_T^4}, \quad (11)$$

explicitly expressing its dependency upon both the total mass M_T of the system and its total angular momentum L_T .

3 Discussion

We have begun with the successful MOND expression $g = \sqrt{g_N a_0}$ using $a_0 = -1.2 \times 10^{-10} \text{ m/s}^2$, with a_0 having this value for all single galaxies. But if we assume that a_0 has this same value for galaxy clusters, then the baryonic mass discrepancy shown in Fig. 1 arises.

According to QCM, there can be two possible causes for the discrepancy between the observed radial acceleration g_{obs} and the predicted MOND value g in the galaxy clusters, the values of total baryonic mass value M_T and the total angular momentum L_T . All the baryonic mass M_T in the gas and stars, etc., has been identified. However, we do not know the total angular momentum L_T of any galaxy cluster.

QCM predicts that the a_0 value depends upon the ratio M_T^7/L_T^4 . We already know the baryonic M_T for the clusters, but there are no published values of L_T for any cluster. Therefore, we must estimate the L_T values for different galaxy clusters if the MOND $g = g_{obs}$ is to hold true.

In some clusters of galaxies the dynamical mass M_{dyn} has been determined to be as much as a factor of 5 larger than the actual observed mass M_{obs} of the hot gas and the stellar content. Therefore, the ratio M_T^7/L_T^4 for a_0 in these galaxy clusters must be up to 5 times larger than for single galaxies in order to have $g_{obs} = \sqrt{g_N a_0}$.

We assume that the expected L_T value is the one that makes the MOND $a_0 = -1.2 \times 10^{-10} \text{ m/s}^2$. Then in the general case, if there is a factor f reduction in the baryonic mass

M_T , QCM requires

$$fa_0 = \frac{G^3 M_T^7}{n^4 L_T^4} \quad (12)$$

which, for $n = 1$ and $M_{obs} = M_T/f$, means

$$L_T^4 = \frac{G^3 M_{obs}^7}{f^8 a_0}. \quad (13)$$

For example, if $f = 2$, the L_T value would be 4 times smaller than expected for the M_{obs} . This L_T value then makes the product $g_N a_0$ guarantee $g = g_{obs}$. Thus, each galaxy cluster could have a unique a_0 value.

There exists several possible sources of a lower angular momentum total than expected:

1. the intracluster (IC) gas that comprises about 90% of the baryonic mass of the cluster could, in part or as a whole, have a slower rotation speed than gas in single galaxies,
2. the IC stars are known to rotate slower than many stars,
3. the angular momentum vectors of the galaxies in the cluster may have a greater variety of directions than expected, thereby decreasing their vector sum.

Whether any or all of these possible sources of lower angular momentum are the cause of the different a_0 values for the galaxy clusters has yet to be determined.

4 Conclusion

Recent measurements have verified that there is not enough baryonic mass for the successful MOND gravitational acceleration expression for single galaxies

$$g = \sqrt{g_N a_0} \quad (14)$$

to be true for clusters of galaxies, where g_N is the Newtonian gravitational radial acceleration and the MOND $a_0 = -1.2 \times 10^{-10} \text{ m/s}^2$ is assumed to be a universal constant.

However, a_0 may not be a universal constant as originally proposed. We briefly reviewed the quantum celestial mechanics (QCM) derivation of a_0 from the general relativistic Hamilton-Jacobi equation to obtain the acceleration

$$g = \frac{r_g^2 c^2}{4n^2 H^2 r} = \sqrt{\frac{GM}{r^2} \left(\frac{G^3 M_T^7}{n^4 L_T^4} \right)}. \quad (15)$$

Therefore, QCM dictates

$$a_0 = \frac{G^3 M_T^7}{n^4 L_T^4}, \quad (16)$$

showing that a_0 depends upon both the total baryonic mass M_T and its total angular momentum L_T of any gravitationally bound system obeying the Schwarzschild metric. For single

galaxies, this QCM expression for a_0 varies less than a few percent and therefore a_0 can be assumed universal.

However, in more massive gravitationally bound systems such as clusters of galaxies, a_0 could have different values in order to satisfy the MOND expression $g = \sqrt{g_N a_0}$. If galaxy clusters possess significantly less angular momentum than is expected for the measured total baryonic mass, this MOND expression can be satisfied still. Several possible reasons for the lesser total angular momentum values were suggested.

We await total angular momentum estimates for galaxy clusters in the near future to establish whether the MOND acceleration a_0 has a different value for galaxy clusters and whether the MOND expression $g = \sqrt{g_N a_0}$ continues to hold true.

Acknowledgements

We thank Sciencegems for continued support and encouragement to investigate various challenges in gravitation.

Received on September 26, 2024

References

1. Rubin V. C., Ford W. K. Jr., Thonnard N. Rotational properties of 21 SC galaxies with a large range of luminosities and radii, from NGC 4605 (R=4kpc) to UGC 2885 (R=122kpc). *Astrophysical J.*, 1980, v. 238, 471–487.
2. Navarro J. F., Frenk C. S., White S. D. M. The Structure of Cold Dark Matter Halos. *The Astrophysical J.*, 1996, v. 462, 563–575.
3. Chen C-Y, Hwang C-Y. Six spiral galaxies lacking dark matter. *Scientific Reports*, 2024, v. 14, 17268.
4. Das A., Kurinsky N., Leane R. K. Dark Matter Induced Power in Quantum Devices. *Phys. Rev. Lett.*, 2024, v. 132, 121801.
5. Mistele T., McGaugh S., Lelli F., Schombert J., Li P. Indefinitely Flat Circular Velocities and the Baryonic Tully-Fisher Relation from Weak Lensing. *ApJL.*, 2024, v. 969 (1), L3.
6. Milgrom M. A modification of the Newtonian dynamics: implications for galaxy systems. *Astrophysical J.*, 1983, v. 270, 384–389.
7. Sanders R. H., McGaugh S. S. Modified Newtonian Dynamics as an Alternative to Dark Matter. *Annual Rev. of Astronomy and Astrophysics*, 2002, v. 40, 263–317.
8. Sanders R. H. Clusters of galaxies with modified Newtonian dynamics. *Monthly Notice of the Royal Astronomical Society*, 2003, v. 342 (3), 901-908.
9. Li P., Tian Y., *et al.* Measuring galaxy cluster mass profiles into the low acceleration regime with galaxy kinematics. arXiv: astro-ph/2303.10175v2.
10. Preston H. G., Potter F. Exploring large-scale gravitational quantization without \hbar in planetary systems, galaxies, and the Universe. arXiv: gr-qc/0303112.
11. Potter F. Multi-planetary exosystems all obey orbital angular momentum quantization per unit mass as predicted by Quantum Celestial Mechanics (QCM). *Prog. in Phys.*, 2013, v. 9 (3), 29–30.

On the Possibility of a Scientific Prognosis of the Weather with the Introduction of Galactic Impacts into Analysis

Nikolai A. Morozov*

In this paper the author gives a preliminary information of his research study concerning cosmic influences on the weather. For this purpose, solar time was converted into sidereal (stellar) time for many thousands of meteorological data taken from the meteorological yearbooks published by meteorological observatories of the world. The resulting more than 200 diagrams identify interesting dependencies indicating a significant influence of the Galactic Centre and some other Galactic sources on the weather.

*Translated from *Bulletin de L'Académie des Sciences de L'URSS, Série Géographique et Géophysique*, 1944, t. VIII, no. 2–3, 63–71.



Nikolai A. Morozov, 1910

Nikolai A. Morozov (1854–1946) was the first child of a Russian millionaire and his freed female slave (slavery in Russia was abolished only 7 years later in 1861). He was a polymath and also a political figure who, while living in Genève, became the main theorist and one of the leaders of the 1881 Russian Bourgeois Revolution: they dreamed of a parliament, constitution, free capitalism, human rights and “liberté, égalité, fraternité” in the sense of Robespierre and Marat, but ended by the assassination of Alexander II, Emperor of Russia, which was not supported by mass people. After returning to Russia in 1881, Morozov was sentenced to life in solitary confinement in the Schlüsselburg Fortress near St. Petersburg, where he spent the next 24 years of his life (1881–1905) in a solitary confinement cell.

After the royal amnesty in 1905, Morozov devoted himself entirely to continuing the theoretical scientific research he had begun before the jail and then continued while in prison. He was immediately elected Professor of chemistry at the Lesgaf Research Institute in St. Petersburg, and then headed the entire Institute, where he remained Director until his death in 1946. His main research works were in the fields of chemistry, physics, astrophysics, meteorology, linguistics and world history. After the fall of the royal regime in Russia, he was elected to the Russian Academy of Sciences.

Being already an old man, in order to conduct experiments necessary for his scientific work, Morozov flew into the stratosphere in a stratospheric balloon. His original periodic table of chemical elements (an alternative to the generally accepted Mendeleev table) extends to elementary particles. In 1919, he conducted a series of original experiments testing the effects of Special Relativity. “Linguistic spectra” he introduced to identify true authors are now widely used in cryptography.

In the first half of the last [19th] century, attempts were made to scientifically process the old folk belief about the connexion between weather changes and the combination of the Sun and Moon, especially with new moons. Indeed, there was much in this belief that deserved attention: due to solar heating, ascending air currents occur, and thanks to them, descending air currents with the formation of cumulus and thunderclouds of local origin, as well as trade winds and non-trade wind air currents, and also cold polar layers that mix air with the warmer layers of the Earth’s temperate zones.

Due to the tidal action of the Moon and the Sun, there must inevitably be ebbs and flows not only in the seas, but also in the atmosphere, and the ebbs and flows of the atmosphere due to the attraction of the Sun, running into the lunar ebbs and flows lagging behind them, must, depending on the time of year, cause various cyclones (the main factors of weather instability on the Earth), depending on the geographical place of their origin.

All this seemed so clear that many astronomers and meteorologists, beginning with the famous François Arago, put a lot of effort into testing the aforementioned idea on a huge number of daily records in meteorological observatories throughout the world. But no matter how they combined these records, bringing them into connexion with the combinations of the positions of the Sun and the Moon, they always came to the same thing: 60 percent of the predictions came true, and 40 percent did not, showing that in addition to the Sun and the Moon, some other cosmic factors influence weather changes, since from a natural-scientific point of view no natural phenomenon can be causeless. Many years ago I also studied this subject. At that time, I had the idea that the missing third fac-

In December 1942, at the age of 88, Morozov volunteered for military service as a sniper and scored a number of confirmed hits, but was demobilized one month later due to health reasons. He died from pneumonia at the age of 92 in 1946 in his mansion, which he inherited from his father.

The presented paper is a preliminary communication outlining the results of his extensive monograph on this subject (unpublished since he passed away in 1946). The staff of the Astronomy Department of the Lesgaf Research Institute, where he was Director, assisted him over many years in the 1930s in calculations and the construction of hundreds of graphs (necessary for this study) based on data from meteorological yearbooks for the entire history of regular meteorological observations over the past 150 years (until the 1940s). — Editor’s remark.

tor in weather changes could and even should be our entire Galactic cosmos, i.e., the entire set of our disk-shaped cluster of stars and, in particular, the centre of their rotation.

But to clarify such an influence and determine its magnitude, it was necessary to re-calculate the records of all meteorological yearbooks from our usual solar time, according to which they are kept, to sidereal (stellar) time, the day of which is 4 minutes shorter than the solar day. And this re-calculation of hundreds of thousands of meteorological observations, necessary to obtain some specific conclusion, would be such a huge job that the work of hundreds of calculators would be required for more than many years.

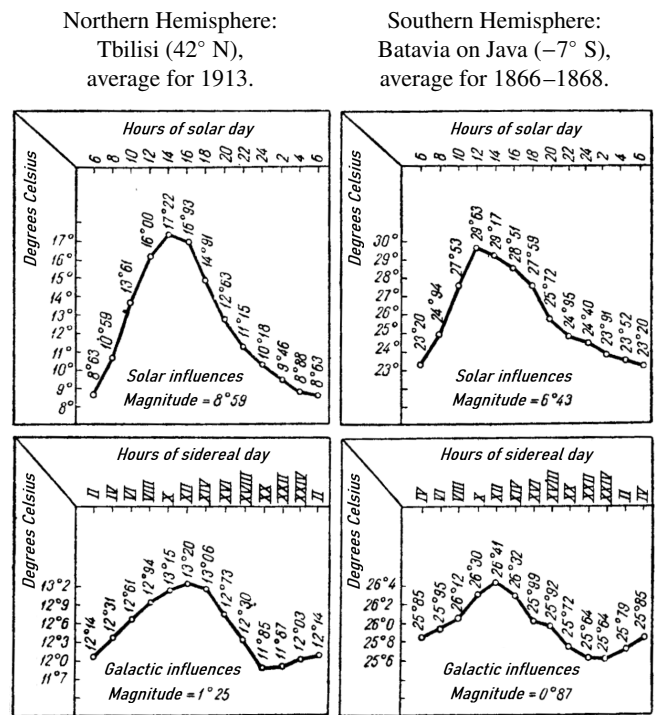
Only seven years ago, after much research on this subject, I succeeded in finding a new method of conversion, using which in one evening it is possible to convert from solar time to sidereal time such a number of meteorological records, which by the method that has existed up to now would have required at least a month. And I immediately set to work. Taking from the library of the [Russian] Academy of Sciences and the library of the Pulkovo Observatory the meteorological yearbooks of the Paris, London, Bombay, Batavia on Java, Leningrad, Moscow, Tbilisi, Cape Town and other observatories over the past few years, I personally made several thousand such conversions. Then, having instructed my assistants [from the Astronomy Department], I continued this work, as a result of which the calculation results were presented in the form of more than 200 diagrams.

Looking at these diagrams, I immediately found that for the sidereal-daily influences of our entire star cluster, clearly expressed diagrammatic configurations of the same type as the configurations of solar influences, only of a different magnitude, were obtained. Among the hundreds of thousands of data calculated, there was not even a single contradictory case in Europe, Asia, Africa, America, or Australia. All my tables and diagrams testified to the same thing: the influences of our entire star cluster cannot be ignored in any way when forecasting the weather.

It turned out to be possible to determine even the places [on the sky] from which the hitherto missing cosmic influences on the weather originate. All the discovered maxima and minima of the sidereal-daily influences on the air temperature unanimously showed that behind the constellation Argo Navis [now divided into Carina, Puppis and Vela], around the VIII-XI hour of right ascension, there is a gigantic accumulation of high-temperature matter, the radiation of which, like a gigantic furnace invisible at night, increases the air temperature above the horizon of any place during its highest ascent by more than one-seventh of the solar heating (Table I).

As this source rises above the horizon, the relative humidity of the air, i.e., its saturation with water gas, also increases. By designating 100% as the saturation at which water gas begins to be released in the form of fog or rain, we obtain very regular diametric arcs for both solar and Galactic influences (Table II), with the magnitude of the arc of Galactic influ-

Table I: Two examples of [air] temperature increase due to solar diurnal period action and galactic action (sidereal-daily period).



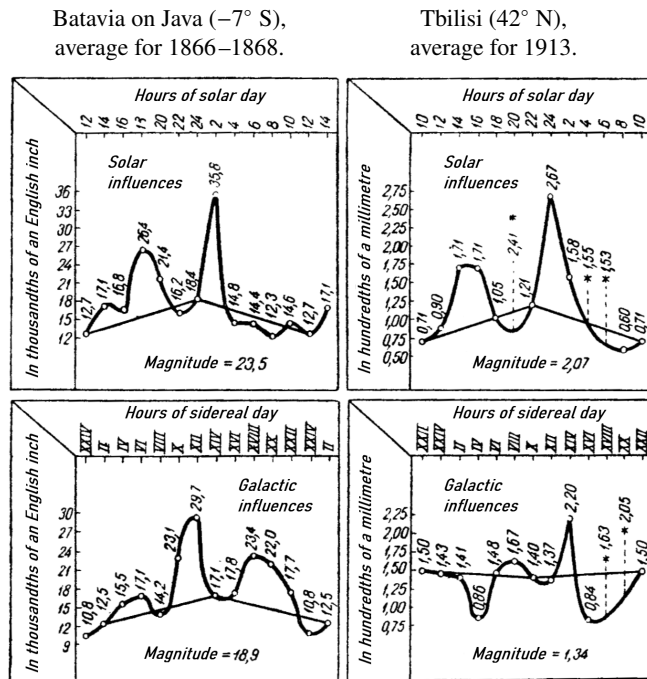
The increase in [air] temperature due to solar action reaches its maximum 2 hours after the Sun passes through the celestial meridian (at 14 solar hours). Similarly, the increase in temperature due to Galactic impact should reach its maximum 2 hours after the X celestial hour passes through the celestial meridian (the Galactic heat emitter is located near the X celestial hour). This Galactic heat emitter is located in the Southern Hemisphere of the sky, since its radiant heat, for example, in Batavia is equal to 1/3 of the solar radiant heat, and in Tbilisi — only 1/6 of the solar.

ence reaching up to half the magnitude of the solar arc in the Earth's temperate climate zones.

The rate of evaporation of the water surface (Table III, left) due to the influence of the rays of this Galactic centre reaches one third of the solar influence. This influence increases by the XII sidereal hour similarly to how the solar influence increases by 14 hours of the solar day, i.e., it occurs from the place of intersection of the XII-hour wing of the starry sky with the Milky Way, where there is a cluster of small stars and several “coal sacks” near the constellation Argo Navis.

Directly related to the evaporation rate, absolute humidity (the same Table III, on the right) has in the tropical zone of the Earth (probably due to the residual accumulation of evaporation) a less sharp peak in the curve of solar influence, so that the maximum of water gas remains undiminished from 14 to 20 hours of solar time. As for Galactic influences, their maximum effect on absolute humidity also falls at approximately the XX hour of sidereal time, but its growth and fall

Table IV: Example of average annual distribution of rainfall (by hours of the day) due to solar influence and Galactic influence.

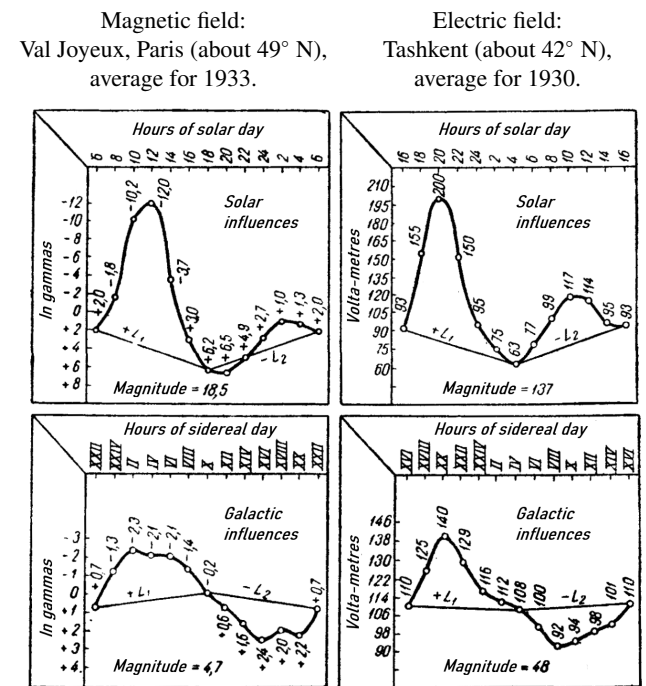


The irregular bends and jumps of these diagrammatic curves, especially — Tbilisi (asterisk) — show that rains depend not only on temperature and barometric pressure drops, but also on the electromagnetic effects of the Sun and the Galactic Centre, and that even more powerful electromagnetic storms than on the Sun permanently occur at this Centre.

tic influences by the hours of the sidereal day. On the left it is given for Batavia on Java (-7° S) and on the right — for Tbilisi in the Caucasus (42° N).

The two main maxima generated after the solar action (at 2 and 24 o'clock in the morning), as well as the evening actions (at 18 and 16 o'clock in the afternoon) show here that the solar actions in Tbilisi are generally the same as in Batavia, although they are delayed by 2 hours compared to Batavia. But why in Tbilisi in 1913 in the 20th, 4th and 6th solar hours the amount of rainfall (they are marked with asterisks) jumped out of the norm so much (see Table IV, upper right), that if I had not excluded them, they would have made the configuration of this diagrammatic curve completely disordered and having nothing in common with Batavia? Why do we see the same thing below in the Galactic influences? Here again we have only one way out: to admit that the distribution of rainfall depends not only on changes in temperature and barometric pressure, but also to a large extent on electromagnetic storms, constantly occurring not only on the Sun, but also on the Galactic Centre now being studied in the constellation Argo Navis. It is even possible that such storms on the Sun are only a resonance of Galactic storms, which must be repeated simultaneously on the Earth, and on

Table V: Examples of solar influences on solar-diurnal variations of the magnetic and electric field strengths and examples of similar galactic influences on the sidereal-diurnal period.



Magnetic Galactic influences from the constellation Argo Navis lag behind solar influences by 8 hours. If they were lagging by 12 hours, this would mean that the magnetic axes of the Sun and the Galactic Centre under study in the constellation Navis Argo are oriented opposite to each other. The lag of 8 hours shows that both of these axes are inclined to each other (as seen from the Earth) at an angle of about 120°.

the Moon, and on all the planets. Otherwise, it would be difficult to imagine why the jumps shown by the stars on our diagrams are repeated not only at midday, when the given horizon is turned toward the Sun, but also at different hours of the day, and why they are distributed in the same way among various sidereal hours. It even turns out that it is as if each stroke of cosmic lightning and protuberances on some Galactic centre is accompanied by multiple echoes on the others. In any case, thunderstorms, constantly accompanied by showers, sufficiently indicate a connexion between these two meteorological manifestations. Therefore, it is appropriate to dedicate a few lines to them in this preliminary message.

In Table V on the right I give an example of solar and Galactic influences on the oscillations of the electric field in Tashkent, and in the same place I give an example of the magnetic influences of the Sun in Val Joyeux near Paris (Table V on the left).

The necessity of brevity of this message of mine enforces me to give here, as an example of the substantiation of my theory, only one example of the most important sidereal-daily influences of the Galaxy, excluding its sidereal-annual influ-

ences. But in my working manuscripts, beginning in 1932, when I first began to study this subject systematically, there are hundreds of such re-calculations based on the systematic records of many geophysical and meteorological observatories of the world, and above all, the two Spitsbergen stations (in Horn Sound and Treyrenberg), the Sondakull station in Iceland, the Pavlovsk (now Slutsk) station, the Main Physical Observatory (in Leningrad), Sverdlovsk, Wilhelmshaven, Greenwich, Val Joyeux (near Paris), Budapest, Petrovsko-Razumovskaya (in Moscow), Cheltenham near Washington, Barcelona, Tbilisi, Tashkent, Caesarea in Lebanon, Tucson in Arizona, Beijing, Hong Kong, Alibag near Bombay, and Singapore.

For the Southern Hemisphere, I had at my disposal the records of the observatories at Batavia on Java, on the Island of St. Helena, at Antananarivo in Madagascar, at Buenos Aires, at Christchurch (New Zealand), and on the South Polar Continent [Antarctic] at the observatories at Cape Royds and Cape Evans.

All these observatories are known to every specialist, and their yearbooks that I have indicated are available in the libraries of the [Russian] Academy of Sciences, the Pulkovo Astronomical Observatory, and the Main Physical Observatory (in Leningrad). And all the hundreds of summary re-calculations for sidereal time compiled by me and my co-workers from these publications, and all the diagrams constructed from the calculations unanimously show that the influence of the Galaxy on the meteorological and geophysical processes of the Earth is of a regular nature and so great that without introducing them into the calculations one cannot even dream of a scientific forecasting of the weather even for a month ahead.

Here, first of all, a cycle of 521 Julian years is manifested, since only after this period do the previous combinations of the Sun, Moon and Galaxy repeat for each specific place on the globe. Such a long period does not, of course, provide any practical help for [weather] forecasting, since during most of it there were no meteorological records. However, another period of 19 years manifests itself, but only according to this period it turns out that a cyclone that, for example, swept over Leningrad today, will sweep in 19 years later somewhere over Irkutsk, then over Tokyo, then over San Francisco, and so forth and so on. And another cyclone that will come to Leningrad will be the one that was 19 years ago somewhere over London, and 38 years ago near New York, etc.

It is impossible not to mention here also the dendrochronological period of 11.35 years, determined by the alternation of the thickness of tree rings and coinciding with the same period of sunspots, with the proviso that this [dendrochronological] period itself can only be explained by the effect on the Sun (and with it of course on the Earth) of the radiation of some luminary rotating around its axis in 11.35 years. There can be no other rational explanation here, just as there can be no 280-year cycle consisting of almost 25 of the same

(exactly 11.35-year) cycles repeating quite regularly on the rings of giant Californian pines *Sequoia Gigantea*, for example, on the pine "Mark Twain", a section of which is kept in the New York Museum of Natural History (this pine was 1341 years old when it was cut down*).

And this period cannot be explained by anything except the fact that in the Galactic space there is an even more powerful centre rotating around its axis in 280 years (\pm a few years).

All this shows that for an absolutely accurate weather forecast it is necessary to determine not only the motion of the Moon, the Sun and Galactic centres above the horizon of the observation point, but also which side of their surface the latter are facing the Earth at that moment.

Of great help in using reference points to determine upcoming weather changes in a specific geographic area should be the already existing predictions of solar and lunar eclipses. Adding to them, Galactic influences will undoubtedly eliminate all cases of failure of predictions based on solar and lunar influences alone, but this requires the work of not one person or group of people, but the work of many meteorological institutions using the entire network of meteorological records throughout the globe.

November 4, 1940

*See A. E. Douglass and Waldo S. Glock, *Carnegie Institution of Washington Supplementary Publications*, July 1934, no. 9, and also, in the same place, *News Service Bulletin*, 1937, v. IV, no. 20.

Yang-Mills Theory in the Framework of General Relativity

Patrick Marquet

Calais, France. E-mail: patrick.marquet6@wanadoo.fr

In our recent publication, we derived a solution that allows the coupling between the Yang-Mills theory and the space-time curvature; *Progr. Phys.*, 2021, v.18, 97–102 [1]. This result was achieved by considering a specific manifold which we named the Weyl-Einstein manifold spanned by the connection coefficients displaying a 4-vector. We then deduced a Weyl-Einstein tensor, which was found to be conserved. The Weyl-Einstein 4-vector was directly identified with the Yang-Mills gauge field vectors as described in the Minkowski space tangent to the Weyl-Einstein manifold. In the present work, we investigate further this topic, and we examine how this coupling fits into the field equations.

Notations

Throughout this text, we assume the Einstein summation, whereby a repeated index implies summation over all values of this index.

4-tensor or 4-vector: small Latin indices $a, b, \dots = 0, 2, 3, 4$.

3-tensor or 3-vector: small Greek indices $\alpha, \beta, \dots = 1, 2, 3$.

Signature of the space-time metric: $(+---)$.

Ordinary derivative: $\partial_a U$.

Riemannian covariant derivative on (M, g) : ∇_a or $(;)$.

1 The Weyl-Einstein field equations

1.1 The Weyl-Einstein tensor

Following Lichnerowicz [2] we defined the semi-metric manifold (M_w, g) spanned by the Weyl-Einstein connexion coefficients expressed here with the metric connexion

$$W_{ab}^c = \frac{1}{2} g^{cd} (\partial_b g_{da} + \partial_a g_{db} - \partial_d g_{ab}) - \frac{1}{2} g^{cd} (J_b g_{da} + J_a g_{db} - J_d g_{ab}), \quad (1.1)$$

$$W_{ac}^c = \frac{1}{2} g^{cd} (\partial_a g_{cd} - J_a g_{cd}), \quad (1.2)$$

where J_a is referred to as the Weyl-Einstein 4-vector.

The Einstein-Weyl-curvature tensor is assumed to keep its original form

$$(R_{adb}^c)_w = \partial_b W_{ad}^c - \partial_d W_{ab}^c + W_{eb}^c W_{ad}^e - W_{ed}^c W_{ab}^e. \quad (1.3)$$

Setting

$$(\Gamma_{ab}^c)_J = \frac{1}{2} g^{cd} (J_b g_{da} + J_a g_{db} - J_d g_{ab}) \quad (1.4)$$

and using the Riemannian covariant derivatives, we found

$$(R_{ab})_w = R_{ab} + \nabla_c (\Gamma_{ab}^c)_J - \nabla_b (\Gamma_{ac}^c)_J + (\Gamma_{ab}^d)_J (\Gamma_{dc}^c)_J - (\Gamma_{ae}^d)_J (\Gamma_{db}^e)_J, \quad (1.5)$$

$$R_w = R - \left(\nabla_a J^a + \frac{1}{2} J^2 \right). \quad (1.6)$$

With these, we derived the Weyl-Einstein tensor as

$$(G_{ab})_w = (R_{ab})_w - \frac{1}{2} (g_{ab} R_w - 2J_{ab}), \quad (1.7)$$

where

$$J_{ab} = (\Gamma_{ab}^d)_J (\Gamma_{dc}^c)_J - (\Gamma_{ae}^d)_J (\Gamma_{db}^e)_J.$$

The Weyl-Einstein tensor was shown to be conserved.

1.2 Massive source

The Weyl-Einstein field equations are now expressed by

$$(G_{ab})_w = \kappa T_{ab}. \quad (1.8)$$

Using the Riemannian covariant derivatives, the Weyl-Einstein tensor conservation law reads

$$\nabla_a (G_b^a)_w = 0. \quad (1.9)$$

The right hand side of (1.8) should also verify

$$\nabla_a T_b^a = 0$$

or

$$\partial_a T_b^a = 0 \quad (1.10)$$

with the tensor density $T_b^a = \sqrt{-g} T_b^a$.

However, inspection shows that

$$\partial_a T_b^a = \frac{1}{2} T^{ca} \partial_b g_{ca} \quad (1.11)$$

or equivalently

$$\partial_a T_b^a = \frac{1}{2} T^{ca} (\partial_b g_{ca} - J_b g_{ca}).$$

Thus the condition (1.10) is never satisfied in a general coordinates system. This circumstance results from the fact that the *global* conservation should hold for the 4-momentum of *both* the matter and its gravitational field.

To keep the equation (1.10) consistent with (1.9), we must look for a solution of the form

$$\partial_a (\mathbf{T}_b^a + \mathbf{t}_b^a) = 0, \quad (1.12)$$

where \mathbf{t}^{ab} is the given tensor's density.

Let us compute

$$\begin{aligned} d\mathbf{g}^{ab} &= d(\sqrt{-g} g^{ab}) = \sqrt{-g} \left(dg^{ab} + \frac{1}{2} g^{ab} g^{cd} \right) dg_{cd} = \\ &= \sqrt{-g} \left(-g^{ae} g^{bd} + \frac{1}{2} g^{ab} g^{cd} \right) dg_{cd}, \end{aligned}$$

therefore

$$(\mathbf{R}_{ab})_w d\mathbf{g}^{ab} = \sqrt{-g} \left(-R_w^{ce} + \frac{1}{2} g^{ce} R_w \right) dg_{ce} = -\kappa \mathbf{T}^{ce} dg_{ce}.$$

Taking into account the Lagrangian form of the Weyl-Einstein Ricci tensor

$$(\mathbf{R}_{ab})_w = \partial^e \left[\frac{\mathbf{L}_w}{\partial (\partial_e \mathbf{g}^{ab})} \right] - \frac{\partial \mathbf{L}_w}{\partial \mathbf{g}^{ab}},$$

where the effective Weyl-Einstein Lagrangian is now

$$\mathbf{L}_w = g^{ab} \sqrt{-g} (W_{ab}^e W_{de}^d - W_{ae}^d W_{bd}^e) \quad (1.13)$$

one obtains

$$\begin{aligned} -\kappa \mathbf{T}^{ab} dg_{ab} &= \left(\partial_c \frac{\partial \mathbf{L}_w}{\partial_c \mathbf{g}^{ab}} - \frac{\partial \mathbf{L}_w}{\partial \mathbf{g}^{ab}} \right) d\mathbf{g}^{ab} = \\ &= \partial_c \left(d\mathbf{g}^{ab} \frac{\partial \mathbf{L}_w}{\partial_c \mathbf{g}^{ab}} \right) - d\mathbf{L}_w, \\ -\kappa \mathbf{T}^{ab} \partial_d g_{ab} &= \partial_c \left(\partial_d \mathbf{g}^{ab} \frac{\partial \mathbf{L}_w}{\partial (\partial_c \mathbf{g}^{ab})} - \delta_d^c \mathbf{L}_w \right) = 2\kappa \partial_c \mathbf{t}_d^c. \end{aligned}$$

From the last equation we find

$$\partial_c \mathbf{T}_a^c = \frac{1}{2} \mathbf{T}^{dc} \partial_a g_{dc} = -\partial_c \mathbf{t}_a^c.$$

In order to satisfy the conservation law (1.12), one clearly sees that the gravitational field energy-momentum tensor density should be described by the Weyl-Einstein extension of the *Einstein-Dirac pseudo-tensor* [3, p.61]

$$\mathbf{t}_d^c = \frac{1}{2} \kappa \left[\partial_d \mathbf{g}^{ab} \frac{\partial \mathbf{L}_w}{\partial (\partial_c \mathbf{g}^{ab})} - \delta_d^c \mathbf{L}_w \right] \quad (1.14)$$

the quantities \mathbf{t}^{ab} are called ‘‘pseudo-tensor density’’ since they can be transformed away by a suitable choice of the reference frame and they are not irreducible [4]. This is why the classical theory stipulates that a (free) gravitational energy cannot be *localizable*.

In the classical General Relativity, the non symmetric tensor $\mathbf{t}_{ab}/\sqrt{-g}$ is symmetrized through the Belinfante procedure [5] to suit the standard symmetric Einstein tensor. The relevant symmetric tensor is denoted t_{ab} .

Unfortunately, the Einstein field equations whatever their transcriptions, are yet unbalanced since they do not exhibit a full real tensor as a source. To remedy this problem, we showed that a slightly variable cosmological term Λ -term induces a stress-energy tensor of vacuum, which restores a true gravitational tensor on the right-hand side of equation (1.6) as it should be [6, 7].

This real tensor is given by

$$(t_{ab})_{\text{vac}} = -\frac{1}{2\kappa} \Lambda g_{ab}. \quad (1.15)$$

The Λ -term was found to be [8]

$$\Lambda = \nabla_a K^a = \theta^2, \quad (1.16)$$

where K^a is a 4-vector and

$$\theta = X_{;a}^a \quad (1.17)$$

is the space-time volume scalar expansion characterizing the vacuum stress-energy tensor $(t_{ab})_{\text{vac}}$, and X^a is a congruence of non intersecting unit time lines $X^a X_a = 1$

$$X_{;a}^a = h^{ab} \theta_{ab}, \quad (1.18)$$

while θ_{ab} stands for the expansion tensor and $h_{ab} = g_{ab} - X_a X_b$ is the projection tensor.

Due to the form of (1.16), the Lagrangian (1.13) differs only from a divergence and varying its action generates the same field equations. The real tensor $(t_{ab})_{\text{vac}}$ which corresponds to the vacuum stress-energy tensor can be added to t_{ab} without affecting the Weyl-Einstein Lagrangian.

With this definition the Weyl-Einstein field equations can be finally written as

$$\begin{aligned} (G_{ab})_w &= (\mathbf{R}_{ab})_w - \frac{1}{2} (g_{ab} R_w - 2J_{ab}) = \\ &= \kappa \left[\rho c^2 u_a u_b + \frac{t_{ab}}{\sqrt{-g}} + (t_{ab})_{\text{vac}} \right]. \end{aligned} \quad (1.19)$$

Here the symmetrization procedure is evaded, because the quantity $\mathbf{t}_{ab}/\sqrt{-g}$ is genuinely antisymmetric.

When gravity is weak and velocities are low compared to c , we have the Newtonian approximation where the massive tensor in (1.19) reduces to

$$T_0^0 = \rho c^2.$$

Inspection then shows that

$$(\mathbf{R}_0^0)_w = R_0^0 = \frac{1}{c^2} \frac{\partial^2 \varphi}{\partial \beta^2}$$

with $g_{00} = 1 + \varphi/c^2$, from which we find the well-known Poisson equation

$$\Delta\varphi = 4\pi G\rho,$$

where G is Newton's constant.

1.3 Electromagnetic contribution

The field equations are expressed by

$$(R_{ab})_w - \frac{1}{2}(g_{ab}R_w - 2J_{ab}) = \varkappa \frac{1}{4\pi} \left(-\partial_a A^c F_{bc} + \frac{1}{4} g_{ab} F_{cd} F^{cd} \right), \quad (1.20)$$

$$F_{ab} = \partial_a A_b - \partial_b A_a.$$

The source tensor is antisymmetric. Its form is derived from the canonical equation

$$(t_a^b)_{\text{elec}} = \frac{\partial_a A_c \partial L}{\partial(\partial_b A_c)} - \delta_a^b L,$$

where $L = -\frac{1}{16\pi} F_{bc} F^{bc}$.

If the Weyl part is neglected, the term $\frac{1}{4\pi} \partial_c A^c F_{bc}$ is classically added so that when charge is absent, holds the relation

$$\frac{1}{4\pi} \partial_c A_a F_b^c = \frac{1}{4\pi} \partial_c (A_a F_b^c).$$

This eventually yields the well-known symmetric energy-momentum tensor of the electromagnetic field

$$\tau_{ab} = \frac{1}{4\pi} \left(-F_a^c F_{bc} + \frac{1}{4} g_{ab} F^{cd} F_{cd} \right).$$

1.4 Charged matter

The Weyl-Einstein field equations are

$$(R_{ab})_w - \frac{1}{2}(g_{ab}R_w - 2J_{ab}) = \varkappa \left[\rho c^2 u_a u_b + \frac{t_{ab}}{\sqrt{-g}} + (t_{ab})_{\text{vac}} + \frac{1}{4\pi} \left(-\partial_a A^c F_{bc} + \frac{1}{4} g_{ab} F_{cd} F^{cd} \right) \right]. \quad (1.21)$$

We easily check that the right hand side of the equations is conserved.

2 Relation to the Yang-Mills gauge fields

We first write the Minkowskian line element ds and the Weyl-Einstein line element ds_w , then we set

$$dJ = dA \left(1 + \text{Log} \frac{ds_w}{ds} \right) \quad (1.22)$$

with the following one-forms

$$dJ = J_a dx^a,$$

$$dA = A_a dx^a.$$

The above 4-vector A_a is a generic gauge vector of the Yang-Mills field defined in the flat space tangent to the Weyl-Einstein manifold.

2.1 Weak interaction SU(2) symmetry

Let us now examine the rôle of the Weyl-Einstein tensor in the field equations. We write the group element of SU(2) as

$$U = \exp[-i T^\beta k_\beta],$$

where k is the group parameter with the generators

$$T^\beta = \frac{1}{2} \sigma^\beta,$$

(here σ^β are the 2×2 Pauli spin matrices) with the coupling constant \hbar , the gauge field transforms as

$$B_a \rightarrow B_a - T^\beta \partial_a k^\beta(x) + i \hbar k^\beta(x) [T^\beta, B_a(x)].$$

Here, the Weyl-Einstein field equations (1.19) apply with the correspondence

$$J_a \rightarrow B_a.$$

2.2 The electromagnetic symmetry U(1)

This symmetry group is the abelian group U(1) with a single commuting generator $T_1 = Q$ satisfying

$$[T_1, T_1] = 0,$$

where Q is the quantity of the charges of the field $\Phi(x)$ proportional to the fundamental charge unit e . Under the phase rotation

$$\Phi(x) \rightarrow \Phi(x) \exp[-ikQ(x)]$$

the vector field $A_a(x)$ transforms as

$$A_a(x) \rightarrow A_a(x) + \partial_a k.$$

Within the Weyl-Einstein field equations (1.20), we have the correspondence

$$J_a \rightarrow A_a.$$

2.3 Combined symmetry U(1) \times SU(2)

Here the Weyl-Einstein field equations for charged matter (1.21) are used, where we simply have

$$J_a \rightarrow A_a + B_a,$$

where A_a is the electromagnetic vector field gauge field and B_a is the gauge vector field of the weak interaction.

Other combinations implying for example strong interaction SU(3) could be derived in the same way.

3 Conclusion

What have we achieved? Our theory relies on the specific form of the connexion coefficients which displays a 4-vector. This connexion form was first considered by H. Weyl by relating this vector to the “segment curvature” next to the Riemann curvature and zero torsion, with the aim to unify electricity and gravitation in a non trivial way [9]. Although we kept the name Weyl-Einstein connexion, the extra segment curvature is not introduced here. On the contrary, we have exploited the Weyl-Einstein 4-vector to connect the Yang-Mills gauge fields through an extended field equations set where both the left and right sides are still conserved. In doing so, such field equations can now display the type of interactions that is considered thus informing us between either electromagnetic field or weak and strong interactions of matter which was basically impossible with the standard field equations.

Submitted on October 8, 2024

References

1. Marquet P. How to couple the space-time curvature with the Yang-Mills Theory. *Progress in Physics*, 2022, v.18, no.2, 97–102.
2. Lichnerowicz A. Les espaces variationnels généralisés. *Annales scientifiques de l'Ecole Normale Supérieure, série 3*, 1945, t.62, 339–384.
3. Dirac P.A.M. General Theory of Relativity. Princeton University Press, 2nd edition, 1975.
4. Landau L. et Lifchitz E. Théorie des champs. Éditions MIR, Moscou, 1964.
5. Rosenfeld L. Sur le tenseur d'impulsion-énergie. *Acad. Roy. de Belgique, Mémoires de Classes de Sciences*, t.18, 1940.
6. Marquet P. The gravitational field: a new approach. *Progress in Physics*, 2013, v.9, no.3, 62–66.
7. Marquet P. Vacuum background field in General Relativity. *Progress in Physics*, 2016, v.12, no.4, 314–316.
8. Marquet P. Some insights on the nature of the vacuum background field in General Relativity. *Progress in Physics*, 2016, v.12, no.4, 366–367.
9. Weyl H. Gravitation und Elektrizität. *Sitzungsberichte der Königlich Preussischen Akademie der Wissenschaften zu Berlin*, 1918, 465–480.

On a Plausible Solution to the Hubble Tension via the Hypothesis of Cosmologically Varying Fundamental Natural Constants

G. G. Nyambuya

National University of Science and Technology, Faculty of Applied Sciences — Department of Applied Physics,
Fundamental Theoretical and Astrophysics Group, P. O. Box 939, Ascot, Bulawayo, Republic of Zimbabwe.
E-mail: physicist.ggn@gmail.com

We herein present what we propose could be a plausible solution to the current, interesting and topical problem in cosmology — the *Hubble Tension*. This problem of the Hubble tension seems to have thrown all of cosmology into a crisis. By employing the seemingly temerarious hypothesis of varying *Fundamental Natural Constants* (FNCs), namely Planck's constant, \hbar , we demonstrate that for the case where the cosmological Interstellar Medium (ISM) is a perfect *vacuo* with a refractive index of unity, the supernovae derived \mathcal{H}_0 -value can be brought down from its current lofty height of: $\mathcal{H}_0^{\text{SNe}} = 73.30 \pm 1.03 \text{ km s}^{-1} \text{ Mpc}^{-1}$, down to a more humble and modest value of: $68.70 \pm 0.30 \text{ km s}^{-1} \text{ Mpc}^{-1}$, and within the margins of error, this new value is in agreement with the Tip of the Red Giant Branch (TRGB) derived \mathcal{H}_0 -value, namely: $\mathcal{H}_0^{\text{TRGB}} = 69.80 \pm 2.20 \text{ km s}^{-1} \text{ Mpc}^{-1}$, and this is much closer to the CMB-derived \mathcal{H}_0 -value: $\mathcal{H}_0^{\text{CMB}} = 67.40 \pm 0.50 \text{ km s}^{-1} \text{ Mpc}^{-1}$. At a 2.2σ -level of statistical significance in discrepancy, this new \mathcal{H}_0 -value reduces the tension by 88%, and this surely is a most welcome development. On the other hand, if the ISM is assumed to be homogeneous and isotropic with a slightly varying, if not near constant refractive index, n_r^{ISM} , for most photon wavelengths, then, a refractive index value of: $n_r^{\text{ISM}} = 1.010 \pm 0.006$, does bring the new SNe-derived \mathcal{H}_0 -value into complete and total concordance with the CMB-derived \mathcal{H}_0 -value, thus resolving the tension altogether. The final concordance \mathcal{H}_0 -value that matches or resolves both measurements after a final correction of the ISM's refractive index is found to be: $\mathcal{H}_0 = 68.00 \pm 0.90 \text{ km s}^{-1} \text{ Mpc}^{-1}$.

Cosmology is peculiar among the sciences for it is both the oldest and the youngest. From the dawn of civilization man has speculated about the nature of the stary heavens and the origin of the world, but only in the present century has physical cosmology split away from general philosophy to become an independent discipline.

Gerald James Whitrow (1912–2000)*

1 Introduction

Without an *iota* of doubt, the Hubble constant, denoted by the symbol \mathcal{H}_0 , is an all important constant in all of modern cosmology and astrophysics [1–4]. It, amongst others, measures the expansion rate of the Universe and is pivotal in the measurement of the age of the Universe [1–4]. Since the theoretical discovery [5] of the expansion of the Universe by the Belgian Catholic priest, theoretical physicist, mathematician, astronomer, and then professor of physics at the Catholic University of Louvain, Georges Henri Joseph Édouard Lemaître (1894–1966), and the subsequent observational confirmation [6] of this hypothetical expansion by the great American astronomer, Edwin Powell Hubble (1889–1953), a great many efforts have been made to measure this constant with the highest and optimum possible precision available at the time. The importance of this parameter in cosmology cannot be overstated. Hence, accurate knowledge of this constant is not only

a *sine qua non*, but very important as all of cosmology and the cosmological models thereof, depend on it.

Rather worrisomely, initial measurements of this constant in the past century were marred by serious scattering with the resultant values thereof ranging from: $\sim 40 \text{ km s}^{-1} \text{ Mpc}^{-1}$ to $\sim 100 \text{ km s}^{-1} \text{ Mpc}^{-1}$ [4]. However, recent 21st century advances in science and technology have made it all possible to obtain very accurate measurements of this constant using at least three different methods — which methods measure the Hubble constant on two different evolutionary epochs of the Universe, namely the early-and-late Universe. Values of \mathcal{H}_0 from the early Universe are typically referred to as global measurements of \mathcal{H}_0 , while those from the late Universe are commonly referred to as local values of \mathcal{H}_0 . Global \mathcal{H}_0 values measure the Hubble constant in the early Universe (distant past) while the local \mathcal{H}_0 values measure this constant in our local neighbourhood which is the present epoch in the Universe.

According to the widely accepted Standard Λ CDM cosmology model that is used to describe the Universe, \mathcal{H}_0 must be the same for any evolutionary epochs of the Universe — be it in early or late Universe, it does not matter, the value of \mathcal{H}_0 ought to be the same. To the chagrin and against the desideratum of the cosmologically searching mind, the local and global values of \mathcal{H}_0 seem to not be in agreement — each yielding at a 4.9σ -level of statistical significance [10], two

*In "Theories of the Universe" (1958)

Table 1: Critical Measurements of the Hubble Constant

Group	Cosmic Epoch	Measurement Type	\mathcal{H}_0 (km s ⁻¹ Mpc ⁻¹)	Reference
Supernova Cosmology (SCG)	Late Universe	Far Local	73.30 ± 1.04	[7]
Carnegie-Chicago Hubble Project (CCHP)	Late Universe	Near Local	69.80 ± 2.20	[8]
Planck Collaboration (PC)	Early Universe	Global	67.40 ± 0.50	[9]

different values that are not only $\sim 10\%$ apart, but also outside of the provinces of their error margins. This interesting and topical problem or discrepancy in the local and global measurements of the Hubble constant has come to be known as the *Hubble tension* and has thrown cosmology into a serious crisis.

From a fundamental theoretical stand point, before suspecting that there possibly may be errors in the measurements and/or systematics thereof, one needs to first trust that — those that have made these measurements have done so meticulously with due and requisite diligence, and with the best precision at hand. Of course, one cannot rule out errors in the measurements and/or systematics — we are human after all, we err. Be that as it may, as our point of departure, we shall assume that these measurements are flawless. With that having been said, we must say that there are three main popular and common techniques used to measure \mathcal{H}_0 :

1. Supernovae Type Ia (SNe Ia) method;
2. Tip-of-the-Red-Giant-Branch (TRGB) method;
3. Cosmic Microwave Background (CMB) radiation method.

We shall discuss in detail these techniques in §4. Our interest in taking a deeper look into these methods is to unravel their dependence on FNCs because it is in these FNCs that we believe the source of our error in the determination of the Hubble constant may lay.

For further clarity, as already aforementioned, we shall elaborate that the methods to measure the Hubble constant fall into two classes: a) *Local* measurements, and, b) *Global* measurements, i.e.:

1. Local \mathcal{H}_0 measurements: measure \mathcal{H}_0 in the present (local) evolutionary epoch of the Universe. The present epoch is the late Universe, hence, these type of measurements are also referred to as late Universe measurements.
2. Global \mathcal{H}_0 measurements: are all-sky measurements of \mathcal{H}_0 , measuring the Hubble constant across the entire sky, hence, they being referred to as global \mathcal{H}_0 measurements. These measurements typically measure, \mathcal{H}_0 , in the very early Universe hence they also being referred to as early Universe measurements.

The TRGB and SNe Ia measurements are classified as local \mathcal{H}_0 measurements as they measure \mathcal{H}_0 in the present (and not past) evolutionary epoch of the Universe. The TRGB method measures \mathcal{H}_0 -values in galaxy systems much closer

to us (yielding: $\mathcal{H}_0^{\text{TRGB}} = 69.80 \pm 2.20$ km s⁻¹ Mpc⁻¹ [8]), while the SNe Ia measurement \mathcal{H}_0 -values in galaxy systems relatively far in the local Universe (yielding: $\mathcal{H}_0^{\text{SNe}} = 73.30 \pm 1.04$ km s⁻¹ Mpc⁻¹ [7]). We shall say that the TRGB method measures \mathcal{H}_0 -values in the near-local Universe, while, the SNe Ia methods measures \mathcal{H}_0 -values in the far-local Universe. The near and far-local \mathcal{H}_0 -values do not agree (69.80 ± 2.20 km s⁻¹ Mpc⁻¹ [8] and 73.30 ± 1.04 km s⁻¹ Mpc⁻¹ [7], respectively), thus, giving raise to yet another tension within an already existing tension.

On the other hand, the CMB \mathcal{H}_0 measurements are classified as a global \mathcal{H}_0 measurements as these measurements are all-sky measurements of \mathcal{H}_0 measuring the Hubble constant across the entire sky, hence, they being referred to as a global \mathcal{H}_0 measurements. The CMB method is a state-of-the-art precision method of global \mathcal{H}_0 measurements by Aghanim *et al.* [9] and this has yielded: $\mathcal{H}_0^{\text{CMB}} = 67.40 \pm 0.50$ km s⁻¹ Mpc⁻¹. A summary of these key measurements is presented in self-explanatory Table 1.

Since Lemaître [5] and Hubble [6]’s initial estimates, there has been numerous measurements of the Hubble constant. For our purposes here, the above three measurements (presented in [7–9], which are summarised in a clear and succinct manner in Table 1) shall constitute our focal point in all the \mathcal{H}_0 measurements as these three important measurements sufficiently capture the morass substance contained in our current musings and at the same time — they drive our point home regarding this important tropical issue of the Hubble tension.

Astronomers, astrophysicists and cosmologists are hard at work to figure out why the discrepancy in the values of \mathcal{H}_0 from the two different methods as a number have wondered if this discrepancy is heralding some hitherto yet unknown physics [3, 11, 12] or there might be some serious, albeit subtle, error in our methods and analysis? We herein present a suggestion to this problem and this suggestion is to the effect that varying Fundamental Natural Constants (FNCs) may be the cause of this tension. As will be demonstrated, a simple hypothesis regarding the nature of the said variation on the FNCs seem to deliver a bold solution to this problem.

In closing this introductory section, we shall give a synopsis of the reminder of this article, i.e.: the reminder of this article is arranged as follows: for no other than smoothness,

completeness and self-containment purpose, we present in the next §2, a pedestrian derivation of the distance modulus formula used in astronomy, astrophysics and cosmology. Thereafter in §3, we discuss distances in cosmology with emphasis on how the luminosity and Light travel distances are used in the distance modulus formula in order to derive the Hubble constant and having done this, in §4, we discuss the three common and popular methods to measure the Hubble constant. In §5, we present what we believe is the source of the problem in our endeavour to compute the Hubble constant leading to the current tension in the measurement of this constant using the two major methods. In §6, we justify the idea of variable fundamental natural constants. It is this idea that our proposed solution to the Hubble tension is to be found, hence there is need to justify the idea. In §7, we present our proposed solution and application of this solution to real data in §8. Lastly, in §10 and §11, we present a general discussion and the conclusion drawn thereof.

2 Distance modulus

In this section, we are going to go through some necessary trivialities and this is for no other purpose other than for self-containment and smooth flow of the paper thereof. As is well known, in astronomy, astrophysics and cosmology, the distance modulus, denoted by the symbol μ , is a way of expressing distances to stellar objects. It is a measure of the difference between the apparent (m) and absolute magnitude (M), of an astronomical object, i.e.: $\mu = m - M$. For a star (or any stellar body of radius, R , mean temperature, T , and, with surface emissivity, ϵ) whose luminosity: $L = 4\pi R^2 \epsilon \sigma_0 T^4$ (where: σ_0 is the Stefan-Boltzmann constant), with a total flux of: $F(d_L)$, and with this flux reaching at the arbitrary distance, d_L , away from the star — the flux received at the said arbitrary distance d_L , obeys the following inverse square law:

$$F(d_L) = \frac{L}{4\pi d_L^2}. \quad (1)$$

The absolute magnitude is by definition defined as follows:

$$M = -2.5 \log_{10} F(d_L), \quad (2)$$

while the apparent magnitude is by definition defined:

$$m = -2.5 \log_{10} F(10 \text{ pc}), \quad (3)$$

where: $F(10 \text{ pc}) = L/4\pi(10 \text{ pc})^2$ is the flux of the given stellar object at a distance: $d_L = 10 \text{ pc}$, away. Hence:

$$\begin{aligned} \mu_L &= m - M, \\ &= -2.5 \log_{10} \left(\frac{F(d_L)}{F(10 \text{ pc})} \right), \\ &= -2.5 \log_{10} \left(\frac{10 \text{ pc}}{d_L} \right)^2. \end{aligned} \quad (4)$$

This further simplifies to:

$$\mu_L = 5 \log_{10} \left(\frac{d_L}{10 \text{ pc}} \right), \quad (5)$$

In cosmology, one often works with distances in mega-parsec (Mpc), so, it is convenient to write (5) with, d_L , in Mpc and not in units of 10pc. Written in the units of Mpc, (5) becomes:

$$\mu_L = 5 \log_{10} \left(\frac{d_L}{\text{Mpc}} \right) + 25. \quad (6)$$

Now, (6) applies in the case where the flux does not experience attenuation as a result of interstellar material along its path — i.e., in the case where there is no extinction of the flux.

In the case where there is extinction, the flux undergoes attenuation. Let, τ , be the optical depth of the Interstellar Medium (ISM) along the intervening spaces along the path of the photons reaching our telescopes and let, F_0 , be the flux at the surface of the star (or stellar body). Then, the flux at distance d_L away is such that:

$$F(d_L) = F_0 \left(\frac{4\pi R^2}{4\pi d_L^2} \right) e^{-\tau}. \quad (7)$$

For the absolute magnitude, we need the flux, $F(10 \text{ pc})$, at a distance of 10 parsecs as this is to be evaluated without extinction, i.e.:

$$F(10 \text{ pc}) = F_0 \left(\frac{4\pi R^2}{4\pi (10 \text{ pc})^2} \right). \quad (8)$$

Therefore, from (7) and (8), it follows that:

$$\frac{F(d_L)}{F(10 \text{ pc})} = \frac{(10 \text{ pc})^2}{d_L^2} e^{-\tau}, \quad (9)$$

hence:

$$\mu_{L'} = 5 \log_{10} \left(\frac{d_{L'}}{10 \text{ pc}} \right) + A_\tau, \quad (10)$$

where:

$$A_\tau = -2.5 \log_{10}(e^{-\tau}) = 5 \log_{10}(e^{0.5\tau}), \quad (11)$$

is the extinction correction term to the distance modulus, and: $\mu_{L'}$, is the extinction-corrected distance modulus. With, d_L , expressed in Mpc, the above can be written as follows:

$$\mu_{L'} = 5 \log_{10} \left(\frac{d_{L'}}{\text{Mpc}} \right) + 25, \quad (12)$$

where:

$$d_{L'} = e^{0.5\tau} d_L, \quad (13)$$

is the extinction-corrected luminosity distance. Eq.(12) is what is used in cosmology in the study of supernovae to estimate the distance to the Cepheid variables that are resident in the Host galaxy of supernovae.

In closing this section, allow us to say that we are very much aware that we have presented an elementary and textbook derivation of the distance modulus formula. We want to rest assure our reader that this has been done for a very good reason and the reason is that there is an esoteric subtlety associated with this derivation that we want to *exegetically* unmask (point out) and “correct”, all this in the hope that this may be one of the problems from which the discrepancy in the measurement of the Hubble constant might lie. Therefore, we kindly ask our reader for their due indulgence as we unpack this esoteric subtlety.

3 Distances in cosmology

If we get our distances wrong in astronomy, astrophysics and cosmology, so is our interpretation of the results — they will be wrong as well. So, the importance of the measures that we use to obtain these distances cannot be overstated. Different distance measures are used in astronomy, astrophysics and physical cosmology. These distance measures give a natural notion of the distance between two objects or events in the Universe. They are often used to tie some observable quantity to another quantity that is not directly observable, but is more convenient for calculations such as the comoving coordinates of quasars, galaxy, *etc.* The observable quantities in question are quantities such as the luminosity of a distant star (or quasar), the redshift of a distant galaxy, or the angular size of the acoustic peaks in the CMB power spectrum. For low redshift objects, these distance measures reduce to the common notion of Euclidean distance. Of particular interest in our present expedition are the luminosity and Light travel distances.

3.1 Light travel distance

Herein denoted by the symbol d_{LT} , the *Light Travel Distance*, is a cosmological concept that refers to the distance Light travels from one point (A) to the other (B), in particular, the distance Light could travel say from one galaxy to our own telescope at the time of observation. The Light travel distance can be important for understanding phenomenon such as the age of the Universe, its expansion rate and the spatial size of the observable Universe for example. Wholly within the framework of Einstein [13–15]’s General Theory of Relativity (GTR), the Light travel distance is calculated with respect to proper time $d\tau$, i.e.:

$$d_{LT} = \int_{\tau_e}^{\tau_r} c d\tau = \int_{\tau_e}^{\tau_r} \left(\frac{c_0}{n_r} \right) d\tau, \quad (14)$$

where in this case: n_r , is the refractive index of the Interstellar Medium (ISM). In most considerations in the definition and calculation of the Light travel distance, the refractive index does not appear in the formulae, the meaning of which is that, the ISM is, in the said cases, being assumed to be a perfect *vacuo* with a refractive index of unity. In the present

expedition, we shall be meticulous and exercise equanimity by not assuming a perfect *vacuo* for the ISM. This is going to help us in our effort to explain the remaining discrepancy in the resulting Hubble constant after the correction of the FNCs has been made.

From the homogeneous and isotropic metric tensor of Friedmann (1924) [16], Lemaître (1933) [17], Robertson (1935, 1933a,b,c) [18–20] and Walker (1937) [21] (hereafter, FLRW-metric), which is what is used in the Λ CDM cosmology model — by setting the proper time in this metric to equal zero for the propagation of Light in an FLRW-Universe — one can show from it that, the Light travel distance, d_{LT} , defined in (14), is such that:

$$d_{LT} = \frac{d_H}{n_r} \int_0^z \frac{dz}{(1+z_\lambda) n_r \sqrt{\Omega}} = d_H f(z_\lambda), \quad (15)$$

where off cause:

$$f(z_\lambda) = \int_0^{z_\lambda} \frac{dz_\lambda}{(1+z_\lambda) \sqrt{\Omega}}, \quad (16)$$

and: $d_H = c_0/\mathcal{H}_0$, is what is called the Hubble distance with:

$$\Omega = \frac{1}{\mathcal{H}_0^2} \dot{a}^2 = \Omega_m + \Omega_\Lambda + \Omega_k. \quad (17)$$

The Ω ’s appearing in (17) are the usual Ω -parameters used in cosmology, with Ω , being the total Ω -parameter; while, Ω_m , is the Ω -matter parameter; Ω_Λ , is the Ω -vacuum parameter for the Λ -cosmological field; and, Ω_k is the Ω -curvature parameter.

Now as is the usual case, using the Light travel distance, d_{LT} , one can calculate from it the corresponding distance modulus, μ_{LT} , of the given supernovae, it is given by:

$$\mu_{LT} = 5 \log_{10} \left(\frac{d_{LT}}{\text{Mpc}} \right) + 25. \quad (18)$$

Inserting (15) into (18), we obtain:

$$\mu_{LT} = 5 \log_{10} [f(z_\lambda)] + K, \quad (19)$$

where:

$$K = 25 + 5 \log_{10} \left(\frac{c_0}{\text{Mpc}} \right) - 5 \log_{10} (n_r \mathcal{H}_0). \quad (20)$$

It is from the value of, K , as given in (20), that one is able to calculate the Hubble constant.

3.2 Luminosity distance

We have already met the concept of luminosity distance in our derivation of the distance modulus in §2, which distance we have denoted by the symbol, d_L . There are two concepts relating to luminosity distance that we shall call the observationally derived luminosity distance and the redshift derived luminosity distance. The former is what we have met. We shall discuss these two concepts below:

1. *Observationally Derived Luminosity Distance*: The observationally derived luminosity, is the luminosity distance that is defined as the distance at which an object would need to be located in order for its observed (apparent) luminosity to match its intrinsic (absolute) luminosity. This is the distance, d_L , as defined in (1). That is to say, the luminosity distance, d_L , is related to the observed (apparent) flux (F) from the given object and its intrinsic (absolute) luminosity (L) through (1). At the instance of (8) leading to (13), the luminosity distance has been corrected for extinction and the extinction-corrected luminosity distance has been denoted by the symbol, d_{L^r} . We will argue in §5 that our understanding of the luminosity may need to be updated if FNCs are variable over cosmic epochs. It is this dearth and paucity of knowledge in our understanding of the luminosity distance that may very well be the cause of the Hubble tension.
2. *Redshift Derived Luminosity Distance*: The redshift derived luminosity distance, $d_L(z_\lambda)$, depends on cosmology under probe and is given by:

$$\frac{d_L(z_\lambda)}{d_H} = \frac{1 + z_\lambda}{a_0} \int_0^{z_\lambda} \frac{dz_\lambda}{\sqrt{\Omega}}, \quad (21)$$

where: $d_H = c_0/\mathcal{H}_0$, is the Hubble distance and Ω is the total Ω -parameter already defined in (17). The cosmology is defined by the total Ω -parameter.

What happens in the supernovae determinations of the Hubble constant is that two distance moduli are constructed and equated and the resulting equation, the Hubble constant is determined. That is to say, from the observationally derived luminosity distance, d_{L^r} , the distance modulus, μ_{L^r} , is constructed as given in (12). From (21), one constructs the corresponding the redshift derived distance modulus:

$$\mu_L(z_\lambda) = 5 \log_{10} \left(\frac{d_L(z_\lambda)}{\text{Mpc}} \right) + 25. \quad (22)$$

Now, from the equation: $\mu_{L^r} = \mu_L(z_\lambda)$, the Hubble constant is determined.

4 Measuring the Hubble constant

The Hubble constant, can be determined through several different methods, each with its own advantages, disadvantages, and limitations. Here are some of the primary methods:

1. The *Distance Ladder Method* makes use of standard candles such as Cepheid variable stars and type Ia supernovae and from these standard candle distance measures and the the corresponding redshift, one can infer the Hubble constant.
2. The *Cosmic Microwave Background* observations from missions like the Planck satellite provide a measurement of the Hubble constant based on the early Universe's conditions.
3. The *Tip-of-the-Red-Giant Method* makes use of stars at the tip of the red giant branch on a IV -color-color diagram. These stars have known fixed intrinsic brightness, hence, they are standard candles. Using this fact other with their redshift, one can infer the Hubble constant.
4. The *Baryon Acoustic Oscillations (BAO) Method* uses the distribution of galaxies to infer distances and hence the expansion rate of the Universe.
5. The *Gravitational Lensing Method* uses the bending of light from distant objects by massive foreground objects as this can be analyzed to estimate the Hubble constant.
6. The *Time Delay Measurements Method* in systems with multiple images of the same astronomical event (like a supernova), the time delays in these systems can be used to calculate the Hubble constant.
7. The *Tying to Local Measurements Method* links the Hubble constant to local measurements in the Solar System, such as the motion of nearby galaxies.
8. The *Galaxy Cluster Dynamics Method* utilizes the motion of galaxies within clusters providing insights into the expansion rate.

In the next two subsections [i.e., §4.1 and §4.2], we shall give an *exegetic exposition* of the first two methods, namely the *Distance Ladder Method* and the *CMB-Method*. The exegesis that we institute is meant to pinpoint the plausible sources of error that may need to be corrected so as to bring about concordance in the \mathcal{H}_0 -values derived from these two state-of-the-art methods.

4.1 SNe Ia distance ladder method

In the SNe Ia method, three things are necessary:

1. A type Ia supernovae and its redshift, z_λ .
2. A host galaxy for the given supernova.
3. A Cepheid variable star or Cepheid variable stars in the supernovae host galaxy.

Cepheids are stars that vary periodically in brightness in a predictable way, and their brightness can be used to determine their distance from Earth. The Cepheid distances are then used to calibrate type Ia supernova luminosities, whose luminosities are then applied to SN Ia out into the far-field to measure \mathcal{H}_0 [22]. With the distance to the supernova known, the distance modulus, μ_{L^r} , corrected for extinction is known. From the calibrated supernova luminosity, the redshift of the supernova is known. With the redshift of the supernova now known, the theoretically derived redshift dependent luminosity distance, $d_L(z_\lambda)$, is then calculated and the value of, \mathcal{H}_0 , is deduced from the equation: $\mu_{L^r} = \mu_{L^r\lambda}$.

4.2 CMB method

BAO experiments essentially measure two quantities, one parallel to the line-of-sight:

$$\beta_{\parallel} = \mathcal{H}(z)r_s(z_\star), \quad (23)$$

and the other perpendicular to the line-of-sight:

$$\beta_{\perp} = \frac{r_s(z_\star)}{D_A(z)} = \theta_s(z_\star), \quad (24)$$

where $\mathcal{H}(z)$ is the Hubble parameter, $r_s(z_*)$ is the comoving sound horizon at recombination (i.e., the standard ruler) and $D_A(z)$ is the comoving angular distance to the observation redshift, z . The latter is computed as:

$$D_A(z) = d_H \int_0^z \frac{dz}{\sqrt{\Omega}}. \quad (25)$$

The standard ruler $r_s(z_*)$ is well constrained by CMB experiments. For the shape of $\mathcal{H}(z)$, one needs to assume some model (such as Λ CDM). Thus, by fitting the theoretical predictions for β_{\parallel} and β_{\perp} to the BAO data, we get indirect constraints on the expansion history of the Universe, $\mathcal{H}(z)$, and thus on the Hubble constant $H_0 = H(z=0)$. In a similar way to other probes of the early Universe (as the CMB), this method gives a value of H_0 that is in tension with the direct measurement in the local Universe (using the cosmic distance ladder). Note that even if BAO observations are made in the late Universe (by looking at the large-scale distribution of galaxies), it is considered as an early probe because it provides a constraint on $r_s(z_*)$, that gives information about the primordial plasma.

To determine, \mathcal{H}_0 , from the CMB data one calculates a *Monte Carlo Markov Chain* (MCMC) which involves evaluation of the likelihood of parameter values and their associated spectra at tens to hundreds of thousands of points in the parameter space, and then one uses this chain to infer the posterior density of, \mathcal{H}_0 , or any other cosmological parameter of interest [12, 23]. Apart from laying down the method leading to the calculation of, \mathcal{H}_0 , what we want at the end of this section is a generic formula of how one proceeds to calculate \mathcal{H}_0 .

The Hubble constant is inferred from CMB temperature anisotropies measurements. That is, measurements of temperature anisotropies in the CMB have revealed a series of (damped) acoustic peaks [12, 23]. These acoustic peaks constitute the esoteric fingerprint of the early Universe's BAO during the era of the pre-recombination plasma — i.e.: sound waves propagating in the baryon-photon plasma prior to photon decoupling, set up by the interplay between gravity and radiation pressure [24–28]. The first acoustic peak is set up by an oscillation mode which had exactly the time to compress once before freezing as photons decoupled shortly after recombination and this peak is precisely determined at: $\theta_s = 1^\circ$.

The first acoustic peak of the CMB carries the indelible imprint of the comoving sound horizon at last scattering $r_s(z_*)$, given by the following:

$$r_s(z_*) = \int_0^{z_*} \frac{c_s(z_\lambda) dz_\lambda}{\mathcal{H}(z_\lambda)} = \frac{c_0}{\mathcal{H}_0} \int_0^{z_*} \frac{c_s(z_\lambda) dz_\lambda}{c_0 \sqrt{\Omega}}, \quad (26)$$

where: $z_* \sim 1100$, denotes the redshift of last scattering, $\mathcal{H}(z_\lambda)$ denotes the expansion rate, and $c_s(z_\lambda)$ is the sound

speed of the photon-baryon fluid. For most of the expansion history prior to last scattering, $c_s(z_\lambda)/c_0 \simeq 1/\sqrt{3}$, before dropping rapidly when matter starts to dominate.

On the other hand, the spatial temperature fluctuations at last scattering are projected to us as anisotropies on the CMB sky. As a consequence, the first acoustic peak actually carries information on the angular scale θ_s (usually referred to as the angular scale of the first peak), given by:

$$\theta_s(z_*) = \frac{r_s(z_*)}{D_A(z_*)}, \quad (27)$$

where: $D_A(z_*)$, is the angular diameter distance to the surface of last scattering, given by:

$$\begin{aligned} D_A(z_*) &= \frac{c_0}{1+z_*} \int_0^{z_*} \frac{dz_\lambda}{\mathcal{H}(z_\lambda)} \\ &= \frac{c_0}{\mathcal{H}_0(1+z_*)} \int_0^{z_*} \frac{dz_\lambda}{\sqrt{\Omega}}, \end{aligned} \quad (28)$$

From this, one can determine the CMB-derived Hubble constant, $\mathcal{H}_0^{\text{CMB}}$, from the following:

$$\mathcal{H}_0^{\text{CMB}} = \frac{\theta_s(z_*)}{r_s(z_*)} \left(\frac{c_0}{1+z_*} \int_0^{z_*} \frac{dz_\lambda}{\sqrt{\Omega}} \right). \quad (29)$$

According (*e.g.*) to Vagnozzi (2020) [12], measurements of anisotropies in the temperature of the CMB, and in particular the position of the first acoustic peak (which appears at a multipole $\ell \simeq \pi/\theta_s$), accurately fix θ_s , therefore, any modification to the standard cosmological model aimed at solving the Hubble tension should not modify θ_s in the process.

In (29), we see that the CMB-derived redshift is not affected by the variation of FNCs. Apart from, \mathcal{H}_0 , the only other FNC in the CMB \mathcal{H}_0 determination is the speed of Light and in accordance with the very strong reservations laid down by [29] and [30], we are not going to vary this. The sound speed, c_0 , in the pre-recombination plasma medium is the only quantity that can depend on FNC *via* the radiation density term, that is to say, the sound speed is such that: $c_s = c_0/\sqrt{3(1+\rho_b/\rho_\gamma)}$, where: ρ_b and ρ_γ , are the densities of baryonic matter and radiation in this plasma, respectively. Because during the plasma era, radiation dominated the Universe, hence, it is generally assumed that: $\rho_b/\rho_\gamma \ll 1$, so that the sound speed in this cosmic plasma medium is approximately equal to $c_0/\sqrt{3}$. Hence, the CMB measurements of, \mathcal{H}_0 , are not affected by the variation of FNCs.

5 Problem

So what is the problem? We are of the strong view that the problem with the discrepancy leading to the Hubble tension may arise from an underestimate of the distance modulus (μ_L) from its determination using the luminosity distance and this underestimate may be a result of the variation of the FNCs:

most probably Planck's constant, \hbar^* . We will show in §7, that if indeed FNCs are to vary with cosmological time, then, this variation will introduce a form of “dark extinction” that is not accounted for in the typical calibrations leading to the Hubble constant and this is so for the case of the cosmic distance ladder method. The reason for this omission is that at present, the idea of a variable FNCs is not taken with the seriousness it so deserves despite observations [31–39] of the FSC strongly pointing to this possibility.

The two distance moduli, μ_{L^*} and μ_{LT} , are determined and then compared (i.e.: $\mu_{L^*} = \mu_{LT}$), with μ_{L^*} being determined from the brightness of the Cepheids resident in the supernovae galaxy, while, μ_{LT} , is determined from the supernova's redshift and in addition to the redshift, it relays on the chosen parameters of the Friedmann model. It is in this comparison: $\mu_{L^*} = \mu_{LT}$, that the Hubble constant, \mathcal{H}_0 , is determined. One thing that one can immediately deduce without fail from this comparison is that $d_{L^*} \neq d_{LT}$. That is to say, from (12) and (18), we have that:

$$\mu_{L^*} = 5 \log_{10} \left(\frac{d_{L^*}}{\text{Mpc}} \right) + 25, \quad (30a)$$

$$\mu_{LT} = 5 \log_{10} \left(\frac{d_{LT}}{\text{Mpc}} \right) + 25, \quad (30b)$$

and from (30), it is not difficult to deduce that the said comparison of μ_{L^*} and μ_{LT} ($\mu_{L^*} = \mu_{LT}$) implies that:

$$d_{L^*} = d_{LT}. \quad (31)$$

So, the luminosity and Light travel distances are generally not equal and are only equal in the case of the ISM having a vanishing optical depth. Now, before we deliver our suggested solution, we shall first motivate for our working model on the variation of FNCs.

6 Variable fundamental natural constants

If we blindly were to go by their verbatim name, then *Fundamental Natural Constants* (FNCs) ought to be what is purported or suggested by their very name “Fundamental”, “Natural” and “Constant”.

1. FUNDAMENTAL — meaning intrinsic, inherent and foundational in all reality where they are involved;
2. NATURAL — meaning that these FNCs must arise naturally in our theories and are not imposed by our finite and limited *intellect, whim, will or desideratum*;
3. CONSTANT — meaning they are sacrosanct and unchanging throughout the entire evolution of the Universe.

Pristinely and succinctly stated, the term *Fundamental Natural Constant* expresses a somewhat “divine” notion of the

*Typically, \hbar is referred to as the reduced or normalized Planck constant. Fully cognisant of this fact, we shall however refer to this constant \hbar , simply as Planck's constant.

sacrosanctity of these seemingly immutable and divinely imposed physical quantities.

How far true is this assumption of sacrosanctity, immutability and constancy of these FNCs? For all we know, physics is an experimental human endeavour where answers to the questions that we pause regarding the inner and outer workings of Nature are to be sought by way of physical enquiry *via* ponderable measurements. That is to say, only measurements can decisively and conclusively answer this deep and very interesting question about the possible variation the FNCs. Fortunately, this question of the possible variation of FNCs is now a question capable of being answered from both experimental and observational science — thanks to the capabilities of modern state-of-the-art precision technology that has made this a reality.

The path to the road of inquiry into the possible variation of the FNCs began sometime in 1935 and 1937 with the great British theoretical physicists Edward Arthur Milne (1896-1950) and Paul Adrian Maurice Dirac (1902-1984). That is to say, Milne [40, 41] and Dirac [42] were perhaps the first (in the recorded scientific literature) to question this *status quo* by suggesting that this long held assumption that Newton's supposed universal constant of gravitation, G , was a sacrosanct and sacred constant of Nature that has remained constant since the Universe came into being.

To that end, if current observations [31–39] indicating the cosmological variation of the *Fine Structure Constant* (FSC) stand up to the most ruthless scientific scrutiny, then Milne [40, 41] and Dirac [42] may have been right after all, albeit not on the possible variation of Newton's constant G , but the cosmological variation of the FSC which involves four FNCs, namely: the electronic charge, $e = 1.602176634 \times 10^{-19}$ C; the permittivity of free space, $\epsilon_0 = 8.8541878128(13) \times 10^{12}$ F m⁻¹; Planck's constant, $h = 6.62607015 \times 10^{-34}$ J s; and, the speed of Light in *vacuo*, $c_0 = 299792458 \times 10^8$ m s⁻¹ (2022, CODATA Values).

The dimensionless FSC, denoted by the symbol α_0 , is such that:

$$\alpha_0 = \frac{e^2}{4\pi\epsilon_0\hbar c_0} = \frac{1}{137.035999074(44)}, \quad (32)$$

hence:

$$\frac{\Delta\alpha}{\alpha_0} = 2 \left(\frac{\Delta e}{e} \right) - \frac{\Delta\epsilon_0}{\epsilon_0} - \frac{\Delta\hbar}{\hbar} - \frac{\Delta c}{c_0}, \quad (33)$$

that is to say, a cosmological variation in α_0 , directly points to a variation in any one, or any possible combination, of the four FNCs: e , ϵ_0 , \hbar , and, c_0 .

At present, there exists no properly constituted and fairly accepted theory that explains why any of the supposed FNCs must vary. Most theories that do make the endeavour to explain the possibility of the variation of the FSC are speculative theories based on exotic and exogenous ideas [43–48] and some of these theories are yet to make contact with experience such as string and string-related theories.

Following Dirac [42] on the variation of the Newtonian gravitational constant that it must vary in proportional to the age of the Universe, which also translates to a variation with respect to the cosmological scale factor $\alpha = \alpha(t)$, we shall assume that the expansion of the Universe is what is responsible for the variation of FNCs. That is to say, if for example, K , is some arbitrary FNC, then, its variation will scale in proportion to the scale factor, α , that is to say: $K \propto \alpha^{\beta_K}$, and as a mathematical equation, this can be written as follows:

$$K = K_H \alpha^{\beta_K} = K_H (1 + z_\lambda)^{-\beta_K}, \quad (34)$$

where: K_H , is the value of this constant at the beginning of time where: $t = \tau_P$, and β_K , is the proportionality index for this constant and α_0 , is the scale factor of the Universe while, α , is the scale factor of the Universe at the time of emission of the photon whose redshift we measure with our telescopes today. We hypothesize that the Universe began when the cosmic clock was reading one Planck second $\tau_P = \sqrt{G\hbar/c_0^5}$. From this, it follows that:

1. If: $\beta_K > 0$, then, the FNC in question increases with time, i.e., its value gets larger as the Universe gets older.
2. If: $\beta_K < 0$, then, the FNC in question decreases with time, i.e., its value gets smaller as the Universe gets older.
3. If: $\beta_K = 0$, then, the FNC in question is indeed a true constant of Nature.

In the present exploration of ideas, we shall assume that one of, or all of, or any possible combination of the four FNCs ($e, \epsilon_0, \hbar, c_0$) making up the FSC will vary with cosmological time, i.e.:

$$e = e_H \alpha^{\beta_e} = e_H (1 + z_\lambda)^{-\beta_e}, \quad (35a)$$

$$\epsilon_0 = \epsilon_{0H} \alpha^{\beta_{\epsilon_0}} = \epsilon_{0H} (1 + z_\lambda)^{-\beta_{\epsilon_0}}, \quad (35b)$$

$$\hbar = \hbar_H \alpha^{\beta_\hbar} = \hbar_H (1 + z_\lambda)^{-\beta_\hbar}, \quad (35c)$$

$$c_0 = c_{0H} \alpha^{\beta_{c_0}} = c_{0H} (1 + z_\lambda)^{-\beta_{c_0}}, \quad (35d)$$

where: $e_H, \epsilon_{0H}, \hbar_H$ and c_{0H} , are the values of the fundamental electronic charge, the permittivity of free space, Planck's constant and the speed of Light in *vacuo* at the beginning of time and: $\beta_e, \beta_{\epsilon_0}, \beta_\hbar$, and, β_{c_0} , are the corresponding indices of the variation of these FNCs, respectively.

We want to be clear to our reader in that we are not proposing that all the four FNCs e, ϵ_0, \hbar , and, c_0 , do vary with cosmic time. What we are saying is that the variation of the FSC allows us to entertain the possibility of the variation of at least one of these four constants. If we were asked our inclination regarding which of the four do we really think are varying, we would say, it is probably Planck's constant. We have our reasons, for we have pondered on this matter in our on-going ideas that we are still working on and are yet to be published; from the said ideas, we strongly holdfast that the speed of Light and as well the electronic charge must be true FNCs, thus leaving \hbar and ϵ_0 as variables.

For our purpose here, it really does not matter as to which FNC is varying, as long just one of them is variable, this would lead to the Stefan-Boltzmann-Planck constant, σ_0 , being a variable as it does depend on the Planck constant and the speed of Light in *vacuo*. That is to say, we know that:

$$\sigma_0 = \frac{2\pi^5 k_B^4}{15\hbar^3 c_0^2} = 5.670374419 \times 10^{-8} \text{ W m}^{-2} \text{ K}^{-4}, \quad (36)$$

where: $k_B = 1.380649 \times 10^{-23} \text{ J K}^{-1}$ (2022, CODATA Value) is Boltzmann's constant. From (36), it follows that if say, \hbar , or, c_0 , did vary with cosmological time, then, σ_0 , will vary cosmologically as well, i.e.:

$$\sigma_0 = \sigma_{0H} \alpha^{\beta_\sigma}, \quad (37)$$

where as before: σ_{0H} , is the Stefan-Boltzmann-Planck constant at the beginning of time and, $\beta_\sigma = 4\beta_{k_B} - 3\beta_\hbar - 2\beta_{c_0}$, is the corresponding index of the cosmological variation of σ_0 . For our purposes here, following the strong advice of Ellis & Uzan [29,30], we shall assume that: $\beta_{c_0} = 0$, and also following our own intuition, we shall assume: $\beta_{k_B} = 0$; hence, we shall have: $\beta_\sigma = -3\beta_\hbar$ and this implies that the luminosity of a star, L , will vary with the scale factor as follows:

$$L \propto \alpha^{-3\beta_\hbar}. \quad (38)$$

Equipped with this seemingly strange and exotic hypothetical idea of the cosmological variation of FNCs, we are going to suggest in the next section a plausible solution to the Hubble tension problem.

7 Proposed solution

From the thesis just laid down in the previous section, it is pristine clear that if FNCs are variable, then there ought to be a discrepancy in the values of early and late measurements of \mathcal{H}_0 , and the reason is simple because these epochs have different values of these FNCs that drive the physics thereof. For example, late-type values are those from the local neighbourhood where the FNCs (k_B, \hbar, c_0) in those galaxies are just about the same as in our own galaxy, whereas in the early-type \mathcal{H}_0 -measurements, the FNCs are significantly different from our own, hence we are comparing two significantly different cosmological epochs. Thus, from the foregoing, it is clear that late-type \mathcal{H}_0 -measurements ought to be the true and correct values of \mathcal{H}_0 , whereas those from the early-type measurements are going to contain a hitherto intrinsic and inherent additional signal (term) which is not accounted for in contemporary measurements, hence the tension.

Now, in order to see how this variation of FNCs comes in, from (38), we now have the FNC variation term, $\alpha^{-3\beta_\hbar}$, in the flux emitted by the source at distance, d , i.e.:

$$F(d_L) = F_0 \left(\frac{4\pi R^2}{4\pi d_L^2} \right) \alpha^{-3\beta_\hbar} e^{-\tau}, \quad (39)$$

where in (39), we see that in comparison to (7), we have in addition to the traditional extinction term, $e^{-\tau}$, there now is supplemented a new extinction term $\alpha^{-3\beta_h}$. Our claim is that it is this term $\alpha^{-3\beta_h}$ that is not accounted for in contemporary cosmology models that do not embrace the variation of the FNCs.

Now, just as before for the absolute magnitude, we need the flux, $F(10\text{pc})$, at a distance of 10 parsecs as this is to be evaluated without any form extinction — either the optical (τ) term or the FNC-variation term (β_h), i.e.:

$$F(10\text{pc}) = F_0 \left(\frac{4\pi R^2}{4\pi(10\text{pc})^2} \right). \quad (40)$$

From (39) and (40), it follows that:

$$\frac{F(d_L)}{F(10\text{pc})} = \frac{(10\text{pc})^2}{d_L^2} \alpha^{-3\beta_h} e^{-\tau}, \quad (41)$$

hence, the *variation* of FNCs corrected-distance modulus, μ'_L , is given by:

$$\mu'_L = \overbrace{5 \log_{10} \left(\frac{d_L}{\text{Mpc}} \right)}^{\mu_{L\tau}} + 25 + A_\tau + \overbrace{5 \log_{10} \left(\alpha^{1.5\beta_h} \right)}^{\mu_D \text{ Dark-Term}}. \quad (42)$$

That is to say, (42) reads: $\mu'_L = \mu_{L\tau} + \mu_D$, where: μ_D , is a new emergent dark-term that arises from the variation of the Planck constant (if the Planck constant is not variable, then it must either be, k_B , and, c_0). Since: $\mu'_L = \mu_{LT}$, it follows that:

$$\begin{aligned} \overbrace{5 \log_{10} \left(\frac{d_L}{\text{Mpc}} \right)}^{\mu_{L\tau}} + 25 + A_\tau + \overbrace{5 \log_{10} \left(\alpha^{1.5\beta_h} \right)}^{\mu_D \text{ Dark-Term}} &= \\ &= 5 \log_{10} \left(\frac{d_{LT}}{\text{Mpc}} \right) + 25. \end{aligned} \quad (43)$$

Taking the dark-term to the right hand-side of (43), we will have:

$$\begin{aligned} 5 \log_{10} \left(\frac{d_L}{\text{Mpc}} \right) + 25 + A_\tau &= \\ &= 5 \log_{10} \left(\frac{d_{LT}}{\text{Mpc}} \right) + 25 - 5 \log_{10} \left(\alpha^{1.5\beta_h} \right). \end{aligned} \quad (44)$$

We can re-write (44), as follows:

$$\begin{aligned} \overbrace{5 \log_{10} \left(\frac{d_{L\tau}}{\text{Mpc}} \right) + 25}^{\text{Flux-Dependent}} &= \\ \underbrace{5 \log_{10} \left(\frac{d_{L\tau}}{\text{Mpc}} \right) + 25}_{\text{Observationally Derived}} &= \\ &= \overbrace{5 \log_{10} \left(\frac{d_{LT}^{\Delta\sigma_0}}{\text{Mpc}} \right) + 25}_{\text{Redshift-Dependent}} = \mu_{LT}^{\delta h}, \\ & \underbrace{\hspace{10em}}_{\text{Theoretically Derived}} \end{aligned} \quad (45)$$

where:

$$d_{LT}^{\Delta\sigma_0} = \alpha^{-1.5\beta_h} d_{LT}, \quad (46)$$

is what we shall call the *FNC variation-corrected Light travel distance*, where in the present case, the FNC for which the Light travel distance has been corrected for, is the Planck constant because it is the particular FNC that we have chosen is variable, while the other two (k_B, c_0) have been held constant.

Now, given that in the Λ CDM cosmology model, the redshift, z_λ , and the scale factor, a , are related as follows: $1+z_\lambda = a_0/a$, i.e.:

$$a = \frac{a_0}{1+z_\lambda}, \quad (47)$$

where: a_0 , is the present day scale factor of the Universe while, a , is the Universe's scale factor at the time of emission of the photon that we receive here on Earth. The present scale factor of the Universe is set: $a_0 = 1$. From this, it follows that if we are to insert this into (42), we will obtain:

$$d_{LT}^{\Delta\sigma_0} = (1+z_\lambda)^{1.5\beta_h} d_{LT}. \quad (48)$$

Now, since: $d_{L\tau} = d_{LT}^{\Delta\sigma_0}$, it follows that:

$$d_{L\tau} = (1+z_\lambda)^{1.5\beta_h} d_{LT} = d_H (1+z_\lambda)^{1.5\beta_h} f(z_\lambda), \quad (49)$$

hence:

$$\mu_{L\tau} = 5 \log_{10} \left[(1+z_\lambda)^{1.5\beta_h} f(z_\lambda) \right] + K, \quad (50)$$

where, K , is no longer as has been defined in (20), but is now defined as follows:

$$K = 25 + 5 \log_{10} \left(\frac{c_0}{\text{Mpc}} \right) - 5 \log_{10} (n_r \mathcal{H}_0). \quad (51)$$

This completes our theoretical exegesis on the plausible origins of the Hubble tension. What is now left is for us to calibrate this result (50) against real data. In order to do this, there is need to first figure out what, $f(z_\lambda)$, is. This function, $f(z_\lambda)$, is dependent on the cosmology model that one adopts. In our present case, we shall adopt a cosmology for which the total Ω -parameter is identically equal to unity, i.e.: $\Omega \equiv 1$. That is to say, Ω , does not happen to be equal to unity in the present epoch of the Universe's evolution, but is eternally so for all times — i.e., from antiquity to eternity. If as declared: $\Omega \equiv 1$, it follows from (16), that:

$$f(z_\lambda) = \ln(1+z_\lambda), \quad (52)$$

hence:

$$\mu_{L\tau} = 5 \log_{10} \left[(1+z_\lambda)^{1.5\beta_h} \ln(1+z_\lambda) \right] + K. \quad (53)$$

Thus, (53) is what we are going to test against observational evidence and we must hasten to say that (53) has not been *priori* designed to fit the observational data that it will excellently fit. It actually came as nothing short of a *non-posteriori* surprise that this model [(53)] agrees very well with empirical evidence.

8 Application of theory

We are now ready to apply our ideas onto some real and tangible data and for this, we are going to use the Supernova Cosmology Project (SCP) Union2.1 dataset spanning the redshift range: $0.015 \leq z_\lambda \leq 1.414$, [49]. This dataset is a compilation of 580 SNe type Ia drawn from 19 datasets [50–67]. We must say that this dataset may very well be the most comprehensive and most accurate SNe data available to date. Further, according to Suzuki *et al.* [49], all SNe were fitted using a single light-curve fitter (SALT2-1) and uniformly analyzed in blind-mode, i.e., without due consideration of a particular cosmology model. With 580 data points in the sufficiently large redshift range: $0.015 \leq z_\lambda \leq 1.414$, we certainly do have a statistically significant dataset to make a meaningful conclusion on the present model (53) of the plausible time variability of FNCs.

What we really want in this section is to test the proposed model presented in (53). We want to find the value of β_h , and, K ; and from the value of K , we can deduce \mathcal{H}_0 . To that end, in Fig. 1, we have plotted the distance modulus, μ_L , vs the redshift, z_λ , of the 580 SNe from the Union2.1 dataset and with this dataset, we perform a non-linear curve fitting on the data and from this non-linear curve fitting exercise, we obtain:

$$\beta_h = +0.77 \pm 0.02, \quad (54a)$$

$$K = 43.20 \pm 0.01 \text{ mag}. \quad (54b)$$

From the value of K , obtained ($43.20 \pm 0.01 \text{ mag}$), we find for the Hubble constant, the value:

$$\mathcal{H}_0 = \frac{68.70 \pm 0.30 \text{ km s}^{-1} \text{ Mpc}^{-1}}{n_r} = \frac{\mathcal{H}_0^{\text{SNe}}}{n_r}. \quad (55)$$

If the ISM is a perfect *vacuo* (which it obviously is not), then:

$$\mathcal{H}_0 = \mathcal{H}_0^{\text{SNe}} = 68.70 \pm 0.30 \text{ km s}^{-1} \text{ Mpc}^{-1}. \quad (56)$$

This value given (56) is the corrected *vacuo* SNe \mathcal{H}_0 -value where the correction made is that hypothesised variation in the Planck constant and the tension in this value when compared with the CMB-value is significant at a 2.2σ -level (97%) of statistical significance.

Of this value, within the provinces of its own error margins, one can safely say that this rather unexpected result is in very good agreement (0.5σ -level of statistical significance in discrepancy) with that of Freedman *et al.* [8]’s TRGB-midpoint value: $\mathcal{H}_0 = 69.80 \pm 2.20 \text{ km s}^{-1} \text{ Mpc}^{-1}$. Further, this value is in agreement with the *Wilkinson Microwave Anisotropy Probe* (WMAP) data for the CMB data — where: $\mathcal{H}_0 = 69.30 \pm 1.60 \text{ km s}^{-1} \text{ Mpc}^{-1}$ [68, 69], and, the *Planck 2013* data — where: $\mathcal{H}_0 = 69.80 \pm 2.20 \text{ km s}^{-1} \text{ Mpc}^{-1}$ [70]. In the \mathcal{H}_0 values of Anderson *et al.* [68], Mehta *et al.* [69] & Ade *et al.* [70], the BAO data has been admitted together with the CMB data, thus allowing Ω_k to be a free parameter [68, 70,

71], and this is unlike in Aghanim *et al.* [9]’s case were the curvature parameter has been tightly constrained to: $\Omega_k \sim 0$. Furthermore, applying the WMAP & CMB constraints to both BAO and SNe data together with the CMB, Blake *et al.* [72] obtained: $\mathcal{H}_0 = 68.70 \pm 1.90 \text{ km s}^{-1} \text{ Mpc}^{-1}$, and Anderson *et al.* [68] obtained: $\mathcal{H}_0 = 69.60 \pm 1.70 \text{ km s}^{-1} \text{ Mpc}^{-1}$. Within the margins of error — all these results are in very good agreement with our result: $\mathcal{H}_0 = 68.70 \pm 0.30 \text{ km s}^{-1} \text{ Mpc}^{-1}$. While this is the case — that our derived value is an improvement in matching the two discontent \mathcal{H}_0 -values, if at all possible, there is need to get a most perfect agreement between these two values and this can be done by considering the fact that the ISM is not a perfect *vacuo*, the meaning of which is that we need not assume a refractive index of unity for the ISM.

9 Concordance \mathcal{H}_0 -value

As stated above, the two discontent \mathcal{H}_0 -values ($\mathcal{H}_0^{\text{SNe}}$ and $\mathcal{H}_0^{\text{CMB}}$) can be brought into concordance by considering the fact that the ISM is not a perfect *vacuo*. That is to say, in the derivation of $\mathcal{H}_0^{\text{SNe}}$, leading to (55), the refractive index was taken into account but later in (56), it (refractive index) was then set to equal unity. We shall drop this assumption that the refractive index is unity. On the same pedestal, we must realize that this same assumption that the refractive index of ISM is unity is employed in the CMB-derivation of $\mathcal{H}_0^{\text{CMB}}$ in (29).

In order for us to take the refractive index into account in (29), what we need to do is to replace c_0 with c_0/n_r . So doing, we obtain:

$$\mathcal{H}_0^{\text{CMB}} = \frac{\theta_s(z_\star)}{r_s(z_\star)} \left(\frac{c_0/n_r}{1+z_\star} \int_0^{z_\star} \frac{dz_\lambda}{\sqrt{\Omega}} \right) = \frac{\mathcal{H}_0}{n_r}. \quad (57)$$

From (57), we obtain: $\mathcal{H}_0 = n_r \mathcal{H}_0^{\text{CMB}}$, and proceeding to substitute this into (55), we obtain:

$$\begin{aligned} n_r &= \sqrt{\frac{\mathcal{H}_0^{\text{SNe}}}{\mathcal{H}_0^{\text{CMB}}}}, \\ &= \sqrt{\frac{68.70 \pm 0.30 \text{ km s}^{-1} \text{ Mpc}^{-1}}{67.40 \pm 0.50 \text{ km s}^{-1} \text{ Mpc}^{-1}}}, \\ \therefore n_r^{\text{ISM}} &= 1.010 \pm 0.006. \end{aligned} \quad (58)$$

In all probity, this value ($n_r^{\text{ISM}} = 1.010 \pm 0.006$) is not at all in bad agreement with the measured refractive index ($n_r^{\text{ISM}} = 1.0001$ to 1.0003 [73–75]) of the ISM. With this ISM refractive index value (1.010 ± 0.006), the concordance \mathcal{H}_0 -value is:

$$\mathcal{H}_0 = 68.00 \pm 0.90 \text{ km s}^{-1} \text{ Mpc}^{-1}. \quad (59)$$

Within the margins of error, this concordance \mathcal{H}_0 -value is in good agreement with Freedman *et al.* [8]’s TRGB \mathcal{H}_0 -value. This good agreement can very well be understood from the fact that the TRGB stars, from which these measurements are inferred, are nearby stars and as a direct result

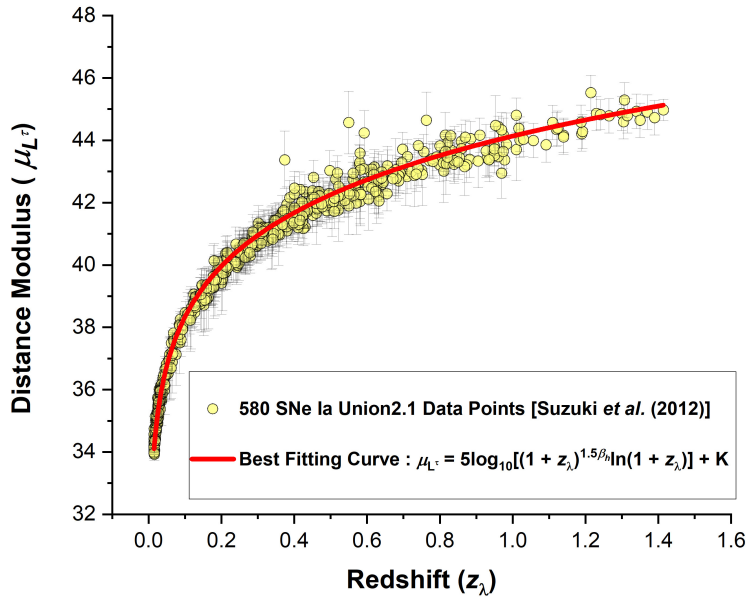


Fig. 1: Graph of Distance Modulus (μ_L) vs Redshift (z_λ) from the Union2.1 data of [49]. The Best Fit Graph (RED) is described by the non-linear curve: $\mu_L = 5 \log_{10} \left[(1 + z_\lambda)^{1.5\beta_h} \ln(1 + z_\lambda) \right] + K$, and, from it we obtain the following best parameter fittings: $\beta_h = 0.77 \pm 0.02$, and, $K = 43.20 \pm 0.01$ mag. The R^2 -value or Coefficient of Determination (COD) of the fit to data is: 99.49%. Assuming an ISM refractive index of unity — i.e.: $n_r^{\text{ISM}} \equiv 1$, the obtaining K -value leads to: $\mathcal{H}_0 = 68.70 \pm 0.30 \text{ km s}^{-1} \text{ Mpc}^{-1}$. In order to bring the CMB and SNe Ia measurements into unity and harmony, an ISM refractive index of: $n_r^{\text{ISM}} = 1.010 \pm 0.006$, is needed and this leads to a concordance \mathcal{H}_0 -value of: $\mathcal{H}_0 = 68.00 \pm 0.90 \text{ km s}^{-1} \text{ Mpc}^{-1}$.

of this fact, the value of Planck's constant for these systems is pretty much the same as the value of Planck's constant here on Earth, hence, the correction of the variation of Planck's constant needed on these measurements may very well be negligible. Be that as it may, there is need to subject TRGB \mathcal{H}_0 -measurements to the present idea of a variable Planck constant.

10 General discussion

We have herein suggested that cosmologically varying FNCs may very well present a viable and perdurable solution to the current crisis in cosmology, namely, the Hubble tension. That is to say, from the same SNe Ia data that usually produces values of the Hubble constant in the range ~ 70 – $76 \text{ km s}^{-1} \text{ Mpc}^{-1}$, we have downgraded this old value to the new concordance \mathcal{H}_0 -value: $68.00 \pm 0.10 \text{ km s}^{-1} \text{ Mpc}^{-1}$, and in the same exercise, the Planck collaboration value of: $67.40 \pm 0.50 \text{ km s}^{-1} \text{ Mpc}^{-1}$ has been upgraded to this concordance \mathcal{H}_0 -value. This has required two major ideas to be evoked, namely, the:

1. Assumption of a cosmologically varying Planck constant, \hbar .
2. Adoption of a non-unity value for the refractive index of the ISM.

The assumption of a cosmologically varying Planck constant reduces the SNe Ia derived value of the Hubble constant from the: 70 – $76 \text{ km s}^{-1} \text{ Mpc}^{-1}$, territory, to exactly: $68.70 \pm$

$0.30 \text{ km s}^{-1} \text{ Mpc}^{-1}$. As pointed out in the penultimate of §4.2, this assumption of a cosmologically variable Planck constant does not apply to the derivation of the CMB-derived Hubble constant because none of the physical parameters that enter in the formulae leading to the $\mathcal{H}_0^{\text{CMB}}$ depend on \hbar . Effectively, what this means is that the tension in $\mathcal{H}_0^{\text{SNe}}$ and $\mathcal{H}_0^{\text{CMB}}$ is reduced and not resolved. The initial tension* (gap in the two values) is: $7.44 \text{ km s}^{-1} \text{ Mpc}^{-1}$, and this is reduced to: $2.10 \text{ km s}^{-1} \text{ Mpc}^{-1}$, and this is an 88% reduction. In order to “resolve” the tension completely, the fact that the ISM is not a perfect *vacuo* is taken into account and this fact affects both measurements — i.e., the CMB and SNe Ia measurement and is seen that a refractive index: $n_r = 1.010 \pm 0.006$, resolves the tension completely, leading to the concordance value: $\mathcal{H}_0 = 68.00 \pm 0.90 \text{ km s}^{-1} \text{ Mpc}^{-1}$.

We candidly must say that our choice in the Planck constant, \hbar , as the likely culprit is informed by what we believe to

*By tension here we mean the difference within the margins of error between the two values: $\mathcal{H}_0^{\text{SNe}} = 68.00 \pm 0.10 \text{ km s}^{-1} \text{ Mpc}^{-1}$, and, $\mathcal{H}_0^{\text{CMB}} = 67.40 \pm 0.50 \text{ km s}^{-1} \text{ Mpc}^{-1}$. That is to say, the difference in: $\text{MIN}(\mathcal{H}_0^{\text{SNe}}) = 71.97 \text{ km s}^{-1} \text{ Mpc}^{-1}$, and, $\text{MAX}(\mathcal{H}_0^{\text{CMB}}) = 67.90 \text{ km s}^{-1} \text{ Mpc}^{-1}$. Clearly, this difference is equal to: $4.07 \text{ km s}^{-1} \text{ Mpc}^{-1}$. Following the same line of thought and reasoning, the tension in the new variable- \hbar corrected: $\mathcal{H}_0^{\text{SNe}} = 68.00 \pm 0.10 \text{ km s}^{-1} \text{ Mpc}^{-1}$, and the old CMB-derived \mathcal{H}_0 -value: $\mathcal{H}_0^{\text{CMB}} = 67.40 \pm 0.50 \text{ km s}^{-1} \text{ Mpc}^{-1}$, is: $0.50 \text{ km s}^{-1} \text{ Mpc}^{-1}$. Clearly, the percentage reduction in tension is: $(1 - 0.50 \text{ km s}^{-1} \text{ Mpc}^{-1} / 4.07 \text{ km s}^{-1} \text{ Mpc}^{-1}) \times 100\% = 88\%$.

be our strong intuition rather than scientific objectivity. Because of a general lack or consensus on the variation of the FSC; without fail, we must say that ideas of variable FNCs are by their nature largely considered to be speculative and may very well be outside of the realm of the general support of contemporary scientific understanding because despite claims of a variable FSC [31–39], at present, there is no direct “incriminating” and invigorating evidence to suggest that the Planck constant could change over cosmic times [76–78].

The most widely considered FNCs to vary over cosmic times is the speed of Light [79–87] but we have our deep-seated reasons for holding back on taking this position*. We are not going to take a position simply because everyone is taking that position because we are aware that no amount of research on the candle would have led mankind to discover the Light bulb. To discover the Light bulb, it was needed to consider ideas alien to our common experience. We have here chosen to take the “road less travelled if not the road not travelled” and vary Planck’s constant.

Because the Planck constant sets the scale for the quantum nature of particles and their interactions with its value determining the granularity of atomic energy levels and the scale at which quantum effects become significant — in a Universe with an increasing Planck constant such as the one that we are suggesting, over cosmic times, the behaviour of the Universe would tend to be more classical rather than quantum mechanical. From a quantum probability calculus view point, this means the initial state of the Universe must have been less probabilistic (i.e., highly unpredictable) and has been evolving into a more probabilistic state (i.e., more predictable). This evolutionary sequence of the Universe resonates well with the *Second Law of Thermodynamics* (SLT) as this implies that the Universe must have started in a state of lowest entropy and has been, and is, evolving into a state of highest entropy.

Further, if the Planck constant \hbar , were to vary as suggested here, it could help solve one of the outstanding problems in the Universe’s expansion to do with the conservation of the photon’s energy and the expansion of the spacetime. The problem is a simple one and is as follows. We know that the energy, E_γ , of a photon is related to the photon’s wavelength, λ , as follows: $E_\gamma = 2\pi\hbar c_0/\lambda$. As a result of cosmic expansion, the wavelength of the photon increases. If \hbar , and, c_0 , are to remain constant as the spacetime expands, it follows that the energy of the photon will diminish without any foreseeable compensation — i.e.: $\Delta E_\gamma \neq 0$, and this obviously violates the *Law of Conservation of Energy*.

*Completely in agreement with Ellis [29] and Ellis & Uzan [30], we are of the view that the speed of Light cannot be varied in a “part or portion of physics” but must be done wholesomely in a consistent manner at a most fundamental level. At the very least, this requires a complete and total rewrite of physics. Varying the speed of Light is unimaginable at the very least. We have held fast in the present exploration the idea of a sacrosanct and invariant speed of Light.

Where does the diminished energy go to? This is something that has bothered the desideratum of the foremost theoretical physicist since this issue was first noticed and to this day, it has not been resolved. In the advent of a time-variable Planck constant and an invariant Light speed c_0 , one can postulate that the photon energy is conserved ($\Delta E_\gamma = 0$) and the compensation in the increase in its wavelength comes in the wake of an equal compensation in the increase of the Planck constant — i.e.:

$$z_\lambda = \frac{\Delta\lambda}{\lambda} = \frac{\Delta\hbar}{\hbar}. \quad (60)$$

What (60) means is that the redshift, z_λ , that we measure must be a measure in the change of the Planck constant.

Regarding the evidence of a varying Planck constant, there have been few direct references in the literature on the subject of a variable Planck constant [88–90]. [88, 89] approaches the subject from a laboratory view point while [90] does this on a purely speculative theoretical standpoint. Searches for a variable Planck constant have been under the guise of a variable FSC [31, 39] which amongst others also implies a variable electronic charge, the speed of Light and/or the permittivity of free space.

Hutchin [89] reports that a gradual and systematic drop has been observed in the decay rates of 8 radionuclides [^{226}Ra , ^{154}Eu , ^{238}Pu , ^3H , ^{54}Mn , ^{60}Co , ^{90}Sr , ^{36}Cl] over a 20 year span by six organizations on three continents (German, American and Russian labs), including beta decay (weak interaction) and alpha decay (strong interaction) and in the search for a common cause, Hutchin [89] hypothesizes that small variations in Planck’s constant might account for the observed synchronized variations in these strong and weak decays.

Hutchin [88] further suggests that this proposed variation of \hbar , may very well be a good candidate for the cause of the Casimir radiation and further proposes that if this Casimir radiation were emitted by stars *via* a changing \hbar , then:

... this could provide an alternative explanation for the Hubble constant, where the distant galaxies are redder simply because \hbar is smaller back in time, making local time move more slowly. In contrast to the expanding model of the Universe, we could now consider whether our Universe might simply be static, where gravity is everywhere balanced on a large scale. Such a conclusion would end the search for dark energy since such a Universe is essentially static while the usual red shift would still be observed.

Unlike Hutchin [88], we do not believe that a variable \hbar necessarily rules out “the expansion of the Universe and points to a *Static Universe*.”

As apparent fissures in the standard model have been emerging, there are also indications that there may be cracks that need attention in the local distance scale as well. For example, the tip of the red giant branch (TRGB) method and the Cepheid distance scale result in differing values of $\mathcal{H}_0 =$

$69.60 \pm 1.90 \text{ km s}^{-1} \text{ Mpc}^{-1}$ [8,91] for the TRGB and $73.30 \pm 1.04, \text{ km s}^{-1} \text{ Mpc}^{-1}$ [7], for the Cepheids. This divergence raises the question of whether the purported tension is being driven by yet-to-be-revealed systematic errors in the local Cepheid data, rather than in the cosmological models.

11 Conclusion

Assuming what has been presented herein is acceptable, we hereby present the following as the logical conclusion that can be drawn thereof:

1. We have shown that the Hubble tension can in principle be alleviated if we assume a cosmologically varying Planck constant and as well as a dispersive non-zero refractive index ISM.
2. Further — we have shown that the current supernovae derived \mathcal{H}_0 -value can be brought down from its current lofty value: $\mathcal{H}_0^{\text{SNe}} = 73.30 \pm 1.03 \text{ km s}^{-1} \text{ Mpc}^{-1}$, down to: $68.70 \pm 0.30 \text{ km s}^{-1} \text{ Mpc}^{-1}$, and this new value is not in dire disagreement with the CMB-derived \mathcal{H}_0 -value: $\mathcal{H}_0^{\text{CMB}} = 67.40 \pm 0.50 \text{ km s}^{-1} \text{ Mpc}^{-1}$. That is to say, at a 2.2σ -level of statistical significance in discrepancy, this new \mathcal{H}_0 -value reduces the tension by 88%.
3. Furthermore — in order to “resolve” the tension completely, the fact that the ISM is not a perfect *vacuo* is taken into account and this fact affects both measurements — i.e., the CMB and SNe Ia measurement and it is seen that a refractive index: $n_r = 1.010 \pm 0.006$, resolves the tension completely, leading to the concordance value: $\mathcal{H}_0 = 68.00 \pm 0.90 \text{ km s}^{-1} \text{ Mpc}^{-1}$.
4. Additionally — apart from providing a viable solution to the Hubble tension problem, a time variable Planck constant has the potential to solve the problem of the conservation of the photon’s energy in an expanding Universe if it is to be assumed that the photon’s redshift, $\Delta\lambda/\lambda$, is compensated by a change in Planck’s constant, $\Delta\hbar/\hbar$. Ultimately, the photon’s redshift under this model emerges as a measure in the change in Planck’s constant.
5. Lastly — as demonstrated herein, the idea of varying FNCs ought to be taken much more seriously than currently done as this has the potential to solve the darkenergy and darkmatter problem because if FNCs are really variable, this variation may bring in “dark” effects that might explain away darkenergy and darkmatter.

Dedication

This reading is dedicated to my friend *Anna Neff*.

Received on September 21, 2024

References

1. Verde L., Schöneberg N. and Gil-Marín H. A tale of many H_0 . arXiv: 2311.13305.
2. Kamionkowski M. and Riess A. G. The Hubble tension and early dark energy. arXiv: 2211.04492.
3. Di Valentino E., Mena O., Pan S., *et al.* In the realm of the Hubble tension — a review of solutions. *Classical and Quantum Gravity*, 2021, v. 38 (15), 153001.
4. Huchra J. P. The Hubble constant. *Science*, 1992, v. 256 (5055), 321–325.
5. Lemaître G. Un univers homogène de masse constante et de rayon croissant rendant compte de la vitesse radiale des nébuleuses extragalactiques (A homogeneous universe of constant mass and increasing radius accounting for the radial velocity of extragalactic nebulae). *Annales de la Société Scientifique de Bruxelles*, 1927, v. A47, 49–59.
6. Hubble E. P. A relation between distance and radial velocity among extra-galactic nebulae. *Proceedings of the National Academy of Sciences*, 1929, v. 15 (3), 168–173.
7. Riess A. G., Yuan W., Macri L. M., *et al.* A comprehensive measurement of the local value of the Hubble constant with $1 \text{ km s}^{-1} \text{ Mpc}^{-1}$ uncertainty from the Hubble Space Telescope and the SH0ES team. *ApJL*, 2022, v. 934 (1), L7.
8. Freedman W. L., Madore B. F., Hatt D., *et al.* The Carnegie-Chicago Hubble Program. VIII. An independent determination of the Hubble constant based on the tip of the red giant branch. *ApJ*, 2019, v. 882 (1), 34.
9. Aghanim N., Akrami Y., Ashdown M., Aumont J. and The Planck Collaboration. Planck2018 Results: VI. Cosmological Parameters. *A&A*, 2020, v.641 (A6).
10. Freedman W. L. Measurements of the Hubble constant: tensions in perspective. *ApJ*, 2021, v. 919 (1), 16.
11. Di Valentino E., Anchordoqui L. A., Akarsu Ö., *et al.* Snowmass 2021 — Letter of interest cosmology intertwined II: the Hubble constant tension. *Astroparticle Physics*, 2021, v. 131, p.102605.
12. Vagnozzi, S. New physics in light of the H_0 tension: an alternative view. *Phys. Rev. D*, 2020, v. 102 (2), p.023518.
13. Einstein A. Kosmologische Betrachtungen zur allgemeinen Relativitätstheorie. *Preussische Akademie der Wissenschaften, Sitzungsberichte*, Bd. 1, 1917, 142–152.
14. Einstein A. Grundgedanken der allgemeinen Relativitätstheorie und Anwendung dieser Theorie in der Astronomie (Fundamental ideas of the General Theory of Relativity and the application of this theory in astronomy). *Preussische Akademie der Wissenschaften, Sitzungsberichte*, Bd. 1, 1915, 315.
15. Einstein A. Zur allgemeinen Relativitätstheorie (On the General Theory of Relativity). *Preussische Akademie der Wissenschaften, Sitzungsberichte*, Bd. 2, 1915, 778–786, 799–801.
16. Friedmann A. A. Über die Möglichkeit einer Welt mit konstanter negativer Krümmung des Raumes. *Zeitschrift für Physik*, 1924, v. 21 (1), 326–332.
17. Lemaître G. Über die Krümmung des Raumes. *Annales de la Société Scientifique de Bruxelles*, 1933, v. A53 (1), 51–85.
18. Robertson H. P. Kinematics and world-structure II. *AJ*, 1936, v. 83, 187–201.
19. Robertson H. P. Kinematics and world-structure III. *ApJ*, 1936, v. 83, 257–271.
20. Robertson H. P. Kinematics and world-structure. *ApJ*, 1935, v. 82, 284–301.
21. Walker A. G. On Milne’s theory of world-structure. *Proceedings of the London Mathematical Society*, 1937, v. 42 (1), 90–127.
22. Anand G. S., Tully R. B., Rizzi L., Riess A. G. and Yuan W. Comparing tip of the red giant branch distance scales: an independent reduction of the Carnegie-Chicago Hubble Program and the value of the Hubble constant. *ApJ*, 2022, v. 932 (1), 15.
23. Knox L. and Millea M. Hubble Constant Hunter’s Guide. *Phys. Rev. D*, 2020, v. 101 (4), 043533.
24. Bassett B. A. and Hlozek R. Baryon Acoustic Oscillations. 2009, 1–42.

25. Bond J.R. and Efstathiou G. The statistics of Cosmic Background Radiation fluctuations. *MNRAS*, 1987, v. 226 (3), 655–687.
26. Bond J.R. and Efstathiou G. Cosmic Background Radiation anisotropies in universes dominated by non-baryonic darkmatter. *ApJ*, 1984, v. 285, L4.
27. Peebles P.J.E. and Yu J.T. Primeval adiabatic perturbation in an expanding universe. *ApJ*, 1970, v. 162, 815.
28. Sunyaev R. A. and Zeldovich Ya. B. The interaction of matter and radiation in the hot model of the Universe, II. *Astrophys. & Space Sci.*, 1970, v. 7 (1), 20–30.
29. Ellis G. F. R. Note on varying speed of light cosmologies. *Gen. Rel. & Grav.*, 2007, v. 39 (4), 511–520.
30. Ellis G. F. R. and Uzan J. P. c is the speed of light, isn't it? *Am. J. Phys.*, 2005, 2005, v. 73 (3), 240–247.
31. King J. A., Webb J. K., Murphy M. T., *et al.* Spatial variation in the fine structure constant — new results from VLT/UVES. *MNRAS*, 2012, v. 422 (4), 3370–3414.
32. Webb J. K., King J. A., Murphy M. T., *et al.* Indications of a spatial variation of the fine structure constant. *Phys. Rev. Lett.*, 2011, v. 107, 191101.
33. Murphy M. T., Webb J. K. and Flambaum V. V. Keck constraints on a varying fine-structure constant: wavelength calibration errors. *Memorie della Società Astronomica Italiana*, 2009, v. 80 (H15), 833–841.
34. Murphy M. T., Webb J. K. and Flambaum V. V. Comment on “Limits on the Time Variation of the Electromagnetic Fine-Structure Constant in the Low Energy Limit from Absorption Lines in the Spectra of Distant Quasars”. *Phys. Rev. Lett.*, 2007, v. 99, 239001.
35. Murphy M. T., Webb J. K. and Flambaum V. V. Revision of VLT/UVES constraints on a varying fine-structure constant. *Lect. Notes Phys.*, 2004, v. 648 (2), 131.
36. Murphy M. T., Webb J. K. and Flambaum V. V. Further evidence for a variable fine-structure constant from Keck/HIRES QSO absorption spectra. *MNRAS*, 2003, v. 345 (2), 609–638.
37. Murphy M. T., Webb J. K. and Flambaum V. V., *et al.* Possible evidence for a variable fine-structure constant from QSO absorption lines: motivations, analysis and results. *MNRAS*, 2001, v. 327 (4), 1208–1222.
38. Webb J. K., Murphy M. T., Flambaum, V. V., *et al.* Further evidence for cosmological evolution of the fine structure constant. *Phys. Rev. Lett.*, 2001, v. 87 (9), 091301.
39. Webb J. K., Flambaum V. V., Churchill C. W., *et al.* Search for time variation of the fine structure constant. *Phys. Rev. Lett.*, 1999, v. 82, 884–887.
40. Milne E. A. Relativity, gravitation and world-structure. *Nature*, 1935, v. 135 (3417), 635–636.
41. Milne E. A. Kinematics, dynamics, and the scale of time. *Proceedings of the Royal Society of London A: Mathematical, Physical and Engineering Sciences*, 1937, v. 158 (894), 324–348.
42. Dirac P. A. M. The cosmological constants. *Nature*, 1937, v. 139 (3512), 323–323.
43. Silva M. F., Winther H. A., Mota D. F. and Martins C. J. A. P. Spatial variations of the fine-structure constant in symmetron models. *Phys. Rev. D*, 2014, v. 89, 024025.
44. Bamba K., Nojiri, S. and Odintsov S. D. Domain wall solution in $F(R)$ gravity and variation of the fine structure constant. *Phys. Rev. D*, 2012, v. 85, 044012.
45. Barrow J. D. and Lip S. Z. W. Generalized theory of varying alpha. *Phys. Rev. D*, 2012, v. 85, 023514.
46. Barrow J. D., Sandvik H. B. and Magueijo J. Behavior of varying-alpha cosmologies. *Phys. Rev. D*, 2002, v. 65 (6), 063504.
47. Olive K. A., Peloso M. and Peterson A. J. Where are the walls? Spatial variation in the fine-structure constant. *Phys. Rev. D*, 2012, v. 86, 043501.
48. Calabrese E., Menegoni, Martins C. J. A. P., Melchiorri A., and Rocha G. Constraining variations in the fine structure constant in the presence of early dark energy. *Phys. Rev. D*, 2011, v. 84, 023518.
49. Suzuki N., Rubin D., Lidman C., *et al.* The Hubble Space Telescope cluster supernova survey: V. Improving the dark energy constraints above $z > 1$ and building an early-type-hosted supernova sample. *ApJ*, 2012, v. 746 (1), 85.
50. Amanullah R., Lidma C., Rubin, D., *et al.* Spectra and Hubble Space Telescope light curves of six Type Ia supernovae at $0.511 < z < 1.12$ and the Union2 compilation. *ApJ*, 2010, v. 716 (1), 712–738.
51. Amanullah R., Stanishev V., Goobar A., *et al.* Light curves of five Type Ia supernovae at intermediate redshift. *A&A*, 2008, v. 486 (2), 375–382.
52. Astier P., Guy J., Regnault N., *et al.* The supernova legacy survey: measurement of Ω_M , Ω_Λ and w from the first year data set. *A&A*, 2006, v. 447 (1), 31–48.
53. Barris B. J., Tonry J. L., Blondin S., *et al.* Twenty-three high-redshift supernovae from the Institute for Astronomy Deep Survey: doubling the supernova sample at $z > 0.7$. *ApJ*, 2004, v. 602 (2), 571–594.
54. Contreras C., Hamuy M., Phillips M. M., *et al.* The Carnegie Supernova Project: first photometry data release of low-redshift Type Ia supernovae. *AJ*, 2010, v. 139 (2), 519–539.
55. Hamuy M., Trager S. C., Pinto P. A., *et al.* A search for environmental effects on Type I[CLC]a/[CLC] supernovae. *AJ*, 2000, v. 120 (3), 1479–1486.
56. Hicken M., Challis P., Jha S., *et al.* CfA3: 185 Type Ia supernova light curves from the CfA. *ApJ*, 2009, v. 700 (1), 331–357.
57. Holtzman Jon A., Marriner J., Kessler R., *et al.* The Sloan Digital Sky Survey-II: photometry and Supernova IA light curves from the 2005 data. *AJ*, 2008, v. 136 (6), 2306–2320.
58. Jha S., Kirshner R. P., Challis P., *et al.* UBVRI light curves of 44 Type Ia supernovae. *AJ*, 2006, v. 131 (1), 527–554.
59. Knop R. A., Aldering G., Amanullah R., *et al.* New constraints on Ω_M , Ω_Λ , and w from an independent set of 11 high-redshift supernovae observed with the Hubble Space Telescope. *ApJ*, 2003, v. 598 (1), 102–137.
60. Kowalski M., Rubin D., Aldering G., *et al.* Improved cosmological constraints from new, old, and combined supernova data sets. *ApJ*, 2008, v. 686 (2), 749–778.
61. Krisciunas K., Garnavich P. M., Challis P., *et al.* Hubble Space Telescope observations of nine high-redshift ESSENCE supernovae. *AJ*, 2005, v. 130 (6), 2453–2472.
62. Miknaitis G., Pignata G., Rest A., *et al.* The ESSENCE Supernova Survey: survey optimization, observations, and supernova photometry. *ApJ*, 2007, v. 666 (2), 674–693.
63. Perlmutter S., Aldering G., Goldhaber G., *et al.*, and The Supernova Cosmology Project. Measurements of ω and λ from 42 high-redshift supernovae. *ApJ*, 1999, v. 517 (2), 565–586.
64. Riess A. G., Strolger L. G., Casertano S., *et al.* New Hubble Space Telescope discoveries of Type Ia supernovae at $z \geq 1$: narrowing constraints on the early behavior of dark energy. *ApJ*, 2007, v. 659 (1), 98–121.
65. Riess A. G., Kirshner R. P., Schmidt B. P., *et al.* [ITAL]BVRI/[ITAL] light curves for 22 Type I[CLC]a/[CLC] supernovae. *AJ*, 1999, v. 117 (2), 707–724.
66. Riess A. G., Filippenko A. V., Challis P., *et al.* Observational evidence from supernovae for an accelerating universe and a cosmological constant. *ApJ*, 1998, v. 116 (3), 1009–1038.

67. Tonry J. L., Schmidt B. P., Barris B., *et al.* Cosmological results from high- z supernovae. *ApJ*, 2003, v. 594 (1), 1–24.
68. Anderson L., Aubourg E., Bailey S., Bizyaev D., and *at al.* The clustering of galaxies in the SDSS-III baryon oscillation spectroscopic survey: baryon acoustic oscillations in the data release 9 spectroscopic galaxy sample. *MNRAS*, 2012, v. 427 (4), 3435–3467.
69. Mehta K. T., Cuesta A. J., Xu X., Eisenstein D. J. and Padmanabhan K. A 2 percent distance to $z = 0.35$ by reconstructing baryon acoustic oscillations — III. Cosmological measurements and interpretation: A 2 percent distance to $z = 0.35$. *MNRAS*, 2012, v. 427 (3), 2168–2179.
70. Ade P. A. R., Aghanim N., Armitage-Caplan C., Arnaud M., Ashdown M., and the Planck Collaboration. Planck2013 Results. XVI. Cosmological parameters. *A&A*, 2014, v. 571 (A16).
71. Tegmark M., Eisenstein D. J., Strauss M. A., Weinberg D. H., *at al.* Cosmological constraints from the SDSS luminous red galaxies. *Phys. Rev. D*, 2006, v. 74 (12), 123507.
72. Blake C., Kazin E. A., Beutler F., *et al.* The WiggleZ Dark Energy Survey: mapping the distance-redshift relation with baryon acoustic oscillations: WiggleZ survey: BAOs in redshift slices. *MNRAS*, 2011, v. 418 (3), 1707–1724.
73. Saintonge A. and Catinella B. The cold interstellar medium of galaxies in the local Universe. *Ann. Rev. A&A*, 2022, v. 60 (1), 319–361.
74. Draine B. T. *Physics of the Interstellar and Intergalactic Medium*. Princeton series in astrophysics, Princeton University Press, Princeton, NJ, 2011. Formerly CIP UK. — Includes bibliographical references and index.
75. Rohlfs K. and Wilson T. L. *Tools of Radio Astronomy*. Springer, Berlin Heidelberg, 2004.
76. Levshakov S. A., Centurión M., Molaro P. and D’Odorico S. VLT/UVES constraints on the cosmological variability of the fine-structure constant. *A&A*, 2005, v. 434 (3), 827–838.
77. Chand H., Srianand R., Petitjean P., and Aracil B. Probing the cosmological variation of the fine-structure constant: results based on VLT-UVES sample. *A&A*, 2004, v. 417 (3), 853–871.
78. Srianand R., Chand H., Petitjean P. and Aracil B. Limits on the time variation of the electromagnetic fine-structure constant in the low energy limit from absorption lines in the spectra of distant quasars. *Phys. Rev. Lett.*, 2004, v. 92 (12), 121302.
79. Sanejouand Y. H. About some possible empirical evidences in favor of a cosmological time variation of the speed of light. *Europhys. Lett.*, 2009, v. 88 (5), 59002.
80. Unzicker A. A look at the abandoned contributions to cosmology of Dirac, Sciama, and Dicke. *Ann. der Physik*, 2009, v. 521 (1), 57–70.
81. Broekaert J. A spatially-VSL gravity model with 1-PN limit of GTR. *Found. Phys.*, 2008, v. 38 (5), 409–435.
82. Magueijo J. New varying speed of light theories. *Reports on Progress in Physics*, 2003, v. 66 (11), 2025–2068.
83. Barrow J. D. Cosmologies with varying light speed. *Phys. Rev. D*, 1999, v. 59 (4), 043515.
84. Moffat J. W. Superluminary universe: a possible solution to the initial value problem in cosmology. *Int. J. Mod. Phys. D*, 1993, V. 02 (03), 351–365.
85. Petit J. P. An interpretation of cosmological model with variable light velocity. *Mod. Phys. Lett. A*, 1988, v. 03 (16), 1527–1532.
86. Giere A. C. and Tan A. A derivation of Hubble’s law. *Chinese J. Phys.*, 1986, v. 24 (3), 217–219.
87. Dicke R. H. Gravitation without a principle of equivalence. *Rev. Mod. Phys.*, 1957, v. 29 (3), 363–376.
88. Hutchin R. A. The physics behind the NASA flyby anomaly. *Optics and Photonics Journal*, 2022, v. 12 (03), 31–51.
89. Hutchin R. A. Experimental evidence for variability in Planck’s constant. *Optics and Photonics Journal*, 2016, v. 6 (6), 124–137.
90. Dannenberg R. Planck’s constant as a dynamical field and path integral. arXiv: 1812.02325.
91. Freedman W. L., Madore B. F., Hoyt T., *et al.* Calibration of the tip of the red giant branch. *ApJ*, 2020, v. 891 (1), 57.

I: Evidence for Phenomena, Including Magnetic Monopoles, Beyond 4-D Space-Time, and Theory Thereof

Richard Ellis

Corpus Christi College (Alumnus), Oxford OX1 4JF, UK

E-mail: r.ellis@physics.oxon.org

This phenomenology paper presents a framework to understand two little-known properties of light. Firstly Brittin and Gamow have shown that sunlight shining on the Earth's surface lowers the entropy level there because $T_s > T_e > T_{\text{space}}$. We have found evidence for this, presented separately, which shows it persists contrary to the second law. Secondly when ferromagnetic particles are strongly illuminated, they move as magnetic monopoles. Mikhailov made repeated measurements and determined that the monopole charge is quantized ($g = ng_D$, $n = 1-5$; $\bar{g} = (0.99 \pm 0.05)g_D$) as predicted by Dirac. But they cease to move as monopoles when the illumination is turned off, and so have been ignored. However, the results are reproducible and we deduce these Dirac monopoles are in another space-time. The chronometric invariant formalism of General Relativity (CIGR) predicts a more complex structure to space-time of 5D, with a second time dimension, mirror time, directed from the future to the past (3,2). We make the hypothesis that light, by lowering the entropy level via the Brittin and Gamow effect, can switch the arrow of time into that of the mirror world of CIGR to reveal phenomena there. We call this the "photo-mirror hypothesis". This reveals magnetic monopoles outside 4D but in mirror space-time, where they are less objective, but reproducible and so real. This explains why monopoles can be observed at low energies (because mirror mass is negative), and the infinite length of the Dirac string.

1 Introduction

Brittin and Gamow have used the quantum theory of radiation to derive an equation which predicts that sunlight shining on the Earth's surface, lowers the entropy level there, apparently contrary to the second law of thermodynamics — see equation (1) below [1]. As we investigated this further, we confirmed the violation of the second law. To explain this, we have found new physics which may help penetrate a number of other unsolved problems in quantum and particle physics, such as magnetic monopoles. However, there are several barriers blocking progress. We start with the theoretical barriers.

1. Murray Gell-Mann said at the Conference in Honour of his 80th birthday "I should like to emphasize particularly... the need to go against certain received ideas. Sometimes they are taken for granted all over the world... Often they have a negative character and they amount to prohibitions of thinking along certain lines... Now and then, however, the only way to make progress is to defy one of these prohibitions that are uncritically accepted without good reason" [2]. Such prohibitions often concern problems from the past. So it follows, contrary to the current view that references should be up-to-date, that some of the references below, are old ones. For example, another peculiar effect of light is the detection of magnetic monopoles only when strongly illuminated, in 1930 [3].

2. Secondly, theory is sometimes biased against experiment. True, it is accepted that experiment is the final arbiter of reality. However, important discoveries often get ignored,

if the correct theoretical interpretation is not given. For example, parity violation was first observed in 1928, but was rejected as an "instrumental effect" [4]. In 1956 Lee and Yang suggested it could be violated theoretically, and Mme Wu "discovered" it shortly after that. Another example is that Irène Curie and Frédéric Joliot failed to discover the neutron because they did not believe Rutherford's neutron hypothesis. Chadwick realised that their January 18th 1932 results were not due to photons but evidence for neutrons, and so made the discovery a few months later. (The Joliot-Curies also failed to discover the positron, even though they had data for it before Anderson.) A fourth example is that the cosmic microwave background radiation from the Big Bang was first observed by A. McKellar in 1941, but misinterpreted [5]. The CMB was rediscovered at the Pulkovo Observatory by Soviet scientist T. A. Shmaonov in 1957 and published in his thesis, where he determined the temperature to be $4 \pm 3^\circ\text{K}$, but it was ignored [6]. Finally in 1964, Penzias and Wilson detected it a third time, and showed the results to Dicke at Princeton, who realised that this was the afterglow of the Big Bang. Finally the discovery was made.

Another example is the case of Felix Ehrenhaft who had the misfortune to make two such discoveries, firstly of fractional electric charges in 1910 onwards, and then magnetic monopoles in 1930, and get rejected for theoretical reasons twice! We go into magnetic monopoles in more detail below.

There is clearly a pattern here of unexpected experimental results being rejected, sometimes for decades, even indefinitely (e.g. Ehrenhaft). One possible explanation was given

by Einstein when he said to Heisenberg: “It is the theory which decides what we can observe” [7]. In effect it is theory which tells us what we can think. This is fine, when the theory is correct. However, experiment is the final arbiter of the truth, and so experimentalists are closer to Nature, and it is Nature which should tell us what to think. Therefore, when unusual experimental results are obtained, experimentalists should be encouraged to develop the theoretical explanation, especially when they can support their reasoning with mathematics already in the literature, as in this paper.

3. One of the prohibitions to thinking is the second law of thermodynamics. It is thought to be absolute, and to lead to the “heat death” of the Universe. This is in effect a classical physics “Theory of Everything”. It is true that (superficially) there is almost overwhelming evidence that entropy tends to increase with time. However, the Universe is a big place and we now know that baryonic matter makes up only about 4% of the Universe. The other 96% consists of dark matter and dark energy; and we do not know what these are, *nor what laws they obey*. So it is illogical to assume that the second law applies to them — it may or it may not. So it is perfectly rational to look for processes which create order out of chaos.

The author has done some experiments on phenomena which apparently violate the second law of thermodynamics, and so are inexplicable [8]. It is the objective of this paper to present a phenomenological framework to understand these results. In the process, we find that this new framework also explains experiments on magnetic monopoles, and observations of fractional electric charges [9].

4. There are also experimental barriers to solving problems in quantum and particle physics. Firstly, particle physics has been re-branded “high energy physics”, which is a technique, not a subject. Low energy particle physics is still an important and active area of research [10]. However, it does not get the support nor attention it deserves, because of high energy physics. High energy experiments are massive technological achievements, so low energy experiments can appear insignificant. It is the purpose of these papers to demonstrate the reverse. We present new approaches, both theoretical and experimental, into magnetic monopoles, quarks, preons, and possibly dark matter.

5. Furthermore, experimental physics is currently based upon determining *objective* facts in 4D space-time, for example, by controlled experiment. However, if one relies upon objective facts only, this assumes that the Universe can be reduced to objective facts, or at least if there are any non-objective aspects, they can be ignored. There is no proof of this, and it could lead to an infinite regression. (For example, if matter in the Universe is made from some fundamental objective substance S_A , then what is this made of? Either it is something non-objective, or it is another objective substance S_B , and so on.) So less-than-objective phenomena could be more fundamental than objective ones.

In order to bring experimental physics up to date and more

in line with theoretical physics (which frequently incorporates other dimensions or space-times), *we propose that the requirement of objectivity should be relaxed*. For example, if one makes measurements in other spaces or dimensions then, assuming it is possible, *there is inevitably some reduction in control and/or objectivity*. It is currently not recognised that such less-objective results do occur occasionally, and so they tend to be rejected because they are not objective (i.e. not in 4-D space time). We argue that such results should be considered physically real *if they can be reproduced*. We have examined the literature and find that magnetic monopoles are an example of this. They are only detected under intense illumination and so may be linked to the Brittin and Gamow effect.

Our method to challenge these barriers, is to reason from experiment upwards, as opposed to that from theoretical principles downwards, *because it is experiment which can guide us to the true nature of reality*. Never-the-less, we include some mathematics when it is available and can help us understand the experiments.

2 Magnetic Monopoles

We present experimental evidence from the literature, for real ($\nabla \cdot \mathbf{B} \neq 0$) magnetic monopoles, as opposed to the pseudo-monopoles ($\nabla \cdot \mathbf{H} \neq 0$) sometimes observed in spin ices or other solid-state phenomena.

Over the last 70 years there have been numerous searches for real magnetic monopoles with mostly negative results. Compilations of these searches conclude that there is no reproducible evidence for magnetic monopoles [11, 12]. But there is an assumption behind this conclusion, namely that magnetic monopoles must be particles which can be detected objectively in 4-D space-time, because that is what controlled experiment is limited too. Firstly, in Dirac’s theory there is a line connecting two monopoles which has to be *infinitely long*, and yet the universe is finite [13]. This infinite length of the Dirac string is normally explained away as an artefact of the calculation. However, it is there in the theory and implies that both monopoles are outside 4-D space-time, just as the Dirac equation implies the existence of antimatter. (In principle one monopole could be inside 4-D space-time and the other outside, but that would require preferential treatment for one monopole over another, which the theory does not provide. So we reject this.) If they are outside 4D space-time, then it would not be possible to detect them objectively by the normal methods of experimental physics (e.g. by controlled experiment). Therefore the conclusion of the above compilations is not strictly correct. It should read “there is no reproducible evidence for magnetic monopoles *in 4-D space-time*”. However, this is not evidence for or against magnetic monopoles because they are not predicted to be in 4-D space-time.

Furthermore, if a phenomenon is not objective, then it is currently rejected by most physicists as *not* being physi-

cally real. Therefore, the above monopole surveys usually omit most, if not all, of the references to the following experiments which provide reproducible evidence for magnetic monopoles, but of a non-objective nature. They are non-objective because *these monopoles are only visible under intense illumination*. When the intense illumination is turned off, they disappear, in the sense that the particle being observed ceases to move as a monopole, and moves as a neutral particle or dipole. *Thus these monopoles do not seem to exist in their own right*. However, these results are reproducible, and so we argue they are physically real. Here is a summary of the published evidence.

2.1 Ehrenhaft

Ehrenhaft first reported observation of single magnetic charges, which were only detectable under intense illumination, in 1930 [3], before Dirac's paper in 1931 [13]. However, Dirac did not recognise Ehrenhaft's results [14, 15]. Not only were Ehrenhaft's results non-objective, but they were obtained at very low energies. So Dirac rejected them, not just because high energies imply objectiveness, but because he thought the very strong force between monopoles would require high energies to separate them. We explain how they can be separated at low energies below.

Dirac's rejection of Ehrenhaft's monopoles creates another problem, namely that there would be two different types of monopole: that predicted by Dirac's theory, and that observed by Ehrenhaft. This is unlikely.

The essence of Ehrenhaft's observations is that when microparticles of ferromagnetic substances (such as iron, nickel or cobalt) are suspended in a gas atmosphere and subjected *simultaneously* to a uniform magnetic field *and to intense illumination by light*, they move as objects carrying single magnetic charges. If the magnetic field \mathbf{H} is reversed, then the direction of motion of the single magnetic charges is reversed (magnetic dipoles would not do this). This effect was confirmed by Benedict and Leng [16].

Ehrenhaft did a number of other experiments [17], and when he did not get the recognition he felt he deserved, he made more extreme claims, such as that "light magnetises matter" [18]. He was convinced that he had discovered free magnetic charges and should get the kind of recognition of someone such as Ampère or Faraday. He claimed he had created a magnetic current by causing the monopoles to move [19]. He also claimed to have discovered "magnetolysis", being the magnetic equivalent of electrolysis [20]. Many physicists were unconvinced that "light makes magnetism", suspected it could be due to surface effects, found the effect not objectively real, and so tended to ridicule the results [21]. Einstein took the observations seriously, but wanted a better explanation [22].

Kemple made a review of experimental searches for monopoles up to 1961, including not only the work of Ehren-

haft, but also by his contemporaries. He noted that other experimenters could not reproduce some of these results, and therefore concluded that this work is not evidence for magnetic monopoles [23]. However, this is not strictly correct, because even though some of the experiments may not have been confirmed, the basic observation of magnetic monopoles under intense illumination, was confirmed by Benedict and Leng [16].

2.2 Mikhailov

There the matter might have rested, had it not been that Mikhailov repeated Ehrenhaft's magnetic charge experiment with better technique, and confirmed the result [24–26]. In his first experiment, he used iron microparticles suspended in an atmosphere of argon, illuminated by a laser with power up to 1 kW/cm², and in the presence of crossed uniform electric and magnetic fields, which were switched by a square waveform with a frequency of a few Hertz. The particles were observed with a microscope, and moved under the influence of the crossed electric and magnetic fields (\mathbf{E} and \mathbf{H}). By observing their motion, one could *select the signs of the electric and magnetic charges of the particles being observed, thereby confirming Ehrenhaft*.

The observed microparticles had a mass $M \leq 10^{-14}$ gram and size $r \leq 10^{-5}$ cm, and their motion was governed by Stokes' law. By making measurements on particles carrying both an electric and a magnetic charge, it was possible to measure the ratio g/q independently of the Stokes' coefficient, and hence of the size of the particle. From observations of 1200 such particles, Mikhailov found that *the magnetic charge is quantized*. But his initial value of g disagreed with Dirac's prediction. However, Akers pointed out that *Mikhailov had ignored components of the particle's velocity orthogonal to \mathbf{E} and \mathbf{H}* , and so this interpretation of the result could be incorrect [27].

Mikhailov reanalysed his results and found that the magnetic charge in this experiment, is in fact the solution of a quadratic equation and so gives *two* possible values. One value is the one he had previously reported, the other being *that predicted by Dirac*. In order to distinguish between these two roots, Mikhailov redesigned the experiment to remove this ambiguity and also possible surface effects.

He condensed super-saturated vapour onto solid ferromagnetic particles in a diffusion chamber, which created a smooth surface round each particle and so eliminated surface effects. These ferromagnetic particles, surrounded by fluid, were allowed to drop through a beam of light, under the force of gravity in a magnetic field \mathbf{H} , which was periodically inverted. Under these conditions, particles exhibiting the magnetic charge effect, fall in a zig-zag path. He observed 428 such tracks with a mean magnetic charge of $\bar{g} = (2.5_{-1.3}^{+1.6}) \times 10^{-8}$ gauss \times cm², which agrees with the value predicted by Dirac of $g_D = 3.29 \times 10^{-8}$ gauss \times cm² within

the errors. In this way, Mikhailov showed unambiguously that he was observing Dirac “monopoles”, and furthermore, these were not due to surface effects on the particles [28].

He also repeated his previous experiment, choosing the correct root, and found that the ferromagnetic particles carried from 1 to 5 magnetic charges. The histogram of magnetic charges clearly shows 5 separate peaks corresponding to $g = ng_D$, where $n = 1$ to 5, with the peaks being gaussian-like with some gaps in between [29]. This confirms that the magnetic charge is quantised as predicted by Dirac, and rules out Schwinger monopoles which have twice the magnetic charge ($g_S = 2g_D$) [30].

The microparticles measured by Mikhailov were composite ($M \leq 10^{-14}$ gram), so the monopoles could be composite pseudo-particles (instantons). However, the charge of these pseudo-particles would then not be quantised with the monopole charge predicted by Dirac [31].

He also reanalysed his previous experiments, selecting the correct root and dividing the data by n , and obtained a narrow bell-shaped distribution centred on $\bar{g} = (3.27 \pm 0.16) \times 10^{-8}$ gauss \times cm² = $0.99 g_D$ with an accuracy of $\pm 5\%$ [31]. Therefore, by these ingenious experiments, Mikhailov has observed Dirac monopoles, *but only when illuminated by light*. The problem is they are non-existent in their own right, because they cease to move as monopoles when the light is turned off. There has been no satisfactory explanation for this.

2.3 Discussion

These results are reproducible, because several experimentalists have observed more than 1600 single magnetic charges. Furthermore, they apparently obey gaussian statistics (e.g. the bell-shaped distribution) and are statistically significant. Therefore we argue, these single magnetic charges *should be considered a real physical phenomena*. However we have shown above that surveys of the objective methods of physics have failed to detect them, and concluded there is no evidence for them in 4-D space-time. *One possible explanation is that the monopoles observed only under intense illumination, are not in 4-D space-time but in another space-time, as predicted by Dirac’s theory.*

Nevertheless, this is not a complete explanation. We also need a theory which predicts the existence of this second space-time, together with a mechanism which enables light to switch space-time into this second space-time. We now present such a combined theory.

3 Sunlight Shining on the Earth’s Surface

We start with an existing theory of an unexpected property of light which does the switching, and then introduce a version of General Relativity which predicts a more complex structure to space-time. The basic idea is that light switches the direction of the flow of time into that of another space-time.

3.1 Brittin and Gamow’s Theory

In a little-known theory, Brittin and Gamow have suggested that sunlight shining on the Earth, pumps entropy out into space, thereby allowing negentropy to accumulate on the Earth’s surface. The Sun’s radiation consists of high temperature photons coming from the surface at $T_s \approx 5,900^\circ$ K, which spreads out in space and becomes diluted. By the time it reaches the Earth’s surface, it’s energy density corresponds to a temperature of the Earth ($T_e \approx 300^\circ$ K), so these photons are not in thermodynamic equilibrium.

Brittin and Gamow use the quantum theory of radiation to show that the net entropy change when sunlight interacts with the Earth’s surface is [1]:

$$\Delta S = \Delta S_s - \Delta S_e = \frac{4}{3} \Delta Q \left(\frac{1}{T_s} - \frac{1}{T_e} \right), \quad (1)$$

which is negative because $T_s > T_e$. So the entropy at the Earth’s surface is reduced. They reason that this is not contrary to the second law of thermodynamics because it is simply due to the temperature gradient $T_s > T_e > T_{\text{space}}$, but see below. (Note this effect can also occur with light from an artificial source, such as an halogen lamp.) However, there is a hidden complication, independent of whether the source is natural or artificial.

The problem is that this mechanism enables negative entropy to build up on the Earth’s surface, only if it can be stored. In the case of sunlight, they calculate that photosynthesis has an efficiency of about 10% for capturing this negative entropy. Brittin and Gamow suggest that this is the source of order for the food chain, which Schrödinger proposed to be a current of negative entropy [32, 33]. If this is the only mechanism for storage, then this is not a purely physical theory because it relies upon plants (and hence biochemistry) to capture the negentropy. However, we now show that there is a mechanism in physics to store the negentropy produced.

3.2 Discussion of Brittin and Gamow Effect

In classical thermodynamics, the entropy increases with the arrow of time [34]. What happens to time when a solar photon interacts with the Earth’s surface, thereby lowering its entropy level? Is the direction of time reversed (e.g. locally), either momentarily or more persistently, when the photon lowers the entropy level? We conclude that it logically must be reversed, because otherwise Eddington’s arrow of time would be violated, and the second law of thermodynamics also. Therefore what is missing from Brittin and Gamow’s theory, is a theory of space-time with a second time dimension which is directed from the future to the past. (Experimental evidence for this reasoning is given in the following reference [8].)

There are a number of theories with two time dimensions, but these are compactified or otherwise unsuitable [35, 36]. However, Köhn has found a solution to the cosmological

problem using two time dimensions. The second time dimension is not compactified, but it is limited to a spacial scale of the Planck length [37]. Elsborg and Köhn have extended this theory to the problem of magnetic monopoles, and developed the theory of magnetic monopoles in this second time dimension [38]. They adopt the orthodox view noted above, that magnetic monopoles have not been observed [11, 12]. Therefore they continue the assumption from Köhn's first paper that the second time dimension only acts on the scale of the Planck length, so that monopoles cannot be observed experimentally at the macroscopic scales now present in the Universe. However, the above evidence for monopoles overrules this aspect of their approach, and requires the second time dimension to be macroscopic. Furthermore, it needs to be directed from the future to the past. Nevertheless, this an interesting paper which provides the mathematical analysis which shows that magnetic monopoles can exist in 5D (3,2) space-time.

There is, however, another theoretical approach. A little-known extension of the theory of General Relativity, has a second macroscopic time dimension directed from the future to the past.

4 General Relativity: Chronometric Invariants

In the 1930s, Landau and others realised that General Relativity is incomplete, because it does not correct for the reference frame of the Observer. As a result, what is observed in a specific reference frame, *is not well defined by the existing theory*. So without the Observer, General Relativity is *incomplete*. The case for including the Observer is thus compelling. Some progress was made by Landau and Lifshitz for specific cases [39]. Zelmanov developed the strict mathematical formalism to calculate the observable values for any tensor quantity in 1944. However this methodology for the general case, was not published until 1956 [40, 41]. The mathematical details of the theory are given in the references. We just present a short summary of the main points here.

Physically observable quantities are obtained by projecting four-dimensional quantities onto the time lines and three-dimensional space of the Observer's reference frame. *Physically observable quantities must be invariant with respect to transformations of time*, and so they are *chronometrically invariant quantities*. Thus the general case of the Observer was incorporated into General Relativity in Russia in the era of the Soviet Union. Cattaneo later obtained similar results [42–44].

This important extension of General Relativity is not well known in the West [45, 46]. Borissova and Rabounski, have developed this theory further. They find that the chronometric invariant equations of motion for mass-bearing particles into the past and into the future, are *asymmetric in time*. They conclude there is a fundamental asymmetry of the directions of time in the in-homogeneous space-time of General Relativity. They hold up a “mirror” to time and find that it does not reflect completely, and that there is a different world “be-

yond the mirror”. The four-dimensional momentum vector for a particle with non-zero rest mass, m_0 is:

$$P^\alpha = m_0 \frac{dx^\alpha}{ds}, \quad P_\alpha P^\alpha = 1, \quad \alpha = 0, 1, 2, 3. \quad (2)$$

When a vector (or tensor) is projected onto the time line and spacial section of an observer, these projections give the physically observable quantities for that observer [40]. Using the properly observable time interval $d\tau = \sqrt{g_{00}} dt + \frac{g_{0i}}{c\sqrt{g_{00}}} dx^i$ [39, 40], the above four-dimensional momentum vector has two projections onto the time line, namely [47, 48]:

$$\frac{P_0}{\sqrt{g_{00}}} = \pm m, \quad \text{where } m = \frac{m_0}{\sqrt{1 - v^2/c^2}} \quad (3)$$

whereas it has only one spacial projection:

$$p^i = \frac{m}{c} v^i = \frac{1}{c} p^i, \quad \text{where } v^i = \frac{dx^i}{d\tau}, \quad i = 1, 2, 3, \quad (4)$$

where p^i is the three-dimensional observable momentum. They conclude that any massive particle, having two time projections, *exists in two observable states*, entangled to each other: the positive mass state is in our world, while the negatively charged mass state is in the mirror world. Using the techniques of chronometric invariants, they find that there are three separate areas: our world (i.e. normal 4-D space-time), the mirror world, and a membrane which separates the two [47].

The flow of time is well defined mathematically in General Relativity. It is determined by the sign of the derivative of the coordinate time t with respect to the proper time ($dt/d\tau$). Using $w = c^2(1 - \sqrt{g_{00}})$ and $v_i = -c \frac{g_{0i}}{\sqrt{g_{00}}}$, Borissova and Rabounski derive the following quadratic equation:

$$\left(\frac{dt}{d\tau}\right)^2 - \frac{2v_i v^i}{c^2 \left(1 - \frac{w}{c^2}\right)} \frac{dt}{d\tau} + \frac{1}{\left(1 - \frac{w}{c^2}\right)^2} \left(\frac{1}{c^4} v_i v_k v^i v^k - 1\right) = 0, \quad (5)$$

the two roots of which are [48]:

$$\left(\frac{dt}{d\tau}\right)_{1,2} = \frac{1}{1 - \frac{w}{c^2}} \left(\frac{1}{c^2} v_i v^i \pm 1\right). \quad (6)$$

This equation has three possible solutions $dt/d\tau > 0$, $dt/d\tau < 0$, and $dt/d\tau = 0$. In our world, $dt/d\tau > 0$ and time flows from the past to the future. *In the mirror world $dt/d\tau < 0$ and so time flows in the opposite direction*. Between the two is a membrane where time has stopped $dt/d\tau = 0$. Thus the two worlds are separate, because of the membrane, but equal. So that to an Observer (in our world), time in the mirror world flows from the future to the past. A summary of their results is shown in Table 1 [49].

The membrane which separates the two worlds, has its own unique three-fold structure. On our world side and the

Table 1: Summary of Spacial Properties of Chronometric Invariant General Relativity.

Mass	Particles	Energies	Class of motion	Area	Time	Entropy
$m > 0$	massive particles	$E > 0$	move at sub-light speeds	our world	$dt > 0$	$\Delta S > 0$
$m = 0$	massless particles (photons)	$E > 0$	move at the speed of light	our world		
$m = 0$	light-like vortices	$E = 0$	moving and rotating at the speed of light	the membrane	$dt = 0$	
$m = 0$	massless particles (photons)	$E < 0$	move at the speed of light	the mirror world		
$m < 0$	massive particles	$E < 0$	move at sub-light speeds	the mirror world	$dt < 0$	$\Delta S < 0$

mirror world side, are streams of light-like particles (photons), moving at the speed of light, but with opposite energies and frequencies. Between the two in the membrane, time has stopped because $dt/d\tau = 0$, and so this region is a void which is purely spacial. However, in this void there are light-like vortices, previously unknown, which have zero relativistic masses (unlike photons which, although massless, have non-zero relativistic masses). These light-like vortices move and rotate at the speed of light, but have no energy because for them time has stopped — they are purely spacial.

In this theory, a mass-bearing particle has two time projections, one in each world, and exists in two observable states. Each particle is in effect a four dimensional dipole object, which exists in two states: in our world with positive mass and energy; in the mirror world with negative mass and energy (NB this negative mass state is not anti-matter, because the inertial mass of anti-matter is positive). However, they cannot “annihilate” or rather “nullify” (since the net energy is zero) because they are separated by the membrane. Furthermore our world and the mirror world have the same background space, and *the three-dimensional momentum remains positive in both sectors*. More details are given in the references above.

This theory of physically observable quantities, is normally referred as the “Chronometric Invariant Formalism of General Relativity”. However, correcting for the Observer’s reference frame in this way, changes the structure of space-time from 4D (3,1) to 5D (3,2) and so it is a major extension of General Relativity. We will refer to this extended theory as “Chronometric Invariant General Relativity” (CIGR), in this and related papers. However, words are important [21], so another name may be adopted. In CIGR, our world (normal 4-D space-time) and the mirror world have the same background space. So time in the mirror world is a macroscopic time dimension. Furthermore, mirror time is directed from the future to the past, so we would expect entropy in the mirror world *to be constant or decrease with our time*.

5 Photo Mirror Hypothesis

We make the hypothesis that light can switch matter into the mirror world state, by means of the Brittin and Gamow effect,

because this reduces the entropy level which reverses the direction of time.

$$\text{normal } (x, t), \frac{dt}{d\tau} > 0 \quad \frac{\Delta S < 0}{\Delta S > 0} \quad \frac{dt}{d\tau} < 0, \text{ mirror } (x, -t). \quad (7)$$

We predict this will occur locally where each photon interacts (in which case $\Delta Q = h\nu$ in equation 1). This reversal could be momentary or persistent depending on the phenomenon being observed. We call this the “photo-mirror hypothesis”.

Note that when it occurs, this is a low energy effect for two reasons. Firstly according to CIGR, any massive particle exists in a 4-dimensional dipole state with positive mass and energy in our world and negative mass and energy in the mirror world. Since the mirror world state already exists, *it does not require any energy to produce it*. All that is required is the reversal of the direction of time *to reveal it*, which can be done by visible photons with energies of a few electron volts (equation 1). The author provides experimental evidence for this in a separate paper [8].

The reader may question why, if photons can switch space-time into the mirror world state, it has not been observed before. Firstly, the effect is subtle and occurs at very low energies. Secondly, physicists are so convinced that the second law of thermodynamics is absolute, that few have looked for the creation of order. Thirdly, it switches space-time into the mirror world where phenomena are less objective and so tend to get ignored or rejected (e.g. the magnetic monopoles above). Furthermore, any random processes which increase entropy will switch the direction of time back to normal (4-D space-time). Limitations of this are discussed below.

5.1 Explanation of Magnetic Monopoles

The explanation for these magnetic monopoles is that photons in the intense illumination, switch the direction of time experienced by the ferromagnetic particles (via the Brittin and Gamow effect), from normal 4D space-time into the mirror world space-time, where the magnetic monopoles exist and can be observed. Therefore the intense illumination does not “make magnetism” as Ehrenhaft claimed, but “reveals magnetic monopoles” in this other space-time.

This overcomes Dirac's objection to Ehrenhaft's monopoles, namely that magnetic monopoles would only be observed at high energies, because of the very strong force between pairs of them [14], in the following way. The monopoles are in mirror space-time where the masses are negative. Therefore the attractive force between two monopoles would cause them *to fly apart*, so dipoles would not form. Thus by switching the direction of time, light can reveal the monopoles at low energies.

Furthermore, Dirac also concludes that a monopole may be connected to a string extending to infinity. If the monopoles are in one space, and the dipole is in another, then the Dirac string between a monopole and the corresponding pole of the dipole, is naturally infinitely long. Therefore observation of monopoles in mirror space-time and of magnetic dipoles in normal 4-D space-time, provides a natural physical explanation for the infinite length of the Dirac string, and confirms this aspect of his theory. In view of these results, Ehrenhaft, Benedict and Leng, and Mikhailov really did observe Dirac monopoles at these very low energies.

6 Limitations

The photo-mirror hypothesis involves both quantum mechanics (the Brittin and Gamow effect) and the chronometric invariant formalism of General Relativity (CIGR), so it implies unification. But quantum mechanics and CIGR have not yet been unified, nor the standard model embedded therein, so there may be limitations. However the author has obtained *independent experimental evidence* for the photo-mirror effect, which justifies its usage above to explain the magnetic monopole data [8].

7 Conclusions

We have made the hypothesis that there may be phenomena which experiment can detect, but which are not completely objective, for example because they are not in normal 4-D space-time. Magnetic monopoles are an example of this, because they can only be detected under intense illumination, so that when the illumination is turned off, they cease to move as monopoles, and so do not seem to exist in their own right. However, if a phenomenon can be detected repeatedly (for example these magnetic monopoles), *we suggest it should be considered physically real*.

We have presented reproducible evidence for magnetic monopoles which appear to exist outside 4-D space-time. We conclude that the current method of experimental physics is flawed, because it limits observations to objective phenomena in 4-D space time. Phenomena beyond 4-D space-time, if they can be observed, are currently rejected. The solution is to relax the criterion of objectivity, and recognise reproducible phenomena as being physically real. This is especially the case if there is a theory for that phenomenon.

Several experimenters have observed more than 1600 magnetic monopoles under intense illumination, so they are reproducible. Mikhailov has determined that these monopoles have the charge predicted by Dirac: $\bar{g} = (3.27 \pm 0.16) \times 10^{-8} \text{ gauss} \times \text{cm}^2 = 0.99 g_D$ with an accuracy of $\pm 5\%$. Furthermore, he determined that this charge is quantised ($g = n g_D$ with $n = 1$ to 5). This rules out Schwinger monopoles because $g_S = 2 g_D$ [30]. This also rules out pseudo-particles (instantons) because they would not be quantised, and certainly not with the Dirac charge [31]. We conclude that Dirac monopoles have been observed, but not in 4-D space-time because they are only observed when they are intensely illuminated.

To explain these monopoles, we combine the Brittin and Gamow effect and Chronometric Invariant General Relativity (CIGR) to make the photo-mirror hypothesis, namely that visible light lowers the entropy level and reverses the direction of time, thereby switching space-time into mirror space-time of CIGR, where time is directed from the future to the past. Therefore the photons of the intense illumination switch the ferromagnetic particles, via the photo-mirror hypothesis, into the mirror world space-time state, where the magnetic monopoles exist and are observed. In this way, *the intense illumination reveals magnetic monopoles in mirror space-time*.

Mirror space-time explains two aspects of Dirac's theory of monopoles: their observation at low energies, and the infinite length of the Dirac string. Firstly, we find the monopoles are in mirror space-time where the masses are negative. Therefore the attractive force between two monopoles would cause them to fly apart, so dipoles would not form. Thus by switching the direction of time, light can reveal the monopoles at low energies. Secondly, observation of magnetic monopoles only in mirror space-time and dipoles only in normal 4-D space-time, provides a natural physical explanation for the infinite length of the Dirac string.

This is evidence for phenomena beyond 4-D space-time. In effect, under certain circumstances, light gives us a window into another world. The photo-mirror hypothesis links a quantum mechanical effect (Brittin and Gamow) with General Relativity (CIGR), which implies unification.

Acknowledgements

The author thanks Dmitri Rabounski for helpful communications. An earlier version of this paper has been published as an e-preprint [50].

Submitted on November 21, 2024

References

1. Brittin W. and Gamow G. Negative entropy and photosynthesis. *Proc. of the Nat. Acad. of Sciences*, 1961, v. 47, 724.
2. Gell-Mann M. Some lessons from sixty years of theorising. *Int. J. Mod. Phys. A*, 2010, v. 25 (20), 3857–3861.
3. Ehrenhaft F. *Phys. Zeitschr.*, 1930, v. 31, 478.

4. Cox R.T., McIlwraith C.G. and Kurrelmeyer B. *Proc. Nat. Acad. Sci.*, 1928, v. 14 (7), 544; Rubbia C., private communication.
5. McKellar A. *Publ. of the Dominion Astrophysical Observatory*, Vancouver, Canada, v. 7 (6), 251–272.
6. Shmaonov T.A. Methodology of absolute measurements for effective radiation temperature with lower equivalent temperature. *Apparatuses and Technics of Experiment*, 1957, v. 1, 83–86.
7. Einstein A., quoted by W. Heisenberg in *Physics and Beyond: Encounters and Conversations*, transl. by A. J. Pomerans, Harper & Row, New York, 1971.
8. Ellis R.J. Preliminary evidence for a second time dimension directed from the future to the past, and for unification. doi:10.5281/zenodo.7347637.
9. Ellis R.J. Preliminary evidence for quarks and preons in mirror space-time. doi:10.5281/zenodo.7671809.
10. Jaeckel J. and Ringwald A. *Ann. Rev. Nucl. Part. Sci.*, 2010, v. 60, 405.
11. Tanabashi M. et al. *Phys. Rev.*, 2018, D98, 030001.
12. Giacomelli G. et al. DFUB 2000-9 Bologna, arXiv: hep-ex/0005041.
13. Dirac P.A.M. *Proc. Roy. Soc.*, 1931, v. A133, 60.
14. Dirac P.A.M. *Phys. Rev.*, 1948, v. 74, 817.
15. Kragh H. *Dirac: A Scientific Biography*. Cambridge University Press, 1990, pp. 216–217.
16. Benedikt E.T. and Leng H.R. *Phys. Rev.*, 1947, v. 71, 454.
17. Ehrenhaft F. *Annales de Physique*, 1940, v. 11/13, 151.
18. Ehrenhaft F. and Banet L. *Nature*, 1941, v. 147, 297.
19. Ehrenhaft F. *Nature*, 1944, v. 154, 426.
20. Ehrenhaft F. *Phys. Rev.*, 1944, v. 65, 287.
21. The late V.L. Telegdi, private communication.
22. Dibner Library, Smithsonian, Washington DC, MSS 2898, Einstein to Ehrenhaft, 20 Feb. 1940.
23. Kemple T.E. The Magnetic Monopole. MSc Thesis, Univ. Missouri, School of Mines and Metallurgy, 1961, pp.36–44 and references therein; scholarsmine.mst.edu/masters.theses/2765
24. Mikhailov V.F. *Phys. Lett.*, 1983, v. B130, 331.
25. Mikhailov V.F. *J. Phys. A: Math. Gen.*, 1985, v. 18, L903.
26. Mikhailov V.F. *Annales de la Fond. Louis de Broglie*, 1987, v. 12, 491.
27. Akers D. *Int. J. Theor. Phys.*, 1988, v. 27, 1019.
28. Mikhailov V.F. *J. Phys. A: Math. Gen.*, 1991, v. 24, 53.
29. Mikhailov V.F. On Interpretation of the Magnetic Charge Effect on Ferromagnetic Aerosols. Preprint, HEPI 88-05, Kazakh Academy of Sciences, Alma-Ata, 1988, see Figure 2.
30. Schwinger J. *Phys. Rev.*, 1966, v. 144, 1087–1093.
31. Mikhailov V.F. Experimental detection of Dirac's magnetic charge? *J. Phys. D: Applied Physics*, 1996, v. 29, 801–804.
32. Schrödinger E. *What is Life?* Cambridge University Press, 1944.
33. Prigogine I. *Bull. Acad. Roy. Belg. Cl. Sci.*, 1945, v. 31, 600.
34. Eddington A.S. *The Nature of the Physical World*. Cambridge University Press, 1928.
35. Bars I. Duality and hidden dimensions. *Frontiers in Quantum Field Theory*, World Scientific, Singapore, 1996, 52; arXiv: hep-th/9604200.
36. Vafa C. Evidence for F-Theory. *Nucl. Phys.*, 1996, v. B469, 403; arXiv: hep-th/9602022.
37. Köhn C. A solution to the cosmological constant problem in two time dimensions. *J. HEP, Grav. and Cosm.*, 2020, v. 6, 640–655.
38. Elsborg J. and Köhn C. Magnetic monopoles in two time dimensions. *Int. J. Modern Phys. A*, 2022, v. 37, 2250141.
39. Landau L.D. and Lifshitz E.M. *The Classical Theory of Fields*. The 4th final edition, Butterworth-Heinemann, 1980.
40. Zelmanov A.L. Chronometric invariants and the accompanying frames of reference in the General Theory of Relativity. *Soviet Physics Doklady*, 1956, v. 1, 227–230; Zelmanov A.L. On the relativistic theory of an anisotropic in-homogeneous Universe. *Proc. of 6th Soviet Conf. on the Problems of Cosmogony*, Nauka, Moscow, 1959, 144–174 (in Russian), see English transl. in *The Abraham Zelmanov Journal*, 2008, v. 1, 33–63.
41. Zelmanov A.L. Chronometric Invariants. English transl. of the 1944 Dissertation, Am. Res. Press, Rehoboth, 2006; see also Rabounski D. and Borissova D. Physical observables in General Relativity and the Zelmanov chronometric invariants. *Progress in Physics*, 2023, v. 19 (1), 3–29.
42. Cattaneo C. *Nuov. Cim.*, 1958, v. 10, 318–337.
43. Cattaneo C. *Nuov. Cim.*, 1959, v. 11, 733–735.
44. Cattaneo C. *Nuov. Cim.*, 1959, v. 13, 237–240.
45. Pollock M.D. Chronometric invariance and string theory. *Mod. Phys. Letts. A*, 2008, v. 23, 797–813.
46. Pollock M.D. Quantum gravity in the chronometrically invariant formalism of Zel'manov. IAEA-ICTP-90-69, 1990.
47. Borissova L. and Rabounski D. *Fields, Vacuum, and the Mirror Universe*. The 3rd revised edition, New Scientific Frontiers, London, 2023 (the 1st ed. published in 2001). See Chapters 1 and 6.
48. Rabounski D. and Borissova L. *Particles Here and Beyond the Mirror*. The 4th rev. edition, New Scientific Frontiers, London, 2023 (the 1st ed. published in 2001).
49. Borissova L. and Smarandache F. Positive, neutral and negative mass-charges in General Relativity. *Progress in Physics*, 2006, v. 2 (3), 51–54.
50. Ellis R.J. I: Evidence for phenomena, including magnetic monopoles, beyond 4-D space-time, and theory thereof. arXiv: 2207.04916.

II: Preliminary Evidence for a Second Time Dimension Directed from the Future to the Past, and for Unification

Richard Ellis

Corpus Christi College (Alumnus), Oxford OX1 4JF, UK

E-mail: r.ellis@physics.oxon.org

Experiments are presented on the effects of visible light shining on water. To understand these, we note that Landau and others realised General Relativity was incomplete because it does not correct for the Observer's reference frame. When this is done for the general case, the chronometric invariant formalism of General Relativity (CIGR) predicts a second time dimension directed from the future to the past, and new phenomena at low (eV) energies. The initial objective was to test Brittin and Gamow's theory that sunlight lowers the entropy level at the Earth's surface. We detected this effect and found it persists for at least 10 months after exposure to sunlight (17 days after halogen light), *contrary to the second law of thermodynamics*. In a previous paper, the (photo-mirror) hypothesis was made that light can switch the arrow of time into the mirror world of CIGR, via the Brittin and Gamow effect. Experimental evidence is presented that visible photons switch small (0.2 to 1.5 microns) "quantized" regions of water into the mirror world state; and their brightness distributions match the energy spectrum of the halogen light source ($\chi^2/DF = 1.49$ and 0.94 respectively) indicating causality. This is detailed evidence for the Brittin and Gamow effect. Furthermore, these domains persist (for 20 and 27 days respectively), which is evidence for the second time dimension, and there is evidence they are surrounded by the membrane also predicted by CIGR. This is also evidence for the photo-mirror hypothesis, which links Quantum Mechanics and Chronometric Invariant General Relativity, and so is preliminary experimental evidence for unification.

1 Introduction

Following on from Landau's work in the 1930s, Zelmanov developed the mathematical apparatus (chronometric invariants) to correct for the reference frame of the Observer in the general case. This was not published until 1956 [1], and confirmed by Cataneo. Since then Borissova and Rabounski have developed the chronometric invariant formalism of General Relativity (which we refer to as CIGR) further, and shown it predicts a more complex structure for space-time: 5D (3,2) [2]. In a previous paper we have made the (photo mirror) hypothesis that visible light can reverse the direction of the arrow of time into that of mirror space-time (predicted by CIGR), by lowering the entropy level via the Brittin and Gamow effect [3]. This provides the theoretical framework for understanding experiments which show evidence, presented below, for phenomena which violate the second law of thermodynamics.

The following experimental work investigates the photo mirror hypothesis, and finds evidence for this joint quantum mechanical-relativistic effect. which enables the second law of thermodynamics to be reversed, and for the reduced entropy levels to persist. This is made possible by mirror space-time, where time is directed from the future to the past. Murray Gell-Mann has said "I should like to emphasize ... the need to go against certain received ideas. ... Often they have a negative character and they amount to prohibitions of think-

ing along certain lines. ... Now and then, however, the only way to make progress is to defy one of these prohibitions that are uncritically accepted without good reason" [4].

One of these prohibitions is the second law of thermodynamics [5, 6]. There are several definitions of the second law. Two early ones by Carnot and Clausius, refer to heat engines [7, 8], which are not the subject of this paper. Furthermore, perpetual motion and similar devices are excluded [9]. Instead we focus on the statistical mechanical approach due to Boltzmann in 1877.

Briefly, in Maxwell's kinetic theory of an ideal gas, heat is due to the motion of the molecules. Each molecule can be in a number of different energy states ϵ_i , but can only be in one state at a time, so many states are empty. In a system of many molecules N , of which g_i could be in the state ϵ_i , but only some of them, N_i , are occupied, where $g_i \gg N_i$ and $N = \sum_i N_i$. In this degenerate system, there are several different configurations which all possess the same total energy and correspond to approximately the same temperature ($N_i \propto e^{-\epsilon_i/k_B T}$). The number of ways N_i indistinguishable molecules can be distributed amongst g_i energy states is $g_i^{N_i}/N_i!$. The number of ways a particular macrostate can be achieved is $\Omega = (g_1^{N_1}/N_1!) \times (g_2^{N_2}/N_2!) \dots$, which increases rapidly with the degeneracy. Boltzmann showed that the entropy $S = k_B \ln \Omega$ where k_B is the Boltzmann constant, and the thermodynamic probability Ω is at its maximum at equilibrium [10]. Therefore the entropy is maximum at equilib-

rium, and is interpreted as a measure of statistical disorder of the system.

Thus the second law was formulated in the 19th century, is considered absolute, and is widely thought to lead to the “heat death” of the Universe. This is in effect a classical physics “Theory of Everything”. It is true that (superficially) there is considerable evidence that entropy (of baryonic matter) tends to increase with time. However, baryonic matter makes up only about 4% of the Universe. The other 96% consists of dark matter and dark energy; and we do not know what these are, *nor what laws they obey*. So it is illogical to assume that the second law applies to them — it may or it may not. Therefore it is perfectly rational to look for processes which create order out of chaos. If an effect is found, then the problem is to understand the results theoretically, so as to facilitate more probing experiments.

This is not a general paper on the violation of the second law of thermodynamics. Our starting point is a little-known theory due to Brittin and Gamow (see equation (1) below). This predicts that sunlight shining on the Earth, pumps entropy out into space, thereby allowing negentropy (i.e. order) to accumulate on the Earth’s surface. This appears to be the beginning of the food chain proposed by Schrödinger [11, 12].

This paper is divided into three sections. In this first section, we present an exploratory experiment which provides evidence that visible light reverses the second law of thermodynamics by producing ordered states in an inanimate closed system (i.e. pure water), *which persist*. This persistence should not occur. Before we could investigate this in more detail experimentally, we needed a theoretical explanation for this persistence to guide the experimental work. This explanation comes from the little-known (chronometric invariant) extension of General Relativity (CIGR) mentioned above, which predicts a more complex structure for space-time. In particular it predicts a second time dimension directed from the future to the past and fundamental new phenomena at low energies. Details of this new theoretical approach, are presented in a previous paper and the references cited there [3].

Section II presents results of experiments to test this theoretical explanation. Section III presents conclusions, discussion, and predictions. We start by presenting the small exploratory experiment to test the Brittin and Gamow effect, which we did before this theoretical framework was developed.

1.1 Brittin and Gamow’s Theory

Photons from the Sun’s surface ($T_s \approx 5,900^\circ\text{K}$) come to the Earth ($T_e \approx 300^\circ\text{K}$), where they interact. Brittin and Gamow use the quantum theory of radiation to show that the net entropy change on the Earth’s surface is [13]:

$$\Delta S = \Delta S_s - \Delta S_e = \frac{4}{3} \Delta Q \left(\frac{1}{T_s} - \frac{1}{T_e} \right), \quad (1)$$

which is negative because $T_s > T_e$. They reason that this is

not contrary to the second law of thermodynamics because it is simply due to the temperature gradient $T_s > T_e > T_{space}$. (NB A similar temperature gradient applies to light from a halogen lamp: $T_h > T_e > T_{space}$ since $T_h \approx 3,000^\circ\text{K}$.)

This quantum effect enables negative entropy to build up on the Earth’s surface, *provided it can be stored* [14]. However, in the absence of a storage mechanism, any reduction in the entropy levels should dissipate as the (closed) system returns to equilibrium. Nevertheless, Brittin and Gamow calculate that photosynthesis has an efficiency of about 10% for capturing this negative entropy. So this is apparently not a purely physical theory because it relies upon plants (and hence biochemistry) to capture the negentropy. Does this mean that biochemistry alone enables plants to violate the second law? Or is there some underlying physical mechanism for storing the negative entropy, produced by visible light?

The focus of this paper is to test the above theory in inanimate systems, specifically in water, by looking for reductions of entropy levels which persist.

1.2 Theory of Exploratory Experiment

In order to investigate this, we have done the following simple experiment to test whether there is an *underlying physical storage mechanism*. 60% of the Earth’s surface is covered by water, life is water-based, and plants are 70% water. So if there is a physical mechanism (i.e. not based on biochemistry) for storing this negative entropy, the most likely place to find it would be in water exposed to sunlight.

1.3 Entropy and Brownian Motion

We decided to expose a bowl of pure water to sunlight and later measure the Brownian motion of particles therein, to determine if there is any persistent entropy change. Brownian motion is a random walk which covers the whole of phase space. As is well known, the probability $\rho(x, t)$ of a suspended particle moving a distance x along the x -axis in time t is [15, 16]

$$\rho(x, t) = \frac{e^{-x^2/4Dt}}{2\sqrt{\pi Dt}}, \quad (2)$$

where D is the diffusion constant. Diffusion takes place when a molecule moves to an unoccupied state, so that the more unoccupied states, the greater the diffusion. Entropy also increases when there are more unoccupied states, so that an increase in the diffusion constant implies an increase in entropy and vice versa. From the Fokker-Planck equation, the Boltzmann-Gibbs entropy $S = -k_B \int_{-\infty}^{+\infty} \rho(x, t) \ln \rho(x, t) dx$ where $\rho(x, t)$ is given by equation (2) above. Hence $S = -k_B (\ln(1/\sqrt{4\pi Dt}) - 0.5)$ so that as the diffusion constant increases, so does the entropy. Conversely, if the entropy has been reduced then the probability $\rho(x, t)$ will become narrower.

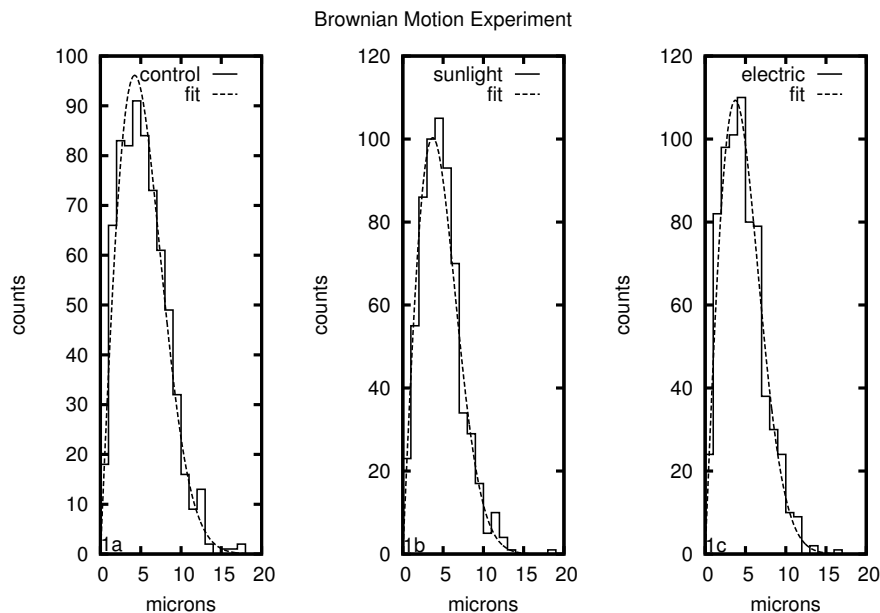


Fig. 1: Distribution of particle displacements every 10 seconds for a) non-irradiated distilled water = control; b) water measured 10 months after exposure to sunlight = signal 1; c) water measured 17 days after exposure to light from an halogen lamp = electric (i.e. signal 2). The dashed curves show the fits — see Table 1 for details. Both the sunlight and electric light samples are narrower than the non-irradiated control by 21% FWHM.

1.4 Details of Exploratory Experiment

Distilled water was exposed to sunlight for 8 days in August in the UK. Another sample was exposed to an halogen lamp ($T_h \approx 3,000^\circ \text{K}$) so as to receive a similar level of illumination. Both samples were bottled and stored in a box away from direct light, at room temperature which varied by a few $^\circ\text{C}$ at most. A third sample was taken directly from the amber Winchester supply bottle without any deliberate exposure to light and used as the control.

After storing the exposed samples, the Brownian motion measurements were made 10 months and 17 days later respectively, as follows. A few drops of the sample were placed on a microscope slide, 1 micron diamond particles were added, it was covered and viewed under a microscope (magnification $\times 1000$), with a video attachment. The Brownian motion of the diamond particles was readily visible and recorded at room temperature.

1.5 Results of Exploratory Experiment

Diamond particles with a diameter of about 0.7 microns were selected for measurement. The distance $r = \sqrt{x^2 + y^2}$ moved in 10 seconds was measured. A number of particles were tracked for each sample, with a total of order 700 data points per sample. The distributions for the three samples are shown in Figure 1. There is little or no background and no long tails. Fits to the two-dimensional form of Einstein’s theory are very good, as shown by the curves in the Figures, and the chi-squares per degree of freedom, shown in Table 1, are all

close to 1. *So we have observed Brownian motion.*

The distributions of the solar and halogen (electric) samples, are *both narrower* than the non-irradiated control. The fits show that sunlight and halogen light have reduced the diffusion constant by about 23% and 22% respectively. (The difference $\delta = -0.01 \pm .029$ between these two signals is not statistically significant.) This translates into a reduction in the entropy by $4.7 \pm 0.7\%$ for water exposed to sunlight and $4.4 \pm 0.7\%$ for halogen light. These correspond to 6.5 and 6.2 standard deviations respectively, so this reduction in entropy is statistically significant. Therefore this is evidence for the Brittin and Gamow effect.

However, this reduction in entropy has *persisted*, despite the samples being closed systems in thermal equilibrium with their surroundings, for 10 months and 17 days respectively, which is far longer than the few hours to reach thermal equilibrium. *So there appears to be a physical mechanism for storing the negentropy.* What is this?

1.6 Discussion and Second Law

In the above experiments, most visible photons pass through the water because it is transparent. A few interact dynamically with water molecules, which can lower the entropy level locally by the Brittin and Gamow effect (see equation (3) below). Then according to the second law, as the water returns to thermal equilibrium, the entropy should return to the maximum. Pippard said that the second law is not violated under any circumstances [5]. Thus the fleeting kinematic effects of photons could not produce a persistent effect unless

Table 1: Exploratory experiment: Determination of Diffusion Constants and Entropy for water exposed to sunlight and halogen light.

Sample type or difference	χ^2/DF	Diffusion constant $\mu\text{m}^2/\text{sec}$	Entropy S $k_B = 1$	ΔS (signal — control)	$\Delta S/\sigma$ (No. of std. devn.)
Signal 1 = solarized water	1.13	$0.691^{+0.019}_{-0.021}$	$2.732^{+0.014}_{-0.015}$	$-4.7 \pm 0.7\%$	6.5
Control = non-irradiated water	0.91	$0.903^{+0.023}_{-0.026}$	$2.866^{+0.013}_{-0.015}$	—	—
Signal 2 = halogen light water	1.15	$0.701^{+0.020}_{-0.022}$	$2.739^{+0.014}_{-0.016}$	$-4.4 \pm 0.7\%$	6.2
δ = (signal 1 — signal 2)		$\delta = -0.01 \pm .029$			

there is some agency which causes or facilitates this persistence. Without such a mechanism, this persistence violates the second law.

In both experiments above (sunlight and halogen), it is just photons in and photons out. Photons are massless and travel at the speed of light, and cannot combine chemically with water. Therefore we rule out the so-called “memory of water” — see Appendix A for details. The interaction of photons with water is purely dynamical. Assuming that the water molecules move at random, one would expect the reductions in entropy to dissipate as the water returns to equilibrium. But this does not happen in the above experiment. There are two possible types of explanation for this. Either this effect is a property of water (e.g. due to its structure), or it is due to some external agency. It is generally accepted that water has some peculiar properties, some of which may be explained by its structure. Theories of the structure of water are summarised in Appendix B, where it is shown that *they do not explain the phenomena observed*. Therefore these isothermal entropy reductions must persist because there is some external agency which causes them too.

For example, when a magnetic field is applied to a perfect spin gas, the spins become aligned and the entropy decreases. This can occur at constant temperature, in which case both the energy levels and their populations change to correspond to the same Boltzmann distribution for that temperature [17]. In general an isothermal entropy change requires *both* the energy levels and their populations to change. However the above results, whilst they show an isothermal entropy decrease, cannot be so explained because there is no external field to entrain the water molecules. The Earth’s gravity and magnetic fields would not do this, nor did they affect the control. Furthermore we present evidence below and in Appendix B, that the structure of water did not cause this persistence. So we need to find an alternative explanation.

There are two additional possibilities: either this simple experiment *and the others below*, are wrong, or there is something we don’t know about the second law. In order to avoid theoretical bias, we decided to accept the experimental results at their face value and investigate an alternative (theoretical)

solution.

One way to understand the above experiment is in terms of the arrow of time. Eddington noted that entropy tends to increase with time [6]. What happens when photons lower the entropy level, as observed above? Does the Brittin and Gamow effect reverse the arrow of time? There are three possibilities:

1. It does not affect the flow of time, in opposition to Eddington’s hypothesis. Therefore the reduction in entropy would dissipate as the system returned to thermal equilibrium, contrary to the observations.

2. The direction of time is reversed momentarily, probably locally where the photon interacts, but returns to normal after the entropy has been reduced. However, the entropy would then increase as the system returned to equilibrium, contrary to the observations.

3. The direction of time is reversed locally *and this persists*. One possibility is that when a photon interacts, it switches the direction of the flow of time into another space-time, where time flows from the future to the past, if such a space-time exists. In this way, this effect would not violate the second law nor the arrow of time. Furthermore, this second type of space-time could provide the external agency required for this phenomenon to persist.

There is a version of General Relativity which predicts another space *where time flows from the future to the past*. We have discussed this in more detail in the theory paper referred to above [3]. However we give a brief summary here.

1.7 Chronometric Invariant General Relativity

In the 1930s, Landau pointed out that General Relativity is not complete because it does not allow for the Observer’s reference frame [18]. Zelmanov correctly introduced the Observer using chronometric invariants [19, 20]. Borissova and Rabounski have shown that Chronometric Invariant General Relativity (CIGR) requires the existence of a second sector (mirror world) with a second time dimension directed from the future to the past [2, 21, 22]. The mirror world is separated from normal space-time by a membrane with three layers, but

shares the same space as normal space-time. We make the following deductions from this theory:

1. This second time dimension is a macroscopic one.
2. This second time dimension enables entropy levels to decrease with respect to our time, and therefore makes the second law of thermodynamics dual.
3. The membrane between the two worlds consists of 3 layers, 2 layers of photons (1 positive energy on the outside, the other negative on the inside) and a middle layer which is purely spacial with no time dimension, so photons cannot traverse it. It is thus opaque to photons and will reflect or scatter them.

4. We make the hypothesis that light, under certain circumstances, can switch space-time into the mirror world state, by means of the Brittin and Gamow effect, in which *light reduces the entropy level and so reverses the direction of time*. We call this the photo-mirror hypothesis [3].

The persistent decrease in the entropy of water exposed to sunlight and of that exposed to halogen light observed above, are preliminary evidence for the photo-mirror hypothesis.

1.8 Conclusions for Section I: Brownian Motion Experiment

1. Brownian motion has been observed in the above experiments.
2. Sunlight and halogen light both reduced the entropy levels in water by approximately the same amount within the errors. This reduction persisted (for at least 10 months and 17 days respectively), so there appears to be a physical mechanism for storing negentropy in water.
3. Theories of the structure of water do not explain this persistence. Therefore it must be due to some external agency.
4. We deduce that the external agency is probably a second space-time. For example, Chronometric Invariant General Relativity has a second macroscopic time dimension, which is directed from the future to the past.
5. We make the hypothesis that visible light can switch, via the Brittin and Gamow effect (when it lowers the entropy level), the direction of time into mirror space-time. We call this the photo-mirror hypothesis. The rest of this paper is directed to finding more specific evidence for this.

2 Light and Water

Light shining on pure water is a physical system. We decided to look for additional evidence for the Brittin and Gamow effect, for this hypothetical second time dimension and for the photo mirror hypothesis. To do this we exposed HPLC grade water to a 400 watt halogen lamp (1100 lux at surface of the water) and took regular samples for up to 6 days.

2.1 Viscometer Experiment

The statistical error in the exploratory experiment above goes as $1/\sqrt{M}$, where M is the number of observations, which

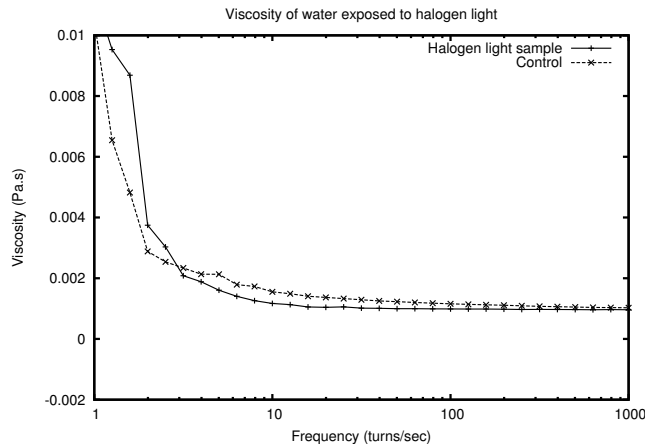


Fig. 2: This rheometer data shows the halogen sample has two components: at low turns per second the viscosity is above the control, and at higher tps it is below the control.

makes it labour intensive to increase the precision. So for $M = 700$ the error is about 4%. There is another equation due to Einstein: $D = RT/6\pi N\eta a$ where R is the gas constant, η is the viscosity, a is the radius of the particle, and N is Avogadro's number; which shows that the diffusion constant D is inversely proportional to the viscosity. The advantage is that viscosity can normally be measured with a precision of about 0.1% using a capillary viscometer (in a constant temperature bath), with a stop watch.

The viscometer used gave precise results for the *untreated* (i.e. not deliberately exposed to light) HPLC grade samples, which agreed with the known viscosity of water at 20° C with a precision of about 0.1% or better, as expected. However, results for all the halogen light *treated* samples tended to be less consistent, even if they had been exposed to halogen light for only a few hours. Repeated measurements of the same halogen light treated sample had a much wider spread, up to five times that for the control (i.e. untreated), despite attention to detail, such as cleansing between samples. (More details of the viscometer technique, are given in the following reference [23].) Despite these larger errors, all the viscosity measurements of treated water were significantly greater than that of untreated pure water, *implying that light lowers the diffusion constant and hence the entropy*, as originally observed. However, there was evidence that irradiated samples had two components, with different viscosities.

2.2 Rheometer Experiment

To investigate this possibility of two components, a sample was exposed to halogen light for 48 hours. Three days later, it was measured using a cone-and-plate rotation rheometer [24]. Distilled water was used as the control. The results are given in Figure 2. Note, the increase in the viscosity of distilled water below 10 turns per second (tps) is an instrumental effect. Nevertheless, the data shows that the water which has been exposed to halogen light, has two components, one with vis-



Fig. 3: The control sample of distilled water, examined using a novel microscope technique. It looks mainly black because there are no “structures” or domains to reflect the light, apart from a bit of noise (e.g. from ambient lighting).

cosity greater than that of the control at low tps, the other with viscosity less than that of the control at higher tps. So the water exposed to halogen light has two components. What are these?

2.3 Theory of light and water

Whilst Brittin and Gamow’s theory (equation 1) is derived from the quantum theory of radiation, it is presented there in terms of the macroscopic energy flow from the Sun to the Earth, and then from the Earth to space. In this experiment, light from a halogen lamp shining onto a bowl of water, consists of individual photons. Water is transparent and so most photons pass straight through, and only occasionally does a photon interact with the water, so that ΔQ is replaced by the energy of that photon $h\nu$:

$$\delta S = \frac{4h\nu}{3} \left(\frac{1}{T_{s/h}} - \frac{1}{T_e} \right). \quad (3)$$

This energy is radiated away by lower energy photons, and there is a small reduction in entropy δS locally in the water. Then by the photo-mirror hypothesis, a small region around this interaction would be switched into the mirror world state. According to CIGR, this will automatically be surrounded by the triple-layer membrane, since the two worlds are separated by this membrane. This enclosed mirror-world region could then persist in the water, because the

momenta of molecules in the mirror state are still positive, and so will balance across the membrane. We will refer to these small mirror-world states as “domains”, or in the case of images or software detection thereof, as “structures” or “sources”.

2.4 Microscope Experiment

In order to make visible these otherwise hidden domains in water, we have used a novel microscope technique developed by Schweitzer [25]. This technique involves first examining the sample with normal illumination to see if it contains any bacteria, dust particles or other impurities. If the sample is clear (as expected for distilled water), then a drop of the water is allowed to evaporate whilst illuminated from the side, approximately orthogonal to the direction of view. When it is about 0.1 mm thick, hidden structures or domains, if present, become visible, provided that the side illumination and other conditions are correct (see Appendix C for details of this technique).

Quite why domains in bulk water are invisible, yet become visible when the thickness is less than about 0.1 mm, is not clear. Perhaps when the water becomes thin enough, the domain membranes become distorted and start to scatter the side illumination. The theory needs to be worked out in more detail. We just report the experimental facts.

Figure 3 shows the results using this technique, for the

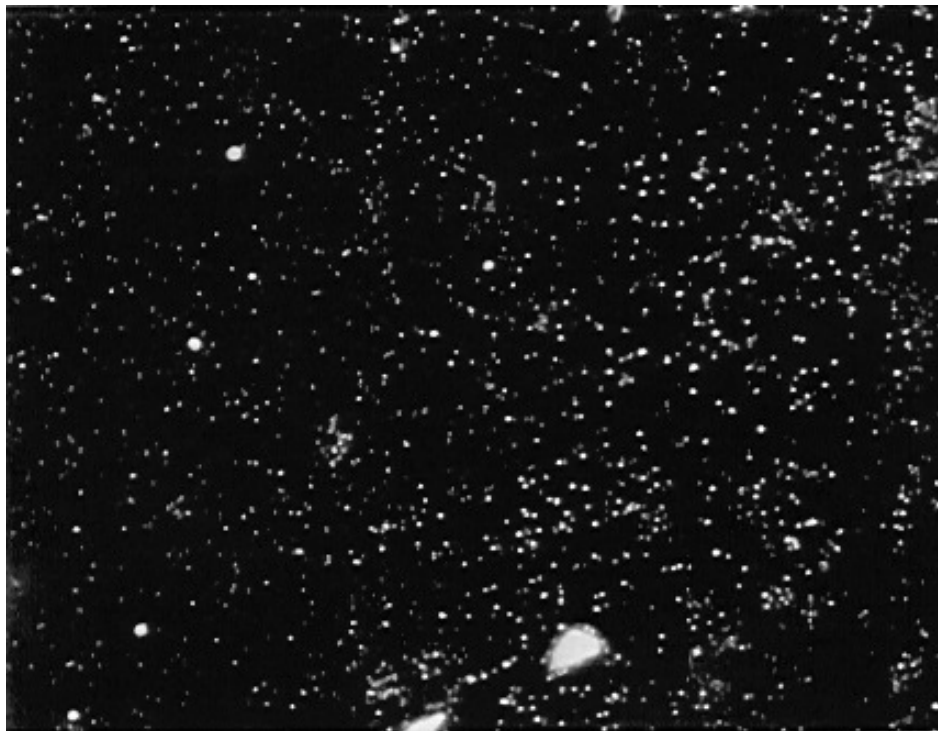


Fig. 4: Hidden domains in water exposed to halogen light for 37.5 hours, revealed by a novel microscope technique using side illumination. These domains are 0.2 to 1.5 microns in size, with a few exceptions.

control sample of distilled water (i.e. not HPLC grade) which has not been deliberately exposed to sunlight nor halogen light (although it may have been exposed to some ambient lighting during the experiment). The process of distillation randomises the water and so breaks up any “structures” or domains, so that this control sample looks mainly black because there are few “structures” or domains to scatter or reflect the light, apart from a bit of “noise”.

Figure 4 shows the first sample, which had been exposed to a 500 Watt halogen lamp for 37.5 hours. Figure 5 shows the second sample which had been exposed to halogen light for 79.5 hours. These are the black and white versions of the original colour CCD images, which are also mainly black and white. There are no signs in the originals, of a range of colours, which could come from diffraction. We conclude that these domains are reflecting or scattering light (from the side illumination) into the microscope. The first image (figure 4) was recorded 20 days after exposure to halogen light, and the second (figure 5) 27 days after exposure. So the effect persists.

2.5 Analysis of Results of Microscope Experiment

In both images there are hundreds of white “sources” which are 0.2 to 1.5 microns across (apart from a few which have started to merge together), *independent of exposure time*. The existence of these 0.2 to 1.5 micron zones in the water suggest that halogen photons have interacted with the water according

to equation (3). If these sources are so produced, then there should be some correlation between their size distribution and the energy spectrum of the photons which produced them. We investigate this and their persistence in more detail below.

These domains look like stars in the night sky, even though they are being observed with a microscope instead of a telescope. The appearance is so similar that we decided to use astronomy software to do pattern recognition on these images [26]. The software was run with the default parameters and found 1288 “sources” in the shorter exposure (figure 4) and 935 in the longer one (figure 5), which is a bit less because of the black regions in that image. The program calculates the isophotal flux which is defined as the sum of the pixel counts above background of all the pixels in a particular “source” ($\sum_{i \in S} p_i$).

The histograms of the isophotal flux, or brightness, for the sources detected in the two images are shown in Figures 6 and 7 respectively, by solid lines. The selection criteria in the software for distinct sources affected the first two bins, so they are excluded. We have also plotted the spectrum of light from the halogen lamp, which has been converted from wavelengths to electron volts [27]. The halogen spectrum (broken line) falls away from the main peak quite quickly down to the secondary peak, and then decreases more slowly after that, matching the two measured brightness distributions well. This suggests the halogen photons have caused these sources. Furthermore, the brightness is independent of the exposure time, being depen-

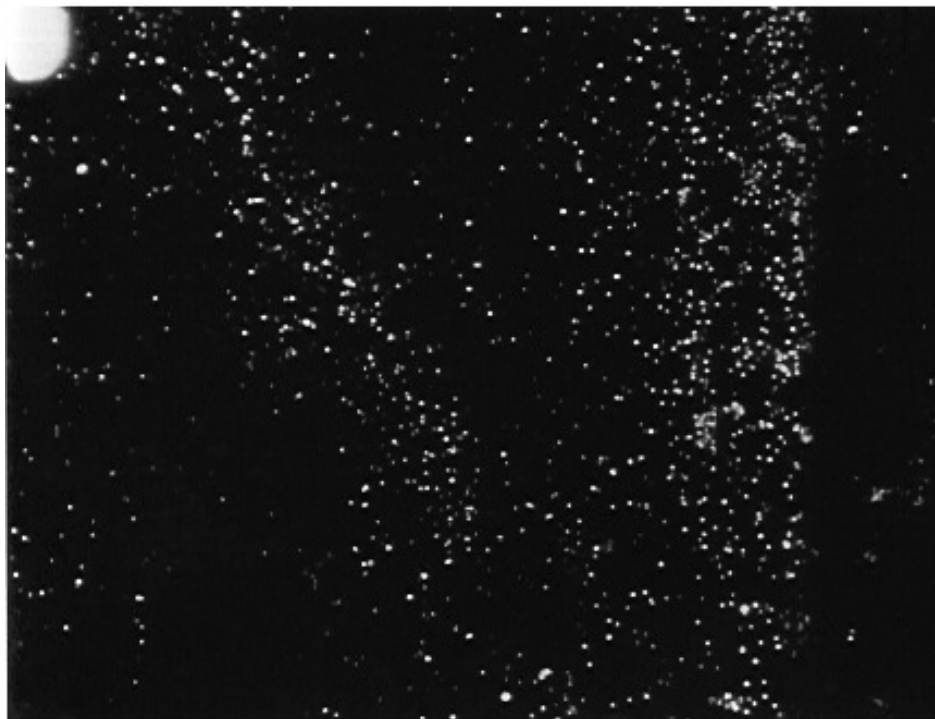


Fig. 5: Hidden domains in water exposed to halogen light for 79.5 hours, revealed by a novel microscope technique using side illumination. These are 0.2 to 1.5 microns in size.

dent on the photon energy, as predicted by equation 3.

We then fitted this spectrum to the data using just three parameters for the least squares fit: an x -axis offset because the photon energy corresponding to zero brightness is about 1.55 eV; an x -axis scaling parameter to convert from electron volts to brightness (counts); and a vertical scaling factor to convert from relative intensity to counts. The chi-squares per degree of freedom are 1.49 and 0.94 in Figures 6 and 7 respectively. So the two brightness distributions have the same shape as the halogen light spectrum, independent of the exposure time, as predicted by equation 3. This confirms that halogen photons have caused these domains via the Brittin and Gamow effect.

The problem with Figure 4 and 5 is that they are pictures. So although we see sources, we do not know if these are produced by the incident halogen photons, or by dust particles, or possibly even bacteria. The advantage of the astronomy software is that enables us to quantify the data and plot the brightness distributions and compare them with the halogen energy spectrum. We see in Figures 6 and 7 that they have almost the same shape, which is confirmed by the fits. Therefore these domains have been produced by halogen photons by the mechanism given in equation 3.

Furthermore, these mirror world domains are correlated with photons whose energies are quantised. Therefore we observe the “quantisation” of regions of water probably in mirror-space-time.

We then combined the two spectra. This is shown in Figure 8 and the chi-square per degree of freedom is 1.67. This is good evidence that the domains are being produced by the photons from the halogen lamp. Nothing material has changed — it is just photons in and photons out. But the state of the water has changed proportionately to the energy of the incident photon, and *the effect persists*.

2.6 Scattering from Surface or Volume of Domains

Do these domains reflect or scatter the side illumination from their surface or from their volume? According to equation 3 the decrease in entropy is proportional to the energy of the interacting photon. If the randomness of water is homogeneous, as one expects from the normal second law of thermodynamics, then the volume of the region generated with this reduced entropy δS will be proportional to the energy of the incident photon. Therefore if scattering is from the volume, then the brightness of these domains will be similar to that of the spectrum from the halogen lamp, as observed above.

However, it is probable that scattering comes from the surface for two reasons. Firstly because bulk water is transparent to the side illumination and appears black (e.g. Figure 3). If it scatters side illumination, then the water has changed in some way, for which there is no explanation, except perhaps CIGR. Secondly CIGR predicts there is a triple layer membrane around these domains which is impenetrable to photons, and therefore the scattering comes from the surface.

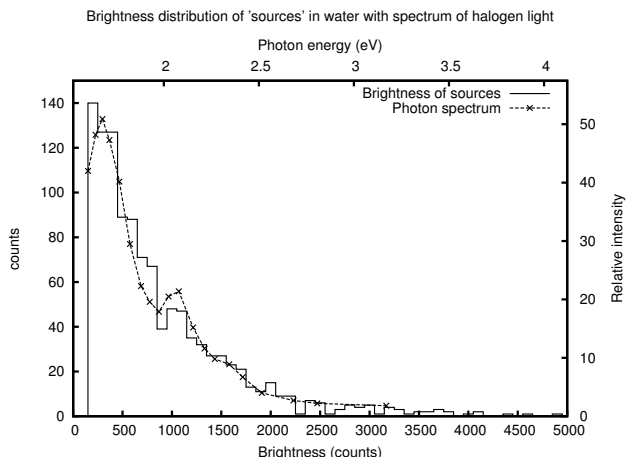


Fig. 6: Brightness distribution after exposure to halogen light for 37.5 hours, plus the spectrum of halogen light in eV. χ^2/DF of fit is 1.49.

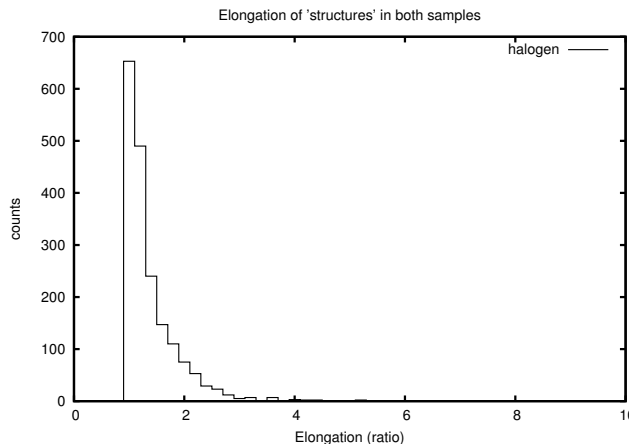


Fig. 9: Histogram of elongation (= major axis/minor axis) for both images.

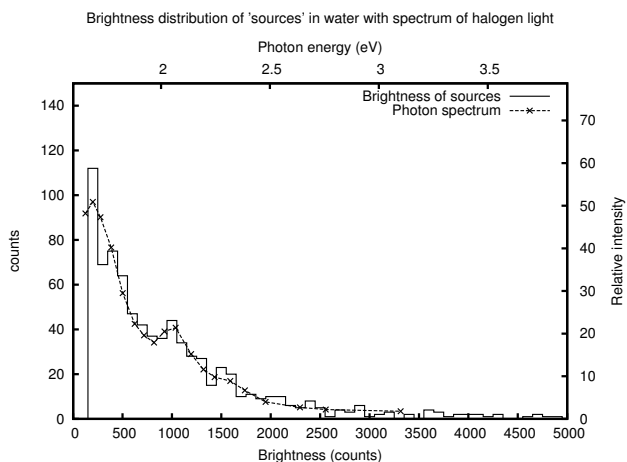


Fig. 7: Brightness distribution after 79.5 hours exposure to halogen light, with halogen spectrum. χ^2/DF of fit is 0.94.

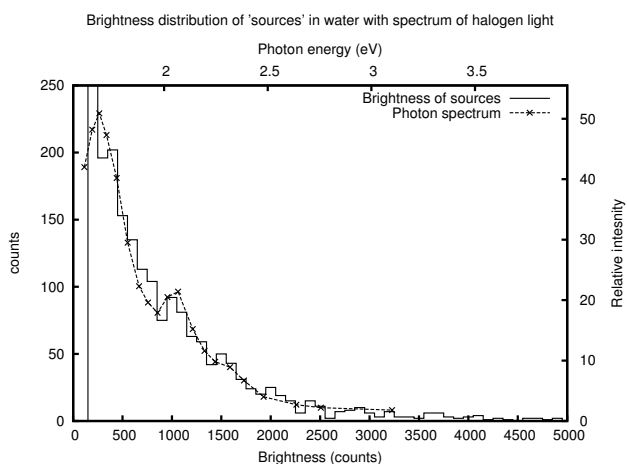


Fig. 8: Combined brightness distributions with halogen spectrum. χ^2 of fit is 1.67.

We investigate the scattering as follows. In the absence of a complete unified theory of CIGR and Quantum Mechanics in water, we reason that these persistent domains probably have a stable shape, such as a spherical one or spheroidal one which is not too elongated. The source extraction software fits an ellipse to each “source” and calculates the major and minor axes, and their ratio, the “elongation”, which is ≥ 1 . The distributions of the elongations for the two images, are very similar, so we have plotted them together in Figure 9. This is quite a narrow distribution: 74% have elongation less than 1.4. So most domains are only slightly elongated, as we expect for stable structures.

We now investigate the brightness distribution for different ranges of elongation El. Figure 10(a) shows the brightness distribution for elongation $El < 1.2$; 10(b) for the elongation in the range 1.2–1.4; and 10(c) for elongation $El \geq 1.4$. We see that the more elongated domains tend to have higher brightness. We have shown above that brighter domains tend to be correlated with more energetic photons. Higher energy photons have higher momenta and will interact over longer distances in the water, and so reduce the entropy level in more elongated regions, as observed. This is evidence for this kinematic effect,

In Figure 10(a) (elongation < 1.2) only 5% of the total, have brightness greater than 1300 counts, whereas in 10(b) 20% have brightness greater than 1300, and in 10(c) 41% have brightness greater than 1300. So brighter domains are there in the data, but hardly any are detected in 10(a) with elongation < 1.2 . Elongated domains must be in this sample, but with their longer axes pointing towards or away from the microscope, so that they do not appear elongated. If these hidden elongated domains were scattering and reflecting side illumination from their volume, then they would show up as brighter domains in 10(a). But they are not there in significant numbers, and so we conclude that they are scattering and/or reflecting the external light source from their surface, as predicted by CIGR.

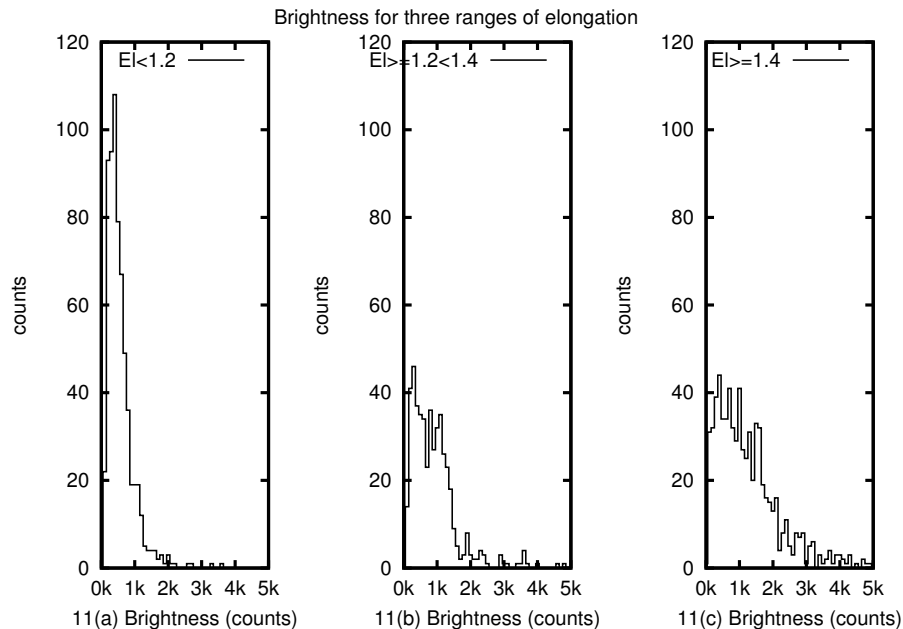


Fig. 10: Brightness distributions for elongation ratio: (a) less than 1.2; (b) in range 1.2-1.4; (c) greater than 1.4. Note the brighter domains are more elongated.

3 Conclusions

In the Brownian motion experiment, we observed reduced entropy levels which persisted, which could not be explained by the structure of water. More details are given in section 1.8: Conclusions for section 1.

We draw the following conclusions from the rheometer and microscope experiments:

1. Light shining on water increases the viscosity and this persists, which confirms the persistent reduction in entropy level previously observed in the exploratory Brownian motion experiment. However the spread in errors is much greater than that for water which has not been significantly exposed to visible light.

2. Measurements with a rheometer provide evidence that light from a halogen lamp produces two components in the water.

3. Water is transparent, so only a small fraction of the photons interact with it. Therefore, it is the small reductions in entropy produced (locally) by the interaction of individual photons (equation 3), which have to be detected,

4. Using a special microscope technique developed by Schweitzer, we have observed hidden domains in water previously exposed to halogen light (0.2 to 1.5 microns in size), which reflect or scatter side illumination, and which persist in time. These domains could be the second component observed in the rheometer experiment above.

5. The brightness distributions of these domains *match the energy spectrum of the halogen lamp well, suggesting that photons have caused these domains.* The brightness distri-

butions are independent of the exposure times (c.f. Figures 6 and 7), as predicted by equation 3. We have previously shown that visible light lowers the entropy level of water. Furthermore, equation 3 predicts that these domains are low entropy regions created by individual photons interacting with the water, and the data confirms this. There are two samples, so this evidence for the Brittin and Gamow effect is reproducible.

6. These reduced entropy states persist for 20 and 27 days respectively, contrary to the normal second law of thermodynamics. The question is, what causes this persistence? Is it the structure of water, or some external agency such as mirror space-time? The most advanced theory of the structure of water at this time is coherent quantum electrodynamics (CQED), which predicts domains of about 100 nm determined by the internal energy levels of water. The domains observed in Figures 4 and 5 are $\times 2$ to $\times 15$ larger, and their brightness distributions shown in Figures 6 and 7, are determined by *the energies of the incident photons*, not the energy levels of water. Therefore they are a different phenomenon from that predicted by CQED. (The significance of this for CQED is discussed in Appendix B.) We therefore need a different theoretical explanation.

7. We conclude that this persistence is caused by some external agency. This could be the second time dimension in the mirror world of CIGR. If this is the case, then the domains will be surrounded by the triple layer membrane which we have predicted will scatter light.

8. We present evidence above that these domains scatter light from their surface (not their volume), which is evidence for the triple-layer membrane around them, predicted

by CIGR. These results are preliminary evidence for the second time dimension of mirror space-time, and the membrane predicted by CIGR.

9. Mirror space-time provides a physical mechanism for storing the negative entropy produced by the Brittin and Gamow effect, hence their persistence. Furthermore, these domains have an “inside” and an “outside” because they are surrounded by the membrane.

10. There is one problem with the above result. We have concluded that there is a second time dimension directed from the future to the past, without any direct evidence. For example, we have not sent a signal from the future to the past. However we have also concluded that the above phenomenon has an “inside” and an “outside”, because of the membrane. Currently our instruments are located on the “outside” and therefore cannot make direct measurements on the “inside”, where the second time dimension is predicted to exist. In the previous paper [3], we have shown that when phenomena occur outside normal 4-D space-time, then they may not be determined completely objectively by experiment. Nevertheless, *if they are reproducible, as above, then they should be considered physically real*. In addition to this, we present experimental evidence for a signal from the future to the past in a separate paper [28].

11. We have thus found evidence for a physical mechanism which reverses the second law of thermodynamics *and creates persistent ordered states*. Note that this occurs outside normal 4-D space-time, so that the second law continues to apply in 4-D space-time.

12. Together these results are evidence for the photo-mirror hypothesis. This effect depends upon Quantum Mechanics and CIGR and so is preliminary evidence for unification (see Appendix D).

3.1 Discussion

In the previous paper [3], we have used the photo-mirror hypothesis to explain the evidence for magnetic monopoles, which are observed only under intense illumination. The independent evidence above for the photo-mirror effect justifies this usage. There are however, two differences. The above results are due to single photons, whereas magnetic monopoles require intense illumination to reveal them. Furthermore, the above domains in water persist, whereas the monopoles disappear rapidly when the illumination is switched off. Both these could be due to the very strong interaction between monopoles. The theory needs to be worked out in more detail.

The chronometric invariant formalism of General Relativity, makes predictions about physically observable quantities which have been confirmed. However, General Relativity does not predict physically observable quantities. For example, it does not predict (as far as the author knows) Galileo’s Principle (that objects with different masses have the same

fall times) nor Newton’s Law of Universal Gravitation. As a result there appear to be two theories of gravitation. Recently, however, the chronometric invariant formalism has been used to predict both Galileo’s Principle and Newton’s Law [29]. So it is the more complete theory.

Furthermore, the evidence presented above for the second time dimension, is evidence for a 5th dimension, so space-time is 5-D (3,2). It is well-known that General Relativity is formulated in 4-D space-time. Therefore it seems to the author (an experimentalist) that the chronometric invariant formalism of General Relativity is actually a new theory, and so deserves its own name. The key point is that putting the Observer into General Relativity has changed the theory so much that the structure of space-time has changed. However this is not for the author to decide, and so for this current series of papers we will continue to refer to chronometric invariant General Relativity (CIGR). But a better name is desirable.

3.2 Predictions

In view of the above evidence for a unified phenomenon (the photo-mirror effect), we make the prediction that Quantum Mechanics can be unified with Chronometric Invariant General Relativity (CIGR), and the standard model embedded within it. The hidden sector of this hypothetical new unified theory would probably be based upon mirror space-time.

We have shown above that water detects individual photons interacting with it precisely, and that this can be explained by mirror space time. In effect the above techniques open a window into another world. We make the prediction that water is sensitive to other unusual phenomena occurring in mirror space-time. For example, it is possible that water can be used to detect some other new type of radiation which lowers entropy levels, if it exists [23].

Without mechanism(s) for the creation and storage of order, there can be no complexity [14]. So the above evidence for a mechanism for the creation of order, and a mechanism for its storage, is possibly the beginning of a theory of complexity, based on fundamental physics. The theory needs to be worked out in more detail.

The incorporation of the Observer into General Relativity (i.e. CIGR) requires a second time dimension, which automatically includes thermodynamics and complexity. Since these have been left out of many unified theories in the past, the unification of Quantum Mechanics with CIGR may well be the way to successful unification. The evidence for magnetic monopoles in mirror space-time [3], and for a new type of radiation in sunlight [23], support this conclusion.

4 Limitations

CIGR has not yet been properly unified with Quantum Mechanics yet, and so this may change some of its predictions, and clarify some of the details above.

Acknowledgements

We thank David Schweitzer for developing this microscope technique, for making measurements of samples we supplied, and providing the photo micrographs of same commercially. We also thank E. Bertin for making the astronomical source extraction software available via open source. We thank Brian Josephson for suggesting we do research into the physics of water as a detector. No Data is associated with this manuscript.

Appendix A: The “Memory of Water”

For completeness we mention the following. Some readers may think that the persistent effects observed above are due to the phenomenon known as the “memory of water”. This may occur when a chemical substance is dissolved in water and then is serially diluted. However, there is no accepted explanation for this latter phenomenon, and so it is disputed. In the above experiments, photons are massless, and cannot be “dissolved” in water. Their interaction is purely dynamical. Nor was anything diluted — it is not even clear how one can dilute pure water. Therefore the above experiment of light shining on water, is investigating a completely different phenomenon from the “memory of water”.

That being said, it is possible that mirror space-time may play a role in explaining the “memory of water”. It is just that the structure of matter (e.g. the solute) is more complex than that of a photon, and its interaction with water also more complex. Therefore the phenomena of photons interacting with water reported in this paper, are different from the “memory of water”.

Appendix B: Theories of Structure of Water

In the various experiments above, it is just photons in and photons out. So how can the decrease in entropy persist, if the water molecules move at random? This raises questions about the structure of water, so we consider theories of this. In 1891 Roentgen suggested that as ice melts, many of the less dense (ice floats) tetrahedral “ice molecules” persist intact in the liquid water as it warms. In this way, he tried to explain one of its more peculiar properties, namely that the density of water increases as its temperature is raised from 0° to a maximum at 4° C [30]. This approach was rejected by Bernal and Fowler for quantum mechanical reasons [31].

Another peculiarity of water is that in addition to the normal chemical bonds, water molecules also interact by the hydrogen bond, which is weaker and directional. Preparata states this is phenomenological in origin [32]. In 1950 Pople presented a quantum mechanical theory of the structure of water [33]. In 1951, Lennard-Jones and Pople showed that there may be a network of hydrogen bonds linking all the molecules together into one large molecule $(\text{H}_2\text{O})_n$ [34]. The problem is that the water molecules move around and the hydrogen bonds, which are highly directional, make or break af-

ter a few picoseconds [35]. As the bonds make or break fluctuating EM fields are produced, and there is also the Earth’s magnetic field, both of which Quantum Mechanics ignores, but quantum electrodynamics (QED) does not.

Preparata and del Giudice have solved the equations of QED for bulk matter and applied it to liquids, solids and water in particular [36]. This theory *replaces* the static picture of chemical bonds linking individual molecules together (“electrostatic meccano” or “erector set”), *with a dynamical interaction between groups of molecules spread over larger distances*. This theory, often referred to a coherent QED or CQED, is a new theory of condensed matter. Their approach is to consider water not to be “molten ice” but “condensed vapour” [37]. When this theory is applied to water, they find that the water molecules form two groups: coherent domains in which the molecules oscillate between the ground state and an excited state, and interstitial water which is random and surrounds these domains.

They predict that the excited state is at 12.07 eV (in the UV region), which produces domains of about 100 nm in extent, and that the radiation is trapped in these domains [38]. Enz agrees that the coherent domains probably exist, but questions whether their boundaries are precisely defined, so the radiation may not be completely trapped [39]. Whilst this theory explains a number of indirect experimental results, there has not been any direct experimental confirmation of these domains in water, nor has any UV radiation been detected leaking out. Therefore this theory has not been proven strictly to be correct.

Furthermore, the results of the experiments above, do not provide any direct evidence to support this theory. For example, Figure 3 does not show any sign of the predicted 100 nm domains in the control sample of distilled water (condensed from vapour). But the microscope experiment was not designed to detect these and so the resolution may not have been good enough. Instead, the domains observed in Figures 4 and 5 are $\times 2$ to $\times 15$ times larger. Furthermore *their size distribution is determined by the energies of the incident photons, not by the internal energy levels of water*. So the phenomena observed are completely different from those predicted by CQED. But this does not necessarily rule out CQED.

CQED predicts coherent domains surrounded by interstitial water which is random. If an incident photon, with an energy of 1 to 3 eV, interacts with a coherent domain of $\approx 10^7$ water molecules oscillating between the ground state and 12.07 eV, then it might be scattered away with little effect on the entropy of that 100 nm domain. However, if it interacts with the interstitial water, then it could lower the entropy level by the Brittin and Gamow effect. *But that reduction would not persist because the interstitial water is random. So even if this is the correct theory of water, then mirror space-time of CIGR is required to explain the observed results*.

Whilst these results do not prove CQED wrong, it does not provide any support for it. Furthermore CQED is clearly

incomplete because it does not include the mirror space-time of CIGR. In fact it is likely that the correct theory of water will be based upon Quantum Mechanics unified with CIGR.

Appendix C: Details of Microscope Technique

The microscope technique used to take the black and white images shown above, was developed by David Schweitzer. The technique requires a good quality high-powered microscope (e.g. a Nikon optifot), with a phase contrast lens and dark filter, a light source, fluorescence adaptor, video camera with CCD image sensor, computer with video card, software and printer. The technique involves first examining the sample with normal illumination to see if it contains any bacteria, dust particles or other impurities. If the sample is clear, as expected for distilled water, then a drop of the water is placed onto a microscope slide and allowed to evaporate at ambient temperature. (If the rate of evaporation is too slow, a gentle source of heat may be applied.) Whilst it is evaporating, it is illuminated horizontally from the side (we call this “side illumination”), the temperature of the light source is adjusted (a reddish white light was used), and it is observed vertically from above. (NB This is not the same as dark-field microscopy.) Schweitzer has found that if there are hidden “structures” present in the water, then these reflect light and become visible when the thickness of the water film has decreased to about 0.1 mm (possibly because of distortion), and the illumination, magnification and other settings are correct. The images shown above, were taken with the solarizing filter phase contrast 4, the Table tilted by 1.95° and microscope magnification of $\times 1000$.

The random walk (Brownian motion) experiment at the beginning of this paper and the black and white images were all obtained using distilled water and exposure was to a 500 watt halogen lamp at 80 cms, which gave 1100 lux at the surface of the water. The viscosity measurements were made with HPLC grade water and a 400 watt halogen lamp (equivalent to 500 watts) also at 80 cms. The software used for the pattern recognition and source extraction was SExtractor version 2.25.0 by E. Bertin.

Appendix D: Unification

“Unification” is a project in physics which dates back to Einstein, who was convinced there is one set of equations which describe the whole Universe. So he spent the last 30 years of his life trying to unify the two main theories of physics, Quantum Mechanics and General Relativity, in order to develop the final theory. However the process of unification dates from before Einstein. For example before Newton’s theory of gravity, it was thought that the laws of motion of a projectile through the air above the Earth’s surface, were different from those of planets in the heavens. Newton’s theory provided a unified explanation of terrestrial and celestial gravitation. (Note that the derivation of Newton’s the-

ory from CIGR, mentioned above, links CIGR to this first step towards unification.) Then before Maxwell, electricity and magnetism were thought to be completely different phenomena. Maxwell’s equations unified the two into electromagnetism. After Einstein in the 1960s, electromagnetism was unified with the weak nuclear interaction (which causes beta-decay) in the electro-weak interaction, which led to the discovery of the W- and Z-bosons.

However, the unification of General Relativity and Quantum Mechanics has stalled, despite herculean efforts (e.g. quantum gravity; string theory; loop quantum gravity, and so on) [40]. In a sense the problem is simple. Quantum mechanics is a “digital” theory of ultra-small phenomena, whilst General Relativity is an analogue theory of large scale phenomena. About the only place where the two might come together is at the event horizon of a black hole, which cannot be easily studied in the laboratory. However, putting the Observer into General Relativity introduces low energy, small scale phenomena, such as thermodynamics, where CIGR and Quantum Mechanics can come together. The above evidence for the photo-mirror effect is highly significant, because it depends upon Quantum Mechanics and CIGR, and so is experimental evidence for unification.

Submitted on November 28, 2024

References

1. Zelmanov A.L. Chronometric invariants and the accompanying frames of reference in the General Theory of Relativity. *Soviet Physics Doklady*, 1956, v. 1, 227–230.
2. Borissova L. and Rabounski D. Fields, Vacuum, and the Mirror Universe. The 3rd revised edition, New Scientific Frontiers, London, 2023 (the 1st ed. published in 2001), Chapters 1 and 6.
3. Ellis R.J. Evidence for Phenomena, including Magnetic Monopoles, Beyond 4-D Space-Time, and Theory Thereof. doi:10.5281/zenodo.7344117; arXiv: 2207.04916.
4. Gell-Mann M. Some lessons from sixty years of theorising. *Int. J. Mod. Phys. A*, 2010, v. 25 (20), 3857–3861.
5. Pippard A.B. Elements of Chemical Thermodynamics for Advanced Students of Physics. Cambridge University Press, 1960, p. 100.
6. Eddington A.S. The Nature of the Physical World. Cambridge University Press, 1928.
7. Carnot S. Réflexions sur la puissance motrice du feu et sur les machines propres à développer cette puissance (Reflections on the Motive Power of Fire and on Machines Fitted to Develop that Power), Bachelier, Paris, 1824.
8. Clausius R. *Annalen der Physik und Chemie*, 1854, v.93 (12), 481–506.
9. Capek V. and Sheenan D. On Challenges to the Second Law of Thermodynamics: Theory and Experiment. Springer, Berlin/Heidelberg, 2005; Special Issue: Quantum Limits to the Second Law of Thermodynamics, *Entropy*, March 2004, v. 6 (1), 1–232; First Int. Conf. on Quantum Limits to the Second Law, *AIP Conf. Proc.*, 2002, v. 643 (1), 3–500; Second law of Thermodynamics: Status and Challenges, *AIP Conf. Proc.*, v. 1411 (1), 1–356.
10. Boltzmann L. *Wissenschaftliche Abhandlungen*, v. I, II and III, Barth, Leipzig, 1909; reissued, Chelsea, New York, 1969; Flamm D. Ludwig Boltzmann — A Pioneer of Modern Physics. arxiv: physics/9710007; Transl. of L. Boltzmann’s paper “On the Relationship between the Second Fundamental Theorem of the Mechanical Theory of Heat and

- Probability Calculations Regarding the Conditions for Thermal Equilibrium”, *Sitzungber. Kais. Akad. Wiss. Wien Math. Naturwiss. Classe*, 1877, v. 76, 373–435, by K. Sharp and F. Matschinsky, *Entropy*, 2015, v. 17(4), 1971–3009.
11. Schrödinger E. *What is Life?* Cambridge University Press, 1944.
 12. Prigogine I. *Bull. Acad. Roy. Belg. Cl. Sci.*, 1945, v. 31, 600; see also Nicolis G. and Prigogine I. *Self-Organization in Nonequilibrium Systems*. John Wiley and Sons, New York, 1977.
 13. Brittin W. and Gamow G. Negative entropy and photosynthesis. *Proc. of the Nat. Acad. of Sciences*, 1961, v. 47, 724. N.B. There is a sign error in equation (14) in this reference, which has been corrected.
 14. Gell-Mann M. What is complexity? *Complexity*, 1995, v. 1(1), 16–19.
 15. Einstein A. *Annalen der Physik*, 1906, v. 19, 289.
 16. Ming Chen Wang and Uhlenbeck G.E. *Rev. Mod. Phys.*, 1945, v. 17, 323–342.
 17. Careri G. *Order and Disorder in Matter*. Benjamin/Cummings, CA, 1984, Chapter 1, Box 1.E.
 18. Landau L.D. and Lifshitz E.M. *The Classical Theory of Fields*. The 4th final edition, Butterworth-Heinemann, 1980.
 19. Zelmanov A.L. Chronometric invariants and the accompanying frames of reference in the General Theory of Relativity. *Soviet Physics Doklady*, 1956, v. 1, 227–230; Zelmanov A.L. On the relativistic theory of an anisotropic in-homogeneous Universe. *Proc. of 6th Soviet Conf. on the Problems of Cosmogony*, Nauka, Moscow, 1959, 144–174 (in Russian), see English transl. in *The Abraham Zelmanov Journal*, 2008, v. 1, 33–63.
 20. Zelmanov A.L. *Chronometric Invariants*. English transl. of the 1944 Dissertation, Am. Res. Press, Rehoboth, 2006.
 21. Borissova L. and Smarandache F. Positive, neutral and negative mass-charges in General Relativity. *Progress in Physics*, 2006, v. 2(3), 51–54.
 22. Rabounski D. and Borissova D. Physical observables in General Relativity and the Zelmanov chronometric invariants. *Progress in Physics*, 2023, v. 19(1), 3–29.
 23. Ellis R.J. Preliminary evidence for a new type of radiation in sunlight. doi:10.5281/zenodo.7347703.
 24. Maxwell T. National Physical Laboratory, Teddington, UK.
 25. David Schweitzer, private researcher, London, UK.
 26. Ishamir L. and Johnston K. recommended SExtractor by E. Bertin, and AstroimageJ.
 27. <http://www.mtholyoke.edu/~mpeterso/classes/~phys301/projects2001/awgachor/awgachor.htm>
 28. Ellis R.J. A new approach to unification: the living universe hypothesis. doi:10.5281/zenodo.11478276.
 29. Borissova L. and Rabounski D. Galileo’s Principle and the origin of gravitation according to General Relativity. *Progress in Physics*, 2024, v. 20(2), 69–78.
 30. Roentgen W.C. Ice and water molecules. *Wied. Ann.*, 1891, v. 45, 91.
 31. Bernal J.D. and Fowler R.H. *J. Chem. Phys.*, 1933, v. 1, 515.
 32. Preparata G. *QED Coherence in Matter*. World Scientific, Singapore, 1995, p. 196.
 33. Pople J.A. A theory of the structure of water. *Proc. Roy. Soc. (London)*, 1950, v. A202, 323; *ibid.* 1951, v. A205, 163; *J. Chem. Phys.*, 1953, v. 21, 2234.
 34. Lennard-Jones J. and Pople J.A. Molecular association in liquids. *Proc. Roy. Soc. (London)*, 1951, v. A205, 155.
 35. Bertolini D. et al. *J. Chem. Phys.*, 1989, v. 91, 1179–1190; Fernandez-Serra M.V. and Artacho E. [arxiv.org: cond-mat/05073193](https://arxiv.org/abs/cond-mat/05073193).
 36. Preparata G. *QED Coherence in Matter*. World Scientific, Singapore, 1995, see Chapter 10.
 37. Bono I., Del Giudice E., Gamberale L., and Henry M. Emergence of the coherent structure of liquid water. *Water*, 2012, v. 4, 510–532.
 38. Arani R., Bono I., Del Giudice E., and Preparata G. QED coherence and the thermodynamics of water. *Int. J. Mod. Phys. B*, 1995, v. 9, 1813–1841.
 39. Enz C.P. *Helv. Phys. Acta*, 1997, v. 70, 141.
 40. Smolin L. *The Trouble with Physics: The Rise of String Theory, the Fall of a Science, and What Comes Next*. Houghton Mifflin, Boston, N.Y., 2006.

PROGRESS IN PHYSICS

An international scientific journal on advanced studies in theoretical and experimental physics, including related themes from mathematics and astronomy. This journal is registered with the Library of Congress (DC, USA).

Electronic version of this journal:
<http://progress-in-physics.com>

Editorial Board

Dmitri Rabounski
Editor-in-Chief
rabounski@yahoo.com
Pierre Millette
pierremillette@sympatico.ca
Andreas Ries
andreasries@yahoo.com
Florentin Smarandache
fsmarandache@gmail.com
Larissa Borissova
lborissova@yahoo.com
Ebenezer Chifu
ebenechifu@yahoo.com

Postal Address

Department of Mathematics and Science,
University of New Mexico,
705 Gurley Ave., Gallup, NM 87301, USA

Copyright © *Progress in Physics*, 2024

All rights reserved. The authors of the articles do hereby grant *Progress in Physics* non-exclusive, worldwide, royalty-free license to publish and distribute the articles in accordance with the Budapest Open Initiative: this means that electronic copying, distribution and printing of both full-size version of the journal and the individual papers published therein for non-commercial, academic or individual use can be made by any user without permission or charge. The authors of the articles published in *Progress in Physics* retain their rights to use this journal as a whole or any part of it in any other publications and in any way they see fit. Any part of *Progress in Physics* howsoever used in other publications must include an appropriate citation of this journal.

This journal is powered by L^AT_EX

A variety of books can be downloaded free from the Digital Library of Science:
<http://fs.unm.edu/ScienceLibrary.htm>

ISSN: 1555-5534 (print)
ISSN: 1555-5615 (online)

Standard Address Number: 297-5092
Printed in the United States of America

December 2024

Vol. 20, Issue 3

SPECIAL ISSUE

Physical Factors of the Historical Process

CONTENTS

Chizhevsky A. L. Physical Factors of the Historical Process	3
Summary	4
Introduction	5
I. Social activities and general influence of the Sun	8
II. On the relationship between the periodic activity of the Sun and the synchronous periodicity of the oscillations of the world-historical process	14
III. Social and psychological characteristics of one complete historical cycle	25
Period I of the historiometric cycle (minimum excitability)	26
Period II of the historiometric cycle (increasing excitability)	26
Period III of the historiometric cycle (maximum excitability)	27
Period IV of the historiometric cycle (decreasing excitability)	34
IV. The influence of geophysical and cosmic factors on the behaviour of individuals and groups of people	37
V. Prospects and conclusion	41

Information for Authors

Progress in Physics has been created for rapid publications on advanced studies in theoretical and experimental physics, including related themes from mathematics and astronomy. All submitted papers should be professional, in good English, containing a brief review of a problem and obtained results.

All submissions should be designed in L^AT_EX format using *Progress in Physics* template. This template can be downloaded from *Progress in Physics* home page <http://www.ptep-online.com>

Preliminary, authors may submit papers in PDF format. If the paper is accepted, authors can manage L^AT_EX typing. Do not send MS Word documents, please: we do not use this software, so unable to read this file format. Incorrectly formatted papers (i.e. not L^AT_EX with the template) will not be accepted for publication. Those authors who are unable to prepare their submissions in L^AT_EX format can apply to a third-party payable service for LaTeX typing. Our personnel work voluntarily. Authors must assist by conforming to this policy, to make the publication process as easy and fast as possible.

Abstract and the necessary information about author(s) should be included into the papers. To submit a paper, mail the file(s) to the Editor-in-Chief.

All submitted papers should be as brief as possible. Short articles are preferable. Large papers can also be considered. Letters related to the publications in the journal or to the events among the science community can be applied to the section *Letters to Progress in Physics*.

All that has been accepted for the online issue of *Progress in Physics* is printed in the paper version of the journal. To order printed issues, contact the Editors.

Authors retain their rights to use their papers published in *Progress in Physics* as a whole or any part of it in any other publications and in any way they see fit. This copyright agreement shall remain valid even if the authors transfer copyright of their published papers to another party.

Electronic copies of all papers published in *Progress in Physics* are available for free download, copying, and re-distribution, according to the copyright agreement printed on the titlepage of each issue of the journal. This copyright agreement follows the *Budapest Open Initiative* and the *Creative Commons Attribution-Noncommercial-No Derivative Works 2.5 License* declaring that electronic copies of such books and journals should always be accessed for reading, download, and copying for any person, and free of charge.

Consideration and review process does not require any payment from the side of the submitters. Nevertheless the authors of accepted papers are requested to pay the page charges. *Progress in Physics* is a non-profit/academic journal: money collected from the authors cover the cost of printing and distribution of the annual volumes of the journal along the major academic/university libraries of the world. (Look for the current author fee in the online version of *Progress in Physics*.)

Physical Factors of the Historical Process

Alexander L. Chizhevsky*

The influence of cosmic factors on the behaviour of organized human masses and on the course of the world-historical process, beginning from the 5th century B.C. and until the present time. This is a short presentation of my research and theory.

*Translated from Chizhevsky A.L. *Physical Factors of the Historical Process*. Kaluga, 1924, 72 pages (in Russian).



Alexander L. Chizhevsky, NY, 1920s

Alexander L. Chizhevsky (1897–1964), also spelled as “Tchijevsky”, was born into a noble Russian family having close relatives among the English, Italian, French and German aristocracy. He was born in Poland, where his father, a Major General of artillery, served in the Russian Royal Army. From his childhood, Chizhevsky was free in English, Italian, French and German (which were the native languages of his aristocratic relatives). Similarly to many young men of that time, he volunteered as a private for World War I, but months later he was demobilized after being wounded in Galicia and awarded the St. George Military Cross of the 4th degree.

Alexander Chizhevsky is known as the discoverer of the effect of solar flares and geomagnetic storms on the human organism, and also the founder of *heliobiology* — the science revealing solar-terrestrial connexions. The presented article is his groundbreaking work on this topic. This is his Doctor of Sciences dissertation, defended by him in 1918 at Moscow University (at the age of 21). This is his main scientific study, which he then expanded and updated with new scientific results throughout his subsequent life. Two decades later, in 1938, he published an extensive “update” of this research in the form of a monograph (3.5 times larger in volume than the first edition of 1924), written by him in French, which was the international language of communication among scientists in those years: *Les épidémies et les perturbations électromagnétiques du milieu extérieur* (Ed. Hippocrate, Paris, 1938, 238 pages).

Chizhevsky’s research was inspired and then reinforced by the discoveries of business cycles linked to solar activity cycles, such as, for example, the 7–11-year investment cycle (Clément Juglar, 1862), the 40-month “inventory” business cycle (Joseph Kitchin, 1923), the 50–60-year cycle of economic booms and depressions (Nikolai Kondratiev, 1925) and 15–25 year waves of infrastructural investment and demographic activity (Simon Kuznets, 1930). Edward Dewey in his 1930–1940s works proved that the entire USA economy, including agriculture, industry, trade, banking, stock exchange, etc., is driven by the mentioned four business cycles (which are

the result of the interference of solar activity cycles).

Based on extensive empirical data from the last thousand years, Chizhevsky proved that all types of social activity (culture, economy, military conflicts and even epidemics) are conditioned by a complex system of solar activity cycles, such as cycles of sunspots, solar flares, etc. This conclusion was later extended by other researchers to long-term cycles in climatology, using data from dendrochronology and radiocarbon analysis. Later, in his studies in the 1950s, Chizhevsky showed that the planets of the Solar System (including the Earth) are in the state of intracellular organs (organelles), while the Sun functions as the cell nucleus.

In the mid-1920s, Chizhevsky left the USSR for Europe, and then for several years in the USA. He was a visiting lecturer at Columbia University in New York, where he met Simon Kuznets (1901–1985), who was also born in Russia; he was sent by the communist government to New York in 1922 to “study the economics of capitalism”, but then refused to return to the USSR. Chizhevsky’s lectures were highly popular among scientists of that time. Simon Kuznets tried to convince him not to return to the USSR and to stay in New York. Svante Arrhenius (1859–1927), the famous Swedish physicist and chemist, told him the same; he offered an academic position to him and to stay in Sweden. But Chizhevsky did not listen to them, because he was sure in his influence and authority, which he had in the USSR. He returned to the USSR, where he headed a personal research laboratory and continued his studies.

However, fate decreed his life differently than he thought. His high-ranking patrons among the USSR officials disappeared one after another in the waves of the Stalin repressions. In 1933, his scientific work was banned in the USSR, and in 1936 his laboratory was closed. In 1939 he was elected Honorary President of the First International Congress on Biophysics in New York, but was unable to travel due to the Iron Curtain covering the USSR. In 1942, he was arrested and sentenced to 8 years in the GULAG camps for anti-Soviet propaganda (in private conversations, he compared his luxurious life in Europe and New York to his impoverished life in the USSR). He was released in 1950 and lived in exile in Kazakhstan until 1958, when he was allowed to return to Moscow. His health was severely undermined by the years he spent in the prisoner camps and his poor heart stopped beating five years later in 1964, when he was at the age of 67.

Later, in 1971, Simon Kuznets (USA) awarded the Nobel Prize in Economic Sciences for his aforementioned discovery in economics, which was directly connected with Chizhevsky’s research.

Here we publish the first complete English translation of this fundamental study by Chizhevsky, performed by me without any omissions or shortenings, in contrast to the very concise English translation published over fifty years ago in the journal *Cycles* (Jan. 1971, 11–27). I have committed myself to do this translation, because French as the language of international communication among scientists was replaced by English in the 1940s, and therefore most contemporary scientists cannot read Chizhevsky’s fundamental monograph published in 1938 in Paris (except for native French speakers, who are not many). My very short corrections to the text are enclosed in square brackets.

We publish here this complete English translation on the 100th anniversary of the first edition of Chizhevsky’s book (1924), from which I made this translation, i.e., we publish it in 2024, which is the year of maximum solar activity. — Editor’s remark, D.R.

Summary

The principles of modern natural science have urged me to investigate whether there did not exist a correlation between the more important phenomena of Nature and events in the social-historical life of Mankind. In this direction, beginning in the year 1915, I have performed a number of researches, but at present I am submitting to the public only those which are directed towards determining the connexion between the periodical sunspot activity and 1) the behaviour of organised human masses and 2) the world historical process.

The following facts are based upon statistics gathered by me while submitting to a minute scrutiny the history of all the peoples and states known to science, beginning with the 5th century B.C. and ending with the present day.

1. As soon as the sunspot activity approaches its maximum, the number of important mass historical events, taken as a whole, increases, approaching its maximum during the sunspot maximum and decreasing to its minimum during the epochs of the sunspot minimum.

2. In each century the rise of the synchronic universal military and political activity on the whole of the Earth's territory is observed exactly 9 times. This circumstance enables us to reckon that a cycle of universal human activity embraces 11 years (in the arithmetical mean); see Fig. 2, Fig. 3 and Fig. 4, and also the historiometric cycle (Table 1).

3. Each cycle according to its historical psychological signs is divided into 4 parts (periods):

- I. Minimum of excitability 3 years;
- II. Growth of excitability 2 years;
- III. Maximum of excitability 3 years;
- VI. Decline of excitability 3 years.

The number of historical events in each cycle are distributed approximately according to the data for 500 years (15th–20th centuries) in the following manner (in the mean); see Fig. 1 for details:

- Period I 5%;
- Period II 20%;
- Period III 60%;
- Period IV 15%.

4. The course and development of each lengthy historical event is subject to fluctuations (periods of activity and inactivity) in direct dependence upon the periodical fluctuations occurring in the Sun's activity. Formula: the state of predisposition of collective bodies towards action is a function of the sunspot periodical activity.

5. Episodical leaps or rises in the Sun's activity, given the existence in human societies of politico-economical and other exciting factors, are capable of calling forth a synchronic rising in human collective bodies. Formula: the rising of the sunspot activity transforms the people's potential energy into kinetic energy; see Fig. 5.

My studies in the field of synthesizing historical material

have enabled me to determine the following morphological law of the historical process:

6. The course of the world historical process is composed of an uninterrupted row of cycles, occupying a period equaling in the arithmetical mean 11 years and synchronizing in the degree of its military-political activity with the sunspot activity. Each cycle possesses the following historio-psychological peculiarities:

a. In the middle points of the cycle's course the mass activity of humanity all over the surface of the Earth, given the presence in human societies of economical, political or military exciting factors, reaches the maximum tension, manifesting itself in psychomotoric pandemics: revolutions, insurrections, expeditions, migrations etc., creating new formations in the existence of separate states and new historical epochs in the life of humanity. It is accompanied by an integration of the masses, a full expression of their activity and a form of government consisting of a majority.

b. In the extreme points of the cycle's course the tension of the all-human military political activity falls to the minimum, ceding the way to creative activity and is accompanied by a general decrease of military or political enthusiasm, by peace and peaceful creative work in the field of state organizations, international relations, science and art, with a pronounced tendency towards absolutism in the governing powers and a disintegration of the masses. See Table 4.

7. The correlation with the sunspot maximum stand:

a. The dissemination of different doctrines political, religious etc., the spreading of heresies, religious riots, pilgrimages etc.

b. The appearance of social, military and religious leaders, reformators etc.

c. The formation of political, military, religious and commercial corporations, associations, unions, leagues, sects, companies etc.

8. It is impossible to overlook the fact, that pathological epidemics also coincide very frequently with the sunspot maximum periods (see Table 3).

9. Thus the existence of a dependence between the sunspot activity and the behaviour of humanity should be considered established.

One cycle of the all-human activity is taken by me for the first measuring unit of the historical process. The science concerned with investigating the historical phenomena from the above point of view I have named historiometria.

At present I am working on a plan of organizing scientific institutes for determining the influence of cosmic and geophysical factors upon the condition of the psychics of individuals and collective bodies, and devising a working method for them.

November, 1922

A. Chizhevsky

Dedicated to the memory
of the astronomer
Rudolf Wolf (1816–1893)

Social evolution proceeds under the direct influence of various economic, political and natural factors.

While the most serious attention has been paid to the detailed clarification of the laws of economics and politics, the study of the influence of natural factors has not received the necessary development.

Our work targets to reveal the rôle of some natural factors in the social movements of human groups.

This paper presents a brief and generally accessible extract from a special study of the influence of a powerful cosmic factor — periodic sunspot activity on the behaviour of organized masses and on the course of the world-historical process.

Introduction

With rare exceptions, in the entire history of Mankind we will not find facts of clear foresight by historical figures of the immediate future of their peoples and states or the final results of wars and revolutions. Historical events, when completed, always gave results different from those that were assumed at their origin. It seemed that what people and entire communities were striving for or wishing for was not what they turned out to be. Throughout its centuries-old culture, accompanied by the gradual development of the exact sciences, humanity has not clarified a single law according to which this or that historical phenomenon or event should proceed. True, the diversity of reactions to identical stimuli in human communities and the heterogeneity of responses to identical stimuli in the historical life of Mankind forced us to assume that chaos lies at the foundations of the fates of history, and the distribution of events in space and time is not subject to any laws.

This view was equally extended to short periods of history, to individual events — wars or revolutions, and to entire epochs, centuries and millennia, embracing human cultures and civilizations. Only the comparative method, applied to the study of history, has recently made some progress in the field of proving the opposite. The true rôle of the comparative method lies in the discovery of commonalities in the development of various historical events and in the discovery of precise rules for this development. Historians have succeeded in showing that both individual events of a more or less similar nature and long historical epochs have many identical features in their progressive movement; in other words, the events of history repeat themselves, which allows us to make appropriate generalizations (K. Lamprecht, O. Spengler). It is not for nothing that J. de Condorcet (1743–1794), in his famous work *Esquisse d'un tableau historique des progrès de l'esprit humain*, insisted on creating a hypothetical history of a single people by selecting facts from the history of all peoples and bringing them closer together.

History, until the present time, has, in all fairness, been more often recognized as a kind of knowledge than as a science.¹ Moreover, the skeptics of the late 17th and early 18th centuries were inclined to consider history simply a “conventional fairy tale” (“L’histoire n’est qu’une fable convenue” — an expression attributed to de Fontenelle, who is Corneille’s nephew).

Indeed, the main property of science is a set of certain laws that subordinate phenomena in all their constituent parts. Identical phenomena, proceeding according to a certain law, must, other things being equal, yield the same results.

The failure of attempts to find historical laws involuntarily had led some researchers to the idea that human destinies are governed by predestination, which has the power to direct the course of the historical process in one way or another.

Others, recognizing chance as a characteristic phenomenon in history, already by this very fact considered history to be devoid of any lawfulness.

Finally, others — in free will, in the absence of visible external correctness in the historical actions of Man, saw the reasons due to which the course of historical phenomena continuously underwent various fluctuations that could not be either taken into account or classified.

Belief in the metaphysical dogma of free will was one of the main reasons hindering the objective study of history. And despite the fact that even today philosophers have not come to any definite conclusion on the question of will, scientists were forced to account for the absence of it even in the smallest and most insignificant actions on the basis of scientific achievements and to put forward a deterministic point of view to explain the most complex phenomena in the mental life of Man.²

Since the statistics of human actions, which has been widely developed since the remarkable works of A. Quetelet (1796–1874), in which he pointed out the regularity existing in them, i.e., when the constancy of various human actions was objectively revealed, the point of view on free will has changed: human manifestations had to be recognized as a reaction to stimuli by diverse agents of the external world.

Thinkers, whose knowledge did not flow from feeble self-affirmation, nor from the desire to distinguish themselves from the background of Nature and to exalt themselves above everything that exists, but from the ability to subtly feel the

¹This opinion was ardently defended by Arthur Schopenhauer (1788–1860) in his opus *Die Welt als Wille und Vorstellung*.

²As an extreme expression of this view, one can point to the assumption made by P. P. Lazarev, a fellow of the Russian Academy of Sciences, based on the works of H. Zwaardemacker. The latter showed that the cause of the irritating properties of potassium salts found in the blood is their radioactivity. This Russian scientist considers it possible to assume that potassium salts accumulated in a certain place in the nervous system produce radioactive decay, which is the cause of irritation and excitation of certain centres in the brain; this should also entail the emergence of a thought process and cause certain actions in humans and animals (see his *Ionic Theory of Excitation*, Moscow, 1923, p. 149).

structure of Nature and directly understand the world as an indivisible whole, came to the same conclusion. The greatest poets Goethe and Tyutchev, with an extraordinary power of inner comprehension, expressed this in the following stanzas:

Nach ewigen, ehrnen,
Grossen Gesetzen
Mtissen wir alle
Unseres Daseins
Kreise vollenden.

Goethe

Imperturbable order in everything,
Complete consonance in Nature;
Only in our illusory freedom
We are aware of discord with it.

Tyutchev

Asserting himself, forming concepts for himself on the basis of personal experience, a person could assume that the course of events of a private or public nature is directly dependent on his arbitrariness. This led to the removal of the course of historical reality from a series of natural phenomena. Such convictions, having no points of contact with genuine science, forced one to see in history not a living consequence of the interactions of Man and the nature surrounding him, but only a posthumous record of events in the life of Mankind in the order of their successive ignitions and extinctions. Many branches of human knowledge made such great strides in the 19th century and in the two decades of the 20th century that they became necessary and irreplaceable in the practical life of people. But what has history given us? We would consider a person who would dare to speak about the “practical goals of history” not entirely sane. Despite the enormous amount of material collected by historians, the sophisticated methods of its development, despite the colossal work that scientists have accomplished, history, as it is, means no more than zero for the social practice of humanity.

History represents knowledge about the dead, about what is unnecessary for the ever-progressing life. It is an archive where inquiries have rarely been made and are being made, and the knowledge of which, all these “history lessons”, have never taught anyone anything! People who were closely acquainted with history made the same mistakes, the same blunders that had already been committed. The latter occurred because the actors in history had no firm points of support, no well-founded landmarks in space and time that could guide their actions and direct the course of the events that they generated.

Thus, as long as Man believed in the teleological dogma of predestination, relying on super-rational intervention, as long as he saw something significant in his will, he could not stumble upon the path of discovering the laws that govern his daily activities, his centuries-old destinies.

It is also necessary to note the fact that the field of exact disciplines did not touch history as a whole at all, even at

the time when it penetrated the fields of psychology, subordinating the processes of consciousness to physical and mathematical laws. True, in the middle of the 19th century, attempts were made to apply the laws of Nature to explain phenomena in human communities. The English historian H. T. Buckle (1821–1862), on the basis of the richest data collected by science in the field of history, geography, economics, statistics, in his work *History of Civilization in England* tried to show that the methods and principles of the natural sciences should be applied to history, for history is the interaction between Man and Nature. Buckle insisted on studying the influence of environmental conditions on a person using statistics. In his opinion, the laws of history can be learned only through statistical observations of the activity of mass people, revealing the regularity of their mass actions. Only through the knowledge of general laws can history reach the level of science, and therefore knowledge of individual facts and personalities does not represent any scientific value.¹

Almost simultaneously with Buckle, the American chemist and historian J. W. Draper (1811–1882) in his outstanding work *History of the Intellectual Development of Europe* (1856) expressed the idea that the historical evolution of peoples is governed by natural laws and is influenced by physical agents of Nature. Due to the fact that physical phenomena proceed according to strict laws, and historical phenomena do not represent the result of the action of free will, but are subject to a certain pattern, which must be discovered sooner or later.

The good attempts of Buckle and Draper, despite all their obvious usefulness, did not lead to a comprehensive study of natural phenomena and the mass movements of humanity occurring simultaneously with them.

And again, the main reason for the absence of such studies must be recognized as a blind, but general conviction in the independence of human mental and social activity from any physical and chemical phenomena occurring in the world around Man.

However, modern scientists strive to reduce psychological phenomena to physiological processes, in which they seek

¹French sociologists and philosophers go even further in this direction, recognizing statistical data on mass movements as the true essence of history. Bourdeau in *L'histoire et les historiens* (1888) sees the ideal of scientific history in depicting history in statistical figures and mass events in formulas, considering the verbal depiction of events to be the subject of literature. There is some truth in such assertions. The fact is that the mechanical explanation of natural phenomena is gradually giving way to statistical explanations. Since the works of Gustav Theodor Fechner (1801–1887), mathematical statistics has included the doctrine of mass phenomena (Kollektiv-masslehre) and has acquired enormous significance in the matter of revealing mass phenomena (Massenerscheinungen). By statistical explanation of a phenomenon we must understand its consideration as the resultant of a large number of complex and unclear phenomena governed by the law of chance. The achievements of science place the statistical method at the forefront of natural science. Biologists and sociologists, thanks to the works of K. Pearson, H. Bruns and others, are already widely using it, trying to understand a number of laws of Nature with the help of statistics and believing that the latter are the laws of statistics.

and then find a physical-chemical basis, and in the latter — the mechanics of elementary particles. This circumstance allows one to penetrate more deeply into the essence of mental life, closely connected with the life of the whole human organism and the external world surrounding Man.

Therefore, should not the methods and principles of physics and mathematics be applied to the study of the historical process and social evolution? The domain of physics is the entire Universe, the whole of it, and therefore physics must have its say in examining any question in the world.

It must illuminate the face of history with its laws on matter, link a human with Mankind, humanity with Nature by establishing laws for organic beings analogous to the laws of the inorganic world. Mathematics in theoretical synthesis must reveal the forms of historical phenomena and reveal the historical paths of peoples and humanity. Modern exact science is gradually entering this path.

The successes of biophysics over the past decades are beginning to deprive Man and his thought processes of that mysterious aura with which these processes have been surrounded for so many millennia. This is happening as a result of the merging of sciences on the basis of physical and mathematical analysis. The latter, when applied to the study of mental processes, gradually eliminates misconceptions about the supernatural origin of consciousness, the functions of which are expressed in physical and chemical transformations and are subject to mathematical formulas. Thus, human will becomes accessible to experience, and Man himself is transferred from the field of miracles to a series of natural physical and chemical phenomena.

Between the latter there are never-breaking connexions and continuous interactions, and therefore every natural phenomenon is dependent on the influences of the environment around it: in the life of Nature everything is consistent and everything is causally connected with each other. The world is a complex system of dependent variables, and not a museum of individual phenomena, nor a list of motionless facts.

In the light of the modern scientific worldview, the fate of Mankind, without a doubt, depends on the fate of the Universe. And this is not only a poetic thought that can inspire an artist to creativity, but a truth, the recognition of which is urgently required by the results of modern exact science. To one degree or another, every celestial body moving in space relative to the Earth, during its motion, has a certain influence on the distribution of the lines of force of the Earth's magnetic field, thereby introducing various changes and perturbations in the state of meteorological elements and affecting a number of other phenomena occurring on the surface of our planet. Moreover, the state of the Sun, the primary source of all movement and all breathing on the Earth, is in a certain dependence on the general state of the electromagnetic life of the world in general and, in particular, on the position of other celestial bodies. Does not this connect the intellectual development of humanity with the life activity of

the entire Universe by amazingly subtle, but at the same time majestic connexions? The world process, embracing all aspects of inorganic and organic evolution, is a phenomenon that is completely lawful and interdependent in all its parts and manifestations. A change in some parts, central and controlling, entails a corresponding change in all parts, peripheral and subordinate.

By including Man and his mental activity in the field of ordinary phenomena of Nature, modern science thereby gives grounds to assume a certain dependence existing between the manifestations of the intellectual and social activity of Man and a number of powerful phenomena of the natural environment. The life of the entire Earth taken as a whole, with its atmosphere, hydrosphere and lithosphere, as well as with all plants, animals and with Mankind inhabiting the Earth, we must consider as the life of one common organism.

Having adopted the above new point of view, it is necessary to admit a priori that the most important events in human communities, embracing entire countries with the participation of the masses of people, occur simultaneously with some fluctuations or changes in the forces of the natural environment. Indeed, any mass social event is a very complex system. To dismember, to break this system into several parts, simple and clear, and thereby simplify the understanding of the phenomena — this is the main task of natural-historical knowledge.

I have conducted a study of the course of historical phenomena in connexion with the periodic activity of the Sun.

The results of my research study in this direction are presented in *A Study of the Relationship Between the Sunspot-forming Activity and the Course of the World-historical Process, Beginning from the 5th Century B.C. and Until the Present Time*.¹

Having discovered a known relationship between solar activity and the military-political activity of Mankind, I expressed my point of view on this phenomenon in the work *Fundamentals of Historiometrics*.

Here I present my proposed theory of periodic changes in the behaviour of organized masses of people, simultaneous with periodic changes in solar activity, as well as the principles of the 11-year cycle of general human, collective and individual, military-political and creative activity that I discovered. In addition, I established the basic and first unit of

¹By "world-historical process" we mean *simultaneously* occurring social evolution in all human communities, dependent or independent of one another in their spatial position on the surface of the terrestrial globe. With this term we somewhat touch upon the long-expressed desire to unite history into a single whole. Thus, already in the 2nd century B.C. the Greek historian Polybius, and then 18 centuries later Bishop J. Bossuet (1627–1704) pointed out the need to develop a common view of history and establish a world-historical point of view. Bossuet in *Discours sur l'histoire universelle* (1681) wrote that, just as a single geographical map generalizes all countries and all peoples, so a common view of history would help to merge the histories of the development of various peoples into a single process of the world history of Mankind.

measurement for counting the time of the historical process and outlined the paths to discovering the *physical* laws that govern the course of social evolution.

I Social activities and general influence of the Sun

Taking into account the huge volume of the Sun, as well as the relatively small distance separating the Sun from the Earth, which is equal to the sum of 107 diameters of the Sun, it can be said that the Earth is under the direct and quite powerful influence of the central body of the Solar System.

The Sun is a colossal source of electrical energy, and its impact on the surrounding space can be divided into two main categories: radiation and induction.¹

The radiation emitted from the Sun originates from the radioactive decay of its matter and carries with it negative and positive electric charges. The Sun is surrounded by an electromagnetic field extending beyond the outer planet of the Solar System — Neptune [Pluto had not yet been discovered at the time of writing], which is also influenced by the Sun, despite the fact that it is 30 times farther from the Sun than the Earth. Therefore, the terrestrial globe with its electromagnetic field is inside the electromagnetic field of the Sun, under its powerful action. The change in the relative positions of the planets and the Sun during their motion has some effect on the state of their electromagnetic fields. It is known that any motion of matter is simultaneously an electromagnetic phenomenon, since matter contains intra-molecular and intra-atomic electric fields that are set in motion when matter moves in space. Changes in the state of the electromagnetic field of the Earth are also influenced by fluctuations in the physical and chemical processes in the substance of the Sun. These processes, which reach enormous power during periods of maximum solar activity, cause electromotive forces to appear in many areas on the Sun; violent vibrations and ruptures of solar matter, motions of sunspot matter, etc. — all this should produce series of electromagnetic waves in the surrounding cosmic space.

The internal life of the Sun does not proceed uniformly, but continuously experiences rhythmic fluctuations of a more or less regular period, externally expressed in the appearance and disappearance of sunspots, their number, as well as other phenomena: sometimes solar activity increases and its face is covered with sunspots, reaching a maximum, then it decreases, falling to a minimum and thus undergoing the following four stages:

1. The stage of minimum;
2. The stage of increasing activity;
3. The stage of maximum;
4. The stage of degradation.

¹Here I will not touch upon theories about the internal constitution of the Sun, its physics and chemistry, the temperature of its surface and internal parts, energy reserves, etc. The reader can find all this information in any astronomy textbook.

A complete cycle, which includes one maximum, one minimum and transitional stages, takes a period of time from 7 to 16 years (more often from 9 to 13 years). The periodicity of solar activity was discovered by H. von Schwabe (1851). In the arithmetic mean this period, as was found later, is equal to 11 years and, therefore, repeats itself 9 times in a century. Assumptions were also made that, in addition to the 11-year period of solar activity, there are also others — longer and shorter than 11 years. De Mairan (1746) already expressed the idea of long periods in solar activity and in the development of the polar lights. The Russian astronomer A. P. Gansky identified this period to be 72 years. Schuster (1906), using harmonic analysis, calculated a series of secondary periods following the 11-year period, namely: 4.48 years, 8.32 years, 9.25 years and 13.5 years. The most important period after the 11-year period, Schuster considers the period of 33.375 years — “one-third-century cycles”, — which he found to be dependent on the period of revolution of the Leonid meteor shower around the Sun. Then, Dr. Elsa Frenkel (1913) found in solar activity a period of 200 and 68.5 days, which is similar to the period of revolution of Venus (224.7 days) and Mercury (87.9 days) around the Sun. Finally, H. Turner in the same year, on the basis of his hypotheses and calculations, came to the conclusion about the existence of a long-term period of 266 years.

The complexity of the spot-forming process [on the Sun] and the divergence of opinions about its periods forced me, due to the importance of solving this problem for my research, to inquire with the most important observatories about the latest (as of 1922) research results in this field.²

Based on a number of answers received, it can be said that, except for the 11-year period, none of the above periods has been firmly verified, and many eminent astronomers are inclined to doubt the real existence of some of them. However, it should be thought that the spot-forming activity of the Sun, in addition to the clearly detectable 11-year period, is subject to fluctuations of other periods, which have not yet been precisely established due to the insignificant amount of relevant material.

The reasons that force solar matter to perform rhythmic pulsations from century to century have not yet been clarified. However, external signs of increased vital activity of the Sun have been established with certainty: sunspots, prominences, torches, flocculi, filaments, alignments, the corona, and others, and their properties and relationships are now being clarified.

Of special interest are sunspots, because the question of the internal constitution of the Sun itself is reduced to them. As is known, spots appear on the Sun in two belts and for approximately 13–14 days, together with the Sun revolving

²Mount Willson Solar Observatory in Pasadena (Prof. Seth B. Nicholson), Eidgenössische Sternwarte in Zürich (Prof. A. Wolfer), Royal Observatory in Greenwich (Prof. F. W. Dyson), Steward Observatory in Arizona (Prof. A. E. Douglass) and others.

around its own axis, they pass along its disc, gradually disappearing behind its edge. Sometimes, after the same period of time, the same sunspots appear again. Sunspot formation has attracted the attention of scientists for a long time. And, despite the fact that many astronomers have carried out a number of observations and studies to explain the nature of sunspots and proposed a number of hypotheses (Herschel, Zöllner, Faye, Secchi, Moreux), however, to this day this question is considered not to have been resolved in its final form and the “great mystery” of sunspots, in the words of Galileo (1564–1642), has not yet been revealed. Only little by little, thanks to the foundation of special solar observatories and the invention of amazingly precise instruments, scientists are beginning to penetrate into their nature. Outstanding works in this area should be considered the research of the American scientist George Ellery Hale and the French scientist H. Deslandres. Based on his spectroheliographic work, Hale put forward the bold idea that sunspots are colossal electric vortices. Meanwhile, it had long been proven that the essence of magnetism comes down to rotation and that during rapid rotation an electrically charged body generates a magnetic field (Rowland). Young in 1892 discovered the splitting of many lines in the spectrum of sunspots, but did not provide an explanation for this phenomenon. Finally, in 1908, a series of studies allowed Hale to discover the Zeeman effect (1896) — the splitting of spectral lines in a magnetic field — in the spectrum of sunspots, and thus the magnetic field of sunspots was proven. Based on these works, one can conclude that a sunspot is an enormous magnet. One pole of it is turned toward us, the other lies deep inside the substance of the Sun. The structure of sunspots (on the photos framed in the spectral line of hydrogen) turned out to be vortex-like (“solar vortices” according to Hale). Astronomers again had to return to the vortex theory of sunspots, proposed already by H. Faye. Indeed, Evershed and St. John noticed motions inside sunspots. Thus, using again spectral analysis, which is the most powerful method of research, a discovery of the greatest importance was made — the secret of the most grandiose electrical processes in solar matter. Consequently, the electrical essence of sunspot formation was discovered, but the reasons for the formation of sunspots themselves have not yet been clarified, despite all attempts.

Sir John Herschel (1792–1871) tried to explain sunspots by the fall of meteoric substance onto the Sun. Peirce (USA) and more recently Stephanie supported this hypothesis. The greatest English physicist Lord Kelvin (1824–1907) admitted such a possibility, explaining the acceleration of the equatorial motion of the Sun’s mass by meteor impacts. H. Turner in 1913 made a splash with a similar hypothesis. Some astronomers explained the periodicity of sunspots by the influence of planets, such as Mercury, Venus, Saturn, Jupiter, the combination of whose revolution around the Sun was linked to the period of sunspots (Warren De la Rue, Balfour Stewart, etc.). Finally, Mrs. Maunder (1907) sought to show that the terres-

trial globe also exerts an influence on the slowing down of the development of sunspots on the side of the Sun facing us.

Highly likely, the Sun is a huge resonator, quickly and sensitively responding to the motion of its Solar System and the influence of electromagnetic oscillations in outer cosmos. In this case, the cause of the appearance of sunspots should be sought inside the Sun itself, while we can admit the influence of external factors on their distribution in time and on the surface of the Sun, as well as on the variability of the strength of the sunspot-forming process.

During the period of maximum activity of the Sun, all phenomena on it assume grandiose proportions. The Sun throws up substances converted into vapors for millions of miles and emits streams of anode and cathode rays [proton and electron streams, respectively]. In this respect, the Sun is quite reminiscent of a radioactive body (A. A. Eichenwald), throwing out negatively and positively charged particles. The latter, rushing at considerable speed into cosmos, are driven away from the Sun by the pressure of light and are partly retained by the planets or their atmosphere. Streams of these particles, in the opinion of some scientists (Birkeland, Arrhenius, Nordmann, Paulsen, Villards), ionize the Earth’s atmosphere, producing certain physical effects in it. Other scientists see the causes of these effects in the action of electromagnetic waves emitted by the Sun. The latter is less likely, since the magnitude of the magnetic fields on the Sun is insufficient to directly affect the Earth (Hale).

It should be noted, however, that the strongest perturbations of the Earth’s magnetism always occur when large sunspots pass through the central meridian of the Sun (Loomis, Lord Kelvin, Terby, etc.). Ricco (1892) showed that magnetic disturbances lag behind by approximately two days from the time the spot is in the region of the central solar meridian. In the annals of astronomy, there are only a few cases, when anomalous movements occurred simultaneously on the Sun and on the Earth; these are the observations of Carrington on September 1, 1859, Trouvelot on August 16, 1885, and Hale on July 15, 1892. They try to explain the lag in the magnetic effect by the time it takes for particles of solar matter to travel from sunspots to the Earth (Arrhenius).¹

The perturbative effect produced by the electrical processes on the Sun on many processes on the Earth is manifested with unvarying force with each increase in solar activity. Indeed, the periodic stresses of the Sun’s spot-forming activity cause periodic fluctuations and disturbances in the physical life of the Earth. Below I cite several physical phenomena on the Earth, the relationships of which with the spot-

¹We will not dwell on the discussion of the opinion of some scientists, which consists in the fact that the activity of the Sun and the physical phenomena on the Earth, synchronous with it, are co-effects of the same extra-solar cause, lying in the electromagnetic environment of outer cosmos. In examining this question, we, on the basis of weighty scientific data, and also, for the sake of easy understanding, accept the spot-forming process on the Sun as “causa efficiens”.

forming process on the Sun have been surely established or are being established now:

- Magnetic storms (Sabine, Wolf, Gautier, 1852);
- Aurora borealis (Fritz 1853, Loomis);
- Cirrus clouds — cirrus, cirro-stratus, cirro-cumulus (Klein, Paulsen);
- Optical effects in the atmosphere — halos;
- Fluctuations of atmospheric electricity (Chree);
- Thunderstorms (Hess, Herbig, Svyatsky);
- Movements in the atmosphere: cyclones, anticyclones, hurricanes, tornadoes, tropical storms (Meldrun);
- Coloration of the sky (Bush);
- Air temperature at the Earth's surface (Köppen, Nordmann, Mielke, 1913);
- Temperature of some seas (for example, the Norwegian Atlantic Stream);
- Polar icebergs;
- Precipitation (Symons, Moreux, etc.);
- Air pressure (Walker, Leist, Fedorov);
- Climate fluctuations or disturbances (Bogolepov);
- Earthquakes.

It should be noted that the parallelism of the three curves, which has long been accepted in science, is a graphic representation of the spot activity of the Sun, the frequency of the polar lights and the fluctuations of the Earth's magnetism. Assumptions have also been made about the influence of sunspot formation on the displacement of the Poles, St. Elmo's fire (Rudolph). Science is still too young to fully reveal the influence of the Sun. Perhaps the Sun is the cause of all regular, periodic phenomena on the terrestrial globe.

The influence of sunspot activity is not limited to the Earth. Scientists have managed to notice that sunspot activity affects many phenomena in cosmic space. The brightness of the colour of some planets, due to the increase in cloudiness and albedo on them¹ — Jupiter, Mars, Venus and the colour of the Moon during eclipses (Vogel, Danjon) change with the change in the number of sunspots. Comets, moving inside the Solar System, experience significant resistance during the periods of maximum solar activity, due to the abundance of electrical particles of solar matter in the space of the Solar System (Backlund). Finally, the tails of comets in the same periods of time have greater brightness, which allows astronomers to discover more of them in these periods of time than in the intermediate years (Berberich, Bosler). In addition, it has been noted that the melting of polar snow on Mars occurs faster in the years of maximum solar activity than in the years of minimum (Antoniadi).

As for the dependence of the organic world of the Earth on the periodic activity of the Sun, this problem is still considered open in the literature on the subject. Meanwhile, the

¹The ratio of the amount of sunlight that a planet's disc reflects to the total amount of light that falls on it.

general influence of the Sun on the development of organic life has been carefully observed by many thinkers since ancient times and has been subjected to detailed study.

In my presentation of this influence, I will begin with the general influence and gradually move to the particular.

People have always felt their dependence on the Sun; they guessed that the destinies of the Earth are closely connected with the destiny of the Sun. Therefore, there is nothing surprising in the fact that from ancient times Man recognized this source of light, heat and life as his main god and represented him in anthropomorphic and zoomorphic images. The Hindu god of the Sun was Sūrya, or otherwise — Savitar², the Persian god of the Sun was Ormuzd; the Assyrians had Izdubar and Nimrod; the Babylonians had Marduk; the Egyptians — Osiris, Ptah, Ra; the Phoenicians — Hercules; the Greeks — Apollo, Helios, Phoebus; the Scandinavians — Odin; the Germans — Balder; the Slavs — Dazhbog, Khore, Veles, Bel-bog, etc. The religions of the ancient East, the cults of Greece and Rome, the cults of Mexico and Peru, and finally the religions of the Lithuanians, Slavs, Germans and other peoples created sects worshiping the Sun and fire, as the earthly prototype of the former. Fire worship was developed in India and Persia. The hymns of the Rig Veda, composed in time immemorial, glorify the god Agni ("ignis" — fire); we find the cult of fire in the teachings of Zoroaster. Slavic holidays — Kolyada, the holiday of Marena, Kupala are associated with pagan rites of worship of the Sun. In Greece, temples were built to the Sun, such as in Corinth, Argos, Luxor. In Baalbek, a temple famous for its architecture was also erected to the Sun. On the island of Rhodes, at the entrance to the harbor, there was a colossal image of the sun god. The Greeks and Romans used sunlight to treat the sick, as indicated by Hippocrates, Oribasius, Antilius, Avicenna, Galien and Celsus. Entire cities were named after the Sun, for example, Heliopolis, near the Nile Delta. It can be assumed that Egypt itself ("Hakapta") received its name from its dedication to the god of the Sun — Ptah. Ancient art, fragments of which have come down to us, is full of deification of the daytime Sun. The cult of the Sun permeates the entire symbolism of the plastic art of the inhabitants of the White and Blue Rivers. Thus, the doctrine of the action of the central eternally life-giving fire, as the primary source of all that exists and the primary substance, occupies a central place in all mythologies, natural philosophies and arts of the peoples of the Old World.

The Sun served as the embodiment of the idea of the power of beauty and fertility. The Greeks called it "Βασιλευς Ηλιος", considering the Sun to be the main manifestation of life, the heart of the world, animating everything with its rays. Let us recall the great wisdom of the inscription on the ancient

²Sūrya and Savitar are names of the Sun in Sanskrit. They mean "to shine" and "to sound" (the root "sū" means "to fertilize"). The Sun was understood not only from the point of view of its "radiant power", but also its fertilizing, creative power.

temple of Diana in Ephesus: “. . . only the Sun with its shining light gives life!” Throughout ancient literature, medieval and modern poetry, one can hear an incessant hymn to our daily luminary — a song of praise, which, finally, in the words of the dying Turner, turns into a prayer: “the Sun is God!” And in our days, one outstanding French astronomer¹, taking into account, on the basis of the data of exact science, the greatest influence of the Sun on the Earth and Man, proposed that the French Astronomical Society petition the French government to establish a universal tax, insignificant in size, but fair in essence, for work on the study of the Sun, for Man’s dependence on the Sun has no boundaries: “The Sun is one who shines for all and grows the crops of all, therefore, a priori, it seems fair that all people should contribute their share to solar research.”

Even ancient thinkers attempted to determine the connexions between the state of the human organism and the fluctuations of the physical environment surrounding it, which depended on the Sun. The ancient Greek historian Herodotus (485–425 B.C.), while traveling, noted a number of facts showing the influence of natural conditions on the physical and mental development of Man. The famous Greek physician Hippocrates (460–377 B.C.), in his work “Περὶ αἰθρῶν ὑδάτων καὶ τόπων” (which means “on the influence of air, water and terrain”) made the first attempt at historical geography. The greatest philosopher of the Antique World, Aristotle (384–322 B.C.), was not alien to this issue. Strabo (born in 54 B.C.), Plinius the Elder (23–79 A.D.) and also Ptolemy (2nd century A.D.) studied the problem of the influence of climate on the development of Mankind. The same influence was pointed out by the Arab pragmatist historian Ibn Khaldun (1332–1406). Thinkers of the 16th–19th centuries, such as J. Bodin (1530–1596), S. de Montesquieu (1689–1755), J. Herder (1744–1803), K. Ritter (1779–1859), F. Ratzel (1844–1904), E. Reclus (1830–1905) and others tried to make all the variability of human races, characters, temperaments, as well as the historical destinies of peoples dependent on geographical conditions, mainly on climate. All this contributed to the creation of a special science about the influence of external nature on Man — anthropogeography. As an extreme expression of such views we can point to the so-called “geographical monism” or “geographical fatalism” (K. von Baer), the roots of which go back to the Middle Ages (Iohann Cochlaeus, 1479–1552).

But what is climate? This term should be understood as the average state of meteorological factors that create certain conditions for the existence of representatives of the organic world. The concept of “climate” is closely related to the concept of “life”, and climatic conditions can only be considered in relation to the plant or animal world. The [ancient] Greeks believed that climate depends on the angle of incidence of the

Sun’s rays (climate, in Greek — κλίμα, κλίματος — means “inclination”) and on the duration of illumination, i.e., on the geographical latitude of the place. However, ancient geographers overlooked the fact that the surface of the Earth is not the same and the terrestrial atmosphere contains vapors. The properties of the Earth’s surface and the state of the atmosphere have a significant impact on climate. But the main factor of climate, its main element is still the radiant energy of the Sun. The great diversity of organic life on the Earth’s surface is caused by those energy flows that burst into the atmosphere in the form of solar radiation. Is it worth dwelling on the long-known and well-known truth that the Sun is the only source for all forms of energy that we observe in the life of nature, beginning with the light breeze of zéphir [ζέφυρος, in Ancient Greek — light Western or Northwestern wind] and the gentle germination of plant seeds and ending with tornadoes and hurricanes, and also the mental activity of Man. All this is the work of the Sun, the creativity of the Sun.

From the point of view of modern science, all the most diverse and varied phenomena on the Earth — both the chemical transformations of the Earth’s crust and the dynamics of the planet itself and its constituent parts, the atmosphere, hydrosphere and lithosphere, occur under the direct action of the Sun. It is known that the nature of chemical processes on the surface of the Earth changes, as a result of changes in temperature, with latitude, reaching the highest rate at the equator, while at the Poles we see only slow chemical reactions. There are, therefore, chemical zones of the Earth (A. Fersman) and they correspond to certain zones of the soil (V. Dokuchaev).

With a change in the latitude of a place and soil, its productive forces, the degree of its population, etc., change. The distribution of plant and animal species on the Earth’s surface depends on the geographical location. As Alexander von Humboldt (1769–1850) showed and then Alphonse de Candolle (1806–1893) formulated in his work *Géographie botanique raisonnée* (1855), the lowest representatives of plants live in cold countries, the highest in hot countries. Each plant species is fully adapted to a strictly defined climate and has a precisely defined “climatic zone” of distribution. Today, four main groups of climates and corresponding zones of distribution of representatives of the organic world are distinguished (E. de Mortonne, I. Brunhes).

It has been established beyond doubt that green plants receive the energy they need for life directly from the Sun, which is thus the main source of their existence, facilitating the preparation of organic substances from inorganic substances. This is the global function of green plants, supporting the life and development of the entire animal kingdom. The process of photosynthesis occurs in the laboratory of chlorophyll grains. With their help, plants literally absorb the energy of the Sun’s rays: the red rays of the spectrum dissociate carbon dioxide and synthesize carbohydrates that feed the plant (K. A. Timiryazev, 1843–1920). Solar heat, released in our organisms, furnaces and machine furnaces, determines all

¹Henri-Alexandre Deslandres, Director of the Meudon and Paris Observatories, who carried out intensive studies on the behaviour of the atmosphere of the Sun.

our movements and all work performed in factories.

Then, the importance of green plants should be considered from another side — from the side of their cosmic role; representing an intermediate link between minerals and animals, plants again, by means of solar energy, complete the circle of chemical transformations and thus facilitate the turnover of substances on the Earth and the replacement of carbon dioxide with oxygen. The annual consumption and expenditure of atmospheric oxygen, according to some estimates, is equal to 400 billion poods [an obsolete royal unit of mass equal to 40 pounds]. The increase in the number of individuals of the animal and human world should cause a gradual decrease in the oxygen supply and an increase in the amount of carbon dioxide. B. Weinberg (1907) came to the conclusion that the period of existence of Mankind under such conditions will not exceed 1 000 years.

Of course, it is premature to make such a pessimistic conclusion.

It should be thought that plants, with the help of sunlight, will continue to restore the chemical composition of the air that is necessary for us.

Plants show extreme sensitivity to sunlight: they make independent movements towards the sunbeam (positive heliotropism), placing their leaves perpendicular to the latter. In the morning, the leaves turn to the East, at midday they are set parallel to the ground, and in the evening they lean towards the West (H. Vöchting), because, in general, plants show the ability to make various movements, like thinking beings (J. Bose). The leaves of many plants have special organs that serve to perceive light — a kind of “eyes” (G. Haberlandt). However, plants do not have the same inclination to every part of the spectrum: the greatest heliotropic effect is shown by ultraviolet and then infrared rays; yellow rays do not have a noticeable effect on plant growth. It is interesting to note that the ultraviolet part of the spectrum has a predominant effect on the development of flowers in plants (J. Sachs). In a word, plants have a great inclination to the Sun. The life-giving influence of our daily luminary is best proven by the spring awakening of the plant world, the richness and splendor of tropical forms. The luxury of vegetation is directly proportional to the strength of sunlight — these words of J. W. Draper sound like a prophecy that has come true.

But light has a destructive effect on most microorganisms, changing their chemical processes within them or disrupting chemical processes in their environment. It is known that in the light, in presence of oxygen, oxidation processes are enhanced, and in the air, under the influence of ultraviolet rays, hydrogen peroxide and ozone are formed. Consequently, light excites disinfectant properties, justifying the Italian proverb: “Where the Sun does not look, there comes the doctor.”

The distribution of animals, according to P. L. Sclater (1829–1913) and Alfred R. Wallace (1822–1913), depends almost equally on the geographical factor: in polar and tem-

perate countries, according to Wallace’s work *Geographical Distributions of Animals* (1876), mammals and birds account for 1/3 of the total number of higher animals.

The physical development of Man and animals is also determined by climatic zones. In this regard, Isidore G. Saint-Hilaire in *Essais de zoologie générale* (1841) wrote that the majority of genera and species reach their maximum growth in the warmest countries and fall to a minimum in cold countries. For example, let us take the south of Russia: in most cases, the isoline of the maximum average height (169–170 cm) of people is superimposed on the isotherm of +10 and +15°C (Ivanovsky).

Thus, the evolutionary stage of representatives of the organic world is in a certain relationship with the degree of strength and quantity of radiant energy of the Sun falling on a given area of the Earth.

Charles Darwin (1809–1882) in his theory of the origin of species, defining evolution as a process of interaction between organisms and their environment, devotes little space to the direct significance of the radiant energy of the Sun, although this energy, as we see, determines the spatial distribution and relative quantity of various forms of flora and fauna. It must be recognized that the electrical structure of solar radiation, revealed by recent achievements in physics, must have not only a secondary, so to speak, facilitating effect on the organic world, but the energy of the Sun, highly likely, is the main factor in the evolution of plant and animal organisms — a factor that acts continuously in relation to geological time and the geographical position of the place. Perhaps the causes of organic evolution, which is believed to arise spontaneously, lie in disturbances in the physical state and chemical composition of the external environment under the influence of sharp fluctuations or disturbances in nature, associated with fluctuations in solar activity. Disturbances in the external environment, as we shall see later, entail corresponding changes in the physical chemistry of organic beings.

Now I shall focus attention on the effects of the direct impact of the radiant energy of the Sun on organic bodies, beginning with the simplest animal organisms (protozoa) and ending with highly organized Man.

The influence of the Sun on living organisms, in the present state of knowledge, cannot yet be expressed by one universal formula, therefore it will be necessary to briefly list the effects of the influence of sunlight on the constituent parts of the animal organism: on cells, tissues, muscles, blood, etc.

For example, ultraviolet rays first excite and then inhibit cells, which is explained by irritation of cell plasma (Hertel). Under the influence of light, there is an increase in oxidative processes in cells (Quincke) and an increase in gas exchange of living muscle and nervous tissue (Moleschott, Fubini). Light affects the movement of the ciliated epithelium of the frog’s esophagus (Uskov). Tissue regeneration occurs incomparably faster in the light than in the dark (Godnev). Intracellular life is also in a certain dependence on light: ul-

traviolet rays, through the hydrogen peroxide they form, affect diastases (Agulhon). The effect of hydrogen peroxide is used to explain the effect of ultraviolet rays on milk (Romer). There are indications of the effect of sunlight on the hypobronchial glands of gastropods.

The change in gas exchange in animals under the influence of sunlight should be considered very important. Moleschott demonstrated in 1855 on a number of animals that light causes an increase in oxygen absorption and an increase in the release of carbon dioxide. In the same direction, I note the experiments conducted by Loeb, von Platon, Speck, Alexander, Ewald, Dürich and others. Nitrogen metabolism is also enhanced under the influence of general gas exchange (Godnev). The maximum effect relates to the yellow and violet parts of the spectrum (Kogan); darkness contributes to a decrease in nitrogen exchange.

A number of authors (Schmidt, Fubini) found a greater weight loss in illuminated cats and frogs than in those in the dark. However, there is an opposite opinion about the effect of light on weight (Borisov); it is believed that light has a stimulating effect on the body, which helps to increase the absorption of food; this can result in an increase in the weight of animals and an increase in their growth. The latter is confirmed by Edwards, Beclard, Fère and others in a number of experiments. Short-length light waves produce a particularly strong effect on growth, as well as on other processes in cells and tissues. Consequently, by influencing the life of cells and tissues, light undoubtedly produces not only a local effect, but also has a certain effect on the general condition of the body. The effect of the Sun on the human body is primarily manifested in the change in the chemistry of the skin pigment, which plays a very significant rôle in heat regulation, in protecting the body from pathogens, etc. The rôle of pigment in connexion with the influence of light on it has been studied by a large number of researchers.

The effect of sunlight on the skin causes hyperemia of the vessels with dilation of the capillaries. This process affects not only the capillaries of the skin, but penetrates into the area of the deep-lying vessels, lowering blood pressure, which continues throughout the entire period of light action (Lenkei, Behring, Hasselbach, Nogier, Aimes). Not all rays of light have the same effect on blood pressure. Blue light increases blood pressure more than red and green (Spirtoff).

When exposing the body to insolation, one can notice an acceleration of the pulse, which, if the sunlight is intense enough, occurs about 10 minutes after the start of the exposure. This is explained by the rapid expansion of the skin vessels, which stimulates the heart to contract faster. Influencing the blood vessels, sunlight does not remain indifferent to the physical chemistry of the blood itself. As Rollier, Revillet, Behring, Marquès and Lenkei claim, exposure of the body to the Sun causes an increase in the number of red blood cells, accompanied by a proportional increase in hemoglobin and a corresponding decrease in poikilocytosis. Careful works

conducted by d'Oelsnitz and Robin established the fact that in the first hours after insolation, there is a progressive increase in the number of leukocytes, as well as polynuclears and eosinophils.

Changes in the chemical composition of the blood necessarily entail corresponding changes in the general condition of the body and its nervous tone. Brown-Séquard also showed that light affects muscle contractility. Moleschott, together with Marmé, exposed frogs to light and found increased excitability of nerves and increased muscular performance. Then Fubini proved that nervous tissue exposed to light releases significantly more carbon dioxide than tissue in the dark, but under the condition of maintaining the central nervous system and muscle activity (Moleschott, Loeb). In a word, the influence of light and the Sun is not limited to the periphery of the body, but extends deep into it — right up to the centres of higher nervous activity.

The fact that sunlight plays a huge role in the body's reactions was known to a number of scientists almost since the time of I. Newton (1642–1727). The great scientist understood what an important role the life-giving forces of light play. "By means of the vibration of this force", he claimed in his famous work *Philosophiae Naturalis Principia Mathematica* (1687), "sensations are excited and the organs of animals are set into voluntary movement, while this force spreads from the external sense organs through dense networks of nerve fibers to the brain and then from the brain to the muscles."

In the nowadays there is a special branch of medical science — phototherapy, which deals with the treatment of various pathological and neuropsychiatric diseases using light. The general effect of the latter, according to V. M. Bekhterev, a fellow of the Russian Academy of Sciences, increases the excitability of neuropsychiatric activity in general. Just as in the case of plants and animals, different parts of the spectrum have a different effect on the human body and mental activity, since different colors cause corresponding changes in the speed of physical and chemical processes in the body, in blood circulation, in the functions of the brain, etc. As early as 1876, the observations of the Italian professor Ponza established the unequal influence of different colours on the mental state of the mentally ill persons.

Another famous Italian scientist, psychiatrist and criminologist S. Lombroso (1836–1910), in his book *Genio e follia* collected interesting data on the influence of the season, i.e., about the influence of a greater or lesser amount of radiant energy of the Sun on the state of human mental abilities. He established the coincidence of the development of insanity with a sharp increase in temperature in spring and summer. The maximum of mental illnesses, according to Lombroso, occurs in July, the minimum — in December.

He also says the same about brilliant minds, whose creative powers reach their peak in May and September, the minimum of creative activity occurs in winter, when this activity

flares up only on the warm days of this time of year.

Consequently, warm and bright months and days turn out to be fruitful not only for plant or animal nature, but also for the human mind.

Indeed, if we trace the conditions for the emergence and development of civilizations, then we will clearly see that the greatest centres of human mental life are initially localized in places with optimum temperatures. This applies to cultures: Chinese, Babylonian, Egyptian, Indian, Antique, Arabic.

The low developed tribes to this day live either in equatorial or polar countries. Indeed, the influence of geographical latitude in history is noticeable. For example, civilized and populous cities lie between the two extreme isothermal lines of +16°C and +4°C. Chicago, New York, Philadelphia, London, Vienna, Odessa, and Beijing lie on the main axis of the climatic and civilized belt with the 0°C isotherm.

Thus, the average amount of radiant energy of the Sun corresponds to the most developed race and culture; the minimum and maximum — are accompanied by a less developed race and culture. *The forces of external nature bind or release the hidden potential of human spiritual essence and compel the intellect to act or to die.*

There is an opinion that warm countries provide people with easy-to-obtain food during their leisure time, which allows them to devote a significant amount of time to mental activities. If this is partly true, then it is also true that the acceleration of physical and chemical reactions in the body can also contribute to a more intense flow of brain activity. Aristotle noted that a rush of blood to the head changes the normal state of people, making them “poets and prophets”. It is now known that a change in temperature correspondingly changes the rate of reactions. According to J. H. van t’Hoff, a 10° increase in temperature increases the rate of chemical reactions approximately twofold. The relative increase in the rate of reaction with a temperature increase of the specified number of degrees is called the temperature coefficient. Reactions occurring in the dark have a temperature coefficient different from reactions occurring in the light, namely, a significantly smaller one. Since at high temperatures the coefficient becomes small, reactions in the light, or photochemical reactions, are quite similar to reactions occurring under the influence of high temperatures. Thus, chemical processes occurring in organic nature are directly dependent on the temperature and lighting imparted to them. Such a dependence has been established for the rate of assimilation of carbon dioxide by plant leaves, the rate of heart contractions, the spread of nervous excitation, mental processes, etc.

It is not difficult to consider what a huge rôle the Sun plays only as a source of heat and light in the life of the entire organic world: starting from the Poles, towards the equator, accompanying the geographic latitudes, together with the increase in the amount of radiant energy of the Sun falling on the Earth, the speed of physical and chemical reactions, the rise of the evolutionary ladder of the plant and animal king-

doms, the growth of plants, animals and humans, the speed of the onset of sexual maturity, marriage, birth rate, etc., increase accordingly.

If the gradual change in the amount of radiant energy of the Sun received by different parts of the Earth, due to the spherical shape of the Earth and the tilt of its axis, has such a decisive influence on the general development of the biopsychic and physical life of the planet, then the question arises: *Are not the powerful fluctuations of solar activity associated with the ejection into space of countless streams of electrically charged particles of solar matter and the radiation of electromagnetic waves also manifested in the organic nature of the Earth?*

II On the relationship between the periodic activity of the Sun and the synchronous periodicity of the oscillations of the world-historical process

Even the 18th century Danish astronomer Christian Horrebow (1718–1776) wrote that observation of solar activity would lead to the discovery of the sunspot period and “only then will the time come to investigate how sunspots affect bodies governed and illuminated by the Sun”.¹ Highly likely, even at that time there were assumptions and guesses that sunspots could not but have some effect on the life of the solar world.

In the 19th century, indications appeared of the relationship between the periodic activity of the Sun and some phenomena in organic nature on the Earth.

One comparison made by Sir William Herschel (1738–1822) is not without interest. He tried to establish a connexion between crop failures and the price of bread with the sunspot period², and Fergusson investigated the issue of crop yield fluctuations in India. In addition to the price of bread, the price of table wines in France, as statistical calculations have shown, is also related to the period of sunspots. Thus, in years of minimums, the price of wine is higher than average, in years of maximums — lower. The English economist W. S. Jevons (1835–1882), who was educated in many ways, both philosophically and scientifically, — not afraid of being known as an original, — pointed out at that time the connexion between phenomena that at first glance may seem to belong to completely different branches of knowledge: in his work *Commercial Crises and Sun-Spots* (1878) he set out his theory of the connexion between industrial crises and the periodic course of solar activity.

The same problem was touched upon by W. S. Jevons in his other work.³

¹Young C. A. *The Sun*. International Scientific Series, D. Appleton & Co., New York, 1881, 321 pages.

²Henry T. Buckle (1821–1862), in his book *History of Civilization in England*, Longmans, Green, & Co., London, 1882, vol. I, p. 32, pointed out that, according to statistical calculations, the number of marriages is not determined by personal feelings, character or temperament, but is in turn in a certain dependence on the price for bread.

³Jevons W. S. *The Variation of Prices. Investigations in Currency and Finances*. Macmillan & Co., London, 1882, pages 145–147.

Indeed, if meteorological conditions are in any way dependent on the activity of the Sun, then, by affecting harvests, they can cause certain economic and financial crises. The latter should affect the course of world trade, which is thus linked to cosmic phenomena.

Then there were fleeting indications of a connexion between the epidemics of Asiatic cholera and the increased activity of the Sun¹, between cod fishing off the coast of Scandinavia and the process of spot formation on the Sun². They tried to establish a connexion between the periods of maximum and minimum sunspots and mass appearances of locusts, identifying these periods as 11 years (W. Köppen). Camille Flammarion, based on 30 years of observations, noted that the time of flowering of chestnuts in Paris reveals a clear periodicity equal to the period of solar activity. The French astronomer Abbot Théophile Moreux in Bourges showed that the influence of sunspots is manifested, in addition to the world grain harvest, also on the grape harvest, the time of lilac blossoming in France and the arrival of swallows. Moreux's diagrammatic curves perfectly illustrate the coincidences of these phenomena.³

In 1918, the US scientist A. E. Douglass (Director of the Steward Observatory in Arizona), published a study that established that the thickness of the annual layers of old trees (such as, for example, 1 000-year-old Sequoia trees and others in Southern California) is directly dependent on fluctuations in solar activity. His research touched upon a deep historical layer of time.⁴

So, this is how the question of the relationship between various states of solar activity and manifestations of organic life on the Earth stood at 1915, when we, observing the sunspot activity of the Sun in the summer months of 1915, discovered the following fact: some periods of increased solar activity coincided with the development and intensification of military events on many fronts of the World War.

Later, Moreux wrote in his article *Le Soleil et nous* that he had noticed the following curious phenomenon, namely: world exhibitions, for example, those in Paris in 1867, 1878, 1889, 1900 and in Ghent in 1910, coincided with the minima of solar activity⁵, and some wars and military campaigns over several decades with its maxima. This issue has recently attracted the attention of some researchers.

In Russia, D. O. Svyatsky in 1917–1918 collected a small but interesting material concerning the same issue and pub-

lished two notes in the journal he edited.⁶

V. M. Bekhterev, a fellow of the Russian Academy of Sciences, in his extensive work *Collective Reflexology*⁷, speaking about the connexion between human activity and external nature, and then establishing the “law of dependent relations”, touched upon this curious issue and pointed out that “dependent relations in the social environment are not limited to the circle of only the surrounding nature of our Earth, but have a significantly broader spatiality, extending into the depths of the Universe with its inexhaustible amount of world energy flowing to us”.⁸

Whether the phenomenon of correspondence that we observed in 1915 was a simple coincidence or whether there really was some kind of relationship between phenomena on the Sun and military events on the Earth, but having become interested in these strange coincidences, I made the first attempt to find one or another explanation for them back then. Assuming that the starting point for the development of any event in human societies is the centres of higher nervous activity, I first of all focused on the question of what influence the formation of a sunspot can have on the behaviour of a person who, despite strategic, diplomatic and other obstacles, strives to intensify his military or social activity simultaneously with the intensification of the activity of our daily luminary. Then, using astronomical data on the Sun and the chronology of history, it was easy to verify the remarkable coincidences of some of the most important events in the life of Mankind over the past 300 years with the maximums of solar activity.

But the events that followed soon after tore me away from my current work for a long time, stopping the implementation of my planned research. Only when the excitement of the last revolution [the 1917 Revolution in Russia] had somewhat died down I got the opportunity to think about independent work and to renew in my memory the main principles of my theory.

Dissatisfied with the coincidences of solar activity and the activity of Man that I have discovered over a comparatively short period, I decided to trace whether the same dependence existed in historical epochs more distant from our time. This work of comparisons, as we will see below, contributed to the establishment of some extremely important facts that I laid as the foundation for a new understanding of the development of social events and the course of the historical process.

First of all, I have to turn to sources that testify to the state

¹This problem was studied in detail and presented in my other work: Chizhevsky A. L. *The Influence of Periodic Activity of the Sun on the Emergence and Development of Pathological Pandemics*.

²Shokalski Yu. M. *Oceanography*. St. Petersburg, 1917, page 523.

³Moreux T. *Le problème solaire*. Ed. Bertaux, Paris, 1900, 343 pages.

⁴Douglass A. E. *Climatic Cycles and Tree-Growth. A Study of the Annual Rings of Trees in Relation to Climate and Solar Activity*. The Carnegie Institution, Washington, 1919, issue 289.

⁵It is interesting to note that the Russian Agricultural Exhibition planned for the summer of 1923 in Moscow will also coincide with a minimum of solar activity.

⁶*Proc. of the Russian Society of World Studies (R.O.L.M.)*, 1918, vol. VI, no. 6(30), page 310, and also 1919, vol. VII, no. 1(31), page 39.

⁷1921, pages 409–412.

⁸Ernest Millard attempted to establish the dependence of historical phenomena on such a natural factor as secular fluctuations in the Earth's magnetism in his work *Une loi historique*. He considered 500-year fluctuations in the Earth's magnetism to be a period in the development of human society (see *Historische Zeitschrift*, 1909, Bd. 102, 654). See also: Reclus E. *L'Homme et la Terre*, en 6 livres, Ed. Librairie Universelle, Paris, 1905–1908, Le livre I — Les Ancêtres, Chapitre 1.

of solar activity in the historical epoch.

Observations of the Sun, the number of spots have been recorded since 1610, since their discovery by Galileo (1564–1642), Johannes Fabricius¹ (1587–1615) and also Father Christoph Scheiner² (1575–1650). At first, these observations were not accurate, were random, telescopes were poor, and there were relatively few observers (in England, the Sun was observed by 6 people, in Germany — by 5, in France — by 4, and in the Netherlands — by 1).

Only in a short period of time, since the observation methods were established and the network of observation points was expanded³, do we have reliable material on the activity on the Sun. But the periods of the first observations, the data about which were carefully collected by Rudolf Wolf (1816–1893) in his *Sonnenflecken Literatur* (1856) provided the opportunity to outline the dates of the maxima and minima of the sunspot activity, which was already given by Wolf in 1749 and then processed and continued to this day by A. Wolfer in tables and graphs (he published in *Astronomische Mitteilungen*, Zürich).

As for the epochs standing older than 1610, astronomy, except for some random indications, had no material for judging the distribution of solar activity cycles in them. Only some information from ancient Chinese (Chinese Annals), Arabic, Russian and Armenian chronicles, as well as from Western European city chronicles and annals (*Chroniken der deutschen Städte*), partly collected by me, partly from already prepared data (de Mairan, Arago, Hiragama, Svyatsky), helped to outline the approximate epochs of maximum solar activity stresses for the period of time from the first Chinese observation in 188 A.D. to the aforementioned period with significant gaps, sometimes reaching several decades.⁴

This information concerned mainly some meteorological

¹Johannes Fabricius was the first to lay the foundation for solar physics by describing his observations in the opus *De maculis in sole observatis et apparente earum cum sole conversione narratio, cui adjecta est de modo educationis specierum visibilium dubitatio* (1611).

²From the manuscripts of Thomas Harriot it is evident that this English astronomer was a competitor [to Galileo] in the discovery of sunspots, for he first observed them on December 8, 1610.

³Kew [a district of London], Zürich, Chicago, Greenwich, Medon, Cape of Good Hope, Kodaikanal, Dehra-Dun, Mount Wilson and others.

⁴While the solar corona was well described by Philostratus and Plutarch, the first date of sunspots being noticed on the Sun should be considered to be 188 A.D., according to Chinese records collected and published by the Japanese astronomer Shin [Makoto] Hirayama (*Observatory*, 1889, v. XII, page 218). They were based on a table of 45 observations of solar Fridays for the period 301–1205 A.D., compiled by the Chinese encyclopedist Ma Duanlin (1245–1322).

True, the evangelists Matthew, Mark and Luke point to the darkening of the Sun, which allegedly occurred after the death of Jesus Christ. Ovid (*Metamorphoses*, XV) and Virgil (*Georgica*, I) speak of the darkening of the Sun at the death of Caesar in 44 B.C. Similar phenomena have been repeatedly described and can be explained by other causes, and not by the presence of colossal sunspots, for example, the so-called, “dry fogs” that sometimes obscure the light of the Sun and were mentioned by Johannes Kepler (1571–1630) and Gemma Frisius (1508–1555) [born Jemme Reinerszoon], a Dutch astronomer in Louvain.

and optical phenomena developing in the atmosphere usually during the time of maximum solar activity. Sometimes there were also direct indications of the size, shape and number of sunspots, observed, of course, with the naked eye. All this data was not distinguished by accuracy and therefore required careful study, verification and careful systematization.

The very first steps in this direction revealed to me a truly amazing picture: the fluctuations of the historical process turned out to be simultaneous with the fluctuations of the physical and chemical processes in solar matter.

Further work showed that *although the historical life of Mankind does not calm down for a minute and continuously flares up now in one, now in another part of the Earth — at the moments of maximum solar activity it receives almost complete development over the entire surface of the planet.*

First of all, I had to develop a method of statistical accounting in equal units and classification of historical phenomena involving masses of people. This work presented many difficulties. It was necessary to resolve the question of what to take as a unit of accounting. Any historical event can be considered both in relation to quality (the significance of the event in the historical life of the people, its influence on other events, etc.), and in relation to quantity (for example, the number of people participating in the event, etc.). However, neither qualitative nor quantitative accounting of all events turned out to be completely impossible, because what could be precisely established for one event was inaccessible for another. In addition, a number of incidental phenomena (the duration of events, the space covered by the event, etc.) made it difficult to establish the feature of the event that interests us.

It was necessary to choose a *general method*, i.e., one that would be suitable for accounting for any historical phenomenon. To accomplish our task, I had decided to take as a unit of measurement the following:

- | | | |
|---|---|---|
| <ol style="list-style-type: none"> 1. The beginning (the first rise of the masses of people) and 2. The highest point of social tension (if such can be determined) | } | of each mass event of more or less major historical significance. |
|---|---|---|

My main attention was paid to the dates of the emergence of historical events, i.e., the dates of the first rise of the masses of people for achieving one or another goal.

The final conclusion was obtained after a long work as a result of a detailed statistical study of the history of the majority of states and peoples [they are listed below], inhabiting all five continents of the globe and known to science, starting from 500 B.C. and ending in 1914, i.e., for 2414 years.

In order to get acquainted in detail with the history of all the listed peoples, countries and states, I used the sources and manuals in ancient and modern languages that were available to me at the time I was living through.

- | | | | |
|--------------------|------------------------|------------------------|--------------------------|
| 1. Europe: | Austria-Hungary, | Indo-China, | Morocco, |
| Greece, | Turkey, | Ceylon, | Congo, |
| Rome, | Romania, | Indonesia, | Other African nations, |
| Italy, | Russia, | Siberia, | European colonies, etc. |
| Germany, | Lithuania, | Asian Russia, | |
| Gaul, | Poland, | Afghanistan, | 4. America: |
| France, | Czech Republic, | Arabia, | Canada, |
| Iberia, | Bulgaria, | Eastern Roman Empire, | California, |
| Spain, | Serbia, etc. | Turkey, | Texas, |
| Portugal, | | Persia, | Other United States, |
| England, | 2. Asia: | Palestine, Israel, | Mexico, |
| Ireland, Scotland, | China, | Other ancient peoples. | Peru, |
| Holland, | Tibet, | | Brazil, |
| Netherlands, | Mongolia, | 3. Africa: | European colonies, etc. |
| Norway, | Japan, | Egypt, | |
| Sweden, | Korea, | Carthage, | 5. Australia: |
| Denmark, | Central Asian peoples, | Mauritania, | European colonies, etc., |
| Switzerland, | Huns, | Sudan, | Tasmania, |
| Hungary, | India, | Abyssinia, | Oceania. |

This work allowed me, on the basis of quantitative relationships, to state the following basic provisions characterizing the course of the world-historical process:

1. On different continents of the Earth, in different countries, among different peoples, dependent or independent of each other in political or economic terms, as well as in relation to the territory they inhabit, the main moments of their historical life, associated with the movement of large masses of people, tend to be synchronous; the number of historical events occurring simultaneously in different parts of the Earth gradually increases with the approach to the maximum of solar activity, reaching the greatest number in the epochs of maximums, and decreases with the approach to the minimum of solar activity.

This allows us to consider each cycle of historical events of the world-historical process as *universal*.

2. In each century, the universal cycle of historical events is repeated exactly 9 times. Throughout the world history of Mankind, beginning with 500 B.C. and until the present time, in each century I have discovered 9 clearly outlined concentrations of the initial moments of historical events.

Thus, it can be considered that each cycle of the general historical, military or social activity of humanity is equal, on average, to 11 years.

3. The epochs of concentrations of historical events are divided among themselves by epochs during which the number of new historical events falls to a minimum.
4. The epochs of concentrations of historical events coincide with the epochs of maxima of solar activity; the epochs of rarefaction coincide with the epochs of minima of solar activity.

For the time since 1610 about the last provisions must be considered fully established, in view of the significant amount of historical data, and then the accuracy of observations of solar activity.¹

5. More or less prolonged historical events, continuing for several years and receiving a decisive manifestation in the era of maximum solar activity, as well as the evolu-

¹In the beginning of my research, I assumed that the abundance of mass movements recorded by history, regardless of their intensity, would have to harm the establishment of quantitative relationships in different periods; however, even minor mass movements of peoples and small episodes, taken on a par with major historical phenomena, could not prevent the discovery of a periodic pattern of concentrations and discharges.

True, in such a case the difference in the number of events during periods of the cycle [of solar activity] opposite in intensity was sometimes not so clearly revealed; but this is simply explained by the presence of a significant number of secondary and minor phenomena taken into account. The objections that can be made in this direction find a sufficiently weighty rebuttal in the following words of P. P. Lazarev, a fellow of the Russian Academy of Sciences: "For the construction of a theory it is especially advantageous if experimental methods and observations do not immediately provide data with a high degree of accuracy, and thus make it possible to ignore the mass of secondary accompanying phenomena that complicate the establishment of simple empirical patterns. In this regard, for example, the observations of Tycho de Brahe, which gave Kepler the material for creating his laws, were precisely sufficient in accuracy to characterize the motions of the planets around the Sun in the first approximation. If, on the contrary, Kepler had obtained those most precise observations that can be had in our time, then, of course, his attempt to find an empirical law could not have led to simple and sufficiently clear results due to the complexity of the entire phenomenon and would not therefore have given Newton the material from which the theory of universal gravitation was created" (Lazarev P. P. *Research in the Ionic Theory of Excitation*, Part I, Moscow, 1916, page 6). In this regard, we remind the reader of one scholastic axiom, which was pointed out by Sir W. Hamilton (Sir W. Hamilton. *Discussions on Philosophy*. 2nd edition, London, 1853, page 630): "Frustra sit per plura quod fieri potest per pauciora" (it would be futile to cite more numerous reasons for something whose origin can be explained with the help of fewer of them).

tion of ideologies, mass sentiments, etc., accompanying these events, proceed according to a general historical cycle, undergoing the following clearly detectable [successive] stages:

- I. The stage of minimum excitability;
- II. The stage of increasing excitability;
- III. The stage of maximum excitability
- IV. The stage of decreasing excitability.

These four stages (let us call them *periods*) tend to coincide completely with the corresponding eras of solar activity: minimum of sunspots, an increase in the number of sunspots to their maximum, their maximum, and then decrease from the maximum with a transition, again, to a minimum of sunspots.

As is known, the transition from minimum to maximum solar activity occurs somewhat faster than the transition from maximum to minimum, i.e., sunspot formation increases faster than it dies down.

Based on the considerations provided in the item 5 [of the above list], I have found it possible to divide each historical cycle synchronous with the solar cycle into 4 periods:

- Period I (minimum excitability) = 3 years;
- Period II (increasing excitability) = 2 years;
- Period III (maximum excitability) = 3 years;
- Period IV (decreasing excitability) = 3 years.

The statistical accounting of world history events for 500 years (from the 15th to the 20th centuries) that I carried out using the method indicated earlier showed their distribution over 4 periods of the cycle, namely:

- During Period I (3 years) 5% of all historical events begin;
- During Period II (2 years) 20% of all historical events begin;
- During Period III (3 years) 60% of all historical events begin;
- During Period IV (3 years) 15% of all historical events begin;

and, therefore,

- During 1 year of Period I 1.7% of all historical events begin;
- During 1 year of Period II 10% of all historical events begin;
- During 1 year of Period III 20% of all historical events begin;
- During 1 year of Period IV 5% of all historical events begin.

The above allows us to consider one world historical cycle, consisting of 4 periods, as a model, as the basic unit of

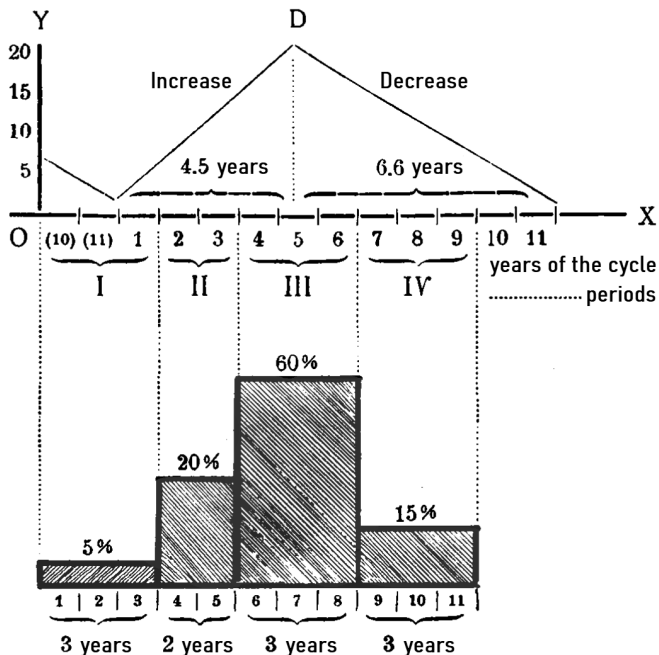


Fig. 1: Percentage ratio of occurrences of historical events to years and periods of the cycle. Average output for 500 years (15th–20th centuries).

time measurement of the historical process, due to the [discovered] fact that the *internal structure of each historical cycle corresponds to the internal structure of all other historical cycles*; then, using the comparative-historical method, I conducted a study of all of the psychological and social manifestations of the mentioned [discovered] cycle, in order to then synthetically derive the laws governing the development of events in each period of the cycle.

I call the new branch of knowledge that arose on the basis of these considerations *historiometry*.¹ The first and basic unit of measurement for counting historical time is one cycle of solar activity, equal, on average, to 11 years.

I call this unit of historical time measurement a *historiometric cycle*, according to the above introduced terminology. Based on some data, we can make an assumption about the existence of other (multiples of the basic) periods in the historical life of Mankind. This issue is currently under my investigation.

A clear confirmation of all that has been said above can be found in the historiometric table and graphic representation of the fluctuations of the world-historical process presented here, compiled from the data attached to [my work] *A Study of the Relationship between the Sunspot-Forming Activity and the Course of the World-Historical Process, Beginning with the 5th Century B.C. and Until the Present Time*.

As we have just said, throughout world history we have discovered 9 historiometric cycles in each century. For ease

¹Measuring historical time using physical units.

Table 1: Historiometric table for the period from the 5th century B.C. to the 20th century A.D.

		5th century B.C.		4th century B.C.		3rd century B.C.	
No.	11-year periods	Historiometric cycles	11-year periods	Historiometric cycles	11-year periods	Historiometric cycles	
1	(500)	494—487	(389)	396—390	(289)	286—278	
2	(489)	480—479	(378)	382—376	(278)	275—271	
3	(478)	470—460	(367)	371—362	(267)	266—260	
4	(467)	457—453	(356)	355—351	(256)	256—249	
5	(456)	450—447	(345)	344—338	(245)	243—237	
6	(445)	435—431	(334)	335—326	(234)	230—227	
7	(434)	428—422	(323)	323—321	(223)	225—215	
8	(423)	418—410	(312)	311—307	(212)	212—206	
9	(412)	407—399	(301)	301—295	(201)	202—195	
		2nd century A.D.		3rd century A.D.		4th century A.D.	
No.	11-year periods	Historiometric cycles	11-year periods	Historiometric cycles	Solar activity (histor. chron.)	Historiometric cycles	
1	(101)	101—106	(201)	197—201	301 ●	303	
2	(112)	114—116	(212)	209—216	311	311—314	
3	(123)		(223)	221—226	322	323	
4	(134)	132	(234)	231—234	342	340	
5	(145)	147	(245)	242	354 ●	351	
6	(156)	162—167	(256)	248—251	359	357—368	
7	(167)	173	(267)	260—269	374 ●	371—378	
8	(178)	178	(278)	272—277(285)	388	383—391	
9	188	184	(289)	295—296	395	394—397	
		8th century A.D.		9th century A.D.		10th century A.D.	
No.	Solar activity (histor. chron.)	Historiometric cycles	Solar activity (histor. chron.)	Historiometric cycles	Solar activity (histor. chron.)	Historiometric cycles	
1	(701)	—	(797)	798—802	(896)	899—904	
2	(712)	711—712	807	808—812	905	907—915	
3	(723)	717—720	(818)	823—824	919—930 (?)	921—929	
4	(734)	732—733	830	832—833	940	937—941	
5	745	737—740	840 ●	841—846	(948)	944—947	
6	(755)	752—759	848 (?)	856—859	956	951—955	
7	765	—	860	865	(966)	961—969	
8	778	772—782	874	875—878	974	973—978	
9	786	787—793	(885)	885—891	979—993 (?)	981—988	
		14th century A.D.		15th century A.D.		16th century A.D.	
No.	Solar activity (histor. chron.)	Historiometric cycles	Solar activity (histor. chron.)	Historiometric cycles	Solar activity (histor. chron.)	Historiometric cycles	
1	1307	1303—1307	1402	1398—1403	(1500)	1499—1502	
2	(1312)	1311—1315	(1403)	1408—1415	(1510)	1509—1512	
3	1325	1322—1330	(1424)	1419—1422	1520—1527	1517—1528	
4	(1336)	1337—1340	1431	1427—1434	1537	1531—1536; 1542	
5	1353 ?	1345—1353	1446	1443—1456	1551 ●	1549—1553	
6	1365	1356—1365	1461	1458—1464	1560 ●	1558—1563	
7	1372 ●	1368—1372	(1472)	1469—1471	1572 ●	1566—1573	
8	1383	1377—1385	(1483)	1476—1485	1581 ●	1578—1582	
9	(1394)	1388—1396	1490	1489—1495	1588 ●	1585—1592	

Table 1: Historiometric table for the period from the 5th century B.C. to the 20th century A.D. (continued).

2nd century B.C.		1st century B.C.		1st century A.D.		
11-year periods	Historiometric cycles	11-year periods	Historiometric cycles	11-year periods	Historiometric cycles	
(189)	191—189	(89)	90—82	(1)	6—9	
(178)	186—183	(78)	78—72	(12)	14—19	
(167)	171—165	(67)	69—62	(23)	—	
(156)	156	(56)	58—51	(34)	—	
(145)	149—143	(45)	49—41	(45)	42—45	
(134)	135—133	(34)	33—31	(56)	58—59	
(123)	126—118	(23)	27—25	(67)	64—70	
(112)	113—108	(12)	16—12	(78)	78—85	
(101)	105—101	(1)	—	(89)	91	
5th century A.D.		6th century A.D.		7th century A.D.		
Solar activity (histor. chron.)	Historiometric cycles	Solar activity (histor. chron.)	Historiometric cycles	Solar activity (histor. chron.)	Historiometric cycles	
401	401—406	502	507—510	603	602—604	
(412)	408—415	(513)	515—517	(614)	614—618	
(423)	419—420	535	529—536	626	622—628	
(434)	429—433	(546)	539—543	(634)	633—637	
450 ●	448—455	(557)	551—555	(645)	641—642	
(467)	465	566 ●	566—568	(656)	653	
(478)	476	577 ●	575	(667)	668—670	
(489)	486—493	585 ●	581	(678)	681—187	
(500)	496	(596)	—	(689)	695—697	
11th century A.D.		12th century A.D.		13th century A.D.		
Solar activity (histor. chron.)	Historiometric cycles	Solar activity (histor. chron.)	Historiometric cycles	Solar activity (histor. chron.)	Historiometric cycles	
1005	1000—1004	1104 ●	1103—1106	1202 ●	1201—1205	
1014	1012—1015	1118 ●	1113—1119	(1213)	1211—1216	
(1025)	1026—1030	1129 ●	1124—1132	(1224)	1223—1228	
1039	1035—1041	1137 ●	1135—1139	1238—1242 {	1234—1238	
(1050)	1044—1052	1145	1143—1147		1239—1246	
(1061)	1056—1059	1157	1154—1162	(1253)	1255—1256	
(1072)	1068—1073	(1168)	1166—1176	1269	1265—1270	
1078 ●	1075—1085	1185 ●	1182—1188	1276	1275—1282	
1096	1093—1100	1193	1191—1197	1292	1285—1293	
17th century A.D.		18th century A.D.		19th century A.D.		
Solar activity		Solar activity		Solar activity		Historiometric cycles
Max.	Min.	Max.	Min.	Max.	Min.	
1605 ●	1610.8	1705.5	1712.0	1805.2	1810.6	1797—1809
1615.5	1619.0	1718.2	1723.5	1816.4	1823.3	1812—1822
1626.0	1634.0	1727.5	1734.0	1829.9	1833.9	1824—1833
1639.5	1645.0	1738.7	1745.0	1837.2	1843.5	1835—1843
1649.0	1655.0	1750.3	1755.2	1848.1	1856.0	1845—1856
1660.0	1666.0	1761.5	1766.5	1860.1	1867.2	1857—1868
1675.0	1679.0	1769.7	1775.5	1870.6	1878.9	1870—1877
1685.0	1689.5	1778.4	1784.7	1883.9	1889.6	1879—1888
1693.0	1698.0	1788.1	1798.3	1894.1	1901.7	1891—1900

Fig. 2: Average curves of fluctuations of the world-historical process for the period from the 5th century B.C. to the 20th century. The abscissa (horizontal line) shows the years, the ordinate (vertical line) shows the number of occurrences of the most important events in the world history of Mankind. The dots show pre-telescopic and then — astronomical data on the intensity of the Sun's activity; the dashes show its minima.

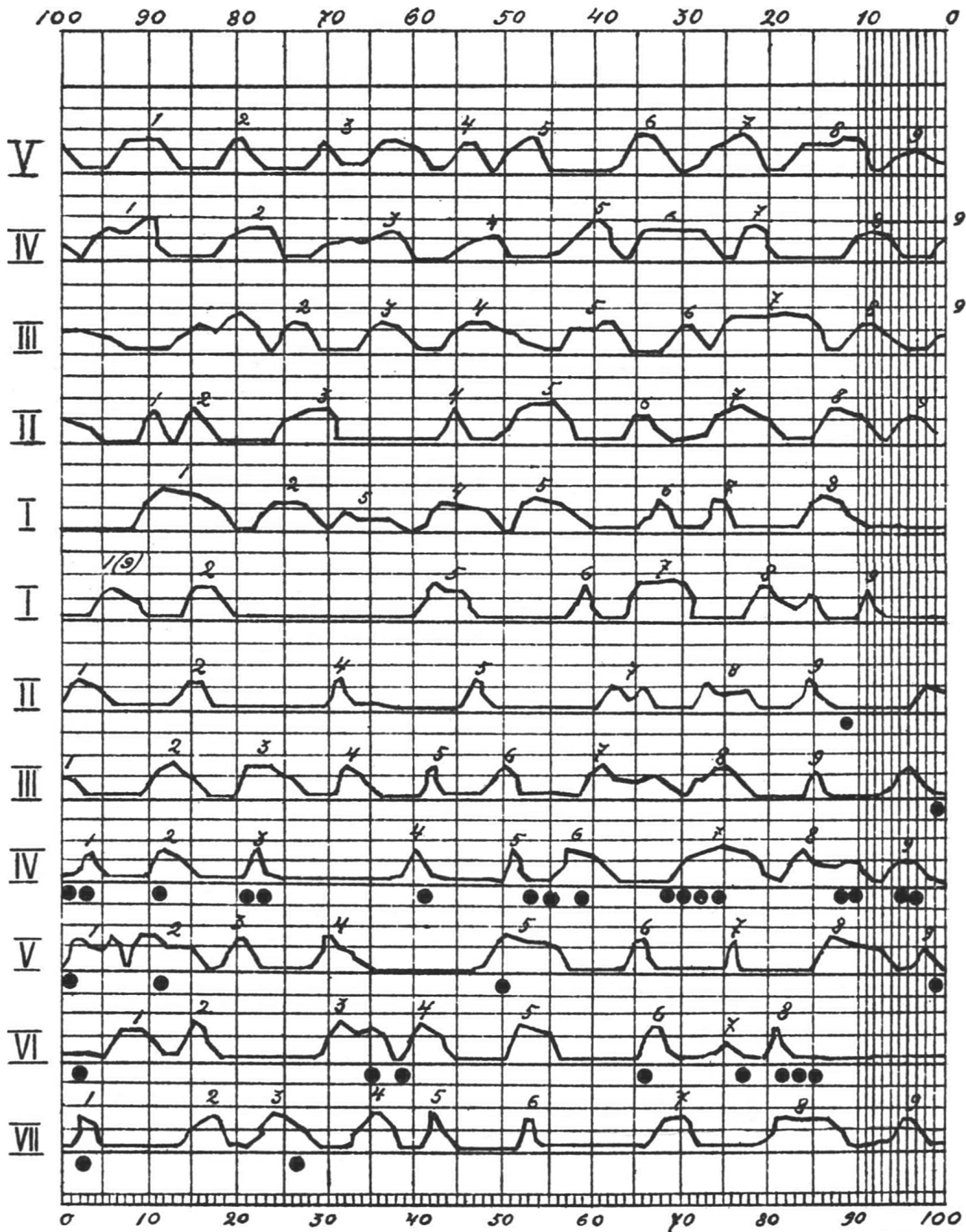


Fig. 3: Average curves of fluctuations of the world-historical process for the period from the 5th century B.C. to the 20th century. The abscissa (horizontal line) shows the years, the ordinate (vertical line) shows the number of occurrences of the most important events in the world history of Mankind. The dots show pre-telescopic and then — astronomical data on the intensity of the Sun's activity; the dashes show its minima (*continued*).

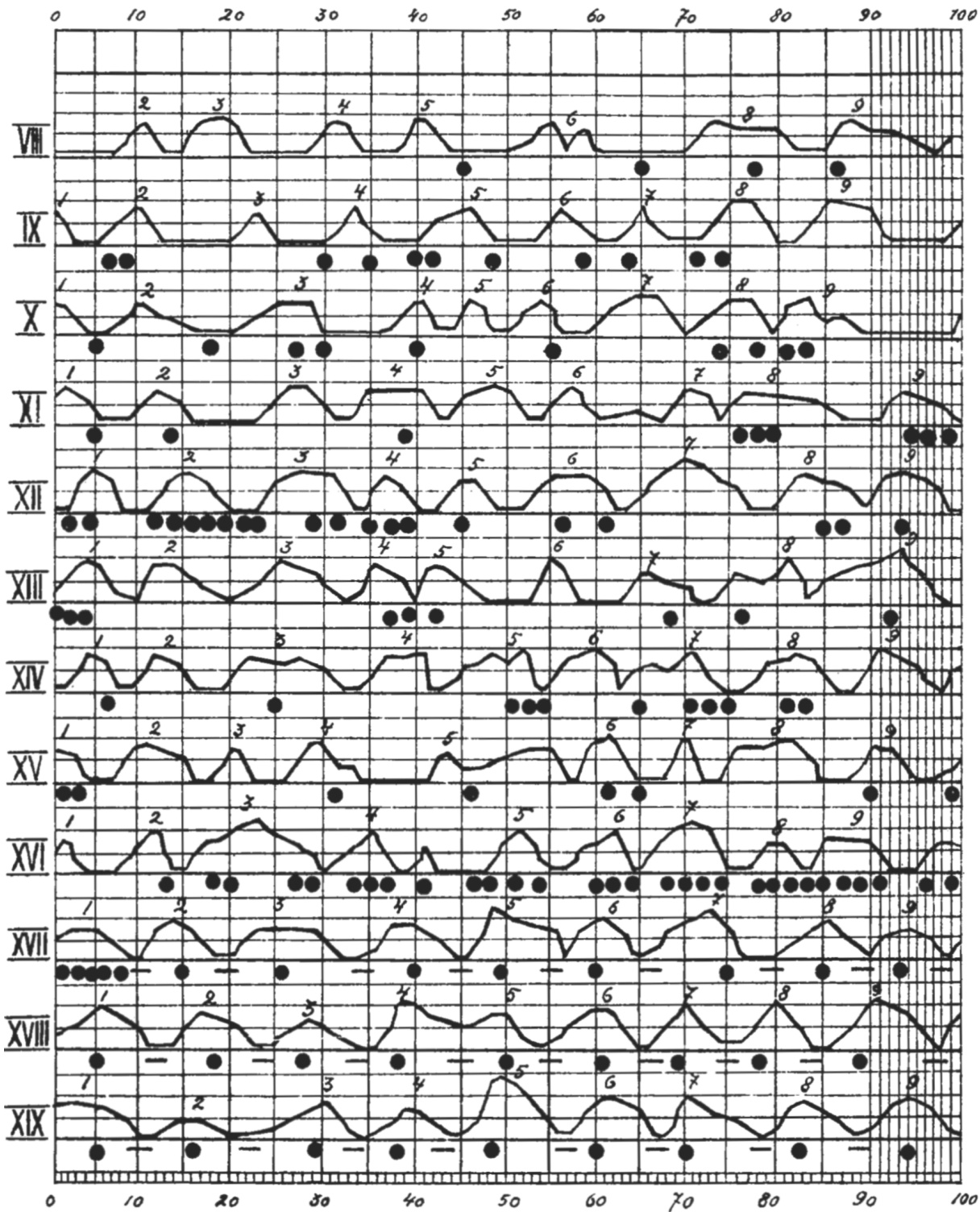


Fig. 4: Parallelism of the curves of sunspot activity (lower curve) and the global military-political activity of humanity (upper curve) from 1749 to the present time (1922).

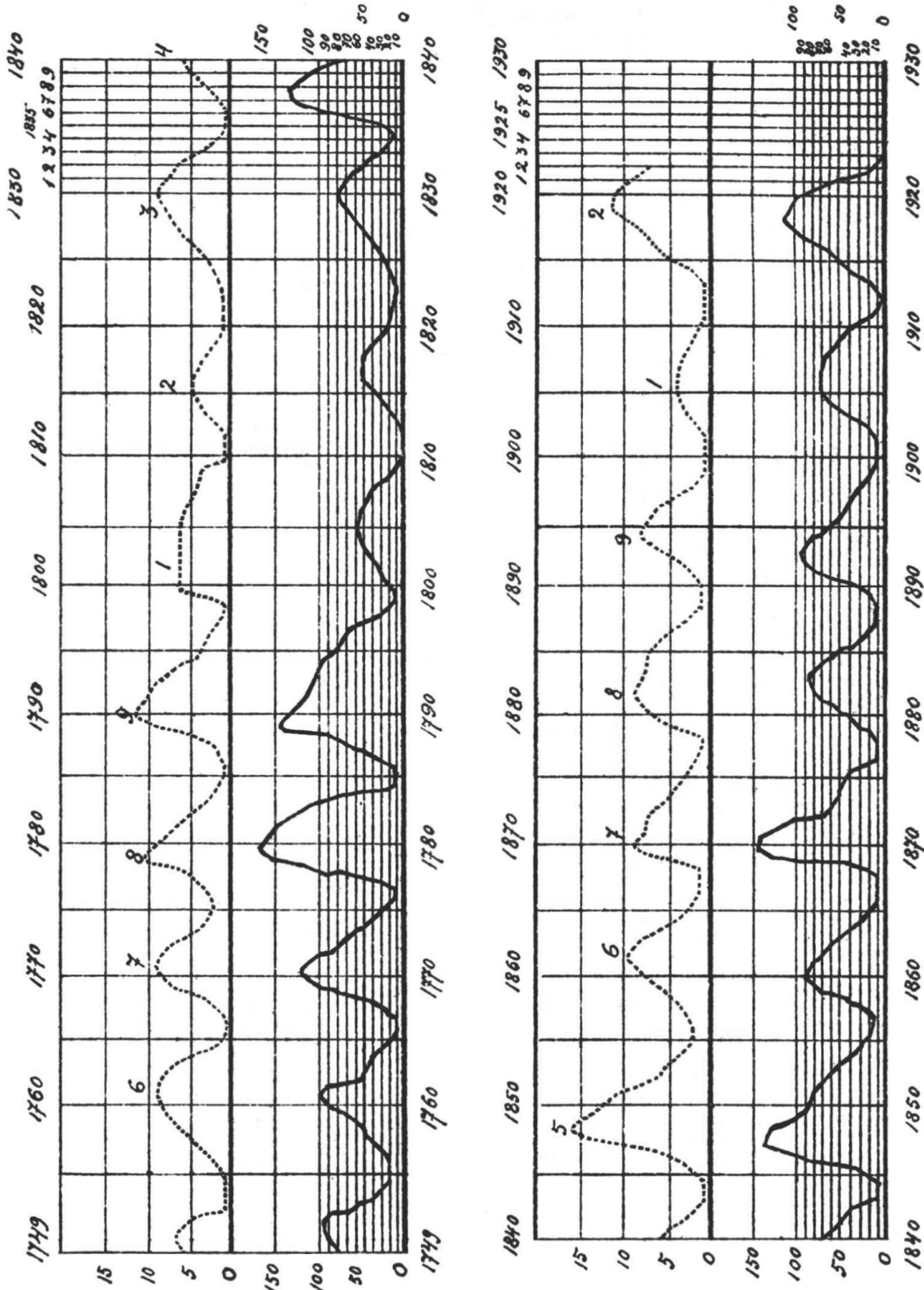
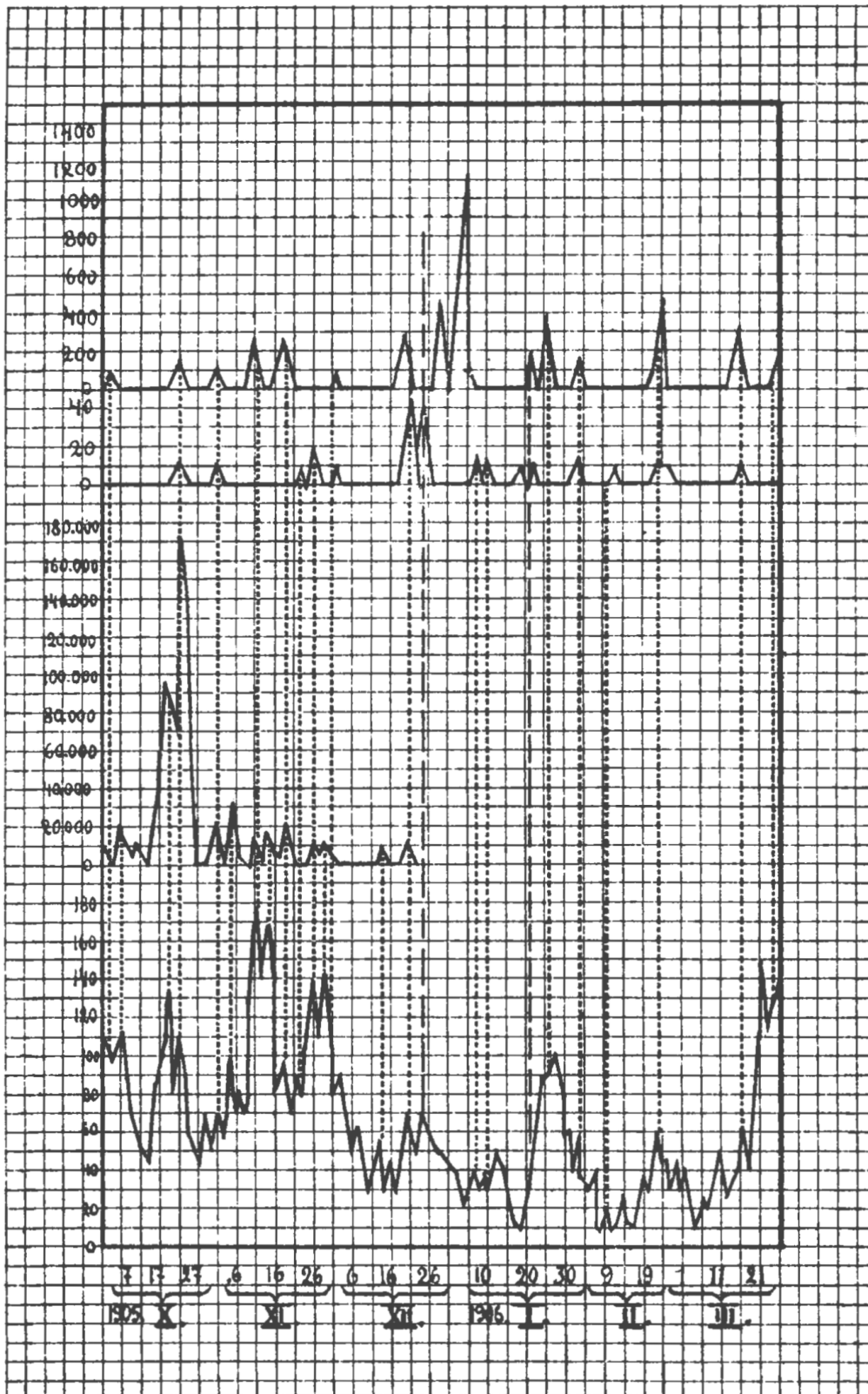


Fig. 5: Coincidences of increases in sunspot formation (lower curve) and outbreaks of revolutionary activity of the masses of people in Russia for the period from October 1, 1905 to April 1, 1906 (rallies and strikes, assassination attempts, immediate repressions).



of distribution they are numbered (from 1 to 9) and then collected in a table, the first attempt¹ at constructing which is attached here and to which significant amendments must be made during further study of the issue.

This table only shows the sizes of clusters (concentrations) of newly emerging historical events, as well as the sizes of pauses between them, i.e., the time of comparative calm and tranquility.

In addition, the historiometric table compares the following to clarify the relationships between the activity of the Sun and the [social] activity of Mankind:

1. From the 5th century B.C. to the 16th century A.D. — equal 11-year time intervals (numbers in brackets).
2. From the 2nd century A.D. to the 12th century — historical data on the state of the sunspot activity of the Sun (probable epochs of maxima are typed in bold; the most reliable of them are marked with dots.²
3. From the 17th century to the 20th century, astronomical data on the maxima and minima of solar activity according to the latest data.³

But the historiographical table does not show the moments of the highest tensions of the ubiquitous and general activity of Mankind.

The latter is clearly represented by the curves in Fig. 2 and Fig. 3, which should be considered fair only in general terms, due to the possible inaccuracy of historical data and some involuntary accounting errors.

The abscissa (horizontal line) shows the years, the ordinate (vertical line) shows the number of initial moments of the most important events in world history. The dots under the curves show the dates before telescopic observations, which testify to the intensity of the Sun's activity in the historical era, and then, starting from the 17th century, also astronomical data. The minima are indicated by dashes. When examining the curves, it is easy to notice that in most cases the curve seems to move away from the dots upwards; the dashes, on the contrary, seem to attract it to themselves. This means that the increase in solar activity is accompanied by the intensity of the combined activity of humanity and vice versa: its decrease coincides with a general calm.

It should be considered very important that most of the rises of our curve reach the highest point of the rise, the so-called points of greatest density, after which they gradually descend. This shows that each historiometric cycle, like the cycle of sunspot activity, has a moment of maximum tension,

¹A more detailed experience of constructing a historiometric table, indicating the activity of the Sun in the historical era according to Douglass and Danjon, is attached to my mentioned work *A Study of the Relationship between the Sunspot-Forming Activity and the Course of the World-Historical Process, Beginning with the 5th Century B.C. and Until the Present Time*.

²*Proceedings of the Russian Society of World Studies (R.O.L.M.)*, 1918, vol. VII, page 232.

³*Meteorologischen Zeitschrift*, Heft 10, 1916, Seiten 327–1922.

when events in the human environment erupt everywhere and intensely.

Some inaccuracy of the found coincidences means only the insufficiency of pre-telescopic observations and partly incompleteness of information about historical events. This has been completely eliminated over the last 4 centuries, when our curve (see Fig. 4) completely coincides with the average curve of solar activity.

The curves presented in Fig. 4 for the period from 1749 to 1922 are the best proof of this. Here we observe almost complete rectilinearity of the coincidence of the curves and the equal value of the corresponding ordinates.

As for the period of ancient history and partly the Middle Ages, as can be seen from Fig. 2, even in these eras we see in each century exactly 9 clearly outlined concentrations of events in world history and moments of maximum tension in human activity. As a result of all the above, it is necessary to admit that the fluctuations of the historical process in ancient times were also closely connected with the fluctuations of the sunspot-forming activity of the Sun and were subject to the same regularity.

III Social and psychological characteristics of one complete historical cycle

The motivation for dividing each [historical] cycle into 4 periods was the data obtained as a result of studies of historical events that developed in parallel with the corresponding changes in solar activity. Analyzing the course of each event separately and then comparing its known stages with similar solar activity stages of other historical events, it was not difficult to arrive at the conclusion that, despite the absence of any connexion between them, they all flow along an identical channel, making similar rises, turns and falls at certain moments. The most diverse events of world history were involved in this analysis, beginning with the ancient Greek and Roman uprisings and military campaigns and ending with the revolutions and wars of modern ages. Formal correspondences in the development of historical phenomena, sometimes having nothing in common with each other either in space or in historical time, but possessing a certain parallelism of evolution, are a motivating reason to assume the existence of some periodically acting factor, independent of local time or spatial conditions and endowing the course of various historical events with an internally obligatory, almost universal regularity and morphological identity. The distinctive features of the latter, although not stationary, are subject to fluctuations only within insignificant limits.

Synthesizing the collected material, I have obtained for each period of the historiometric cycle the following characteristics, briefly outlined here, a kind of ideal of the form underlying each historiometric cycle, which is free from various accidents and superficial phenomena of temporary or local significance.

Period I of the historiometric cycle (the period of minimum excitability)

The characteristic features of this period are the following: disunity of human masses, indifference of the human masses to political and military issues, peace-loving mood of the human masses, compliance, tolerance, etc.

The appearance of these psychological signs in the historically active human masses in the 1st period of the cycle is usually accompanied by the absence of any desire for any struggle for an idea or right, and therefore entails easy capitulation, surrender, throwing down of arms, flight from the battlefield, etc.

Such behaviour of individuals or entire groups of people forces the ruling circles of the state to appropriate measures: concluding a series of truces with the enemy and, finally, peace; capitulation under harsh conditions, opening of diplomatic relations, declaration of neutrality, then disbandment of troops, etc.

In the memoirs of contemporaries and in historical studies, this period is noted for its general peace-loving mood, unwillingness to enter into any disputes, the end of most military actions and the triumph of the principle of non-intervention in international and national military-political life. Historians try to explain these facts by the exhaustion of moral and physical strength, mental fatigue after the unrest experienced, the breakdown of state unity, the cessation of the influence of the previously unifying cause, incapacity for combat, the fall or departure of the [former] leaders who had lost the trust of the masses of people and power over them, etc.

The aspirations of humanity in other fields of social activity also change: the flow of social life, falling into the channel of calm and peace, gets the opportunity to apply its quiet course to the achievement of other goals, to the solution of other problems.

Here the spiritual activity of Man begins, cultural values are created, pure art and science are placed in the corner of social life, replacing the stormy turmoil of recent days and devaluing with their achievements everything created hastily and precariously. In the period of minimum, humanity strives for calm, rests from the worries of previous years and gathers physical strength for the inevitably approaching new era of [social] unrest.

A study of the historical events that took place in the 1st period allowed us to establish a number of facts, according to which the period of minimum excitability contributes to [the following actions]:

1. The conclusion of peace treaties;
2. Conquest expeditions of a non-mass character;
3. Capitulation;
4. Occupation;
5. Maximum reduction of parliamentarism;
6. Strengthening of autocracy or rule by a few.

Period II of the historiometric cycle (the period of increasing excitability)

The psychological and historical complexity of this period required very extensive research, as a result of which I have collected considerable data relating to this period. Here I am forced to limit myself to only a general remark.

Already the beginning of this period in historical studies is characterized by a significantly greater rise in the excitement of human masses than in the preceding period. There is still no unity of the masses of people; only little by little do the parties and groups that had fallen apart during the period of minimal excitability begin to reorganize, leaders are outlined, programs are defined. The power of suggestion manifests itself among the human masses: statesmen, military leaders, orators, the press are regaining their importance. Questions, political and military, begin to appear from behind the horizon of public life and gradually become more acute. The tendency to perseverate homogeneous thoughts is noticeable everywhere, filling the mental activity of the human masses. In spite of the will of individuals, the concentration on the same military or political themes, in the presence of, of course, favorable reasons for this, gradually increases; ideas circulating among the human masses begin to dominate.

There is still hesitation and indecision in resolving important state issues, the conclusions have not yet matured completely, but preparations for war may already be thundering, the international situation is becoming complicated. However, the rulers do not yet decide to enter into open struggle or declare war: they are still hesitating, waiting for the right moment and anticipating its gradual growth of the general excitement of the masses of people. Indeed, soon, in a year or two, and sometimes less, the unanimous demand of the masses of people, aimed at resolving one or another issue, gains the upper hand. Now even persons who are far from military or political affairs are forced to join one or another political or military group.

At the end of the 2nd period, which can gradually assume a stormy character and reveal the impatience and nervousness of the masses of people, we notice one of the most important phenomena of the military-political life of communities, namely: the desire to unite the various nationalities that make up a given community for the purpose of defense or attack, and the merging of various political groups to counter other political groups.

The significance of this period is that it lays the foundation for the further development of historical events during a given cycle in a given human community and, in part, even predetermines their course during the period of maximum excitability.

The period in question does not always and in all human communities occupy the same period of time; its duration or brevity is determined by the state of solar activity on the one hand, and by the diversity of political, economic and other

factors on the other. In addition, this period, depending on the same reasons, takes on various forms of manifestation.

During the 2nd period, three main phases should be distinguished in the order of their gradual development: 1) the emergence of ideas among the masses of people; 2) the grouping of ideas, and 3) the identification of one main idea among the masses of a given human community by the initial moment of the 3rd period.

1. The emergence of main ideas during the first phase of the period of increasing excitability is directly dependent on internal state policy, economic and international military-political factors, which in this case are of equal importance: the economic condition of the state, the degree of organization and stability of power and the state apparatus; the international situation — the threat of war, blockade, occupation, etc., as well as on various moods and ideas wandering among large masses of people. If at a given moment in a given community there are no factors of dissatisfaction with the existing system or order of things, the above phenomena may not arise, which will cause a more or less calm course of the historiometric cycle. However, there are still no guarantees that sharp complications will not arise in the further development of the cycle; indeed, almost always, even with minimal presence of exciting causes, the subsequent period can be marked by some private events with local participation of human masses.
2. The bearers of ideas that have arisen in this way become a psychic centre for the formation of groups of people united by one basic idea. This process takes place in accordance with class consciousness, the financial level and the personal qualities of each individual. The groups of people that have formed in this way can put forward a new leader from among themselves in order to subordinate their psychic imbalance to a certain psychic centre, where incoming ideas are summarized, transformed into uniform directives and creating certain formulas of action for the organized group.
3. The third phase develops from the second and consists of: a) the identification of one supreme idea that absorbs many group ideas; b) the unification of a number of separate groups around the supreme psychic centre that subordinates the mass [of people], and c) the mass focusing [of people] onto one idea.

All three phases of the 2nd period sometimes develop quite mechanically, without the organizing participation of active individuals, completely unexpected effects of mass unity, for which they prepare for the approaching beginning of the 3rd period of the historiometric cycle — the period of maximum excitability. Thus, the need matures to resolve, first of all, the first fundamental question that worries the masses in the human community.

Period III of the historiometric cycle (the period of maximum excitability)

This is the main stage of development of each cycle, resolving the world-historical problems of humanity and founding new historical epochs. It incites humanity to the greatest follies and the greatest benefactions: it embodies ideas in life by means of the shedding of blood and the clanking of iron. If we wished to give a comparative-historical characteristic of this period, we would have to repeat the main events of world history: all of them, as the comparisons of the activity of the Sun and Man have shown, occurred in epochs of intense solar activity. In this period, the greatest revolutions and the greatest clashes of peoples took place, beginning new eras in the life of humanity and justifying with this the terrible formula of Heraclitus the Dark (ca. 535–475 B.C.): “*Polemos panton esti pater kai basileus*” — war is the father and king of everything. The parallelism of the activity of two substances remote from each other — solar matter and brain matter — manifests itself with particular clarity and clarity precisely during this period.

Here we cannot consider the significant amount of the [historical] material collected by me during the study of the period of maximum excitability. In [my work] *Fundamentals of Historiography* this problem is devoted many pages. Here I will point out only those main factors, the presence of which in the human masses determines the emergence and development of decisive events in human communities:

1. The stimulating effect of popular leaders, military leaders, orators, the press, etc. on human masses;
2. The stimulating effect of moods and ideas circulating in the human masses;
3. The speed of excitability from the unity of the psychic centre;
4. The size of the territorial scope of the mass movement of people;
5. The integration and individualization of the masses of people.

Never does the influence of leaders, military leaders, orators, the press, etc., reach such a tremendous force as during the period of maximum intensity of the sunspot-forming activity of the Sun. During this period, sometimes one well-timed word or one gesture is enough to move entire armies and the masses. One wave of the leader draws under the banners heterogeneous nationalities, which are part of the state, opposing parties, which make up the human community. In this era, the leader's word – his winged word – does an amazing job: the masses of people listen to him, obey him, while the whole streams of exhortations that were heard at every step during the period of the minimum could not lead to the desired result. Now even the leader's name, pronounced aloud, causes a powerful surge of inspiration. The masses follow the leader blindly, without thinking, carried away by a

whirlpool of acute excitement and ecstasy.

The power of the leaders' influence mechanically advances gifted individuals above the masses of people, without regard for traditional norms and established laws. And so, at the top of mass movements we see the greatest military and political geniuses that humanity has ever known, spiritual leaders, champions of freedom, founders of various human associations. All of them, having broken through the thickness of nations, as bright embodiments of the aspirations of the human masses of the given moment, are already leading them and with their help lay the foundations for new human formations, new forms of social life, new types of spiritual quests. Such advances, as a special study of general history shows, can only occur in the case of the unity of the masses of people, and the latter is observed exclusively in epochs and moments of increased activity of the Sun.

Of no less importance are ideas that appeal to the human masses during the period of maximum excitability. In this case, the influence of oral agitation, as well as the press, can acquire a decisive significance on the outcome of one or another political or military movement.

The period of maximum excitability may just be called the period of the emergence of the face of human masses and the sounding of the voice of the people. Historians are at a loss before the facts, which indicate that ideas which no one dared to speak of a year or two ago were now expressed openly and boldly; the human masses became more impatient, more restless, more excited; they began to raise their voices, to demand and to arm themselves. Demonstrations became more malicious and hostile, popular assemblies did not proceed peacefully: the masses of people imperiously demanded, sword in hand, recognition of their decisions; impulses were no longer restrained and, immediately seized upon by the masses of people, led to the overthrow of everything that agitated and disturbed the minds. Individual whims and pranks immediately became law, and punishment was meted out to anyone who attempted to contradict them; the [human] population was seized by a profound hatred for their enemies, who were given over to extermination, being paralyzed by some wondrous magic.

During the period of maximum excitability, sometimes the slightest pretext is enough for the human masses to flare up, rise up in uprising, or volunteer to a war. Even one rumor, put into circulation among the human masses, can lead to general unrest and uprising. What usually causes calm discussion during the period of minimum, at the time in question excites the human masses and leads to uprisings, wars, bloody episodes. The masses of people thirst for movement, the troops are restrained with difficulty, the soldiers are inclined to mutiny, and the people — to anarchy. In a word, the excitement increases unusually and the human organism seems to demand a discharge. This is explained by the fact that the combination of the above reasons causes a sharp change in the nervous and mental tone of the human masses, increas-

ing their nervous and mental reaction to external stimuli. Individuals are unable to suppress their heightened reflex excitability, exhibiting very significant reactions even to weak and insignificant stimuli.

The memoirs of contemporaries testify to the astonishing speed of the spread of popular uprisings and mass [social] movements in general, which took place during the period of maximum excitability. Here, for example, are several descriptions of the speed of the spread of uprisings, taken from various sources: the uprising engulfed the country with extraordinary speed; in a few days, huge areas were raised to their feet; the entire population joined the rebels, as if by the wave of a magic wand; the uprising spread throughout the state with the speed of a hurricane; the uprising broke out almost simultaneously in different parts of the country; attracting huge crowds of people to its banners; the roar of the uprising rolled over the entire country with the speed of a thunderclap; the flames of international war engulfed vast spaces and the entire population — from small to great took part in the uprising. It is not for nothing that Titus Livius called social conflicts "infectious pestilence".

In addition to the speed of spread of mass movements of people, it is also worth noting the significance of territorial scope. Indeed, an uprising that began somewhere in one state can, given certain conditions, penetrate into neighboring countries. History knows examples when wars, uprisings and other mass movements, in a short period of time, covered huge areas — the lands of many peoples and even entire continents.

The basis of the above is the unanimity of the masses of people, which is especially clearly outlined in this period when resolving any military or political issues. Now, at the call of a leader, tens, hundreds of thousands of people can gather under the battle flags, inspired by one thought, one desire. In place of hostility, unanimity reigns and a common thought inflames minds. This unanimity in a period of maximum excitement is capable of miracles; even recent enemies can become friends in order to confront together the strongest and most formidable danger or to resolve a common and important issue for all. At such moments, nationality, party affiliation, and social status are partly obscured; private feuds subside and all who must, hasten to the designated assembly points. In a word, in the name of any military campaigns, uprisings, etc., complete agreement and peace are established in the country between the contradictory and previously hostile elements of the state. At such moments the whole country, as one person, is ready to pursue the intended goal. This consciousness of unity and complete solidarity in the masses of people destroys all disputes and squabbles. Mental contagion or mutual suggestion reaches its highest point, and the human masses turn into a collective personality — the [human] collective becomes individualized.

This brings with it various phenomena characteristic of any struggle, and mass movements of people usually undergo

abnormal deviations. Sometimes the height of the struggle reveals the entire vast area of human madness, instability and passion. Elemental violence, bitterness, frenzy, thirst for revenge, epidemics of murder, panic, pogroms, devastating raids, desperate battles, mass exterminations, bloodbaths, as well as uprisings, mutinies, coupled with the manifestation of fanaticism and heroism — reach their apogee. Crowds of people can rejoice at the sight of the most terrible violence, atrocities, murders. They invent the most excruciating executions. Madness is embodied in life. What was considered impossible and wild in the period of minimum excitability, in the period of maximum may well go hand in hand with morality and the loftiness of the ideals pursued. Before these impulses and manifestations of both the masses and individuals, as a result of the extraordinary state of psychic excitement, the feelings of danger, self-preservation, even instinct must die out.

Thus, the ground is prepared for the solution of questions of a world-historical nature — the ground on which systems of human communities are erected. Here events occur that hardly have equals in other periods of the historiometric cycle. We state the fact that the greatest revolutions, wars and other mass movements of people that created systems of states, laid the foundation for turning points in history and shook the life of Mankind on the territories of entire continents, tend to coincide with the epoch of maximum tension of solar activity and develop the highest intensity at the moments of its highest tensions.

The study of historical events that took place in the 3rd period allowed us to establish a number of facts, according to which the period of maximum excitability contributes to:

1. Unification of human masses;
2. Advancement of leaders, military leaders, statesmen;
3. Triumph of ideas supported by the human masses;
4. Maximum development of parliamentarism;
5. Democratic and social reforms;
6. People's power and limitation of autocracy;
7. Uprisings, unrest, riots, rebellions, revolutions;
8. Wars, campaigns, expeditions;
9. Emigrations, re-settlements, persecutions and other outbreaks of mass human activity.

Several examples from the huge number of coincidences of solar and human activity encountered throughout world history can serve as an illustration of the above.

The numbers indicate the dates of the eras of maximum solar activity (according to annals, chronicles and astronomical data) *completely synchronous* with the most important historical events (deviations do not exceed 2–3 years).

Based on this list, we can assume that such outstanding figures of antiquity as Miltiades, Themistocles, Cimon, Pericles, Lysander, Pelopidas, Epaminondas, Hannibal, Marius,

TURNING POINTS IN WORLD HISTORY:

- 1492 — fall of the Muslim states in Spain; discovery of America; beginning of Modern History;
- 1789 — the Great French Revolution; beginning of Modern History;
- 1917 — Revolution in Russia, which has a historical significance for the world.

THE MOST IMPORTANT UPRISINGS AND REVOLUTIONS:

- 1306 — the great uprising in England;
- 1358 — the great uprising in France;
- 1368 — the great uprising in China;
- 1381 — the great uprising in England;
- 1526 — the great uprising in Germany;
- 1648 — revolution in England;
- 1789 — revolution in France;
- 1830 — the July Revolution (France);
- 1848 — the February Revolution (France) and the pan-European crisis;
- 1860 — uprising in Italy;
- 1870 — the Paris Commune;
- 1917 — revolution in Russia.

CRUSADES:

- 1094–1096 — 1st Crusade
- 1147 — 2nd Crusade
- 1187 — 3rd Crusade
- 1194 — 4th Crusade
- 1212 — Children's Crusade
- 1224 — 5th Crusade
- 1270 — 7th Crusade

P.S. The Crusade that began in 1248 (minimum solar activity) was not carried out by masses of people, but by Louis IX with a small number of troops.

THE GREAT MIGRATION OF PEOPLES:

Years: 374; 409; 449–451–452; 568.

MASS PERSECUTION OF JEWS:

- 1093 — Southern Europe;
- 1144 — Germany and Italy;
- 1182 — France;
- 1215 — Western Europe;
- 1290 — England;
- 1306 — France;
- 1348 — Europe;
- 1391–1394 — Spain, France;
- 1481 — Spain;

1491–1494 — Spain, Lithuania;
 1704 — Ukraine;
 1830 — Europe;
 1849 — Europe;
 1881–1882 — Russia, Hungary, etc.

PERSECUTION OF CHRISTIANS:
 Years: 303; 362; 575; and others.

BLOODY EPISODES OF WORLD HISTORY:

1185 — massacre of the Latins in Thessalonica;
 1204 — destruction of Byzantium;
 1520 — massacre in Stockholm;
 1560 — massacre in Vassy;
 1572 — St. Bartholomew's Day massacre in France;
 1588 — London executions;
 1739 — Delhi massacre;
 1768 — Uman massacre;
 1792 — September massacres in France (the next minimum — in 1799);
 1860 — massacre of Christians in the East;
 1896 — massacre in Constantinople and many others.

THE RISE OF POPULAR AND SPIRITUAL LEADERS, REFORMERS, MILITARY LEADERS AND OFFICIALS:

395 — Alaric;
 444 — Attila;
 536 — Vitiges;
 536 — Belisarius;
 622 — Mohammed;
 719 — Charles Martel;
 1096 — Peter of Amiens;
 1146 — Bernard of Clairvaux;
 1306 — Robert the Bruce;
 1365 — Wycliffe;
 1367 — Tamerlane;
 1381 — Wat Tyler;
 1402, 1412 — Jan Hus;
 1420 — Ivan Zizka;
 1429 — Joan of Arc;
 1489 — Savonarola;
 1519–1525 — Luther, Zwingli, Vasa, Müller;
 1537 — Ignatius Loyola;
 1605 — False Dmitry;
 1605 — Vasily Shuisky;
 1612 (max. 1615) — Minin, Pozharsky;
 1625 — Zhmaila;

1625 — Richelieu;
 1626 — Wallenstein;
 1637–1639 — Pavlyuk, Gunya, Ostranitsa, Alexander Leslie;
 1648 — Bogdan Khmelnytsky;
 1648 — Oliver Cromwell;
 1683 — Eugene of Savoy;
 1769 — Haider Ali;
 1777 — Lafayette;
 1777 — Washington;
 1788 — Suvorov;
 1805 — Wellington;
 1839 — Shamil;
 1848, 1860 — Garibaldi;
 1870 — Moltke;
 1870 — Gambetta;
 1917 — Kerensky;
 1917 — Lenin.

Sulla, Spartacus, Catelina, Vercingetorix, Caesar, Germanicus, Civilis and many others first appeared on the arena of public life or first acquired public significance in the epochs of maximum sunspot activity¹

Let us pay attention to Table 2, which represents the time distribution of all the most important battles from the 5th century B.C. to the year 1 A.D.

Having arranged the dates of the most remarkable battles of antiquity for these 5 centuries by centuries and decades, it is easy to discern two striking patterns that are observed in the distribution of these events in time. The first of them is the amazing coincidence of the digits standing in place of the units and tens of any historical date of one century with the digits standing in place of the corresponding units and tens in the historical date of another century or after one, two or three centuries. For example:

496–394–295–197	340–241–42
490–390–191/190	433–333/331–30
480/479–280/279	525–425–225
371–272–74/72	418–218
168–69	410–212
466–66	606/604–406/405
362–260	401–301–202–101/102

Another pattern is observed in the distribution of these same dates in each century. It turns out that the dates of the indicated battles are separated from each other, in most cases, by numbers multiple of 10–11 years, i.e., by the time inter-

¹From the historiometric table it is easy to see that the listed persons came to the fore precisely in the middle of concentrations of historical events.

Table 2: The most important battles of the 7th–1st centuries B.C.

years	7th–6th cent.	5th century	4th century	3rd century	2nd century	1st century
100		496. Lake Regillus	394. Cnidus & Coronea	295. Sentinum	197. Cynoscephalae	
90		490. Marathon	390. Allia brook		{ 191. Thermopylae 190. Magnesia	
80						{ 86. Chaeronea 85. Orchomenus
		{ 480. Thermopylae, Artemision, Salamis 479. Plataea, Mycale		{ 280. Heraclea 279. Asculum 275. Beneventum 272. Taranto		{ 74. Cyzicus 72. Sertorius
70			371. Leuctra			69. Tigranocerta
60		466. Eurymedon	362. Mantinea	260. Lipari Islands	168. Pydna	66. Euphrates
50						
				241. Aegates		{ 46. Thapsus 45. Munda 42. Philippi
40			{ 340. Vesuvius 333. Chaeronea			30. Actium
			{ 334. Granicus 333. Issus 331. Arbela (Gaugamela)			
30		434. Actium 433. Sybota				
	525. Pelusium	{ 425. Pylos, Sphacteria 422. Amphipolis		{ 225. Telamon 222. Sellasia		
20		{ 418. Mantinea 415. Syracuse		{ 218. Ticinus & Trebia 217. Lake Trasimene & Metaurus 216. Cannae 212. Syracuse		
10		410. Cyzicus				
	{ 606. Harran 604. Carchemish	{ 406. Arginusae 405. Aegospotami				
		401. Cunaxa	301. Ipsus	202. Zama	{ 102. Aquae Sextiae 101. Vercellae	

375–476 (101 years)	the main waves of the Great Migration of Peoples;
622–632 (10 years)	the era of Muhammad’s activity;
1224–1235 (11 years)	the main waves of the Tatar invasion to Russia;
1380–1480 (100 years)	the main stages of the overthrow of the Tatar yoke;
1389–1448 (59 years)	the main stages of the struggle of the Turks with the Christian world; the 1st and 2nd battles on the Kossovo field;
1460–1471 (11 years)	the main stages of the War of the Scarlet and White Roses in England;
1481–1492 (11 years)	the main stages of the struggle with the Moors in Spain;
1489–1498 (9 years)	the era of Savonarola’s activity;
1562–1572 (10 years)	two bloody episodes: the massacre in Vassy and the St. Bartholomew’s Day Massacre;
1614–1789 (max.–max.)	the years of two convocations of États généraux in France; from 1614 (max. solar activity) to 1789 (max. solar activity) États généraux were not convened at all;
1702–1714 (12 years)	the War of the Spanish Succession;
1789–1804 (15 years, max.–max.)	the final stages of the republican system of the Great French Revolution;
1830–1848 (max.–max.)	July Revolution — February Revolution in France, and also pan-European crisis;
1848–1860 (max.–max.)	Garibaldi uprisings;
1905–1917 (max.–max.)	1st and 2nd revolutions in Russia.

val between one and another maximum of solar activity. For example:

5th century:	490–480; 466–433; 433–425; 425–415; 415–405;
4th century:	390–371; 371–362; 362–340; 340–381; 381–301;
3rd century:	280–272; 272–260; 260–241; 241–222; 222–212; 212–202;
2nd century:	197–190; 190–168; 168–102;
1st century:	86–74; 74–66; 66–46; 46–30.

Here are some more examples showing the same multiple dates for many historical events (many similar examples could be given); see on top of this page.

Thus, according to the epochs of solar activity maxima, from maxima to maxima, and sometimes through several maxima, the historical life of nations fluctuates, following the indications of this cosmic factor. These fluctuations can be found throughout the history of Mankind. If we, for example, try to outline the main stages in the life of the states of Ancient Greece and Ancient Rome, we will be convinced of their remarkable distribution.

All other mass phenomena in human communities are in the same connexion with the activity of the Sun, namely:

1. Formation of religious, military, political, artistic, trade corporations, associations, unions, leagues and partnerships, etc. For example:

Lombard Cities League	1167 (max. sol. activity)
Hanseatic Cities League	1241 (max. sol. activity)
Swiss Cities League	1352 (max. sol. activity)
Swabian Cities League	1381 (max. sol. activity)
Cambrai League	1508 (max. sol. activity)
Ratisbon League	1524 (max. sol. activity)
Schmalkaldic League	1530 (max. sol. activity)
Sacred Union League	1576 (max. sol. activity)
Maximum activity of the Sacred Union	1587–88 (max. sol. act.)
Augsburg League	1686 (max. sol. activity)

2. The spread of various teachings — political, religious, etc.; the spread of heresies, religious unrest, pilgrimages, political conspiracies are subject to the same regularity. For example, social theories were spread mainly during periods of maximum excitement: the Genève and Lyon anarchists (1880–1882), the Paris and Liège anarchists (1892).

Let us briefly trace the history of the revolutionary movement in Russia in the 19th century (according to Prof. Alphons Thun and others):

1815	the literary society “Arzamas”;
1816 (max.)	the first political society in Russia;
1817	the first secret society in Russia;

1825 (max. begins) ... the Decembrist uprising;
 1837 (max.) ... Stankevich's circle;
 1848 (max.) ... Petrashevsky's circle;
 1861 (max.) ... the abolition of slavery in Russia;
 1862 ... unrest in Russia;
 1868 (min.) ... "The Bell" magazine closed due to falling circulation;
 1869 (max. in 1870) ... beginning of the spread of socialist teachings;
 1870 ... "People's Cause"; a brief revival of "The Bell"; Tchaikovsky's circle;
 1871 ... the Nechayev trial;
 1872 ... activities of the anarchists Bakunin and Lavrov; movements "going to the people"; Dolgushin's society;
 1875 (to min.) ... disorganization of socialist propaganda in Russia;
 1876–1877 ... the revolutionary societies "Land and Freedom", "Common Cause";
 1878–1879 ... maturing of solar activity was marked by the transition to terrorism;
 1879 ... the revolutionary workers' organization "Executive Committee";
 1880–1881 (to max.) ... the revival of the revolutionary movement: peasant unrest, riots, armed resistance to the police and troops, assassinations, murders, mass Jewish pogroms;
 1879–1882 ... the revolutionary societies "People's Will", "Black Redistribution", "Corn"; "Free Word", "Baltic Federalist", "Truth" and others;
 1887 (to min.)–1895 ... lull in the revolutionary movement in Russia.

3. Localization of excitation on various ideas, entertainment, spectacles, etc. The ideas of all 8 crusades, without exception, originated and were especially intensively spread during the periods of maximum solar activity. The idea of doomsday, which was supposed to happen in 1000 A.D., began to excite the medieval world 10 years before the expected event (993 — max. sol. act.). The idea of the "peace of the Lord" arose in 1030 (max.), then spread throughout Europe in 1040 (max.). The Fronde in France 1648–1653 (max.); the Dreyfus trial 1894–1896 (max.) and many others.

4. Mass morbid manifestations of human neuropsychic activity develop mainly in the periods of spot formation tension. For example¹:

1374 ... St. Vitus' Dance;
 1500 ... mental epidemic in Ouvre;
 1630 ... mental epidemic in Madrid;
 1642 ... mental epidemic in Louviers;
 1728, 1738 ... Saint-Médard mental epidemic.

5. It is also impossible not to note the fact that pathological epidemics and pandemics very often coincide with the period of maximum.

Let us now focus our attention on the development of cholera epidemics (cholera asiatica).

Historical information about cholera is small. According to Ozanam, cholera was known even in the time of Hippocrates, raged mainly in China, when it was described by the Chinese doctor Jang Chon Ko. According to Haeser, the cholera epidemic in the first half of the 11th century affected significant areas in India, part of the Asian continent and appeared in Constantinople.

The first precise indications of devastating cholera epidemics in the 14th century are found in Persian writers between 1364 and 1376. Russian chronicles mention observations of sunspots in 1365. Chinese chroniclers (according to Hirayama) wrote about large spots on the Sun, visible to the naked eye in 1370, i.e., just during the period of the strongest cholera epidemics described by the Persians. According to Riegler, the cholera epidemic appeared in Constantinople, Syria, Arabia, Egypt shortly before the conquest of Byzantium by the Turks.

The French traveler Sonnerat described a devastating cholera epidemic in India, where it claimed about 60 000 victims in three years from 1768 to 1771. An increase in solar activity was noted by Jean Gaspard Staudacher in Nürnberg and other observers in 1769, i.e., exactly during the period of the spread of cholera in India. There is undoubted evidence of significant cholera epidemics on the Coromandel Coast in 1774–1780. Maximum solar activity was attributed to 1778. An epidemic is known in Tranquebar, Madras and other places in India in 1787–1790. Maximum sunspot formation was noted by astronomers in 1788. Since about this time, thanks to the development of medical knowledge, strict records have been kept of the epidemic spread of cholera, which periodically makes round-the-world trips and systematically visits Europe, where it first appeared in 1830 (max. solar activity), if you do not count its short-term, quickly extinguished stay in the city of Astrakhan in 1823 (min. solar activity).

In studying the spread of cholera epidemics and pandemics (i.e., general epidemics), I adhered to the order currently accepted in medical epidemiology, although it should be noted that dividing cholera movements into any periods is not entirely accurate. The fact is that cholera never disappears from the Earth, but only calms down from time to time, concentrating in some area, in order to again conquer vast areas with the same force. These periods of calm strikingly

¹The question of the dependence of the development of mental epidemics on solar activity is presented by me in a separate other work.

Sunspot activity		Pandemic number	Cholera pandemics		
Maximum	Minimum		Beginning of the pandemic	Period of maximum spread of the pandemic	End of the pandemic
1816	1823	1	1816	1817	1828
1829 1837	1883	2	1827	1829—31 + 1837	1833 +
1848	1856	3	1844	1848	1857
1860 1870	1867 1878	4	1863	1863—66 1870—72	1875
1883	1889	5	1883	1883—86	1889
1894	1900	6	1890	1892,94	—

Table 3: The relationship between the development of cholera pandemics in the 19th century and sunspot activity.

coincide with the lull in the sunspot-forming activity on the Sun. On the contrary, with the increase in the vital activity of our daily luminary, cholera epidemics sometimes take on a general, threatening character.

What has been said is expressed with sufficient clarity in Table 3, borrowed, in some abbreviation, from my special study of this issue.

Plague epidemics and pandemics somewhat deviate from exact simultaneity with the course of periodic processes on the Sun, but statistical calculations show that the state of the Sun and the state of humanity associated with it are also reflected in the development and spread of plague microorganisms. Over a period of several centuries, plague pandemics coincided with the era of solar activity maxima about 30 times, with the era of minima — 8 times; between maximum and minimum — 6 times, and between minimum and maximum — 2 times¹.

The most severe epidemics of infectious diseases, as comparisons have shown, also very often coincide with solar activity maxima.

Period IV of the historiometric cycle (the period of decreasing excitability)

The period of decline in excitability is even no less interesting from a historical and psychological point of view than the periods preceding it. It can also abound in major events, but usually only those that arose earlier are completed during this period.

The period of decline in excitability is, as it were, an echo of the stormy period of struggle and unrest that preceded it, the highest degree of tension of which has already passed, and a general need for calm and peace is felt. If there is a

¹My study of this issue is not yet complete.

war, its heat gradually dies down, sluggishness is observed in military actions, their tempo slows down.

Now for the first time one begins to feel satiety with war, robbery, blood. Observance of military obligations and treaties is no longer necessary; allied countries do not provide combat support; separatism begins to appear more and more often; military alliances disintegrate.

The still continuing movements of troops resemble the convulsions of a dying person, and crowds of soldiers with the same impatience thirst for peace as they recently thirsted for war. At this time, the movement of enemy troops, if the latter are still sufficiently disciplined, does not meet with serious resistance. Meanwhile, so recently the entire country met the appearance of enemies with fire and sword. Gradually, armies turn into a disobedient herd and quickly thin out; soldiers scatter in crowds, rushing home, and the general warlike mood in the masses is replaced by a peace-loving one.

Leaders, commanders, orators lose those forces that in the preceding period fettered the masses and forced them to obedience. The masses are already subject to suggestion with difficulty.

Newly emerged wars or uprisings do not flare up, but quickly subside, ending in peace on lenient terms. If a year or two earlier it would have been possible to raise an uprising, now it does not work and all attempts will lead to nothing. Historians are often surprised by the fact that the elements of opposition do not gather together, as was the case in the life of the country so recently, do not rebel, do not rise up simultaneously in many places, but, on the contrary, hesitate, do not decide, acting by their slowness in a destructive way on all military or political alliances.

This lack of unanimity in the 4th period of the historiometric cycle can be called a stumbling block on which any newly-begun uprising, any mass activity risks being wrecked, since concentrated action, due to the reduction and relaxation of the connecting forces, becomes impossible. The military campaigns or invasions that were started are prepared without enthusiasm, even with obvious lack of sympathy. The enthusiastic mood of the masses of people in favor of reforms, popular representation, wars, uprisings, and so on weakens, giving way to complete indifference. Indeed, everyone expresses a tendency toward reconciliation, and talk of peace begins. These talks are heard in the most warlike countries.

The decline in the degree of unanimous communication of the masses of people causes disputes and discord in groups, unions, and states. The latter circumstance makes all human groups ineffective and indecisive.

The above in its complex totality leads to a renunciation of recent claims, and demands that were previously defended with foam at the mouth are reduced to a minimum.

Finally, the general decline in excitability is replaced by a psycho-physical state that can be called enervation. Popular assemblies and representations are dispersed without protest, uprisings are easily suppressed, wars do not flare up, and also

Table 4: Schematic presentation of data from one complete historiometric cycle.

The arithmetic mean is 11.124 years				1 sunspot formation cycle	Sunspot activity of the Sun
Number of spots					
5.96 years		Number of sunspots		5.16 years	
IV.	III.	II.	I.	Period	☉
Number of sunspots and their groups is decreasing	Maximum	Number of spots and their groups is increasing	Minimum	Relative number of sunspots	
The arithmetic mean is 11 years				1 historiometric cycle	Social activity of human masses
3 years (arithm. mean)	3 years (arithm. mean)	2 years (arithm. mean)	3 years (arithm. mean)	Periods of historiometric cycle	
Period of decreasing excitability	Period of maximum excitability (era of concentration)	Period of increasing excitability	Period of min. excitability (era of irritation)	Names of the periods	
Decreasing number of mass social movements	Maximum	Growing number of mass social movements	Minimum of mass social movements	Relative number of historical events	
150%	600%	200%	50%	Number of hist. events, % (aver.)	
50%	200%	100%	1.70%	Number of hist. events per year, % (average)	
Progressive slowness of society's reactions to stimuli; degradation of concentrated action, enthusiasm, inspiration, etc.	1. a) Affecting human masses by popular leaders, mil. commanders, mass media, orators, etc. b) Affecting by the ideas circulating among the masses. 2. a) Rapid rise of mass movements; b) Wide territory covered; c) Integration of the masses; d) Individualization of groups; e) Dynamic state of the masses	1. Rise of the ideas of social order, collective concentration begins; 2. Grouping of the ideas and masses; 3. Emergence of a single basic idea and the unity of the masses	Differentiation of human masses, indifference to social problems, peaceful moods among the masses, compliance, tolerance, depression, static state of the masses, etc.	Socio-psychological behaviour of human masses during each period of the cycle	
	Phenomena that develop in society if there are exciting factors of a military, political or other nature			Comment	
Disintegration of military and political organizations; separatism, renunciation of international or domestic claims, dispersal or disintegration of popular assemblies, completion of events that began in the previous period	Rise of leaders, military leaders, and officials; triumph of ideas supported by human masses; triumph of parliamentarism; democratic and social reforms; democracy, limitation of autocracy. Revolutions, uprisings, turmoil, rebellions, wars, invasions, emigrations, resettlements, persecutions, and other outbreaks of mass human activity	Indecision in resolving military and political issues, preparation for war, complication of foreign affairs, beginning of conspiracies; determination of military and political tendencies	Conclusion of peace treaties, non-massive invasions of conquest, captivities, occupations; maximum reduction of parliamentarism, strengthening of autocracy	Historical phenomena that occur during each period of the cycle	

peace negotiations are mechanically caused by the depressive state of the masses of people, which is often facilitated by physical exhaustion and fatigue.

Such is, in brief, the morphological identity of all historical cycles — “universal” changes in the behaviour of the active masses of humanity during each historiometric cycle.

Here we schematize in a certain way the historical phenomena connected with the state of solar activity. There can be no doubt that all these phenomena are much more complex and intricate than they are presented here. But, using this schematization, which in many respects should be considered as *preliminary*, we can move forward in an objective study of this question. Let us now dwell on some general remarks concerning the course of the historiometric cycle.

Changes in the behaviour of humanity are especially prominent in the development of long-term historical phenomena. Here, stages of enormous energy, upsurge and inspiration, then a gradual decline of this energy with a transition to a state of fatigue and apathy are clearly outlined. Then, after some time, a general revival, excitement, growing agitation and finally a rise in political or military enthusiasm, characteristic of the period of maximum, are again observed. Long-term historical phenomena that began with the second period of the historiometric cycle provide an ideal example of changes throughout the cycle. All major historical events, covering entire countries and lasting for several decades, were subject to cyclic fluctuations in their development, which is easy to see when studying any [historical] event in connexion with changes in sunspot formation processes on the Sun.

True, such a clear distinction between the various periods of the historiometric cycle is not always feasible; sometimes it is necessary to simply grope our way to their definition, guessing the boundaries by the mood of the masses of peoples, by their aspirations, by the spirit of history of the given moment.

As is well known, the disturbance of solar matter, expressed in the appearance of sunspots, sometimes arises somewhat faster than it subsides, although the time interval between the minimum and the next nearest maximum is, on average, almost equal to the time interval between the maximum and the next nearest minimum.

The number of historical events and, most importantly, the degree of intensity of their development tend to follow in all details the changes in the curve of solar activity, but in some periods of the historiometric cycle they undergo significant deviations. Thus, sometimes general human activity reaches its maximum shortly before the maximum of solar activity and remains at the same height for some time at the beginning of the 4th period. It also happens that the maximum of general human military and political activity does not occur exactly simultaneously with the solar maximum, but is somewhat delayed. But if we draw the average curve of

several periods of the sunspot-forming activity, it completely coincides with the average curve of several historiometric cycles. This shows the undoubted connexion that exists between these two phenomena.

In addition, irregularities are often observed in relation to the gradual increase in the number of historical events with an average increase in solar activity. Then the curve of the historiometric cycle only vaguely resembles the sinusoidal course of the phenomenon; it is more like the daily course of the temperature of a typhoid patient, like the teeth of a semicircular saw. Here, sharp rises and falls, shifts and interruptions are observed. All of them depend on the most diverse, incalculable, private, military and political reasons that occur in human communities. However, it should be noted that rises and falls in the course of the curve of the historiometric cycle can arise as a result of sharp fluctuations in solar activity. This is a fact of the greatest importance.

It should also be added here that the rapid increase in sunspot formation after a minimum sometimes causes a series of historical phenomena that quickly fade away, but arise again by the period of maximum excitation, gradually increasing the intensity of their manifestations.

The aforementioned questions, as well as many other questions concerning the theory we are substantiating, are investigated and presented in my other works.

Having completed a brief review of the characteristic features of each part of the historiometric cycle and having established the relationship between the activity of the Sun and humanity, we present here the *basic morphological law of historiometry*, formulated by me as follows:

THE BASIC MORPHOLOGICAL LAW OF HISTORIOMETRY: The course of the world-historical process is made up of a continuous series of cycles, each of which lasts for a period of time equal in average to 11 years, and which are synchronous in the magnitude of their activity with the periodic spot-forming activity of the Sun.

Each cycle has the following historical and psychological features:

1. At the midpoints of the course of the cycle, the mass activity of humanity on the entire surface of the Earth, in the presence of economic, political or military stimulating factors in human communities, reaches maximum tension, expressed in pandemics, revolutions, uprisings, wars, campaigns of conquest, migrations, creating new formations in the life of individual states and new historical epochs in the life of humanity, and accompanied by the integration of the masses of people, the revelation of their activity and the rule of the majority.
2. At the end points of the cycle, the tension of universal human activity of a military or political nature decreases to a minimum limit, giving way to creative activity and accompanied by a general decline in politi-

cal or military enthusiasm, peace and calmed creative work in the field of organizing state foundations, international relations, science and art with the disintegration and depression of the human masses and the strengthening of absolutist tendencies of power.

All conceivable deviations from the above basic law are caused by reasons that lie outside the mentioned cosmic factor, and are only a consequence of the main events that arose during the period of maximum excitability, but did not have time, for one reason or another, to end within the period that caused them.

IV The influence of geophysical and cosmic factors on the behaviour of individuals and groups of people

The successive changes in the global activity of Mankind during each of the cycles required an explanation from the point of view of modern biophysics.

However, it was necessary to clarify first the question of how the activity of the Sun influences the centres of the higher nervous system of Man — directly or indirectly, i.e., directly on the organ of mental activity or with the participation of such factors as famine, which arose as a result of drought (which, in turn, could be a consequence of the activity of the Sun) and caused war or the high cost of food, which prompted the people to revolt, etc. The study of this question showed that the indirect factor, although often accompanying, is by no means necessary.

In fact, the same number of concentrations of historical events in each century and their simultaneity in many regions of the Earth quite clearly indicate that these phenomena are caused not by some local natural factor with a limited area of action, but by some forces that strictly periodically influence humanity, regardless of what area of the globe it inhabits. Here, precisely this simultaneity of mass unrest or even disturbances throughout the globe is striking. Therefore, it is necessary to conclude that the disturbing forces act everywhere at one and the same absolute time.

If the course of historical events were left entirely to itself and not a single cosmic factor influenced it, we would never have discovered in it regular fluctuations of a more or less precise period and their simultaneity throughout the entire territory of the planet.

From what has been said, it follows that there is some extraterrestrial force that influences the development of events in human communities from the outside. The simultaneity of the fluctuations of solar and human activity serves as the best indication of this force.

So, for now we must admit that the electrical energy of the Sun is that external natural factor that influences the course of the historical process. Now let us turn to an examination of the dependence that exists between the human organism and the various fluctuations of the space surrounding it. It should be remembered that this dependence between Man, as well

as animals and plants — on the one hand, and the inorganic world — on the other, is extremely strong, although subtle to the point of elusiveness.

The environment in which our organisms are immersed is constantly mobile and is subject to the most diverse micro and macro-oscillations and pulsations. The slightest deviation from a strictly horizontal surface, the movement of air or any nearby body, changes in the strength of sunlight, temperature and degree of humidity, soil emanation, etc., continuously fluctuate the potential of atmospheric electricity, since the atmosphere itself is a huge electric field.

Our organism, the colloidal system of which undergoes continuous changes, has a refined sensitivity to all external influences and fluctuations. Experiencing these fluctuations that disrupt the balance, the [human] organism is forced to continuously expend a certain amount of energy to restore this balance.

Many of these fluctuations do not reach the threshold of consciousness, and, usually, strong and healthy organisms react weakly to them; the process of restoring balance occurs unconsciously. But sharp fluctuations in the physical environment even in strong organisms cause certain disturbances, change the sign of the tone of higher nervous activity and create what in society is called a “change of mood”, without any apparent reason.

Herbert Spenser (1820–1903) considered life as maintaining a mobile equilibrium, as a continuous adaptation of internal relations to external ones.

The famous Russian physiologist I. P. Pavlov, a fellow of the Russian Academy of Sciences [who won the Nobel Prize for Physiology or Medicine in 1904], wrote the following about these equilibrations: “As a part of Nature, each animal organism is a complex isolated system, the internal forces of which, every moment, as long as it exists, as such, are balanced with the external forces of the environment. The more complex the organism, the more subtle, numerous and varied the elements of balancing. For this purpose, analyzers and mechanisms of both permanent and temporary connexions serve, establishing the most precise relationships between the smallest elements of the external world and the most subtle reactions of the animal organism. Thus, all life from the simplest to the most complex organisms, including, of course, Man, is a long series of increasingly complex balancing of the external environment to the highest degree. The time will come — albeit a distant one — when mathematical analysis, relying on natural science, will embrace all these equilibrations with majestic formulas of equations, including in them, finally, itself.”¹

Another Russian scientist, the famous meteorologist Prof. A. V. Klossovsky, wrote the following regarding the influence of external phenomena on the body: “Organic life on the

¹Pavlov I. P. *Twenty Years of Objective Study of Higher Nervous Activity (Behavior) of Animals. Conditioned Reflexes*. State Publishing House, Moscow-Petrograd, 1923, page 77.

Earth's surface occurs under the direct influence of a number of continuously changing climatic factors. Quantitative and qualitative changes in each of these factors entail corresponding changes in the functions of our body and, under certain unfavorable conditions, can cause a number of morbid phenomena. In general, the vital activity of our body is closely connected and dependent on meteorological factors." He then continued: "Changes in the quantity and voltage of solar insolation and atmospheric electricity also play an important role. If we could plot the changes of each of the numerous meteorological elements over a known period of time, then perhaps the curve of morbidity and mortality would be the result of a kind of interference of all meteorological elements. Finally, the influence of meteorological conditions is reflected in the activity of our organism not only directly, but also indirectly. These factors consist in the fact that they create more or less favorable conditions for the development and reproduction of pathogenic bacteria."¹

Diseased and nervous organisms, like the precise and sensitive instruments of a physicist, already sense to a significant degree the slightest fluctuations of the environment. This same phenomenon is clearly expressed in persons deprived from childhood or by nature of the main sense organs, for example, in the deaf-blind-mute. Possessing only the sense of touch and smell, they acquire amazing abilities to recognize many changes in the space around them, which can by no means be called a mere refinement of the senses remaining to them. The most diverse phenomena of the external world, beginning with the influence of objects on air layers and ending with the recognition of the mood of people around them, right up to guessing thoughts — are transmitted to them directly, without direct contact (Helen Keller).

For sick human organisms, insignificant changes in the physical environment sometimes play a rôle; these changes, affecting the entire system of the organism, make a person experience a range of diverse sensations, and sometimes make it possible to foresee the onset of some meteorological or volcanic phenomena several hours or even days in advance. In the scientific literature, there are indications that there are some individuals who predict, on the basis of various changes in their organism, earthquakes, thunderstorms, tornadoes and weather fluctuations in general. This is explained by the fact that all major meteorological and tectonic phenomena are preceded by known fluctuations in the physical environment. For example, before earthquakes, magnetic storms break out a day or more before, which are believed to appear as a result of violent movements of magma in layers of the Earth's crust, significantly removed from the surface. There are also indications that volcanic phenomena affect the force of magnetism (Fitzroy, Orlov). It is known that magnetism, in turn, has a very strong effect on the nervous system of sick and mentally

abnormal people, who, blindfolded, automatically obey the slightest movement of a magnet in the hands of a doctor, and can assume the most unnatural poses for a healthy person. According to the observations of the Japanese seismologist [Fusakichi] Omori, some animals exhibit remarkable sensitivity to ground vibrations. According to the ten-point Forel-Mercalli scale, even the lightest earthquakes are felt by very nervous people, while all others remain completely indifferent to micro-vibrations of the soil. But there are individuals with such a heightened activity of the nervous system that some time before the onset of an earthquake, detected later by the most accurate and sensitive seismic devices, they sense its approach. For example, at the [railway] station Ala in South Tyrol on January 27, 1897, two underground tremors were observed, which were predicted by a hysterical girl 1/4 and 1/2 hours before.²

A number of nervous and pathological diseases are closely connected with periodic or non-periodic changes of the electric or magnetic field surrounding the organism, which depend on the position of the celestial bodies. It has been known since ancient times that the position of the Sun and the phases of the Moon influence many diseases. For example, attacks of sleepwalking or a temporary semi-cataplexy of the human organism coincide with the new moon; acute brain disease — epilepsy also most often appears during the new moon, which gives reason to talk about the influence of the Moon on it; neuro-rheumatic diseases such as: sciatica, lumbago, migraine, tic, etc., as has been noted by patients, are in some relationship with the celestial bodies. The new moon worsens many nervous diseases — neuralgia, tabes, etc. We should also note the fact that women and female animals have a better chance of getting pregnant when their periods coincide with the full moon. In the medical literature there are indications of the possible influence of the Sun and Moon on other diseases and functions of the human body. Arrhenius showed³ that various changes in atmospheric electricity associated with the position of the Moon affect menstruation, birth rate, mortality, epilepsy, etc. Med. Dr. Dexter (London, 1904) published his research on the influence of meteorological factors on attention, behaviour, success in studies, as well as on the manifestation of crime, drunkenness, suicide, etc. Lehmann and Pedersen (Copenhagen, 1907) collected interesting data on the relationship between meteorological factors and human performance. We have already spoken above about Lombroso's work in this direction.

On the same issue, some interesting thoughts have recently been expressed by Nordmann. This French astronomer believes that even the most insignificant fluctuations in the external environment should influence the general state of the

²Klossovsky A. V. *The Physical Life of Our Planet Based on Modern Views*. Mathesis, Odessa, 1908, page 38.

Milne devoted a special work to this issue, published in 1896.

³Arrhenius S. *On the Influence of Cosmic Conditions on Physiological Functions*. *Scientific Review*, 1900, no. 2, page 297.

¹Klossovsky A. V. *Climatology in Connexion with Climatotherapy and Hygiene*. Mathesis, Odessa, 1904.

human nervous system and change his mental activity. In the laboratory instrument — the electroscope — Nordmann sees one of the powerful forces of the future state, a regulator of the social structure, the behaviour of citizens and the welfare of the country. Here the words of the English psychiatrist [Henry] Maudsley involuntarily come to mind: “We vibrate in unison with such individual influences of heaven and earth that our science cannot yet measure.” And not only humans are capable of responding to all these external changes, but also animals and plants, whose condition sometimes (for example, at the moment of the onset of atmospheric fluctuations) clearly reveals the abnormal state of their organism. The French entomologist Fabre published his very curious observations on the degree of sensitivity to external fluctuations of some insects. Among plants there are also species that show certain changes with fluctuations in humidity, pressure and potential fluctuations of atmospheric electricity. The vital functions of plants are closely connected with the development of a significant amount of electricity and, conversely, under the influence of electricity the vital activity of a plant undergoes certain changes. Undoubtedly, fluctuations in the electric and magnetic field, arising from cosmic or geophysical causes, have a huge impact on the life, development and morbidity of all plant and animal organisms.

It is known that the electrical action of sunlight on the atmosphere causes a number of chemical transformations in it. Ultraviolet rays of sunlight produce a chemical action. They transform an oxygen molecule O_2 into an ozone molecule O_3 . As early as 1874, Moffat tried to prove that in years of increased solar activity the average amount of atmospheric ozone is greater than during the minimum.¹ Then, under the influence of electricity, nitrogen in the air partially combines with hydrogen, water vapor and oxygen, forming ammonia compounds, nitrites and nitrates. Finally, exposure to sunlight causes the so-called Hallwachs photoelectric effect — the outflow of negative electrical charges from many rocks on the Earth’s surface (Stoletov, Righi).

A change in the chemical composition of the air is inevitably followed by a disruption of normal functions in the organism and a change in the course of chemical reactions in some of the most important organs.² The latter, through blood

¹Above we have already seen how the movement of cholera, plague and other infectious diseases flexibly corresponds to the course of solar activity. The idea that the spread of cholera is predisposed by the increase in negative electricity in the atmosphere has been repeatedly expressed by different scientists (Inozemtsev, Grauvogel and Schweickart).

²Already de Lamarck (1744–1829), and more recently Eimer, claimed that the biological process is determined entirely by external influences. This would mean that the diverse (physical and neuropsychic) variability of living organisms should be considered as a reaction to external influences, such as air pressure, temperature, light, water, climate, food, the entire surrounding physical and chemical environment, etc. Indeed, science knows many facts that fully confirm this point of view. For example, the convergence of the eyes of the embryos of the fish *Fundulus* occurs due to the addition of magnesium chloride to the water in which they are located; the enlargement of the gills in the tadpoles of one frog (*Rana arvalis*) is caused by a decrease in

circulation, can affect the state of the psyche, stimulating or depressing it, since modern science holds the view that psychic activity is a product of physico-chemical transformations in the nerve centres.

Therefore, it is very significant that until now no extensive research and observations have been made into the influence of periodic fluctuations in solar activity on the course of organic life on the globe in general and the psychic life of Man and animals in particular. True, the absence of work in this direction is justified by the fact that only recently has the science studying the higher nervous activity of Man taken the proper ground of physico-mathematical analysis. Until now, the influence of the environment on the nervous system has been studied primarily in relation to subjective reactions. But an objective observer states the real relationships that exist between the observed phenomena, confirming them with a mathematical formulation.

The study of nervous activity in some laboratories is now carried out using the methods of physics and chemistry and the application of mathematical analysis. The works of leading US and European scientists (J. Loeb, W. Nernst, etc.), among whom a prominent place is occupied by P. P. Lazarev, a fellow of the Russian Academy of Sciences and the Director of the Institute of Biological Physics (Moscow), who works in this field, have shown that nervous activity is based on a physico-chemical process.

Any irritation of the ends of the sense organs causes a chemical reaction in them, accompanied by the movement of ions. This movement is successively transmitted along the constituent parts of the nerve to the nerve cells and causes the appearance of corresponding reactions here, perceived by us as sensations. The latter, therefore, can arise only in the case of a physico-chemical process.

the amount of oxygen in the water containing them. The experiments carried out in this direction by Loeb are very instructive. Thus, external influences can modify organisms and affect the state of their bio-tonus. This variability of organisms under the influence of external agents has the following physico-chemical basis: the fact is that proteins, which represent a special most important part of organisms, are distinguished by chemical instability and, like colloids, have the ability to easily change their physical state.

On the other hand, in the organism itself there are organs whose activity can determine one or another state of the neuropsychic sphere. The studies of hormones (Sterling) showed the greatest valence of the functioning of the glands of the internal secretion. In addition to the fact that the development of the organism and the nervous formations in it, as well as the development of the sexual sphere, growth, vegetation, variability of appearance and mental activity depend on the chemical products produced by the pineal, thyroid glands, pituitary gland, etc., — in addition to all this, it has been established that the functioning of these internal laboratories, which are most important for the entire organism, changes greatly under the influence of external factors: an increase in temperature predisposes the thyroid gland to accelerated functions; carbohydrate and fatty foods inhibit the internal secretion of the pancreas, etc. The latter, in turn, affects the general state of mental activity, stimulating or inhibiting it. Consequently, one of the important elements that create the final result of a person’s neuropsychic activity, his behaviour, must also be considered the chemical functions of his internal organs. All this gives rise to a complex set of interdependent phenomena of external and internal order.

The act of thinking is accompanied by a physico-chemical reaction that exhibits periodicity. These reactions, which take place in the nerve centres of the cerebral cortex, are accompanied by the appearance of periodic electromotive forces that cause electromagnetic processes in the surrounding space.

The above provisions are a consequence of the totality of data available to modern biophysics and a necessary conclusion of Lazarev's ionic theory of excitation.

But if every act of thinking is accompanied by electromagnetic waves, it must be assumed that the corresponding nerve centres can serve as successors to these waves and thus directly perceive thought.

The hypothesis of direct transmission of thought has already been repeatedly expressed from the point of view of other theories, and this question can be considered close to a final solution. V. M. Bekhterev, a fellow of the Russian Academy of Sciences, wrote on this subject: "Is it possible for one individual to directly induce another, i.e., for one person to influence another without the use of any signs or other intermediaries in this matter? The question posed in this way, as it seems to me, has been resolved in a positive sense."¹

In order to discover the direct transmission of thought, many researchers have conducted experiments on animals and humans, which confirmed the possibility of direct communication (Richet, Lehmann, Bekhterev, etc.). In this case, the phenomena of suggestion — individual and mass suggestions — can be explained by electromagnetic excitation of the centres of one individual by the corresponding centres of another.

History abounds with eloquent facts of mass suggestion. In fact, not a single historical event has occurred with the participation of masses of people, where suggestion suppressing the will of individuals could not be noted. This suggestion in some cases was not limited to just a certain group of people, but covered cities and entire countries, and traces of it were preserved for a long time in political or military parties, passed on from generation to generation and reflected in various artworks. Thus, suggestion in the course of the historical process and the psychic evolution of Mankind acquires enormous significance of primary importance. Its role was formulated by [Gabriel] Tarde.²

Based on known data, which still need verification and substantiation, it can be assumed that the power of suggestion — the influence of individuals on human masses — increases with the intensification of the sunspot-forming activity. Our analysis of numerous historical events has shown that the influence of orators, popular leaders, and military leaders on human masses does not always have the same strength and fluctuates not only periodically according to the stages of the solar cycle, but even according to the seasons. The first can

be obtained from the fact of the integration of the masses in the 2nd period of the cycle and their unity during the period of maximum excitement. The second was noted by sociologists who studied the behaviour of crowds.³

Therefore, the assumption arises that the increase in the sunspot activity associated with the increase in its electrical energy has a very strong effect on the state of the electromagnetic field of the Earth, in one way or another exciting human masses to action and promoting suggestion. Chemical reactions within the human organism, taken as a whole, with sharp fluctuations or disturbances in the voltage of the electrical state of the atmosphere and soil, inevitably undergo changes, which should be reflected in the general state of the organism all the more sharply and quickly, the stronger and more sudden these changes are. In addition, perturbations of the magnetic and electrical fields of the Earth should produce quite direct, corresponding paroxysms in the nervous, as well as vascular systems of the organism. Thus, a complex of indirect and direct effects is obtained.

Significant disturbances on the Sun, accompanied by the radiation of electromagnetic waves and radioactive decay of solar matter, cause in human masses, in the presence of a factor uniting them, an explosion of unity, unanimity, immediately disposing them to certain actions. Consequently, *increases in solar activity transform the potential energy (energy of accumulation) of human masses into their kinetic energy (energy of movement)*.

Studying ancient annals, chronicles and annals of Asian and European peoples, we often encountered descriptions of social or military movements, linked to simultaneously occurring celestial phenomena, mainly with the northern lights, halos around the Sun or Moon and other optical effects that occur during large spots across the central meridian of the Sun. Ancient superstition attributed mysterious forces influencing people to these celestial phenomena, considering them — signs (signum). In the quivering lights of the polar lights (aurora borealis), in the circles around the Sun (fascia), etc., our ancestors saw omens of wars, natural disasters and pestilence. The noises accompanying meteorological phenomena were taken by them for threatening and punishing "voices of prophecy" (voces exprobatonis).

During World War I, we observed strange coincidences of the appearance of large spots on the Sun and the immediate intensification of military actions on many fronts. We made the first observation in mid-June 1915, when a large group of spots passed the central meridian of the Sun, when the polar lights, seen in Russia and North America, shone in the north, and magnetic storms continuously disrupted the movement of telegrams and people stubbornly and cruelly measured their strength in sea and land battles: Germans vs Russians, Austrians vs Montenegrins, Germans vs Englishmen. These observations laid the foundation for our research in this field.

¹*Ibid.*, pages 122–123.

²Tarde G. *Les Lois de l'imitation: étude sociologique*. Ed. Félix Alcan, Paris, 1890.

³Tarde G. *L'opinion et la foule*. Ed. Félix Alcan, Paris, 1901.

We can also cite two striking examples, noticed by many, confirming the above in the most illustrative way: let us recall that the February and October revolutions in Russia, as well as the revolutions in Germany and Austria, were preceded by unusually powerful upsurges of the sunspot-forming process on the Sun.

There are indications that on days of a large number of sunspots, the number of psychomotor excesses increases significantly. In order to discover such a connexion, I conducted a special study, which showed that the days of the greatest unrest among the masses of people, the days of mass socio-political movements coincided in time with major perturbations in the substance of the Sun. These amazing coincidences in their significance give such a probability to the positions we express that they fully justify a thorough and painstaking study of the subject.

Thus, historical events develop by means of a series of shocks caused by fluctuations in the sunspot-forming process on the Sun. The speed of action of these shocks, as well as the magnitude of their intensity, in all probability, are in a certain dependence on the elements of each individual fluctuation in the substance of the Sun, also caused by the position in a particular period of the sunspot-forming cycle.

Fig. 5 graphically depicts the complete coincidence of outbreaks of revolutionary activity of the human masses in Russia in the period 1905–1906 with episodic jumps in solar activity. True, the mathematical theory of correlation, when applied to these curves, will not give indications of a linear dependence, but the latter nevertheless perfectly illustrate the above formula. It can be said that social evolution, like evolution in the inorganic (shift laws, quantum theory) and organic (mutation theory) world, does not occur smoothly, but by means of sharp disturbances.

Thus, rapid episodic increases in solar activity can cause sharp changes in the mental state of human masses and sharply change their behaviour. Equally rapid falls in solar activity obviously cause changes in the mental state of the opposite nature. In other words, the *state of predisposition to the behavior of organized masses of people is a function of the activity of the Sun.*

Consequently, the critical resolution of mass movements of people is in a certain dependence on the course of the sunspot-forming processes on the Sun, as well as on the rotation of the Sun around its axis. This latter is noted by us because the rotation of the Sun can cause the disappearance or appearance of disturbed areas of solar matter, disrupting the course of some processes on the Earth.

There is every reason to recognize that there is a direct relationship between the periodic activity of the Sun and the social activity of humanity.

The possibility of such a dependence was perfectly foreseen by P. P. Lazarev, a fellow of the Russian Academy of Sciences, on the basis of his works in the field of his ionic theory of excitation: “The mechanical view of the nature of

higher nervous activity, which controls all human actions, has made such great strides in the field of natural science in recent times that it should become the basis for the study of mass phenomena in human society in the future. *The study of social phenomena in connexion with geophysical and cosmic phenomena should shed some light on the general law governing the mass actions of people, and provide the possibility of scientific substantiation of the laws of human society*” (here the Italic is mine A. L. Chizhevsky).¹

Perhaps, to an absolutely objective observer, the mass activity of people would appear to us as jumping elder balls in the simplest experiment proving electrical influence, or moving iron filings obeying every displacement of a magnet. The known properties inherent in the elder balls or filings can manifest themselves only when they receive a certain impulse from the conductor of an electrostatic machine or a magnet.

Therefore, it would be completely erroneous to assume that the periodic activity of the Sun is the main cause of these or those historical events. Every such event is a dynamic reaction of human masses from all the political and economic, as well as natural stimuli acting on them, changing their behaviour and determining the intellectual and social development of Mankind. The term “behaviour” applied to military-political movements of human masses would be entirely appropriate and should signify an attempt not at a historical-sociological, but at an objective natural-scientific study of mass phenomena among humanity.

V Prospects and conclusion

The theory of the dependence of human mass behavior on cosmic influence that we are substantiating is a conclusion from the main provisions of modern biophysics and can serve as some confirmation of them. The remarkable successes of this science in the field of studying higher nervous activity by means of physical and mathematical analysis force us to assume that Man, with his entire being, must be under the influence of powerful cosmic and geophysical factors.

And despite the fact that the greatest minds, beginning with Newton (1642–1727) and Kant (1724–1804) and ending with von Helmholtz (1821–1894) and Poincaré (1854–1912), have long recognized the physical-mathematical method as the highest and only scientific way of knowing Nature, even in our time there are scientists who hold opposing views and consider introspection and direct impression to be the best way of knowing Man and Nature, and naive realism to be the best philosophy. Convictions of this kind, devoid of a serious scientific basis, have an extremely detrimental effect on the development of some sciences, which to this day are filled with pseudo-scientific terms and an overwhelming abundance of dialectical material. But it is to be hoped that the social sciences, important to Man, will soon, thanks to the advances of

¹Lazarev P. P. *Physicochemical Foundations of Higher Nervous Activity*. Moscow, 1922, pages 59–60.

biophysics, be able to establish their positions on human relationships by applying precise disciplines. This will be an important step forward towards discovering the regularity in the social evolution of Mankind, the laws of which are undoubtedly no exception to the general principles of Nature.

Since the time of the ancient Chaldean thinkers, regularity has been elevated to the basis of the world process, and modern science with each of its forward movements only confirms this philosophical view of ancientry. Indeed, if chaos were realized in the world, obviously, not only would we, thinking beings who appeared as a result of a million-year manifestation of regularity, not exist, but also less complex, but equally amazingly coordinated organic and inorganic formations. We observe regularity both in the motion of celestial bodies that make up the visible stellar world, and in the motion of electrons that make up the atoms of matter. The functions of living organisms, which have their own periods and phases, are also subject to it. Indeed, the surrounding nature has been the source of the conviction in the human mind since ancient times that the regular periodicity or recurrence of phenomena in space and time is the fundamental property of the world, which is governed by the same laws, which apply equally to all parts of nature, regardless of how Man divides and dissects them: both inorganic and organic matter, with all its mental activity, are subject to the same principles common to the entire Universe.

Therefore, with necessary compulsion, the consequence follows that the historical development of humanity, taken as a whole, must proceed in a certain, completely lawful manner, according to the resultant of all the internal forces of social order and external forces of the surrounding nature acting on humanity.

The theory of the physical foundations of the historical process that here allows us to state the fact of the presence of a certain kind of rhythm in the mental activity of all humanity and periodic fluctuations in the course of the world-historical process, as an expression of this rhythm. Consequently, both the collective life of all Mankind and the life of individuals are subject to strict and unchanging laws of rhythm, which can be discovered through research that covers in its material the actions of large human masses and large periods of historical time.

Various phenomena and events of the world history of Mankind, in the light of the theory presented here, acquire a new meaning and significance. Of extreme importance, both in a purely scientific and practical sense, is the establishment of the fact that historical and social phenomena occur *not arbitrarily, not whenever, not indifferently with respect to time*, but are subject to physical laws in connection with the physical phenomena of the world around us and can arise *only when* the entire complex set of interactions of political, economic and other factors in the human world and physical factors in the world of inorganic nature is favorable to this. Thanks to the regularity to which the course of events in time

is subject, every phenomenon in the life of individual communities or in the international life of all Mankind receives a certain explanation, *elevating history to the level of exact disciplines endowed with exact laws*. We have already said above that science is knowledge of the measurable. To make history a science, and not a “conventional fairy tale”, to free it from metaphysics, from the arbitrariness of subjectivism, from everything incommensurable, to give it, as well as its sister, sociology, measuring units and laws — this is the direct task of the near future.

On the way to this, even with the first experiments, perhaps weak and insufficient, the changes and gradations of the mood of the masses of people and the military or political events associated with them become clear to us. We see that all of them are not accidental, but, on the contrary, are subject to laws that compel the masses of humanity, in the presence of disposing reasons, to strictly defined actions. Thus, little by little, the exact sciences begin to penetrate the chaos of history, to measure it with units of historical time that have equal significance and to explain phenomena that occurred in very distant epochs. History is turning into a science of the living, of the necessary, of the near. Events covered with centuries of dust come to life again and begin live intensively and significantly. Every historical figure, every historical phenomenon becomes understandable to us. All of them occurred under the direct influence of the same periodic disturbances or calms in the nature of the Earth that are occurring now and will most likely occur in the distant future of humanity. Now history is given a place not next to Nature, but in it itself, as Karl Ritter said. Therefore, in our opinion, it will be necessary to create other methods for studying history than those that have been accepted until now.

A deep and comprehensive formulation of this problem reveals a whole series of facts, large and small, requiring the most careful scientific analysis. I have considered a significant part of them, to the best of my ability, in my other works. Therefore, here I consider it necessary only to briefly dwell on those points that urgently require illumination, study and resolution.

From the above, it was easy to conclude how amazingly flexible historical events, accomplished by human masses, follow the imperative orders of our daily luminary.

Elemental changes in processes on the Sun, in one way or another, entail changes in material processes in the organs of higher nervous activity, and these latter violate the line of behaviour of all Mankind, the line that we call the historical process. Therefore, the question arises: are we not in bondage to the Sun, are we not in slavery to its electrical forces? If you like — yes, but our bondage is relative, and we ourselves can control the chains that are put on our wrists and the work that is destined for us to do. The Sun does not enforce us to do this or that, but it makes us do something. But humanity follows the line of least resistance and plunges itself into the oceans of its own blood.

As we have seen before, the maximum of solar activity promotes the excitement and unification of the masses in the name of fulfilling some general need, put forward by economic and other reasons. During this period, rulers, military leaders, and leaders appear and mass actions begin: wars, uprisings, etc. However, all these movements are not necessary: everything depends on the events that preceded them. Thus, for example, if a war has already been waged before the period of maximum excitability, then the general excitement can result in the desire for peace — peace at any cost. The conclusion of peace in the 3rd period of the cycle is not an exception to this theory; on the contrary, in this case it was the result of the same manifestation of human masses, the general demand of the masses. History knows excellent examples of mass agitations of people during the period of maximum, having nothing in common with bloody events, namely: religious movements, pilgrimages, the rise of parliamentarism, localization of public attention on trials, reforms, constructions, etc. This gives reason to cherish the wonderful hope that the future culture will find ways of humanely using mass upsurge by means of preliminary propaganda of some socially important and interesting matter, and its implementation during the period of maximum excitability. Then collective theatrical art, collective artistic creativity, with the participation of the masses of people, scientific expeditions, sports competitions, the organization of grandiose structures, cities, canals and so on will have to replace the bloody slaughter usual to Mankind.

It is easy to conclude what an important rôle propaganda or the presence of some idea in the masses of people plays. In the brief essay on the 2nd period of the cycle, we indicated that in most cases it is precisely in this period that certain ideological trends arise in human masses, which determine the course of the entire cycle, manifesting themselves in the form of popular movements during the period of maximum excitability. The life of ideas in human masses during the 2nd period of the cycle is what should interest every statesman.

Indeed, if an idea is given and implanted which is readily accepted by the masses of people as an expression of their desires at the given moment, the government's cause will be won, because the masses will be with them. The harmonious balance of the people and the government will be maintained. But if there is disagreement among the statesmen who give tone and direction to all the [governmental] apparatus of the country, if they fail to approach the human masses psychologically and skillfully and introduce into their midst some ideas which symbolize their aspirations and needs, and finally, if this or that mechanism which unites the masses functions poorly, this government will never succeed in achieving the precise realization of its goals. The relationship between the government and the people is subject to fluctuations depending on the period of sunspot activity. Taking this point of view, one can understand the true significance of the official mass media and political literature in general. At moments of maximum excitement, when sensitivity to the perception

of ideas reaches its highest degree, the slightest fluctuation in the political situation is sometimes enough to undermine the old and give birth to a new object of social concentration and thereby change the mood of human masses and lead them to other decisions, to other political results. We do not yet know, but we dare to assume that the movement of ideas and teachings in the human masses is in a certain relationship with the gradual changes in the influence of the cosmic factor considered here. A comparative study of this problem would allow us to establish the laws of their evolution and resolve one of the most interesting and important problems of sociology. The question of whether all possible manifestations of the intellectual and social activity of Mankind are dependent on a *series* of influences of cosmic factors and even on a certain number of them is also not without scientific significance. There is nothing incredible in the assumption that the presence of a periodically acting factor causes a number of such phenomena which, although they do not have precise boundaries in time, the periodicity of which can be discovered through careful research.¹

Thus, the significance of the presented theory should be considered from the point of view of political science. This theory indicates to the state authorities the methods of action that are in accordance with the mental state of the masses of people who are dependent on the fluctuations of the electric energy of the Sun. The greatest mistakes and failures of rulers, military leaders, and leaders of the people could often be caused by the fact that, without taking into account the state of the mental predisposition of the human masses, they either demanded from them the impossible, not corresponding to the state of their psyche, or mistakenly counted on their support at a time when the masses were deprived of the unity that binds them together, external factors had not begun to exert their influence on them, or the latter was already ending. From this assumption, which has good grounds, it is not difficult to draw a conclusion about the horizons that are opening up for the leaders of the people, diplomacy, strategy, etc. Without fear of falling into the spirit of science fiction novels, one could say that from now on there will be no more false steps, unsuccessful attempts, illegitimate aspirations!

The state power must know about the state of the Sun at any given moment. Before making this or that decision, the government must know about the state of our daylight: is its face bright, clear or darkened by spots? The Sun is a great military-political indicator: its readings are infallible and universal. Therefore, the state power must align itself with its arrows: diplomacy — by the monthly arrow, strategy

¹Attempts have been made repeatedly to find and define these principles of periods that are constant for all cultures and peoples, beginning with Giambattista Vico (1668–1744) and his work *Principi di una scienza nuova intorno alla comune natura delle nazioni* (1726) and ending with Ottokar Lorenz (1832–1904) "Die Geschichtswissenschaft in their Hauptrichtungen und Aufgaben kritisch erörtert" (1886) and the bold concepts of our contemporary Oswald Spengler in his *Der Untergang des Abendlandes* (1920).

— by the daily arrow. Before each battle, military commanders must know what is happening on the Sun. Consequently, the immediate branches of historiography should become one of the most important experimental sciences of political science, and astronomy — an applied science. The time before the historiometric understanding of social phenomena can be, in all fairness, compared with those distant epochs when the navigator did not yet know the compass and had not learned to distinguish directions by the stars. His fragile ship was arbitrarily drawn by the water element, and he did not know where to return the rudder, so as not to wander on the waves, exposing himself to danger at any moment.

The division of all history into cycles — units of historical time — has the task, as we have already seen above, of a comparative study of the four main parts of each cycle and the derivation of laws of behaviour of large human masses. In the work cited earlier, I show, on the basis of well-known data, the possibility of establishing such laws. Of course, even the most detailed analysis of general history is by no means sufficient for this. Direct observation and study of the behaviour of human masses in all states on the Earth from the point of view of the principles briefly outlined here are also necessary.

Then, when these laws will be established empirically, carefully verified and converted into causal ones, by introducing causal connections, Mankind will acquire new knowledge — foresight of the near future. This knowledge is so far characteristic only of the exact sciences, which predetermine the entire course of this or that phenomenon. It is easy to conclude about the greatest consequences that follow from the implementation of the above: *tantum possumus quantum scimus*.

Then the possibility of forecasting the near future will open up, both in relation to time, and in relation to the quality and intensity of military or political events, which until now neither knowledge of history nor the wisdom of statesmen has provided. Now we have in our hands a simple but effective scheme: the nature of the Sun and the Earth rages — people are agitated; the nature of the Sun and the Earth has calmed down — people have calmed down. Therefore, politicians or military leaders should not cherish hopes for the possibility of this or that event. They must know what will really appear with that immutable necessity which characterizes the phenomena of the physical world, completely independent of personal hopes or governmental plans.

Not only the field of military or political science will gain from the study of the behaviour of human masses according to the periods of solar activity — the establishment of laws governing each period will entail a revision of many aspects of human life and the establishment of firm limits for diverse collective and individual activity. Then it will be possible, with the aim of greater productivity of work, to establish norms and forms of activity for each individual in the field of his special profession. Such a delimitation of human life according to the hours of solar activity may give Man

the means of extracting from his psyche the maximum of its energy. Then the methods of upbringing, education and professional work will have to be radically modified.

Moreover, we are convinced that further study of the influence of cosmic and related geophysical factors on human behaviour will have to open up the most extensive horizons for amazingly curious research. Perhaps the eternal and everyday episodes in the life of individual human groups, families, clans, societies, not to mention peoples, nations, states, — are in direct connection with one or another influence of these factors.

Discords and agreements in families, associations, partnerships; the stormy or peaceful course of parliamentary sessions, at which state questions of primary importance are discussed, leading the country to one or another decision; the height of battles or truce on the fronts of wars or revolutions — all of them, on the average, depend on the given state of the central body of our system, on the changes it introduces into the physical environment of the Earth.

Fluctuations in the personal life of individuals are to one degree or another subordinated to the course of the periodic activity of the Sun or are even caused by it. This is especially clear and distinct in the lives of great statesmen, rulers, military leaders, reformers, etc. It is enough to take the biography of any of them to be convinced of the constant correlation between the life of a given person and the changes in the course of the synchronous curve of relative Wolff numbers. This is a fact worthy of astonishing attention and study. Let us take as an example the life of Napoleon Bonaparte (Napoleon I), who troubled Europe for such a long time. It turns out that he, this giant of personal tyranny, had to submit with precision and obedience in his actions to the inexorable influence of the cosmic factor. Thus, the height of his activity can be attributed to the era of maximum solar activity; conversely, the minimum of the military-political activity of this Corsican coincides with the minimum of sunspot formation. This is clearly evident in the period from the end of 1809 to the beginning of 1811, when, according to Wolf's table, we have a minimum of spots and Napoleon did not undertake a single campaign of conquest, only made a number of bloodless acquisitions, and Napoleon himself found time in this era to think "pro domo sua". This period was the apogee of his peaceful autocracy and a time of quiet cabinet work. Meanwhile, the year of the preceding maximum (1804) raised the name of Napoleon to an unattainable height of glory and crowned him with the imperial crown, and the year of the following maximum (1816) placed him on the island of St. Helena. Napoleon's consulate began precisely at the minimum of solar activity (1799), when the revolutionary masses of France had become quiet, and absolutist inclinations could freely flare up in this ambitious artillery officer.

From this it is easy to understand what a great significance for many social sciences a comprehensive study of the question touched upon here must have; the solution of the lat-

ter may entail a radical break in the most diverse aspects of social life that have taken root among Mankind. Its solution will immediately have to be reflected in jurisprudence, diplomacy, labor, artistic and scientific creativity, not to mention, of course, the military or political branches of knowledge.

We do not at all pretend to the absolute reliability and, even less, the categorical nature of our considerations and statements on this subject. They must only show that an objective study of the connexion between some and other phenomena of Nature, which have hitherto been considered independent of each other, can throw light on the most diverse cases of the mental and social life of Man.

Of course, no truth is obtained immediately, like “*deus ex machina*”; a whole series of diverse, sometimes mutually contradictory and mutually exclusive hypotheses and theories precede it. Even in such an exact science as the “queen of sciences” — astronomy — we encounter essentially diametrically opposed opinions on the most important astronomical problems; this is especially evident on the question of the structure of Mars. But the task of a synthetic judgment is precisely to embark on the path of broad generalizations and find a relationship between the phenomena that seem to belong to completely different areas of knowledge and life without fear or apprehension before a judgement of blindly prejudiced, sometimes ignorant criticism. These attempts are led by a combined knowledge of philosophical, natural and historical disciplines.

Therefore, if one may not agree with some of the propositions briefly expressed in this work, this only shows that every truth is necessarily preceded by a time of searching, experimentation, disagreement, and debate. I am also sure that there will be skeptics who, without taking the trouble to familiarize themselves in detail with the theory and other of my studies, on which this theory is based, will deny and dispute it. But we know that bare denial is always fruitless. It is better to doubt something than to refute it, for doubts lead to discoveries. The most unsuccessful assumptions also indirectly direct us to them, stimulating our minds to research.

In the field of exact knowledge, discoveries can be divided into two categories. The first of these are those which represent additions to previously established truth, its continuation, an extension of its boundaries. To verify them, only a certain amount of patience and a quite ordinary mind are required. But there are discoveries which involve a radical break with old views on the nature of a given phenomenon. To evaluate such a discovery, an appropriate expert with a broad intellectual horizon must be selected, a kind of “knight without fear and reproach”, who, without fear of the loud judgments of the ignorant, could defend the discovered facts in the face of an astonished and distrustful world. Such knights are not often encountered: the history of science is full of examples of the opposite nature. We meet such examples everywhere; there are many of them in the last century. At the end of the 1840s, ideas about the conservation of energy met with a harsh atti-

tude from their contemporaries, and the most important scientific journal *Annalen der Physik und Chemie* did not accept von Helmholtz’s famous memoir. Robert Mayer has had his share of troubles. And there are tons of such facts! I believe that a favorable attitude toward a new, sufficiently substantiated theory or a new method is an indispensable sign of a high mind, for it indicates the breadth of its intellectual sphere and the ability to think independently. Most people are not endowed with these qualities: their knowledge conceals in its foundation school rules, forever memorized, and their minds do not know how to respond with due sensitivity to newly discovered truths, which always seem false to them and the facts cited in their confirmation, a simple accident or, even worse, a manipulation. It would be completely unfounded to think that the materials cited in this article were chosen with the calculation to produce an effect. Due to the novelty of the issue under study, mistrust and surprise at the conclusions obtained, we foresee such judgments. It would also be unfounded to think that our curves, which, in fact, can easily be given any form, pursue the same goal and do not correspond to the actual state of affairs. More credulous people may assume, however, that when proving something, a person involuntarily strives to choose for proof what he needs, discarding everything that hinders or harms the course of the proof.

I consider it my duty to categorically reject such assumptions and accusations, and I refer anyone who will not consider it a hassle to check the materials to my main research cited in the Introduction. From this point of view, I consider the question exhausted in a positive sense, despite the additions and corrections that may follow in future work in this direction (for my work is by no means finished), but which will only change the configuration of the mentioned curves to an insignificant degree. The probability of the reliability of the main provisions of the question under study is so great that it leaves no room for fundamental objections. I do not overestimate the results of my work and regard my work as the first modest initiative that can give rise to deeper and more complete research. However, no matter how successful the objections made to me, no matter how convincing and even supported by appropriate arguments, I still have every reason to think that no dialectic, no matter how talented it may be, is capable of belittling conclusions based on facts, numerical relationships and the latest achievements of science. These achievements, I repeat here once again, require an exact explanation of all the phenomena of Nature, devoid of any metaphysical premises, including Man with his diverse mental activity. And in the field of the exact sciences, nothing should be astonished, nothing should be denied a priori and nothing should be neglected. The history of scientific thought abounds in examples of gross errors. Let us recall at least the most prominent philosopher and scientist of the last century, Auguste Comte, who in 1842, several years before the brilliant works of Bunsen and Kirchhoff, in his work *Cours de*

philosophie positive denied the possibility of ever accurately knowing the chemical composition of celestial bodies.

Science is moving forward with slow steps, revealing the regularity in all manifestations of the organic and inorganic world. The time has not yet come to subject the social evolution of Mankind to precise laws and embrace one general universal theory, as has been done for the cosmic bodies of the Solar System, but we must believe that this time will come, as it is already approaching, to establish the regularity of stellar movements, previously considered to be unrelated to each other and arbitrarily occurring in the infinity of space. And just as a number of astronomers in many countries of the world diligently accumulate materials about the stars in the form of radial velocities, proper motions and distances to the stars, so the immediate task facing scientists is to study the influence of the slightest fluctuations in the environment on human mood and behaviour.

For these purposes, special scientific institutes should be organized in all countries of the world to keep the most accurate records of all social fluctuations and movements in their origins, development, and modifications. Strikes at factories and plants, walkouts, meetings, peasant unrest, manifestations of mass enthusiasm, demonstrations, episodes involving crowds of people, and so on, not to mention, of course, larger events, should be subject to accurate records, diagnosis, and classification. The methodology for this work is currently being developed by me¹. From the data collected, graphs of fluctuations in individual types of mass human activity in each country, and then on the entire Earth, will be constructed. Finally, daily data on various types of mass activity will be compared with daily data from astronomy and meteorology. These comparisons will have to reveal the relationship that exists between these two phenomena — and in this way provide access to the field of studying the laws governing human actions under the influence of cosmic and geophysical factors.

In the international and national organization of such institutions I see the guarantee of the future well-being of all Mankind. We must remember that the influence of cosmic factors is reflected more or less uniformly on all the billions of human individuals who now inhabit the Earth — *sol lucit omnibus*, — and it would be crime to ignore the study of their influence, no matter how subtle and elusive at first glance it may not be.

In 1927–1929 we should expect the onset of the maximum of solar activity. If we allow the existence of periods of 60 years (Young) and 35 years (Lockyer), which are added to the main oscillation of 11 years, then the nearest future maximum should be especially intense (maximum maximum), since the maximum of 1870 was distinguished by great strength. In all probability, in these years, due to the presence

of factors of a socio-political nature, major historical events will occur that will again change the geographical map. It would be very desirable by this time to prepare the possibility of a scientific experiment in the field of research into the behavior of individuals and human masses. The latter can be realized only if the researchers meet with sympathy from the government. Otherwise, such an important field of knowledge for humanity will languish in vain for a long time, remaining unnoticed and unstudied by anyone.

It may take many decades of hard work before the plans that are only being projected now are realized. Much work remains to be done, and it is not we who will have to reap the fruits from the tree that we have planted and nurtured. But such is the lot of workers in science: it bears fruit not to those who are ready to die for it and, indeed, sacrifice their lives, but to those who treat it, if without hatred, then, probably, without love and filial devotion.

But those who, in the name of science, are ready to endure all privations and all troubles, starving for years and walking in rags, have one great consolation, one great joy, worth all the blessings and all the pleasures of the world, making them independent of human vulgarity and human judgments, and elevating them: they are closest to the knowledge of the secret laws that govern the mighty life activity of Nature. They already know its internal mechanisms, grasp the connections between shafts and wheels and, in indescribable delight, approach that lever, one push of which is capable of immediately changing the distribution of the parts of the eternally working mechanism and thereby regulating the phenomena of Nature itself — phenomena that until that moment moved in mysterious ways. They are approaching the possibility of controlling great events.

In unity there is strength! I believe that the world solidarity of scientists will help to overcome all difficulties and break down all barriers in the name of protecting life on the Earth and transforming it.

When Man acquires the ability to control the events of his social life entirely, those qualities and impulses will develop in him which sometimes even now shine on his forehead, but which will shine ever brighter and stronger, and finally will completely illuminate with a light similar to the light of the Sun the paths of perfection and well-being of the human race. And then it will be justified and proclaimed: the closer to the Sun, the closer to the Truth.

November 1922, supplemented in 1923

¹See the work to be published: Chizhevsky A. L. *The Necessity of Creating International Scientific Institutes to Study the Influence of Natural Factors on the Behavior of Individuals and Collectives*.

Progress in Physics is an American scientific journal on advanced studies in physics, registered with the Library of Congress (DC, USA): ISSN 1555-5534 (print version) and ISSN 1555-5615 (online version). The journal is peer reviewed.

Progress in Physics is an open-access journal, which is published and distributed in accordance with the Budapest Open Initiative. This means that the electronic copies of both full-size version of the journal and the individual papers published therein will always be accessed for reading, download, and copying for any user free of charge.

Electronic version of this journal: <http://progress-in-physics.com>

